Arthritis & Rheumatology

An Official Journal of the American College of Rheumatology
www.arthritisrheum.org and wileyonlinelibrary.com

Cover design: Todd Machen

♾ This journal is printed on acid-free paper.

Arthritis & Rheumatology
An Official Journal of the American College of Rheumatology
www.arthritisrheum.org and wileyonlinelibrary.com

VOLUME 69 MAY 2017 NO. 5

Cover image: The figure on the cover (from Brunger et al, page 1114) illustrates a method for generating induced pluripotent stem cells resistant to interleukin-1 signaling. Guide RNAs (gRNAs) target Cas9, a gene editing nuclease, to exon 2 of the interleukin-1 receptor *Il1r1* gene, which results in deletion of the receptor's signal peptide sequence. Stem cells engineered using this technique do not respond to the proinflammatory cytokine interleukin-1.

ACR ANNOUNCEMENTS

AMERICAN COLLEGE OF RHEUMATOLOGY
2200 Lake Boulevard NE, Atlanta, Georgia 30319-5312
www.rheumatology.org

ACR Meetings

Annual Meetings
November 3–8, 2017, San Diego
October 19–24, 2018, Chicago

Pediatric Rheumatology Symposium
May 17–20, 2017, Houston

For additional information, contact the ACR office.

Nominations for ACR Awards of Distinction and Masters Due May 15

The ACR has many Awards of Distinction, including the Presidential Gold Medal. Members who wish to nominate a colleague or mentor for an Award of Distinction must complete the online form at www.rheumatology.org. The nomination process includes a letter of nomination, 2 additional letters of recommendation, and a copy of the nominee's curriculum vitae. Recognition as a Master of the American College of Rheumatology is one of the highest honors the ACR bestows. The designation of Master is conferred on ACR members age 65 or older who have made outstanding contributions to the field of rheumatology through scholarly achievements and/or service to their patients, students, and the profession. To nominate someone for a Master designation, members must complete the online nomination form at www.rheumatology.org and include a letter of nomination, 2 supporting letters from voting members of the ACR, and the nominee's curriculum vitae. Nominees for ACR Master must have reached the age of 65 before October 1, 2017.

ACR Invites Nominations for Volunteer Positions

The ACR encourages all members to participate in forming policy and conducting activities by assuming positions of leadership in the organization. Positions are available in all areas of the work of the American College of Rheumatology and the Rheumatology Research Foundation. Please visit www.rheumatology.org for information about nominating yourself or a colleague for a volunteer position with the College. The deadline for volunteer nominations is June 1, 2017. Letters of recommendation are not required but are preferred.

2017 Pediatric Rheumatology Symposium

The 2017 Pediatric Rheumatology Symposium, taking place May 17–20 in Houston, Texas, will provide a venue for attendees not only to hear about cutting-edge updates in the practice of pediatric rheumatology, but also to attend scientific sessions reporting findings that have yet to be published. The symposium will focus on closing the gap between clinical experience and practice through expert lectures, plenary sessions, and oral and poster abstract presentations. Attendees can participate in lunchtime sessions and informal roundtable discussions on a wide variety of topics. For additional information and to register, visit www.rheumatology.org/Learning-Center/Educational-Activities.

In this Issue

Highlights from this issue of *A&R* | By Lara C. Pullen, PhD

Multi-Biomarker Disease Activity Score May Be Useful for Guiding RA Treatment

In this issue, Hambardzumyan et al (p. 953) sought to determine whether the Multi-Biomarker Disease Activity (MBDA) score could be a valuable tool for predicting which second-line treatment would be preferable in a patient with rheumatoid arthritis (RA) who has not responded adequately to methotrexate (MTX) monotherapy. The investigators classified patients according to MBDA score, which is based on measurement of 12 serum biomarkers and is designed to correlate with the 28-joint Disease Activity Score using the C-reactive protein level. They studied 157 RA patients who did not respond well to MTX and found that 12% had a low MBDA score, 32% had a moderate MBDA score, and 56% had a high MBDA score.

p. 953

The team discovered that MBDA score categories were differentially associated with response to subsequent therapies. For example, 88% of individuals with a low MBDA score responded to subsequent triple therapy (MTX plus sulfasalazine plus hydroxychloroquine), but only 18% with a low MBDA score responded to MTX plus infliximab. In other words, individuals who experienced post-MTX biochemical improvements were more likely to respond to triple therapy than to MTX plus infliximab. In the case of individuals with a high MBDA score, 35% responded to triple therapy and 58% responded to MTX plus infliximab.

When the investigators used 38 as a cutoff for the MBDA score, the differential associations with response to triple therapy versus MTX plus infliximab were 79% versus 44% for patients with a lower MBDA score and 36% versus 58% for patients with a higher MBDA score. These results suggest that the MBDA score is a better predictor of response to triple therapy or to MTX plus infliximab than clinical and inflammatory markers. The authors concluded that, if their findings are confirmed, the results may contribute to a better treatment algorithm for RA.

Gut Microbe Associated With RA

The intestinal microbe *Prevotella copri* is known to overexpand in stool samples from patients with new-onset rheumatoid arthritis (RA). Up until now, however, no clear relationship between the organism and RA pathogenesis had been identified. In this issue, Pianta et al (p. 964) report that subgroups of patients with RA have differential IgG or IgA immune reactivity to *P copri*.

p. 964

The investigators used peripheral blood mononuclear cells (PBMCs) from RA patients, and for comparison, Lyme arthritis patients to search for HLA–DR–presented peptides derived from *P copri*. In RA PBMCs, they identified a peptide derived from a 27-kd protein (*Pc*-p27) that was able to stimulate Th1 responses in 42% of patients with new-onset RA. The investigators then tested for antibody responses to *P copri* in patients with new-onset RA as well as those with chronic RA.

When they evaluated patients with new-onset RA and those with chronic RA, they found that 1 subgroup had IgA antibody responses to either *Pc*-p27 or the whole organism. This response correlated with Th17 cytokine responses and frequent anti–citrullinated protein antibodies (ACPAs). The other subgroup had IgG *P copri* antibodies that were associated with *Prevotella* DNA in synovial fluid as well as *P copri*–specific Th1 responses and less frequent ACPAs. The investigators also noted that the *P copri* antibody responses were rarely found in patients with other rheumatic diseases or in healthy controls. These antibodies thus appear to be specific for RA and provide evidence that *P copri* is immune-relevant in RA pathogenesis.

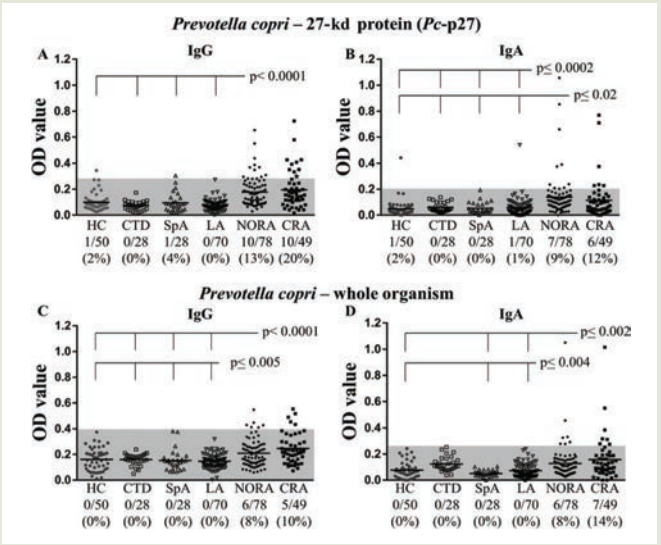

Figure 1. IgG and IgA responses to *Prevotella copri* in rheumatoid arthritis (RA) patients and control subjects. Serum samples from 303 individuals (healthy control [HC] subjects and patients with connective tissue diseases [CTDs], spondyloarthritides [SpA], Lyme arthritis [LA], new-onset RA [NORA], or chronic RA [CRA]) were tested for *P copri* antibodies. Enzyme-linked immunosorbent assays were performed to measure levels of IgG (**A**) and IgA (**B**) against the *P copri* 27-kd protein (*Pc*-p27) as well as levels of IgG (**C**) and IgA (**D**) against 1% formalin–inactivated *P copri* (whole organism). A positive response was defined as a value >3 SD above the mean in healthy controls (area above the shaded region). Each symbol represents a single subject; horizontal lines show the mean. **Star** represents patient RA1. Only significant *P* values relative to healthy controls are shown.

Analysis of Arab Population Reveals New RA Risk Loci

Genetic association studies in rheumatoid arthritis (RA) and meta-analyses of these associations can be useful in uncovering novel risk alleles for disease. p.976 Such studies have primarily been performed in European and East Asian populations, leaving the Arab population largely unstudied. Consequently, genetic factors underlying susceptibility to RA in the Arab population are largely unknown.

In this issue, Saxena et al (p. 976) describe the results of the Genetics of Rheumatoid Arthritis in Some Arab States Study. Theirs is the first RA genome-wide association study in the Arab population. All subjects in the study were nationals of 1 of the 22 countries of the Arab world and were enrolled from centers in Jordan, the Kingdom of Saudi Arabia, Lebanon, Qatar, and the United Arab Emirates. The investigators based their definition of Arab ancestry on self-report, and they analyzed >7 million single-nucleotide polymorphisms (SNPs) for association with RA. The researchers also looked specifically at SNPs in 794 RA cases and 573 healthy controls to determine associations between SNPs and seropositive and seronegative RA.

Their study revealed that the genetic architecture of RA in the Arab population is similar to that in other ethnic groups. The investigators also found that *HLA*-region and RA risk alleles identified in Europeans and East Asians contribute strongly to the risk and severity of disease in Arabs. In particular, they found that 3 loci reached genome-wide significance in the analyses of associations with RA and with seropositive RA. All 3 loci also demonstrated evidence of independent replication. Moreover, the researchers found that, as in other populations, the strongest association was between RA and *HLA–DRB1* amino acid position 11.

A weighted genetic risk score of 68 previously associated RA loci was found to be associated with both RA and seropositive RA in the Arab population. The investigators were also able to contribute population-specific insights into the pathophysiology of RA by identifying 2 novel RA risk loci in Arabs. The 2 novel associations were found at the 5q13 and 17p13 loci.

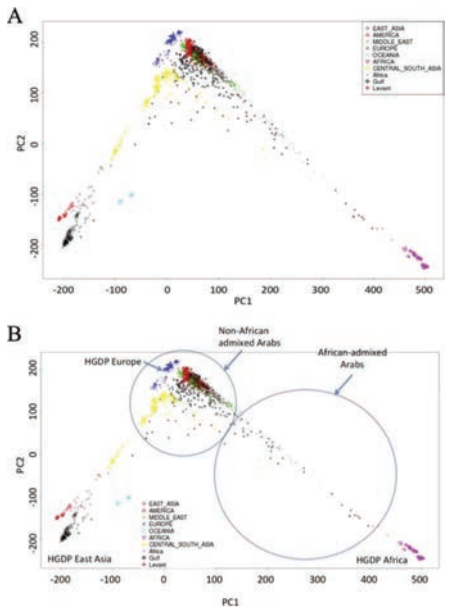

Figure 1. Principal components (PC) analyses of the entire rheumatoid arthritis case–control discovery cohort of Arabs (**A**) and the subgroups of Arab populations (African-admixed and non–African-admixed) defined for secondary analysis (**B**), relative to Human Genome Diversity Project (HGDP) populations. The first PC (PC1) and second PC (PC2) are shown in the plots.

Early Mortality in Systemic Sclerosis Is Substantial

In this issue, Hao et al (p. 1067) report results from the largest study to date (n = 1,070) to examine mortality and causes of death in an inception cohort with systemic sclerosis (SSc). They found that early mortality in SSc is substantial. p.1067 Specifically, the investigators identified 140 deaths (13%) over a median follow-up of 3.0 years. In most cases (62.1%), the primary causes of death were SSc-related. The most common non–SSc-related causes of death were malignancy, sepsis, cerebrovascular disease, and ischemic heart disease. The researchers also calculated a pooled standardized mortality rate (SMR) of 4.06 in the inception cohort, with up to 22.4 years of life lost in women and up to 26.0 years of life lost in men. Of particular note, mortality in the diffuse disease subtype was 24.2% at 8 years. Male sex, older age at disease onset, diffuse disease subtype, pulmonary arterial hypertension, and renal crisis were all predictors of early mortality.

In contrast, the investigators calculated that their prevalent cohort of 3,218 had a pooled SMR of 3.39. The authors concluded that use of prevalent cohorts underestimates mortality in patients with SSc because it fails to capture early deaths, particularly deaths that occur in men and in individuals with diffuse disease.

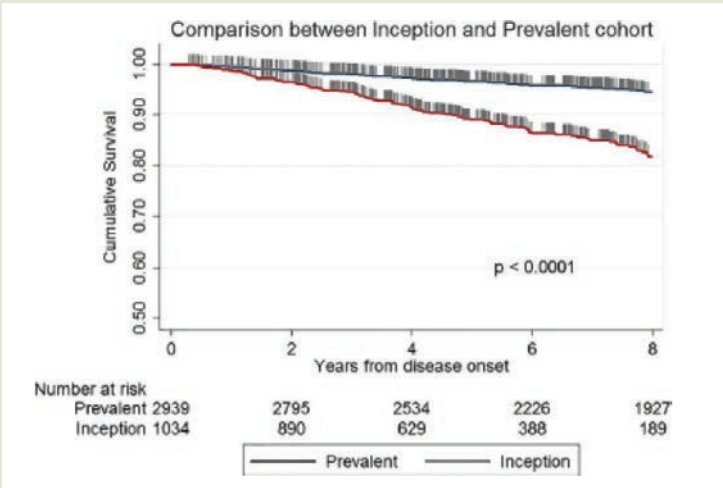

Figure 1. Kaplan-Meier analysis of overall survival in the first decade following disease onset in the combined inception cohort and combined prevalent cohort. The survival of the combined inception cohort was significantly lower than that of the combined prevalent cohort (99.0%, 94.8%, 88.9%, and 81.3% versus 99.5%, 98.0%, 96.7%, and 94.6% at 1, 3, 5, and 8 years, respectively; $P < 0.0001$ by log rank test).

Clinical Connections

CRISPR/Cas9 Editing of Murine Induced Pluripotent Stem Cells for Engineering Inflammation-Resistant Tissues

Brunger et al, *Arthritis Rheumatol* 2017;69:1111–1121.

CORRESPONDENCE

Charles A. Gersbach, PhD: charles.gersbach@duke.edu
Farshid Guilak, PhD: guilak@wustl.edu

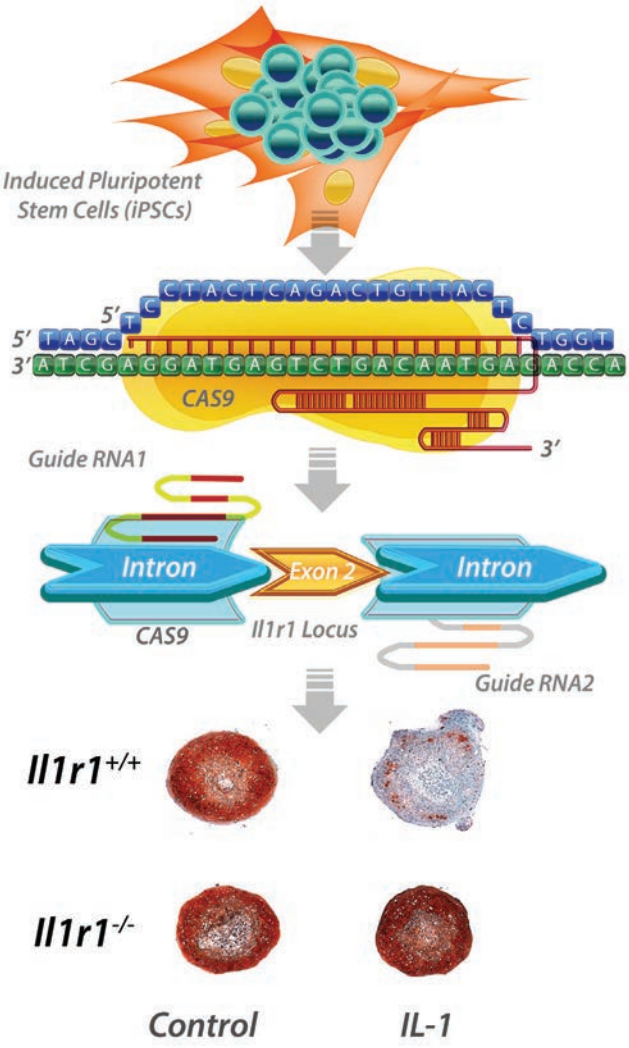

KEY POINTS

- Proinflammatory cytokines such as IL-1 are elevated in the joints following injury or arthritis.
- Exogenous stem cells used for cartilage repair are highly sensitive to IL-1, which inhibits stem cell chondrogenic differentiation and degrades newly formed repair cartilage.
- Genome engineering using the CRISPR/Cas9 method was used to create murine iPSCs that lack the IL-1 receptor 1.
- Cartilage synthesized by these engineered cells was immune to IL-1 signaling and showed no degradation or inflammatory signaling in response to IL-1

SUMMARY

Proinflammatory cytokines such as interleukin 1 (IL-1) are elevated in arthritic or injured joints and promote the degradation of articular cartilage while preventing stem cell differentiation and repair by engineered tissue replacements. To engineer cells and tissues that are resistant to these inflammatory effects, targeted deletion of *Il1r1*, the IL-1 receptor 1, was achieved in murine iPSCs using the RNA-guided, site-specific CRISPR/Cas9 genome engineering system. Cartilage engineered from iPSCs derived from Il1r1$^{-/-}$ mice was found to be resistant to IL-1–mediated degradation, as measured by gene expression, histologic, and biomechanical assays. This work demonstrates proof-of-concept of the ability to engineer stem cells that are immune to proinflammatory cytokines as a potential cell source for tissue engineering of articular cartilage for treating joint injury or arthritis. .

ARTHRITIS & RHEUMATOLOGY
Vol. 69, No. 5, May 2017, pp 873–877
DOI 10.1002/art.40061

Arthritis & Rheumatology
An Official Journal of the American College of Rheumatology
www.arthritisrheum.org and wileyonlinelibrary.com

EDITORIAL

Prevention of Rheumatoid Arthritis: Now Is the Time, but How to Proceed?

Kevin D. Deane, Christopher C. Striebich, and V. Michael Holers

In rheumatoid arthritis (RA), current clinical practice as well as the vast majority of reported studies focus on the ability of certain treatments to ameliorate existing disease activity or to prevent worsening disease in patients with established and classifiable disease. In addition, however, several trials have tried to address prevention of the development of classifiable RA in patients with undifferentiated arthritis (UA) or joint symptoms defined as arthralgia and autoantibody positivity without inflammatory arthritis, with overall mixed results (1–4). In particular, one important contribution to RA prevention is designated Probable Rheumatoid Arthritis: Methotrexate versus Placebo Treatment (PROMPT), an innovative and forward-looking clinical trial designed to stop disease progression from UA to classifiable RA.

The findings from this study have been reported in several stages. In the original study that was reported in 2007, 110 disease-modifying antirheumatic drug (DMARD)–naive patients with synovitis at baseline yet who did not meet the American College of Rheumatology (ACR) 1987 revised criteria for RA (5) were randomized to receive methotrexate (MTX; starting dosage 15 mg/week orally) or placebo, without other DMARDs or steroids (6). After follow-up of up to 30 months, there was no overall difference between groups in those whose disease progressed to classifiable RA (5). However, there was a delay in progression to RA in the MTX-treated group, and at 18 months, patients treated with MTX had less radiographic progression. Furthermore, in subgroup analyses solely of patients who were seropositive for anti–citrullinated protein antibodies (ACPAs), those who received MTX had less frequent progression to classifiable RA (67% versus 93%; $P < 0.001$).

The authors concluded in their original article that intervention in this "early" period of RA, especially in individuals who are ACPA positive, may result in longer-term benefits. However, in a follow-up study that included 5 years of follow-up (7), there was no lasting benefit from the initial course of MTX in terms of development of RA, radiographic damage, or drug-free remission, and the conclusion that followed was that perhaps early treatment did not result in lasting improvement in longer-term outcomes, which was somewhat contrary to many findings demonstrating that earlier treatment in RA leads to improved long-term outcomes (8).

In this issue of *Arthritis & Rheumatology*, the PROMPT investigators (Burgers LE, et al) report a further analysis of the data from the original study, this time to address the issue that perhaps earlier analyses yielded false-negative results because patients at low risk of developing classifiable RA were included (9); as such, if the individuals at highest risk of future RA could be identified, a benefit of treatment might be apparent. With this new approach, Burgers et al stratified individuals at baseline as being at high risk of future RA by applying the Leiden prediction rule, a 9-item instrument that includes clinical and biomarker factors and was developed and validated to determine the UA patients in whom disease may progress to classifiable RA (10,11). In this reanalysis, the primary outcome measure was the fulfillment of the ACR 1987 revised criteria, and the secondary outcome measure was the proportion of patients who achieved drug-free remission.

Kevin D. Deane, MD, PhD, Christopher C. Striebich, MD, PhD, V. Michael Holers, MD: University of Colorado Denver School of Medicine.

The content herein is solely the responsibility of the authors and does not necessarily represent the official views of the National Institutes of Health.

Drs. Deane, Striebich, and Holers' work was supported by the University of Colorado Autoimmunity Center of Excellence through award UM1-AI-110503 from the National Institute of Allergy and Infectious Diseases (NIAID), NIH. Drs. Deane and Holers' work was supported by NIAID grant U01-AI-101981.

Address correspondence to Kevin D. Deane, MD, PhD, University of Colorado Denver School of Medicine, 1775 Aurora Court, Mail Stop B-115, Denver, CO 80045. E-mail: kevin.deane@UCDenver.edu.

Submitted for publication December 29, 2016; accepted in revised form January 31, 2017.

After applying the Leiden rule, 22 of the original 110 subjects were identified as having been at high risk of RA, and fortuitously this small subgroup was originally randomized equally to receive MTX or placebo (11 in each group). Among these patients, during the overall follow-up period of 5 years, 6 of the 11 MTX-treated patients (55%) developed classifiable RA compared to 11 of 11 subjects (100%) in the placebo arm ($P = 0.011$). In addition, classifiable RA was significantly delayed in MTX-treated patients (median 22.5 months versus 3 months; $P < 0.001$), and drug-free remission was more common as well (36% versus 0%; $P = 0.027$). Furthermore, when the data were analyzed using only high-risk patients who were additionally ACPA positive (n = 18), classifiable RA was again noted to be significantly delayed, and there was a trend toward a greater preventive effect of MTX treatment. Finally, in subjects who were not at high risk, no benefit of MTX was identified. Based on these findings, the authors concluded that in order to see a benefit of intervention, it would be necessary in future studies to more accurately classify subjects as being at high risk, and to enter only those individuals into RA prevention trials.

There are several issues to consider when applying the specific findings from the PROMPT study to future prevention studies in RA, particularly those studies that target the stage of disease development between the appearance of the first clinically apparent synovitis and classifiable RA. First, the study by Burger et al was a very small study using retrospective analyses that may introduce bias, and therefore much larger studies will be needed to determine the best approaches for treating individuals who present with UA. Second, in this latest analysis, while some subjects had sustained MTX-free remission, 6 of 11 (55%) MTX-treated subjects still had disease that progressed to classifiable RA. This may have been due to a too-low dose of MTX (starting dosage of 15 mg/week), a too-short course of treatment (1 year), or the possibility that MTX targets the wrong pathway at this pathophysiologic stage of RA development. Further studies are needed to identify the best therapeutic agent(s) to optimize responses in this early stage of RA development.

Third, in this reanalysis, 18 of the 22 subjects (~82%) who the PROMPT investigators determined to be at high risk based on the Leiden rule also met the ACR/European League Against Rheumatism (EULAR) 2010 classification criteria for RA (12) at the time of study entry. The authors also found that the high-risk designation from the Leiden score performed better than the 2010 ACR/EULAR criteria in identifying those in whom MTX was most effective at preventing RA according to the ACR 1987 revised criteria, although the small sample size in the subanalysis limits the conclusions that can be made. However, because the 2010 ACR/EULAR criteria are used widely in clinical practice to guide treatment, it remains to be studied in larger trials how the Leiden prediction rule compares to those criteria in guiding clinical care. Furthermore, given the growing understanding of the pathophysiology of RA and the expansion of blood-based biomarkers and imaging that are available to assess and monitor disease (13), it will be important to determine how models that include additional autoantibodies, autoantibody levels, breadth of autoantibody reactivity, and other imaging or blood-based measures of inflammation can be used to identify individuals with UA who are at high risk of their disease progressing to classifiable RA. In addition, all of these factors may ultimately need to be incorporated into the "standard" classification criteria for RA in order to ensure that classification criteria truly match the biology of disease.

Finally, while the Leiden rule incorporates duration of symptoms as 1 of the 9 items assessed, Burgers et al did not formally assess duration of symptoms in this reanalysis, although in the original publication it was reported that the duration of symptoms was longer in the MTX-treated group (312 days versus 263 days; no *P* value provided) (6). This could impact findings, because in other studies the duration of disease prior to the initiation of therapy has been found to be an important factor in response to therapy (8).

Of note, until now we have avoided using the "classic" definitions of the stages of prevention, which include primary, secondary, and tertiary prevention, in consideration of the PROMPT study as a prevention trial. That is because the application of these terms depends to a large extent on when disease is considered to occur. Importantly, the determination of the presence or absence of a disease depends on an understanding of the natural history and pathophysiology of the disease, as well as on classification criteria that may be determined in an arbitrary manner (14,15). In particular, defining when disease is present in RA has been affected by the use of 2 classification schemes (the 1987 and 2010 criteria) that have some variability in their performance and that therefore may not identify exactly the same subjects or the same stage of disease development (5,12,16). The definition of "disease" in RA has been further challenged by the identification of a preclinical phase during which the levels of RA-related biomarkers, including rheumatoid factor (RF) and ACPAs are elevated years prior to the development of clinically detectable synovitis or classifiable RA (17) (Figure 1). Specific definitions that apply to the preclinical phase of RA are in development (18), although as of yet there is no widely accepted approach to uniformly define preclinical RA. Because of these issues, until consensus guidelines are developed, it may be more appropriate in RA to define

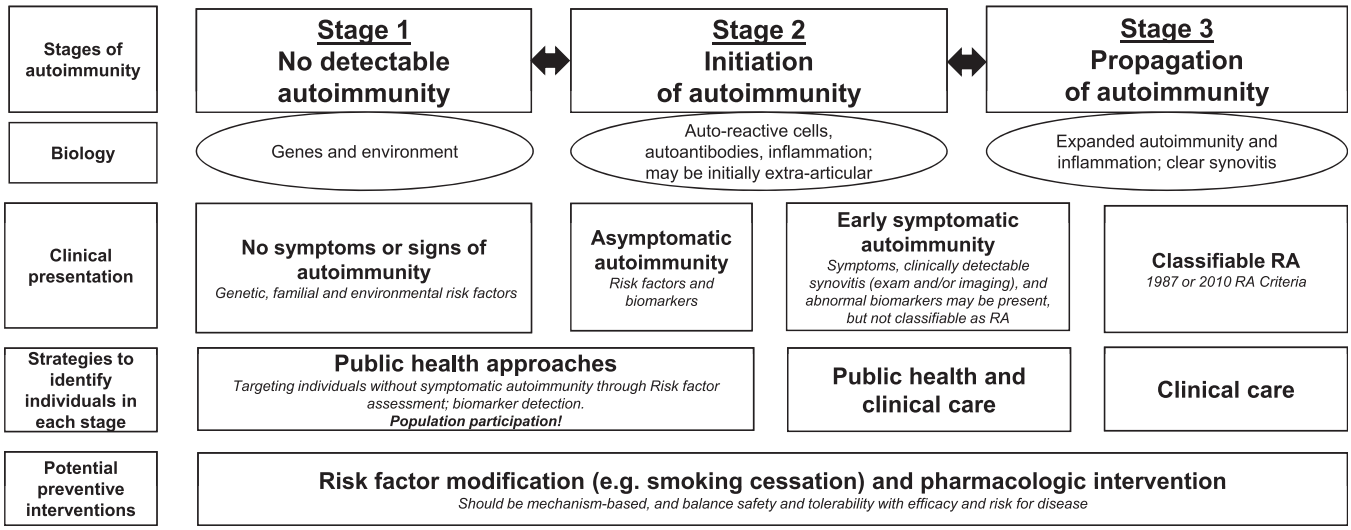

Figure 1. Model for rheumatoid arthritis (RA) development. In this model, RA develops in 3 general stages: 1) no detectable autoimmunity, 2) initiation of autoimmunity, and 3) propagation of autoimmunity. At each stage, the biology of disease can be defined through a variety of factors. Each stage is also characterized by clinical presentation that may be asymptomatic, unclassifiable signs and symptoms (the Probable Rheumatoid Arthritis: Methotrexate versus Placebo Treatment study), and ultimately classifiable RA using established criteria (e.g., 1987 or 2010 criteria). Identifying individuals at each stage requires different approaches such as autoantibody screening to identify asymptomatic or early symptomatic autoimmunity that may be difficult to recognize as related to RA, or clinical evaluation if signs and symptoms of synovitis are present. At each stage, major challenges are to 1) accurately identify individuals who are in each stage, 2) precisely define the risk for progression to the next "worse" stage, and 3) define the biology so that effective interventions can be applied to maintain or improve disease status or even facilitate transition of an individual's disease back to a prior stage. Of note, genes and environment likely act throughout all stages. In addition, the specific duration of each stage may vary across individuals.

prevention more broadly as a means to avoid progression from one stage of disease to another, more severe, stage.

With these issues in mind, it is not yet clear how the findings from the PROMPT study will directly apply to other types of prevention trials in RA that may target different, and earlier, stages of disease. In particular, several studies are currently underway (or were recently completed) to evaluate whether interventions that are given prior to the first clinical evidence of synovitis may prevent future classifiable disease (19–21). Since these studies target an earlier phase of RA development than that in the PROMPT study, the same methods (e.g., Leiden score) to identify an individual with clinically apparent synovitis that will progress to classifiable RA may not be appropriate to identify an individual with preclinical RA who is at risk of developing clinically apparent synovitis in a joint for the first time. Instead, identifying individuals whose disease will progress from preclinical RA to classifiable disease or even to UA may rely more heavily on biomarkers than on clinical symptoms. Indeed, in the prevention studies mentioned above, the inclusion criteria depend heavily on RA-related autoantibody positivity and particularly on ACPA positivity.

Furthermore, it will be imperative for future prevention studies in RA to identify the right targets for prevention for each stage of disease development. Specifically, as discussed above, MTX halted progression to classifiable RA in some of the high-risk PROMPT patients, and it is well known to be useful in treating patients with classifiable RA; however, MTX may not be appropriate to use in the earlier stages of RA because this drug and others have been optimized for the treatment of clinically apparent synovitis, a disease process that may be distinctly different from preclinical autoimmunity (13). Additionally, with the increasing understanding that preclinical RA is associated with and perhaps driven by mucosal inflammation (22), in some cases it may be more appropriate to approach prevention through modulation of that process. Furthermore, studies are needed to assess how changes in biomarkers or other measures over time can be used to assess efficacy of an intervention. The field is currently accustomed to "treating to target" in patients with classifiable RA, and in other diseases such as cardiovascular disease, specific lipid biomarkers are repeatedly assessed over time to gauge response to therapy. Similar approaches may be applied in RA prevention, although the targets may need to change in order to reflect underlying immunopathology rather than counts of tender and swollen joints, which are highly weighted in most tools that are currently used to assess disease activity in individuals who have clinically apparent synovitis.

Despite these caveats, this reevaluation of the PROMPT data addresses a critically important concept of identifying the right individuals to include in any type of prevention study in RA. Certainly, this concept is not new, as investigators have long tried to enroll the "right" patients in studies in order to optimize the identification of meaningful interventions. However, in prevention trials in which the success of the trial may rest heavily on the number of strictly defined outcomes as dichotomous variables (e.g., RA present or absent), it is likely even more important a priori to accurately identify adequate risks of development of classifiable RA in order to have sufficient outcomes for analyses during defined study periods. Moreover, given the temporal limits of clinical trials, inclusion criteria will need to incorporate both the likelihood of an important outcome and the timing of that outcome. For example, in studies of preclinical RA, this means that inclusion criteria will need to provide estimates of the number of individuals who will develop classifiable RA as well as an estimate of how many of those events will occur during the study period. Furthermore, when inclusion criteria adequately reflect the underlying biology of disease, they can help identify the patients with the "right" biology that will respond to a specific intervention. These critical issues for prevention trials can be summed up as follows: right individuals, right time, and right drug/intervention—all of which can be informed by robust inclusion criteria.

As such, great efforts should be put into identifying the right set of inclusion criteria for clinical prevention trials, with these criteria being based on sound understanding of the natural history of disease and its underlying biology. The several trials seeking to prevent the development of classifiable RA in autoantibody-positive individuals who do not have clinically apparent synovitis at baseline are already building on significant data showing that the presence of ACPAs with or without RF positivity is highly predictive of the future onset of classifiable RA (17). However, as knowledge about preclinical RA grows from these and other studies on the natural history of RA, we should be prepared to perform additional stratification that can be informed by a variety of clinical, biomarker, and imaging factors that will allow for delivery of "precision medicine" in prevention (23).

In relation to the above issues, it is important to consider the planned duration of preventive trials, especially if a planned intervention may take a long time to demonstrate its effect. For example, while one may expect a large and "quick" preventive effect on future classifiable RA from a DMARD, it may take much longer for a lifestyle intervention to result in demonstrable outcomes (24). Specifically, retrospective studies suggest that it may take 10–20 years to see an effect of smoking cessation on the future development of RA (25). As such, an RA prevention trial in which the intervention was smoking cessation would require very prolonged follow-up in order to adequately assess outcomes. Although this appears to be a daunting issue, improvements in cardiovascular disease outcomes using interventions such as statins have been measured not only in years but also in decades (26), so such approaches are possible.

In addition, to date the majority of RA prevention studies, including the PROMPT study, have enrolled subjects who have come to attention because they have sought medical care for symptoms. However, to identify individuals even earlier in the natural history of RA, different strategies will have to be employed that may require more public health–type approaches (Figure 1) and investment by clinicians, investigators, and funding agencies, as well as individuals at risk of rheumatic diseases whose participation in preventive trials will be critical to move the field forward. In particular, some prevention studies that are underway, including Strategy for the Prevention of Onset of Clinically-Apparent RA (19), are seeking to identify some study subjects even prior to their presentation to clinical care through serum ACPA screening of populations at higher risk, such as first-degree relatives of patients with RA, an approach that has both advantages and disadvantages but that is more akin to prevention of cardiovascular disease and cancer.

Overall, however, it is exciting that rheumatology is at the point where prevention in RA can be addressed more comprehensively. We hope that as the understanding of the pathophysiology and natural history of RA as well as that of other rheumatic diseases (e.g., lupus [27]) improves, the development of robust inclusion criteria for prevention studies as well as the addressing of other issues will find the right balance among 1) accurately classifying individuals in each stage of RA development, 2) precisely predicting risk of progression to the next "worse" stage of disease, and 3) understanding the biology of disease in each stage and on an individual level so that optimal interventions can be applied. We hope that addressing these issues will soon culminate in investigators being able to demonstrate conclusively that preventive interventions work in rheumatic disease.

AUTHOR CONTRIBUTIONS

All authors were involved in drafting the article or revising it critically for important intellectual content, and all authors approved the final version to be published.

REFERENCES

1. Emery P, Durez P, Dougados M, Legerton CW, Becker JC, Vratsanos G, et al. Impact of T-cell costimulation modulation in patients with undifferentiated inflammatory arthritis or very early rheumatoid arthritis: a clinical and imaging study of abatacept (the ADJUST trial). Ann Rheum Dis 2010;69:510–6.

2. Machold KP, Landewé R, Smolen JS, Stamm TA, van der Heijde DM, Verpoort KN, et al. The Stop Arthritis Very Early (SAVE) trial, an international multicentre, randomised, double-blind, placebo-controlled trial on glucocorticoids in very early arthritis. Ann Rheum Dis 2010;69:495–502.
3. Verstappen SM, McCoy MJ, Roberts C, Dale NE, Hassell AB, Symmons DP. Beneficial effects of a 3-week course of intramuscular glucocorticoid injections in patients with very early inflammatory polyarthritis: results of the STIVEA trial. Ann Rheum Dis 2010;69:503–9.
4. Bos WH, Dijkmans BA, Boers M, van de Stadt RJ, van Schaardenburg D. Effect of dexamethasone on autoantibody levels and arthritis development in patients with arthralgia: a randomised trial. Ann Rheum Dis 2010;69:571–4.
5. Arnett FC, Edworthy SM, Bloch DA, McShane DJ, Fries JF, Cooper NS, et al. The American Rheumatism Association 1987 revised criteria for the classification of rheumatoid arthritis. Arthritis Rheum 1988;31:315–24.
6. Van Dongen H, van Aken J, Lard LR, Visser K, Ronday HK, Hulsmans HM, et al. Efficacy of methotrexate treatment in patients with probable rheumatoid arthritis: a double-blind, randomized, placebo-controlled trial. Arthritis Rheum 2007;56:1424–32.
7. Van Aken J, Heimans L, Gillet-van Dongen H, Visser K, Ronday HK, Speyer I, et al. Five-year outcomes of probable rheumatoid arthritis treated with methotrexate or placebo during the first year (the PROMPT study). Ann Rheum Dis 2014;73:396–400.
8. Van Nies JA, Krabben A, Schoones JW, Huizinga TW, Kloppenburg M, van der Helm-van Mil AH. What is the evidence for the presence of a therapeutic window of opportunity in rheumatoid arthritis? A systematic literature review. Ann Rheum Dis 2014;73:861–70.
9. Burgers LE, Allaart CF, Huizinga TW, van der Helm-van Mil AH. Clinical trials aiming to prevent rheumatoid arthritis cannot detect prevention without adequate risk stratification: a trial of methotrexate versus placebo in undifferentiated arthritis as an example. Arthritis Rheumatol 2017;69: Arthritis Rheumatol doi: http://onlinelibrary.wiley.com/doi/10.1002/art.40061/abstract. E-pub ahead of print.
10. Van der Helm-van Mil AH, le Cessie S, van Dongen H, Breedveld FC, Toes RE, Huizinga TW. A prediction rule for disease outcome in patients with recent-onset undifferentiated arthritis: how to guide individual treatment decisions. Arthritis Rheum 2007;56:433–40.
11. McNally E, Keogh C, Galvin R, Fahey T. Diagnostic accuracy of a clinical prediction rule (CPR) for identifying patients with recent-onset undifferentiated arthritis who are at a high risk of developing rheumatoid arthritis: a systematic review and meta-analysis. Semin Arthritis Rheum 2014;43:498–507.
12. Aletaha D, Neogi T, Silman AJ, Funovits J, Felson DT, Bingham CO III, et al. 2010 rheumatoid arthritis classification criteria: an American College of Rheumatology/European League Against Rheumatism collaborative initiative. Arthritis Rheum 2010;62:2569–81.
13. Arend WP, Firestein GS. Pre-rheumatoid arthritis: predisposition and transition to clinical synovitis. Nat Rev Rheumatol 2012;8:573–86.
14. Starfield B, Hyde J, Gervas J, Heath I. The concept of prevention: a good idea gone astray? J Epidemiol Community Health 2008;62:580–3.
15. Tinetti ME, Fried T. The end of the disease era. Am J Med 2004;116:179–85.
16. Biliavska I, Stamm TA, Martinez-Avila J, Huizinga TW, Landewé RB, Steiner G, et al. Application of the 2010 ACR/EULAR classification criteria in patients with very early inflammatory arthritis: analysis of sensitivity, specificity and predictive values in the SAVE study cohort. Ann Rheum Dis 2013;72:1335–41.
17. Deane KD, El-Gabalawy H. Pathogenesis and prevention of rheumatic disease: focus on preclinical RA and SLE. Nat Rev Rheumatol 2014;10:212–28.
18. Gerlag DM, Raza K, van Baarsen LG, Brouwer E, Buckley CD, Burmester GR, et al. EULAR recommendations for terminology and research in individuals at risk of rheumatoid arthritis: report from the Study Group for Risk Factors for Rheumatoid Arthritis. Ann Rheum Dis 2012;71:638–41.
19. National Institute of Allergy and Infectious Diseases, sponsor. Strategy for the prevention of onset of clinically-apparent rheumatoid arthritis (StopRA). ClinicalTrials.gov identifier: NCT02603146; 2015.
20. Guy's and St. Thomas' NHS Foundation Trust, sponsor. Arthritis prevention in the pre-clinical phase of RA with abatacept. ISRCTN 46017566; 2014.
21. Academic Medical Center, Division of Clinical Immunology and Rheumatology, sponsor. Prevention of clinically manifest rheumatoid arthritis by B cell directed therapy in the earliest phase of the disease (PRAIRI). NTR 2442; 2010.
22. Demoruelle MK, Deane KD, Holers VM. When and where does inflammation begin in rheumatoid arthritis? Curr Opin Rheumatol 2014;26:64–71.
23. Mirnezami R, Nicholson J, Darzi A. Preparing for precision medicine. N Engl J Med 2012;366:489–91.
24. Gerlag DM, Norris JM, Tak PP. Towards prevention of autoantibody-positive rheumatoid arthritis: from lifestyle modification to preventive treatment. Rheumatology (Oxford) 2016;55:607–14.
25. Costenbader KH, Feskanich D, Mandl LA, Karlson EW. Smoking intensity, duration, and cessation, and the risk of rheumatoid arthritis in women. Am J Med 2006;119:503.e1–9.
26. Chou R, Dana T, Blazina I, Daeges M, Jeanne TL. Statins for prevention of cardiovascular disease in adults: evidence report and systematic review for the US Preventive Services Task Force. JAMA 2016;316:2008–24.
27. Olsen NJ, Karp DR. Autoantibodies and SLE: the threshold for disease. Nat Rev Rheumatol 2014;10:181–6.

ARTHRITIS & RHEUMATOLOGY
Vol. 69, No. 5, May 2017, pp 878–884
DOI 10.1002/art.40063

EDITORIAL

A New Classification of Adult Autoimmune Myositis

Jean-Luc Senécal,[1] Jean-Pierre Raynauld,[1] and Yves Troyanov[2]

Since Bohan and Peter first described their original classification and diagnostic criteria for polymyositis (PM) and dermatomyositis (DM) in 1975 (1), rheumatologists have witnessed remarkable progress in the understanding of the heterogeneous nature of these diseases. Notwithstanding major advances made in other aspects of PM and DM such as skeletal muscle histopathology (2,3), progress has been afforded notably by the discovery of serum autoantibodies associated with myositis, which were unknown at the time that the Bohan and Peter criteria were first described (4,5). We focus herein on advances in the nosology of PM and DM brought forward by these autoantibodies and attempt to integrate emerging concepts into a new classification. We also focus on some implications for trial design and outcome measures that stem from this novel classification.

Clinicoserologic analysis of the associations of newly identified autoantibodies has allowed separation of classic PM and DM into newly recognized disease subgroups with distinct phenotypes, i.e., distinct clinical features, course, prognosis, association with cancer, and even therapeutic responses. In addition to the discovery of these autoantibodies, immunogenetic as well as pathophysiologic studies (6) have provided strong evidence of an autoimmune pathogenesis in most PM and DM subgroups, warranting their classification under the more specific terminology of "autoimmune myositis" (AIM) in replacement of "idiopathic inflammatory myopathies."

As shown in Table 1, 5 major syndromes/disease entities are now classified under the AIM banner: overlap myositis (OM) (7), pure (classic) DM, necrotizing autoimmune myositis (NAM) (8), PM, and possibly, sporadic inclusion body myositis. In this article, we focus on adult OM, DM, and NAM, which account for >90% of adult AIM patients seen by rheumatologists in an academic setting.

The concept of overlap myositis

Since the terminology of OM was originally proposed (7), this concept has gained acceptance (8–12). OM is defined by the association of myositis with overlap connective tissue disease features, such as Raynaud's phenomenon, arthritis, and interstitial lung disease (ILD), as well as features of systemic sclerosis (SSc) and lupus, which most commonly are present at the time of myositis diagnosis (Table 1) (7,13). However, although ~15% of OM patients present without overlap clinical features, an overlap autoantibody is present, often with suggestive biopsy findings (3,14), and overlap features typically develop at follow-up (7).

OM is the most frequent AIM subgroup, accounting for ~50% of patients. Although Bohan and Peter did include in their classification "PM or DM associated with collagen-vascular disease," emergence of OM as a distinct entity within the AIM spectrum was triggered by 2 factors. First, the realization that histopathologically defined PM was rare, and that "nonspecific myositis" was a surprisingly common pathologic diagnosis, suggested that PM was an overdiagnosed entity (15). Second, support for the concept of OM stemmed from the identification of >15 specific autoantibodies and recognition of their striking association with distinct clinical phenotypes (12,13,16). A complete list of autoantibody specificities observed in OM patients, i.e., overlap autoantibodies (7), is shown in Table 1.

OM with autoantibodies to synthetases define the antisynthetase syndrome

When OM patients are classified clinicoserologically, i.e., according to both their clinical features and the presence of overlap autoantibodies, phenotypic profiles emerge. Intriguingly, the phenotypic profiles differ depending on the cytoplasmic or nuclear localization of the corresponding autoantigens (Table 1) (12). The extramuscular phenotype of OM

[1]Jean-Luc Senécal, MD, FRCPC, Jean-Pierre Raynauld, MD, FRCPC: University of Montreal Faculty of Medicine and Centre hospitalier de l'Université de Montréal, Montreal, Quebec, Canada; [2]Yves Troyanov, MD, FRCPC: University of Montreal Faculty of Medicine, Centre hospitalier de l'Université de Montréal, and Hôpital du Sacré-Coeur, Montreal, Quebec, Canada.

Address correspondence to Jean-Luc Senécal, MD, FRCPC, Division of Rheumatology, M-4243, Centre hospitalier de l'Université de Montréal, 1560 East Sherbrooke Street, Montreal, Quebec H2L 4M1, Canada. E-mail: dr.j.l.senecal.md@gmail.com.

Submitted for publication June 1, 2016; accepted in revised form January 31, 2017.

Table 1. New clinicoserologic classification for adult autoimmune myositis with emphasis on extramuscular organ involvement and autoantibodies as potential outcome measures for therapeutic trials*

	Major syndromes				
			Polymyositis phenotype		
Characteristic	Overlap myositis	Pure classic dermatomyositis	Necrotizing autoimmune myositis†	Pure polymyositis, exclusion diagnosis	Sporadic inclusion body myositis‡
Acronym	OM	DM	NAM	PM	IBM
Overall frequency, %	50	30–35	10–15	≤5%, must exclude mimickers	≤5%
Skeletal muscle involvement	Yes§	Yes§	Yes	Yes	Yes
Rashes of DM	Yes¶	Yes	No	No	No
Overlap features#	Raynaud's phenomenon Arthritis Mechanic's hands Interstitial lung disease Trigeminal neuropathy Lower esophageal dysmotility Scleroderma features SLE features SS features	No	No	No	No
First manifestation	Overlap features	Rash	Muscular	Muscular	Muscular
Cancer	<5%	Yes, up to 50%	No in anti-SRP NAM and in statin-exposed anti-HMGCR NAM; yes in statin-naïve anti-HMGCR and in seronegative NAM	No	No
Major autoantibodies, autoantigen cellular localization, and name	Cytoplasmic:** Jo-1†† and non–Jo-1 synthetases, MDA-5†† (CADM140). Nuclear: U1 RNP,†† U3 RNP (fibrillarin), U5 RNP, U11–12 RNP, PM-Scl, Ku, nup†† (nucleoporins), CENP-B, Th/To, RuvB-like 1/2, DNA topoisomerase I,†† RNA polymerase III, SMN, native DNA	Nuclear: Mi-2, TIF-1γ (p155/140), NXP-2 (MJ), SAE	Cytoplasmic:** SRP,†† HMGCR††	Undefined	Cytoplasmic: Cytosolic 5′-nucleotidase 1A (also present in systemic autoimmune diseases)
Abnormal nailfold capillaries and capillary microscopy	Yes	Yes	No	No	No

* SLE = systemic lupus erythematosus; SS = Sjögren's syndrome; anti–HMGCR = anti–hydroxymethylglutaryl-coenzyme A reductase; TIF-1γ = transcription intermediary factor 1γ; NXP-2 = nuclear matrix protein 2; SMN = survival of motor neuron complex; SAE = small ubiquitin-like modifier activing syndrome.
† Also known as immune-mediated necrotizing myopathy.
‡ The place of sporadic inclusion body myositis as a member of the autoimmune myositis family has yet to be clarified.
§ Both OM and pure DM may present occasionally as clinically amyopathic DM (CADM).
¶ The subset of DM sine dermatitis is seen almost exclusively in OM. Mechanic's hands are seen almost exclusively in OM.
# As detailed in refs. 7 and 10.
** In OM, cytoplasmic fluorescence suggests an antisynthetase, as anti–melanoma differentiation–associated protein 5 (anti–MDA-5) staining is often very weak or negative. In suspected NAM, cytoplasmic fluorescence is suggestive of anti–signal recognition particle (anti-SRP).
†† Fluctuation of titer in parallel with disease activity/severity.

Table 2. Clinical features that differentiate pure DM from overlap myositis with DM features at the time of myositis diagnosis*

Pure DM	Overlap myositis with DM features
DM rashes as first manifestation of disease, followed by proximal muscle weakness	Proximal muscle weakness but not DM rash as first manifestation of disease
Classic and extensive DM rashes that are chronic/refractory	Isolated heliotrope rash or Gottron's papules
	Discrete and transient DM rashes
	DM sine dermatitis (adermatopathic DM)
Significant oropharyngeal dysphagia at myositis presentation	Mechanic's hands
	Palmar papules, with or without ulcerations
No significant overlap clinical features	Significant overlap clinical features
DM-specific autoantibodies by specific, rather than sensitive, testing	Overlap autoantibodies by specific, rather than sensitive, testing
No overlap autoantibodies	No DM-specific autoantibodies
Association with cancer within 3 years of diagnosis	No associated cancer within 3 years of diagnosis

* Both pure dermatomyositis (DM) and overlap myositis with DM features may present as clinically amyopathic DM.

patients with autoantibodies to the cytoplasmic autoantigens Jo-1, non–Jo-1 synthetases, and melanoma differentiation–associated protein 5 (MDA-5) is dominated by ILD and a rheumatoid arthritis (RA)–like polyarthritis.

Anti–Jo-1 and autoantibodies to non–Jo-1 synthetases are associated with the antisynthetase syndrome, i.e., a peculiar set of overlap features that includes Raynaud's phenomenon, arthritis, puffy hands, ILD, fever, mechanic's hands, and myositis (17,18). Although myositis is often prominent, relapsing, and refractory, this syndrome may present with ILD or polyarthritis, and myositis may be absent or minimal or present as clinically amyopathic DM (19). Phenotypic differences have been noted between patients with different antisynthetases (19). Moreover, patients with non–Jo-1 anti–transfer RNA synthetase autoantibodies have worse survival than anti–Jo-1–positive patients. In the Rituximab in Myositis (RIM) trial, patients with treatment-refractory myositis and antisynthetase autoantibodies responded well to rituximab (20), suggesting that autoantibody profiling may guide therapeutic choices. The striking link between OM autoantibodies and clinical phenotypes is also supported by identification of histopathologic features specific for antisynthetase autoantibodies, such as myonuclear actin filament inclusions (3,14).

These characteristics have an impact on future trials. First, given the prominent overlap features that define the antisynthetase syndrome, it appears untenable at the present time to sustain its classification as pure PM. Second, given that arthritis and ILD are key features, it follows that outcome measures should take into account these manifestations.

Anti–MDA-5–associated overlap myositis

In addition to classic DM rashes, a peculiar rash with papules on the palmar surface of the hands emerges as the disease-defining feature of an "anti–MDA-5"overlap syndrome (21). Cutaneous ulceration and digital ischemia are also seen, while myositis is mild or absent. Overlap features such as ILD are prominent. ILD may be rapidly progressive and is associated with high mortality (22). Given that rapidly progressive ILD, cutaneous manifestations, and arthritis, but not myositis, are the major therapeutic challenges in anti–MDA-5–positive OM, it ensues that outcome measures should focus on these manifestations. However, given the high mortality associated with rapidly progressive ILD, it may be best in therapeutic trials targeting myositis to exclude patients with anti–MDA-5.

Overlap myositis with autoantibodies to nuclear autoantigens (ANAs)

In contrast to anti–MDA-5 and antisynthetases, OM with ANAs such as anti–U1 RNP, anti–PM-Scl, and anti-Ku are associated with SSc and systemic lupus erythematosus manifestations and even with erosive and seropositive arthritis in the anti-nup syndrome (13,23). Moreover, within these various overlap manifestations, each ANA seems to be associated with a different OM phenotypic profile. Although outcome measures focused on muscle weakness and serum creatine kinase (CK) levels are relevant in these ANA-associated OM subgroups, myositis is not a major prognostic determinant, and outcome measures should include extramuscular involvement.

Overlap myositis with DM rashes

To properly classify AIM patients, greater awareness is needed that DM rashes are not restricted to pure (classic) DM, and as such, rashes may occur in OM as well (8,24). Table 2 shows distinguishing features that assist clinicians in classifying patients as having pure DM versus

OM with DM features. Thus, pure DM presents with classic and extensive rashes that are chronic and treatment-refractory and is not associated with overlap features or overlap autoantibodies. In contrast, OM with DM features presents with muscle weakness followed by discrete and transient DM rashes and is typically associated with overlap clinical features and autoantibodies such as anti–Jo-1, anti–non–Jo-1 synthetases, anti–MDA-5, anti–PM-Scl, and anti–U1 RNP (19,24). Moreover, OM with DM features is not associated with cancer within 3 years of diagnosis (Table 2).

Thus, DM rashes do occur in OM patients, and the presence of a DM rash does not automatically warrant classification as pure DM. This concept has important diagnostic and prognostic implications for clinicians.

Overlap myositis, a heterogeneous syndrome

Overall, the emerging global concept is that OM itself is a syndrome that encompasses as many diseases as there are autoantibody-associated phenotypes (12,13). Not only does clinicoserologic patient profiling identify distinct clinical phenotypes but it also provides important prognostic information. As a corollary, autoantibody status appears to be of paramount importance in patient stratification for therapeutic trials and studies aimed at defining outcome measures.

Autoantibodies define novel subgroups in pure DM

As in the case of OM, the classification of pure DM is evolving due to the successive discoveries of specific autoantibodies that allow recognition of distinct disease phenotypes not associated with overlap features (Table 1). Thus, in 1985, Targoff and Reichlin had described anti–Mi-2 antibodies in adult DM patients (4). In addition to the heliotrope rash and Gottron's papules, anti–Mi-2 antibodies are associated with classic and extensive DM rashes such as the shawl sign, V-sign, and holster sign and with markedly elevated serum CK levels (Table 2).

Anti–transcription intermediary factor 1γ (anti–TIF-1γ) and anti–nuclear matrix protein 2 (anti–NXP-2) are specificities recently reported in pure DM (5). Anti–TIF-1γ is also the most frequent autoantibody in clinically amyopathic DM. Moreover, the anti–TIF-1γ phenotype includes muscle weakness despite a normal serum CK level and treatment-resistant DM rashes. Importantly, in adult DM, both anti–TIF-1γ and anti–NXP-2 are strongly associated with cancer (12). These autoantibodies were found in 55% of adult DM patients and identified 83% of patients with cancer-associated DM (25). Thus, in pure DM, phenotypes are strongly linked to the associated autoantibody, suggesting that pure DM, like OM, is a syndrome composed of autoantibody-defined diseases.

Cancer is a potential major confounder in trial design, given its association with treatment-refractory myositis. This raises the question of whether adult patients with these autoantibodies should be excluded from trials during the 3 years after diagnosis.

Subsetting necrotizing autoimmune myositis with anti–signal recognition particle (anti-SRP) and anti–hydroxymethylglutaryl-coenzyme A reductase (anti-HMGCR) autoantibodies

In contrast to other subgroups of AIM characterized by inflammatory cells, skeletal muscle in NAM displays prominent fiber necrosis and regeneration with no or scant inflammatory cells (26). Like OM and DM, NAM is likely a syndrome, as it is associated with different autoantibodies and causes, including cancer (26). Two autoantibodies strongly associated with NAM are anti-SRP (27) and anti-HMGCR (28). A third NAM subset consists of seronegative patients (Table 1).

Anti-HMGCR–positive NAM is associated with statin use, although as many as one-third of patients have not been exposed to statins (28). Patients with anti-SRP autoantibodies are not at increased risk of cancer, nor are statin-exposed patients with anti-HMGCR–positive NAM. However, synchronous cancer was noted in 11% of statin-naive NAM patients with anti-HMGCR autoantibodies (29).

Phenotypically, NAM subsets present with subacute proximal limb muscle weakness and a high serum CK level in the absence of DM rashes and overt overlap features. Differentiating features between the subsets include early weakness, prominent oropharyngeal dysphagia, and irreversible muscle damage in patients with anti-SRP autoantibodies, whereas patients with anti-HMGCR autoantibodies and statin exposure have late-onset weakness that is reversible with aggressive therapy.

Pure PM is rare and at high risk for mimickers

As the concept of OM gained acceptance, and as NAM was identified as a distinct entity, the frequency of pure PM inexorably decreased. From the perspective of rheumatologists and even neurologists, PM now accounts for only 5% of AIM patients (8). Because of referral bias, clearly among neurologists, dermatologists, and rheumatologists, AIM subgroups are not equally distributed (30). Nevertheless, PM has become rare and remains a diagnosis of exclusion, because its nonspecific phenotype (subacute proximal myopathy without overlap features or autoantibodies) is at high risk for mimickers (8) (Table 1).

As a corollary, we raise the question of whether pure PM should be excluded from therapeutic trials and the validation of novel AIM outcome measures.

Autoantibodies are present in 60–80% of AIM patients

Autoantibodies against nuclear RNAs or cytoplasmic autoantigens are now detected in up to 60% of AIM patients (8). Moreover, in one study using multiple methods to detect autoantibodies to a panel of 21 AIM-related autoantigens, one or more autoantibodies encompassing 19 specificities were present in 80% of patients (13). Among "seronegative" patients, some have unidentified bands by immunoprecipitation that may become autoantibody positive as new specificities are discovered. However, some patients currently have no detectable autoantibodies (20).

Despite these advances, many clinicians and investigators among rheumatologists and neurologists do not yet have equal access to accurate and full autoantibody testing, including the onerous immunoprecipitation methods required to best identify some of these autoantibodies. Newer techniques offer the promise of sensitivity and a rapid serologic diagnosis but are hampered by lack of standardization and specificity issues (Table 1). Results of autoantibody tests should always be correlated with clinicopathologic findings and with ANA results as detected by immunofluorescence on substrates such as HEp-2 cells (16). This situation may cause inaccurate estimation of the frequency of these autoantibodies and lead to diagnostic uncertainty. Furthermore, it may well place researchers investigating AIM therapy in the predicament of comparing apples to oranges when it comes to results.

Novel outcome measures to evaluate the therapeutic clinical response in autoimmune myositis

A major incentive for improving the classifications of AIM is to stratify and assemble homogeneous groups of patients in therapeutic trials. In turn, this allows optimal evaluation and comparison of the results of such trials. However, despite a major need for improved therapeutic approaches in AIM, outcome measures defining clinical response in therapeutic trials have been difficult to develop due to the rarity and heterogeneity of these diseases.

In this issue of *Arthritis & Rheumatology*, an international collaborative group of expert AIM investigators proposes novel criteria for minimal and moderate clinical responses in adult PM and DM (31). The rationale for this major study by Aggarwal et al is similar to the motives that led to the modified Rodnan skin thickness score in SSc (32) and the American College of Rheumatology 20%, 50%, 70% improvement criteria outcome measures in studies of RA treatment (33), i.e., with advances in therapeutic agents that target biologic pathways, there is a need for clinical trials using validated outcome measures.

Using state-of-the art statistical and consensus methodologies (34), a conjoint analysis–based hybrid definition based on a continuous improvement score using absolute percent change in core set measures was selected as the response criterion to be used for adult DM/PM and for combined DM/PM and juvenile DM clinical trials (34). Performance characteristics were evaluated on consensus patient profiles, using Delphi method–based consensus of the experts as the gold standard, and further validated using, in particular, data from the RIM randomized controlled trial (35). The new clinical response criteria proposed are a major advance and will undoubtedly be of great importance in future therapeutic trials.

There are 3 limitations to this study. First, as acknowledged by Aggarwal et al (31), patients were classified based on the Bohan and Peter criteria. As pointed out, PM now encompasses several entities, such as OM and NAM, that are distinct from PM as defined by Bohan and Peter, and pure PM has become rare. Similarly, classification as DM according to the Bohan and Peter criteria is based simply on the presence or absence of a DM rash (1). However, as discussed, DM rashes are seen in OM, and pure DM itself now encompasses distinct subgroups. Moreover, autoantibody-defined phenotypes do not appear to have been used to assist in the classification of patients (31). Thus, it is difficult to ascertain which specific contemporary diagnoses would correspond to the patients classified as having PM or DM. Moreover, it is difficult to know how the proposed clinical response criteria would perform if the patients were classified according to Table 1. Therefore, it will be important in future studies to ascertain the clinical response criteria using more recent and refined AIM classifications.

A second limitation is that it is difficult to know whether the response criteria were tested and validated over the full clinical spectrum of active myositis (e.g., in de novo active untreated myositis versus chronic refractory myositis) or if the study focused primarily on refractory myositis (31). The latter is suggested by validation using data from the RIM trial, in which all patients had treatment-refractory PM or DM (35). In clinical practice, many patients with active untreated myositis, for example, those with anti–Mi-2, anti–U1 RNP, or anti-nup autoantibodies, respond well and with increasing muscle strength to corticosteroids in combination with another immunomodulating agent. However, in treatment-refractory myositis, evaluation of clinical response is confounded by previous immunosuppression, corticosteroid-induced myopathy, muscle atrophy, osteonecrosis, and osteoporotic fractures. Thus, sensitivity

to change of the response criteria, including manual muscle testing, may be greater in the former patients, and such patients should be included in future evaluations.

A last limitation is that the response criteria are almost exclusively centered on skeletal muscle. Extramuscular features were assessed only by an undefined Extramuscular Global Activity visual analog measurement scale. Consequently, one wonders whether the consensus measures developed could be applied with confidence to patients who belong to extremely different phenotypic and serologic groups, and in whom extramuscular manifestations are a major therapeutic and prognostic determinant. In other words, would the response criteria perform as well in autoantibody-defined and phenotypically defined AIM subgroups? Similarly, in DM patients, the confounding effect of cancer on myositis response was not addressed. As a corollary, shouldn't distinct outcome measures be defined for distinct patient subgroups?

Overall, these comments highlight the difficulty of applying uniform outcome measures to heterogeneous patients with rare diseases. Aggarwal et al logically opted, as a starting point, to evaluate response criteria that are myocentric, but clearly this approach does not represent the full clinical spectrum of AIM. It will be of great interest to see these questions addressed in future studies.

Two additional outcome measures that are worthy of further study are shown in Table 1. First, nailfold capillary abnormalities reflect systemic microvascular damage (related to disease pathophysiology) as well as global disease activity and severity, predict disease progression, and are readily assessed by noninvasive sequential nailfold capillary microscopy and videomicroscopy (36,37). Thus, further study of nailfold capillary abnormalities in OM and in adult DM may be of interest. Second, the levels of anti–Jo-1, anti-nup, anti–MDA-5, anti-HMGCR, anti–TIF-1γ, anti–Mi-2, and anti-SRP fluctuate in parallel with myositis activity (23,38). Further serial measurements as a clinical response measure will be of great interest.

Time to say farewell to the Bohan and Peter classification criteria

In conclusion, classification of AIM is a work in progress. The time has come to say farewell to the Bohan and Peter criteria in favor of a classification that better reflects the heterogeneity of AIM, notably OM, DM, and NAM and associated autoantibodies, and advances in the field. The clinicoserologic classification outlined in Table 1 is one such approach and has the advantage of being readily understandable by clinicians. Undoubtedly, in the future, phenotype- and autoantibody-based classifications will converge and eventually merge with classifications focused on pathology (2,14), i.e., evolve into clinicopathologic classifications.

The tight link between autoantibodies and phenotypes raises fundamental questions regarding the pathophysiologic events that initiate and perpetuate these immune responses and how these autoantibodies and their cognate autoantigens are involved in pathogenesis (6,39).

Future studies will be of interest in validating clinical response criteria in phenotypically homogeneous groups of patients that better reflect the heterogeneity of AIM and the full clinical extramuscular spectrum of OM. After all, as thoughtfully pointed out by Bohan and Peter 40 years ago, "The natural history of such heterogeneous myopathic syndromes is surely influenced by the concomitant connective-tissue disorder."

AUTHOR CONTRIBUTIONS

All authors were involved in drafting the article and revising it critically for important intellectual content, and all approved the final version to be published.

REFERENCES

1. Bohan A, Peter JB. Polymyositis and dermatomyositis. Parts 1 and 2. N Engl J Med 1975;292:344–7, 403–7.
2. Hoogendijk JE, Amato AA, Lecky BR, Choy EH, Lundberg IE, Rose MR, et al. 119th ENMC international workshop: trial design in adult idiopathic inflammatory myopathies, with the exception of inclusion body myositis, 10-12 October 2003, Naarden, The Netherlands. Neuromuscul Disord 2004;14:337–45.
3. Stenzel W, Preuße C, Allenbach Y, Pehl D, Junckerstorff R, Heppner FL, et al. Nuclear actin aggregation is a hallmark of anti-synthetase syndrome-induced dysimmune myopathy. Neurology 2015;84:1346–54.
4. Targoff IN, Reichlin M. The association between Mi-2 antibodies and dermatomyositis. Arthritis Rheum 1985;28:796–803.
5. Targoff IN, Mamyrova G, Trieu EP, Perurena O, Koneru B, O'Hanlon TP, et al. A novel autoantibody to a 155-kd protein is associated with dermatomyositis. Arthritis Rheum 2006;54:3682–9.
6. Plotz PH. The autoantibody repertoire: searching for order. Nat Rev Immunol 2003;3:73–8.
7. Troyanov Y, Targoff IN, Tremblay JL, Goulet JR, Raymond Y, Senécal JL. Novel classification of idiopathic inflammatory myopathies based on overlap syndrome features and autoantibodies: analysis of 100 French Canadian patients. Medicine (Baltimore) 2005;84:231–49.
8. Dalakas MC. Inflammatory muscle diseases. N Engl J Med 2015;372:1734–47.
9. Benveniste O, Dubourg O, Herson S. New classifications and pathophysiology of the inflammatory myopathies. Rev Med Interne 2007;28:603–12. In French.
10. Fernandez C, Bardin N, de Paula AM, Salort-Campana E, Benyamine A, Franques J, et al. Correlation of clinicoserologic and pathologic classifications of inflammatory myopathies: study of 178 cases and guidelines for diagnosis. Medicine (Baltimore) 2013;92:15–24.
11. De Visser M. The efficacy of rituximab in refractory myositis: the jury is still out [editorial]. Arthritis Rheum 2013;65:303–6.
12. Gunawardena H. The clinical features of myositis-associated autoantibodies: a review. Clin Rev Allergy Immunol 2017;52:45–57.

13. Koenig M, Fritzler MJ, Targoff IN, Troyanov Y, Senécal JL. Heterogeneity of autoantibodies in 100 patients with autoimmune myositis: insights into clinical features and outcomes. Arthritis Res Ther 2007;9:R78.
14. Pestronk A. Acquired immune and inflammatory myopathies: pathologic classification. Curr Opin Rheumatol 2011;23:595–604.
15. Van der Meulen MF, Bronner IM, Hoogendijk JE, Burger H, van Venrooij WJ, Voskuyl AE, et al. Polymyositis: an overdiagnosed entity. Neurology 2003;61:316–21.
16. Satoh M, Tanaka S, Ceribelli A, Calise SJ, Chan EK. A comprehensive overview on myositis-specific antibodies: new and old biomarkers in idiopathic inflammatory myopathy. Clin Rev Allergy Immunol 2017;52:1–19.
17. Love LA, Leff RL, Fraser DD, Targoff IN, Dalakas M, Plotz PH, et al. A new approach to the classification of idiopathic inflammatory myopathy: myositis-specific autoantibodies define useful homogeneous patient groups. Medicine (Baltimore) 1991;70:360–74.
18. Cavagna L, Nuno L, Scire CA, Govoni M, Longo FJ, Franceschini M, et al. Clinical spectrum time course in anti Jo-1 positive antisynthetase syndrome: results from an international retrospective multicenter study. Medicine (Baltimore) 2015;94:e1144.
19. Hamaguchi Y, Fujimoto M, Matsushita T, Kaji K, Komura K, Hasegawa M, et al. Common and distinct clinical features in adult patients with anti-aminoacyl-tRNA synthetase antibodies: heterogeneity within the syndrome. PLoS One 2013;8:e60442.
20. Aggarwal R, Bandos A, Reed AM, Ascherman DP, Barohn RJ, Feldman BM, et al. Predictors of clinical improvement in rituximab-treated refractory adult and juvenile dermatomyositis and adult polymyositis. Arthritis Rheumatol 2014;66:740–9.
21. Hall JC, Casciola-Rosen L, Samedy LA, Werner J, Owoyemi K, Danoff SK, et al. Anti–melanoma differentiation–associated protein 5–associated dermatomyositis: expanding the clinical spectrum. Arthritis Care Res (Hoboken) 2013;65:1307–15.
22. Moghadam-Kia S, Oddis CV, Sato S, Kuwana M, Aggarwal R. Anti–melanoma differentiation–associated gene 5 is associated with rapidly progressive lung disease and poor survival in US patients with amyopathic and myopathic dermatomyositis. Arthritis Care Res (Hoboken) 2016;68:689–94.
23. Senécal JL, Isabelle C, Fritzler MJ, Targoff IN, Goldstein R, Gagné M, et al. An autoimmune myositis-overlap syndrome associated with autoantibodies to nuclear pore complexes: description and long-term follow-up of the anti-nup syndrome. Medicine (Baltimore) 2014;93:383–94.
24. Troyanov Y, Targoff IN, Payette MP, Raynauld JP, Chartier S, Goulet JR, et al. Redefining dermatomyositis: a description of new diagnostic criteria that differentiate pure dermatomyositis from overlap myositis with dermatomyositis features. Medicine (Baltimore) 2014;93:318–32.
25. Fiorentino DF, Chung LS, Christopher-Stine L, Zaba L, Li S, Mammen AL, et al. Most patients with cancer-associated dermatomyositis have antibodies to nuclear matrix protein NXP-2 or transcription intermediary factor 1γ. Arthritis Rheum 2013;65:2954–62.
26. Basharat P, Christopher-Stine L. Immune-mediated necrotizing myopathy: update on diagnosis and management. Curr Rheumatol Rep 2015;17:72.
27. Hengstman GJ, ter Laak HJ, Vree Egberts WT, Lundberg IE, Moutsopoulos HM, Vencovsky J, et al. Anti-signal recognition particle autoantibodies: marker of a necrotising myopathy. Ann Rheum Dis 2006;65:1635–8.
28. Mammen AL. Statin-associated autoimmune myopathy. N Engl J Med 2016;374:664–9.
29. Allenbach Y, Keraen J, Bouvier AM, Jooste V, Champtiaux N, Hervier B, et al. High risk of cancer in autoimmune necrotizing myopathies: usefulness of myositis specific antibody. Brain 2016; 139:2131–5.
30. Klein RQ, Teal V, Taylor L, Troxel AB, Werth VP. Number, characteristics, and classification of patients with dermatomyositis seen by dermatology and rheumatology departments at a large tertiary medical center. J Am Acad Dermatol 2007;57:937–43.
31. Aggarwal R, Rider LG, Ruperto N, Bayat N, Erman B, Feldman BM, et al. 2016 criteria for minimal and moderate clinical response for adult dermatomyositis and polymyositis: an American College of Rheumatology/European League Against Rheumatism/International Myositis Assessment and Clinical Studies Group/Paediatric Rheumatology International Trials Organisation collaborative initiative. Arthritis Rheumatol 2017;69:898–910.
32. Clements P, Lachenbruch P, Seibold J, White B, Weiner S, Martin R, et al. Inter and intraobserver variability of total skin thickness score (modified Rodnan TSS) in systemic sclerosis. J Rheumatol 1995;22:1281–5.
33. Felson DT, Anderson JJ, Boers M, Bombardier C, Furst D, Goldsmith C, et al. American College of Rheumatology preliminary definition of improvement in rheumatoid arthritis. Arthritis Rheum 1995;38:727–35.
34. Rider LG, Ruperto N, Pistorio A, Erman B, Bayat N, Lachenbruch PA, et al. 2016 development of adult dermatomyositis and polymyositis and juvenile dermatomyositis response criteria: methodological aspects: an American College of Rheumatology/European League Against Rheumatism/International Myositis Assessment and Clinical Studies Group/Paediatric Rheumatology International Trials Organisation collaborative initiative. Rheumatology (Oxford). In press.
35. Oddis CV, Reed AM, Aggarwal R, Rider LG, Ascherman DP, Levesque MC, et al. Rituximab in the treatment of refractory adult and juvenile dermatomyositis and adult polymyositis: a randomized, placebo-phase trial. Arthritis Rheum 2013;65: 314–24.
36. Selva-O'Callaghan A, Fonollosa-Pla V, Trallero-Araguás E, Martínez-Gómez X, Simeon-Aznar CP, Labrador-Horrillo M, et al. Nailfold capillary microscopy in adults with inflammatory myopathy. Semin Arthritis Rheum 2010;39:398–404.
37. Koenig M, Joyal F, Fritzler MJ, Roussin A, Abrahamowicz M, Boire G, et al. Autoantibodies and microvascular damage are independent predictive factors for the progression of Raynaud's phenomenon to systemic sclerosis: a twenty-year prospective study of 586 patients with validation of proposed criteria for early systemic sclerosis. Arthritis Rheum 2008;58: 3902–12.
38. Aggarwal R, Oddis CV, Goudeau D, Koontz D, Qi Z, Reed AM, et al. Autoantibody levels in myositis patients correlate with clinical response during B cell depletion with rituximab. Rheumatology (Oxford) 2016;55:1710.
39. Rosen A, Casciola-Rosen L. Autoantigens as partners in initiation and propagation of autoimmune rheumatic diseases. Annu Rev Immunol 2016;34:395–420.

ARTHRITIS & RHEUMATOLOGY
Vol. 69, No. 5, May 2017, pp 885–897
DOI 10.1002/art.40068

REVIEW

Innate Lymphoid Cells

Sparking Inflammatory Rheumatic Disease?

Mark H. Wenink,[1] Emmerik F. A. Leijten,[2] Tom Cupedo,[3] and Timothy R. D. J. Radstake[2]

Introduction

Immunology research is in a constant state of flux with new cell types being described on a regular basis. While most rheumatologists are familiar with the role that "T cell cytokines" such as tumor necrosis factor (TNF), interferon-γ (IFNγ), and interleukin-17A (IL-17A) play in the pathogenesis of rheumatic diseases, what many may not know is that an array of innate counterparts to the conventional T cells have recently been discovered that are capable of rapidly producing these same effector cytokines. These innate counterparts include γ/δ T cells, invariant natural killer (iNK) cells, mucosa-associated invariant T (MAIT) cells, and innate lymphoid cells (ILCs). An insightful overview of γ/δ T cells, iNK cells, and MAIT cells in rheumatic disease has recently been published (1); therefore, the current review focuses on ILCs. Strikingly, some of the ILCs have only recently been discovered, in part due to their relative scarcity in peripheral blood, and their presence in numerous organs of the human body has subsequently been described. In this review, we provide the newest insights into the potential role of ILCs in the field of rheumatology and provide recommendations for future ILC research that will help to promote our understanding of rheumatic diseases even further.

[1]Mark H. Wenink, MD, PhD: Sint Maartenskliniek, Nijmegen, The Netherlands; [2]Emmerik F. A. Leijten, MD, Timothy R. D. J. Radstake, MD, PhD: University Medical Center Utrecht, Utrecht, The Netherlands; [3]Tom Cupedo, PhD: Erasmus University Medical Center, Rotterdam, The Netherlands.

Drs. Wenink and Leijten contributed equally to this work.

Address correspondence to Timothy R. D. J. Radstake, MD, PhD, Department of Rheumatology and Clinical Immunology, Laboratory of Translational Immunology, University Medical Center Utrecht, Heidelberglaan 100, Internal post/room F02.127, PO Box 85500, 3508 GA Utrecht, The Netherlands. E-mail: T.R.D.J.Radstake@UMCUtrecht.nl.

Submitted for publication September 29, 2016; accepted in revised form February 7, 2017.

Essential background on recently discovered ILCs

ILCs as innate counterparts to T cells. Considerable phenotypic and functional overlap exists between ILCs and Th cells, yet there are important differences in activation pathways and tissue localization enabling distinct roles in inflammation. The priming of Th cells requires the recognition of peptide-loaded major histocompatibility complex (MHC) class II molecules provided by professional antigen-presenting cells such as dendritic cells (DCs). In contrast, ILCs do not express rearranged antigen receptors capable of recognizing antigens in a major histocompatibility complex. Activation of ILCs is instead mediated by a wide array of soluble mediators and stress molecules released and expressed by immune and stromal cells. In further contrast to Th cells, ILCs are continuously present at the peripheral barrier tissues in the body, readily able to produce the first waves of cytokine production upon damage or infection and to strongly shape the ensuing immune response (2). From an evolutionary point of view, the comparable role of ILCs and T cells shows apparent redundancy (3), and while ILC depletion in humans may not be critical for survival (4), ILCs can contribute to the pathogenesis of many diseases (for review, see ref. 5).

Conventional NK cells fall within the overarching group of ILCs but are genealogically different from the more recently identified "helper-like" ILCs, which are covered in this review. While the major function of conventional NK cells is inducing cytotoxicity, all other ILCs lack classic cytotoxicity-inducing capacity, and therein lies the distinction between "cytotoxic" and "helper-like" ILCs. Helper-like ILCs are defined by the presence of lymphoid morphology, expression of CD127 (IL-7

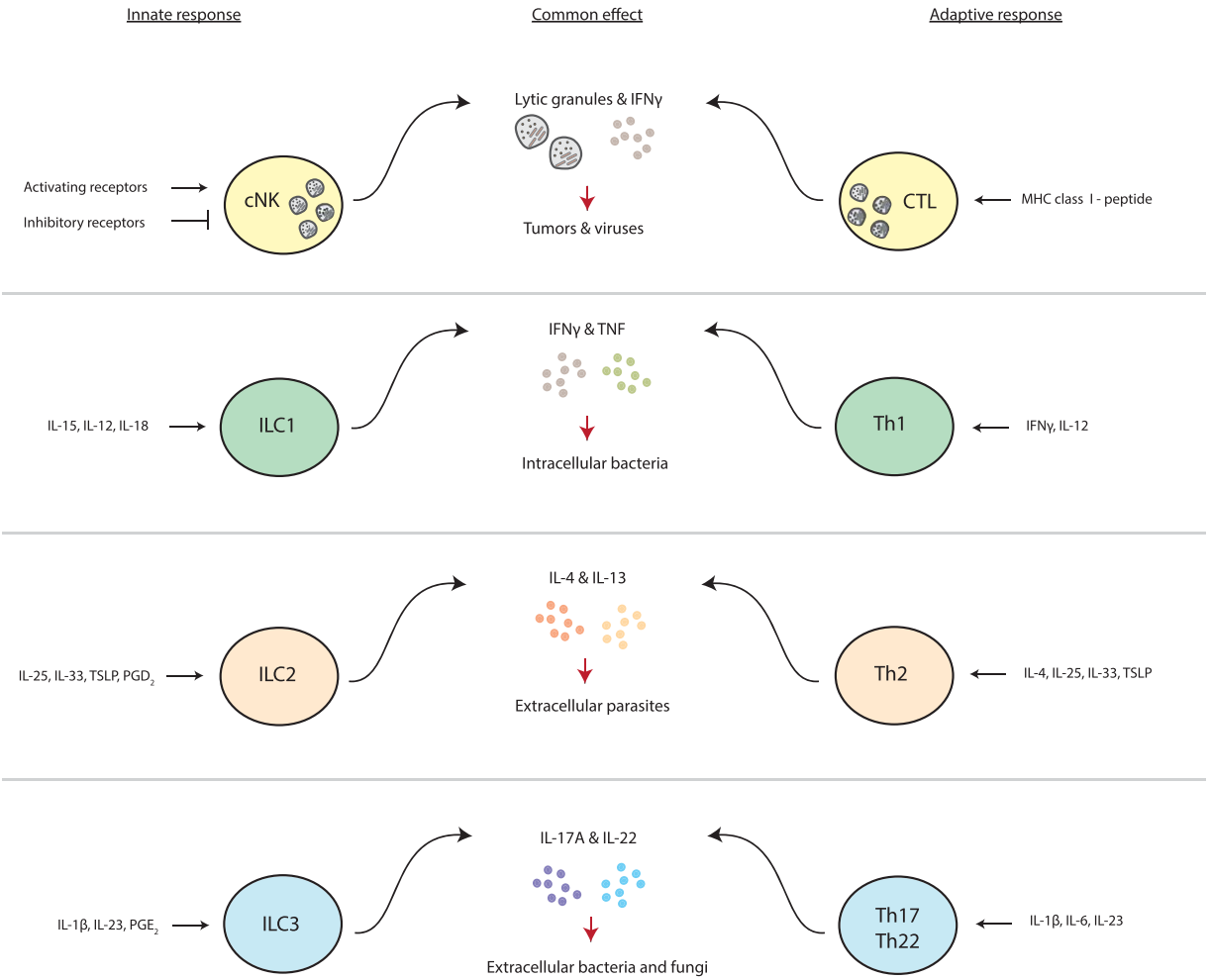

Figure 1. Innate lymphoid cells (ILCs) and their T cell counterparts. Effector functions of ILCs overlap greatly with those of their T cell counterparts. ILCs induce a rapid, innate response (left) that is followed by a slower, adaptive response in T cells (right) targeting the same pathogens. Upstream factors that determine the effector cytokines produced by ILCs and T cells also show considerable overlap. For instance, interleukin-23 (IL-23) is a cytokine involved in the polarization of Th17 cells and is also known to enhance the production of effector cytokines by group 3 ILCs (ILC3s). cNK = conventional natural killer; IFNγ = interferon-γ; CTL = cytotoxic T lymphocyte; MHC = major histocompatibility complex; TNF = tumor necrosis factor; TSLP = thymic stromal lymphopoietin; PGD_2 = prostaglandin D_2.

receptor α-chain [IL-7Rα]), and lack of lineage markers that are present on other cells (for instance, DCs or T cells). ILCs can be further classified into group 1 (ILC1s), group 2 (ILC2s), and group 3 (ILC3s), which to a great extent mimics the nomenclature that is used for the Th cell groups Th1, Th2, and Th17/Th22, respectively (6). An overview of ILCs and their T cell counterparts is shown in Figure 1.

ILC development. Helper-like ILCs are proposed to develop from a "common helper ILC precursor" or CHILP. Various transcription factors are involved in the differentiation of earlier precursors into CHILP. In mice, Id2, NFIL3, and Tox are crucial for the occurrence of all ILCs, while Runx3 is required for the normal development of ILC1s and ILC3s by regulating expression of retinoic acid receptor–related orphan nuclear receptor γt (RORγt) and aryl hydrocarbon receptor (AHR) (7–9). Promyelocytic leukemia zinc-finger protein (PLZF) is a key transcription factor that is required for (most) helper-like ILCs to develop, while PLZF is not needed for conventional NK cell development (10). Studies in mice have also taught us that the transcription factor GATA-3, the prototypical transcription factor of ILC2s, may also be important for the development and function of other ILC groups (11). In mice, GATA-3 is necessary for development of IL-7Rα–expressing ILCs and homeostasis of ILC3s (12). In summary, the balance among the 3 key transcription factors

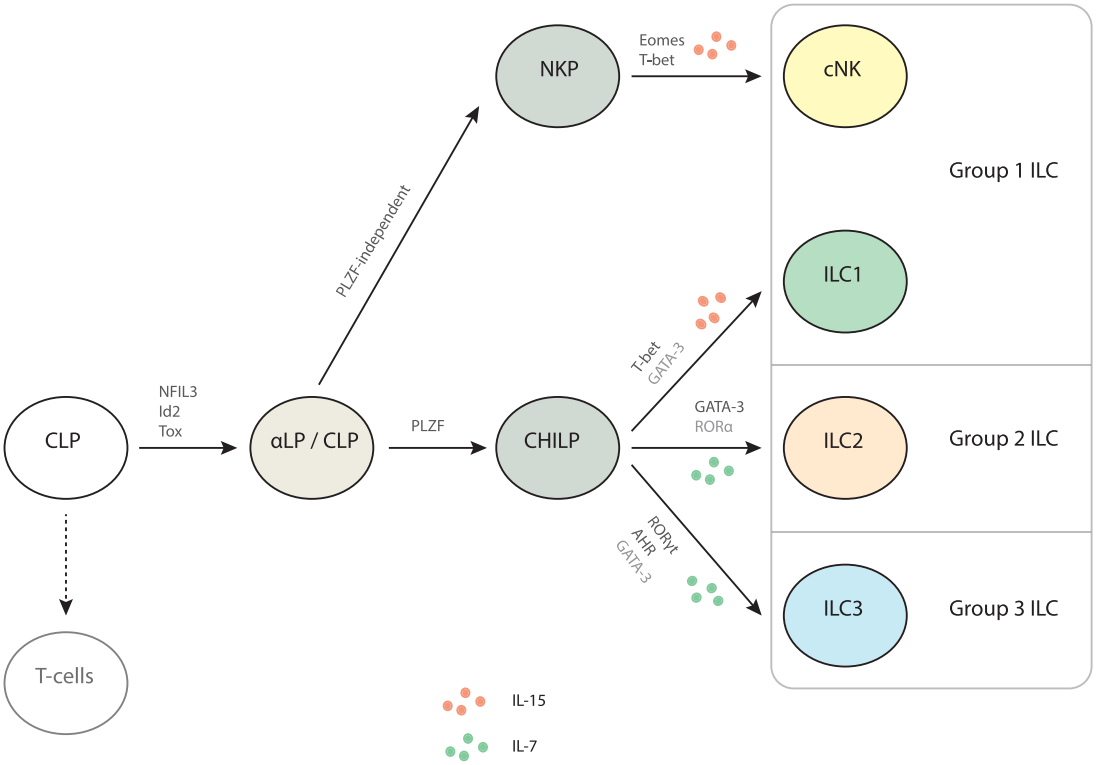

Figure 2. Development and classification of innate lymphoid cells (ILCs). ILCs develop from the common lymphoid progenitor (CLP), which also gives rise to T cells. The development of the $\alpha 4\beta 7$ integrin–expressing lymphoid progenitor (αLP) is dependent on 3 key transcription factors: NFIL3, Id2, and Tox. After this point, the development splits into natural killer cell precursors (NKP) and a common helper ILC precursor (CHILP), the latter being critically dependent on the transcription factor promyelocytic leukemia zinc finger protein (PLZF). Interleukin-15 (IL-15) is necessary for group 1 ILC (ILC1) development and IL-7 is necessary for ILC2 and ILC3 development. The CHILP gives rise to the 3 helper-like ILCs, each characterized by key transcription factors, namely T-bet, GATA-3, and retinoic acid receptor–related orphan nuclear receptor γt (RORγt) for ILC1s, ILC2s, and ILC3s, respectively. The current model of ILC development, depicted in the figure, stems from murine data. It should be noted that alternate developmental pathways may be possible in humans. For instance, lymphoid tissue inducers, a subset of ILC3s important for lymphoid neogenesis, may not follow the depicted developmental program. In addition, a recent study on ILC progenitors from human secondary lymphoid tissues revealed that a common RORγt-expressing ILC progenitor, probably upstream of the CHILP, was capable of giving rise to all ILCs and that all human ILCs, including conventional natural killer cells (cNK), still express RORγt to some extent (18). Eomes = eomesodermin; AHR = aryl hydrocarbon receptor.

RORγt, GATA-3, and T-bet determines the fate of ILCs in mice (5,11,13). IL-7R signaling not only drives proliferation of ILC3s in mice and humans (4,14), but also stabilizes the ILC3 phenotype in adult mice (15).

The current model of ILC development, depicted in Figure 2, stems from murine data and may not fully mimic the process in humans. A recent review has critically summarized the data on ILC development in humans (16), but a full developmental scheme for ILCs in humans is still lacking. We do know that human CD34+ hematopoietic progenitor cells can, under specific culture conditions, give rise to ILCs (17–19). One group has detected human ILC progenitors in the tonsil and gut lamina propria that developed preferentially into ILC3s when cultured with stem cell factor and AHR signaling, while culture conditions with IL-15 favored the development of conventional NK cells (17). More recently, a similar progenitor population expressing RORγt and Id2 was identified that in vitro gave rise to all ILC subsets, including conventional NK cells. These ILC progenitors did not develop into other leukocyte lineages and were found exclusively in secondary lymphoid tissues (18). Uncovering the stages of ILC development in humans remains a challenge in the field (16).

ILC subsets. The system of ILC subset classification is based on their developmental pathways, key transcription factors, and function in the form of signature cytokines being produced (6). Briefly, ILC1s express the transcription factor T-bet and produce IFNγ; ILC2s express the transcription factor GATA-3 and produce IL-4, IL-5, and IL-13; and ILC3s express the transcription factor RORγt and produce IL-17A

Table 1. Cell surface markers used to identify subsets of ILCs in humans*

Surface marker	Conventional NK cells	ILC1s	ILC2s	ILC3s	Interpretation
KIR	Yes	No	No	No	Only expressed on conventional NK cells
CD94	Yes	No	No	No	Differentiates between conventional NK cells and helper-like ILCs
CD56	Yes	Some	No	Some	High or moderate expression on conventional NK cells as well as expression on some (activated) helper-like ILCs
CD127 (IL-7Rα)	No	Yes	Yes	Yes	Expressed on all helper-like ILCs
CD117 (c-Kit)	No	No	Some	Yes	Expressed on ILC3s and some ILC2s
CD294 (CRTH2)	No	No	Yes	No	Only expressed on ILC2s
NKp44	Yes	Some	No	Some	Expressed on conventional NK cells, some ILC3s, and some ILC1s

* Some of the most common markers used to identify innate lymphoid cells (ILCs) in humans and separate them from conventional natural killer (NK) cells are shown. Within the helper-like ILC group, group 1 ILCs (ILC1s) are defined as CD127+CD117−CD294−; group 2 ILCs are defined as CD127+CD294+; and group 3 ILCs are defined as CD127+CD117+. KIR = killer cell immunoglobulin-like receptor; IL-7Rα = interleukin-7 receptor α-chain; CRTH2 = chemoattractant receptor–like molecule expressed on Th2 cells; NKp44 = natural killer p44.

and/or IL-22. Human ILC subsets can be distinguished by the expression of specific cell surface markers (Table 1). Natural cytotoxicity receptors are activating receptors best studied in the context of triggering conventional NK cells, when tumor and virus-infected cells up-regulate their ligands (many of which are still unknown). The natural cytotoxicity receptors include natural killer p30 (NKp30), NKp44 (only expressed in humans), and NKp46, which are also expressed by certain ILCs (20), as will be discussed below.

ILC1s. ILC1s have been proposed to include conventional NK cells and CD127+ and CD103+ ILCs. Although conventional NK cells and ILC1s share many features (e.g., IFNγ production), it is becoming clear that these 2 subsets have different progenitors as well as unique tissue distributions and functions (13,19). ILC1s have been found in intestinal mucosa, salivary gland, liver, and the female reproductive tract; there is a relative paucity of them in blood and lymphoid structures (21,22). On the other hand, conventional NK cells can make up to 15% of peripheral blood lymphocytes, and substantial numbers of them are present in lymphoid structures. ILC1s are thought to differ from conventional NK cells in that they lack expression of eomesodermin and do not exert cytolytic activity. Overall, ILC1s are a diverse group consisting of subsets that vary depending on their tissue microenvironment and the context of their circumstances (8). For example, small intestine intraepithelial ILC1s have been characterized that did express eomesodermin (23), while mouse ILC1s from salivary glands are capable of TRAIL-mediated cytotoxicity (24). ILC1s have been suggested to rely on the cytokines IL-15, IL-12, and IL-18, and they produce copious amounts of IFNγ and TNF. ILC1s protected mice from infection with *Clostridium difficile* and *Toxoplasma gondii* in 2 different infection models, and the ILCs constituted the (early) majority of IFNγ-producing cells (13,25). Judging from those studies, the protective role of ILC1s against infections is important. However, exaggerated or insufficient immune responses by ILC1s might lead to immunopathology.

ILC2s. Consistent with Th2 cells, the transcription factor GATA-3 is the prototypical element required for the development, maintenance, and function of ILC2s. ILC2s are found in increased numbers in the lung, skin, and adipose tissue. They respond to cytokines such as epithelial cell–derived IL-25, IL-33, and thymic stromal lymphopoietin (TSLP) by producing allergy- and fibrosis-related cytokines, such as IL-4, IL-9, and IL-13. Unlike the other ILCs, ILC2s express the prostaglandin D_2 (PGD_2) receptor chemoattractant receptor–like molecule expressed on Th2 cells (CD294). PGD_2 induces the migration of ILC2s and potentiates their cytokine production (21). For instance, ILC2s express NKp30, which responds to keratinocyte membrane–expressed B7-H6, leading to the production of IL-13, and skin from patients with atopic dermatitis expressed increased levels of B7-H6 (26). ILC2s have diverse functions; they have been shown to promote immunity against extracellular parasites (27), induce tissue repair by producing amphiregulin (28), and promote beige fat and reduce insulin resistance (29). However, deleterious roles of ILC2s have also been described. They are

associated with allergies, asthma, and atopic dermatitis. In addition, ILC2s were required for the occurrence of fibrosis in a mouse model of hepatic fibrosis (30).

ILC3s. ILC3s are developmentally dependent on expression of the nuclear hormone receptor RORγt (31,32), although in mature ILC3s, this receptor is dispensable for survival and antimicrobial functionality (33). Several subsets of ILC3s have been identified based on function and surface marker expression. The prototypical ILC3s are the lymphoid tissue inducers. These cells are present during fetal development in mice and humans and are responsible for initiation and organization of secondary lymphoid tissues (34–36). Lymphoid tissue inducers interact with stromal and endothelial cells at sites of lymphoid organ development (37,38) and by induction of chemokines and adhesion molecules initiate a cascade of well-described events culminating in the formation of lymph nodes and Peyer's patches (39).

After birth and throughout adulthood, 2 additional ILC3 subsets are present, characterized by the mutually exclusive expression of the natural cytotoxicity receptor NKp46 and the chemokine receptor CCR6 (40,41). Both reside within secondary lymphoid organs as well as in mucosal tissues such as the intestines (36,42–45). Functionally, ILC3s are characterized by the secretion of cytokines associated with Th17 cell immunity, including IL-22, granulocyte–macrophage colony-stimulating factor (GM-CSF), and IL-17A (36,42–46). This cytokine profile and the location of ILC3s at barrier surfaces such as the intestines makes these cells form an integral part of the body's immediate antimicrobial immune response (40,46–48). ILC3s control epithelial production of antimicrobial peptides whose function is to prevent attachment and translocation of intestinal microorganisms (49). In doing so, ILC3s boost the intestines' innate immunity and prevent bacterial dissemination in the wake of maturation of adaptive immunity (50). Taken together, ILC3s are essential for the maintenance of gut homeostasis, for which they use several mechanisms.

Plasticity. It is important to acknowledge the plasticity of ILCs. For example, ILC3s have been demonstrated to differentiate into ILC1-like cells and vice versa under specific inflammatory conditions (51–54). Shifts between other ILCs have also been described (55–57) that help to explain the class, phenotype, and effector function of ILCs detected in diverse tissues under varying environmental circumstances, and plasticity should be taken into account when interpreting the frequency of ILC subsets in rheumatic disease. An overview of the environmental factors that have been shown to steer plasticity between ILC subsets in vitro is shown in Figure 3.

Lessons from psoriasis and inflammatory bowel disease (IBD)

Psoriasis. IL-22 and IL-17A are key players in the pathogenesis of psoriasis, and it has become evident that conventional T cells are not the only contributors to the production of these effector cytokines (58). Although the NKp44+ ILC3 population is very scarce in the peripheral blood, these cells represent a major proportion of the ILC population in healthy skin (58–60), and numerous independent studies have shown that NKp44+ ILC3s are even more abundant in skin and blood samples from patients with psoriasis (58–62).

One very interesting finding pops up from studies of ILCs in psoriasis. The frequency of specifically NKp44+ ILC3s in the unaffected skin of psoriasis patients is equal to if not higher than the frequency of NKp44+ ILC3s in affected skin (58,59). This altered composition of ILCs in what would clinically appear to be unaffected skin of psoriasis patients raises the key question: are these NKp44+ ILC3s pathogenic or protective? The most common interpretation is that NKp44+ ILC3s in unaffected skin are prepositioned to initiate an inflammatory cascade (58–60,62). Animal models show that IL-22 causes skin lesions reminiscent of psoriasis, which supports the notion that NKp44+ ILC3s are necessary and critical for this process (63,64). Under culture conditions, the cytokines IL-1β and IL-23 can shift ILC1 and NKp44− ILC3 populations toward NKp44+ ILC3s (51,62). Recent gene expression profiling shows convincingly that "unaffected" psoriatic skin is quite different from skin of healthy individuals, with "already" significantly increased transcripts of IL-1β, IL-22, and IL-17 (65). Taken together with the established genetic background of psoriasis patients that includes single-nucleotide polymorphisms (SNPs) in IL-23R (66), these findings might explain why ILC composition in unaffected skin of psoriasis patients is altered.

Our knowledge of ILC3 *function* mainly stems from mouse models or, in humans, from tonsil- or gut-derived ILCs. It is known that NKp44+ ILC3s from psoriatic skin lesions are capable of producing IL-22 to a much greater extent than IL-17A (62), but it would be an oversimplification to view IL-22 as purely pathogenic, since this cytokine has essential regulatory and regenerative functions (for review, see ref. 67) highlighted below.

IBD. ILCs have important functions in homeostasis of the intestinal tract and in establishing immune

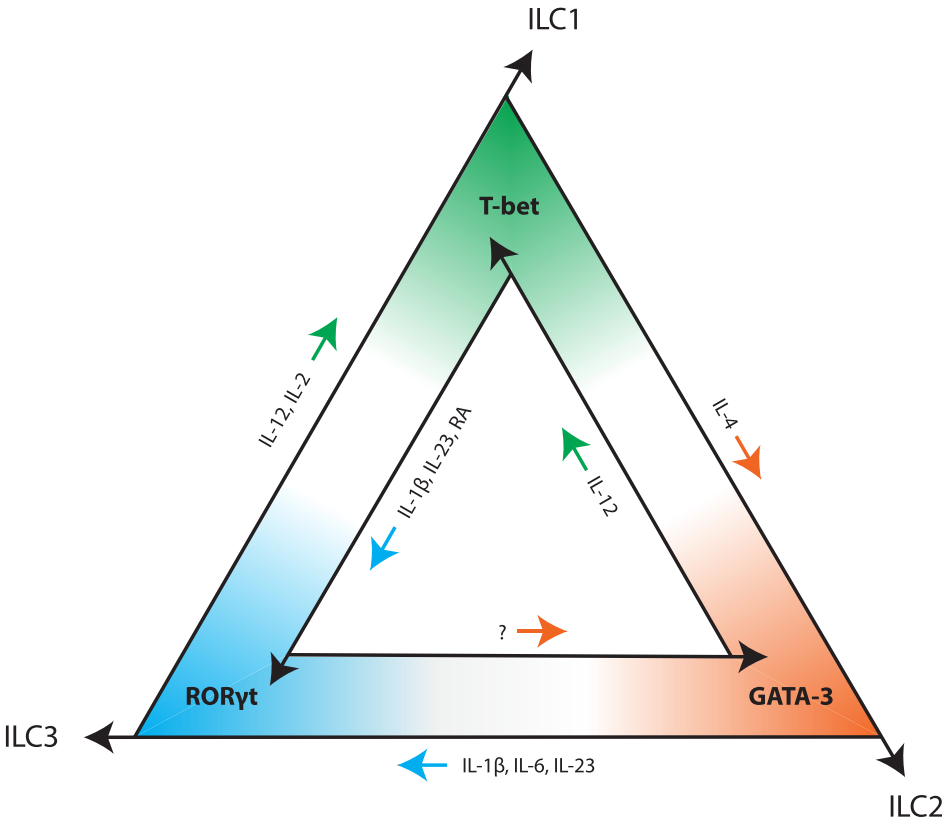

Figure 3. Plasticity of ILCs. Similar to the known plasticity of Th cells, ILCs can also adapt based on environmental cues, and shifts between ILC groups is a well-established phenomenon. Specific cytokines are depicted that, under culture conditions, have been shown to alter the ILC transcriptional program, cell surface markers, and effector cytokines being produced. Plasticity between ILC1s and ILC3s has been well studied. IL-1β, IL-23, and retinoic acid (RA) induce plasticity toward ILC3s, while IL-12 and IL-2 shift the balance toward ILC1s (51–54). The cytokines IL-1β, IL-6, and IL-23 have also been shown to induce ILC3-like phenotype and function in ILC2s (56), but it is unclear (?) whether reciprocal plasticity from ILC3s to ILC2s can occur. IL-4 and IL-12 have been shown to balance the plasticity between ILC1s and ILC2s (55,57). See Figure 2 for other definitions.

equilibrium with commensal bacteria (41). It is therefore not surprising that the loss of intestinal homeostasis and subsequent pathologic antimicrobial immunity that drive IBD are associated with alterations in intestinal ILCs (for review, see ref. 68).

In stark contrast to healthy skin, under homeostatic conditions the healthy gut is characterized by an abundant, protective NKp44+ ILC3 population, which reciprocally shifts toward a predominance of ILC1s in IBD, meaning a significantly increased proportion of ILCs that secrete IFNγ (23,51,52,69). Additionally, ILC3s from healthy gut mainly produce the homeostatic cytokine IL-22, while ILC3s in IBD also secrete proinflammatory IL-17A (70). Animal models have also taught us that ILC3s can dampen pathogenic CD4+ T cell responses (48) and that ILC3-derived IL-22 protects against colitis (71) and induces tolerance to commensal bacteria (47,72). The differential phenotype and function of ILCs in psoriasis versus IBD emphasizes that the outcome of ILC function (pathogenic versus protective) is highly dependent on the environment and tissue in which these cells are located.

Studies of ILCs in rheumatic disease

Psoriatic arthritis (PsA). ILCs have been found in increased numbers in synovial fluid from PsA patients (61). Synovial fluid from PsA patients and patients with rheumatoid arthritis (RA) showed an increase in frequency of ILC1s as compared to the frequency of ILC1s in peripheral blood, while the frequency of ILC2s was unaltered. Interestingly, only synovial fluid from PsA patients contained a major increase in NKp44+ ILC3s, which distinguished the synovial compartment in PsA from that in RA. The increased presence of synovial fluid ILC3s also coincided with up-regulated expression

of CCR6. In contrast, peripheral blood from PsA patients contained fewer CCR6+ ILCs than did peripheral blood from healthy controls, and the frequency of CCR6+ ILC3s was inversely related to disease activity measures, which could indicate specific targeting of these ILC3s to the joint in patients with PsA. ILC3s in synovial fluid from PsA patients were capable of IL-17A production, implicating their role in PsA pathogenesis (61).

PsA has recently been thought of as a disease that starts at the enthesis with microtrauma and culminates in chronic inflammation. In contrast to mouse models of psoriasis and colitis, the role of ILCs has not been studied in experimental models of PsA. It is of particular interest to determine the relative importance of ILC3s and other innate lymphocytes, such as IL-17A–producing γ/δ T cells, as the latter have been demonstrated to be present in mouse models of enthesitis (73,74). Only one group has described the presence of ILC3s and ILC2s in nonrheumatic human spinal, anterior cruciate ligament, and Achilles tendon entheses, yet these data need to be published to be fully appreciated (75). Future work should evaluate which activating/inhibitory receptors are expressed by ILCs found in the joint and determine how their ligands expressed by tissue resident cells influence disease pathogenesis (76–79), for instance, by affecting production of proinflammatory cytokines by ILCs.

Ankylosing spondylitis (AS). AS is characterized by inflammatory back pain and axial new bone formation. Our current view of AS is that the cytokines TNF, IL-17, and IL-22 are critical drivers of its pathogenesis (73,80,81). Animal models have further shown that innate counterparts to T cells can produce these cytokines, mimicking the clinical manifestations of AS (73,74,81). ILC3s have been described in nonrheumatic enthesis (75), and there is evidence of the increased presence of IL-22–producing NKp44+ ILC3s in other tissues from AS patients. Ciccia et al described a cell subset consisting of CD56+NKp44+ cells, possibly ILC3s, to be the main producers of IL-22 in the gut of AS patients. In contrast, in Crohn's disease, CD4+ T cells were the main producers of IL-22 (82). In a follow-up study, Ciccia et al found an increased presence of $\alpha4\beta7$ integrin–positive IL-17+ and IL-22+ ILC3s in the gut, blood, synovial fluid, and bone marrow (83). The interesting hypothesis was put forward that gut-derived ILC3s might home to inflamed (sacroiliac) joints and contribute to the disease process by producing IL-17 and IL-22 (83). A role for gut-derived immune cells is underscored by the transgenic HLA–B27 rat model of AS, in which the gut microbiome is necessary for the occurrence of disease (84,85). Consistent with PsA, a genetic background could enhance the role of ILC3s in the pathogenesis of AS. IL-23R, RUNX3, and MICA have all been linked to AS susceptibility (86).

A recent study further demonstrated that PGE_2, via the EP_4 receptor, potentiates gut ILC3 proliferation and IL-22 production (87). The effect of nonsteroidal antiinflammatory drugs on ILC3 proliferation and IL-22 production deserves investigation in the context of AS.

RA. RA is a disease driven by MHC class II molecules and adaptive immune responses, exemplified by the effectiveness of drugs targeting B cells and the interaction between costimulatory molecules and CD28 (CTLA-4Ig). ILCs have been implicated in supporting antibody production by B cells via diverse pathways, including lymphotoxin, CD40, and BAFF/APRIL signaling (88). Adult ILC3s can sustain CD4+ T cell memory-enhancing germinal center reactions and subsequent antibody production (89). As discussed in the section on ILC3s, these cells are important in the development and homeostasis of secondary lymphoid tissue (82). Under inflammatory conditions, so-called tertiary lymphoid structures can develop, which are germinal center–like structures that arise after birth at sites not originally in need of lymphoid structures.

This prompted a study to investigate if ILCs could be found in tertiary lymphoid structures of RA synovial tissue, but hardly any ILC3s were detected (90). Another research group set out to characterize ILCs in inguinal lymph nodes in patients with preclinical RA (arthralgia patients positive for rheumatoid factor and/or anti–citrullinated protein antibodies), patients with established RA, and healthy controls (91). Although ILCs were sparsely present and there were no differences in total ILC numbers, it was found that in the lymph nodes of patients with preclinical RA, the ILC1/2 group (the study was hampered by not distinguishing between ILC1s and ILC2s) made up a larger proportion of the ILCs than in the lymph nodes of healthy controls. Interestingly, there was a shift in the ILC3 population from NKp44− ILC3s to NKp44+ ILC3s in patients with established RA and a clear tendency toward fewer NKp44− ILC3s in patients with preclinical RA. Since NKp44− ILC3s are thought to be involved in maintaining secondary lymphoid tissue homeostasis (lymphoid tissue inducers), it was hypothesized that the loss of these cells may result in an autoimmune disease–prone lymph node microenvironment (91).

The above-described paucity of ILC3s in RA synovial tertiary lymphoid structures (90) is consistent with the relative lack of ILC3s described in RA synovial fluid (61) and makes a role for ILC3s in the local RA

disease process less likely. In contrast to ILC3s and ILC2s, ILC1s can readily be found in the RA synovial cavity, and the frequency of ILC1s there is strongly increased compared to the frequency of ILC1s in peripheral blood (61). It appears that if ILCs play a role in local RA pathology, then ILC1s are the subset to look at and could contribute to the production of TNF and IFNγ.

Sjögren's syndrome (SS). ILCs have been identified in the salivary glands of mice (22,24,92) and humans (93). The established role of ILCs in producing IL-22 and IL-17A, which are involved in the pathogenesis of primary SS (94), along with their presence at epithelial sites of the body poses ILCs as candidate contributors to the pathogenesis of primary SS. Specifically, it was shown that IL-22–producing NKp44+ ILC3s were more abundant in the salivary glands of patients with primary SS than in the salivary glands of patients with sicca syndrome without SS, and that the frequency of the ILC3s was positively correlated with the lymphocytic focus score (93). Additional studies will be needed to confirm these results and to further evaluate the *function* of ILC3s in salivary glands of patients with primary SS.

Three key areas deserve subsequent exploration in the setting of primary SS. First, ILCs from mice appear to be "tissue resident" in the salivary gland, meaning that they are barely replenished from circulating (precursor) ILCs that would subsequently migrate into the salivary gland (22,92). Second, the histopathology of SS is marked by the formation of tertiary lymphoid structures in salivary glands, which suggests the involvement of ILCs (36,95). Finally, SNPs in NKp30 that cause decreased expression of this receptor are less common in patients with primary SS, and, indeed, patients with primary SS have increased expression of NKp30 on conventional NK cells (96). Helper-like ILCs can also express this receptor, and it is known that the ligand for NKp30, namely B7-H6, is expressed by salivary gland epithelial cells (96). Taken together, these observations highlight the potential role of ILCs in primary SS and justify future research.

Systemic lupus erythematosus (SLE). ILCs have been described in patients with SLE as part of a control cohort for a study on systemic sclerosis (SSc), and the frequency of ILC2s was found to be increased in their circulation compared to that in healthy controls (97). The noted elevated frequency of ILC2s is difficult to reconcile with the established effect of IFNs of decreasing ILC survival and function. SLE is clearly marked by an IFN signature (98), yet studies in mice have shown that ILC3s undergo CD95/FasL-mediated apoptosis following the production of type I IFNs by plasmacytoid DCs (99). Similarly, type I IFNs also increase cell death and decrease cytokine production by ILC2s (100).

Patients with SLE are prone to develop skin lesions (e.g., butterfly rash) following sunlight exposure (ultraviolet B) that induces excessive keratinocyte apoptosis (101). ILCs are important in skin homeostasis, and this function is mediated by production of IL-22, a key cytokine that helps prevent keratinocyte damage (102,103). In this context, the (protective) role of IL-22–producing ILCs in epithelial homeostasis is an interesting avenue for investigation that could shed light on some of the cutaneous manifestations of the disease (104).

SSc. SSc is marked by low-grade inflammation, vascular injury, and subsequent fibrosis of skin and internal organs. In a recent study, ILC2s were present in markedly increased numbers in the skin and blood of SSc patients. Numbers of ILC2s were elevated the most in patients with diffuse cutaneous SSc and correlated with the modified Rodnan skin thickness score (97,105). In light of the IFN signature (which is strongest in early and nonfibrotic SSc [106]) and the suppressive effect of IFN on ILC2s (100), the increased numbers of ILC2s in more advanced stages of the disease is noteworthy (97). The increased presence of ILC2s in SSc was not found in another study that compared 38 clinically undefined SSc patients with matched healthy controls (107). It is unclear why there was such a difference in outcome between the 2 studies, but different methodologies (e.g., different cell markers and gating strategy used) could help explain the discrepancy.

With regard to the occurrence of fibrosis in SSc, the ILC2 subset is of particular interest. In mice, ILC2s were required for the occurrence of hepatic fibrosis, and IL-13 released by ILC2s was sufficient for collagen deposition in a mouse model of pulmonary fibrosis (30,108). ILC2s are activated, start producing cytokines (e.g., IL-13), and proliferate upon exposure to epithelial alarmin cytokines, such as IL-25, IL-33, and TSLP, all of which are found to be elevated in SSc (109). ILC2–derived IL-13 induces collagen deposition from fibroblasts and differentiates macrophages toward a profibrotic phenotype (108).

NKp44+ ILC3s are an important source of IL-17A in skin inflammation, and IL-17A has been implicated in the generation of pulmonary and skin fibrosis (110). In patients with SSc, the NKp44+ ILC3 population was slightly increased in blood, while the NKp44− ILC3 population was decreased compared to that in healthy controls (107). In addition, the same study found an increase in CD4+ ILC1s, which were potent producers of TNF and GM-CSF, in the peripheral blood of SSc patients (107). Future studies should examine the presence and function of ILCs at affected sites, such as the skin, to better understand their potential contribution to SSc.

Conclusions

Over the past few years, it has become clear that ILCs play a pivotal role in orchestrating the first waves of the immune response in human tissue upon receiving danger signals, thereby contributing toward effective clearance of the initiating event. On the other hand, numerous studies have shown the relevance of ILCs in upholding tissue homeostasis. Clear evidence of this balancing act has been well studied in skin and gut disease, yet an overview of the contribution of ILCs to rheumatic disease has been lacking. In this review, we provide a comprehensive overview of the recent research that has been performed on helper-like ILCs in rheumatic diseases (Table 2). Recent reports have begun to shed light on ILC aberrations in patients with IBD-associated arthritis (111) and antineutrophil cytoplasmic antibody–associated vasculitis (112). Many other rheumatic diseases, such as Behçet's disease and reactive arthritis, await and deserve further exploration into the role of ILCs, and more work is needed on the diseases highlighted in this review.

We believe that future work should focus on 3 key issues. At first, due to the rarity of ILCs, our knowledge of these cells is largely based on flow cytometric phenotyping. Hence, we encourage the ILC field to adhere to the established framework for ILC gating to improve comparability between studies and between different clinical conditions as well as to use standardized measures before and after initiation of therapeutic intervention. Second, the low frequency of ILCs challenges our ability to isolate ILCs from human tissues for the purpose of functional assays. For instance, the culturing of ILCs to focus on their functional roles in health and disease poses challenges that hinder development of drugs to target pathologic processes that they orchestrate. Until now, our current knowledge of ILC

Table 2. Studies implicating ILCs in rheumatic and related epithelial diseases in humans*

Disease, implicated ILCs	Role in pathogenesis (ref.)
Psoriasis	
NKp44+ ILC3s	Increased frequency in blood and in unaffected and affected skin (58–62)
IBD	
ILC3s	Increased IL-17A production by ILC3s (70)
ILC1s	Overall shift from ILC3s toward IFNγ-producing ILC1s (23,52)
PsA	
ILC3s and ILC2s	Present in nonrheumatic enthesis (75)
CCR6+ ILC3s	Shift from blood to synovial cavity correlates with disease severity (61)
NKp44+ ILC3s	Highly increased presence in synovial joint in PsA patients in comparison to blood and in comparison to RA patients (61)
IBD-associated arthritis	
IFNγ+ ILCs and IL-17A+ ILCs	Increased frequency in blood compared to IBD patients without arthritis (111)
AS	
ILC3s and ILC2s	Present in nonrheumatic enthesis (75)
α4β7 integrin–positive IL-17+ and IL-22+ ILC3s	Increased presence in gut, blood, bone marrow, and joints in AS (83)
RA	
ILC1s	Selectively increased in synovial fluid of RA patients (61)
NCR− ILC3s	Reduced numbers in lymph nodes in (preclinical) RA (91)
SS	
NKp44+ ILC3s	Increased in salivary gland and correlate with lymphocytic focus score (93)
SLE	
ILC2s	Elevated frequency in blood (97)
ANCA-associated vasculitis	
ILC2s and ILC3s	Decreased frequency in blood of patients with acute disease (112)
SSc	
ILC2s	Increased in skin and blood of SSc patients, and numbers correlated with skin fibrosis and ILD (97); no increased numbers found in another study (107)
NKp44+ ILC3s and NKp44− ILC3s	Found increased and decreased, respectively, in blood (107)
CD4+ ILC1s	Increased in blood of SSc patients (107)

* ILCs = innate lymphoid cells; NKp44 = natural killer p44; ILC3s = group 3 ILCs; IBD = inflammatory bowel disease; IL-17A = interleukin-17A; IFNγ = interferon-γ; PsA = psoriatic arthritis; RA = rheumatoid arthritis; AS = ankylosing spondylitis; NCR = natural cytotoxicity receptor; SS = Sjögren's syndrome; SLE = systemic lupus erythematosus; ANCA = antineutrophil cytoplasmic antibody; SSc = systemic sclerosis; ILD = interstitial lung disease.

development and function has been mainly based on experimental models, which leaves its relevance for humans to be determined. The use of alternative, novel techniques that give an understanding of human ILC function and development (e.g., single-cell sequencing [113,114]) should therefore be exploited further.

Finally, strategies aimed at targeting ILC pathology by blocking their developmental fate, plasticity, and/or effector function deserve further investigation (115). Do therapies targeting the IL-23/IL-17 axis given to patients with psoriatic skin disease also halt aberrant ILC function in the joint or enthesis, preventing the transition toward concomitant joint disease? If this hypothesis holds true, we may go on to apply similar ways of delivering preventative medicine to patients with other rheumatic diseases, shifting our focus away from targeting the chronic effects of immune-mediated disease and toward disease interception, possibly by tackling the ILCs.

AUTHOR CONTRIBUTIONS

All authors were involved in drafting the article or revising it critically for important intellectual content, and all authors approved the final version to be published.

REFERENCES

1. Exley MA, Tsokos GC, Mills KH, Elewaut D, Mulhearn B. What rheumatologists need to know about innate lymphocytes. Nat Rev Rheumatol 2016;12:658–68.
2. Bando JK, Colonna M. Innate lymphoid cell function in the context of adaptive immunity. Nat Immunol 2016;17:783–9.
3. Vivier E, van de Pavert SA, Cooper MD, Belz GT. The evolution of innate lymphoid cells. Nat Immunol 2016;17:790–4.
4. Vély F, Barlogis V, Vallentin B, Neven B, Piperoglou C, Ebbo M, et al. Evidence of innate lymphoid cell redundancy in humans. Nat Immunol 2016;17:1291–9.
5. Klose CS, Artis D. Innate lymphoid cells as regulators of immunity, inflammation and tissue homeostasis. Nat Immunol 2016;17:765–74.
6. Spits H, Artis D, Colonna M, Diefenbach A, Di Santo JP, Eberl G, et al. Innate lymphoid cells: a proposal for uniform nomenclature. Nat Rev Immunol 2013;13:145–9.
7. Gronke K, Nielsen MK, Diefenbach A. Innate lymphoid cells, precursors and plasticity. Immunol Lett 2016;179:9–18.
8. Fuchs A. ILC1s in tissue inflammation and infection. Front Immunol 2016;7:104.
9. Ebihara T, Song C, Ryu SH, Plougastel-Douglas B, Yang L, Levanon D, et al. Runx3 specifies lineage commitment of innate lymphoid cells. Nat Immunol 2015;16:1124–33.
10. Constantinides MG, McDonald BD, Verhoef PA, Bendelac A. A committed precursor to innate lymphoid cells. Nature 2014;508:397–401.
11. Zhong C, Cui K, Wilhelm C, Hu G, Mao K, Belkaid Y, et al. Group 3 innate lymphoid cells continuously require the transcription factor GATA-3 after commitment. Nat Immunol 2016;17:169–78.
12. Yagi R, Zhong C, Northrup DL, Yu F, Bouladoux N, Spencer S, et al. The transcription factor GATA3 is critical for the development of all IL-7Rα-expressing innate lymphoid cells. Immunity 2014;40:378–88.
13. Klose CS, Flach M, Möhle L, Rogell L, Hoyler T, Ebert K, et al. Differentiation of type 1 ILCs from a common progenitor to all helper-like innate lymphoid cell lineages. Cell 2014;157:340–56.
14. Schmutz S, Bosco N, Chappaz S, Boyman O, Acha-Orbea H, Ceredig R, et al. Cutting edge: IL-7 regulates the peripheral pool of adult RORγ^+ lymphoid tissue inducer cells. J Immunol 2009;183:2217–21.
15. Vonarbourg C, Mortha A, Bui VL, Hernandez PP, Kiss EA, Hoyler T, et al. Regulated expression of nuclear receptor RORγt confers distinct functional fates to NK cell receptor-expressing RORγt^+ innate lymphocytes. Immunity 2010;33:736–51.
16. Juelke K, Romagnani C. Differentiation of human innate lymphoid cells (ILCs). Curr Opin Immunol 2016;38:75–85.
17. Montaldo E, Teixeira-Alves LG, Glatzer T, Durek P, Stervbo U, Hamann W, et al. Human RORγt^+CD34$^+$ cells are lineage-specified progenitors of group 3 RORγt^+ innate lymphoid cells. Immunity 2014;41:988–1000.
18. Scoville SD, Mundy-Bosse BL, Zhang MH, Chen L, Zhang X, Keller KA, et al. A progenitor cell expressing transcription factor RORγt generates all human innate lymphoid cell subsets. Immunity 2016;44:1140–50.
19. Renoux VM, Zriwil A, Peitzsch C, Michaëlsson J, Friberg D, Soneji S, et al. Identification of a human natural killer cell lineage-restricted progenitor in fetal and adult tissues. Immunity 2015;43:394–407.
20. Kruse PH, Matta J, Ugolini S, Vivier E. Natural cytotoxicity receptors and their ligands. Immunol Cell Biol 2014;92:221–9.
21. Montaldo E, Vacca P, Vitale C, Moretta F, Locatelli F, Mingari MC, et al. Human innate lymphoid cells. Immunol Lett 2016;179:2–8.
22. Gasteiger G, Fan X, Dikiy S, Lee SY, Rudensky AY. Tissue residency of innate lymphoid cells in lymphoid and nonlymphoid organs. Science 2015;350:981–5.
23. Fuchs A, Vermi W, Lee JS, Lonardi S, Gilfillan S, Newberry RD, et al. Intraepithelial type 1 innate lymphoid cells are a unique subset of IL-12- and IL-15-responsive IFN-γ-producing cells. Immunity 2013;38:769–81.
24. Schuster IS, Wikstrom ME, Brizard G, Coudert JD, Estcourt MJ, Manzur M, et al. TRAIL+ NK cells control CD4+ T cell responses during chronic viral infection to limit autoimmunity. Immunity 2014;41:646–56.
25. Abt MC, Lewis BB, Caballero S, Xiong H, Carter RA, Sušac B, et al. Innate immune defenses mediated by two ILC subsets are critical for protection against acute Clostridium difficile infection. Cell Host Microbe 2015;18:27–37.
26. Salimi M, Xue L, Jolin H, Hardman C, Cousins DJ, McKenzie AN, et al. Group 2 innate lymphoid cells express functional NKp30 receptor inducing type 2 cytokine production. J Immunol 2016;196:45–54.
27. Neill DR, Wong SH, Bellosi A, Flynn RJ, Daly M, Langford TK, et al. Nuocytes represent a new innate effector leukocyte that mediates type-2 immunity. Nature 2010;464:1367–70.
28. Turner JE, Morrison PJ, Wilhelm C, Wilson M, Ahlfors H, Renauld JC, et al. IL-9-mediated survival of type 2 innate lymphoid cells promotes damage control in helminth-induced lung inflammation. J Exp Med 2013;210:2951–65.
29. McKenzie AN, Spits H, Eberl G. Innate lymphoid cells in inflammation and immunity. Immunity 2014;41:366–74.
30. McHedlidze T, Waldner M, Zopf S, Walker J, Rankin AL, Schuchmann M, et al. Interleukin-33-dependent innate lymphoid cells mediate hepatic fibrosis. Immunity 2013;39:357–71.
31. Eberl G, Marmon S, Sunshine MJ, Rennert PD, Choi Y, Littman DR. An essential function for the nuclear receptor RORγt in the generation of fetal lymphoid tissue inducer cells. Nat Immunol 2004;5:64–73.

32. Sun Z, Unutmaz D, Zou YR, Sunshine MJ, Pierani A, Brenner-Morton S, et al. Requirement for RORγ in thymocyte survival and lymphoid organ development. Science 2000;288:2369–73.
33. Withers DR, Hepworth MR, Wang X, Mackley EC, Halford EE, Dutton EE, et al. Transient inhibition of ROR-γt therapeutically limits intestinal inflammation by reducing TH17 cells and preserving group 3 innate lymphoid cells. Nat Med 2016;22:319–23.
34. Mebius RE, Rennert P, Weissman IL. Developing lymph nodes collect CD4+CD3− LTβ+ cells that can differentiate to APC, NK cells, and follicular cells but not T or B cells. Immunity 1997;7:493–504.
35. Van de Pavert SA, Mebius RE. New insights into the development of lymphoid tissues. Nat Rev Immunol 2010;10:664–74.
36. Cupedo T, Crellin NK, Papazian N, Rombouts EJ, Weijer K, Grogan JL, et al. Human fetal lymphoid tissue-inducer cells are interleukin 17-producing precursors to RORC+ CD127+ natural killer-like cells. Nat Immunol 2009;10:66–74.
37. Onder L, Danuser R, Scandella E, Firner S, Chai Q, Hehlgans T, et al. Endothelial cell-specific lymphotoxin-β receptor signaling is critical for lymph node and high endothelial venule formation. J Exp Med 2013;210:465–73.
38. Yoshida H, Naito A, Inoue JI, Satoh M, Santee-Cooper SM, Ware CF, et al. Different cytokines induce surface lymphotoxin-αβ on IL-7 receptor-α cells that differentially engender lymph nodes and Peyer's patches. Immunity 2002;17:823–33.
39. Randall TD, Carragher DM, Rangel-Moreno J. Development of secondary lymphoid organs. Annu Rev Immunol 2008;26:627–50.
40. Spits H, Cupedo T. Innate lymphoid cells: emerging insights in development, lineage relationships, and function. Annu Rev Immunol 2012;30:647–75.
41. Artis D, Spits H. The biology of innate lymphoid cells. Nature 2015;517:293–301.
42. Luci C, Reynders A, Ivanov II, Cognet C, Chiche L, Chasson L, et al. Influence of the transcription factor RORγt on the development of NKp46+ cell populations in gut and skin. Nat Immunol 2009;10:75–82.
43. Sanos SL, Bui VL, Mortha A, Oberle K, Heners C, Johner C, et al. RORγt and commensal microflora are required for the differentiation of mucosal interleukin 22-producing NKp46+ cells. Nat Immunol 2009;10:83–91.
44. Satoh-Takayama N, Vosshenrich CA, Lesjean-Pottier S, Sawa S, Lochner M, Rattis F, et al. Microbial flora drives interleukin 22 production in intestinal NKp46+ cells that provide innate mucosal immune defense. Immunity 2008;29:958–70.
45. Cella M, Fuchs A, Vermi W, Facchetti F, Otero K, Lennerz JK, et al. A human natural killer cell subset provides an innate source of IL-22 for mucosal immunity. Nature 2009;457:722–5.
46. Spits H, Di Santo JP. The expanding family of innate lymphoid cells: regulators and effectors of immunity and tissue remodeling. Nat Immunol 2011;12:21–7.
47. Goto Y, Obata T, Kunisawa J, Sato S, Ivanov II, Lamichhane A, et al. Innate lymphoid cells regulate intestinal epithelial cell glycosylation. Science 2014;345:1254009.
48. Hepworth MR, Monticelli LA, Fung TC, Ziegler CG, Grunberg S, Sinha R, et al. Innate lymphoid cells regulate CD4+ T-cell responses to intestinal commensal bacteria. Nature 2013;498:113–7.
49. Sonnenberg GF, Fouser LA, Artis D. Border patrol: regulation of immunity, inflammation and tissue homeostasis at barrier surfaces by IL-22. Nat Immunol 2011;12:383–90.
50. Sonnenberg GF, Monticelli LA, Elloso MM, Fouser LA, Artis D. $CD4^+$ lymphoid tissue-inducer cells promote innate immunity in the gut. Immunity 2011;34:122–34.
51. Bernink JH, Krabbendam L, Germar K, de Jong E, Gronke K, Kofoed-Nielsen M, et al. Interleukin-12 and -23 control plasticity of Cd127+ group 1 and group 3 innate lymphoid cells in the intestinal lamina propria. Immunity 2015;43:146–60.
52. Bernink JH, Peters CP, Munneke M, te Velde AA, Meijer SL, Weijer K, et al. Human type 1 innate lymphoid cells accumulate in inflamed mucosal tissues. Nat Immunol 2013;14:221–9.
53. Klose CS, Kiss EA, Schwierzeck V, Ebert K, Hoyler T, D'Hargues Y, et al. A T-bet gradient controls the fate and function of $CCR6^-RORγt^+$ innate lymphoid cells. Nature 2013;494:261–5.
54. Cella M, Otero K, Colonna M. Expansion of human NK-22 cells with IL-7, IL-2, and IL-1β reveals intrinsic functional plasticity. Proc Natl Acad Sci U S A 2010;107:10961–6.
55. Lim AI, Menegatti S, Bustamante J, Le Bourhis L, Allez M, Rogge L, et al. IL-12 drives functional plasticity of human group 2 innate lymphoid cells. J Exp Med 2016;213:569–83.
56. Huang Y, Guo L, Qiu J, Chen X, Hu-Li J, Siebenlist U, et al. IL-25-responsive, lineage-negative $KLRG1^{hi}$ cells are multipotential "inflammatory" type 2 innate lymphoid cells. Nat Immunol 2015;16:161–9.
57. Bal SM, Bernink JH, Nagasawa M, Groot J, Shikhagaie MM, Golebski K, et al. IL-1β, IL-4 and IL-12 control the fate of group 2 innate lymphoid cells in human airway inflammation in the lungs. Nat Immunol 2016;17:636–45.
58. Villanova F, Flutter B, Tosi I, Grys K, Sreeneebus H, Perera GK, et al. Characterization of innate lymphoid cells in human skin and blood demonstrates increase of NKp44+ ILC3 in psoriasis. J Invest Dermatol 2014;134:984–91.
59. Dyring-Andersen B, Geisler C, Agerbeck C, Lauritsen JP, Gúdjonsdottir SD, Skov L, et al. Increased number and frequency of group 3 innate lymphoid cells in nonlesional psoriatic skin. Br J Dermatol 2014;170:609–16.
60. Brüggen MC, Bauer W, Reininger B, Clim E, Captarencu C, Steiner GE, et al. In situ mapping of innate lymphoid cells in human skin: evidence for remarkable differences between normal and inflamed skin. J Invest Dermatol 2016;136:2396–405.
61. Leijten EF, van Kempen TS, Boes M, Michels-van Amelsfort JM, Hijnen D, Hartgring SA, et al. Enrichment of activated group 3 innate lymphoid cells in psoriatic arthritis synovial fluid. Arthritis Rheumatol 2015;67:2673–8.
62. Teunissen MB, Munneke JM, Bernink JH, Spuls PI, Res PC, te Velde A, et al. Composition of innate lymphoid cell subsets in the human skin: enrichment of NCR^+ ILC3 in lesional skin and blood of psoriasis patients. J Invest Dermatol 2014;134:2351–60.
63. Pantelyushin S, Haak S, Ingold B, Kulig P, Heppner FL, Navarini AA, et al. Rorγt+ innate lymphocytes and γδ T cells initiate psoriasiform plaque formation in mice. J Clin Invest 2012;122:2252–6.
64. Ma HL, Liang S, Li J, Napierata L, Brown T, Benoit S, et al. IL-22 is required for Th17 cell-mediated pathology in a mouse model of psoriasis-like skin inflammation. J Clin Invest 2008;118:597–607.
65. Chiricozzi A, Suárez-Fariñas M, Fuentes-Duculan J, Cueto I, Li K, Tian S, et al. Increased expression of interleukin-17 pathway genes in nonlesional skin of moderate-to-severe psoriasis vulgaris. Br J Dermatol 2016;174:136–45.
66. Nair RP, Duffin KC, Helms C, Ding J, Stuart PE, Goldgar D, et al. Genome-wide scan reveals association of psoriasis with IL-23 and NF-κB pathways. Nat Genet 2009;41:199–204.
67. Dudakov JA, Hanash AM, van den Brink MR. Interleukin-22: immunobiology and pathology. Annu Rev Immunol 2015;33:747–85.
68. Peters CP, Mjösberg JM, Bernink JH, Spits H. Innate lymphoid cells in inflammatory bowel diseases. Immunol Lett 2016;172:124–31.
69. Buonocore S, Ahern PP, Uhlig HH, Ivanov II, Littman DR, Maloy KJ, et al. Innate lymphoid cells drive interleukin-23-dependent innate intestinal pathology. Nature 2010;464:1371–5.
70. Geremia A, Arancibia-Cárcamo CV, Fleming MP, Rust N, Singh B, Mortensen NJ, et al. IL-23-responsive innate lymphoid cells are increased in inflammatory bowel disease. J Exp Med 2011;208:1127–33.
71. Sawa S, Lochner M, Satoh-Takayama N, Dulauroy S, Bérard M, Kleinschek M, et al. $RORγt^+$ innate lymphoid cells regulate intestinal homeostasis by integrating negative signals from the symbiotic microbiota. Nat Immunol 2011;12:320–6.

72. Hepworth MR, Fung TC, Masur SH, Kelsen JR, McConnell FM, Dubrot J, et al. Group 3 innate lymphoid cells mediate intestinal selection of commensal bacteria-specific $CD4^+$ T cells. Science 2015;348:1031–5.
73. Reinhardt A, Yevsa T, Worbs T, Lienenklaus S, Sandrock I, Oberdörfer L, et al. Interleukin-23–dependent γ/δ T cells produce interleukin-17 and accumulate in the enthesis, aortic valve, and ciliary body in mice. Arthritis Rheumatol 2016;68:2476–86.
74. Ono T, Okamoto K, Nakashima T, Nitta T, Hori S, Iwakura Y, et al. IL-17-producing $\gamma\delta$ T cells enhance bone regeneration. Nat Commun 2016;7:10928.
75. Cuthbert R, Fragkakis E, Millner P, Dunsmuir R, El-Sherbiny Y, McGonagle D. A1.26 innate lymphoid cells are present at normal human enthesis providing a potential mechanism for spondyloarthropathy pathogenesis. Ann Rheum Dis 2016;75 Suppl 1:A11.
76. Tang F, Sally B, Ciszewski C, Abadie V, Curran SA, Groh V, et al. Interleukin 15 primes natural killer cells to kill via NKG2D and cPLA2 and this pathway is active in psoriatic arthritis. PLoS One 2013;8:e76292.
77. Nielsen N, Pascal V, Fasth AE, Sundström Y, Galsgaard ED, Ahern D, et al. Balance between activating NKG2D, DNAM-1, NKp44 and NKp46 and inhibitory CD94/NKG2A receptors determine natural killer degranulation towards rheumatoid arthritis synovial fibroblasts. Immunology 2014;142:581–93.
78. Carrega P, Loiacono F, Di Carlo E, Scaramuccia A, Mora M, Conte R, et al. NCR^+ILC3 concentrate in human lung cancer and associate with intratumoral lymphoid structures. Nat Commun 2015;6:8280.
79. Białoszewska A, Baychelier F, Niderla-Bielińska J, Czop A, Debré P, Vieillard V, et al. Constitutive expression of ligand for natural killer cell NKp44 receptor (NKp44L) by normal human articular chondrocytes. Cell Immunol 2013;285:6–9.
80. Baeten D, Sieper J, Braun J, Baraliakos X, Dougados M, Emery P, et al. Secukinumab, an interleukin-17A inhibitor, in ankylosing spondylitis. N Engl J Med 2015;373:2534–48.
81. Sherlock JP, Joyce-Shaikh B, Turner SP, Chao CC, Sathe M, Grein J, et al. IL-23 induces spondyloarthropathy by acting on ROR-γt^+ $CD3^+CD4^-CD8^-$ entheseal resident T cells. Nat Med 2012;18:1069–76.
82. Ciccia F, Accardo-Palumbo A, Alessandro R, Rizzo A, Principe S, Peralta S, et al. Interleukin-22 and interleukin-22–producing NKp44+ natural killer cells in subclinical gut inflammation in ankylosing spondylitis. Arthritis Rheum 2012;64:1869–78.
83. Ciccia F, Guggino G, Rizzo A, Saieva L, Peralta S, Giardina A, et al. Type 3 innate lymphoid cells producing IL-17 and IL-22 are expanded in the gut, in the peripheral blood, synovial fluid and bone marrow of patients with ankylosing spondylitis. Ann Rheum Dis 2015;74:1739–47.
84. Taurog JD, Richardson JA, Croft JT, Simmons WA, Zhou M, Fernández-Sueiro JL, et al. The germfree state prevents development of gut and joint inflammatory disease in HLA-B27 transgenic rats. J Exp Med 1994;180:2359–64.
85. Asquith MJ, Stauffer P, Davin S, Mitchell C, Lin P, Rosenbaum JT. Perturbed mucosal immunity and dysbiosis accompany clinical disease in a rat model of spondyloarthritis. Arthritis Rheumatol 2016;68:2151–62.
86. Zhou X, Wang J, Zou H, Ward MM, Weisman MH, Espitia MG, et al. MICA, a gene contributing strong susceptibility to ankylosing spondylitis. Ann Rheum Dis 2014;73:1552–7.
87. Duffin R, Connor RA, Crittenden S, Forster T, Yu C, Zheng X, et al. Prostaglandin E_2 constrains systemic inflammation through an innate lymphoid cell-IL-22 axis. Science 2016;351:1333–8.
88. Magri G, Cerutti A. Role of group 3 innate lymphoid cells in antibody production. Curr Opin Immunol 2015;33:36–42.
89. Withers DR, Gaspal FM, Mackley EC, Marriott CL, Ross EA, Desanti GE, et al. Cutting edge: lymphoid tissue inducer cells maintain memory CD4 T cells within secondary lymphoid tissue. J Immunol 2012;189:2094–8.
90. Noort AR, van Zoest KP, van Baarsen LG, Maracle CX, Helder B, Papazian N, et al. Tertiary lymphoid structures in rheumatoid arthritis: NF-κB-inducing kinase-positive endothelial cells as central players. Am J Pathol 2015;185:1935–43.
91. Rodríguez-Carrio J, Hähnlein JS, Ramwadhdoebe TH, Semmelink JF, Choi IY, van Lienden KP, et al. Altered innate lymphoid cell subsets in human lymph node biopsy specimens obtained during the at-risk and earliest phases of rheumatoid arthritis. Arthritis Rheumatol 2017;69:70–6.
92. Cortez VS, Cervantes-Barragan L, Robinette ML, Bando JK, Wang Y, Geiger TL, et al. Transforming growth factor-β signaling guides the differentiation of innate lymphoid cells in salivary glands. Immunity 2016;44:1127–39.
93. Ciccia F, Guggino G, Rizzo A, Ferrante A, Raimondo S, Giardina A, et al. Potential involvement of IL-22 and IL-22-producing cells in the inflamed salivary glands of patients with Sjögren's syndrome. Ann Rheum Dis 2012;71:295–301.
94. Nocturne G, Mariette X. Advances in understanding the pathogenesis of primary Sjögren's syndrome. Nat Rev Rheumatol 2013;9:544–56.
95. Magri G, Miyajima M, Bascones S, Mortha A, Puga I, Cassis L, et al. Innate lymphoid cells integrate stromal and immunological signals to enhance antibody production by splenic marginal zone B cells. Nat Immunol 2014;15:354–64.
96. Rusakiewicz S, Nocturne G, Lazure T, Semeraro M, Flament C, Caillat-Zucman S, et al. NCR3/NKp30 contributes to pathogenesis in primary Sjögren's syndrome. Sci Transl Med 2013;5:195ra96.
97. Wohlfahrt T, Usherenko S, Englbrecht M, Dees C, Weber S, Beyer C, et al. Type 2 innate lymphoid cell counts are increased in patients with systemic sclerosis and correlate with the extent of fibrosis. Ann Rheum Dis 2016;75:623–6.
98. Reefman E, Kuiper H, Limburg PC, Kallenberg CG, Bijl M. Type I interferons are involved in the development of ultraviolet B-induced inflammatory skin lesions in systemic lupus erythaematosus patients. Ann Rheum Dis 2008;67:11–18.
99. Zhang Z, Cheng L, Zhao J, Li G, Zhang L, Chen W, et al. Plasmacytoid dendritic cells promote HIV-1-induced group 3 innate lymphoid cell depletion. J Clin Invest 2015;125:3692–703.
100. Duerr CU, McCarthy CD, Mindt BC, Rubio M, Meli AP, Pothlichet J, et al. Type I interferon restricts type 2 immunopathology through the regulation of group 2 innate lymphoid cells. Nat Immunol 2016;17:65–75.
101. Bijl M, Kallenberg CG. Ultraviolet light and cutaneous lupus. Lupus 2006;15:724–7.
102. Gimblet C, Loesche MA, Carvalho L, Carvalho EM, Grice EA, Artis D, et al. IL-22 protects against tissue damage during cutaneous Leishmaniasis. PLoS One 2015;10:e0134698.
103. Avitabile S, Odorisio T, Madonna S, Eyerich S, Guerra L, Eyerich K, et al. Interleukin-22 promotes wound repair in diabetes by improving keratinocyte pro-healing functions. J Invest Dermatol 2015;135:2862–70.
104. Méndez-Flores S, Hernández-Molina G, Enríquez AB, Faz-Muñoz D, Esquivel Y, Pacheco-Molina C, et al. Cytokines and effector/regulatory cells characterization in the physiopathology of cutaneous lupus erythematous: a cross-sectional study. Mediators Inflamm 2016;2016:7074829.
105. Clements P, Lachenbruch P, Seibold J, White B, Weiner S, Martin R, et al. Inter and intraobserver variability of total skin thickness score (modified Rodnan TSS) in systemic sclerosis. J Rheumatol 1995;22:1281–5.
106. Brkic Z, van Bon L, Cossu M, van Helden-Meeuwsen CG, Vonk MC, Knaapen H, et al. The interferon type I signature is present in systemic sclerosis before overt fibrosis and might contribute to its pathogenesis through high BAFF gene expression and high collagen synthesis. Ann Rheum Dis 2016;75:1567–73.
107. Roan F, Stoklasek TA, Whalen E, Molitor JA, Bluestone JA, Buckner JH, et al. CD4+ group 1 innate lymphoid cells (ILC) form a functionally distinct ILC subset that is increased in systemic sclerosis. J Immunol 2016;196:2051–62.

108. Hams E, Armstrong ME, Barlow JL, Saunders SP, Schwartz C, Cooke G, et al. IL-25 and type 2 innate lymphoid cells induce pulmonary fibrosis. Proc Natl Acad Sci U S A 2014;111:367–72.
109. Hams E, Bermingham R, Fallon PG. Macrophage and innate lymphoid cell interplay in the genesis of fibrosis. Front Immunol 2015; 6:597.
110. Lei L, Zhao C, Qin F, He ZY, Wang X, Zhong XN. Th17 cells and IL-17 promote the skin and lung inflammation and fibrosis process in a bleomycin-induced murine model of systemic sclerosis. Clin Exp Rheumatol 2016;34 Suppl 100:14–22.
111. Triggianese P, Conigliaro P, Chimenti MS, Biancone L, Monteleone G, Perricone R, et al. Evidence of IL-17 producing innate lymphoid cells in peripheral blood from patients with enteropathic spondyloarthritis. Clin Exp Rheumatol 2016;34:1085–93.
112. Braudeau C, Amouriaux K, Néel A, Herbreteau G, Salabert N, Rimbert M, et al. Persistent deficiency of circulating mucosal-associated invariant T (MAIT) cells in ANCA-associated vasculitis. J Autoimmun 2016;70:73–9.
113. Björklund ÅK, Forkel M, Picelli S, Konya V, Theorell J, Friberg D, et al. The heterogeneity of human CD127^{+} innate lymphoid cells revealed by single-cell RNA sequencing. Nat Immunol 2016;17:451–60.
114. Yu Y, Tsang JC, Wang C, Clare S, Wang J, Chen X, et al. Single-cell RNA-seq identifies a PD-1^{hi} ILC progenitor and defines its development pathway. Nature 2016;539:102–6.
115. Huang T, Hazen M, Shang Y, Zhou M, Wu X, Yan D, et al. Depletion of major pathogenic cells in asthma by targeting CRTh2. JCI Insight 2016;1:e86689.

ARTHRITIS & RHEUMATOLOGY
Vol. 69, No. 5, May 2017, pp 898–910
DOI 10.1002/art.40064

SPECIAL ARTICLE

2016 American College of Rheumatology/European League Against Rheumatism Criteria for Minimal, Moderate, and Major Clinical Response in Adult Dermatomyositis and Polymyositis

An International Myositis Assessment and Clinical Studies Group/Paediatric Rheumatology International Trials Organisation Collaborative Initiative

Rohit Aggarwal,[1] Lisa G. Rider,[2] Nicolino Ruperto,[3] Nastaran Bayat,[2] Brian Erman,[4] Brian M. Feldman,[5] Chester V. Oddis,[1] Anthony A. Amato,[6] Hector Chinoy,[7] Robert G. Cooper,[8] Maryam Dastmalchi,[9] David Fiorentino,[10] David Isenberg,[11] James D. Katz,[2] Andrew Mammen,[12] Marianne de Visser,[13] Steven R. Ytterberg,[14] Ingrid E. Lundberg,[9] Lorinda Chung,[10] Katalin Danko,[15] Ignacio García-De la Torre,[16] Yeong Wook Song,[17] Luca Villa,[3] Mariangela Rinaldi,[3] Howard Rockette,[1] Peter A. Lachenbruch,[2] Frederick W. Miller,[2] and Jiri Vencovsky,[18] for the International Myositis Assessment and Clinical Studies Group and the Paediatric Rheumatology International Trials Organisation

This criteria set has been approved by the American College of Rheumatology (ACR) Board of Directors and the European League Against Rheumatism (EULAR) Executive Committee. This signifies that the criteria set has been quantitatively validated using patient data, and it has undergone validation based on an independent data set. All ACR/EULAR-approved criteria sets are expected to undergo intermittent updates.

The ACR is an independent, professional, medical and scientific society that does not guarantee, warrant, or endorse any commercial product or service.

This article is published simultaneously in the May 2017 issue of *Annals of the Rheumatic Diseases*.

Supported in part by the American College of Rheumatology, the European League Against Rheumatism, Cure JM Foundation, Myositis UK, Istituto G. Gaslini and the Paediatric Rheumatology International Trials Organisation (PRINTO), the Myositis Association, and the NIH (National Institute of Environmental Health Sciences [NIEHS], National Center for Advancing Translational Sciences, and National Institute of Arthritis and Musculoskeletal and Skin Diseases). Dr. García-De la Torre's work was supported in part by CONACYT (Programa Nacional de Posgrados de Calidad). Dr. Song's work was supported by the Korea Health Technology R & D Project through the Korea Health Industry Development Institute, funded by the Ministry of Health & Welfare, Republic of Korea (grant HI14C1277). Dr. Vencovsky's work was supported by the Ministry of Health, Czech Republic (Institute of Rheumatology project for conceptual development of a research organization, 00023728).

[1]Rohit Aggarwal, MD, MSc, Chester V. Oddis, MD, Howard Rockette, PhD: University of Pittsburgh, Pittsburgh, Pennsylvania; [2]Lisa G. Rider, MD, Nastaran Bayat, MD, James D. Katz, MD, Peter A. Lachenbruch, PhD, Frederick W. Miller, MD, PhD: NIEHS, NIH, Bethesda, Maryland; [3]Nicolino Ruperto, MD, MPH, Luca Villa, MA, Mariangela Rinaldi, MEng: Istituto Giannina Gaslini, Pediatria II - Reumatologia, PRINTO, Genoa, Italy; [4]Brian Erman, MS: Social and Scientific Systems, Inc., Durham, North Carolina; [5]Brian M. Feldman, MD, MSc, FRCPC: The Hospital for Sick Children, Toronto, Ontario, Canada; [6]Anthony A. Amato, MD: Brigham and Women's Hospital and Harvard Medical School, Boston, Massachusetts; [7]Hector Chinoy, PhD, MRCP: Central Manchester University Hospitals NHS Foundation Trust, University of Manchester, Manchester, UK; [8]Robert G.

Objective. **To develop response criteria for adult dermatomyositis (DM) and polymyositis (PM).**

Methods. **Expert surveys, logistic regression, and conjoint analysis were used to develop 287 definitions using core set measures. Myositis experts rated greater improvement among multiple pairwise scenarios in conjoint analysis surveys, where different levels of improvement in 2 core set measures were presented. The PAPRIKA (Potentially All Pairwise Rankings of All Possible Alternatives) method determined the relative weights of core set measures and conjoint analysis definitions. The performance characteristics of the definitions were evaluated on patient profiles using expert consensus (gold standard) and were validated using data from a clinical trial. The nominal group technique was used to reach consensus.**

Results. **Consensus was reached for a conjoint analysis–based continuous model using absolute percent change in core set measures (physician, patient, and extramuscular global activity, muscle strength, Health Assessment Questionnaire, and muscle enzyme levels). A total improvement score (range 0–100), determined by summing scores for each core set measure, was based on improvement in and relative weight of each core set measure. Thresholds for minimal, moderate, and major improvement were ≥20, ≥40, and ≥60 points in the total improvement score. The same criteria were chosen for juvenile DM, with different improvement thresholds. Sensitivity and specificity in DM/PM patient cohorts were 85% and 92%, 90% and 96%, and 92% and 98% for minimal, moderate, and major improvement, respectively. Definitions were validated in the clinical trial analysis for differentiating the physician rating of improvement ($P < 0.001$).**

Conclusion. **The response criteria for adult DM/PM consisted of the conjoint analysis model based on absolute percent change in 6 core set measures, with thresholds for minimal, moderate, and major improvement.**

Idiopathic inflammatory myopathies are a group of acquired, heterogeneous, systemic connective tissue diseases that include adult dermatomyositis (DM) and polymyositis (PM) and juvenile DM (1). Despite significant morbidity and mortality associated with DM/PM, there are currently no therapies approved for these syndromes by the Food and Drug Administration or the European Medicines Agency based on randomized controlled trials. However, with the advancement in novel therapeutic agents that target various biologic pathways implicated in the pathogenesis of DM/PM (2), there is a need for well-designed clinical trials using validated and universally accepted outcome measures. Recently completed clinical trials in adult DM/PM and juvenile DM have used varying response criteria (3–5), again highlighting the need for both data- and consensus-driven criteria to be used uniformly in future studies. Core set measures of myositis disease activity for adult DM/PM clinical trials have been established and validated by the International Myositis Assessment and Clinical Studies Group (IMACS) (6–8); these measures were used as the foundation for the current study. We undertook this study because there is a need for composite response criteria in myositis, given the heterogeneity of the disease and the fact that no single core set measure adequately covers all the domains in myositis. For example, muscle enzyme levels can be normal in active DM, and active muscle weakness in DM can occur without active rash.

Preliminary response criteria for adult DM/PM had been developed and partially validated by IMACS; these criteria were based on at least 20% improvement in 3 of 6 core set measures, with no more than 2 core set measures worsening by at least 25% (which cannot be muscle strength) (8,9). However, those criteria were considered preliminary, because they were not prospectively validated. Moreover, newer methodologies such as conjoint analysis and other continuous or hybrid approaches for developing response criteria had not been evaluated (10–14). The preliminary criteria had other potential limitations, including equal weights being applied to each core set measure and the lack of quantitative or continuous outcomes. With the growing repertoire of potential therapeutic agents, some of which may yield better results than only minimal clinical improvement, there is also a need to develop criteria for moderate and major clinical improvement.

Cooper, MD: University of Liverpool, Liverpool, UK; [9]Maryam Dastmalchi, MD, PhD, Ingrid E. Lundberg, MD, PhD: Karolinska University Hospital, Karolinska Institute, Stockholm, Sweden; [10]David Fiorentino, MD, PhD, Lorinda Chung, MD: Stanford University, Redwood City, California; [11]David Isenberg, MD: University College London, London, UK; [12]Andrew Mammen, MD, PhD: Johns Hopkins University School of Medicine, Baltimore, Maryland; [13]Marianne de Visser, MD, PhD: Academic Medical Center, Amsterdam, The Netherlands; [14]Steven R. Ytterberg, MD: Mayo Clinic, Rochester, Minnesota; [15]Katalin Danko, MD, PhD, DSc: University of Debrecen, Debrecen, Hungary; [16]Ignacio Garcia-De la Torre, MD: Hospital General de Occidente de la Secretaría de Salud and University of Guadalajara, Guadalajara, México; [17]Yeong Wook Song, MD, PhD: Graduate School of Convergence Science and Technology and Seoul National University Hospital, Seoul, Korea; [18]Jiri Vencovsky, MD, PhD: Charles University, Prague, Czech Republic. See Appendix A for members of the International Myositis Assessment and Clinical Studies Group and the Paediatric Rheumatology International Trials Organisation who contributed to developing the response criteria.

Drs. Aggarwal and Rider contributed equally to this work. Drs. Miller and Vencovsky contributed equally to this work.

Address correspondence to Rohit Aggarwal, MD, MSc, Division of Rheumatology and Clinical Immunology, Department of Medicine, University of Pittsburgh, 3601 5th Avenue, Suite 2B, Pittsburgh, PA 15261. E-mail: aggarwalr@upmc.edu.

Submitted for publication February 11, 2016; accepted in revised form January 31, 2017.

For these reasons, and with support from the American College of Rheumatology, European League Against Rheumatism, IMACS, and the Paediatric Rheumatology International Trials Organisation (PRINTO) (15), a collaboration was established to develop a data- and consensus-driven process involving multiple clinical data sets and the international myositis community in order to develop and validate response criteria for adult DM/PM and juvenile DM. This effort involved a comprehensive approach to developing candidate definitions for the response criteria, including continuous or hybrid definitions, using conjoint analysis (13,14,16–19), and for developing criteria for minimal as well as greater degrees of improvement. This article focuses on the criteria for minimal and moderate improvement for adult DM/PM, whereas the threshold for major improvement is considered preliminary. A companion article focuses on the juvenile DM response criteria (20).

Methods

Core set measures and patient profile consensus. To develop patient profiles as well as candidate definitions for response criteria in adult PM and DM, we used previously validated IMACS myositis core set measures for patients with adult DM/PM, which include physician and patient global activity on a 10-cm visual analog scale (VAS), muscle strength measured by manual muscle testing (MMT), physical function measured by the Health Assessment Questionnaire (HAQ) (21), extramuscular global activity measured by the physician on a 10-cm VAS, and the most abnormal serum muscle enzyme (8,22). The entire process, from the development of these profiles and candidate definitions through final consensus voting, is shown in the flow diagram in Figure 1 (23,24). Details of the methodology used to develop patient profiles, candidate definitions, validation, and expert consensus will be described in a separate publication (24). Briefly, patient data from natural history studies and uncontrolled clinical trials were used to develop patient profiles, which were then rated by adult myositis experts to achieve consensus as to whether improvement was none, minimal, moderate, or major. The expert consensus of improvement was used as the gold standard to validate various candidate definitions. The Bohan and Peter classification was used to designate definite or probable adult DM/PM (25).

Candidate definitions of response criteria. Six different types of candidate definitions for minimal, moderate, and major response (Table 1) were developed (23,26): 3 types of definitions were traditional (categorical), and 3 were continuous (hybrid). Traditional definitions provide only categorical outcomes of minimal, moderate, and major improvement, or not improved, based on the criteria, whereas continuous definitions yield an improvement score as a continuous outcome measure, with thresholds of minimal, moderate, and major improvement serving as categorical outcomes. Continuous definitions are considered hybrid definitions, because the same definition can be used as a continuous or categorical outcome measure based on the study requirements. Definitions utilizing either absolute percent change (final minus baseline divided by range and multiplied by 100) or

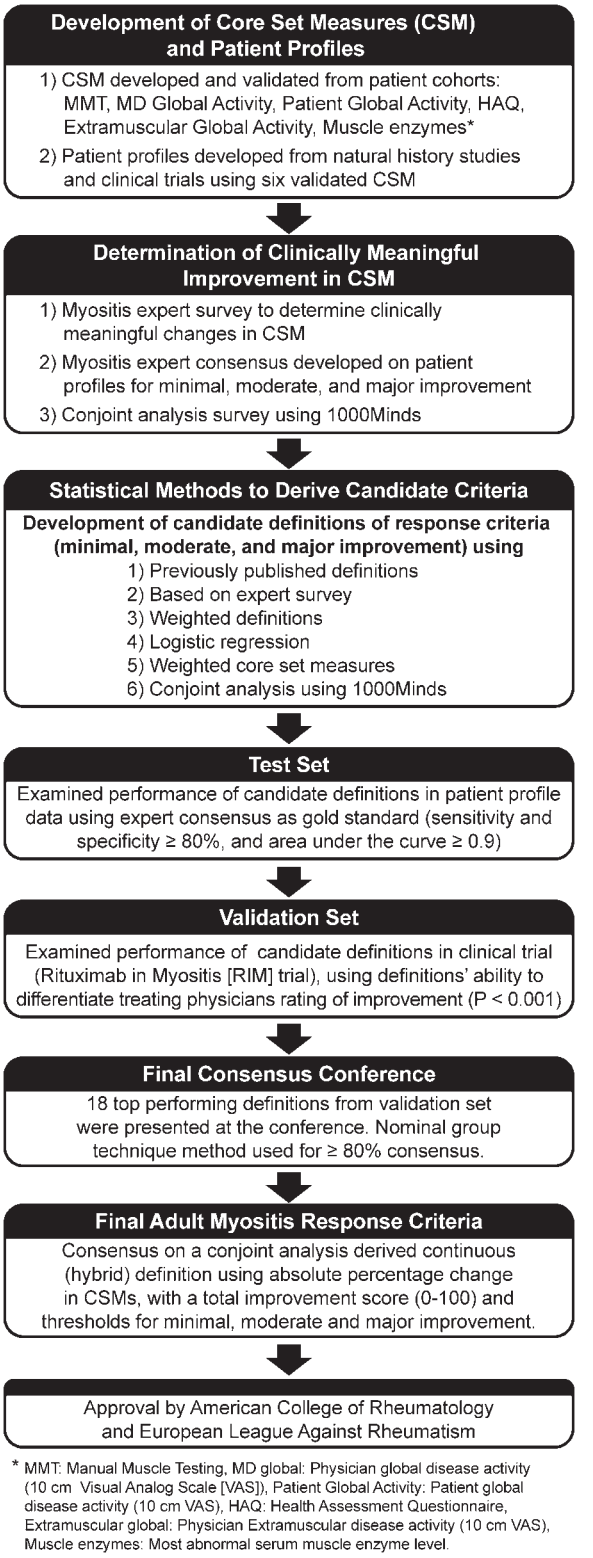

Figure 1. Flow diagram of the entire process used to develop and validate the approved response criteria for adult dermatomyositis and polymyositis.

Table 1. Types of candidate definitions for response criteria that were developed and tested*

Type of candidate definitions of response	Description	Example of candidate definition for the response criteria
Previously published (categorical definition)	Previously published definitions of improvement that were retested	Minimal. Three of any 6 improved by ≥20%, no more than 2 worse by >25% (which cannot be MMT) (9) Moderate. Three of any 6 improved by ≥50%, no more than 2 worse by >25% (which cannot be MMT) Major. Three of any 6 improved by ≥70%, no more than 2 worse by >25% (which cannot be MMT)
Newly drafted (categorical definition)	Drafted relative or absolute % change candidate definitions of response, based on recent CSM survey	Minimal. Two of any 6 improved by ≥30%, no more than 1 worse by >30% (which cannot be MMT) Moderate. Two of any 6 improved by ≥50%, no more than 1 worse by >30% (which cannot be MMT) Major. Two of any 6 improved by ≥75%, no more than 1 worse by >30% (which cannot be MMT)
Weighted (categorical definition)	Applied conjoint analysis relative weights to CSM in newly drafted definitions; each CSM receives improvement points (corresponding relative weights), when it reaches the threshold for minimal, moderate, or major improvement; worsening points are applied similarly; improvement is calculated based on a total score of improvement versus worsening	Improvement = at least 2.5 total improvement points of a maximum possible score of 8, and no more than 2.5 worsening points, where MD global = 1.5 points, patient global = 1 point, MMT = 2 points, HAQ = 1.5 points, extramusc = 1.5 points, enzyme = 0.5 point Minimal. Improvement points given when CSM ≥30%; worsening points given when CSM worse by >25% Moderate. Improvement points given when CSM ≥50%; worsening points given when CSM worse by >25% Major. Improvement points given when CSM ≥75%; worsening points given when CSM worse by >25%
Logistic regression (continuous definition)	Model of improvement using combination of CSM with different weights, as developed in the logistic regression model and rounded for better feasibility; total scores derived, with different cutoffs, for minimal, moderate, and major improvement	Improvement score = 5 × (MD global % change) + 3 × (patient global % change) + (MMT % change) + 2 × (HAQ % change) + 2 × (extramusc % change) + 2.5 × (enzyme % change) Minimal. Improvement score ≥250 Moderate. Improvement score ≥500 Major. Improvement score ≥750
Core set measure–weighted (continuous definition)	Multiply the % change in each CSM by the weights derived from conjoint analysis, then sum (% change in each CSM × conjoint analysis weights) to get final total improvement score; different thresholds for minimal, moderate, and major improvement established based on consensus profile ratings as gold standard	Improvement score = 2 × (MD global % change) + (patient global % change) + 3 × (MMT % change) + 1.5 × (HAQ % change) + 1.5 × (extramusc % change) + (enzyme % change) Minimal. Improvement score ≥100 Moderate. Improvement score ≥250 Major. Improvement score ≥400
Conjoint analysis (continuous definition)	For a given range in the level of improvement in each CSM, a score is assigned, as developed by the conjoint-analysis survey results and modeling; greater degrees of improvement receive higher scores; a patient is minimally improved if the improvement score is above the cutoff for minimal improvement; similarly, for moderate and major improvement	Cut points for the model are: Minimal. Improvement score ≥20 Moderate. Improvement score ≥40 Major. Improvement score ≥60†

* MMT = manual muscle testing; CSM = core set measure; MD global = physician global activity score; patient global = patient global activity score; HAQ = Health Assessment Questionnaire; extramusc = extramuscular global activity; enzyme = most abnormal serum muscle enzyme value among aldolase, alanine aminotransferase, aspartate aminotransferase, lactate dehydrogenase, and creatine kinase.
† See Table 3 for cut points for the full model.

relative percent change (final minus baseline, divided by baseline and multiplied by 100) were evaluated as candidate definitions.

Conjoint analysis surveys. Conjoint analysis surveys were administered to myositis experts using 1000Minds online software (11). Experts were presented with pairs of hypothetical patient scenarios; each patient had different levels of improvement in the same 2 core set measures, assuming other core set measures remained the same. Experts rated which of the 2 scenarios had greater improvement. Based on the rater's response, all other hypothetical patients that could be pairwise ranked were eliminated via the property of transitivity, thereby significantly reducing the number of scenarios presented. The PAPRIKA (Potentially All Pairwise Rankings of All Possible Alternatives) method was used to determine the relative importance of the core set measures. Relative weights of core set measures and their levels of improvement were used to develop a scoring system by mathematical methods based on linear programming (13), such that when all 6 core set measures are considered together, the maximum score (total improvement score) possible for representing a patient's improvement is 100 and the minimum score is 0. The thresholds for minimal, moderate, and major improvement in the total improvement score were based on optimum sensitivity and specificity (using the Youden index [27]) in the subset of patient cohort data.

Validation of candidate response criteria. The performance characteristics of candidate criteria were evaluated using consensus profile ratings as the gold standard, assessing sensitivity, specificity, and area under the curve (AUC) to compare the performance of these candidate definitions. Those that performed well in the consensus profiles (sensitivity and specificity ≥80%, AUC ≥0.9 for minimal improvement, and AUC ≥0.8 for moderate and major improvement) were externally validated using data for adult DM/PM patients (n = 142) enrolled in the Rituximab in Myositis (RIM) trial (3). The treating physician's rating of improvement (0–7 scale) at 24 weeks in the RIM trial was used for validation, and a 1-point change in the physician's rating was considered clinically significant (3). We then selected the top candidate definitions (up to 4 top-performing definitions from each of the 6 different types of candidate definitions) for consideration at the final consensus conference, in order to discuss a manageable number of definitions at the conference.

Consensus conference. The nominal group technique (NGT) was applied to develop consensus among experts in adult DM/PM regarding the top-performing candidate definitions for minimal and moderate improvement in adult DM/PM (28–30). Experienced moderators (RA and FWM) led the NGT consensus-development process for the adult working group and the combined adult and pediatric working group (RA, LGR, NR, and FWM). Given the paucity of data on major improvement, we considered the major improvement thresholds as preliminary for the final consensus meeting. For each candidate definition, the methodologic details used to develop it and its performance characteristics in the consensus patient profiles and the RIM trial were presented to the adult working group. Each of the 12 participants in the adult working group independently reviewed the performance characteristics of all 18 top candidate definitions for adult DM/PM. Detailed data for each candidate definition, including sensitivity, specificity, and AUC as well as kappa values and odds ratios for minimal, moderate, and major improvement, were provided. The AUC was determined from the receiver operating characteristic curve as a plot of sensitivity versus (1 – specificity) for total improvement scores as well as for thresholds (27).

Adult working group. The primary goal for the adult working group was to develop consensus response criteria for minimal and moderate clinical improvement in adult DM/PM based on the data presented, as well as the face validity, feasibility, and generalizability of the proposed candidate criteria. The experts in the adult working group included internationally recognized rheumatologists, neurologists, and dermatologists who have considerable experience in myositis and with the core set measures. Voting was conducted in an independent, anonymous, and systematic manner via a web-based system developed by staff at the PRINTO coordinating center (31,32). In the initial rounds of voting, participants were asked to rank their top 5 choices. The results were compiled, and aggregate votes and rank of each candidate definition were shared with the group after each round of voting. Participants were then asked in a random manner to discuss their top-ranked and bottom-ranked choices. Candidate definitions receiving a small proportion of votes were eliminated. In subsequent voting rounds, participants were asked to re-rank their choices after reviewing the previous round's voting and discussion. When fewer than 5 candidate definitions remained, each participant selected one as the top response criteria. The objective was to continue the rounds of voting in the same manner until a single candidate definition reached consensus (≥80% of the votes) or until it was clear that consensus would not be reached.

Combined adult and pediatric working group. After consensus was achieved by each working group, both groups then came together to vote on common response criteria to be used for both adult DM/PM and juvenile DM (20) as the outcome measure for combined clinical trials. For this voting round, the top candidate definitions from the final round of voting in each working group were considered, and a similar online voting system and the NGT were used until consensus of ≥80% was reached (28–30). For determining the thresholds of improvement for the selected definition, the required consensus was ≥70%, which was done by post-conference voting.

Results

Candidate definitions. A total of 287 adult DM/PM candidate response criteria were drafted or derived using data-driven methods. Included were 10 previously published definitions, 134 newly drafted definitions based on expert survey results, 63 weighted definitions, 68 logistic regression definitions, 6 conjoint analysis definitions, and 6 definitions in which differential weights were applied to the improvement achieved in each core set measure. Among these definitions, 163 used relative percent change and 124 used absolute percent change in the core set measures.

Validation. Candidate definitions with a sensitivity and specificity of ≥80%, AUC ≥0.9 for minimal, and AUC ≥0.8 for moderate and major improvement in the patient profile analysis using expert consensus rating as the gold standard were evaluated for external validation using RIM clinical trial data (3) (see Supplementary Table 1, available on the *Arthritis & Rheumatology* web site at

Table 2. Detailed performance characteristics of patient profiles and clinical trial data for the top 5 candidate response criteria definitions presented at the consensus conference*

Candidate definitions for response criteria, improvement category, core set measure	Profiles (n = 270)†				RIM trial (n = 147)			
	Sensitivity, %	Specificity, %	Threshold AUC	Total AUC	Candidate definition, improved physician's rating‡	Candidate definition, not improved physician's rating‡	*P*	Rank
Conjoint analysis absolute % change (model 3)§								1
Minimal (improvement score ≥20)	85	92	0.89	0.96	2.0	4.0	<0.001	
Moderate (improvement score ≥40)	90	96	0.93	0.99	2.0	3.0	<0.001	
Major (total improvement score ≥60)	92	98	0.95	1.00	2.0	3.0	<0.001	
Conjoint analysis relative % change (model 1)¶								2
Minimal (improvement score ≥33)	94	90	0.92	0.98	2.0	4.0	<0.001	
Moderate (improvement score ≥55)	93	93	0.93	0.99	2.0	3.0	<0.001	
Major (improvement score ≥70)	100	95	0.97	0.99	2.0	3.0	<0.001	
Conjoint analysis relative % change (model 2)¶								3
Minimal (improvement score ≥30)	94	92	0.93	0.98	2.0	4.0	<0.001	
Moderate (total improvement score ≥45)	94	88	0.91	0.98	2.0	3.0	<0.001	
Major (improvement score ≥65)	100	98	0.99	1.00	2.0	3.0	<0.001	
Weighted core set measure relative % change#								4
Minimal (improvement score ≥100)	92	91	0.91	0.97	2.0	3.0	<0.001	
Moderate (improvement score ≥250)	94	91	0.93	0.98	2.0	3.0	<0.001	
Major (improvement score ≥400)	100	94	0.97	1.00	2.0	3.0	<0.001	
Logistic regression relative % change**								5
Minimal (improvement score ≥75)	89	93	0.91	0.97	2.0	3.0	<0.001	
Moderate (improvement score ≥150)	94	88	0.91	0.98	2.0	3.0	<0.001	
Major (improvement score ≥300)	100	96	0.98	1.00	2.0	3.0	<0.001	

* Supplementary Table 2 (available on the *Arthritis & Rheumatology* web site at http://onlinelibrary.wiley.com/doi/10.1002/art.40064/abstract) shows definitions 6–18 from the consensus conference ratings. The threshold area under the curve (AUC) was calculated as the AUC from the receiver operating characteristic (ROC) curve for the total improvement score and the threshold for minimal, moderate, and major improvement. The total AUC was calculated as the AUC from the ROC curve, using the total improvement score and the threshold cutoffs for minimal, moderate, and major improvement, and applies only to continuous definitions.

† The reference standard for sensitivity and specificity was myositis expert consensus rating of improvement.

‡ Physician's rating is the treating physician's rating on a Likert scale of 1–7, where lower scores represent a greater degree of improvement, at week 24 of the Rituximab in Myositis (RIM) trial (3). A 1-point difference in the physician's rating of improvement from no improvement to minimal improvement was considered not only statistically significant but also clinically significant.

§ Conjoint analysis–based continuous candidate response criteria using absolute percent change in core set measures (absolute percent change model) is shown in Table 3. These criteria are also the top response criteria for juvenile dermatomyositis (DM), but with different thresholds in the total improvement score for minimal, moderate, and major improvement (20).

¶ Conjoint analysis–based continuous candidate response criteria using relative percent change in core set measures are shown in Supplementary Table 3 (available on the *Arthritis & Rheumatology* web site at http://onlinelibrary.wiley.com/doi/10.1002/art.40064/abstract). These criteria are also the second- and third-choice criteria for juvenile DM, but with different thresholds in the total improvement score for minimal, moderate, and major improvement (20).

The total improvement score is calculated as 2 × (MD global % change) + (patient global % change) + 3 × (MMT % change) + 1.5 × (HAQ % change) + 1.5 × (extramusc % change) + (enzyme % change). (MD global = physician global activity; patient global = patient global activity; MMT = manual muscle testing; HAQ = Health Assessment Questionnaire; extramusc = extramuscular; enzyme = most abnormal serum muscle enzyme value among aldolase, alanine aminotransferase, aspartate aminotransferase, lactate hydrogenase, and creatine kinase.)

** The total improvement score is calculated as (MD global % change) + (patient global % change) + (MMT % change) + (HAQ % change) + (extramusc % change) + (enzyme % change).

http://onlinelibrary.wiley.com/doi/10.1002/art.40064/abstract). Thus, of 122 adult DM/PM candidate definitions evaluated using the RIM trial data, 36 adult DM/PM candidate definitions, including 25 using relative and 11 using absolute percent change in core set measures, had AUC ≥0.7 and showed validation in the clinical trial analysis.

Top candidate definitions. Of 36 validated definitions, 17 top-performing adult candidate definitions and the top pediatric response criteria (20) were considered by the adult working group at the consensus conference so that, in total, 18 candidate definitions were evaluated (Table 2 and Supplementary Table 2, available on the *Arthritis & Rheumatology* web site at http://onlinelibrary.wiley.com/doi/10.1002/art.40064/abstract). They included 9 categorical definitions and 9 continuous definitions, in which 14 used relative percent change and 4 used absolute percent change in core set measures. In each categorical definition, a patient would either meet or not meet the response criteria of minimal, moderate, or major improvement based on the degree of improvement or worsening in each core set measure. In

the continuous definitions, however, each subject generates a total improvement score on a continuous scale, such that a greater degree of improvement corresponds to a higher score. Furthermore, patients could be categorized as achieving minimal, moderate, or major clinical improvement based on reaching the pre-set threshold score on the continuous scale. Table 2 shows the performance characteristics of the top 5 candidate definitions for the response criteria selected at the consensus conference (see Supplementary Table 2 for definitions 6–18).

In the patient profiles, with expert consensus as the gold standard, all top candidate definitions presented at the conference had excellent performance characteristics, with median sensitivity of 87% (interquartile range [IQR] 84–90%) and specificity of 94% (IQR 92–95%) for minimal improvement with a median AUC of 0.91 (IQR 0.90–0.92) (Table 2 and Supplementary Tables 1 and 2, available on the *Arthritis & Rheumatology* web site at http://onlinelibrary.wiley.com/doi/10.1002/art.40064/abstract). Sensitivity, specificity, and AUC were similarly high for moderate and major improvement criteria for these definitions (Table 2 and Supplementary Tables 1 and 2). All candidate definitions presented at the conference were validated using the RIM trial data at the 24-week time point and were shown to differentiate ($P < 0.001$) between the treating physician's improvement score at week 24 in patients rated as improved versus not improved (3) (Table 2 and Supplementary Tables 1 and 2).

Consensus conference voting. The top-choice definition for the adult working group, which received 80% of the votes, was the conjoint analysis–based continuous definition model 1, which includes relative percent change in core set measures, including physician and patient global activity, muscle strength, physical function, most abnormal serum enzyme level, and extramuscular activity (Supplementary Table 3, available on the *Arthritis & Rheumatology* web site at http://onlinelibrary.wiley.com/doi/10.1002/art.40064/abstract). The second-choice definition, receiving 20% of the votes, was the conjoint analysis–based continuous model 2, which also includes relative percent change in core set measures (see Supplementary Table 3). Models 1 and 2 differ only in the scores associated with each level of improvement in each core set measure.

However, in the final round of voting and discussion, adult working group participants reached unanimous consensus that the response criteria for adult DM/PM would be identical to the top-choice response criteria for juvenile DM, which is a conjoint analysis–based continuous definition (model 3) using absolute percent change in core set measures (Table 3) (20). Participants favored using the same response criteria for adult DM/PM and juvenile DM so that data from different studies can be harmonized more effectively and to facilitate combined trials, especially given that the definitions were similar with similar performance characteristics. Moreover, the absolute percent change in core set measures (model 3 [Table 3]) was thought to be more representative of meaningful clinical change compared with relative percent change in core set measures (models 1 and 2 [Supplementary Table 3]). Participants also voted to evaluate all top 5 candidate definitions from the adult working group in future clinical trials, with the other 4 as secondary outcome measures. The top 3 of these criteria, the conjoint analysis definitions, are the same for both adult DM/PM and juvenile DM, with different thresholds of improvement.

The sensitivity and specificity of the top-choice criteria, the conjoint analysis absolute percent change (Table 3), were 85% and 92% for minimal improvement, 90% and 96% for moderate improvement, and 92% and 98% for major improvement, respectively (Table 2). The AUC was 0.96 for the total improvement score and 0.89, 0.93, and 0.95 for minimal, moderate, and major improvement thresholds, respectively (Table 2). In the RIM trial (3), these response criteria showed a significant difference in the physician's rating of improvement when the response criteria rated the patient as improved versus not improved for minimal, moderate, and major improvement ($P < 0.001$) (Table 2 and Supplementary Table 2, available on the *Arthritis & Rheumatology* web site at http://onlinelibrary.wiley.com/doi/10.1002/art.40064/abstract). Myositis experts in the consensus conference favored the conjoint analysis–based continuous response criteria because the total improvement score is a continuous measure that corresponds to the magnitude of improvement in a patient and provides the ability to categorize a patient's degree of improvement as minimal, moderate, or major (making it truly a hybrid definition). Moreover, the differential weights for various core set measures were also thought to be congruent with an expert's assessment of the relative importance of each core set measure. An important consideration in the final selection was that the top-choice definition be based on absolute percent change in the core set measures, which was favored by the participants because, given the various VAS measurements used, the absolute percent change was thought to be more representative of meaningful clinical change.

Top candidate definitions considered by the combined pediatric/adult working group. Three candidate definitions were considered by the combined adult/pediatric working group; these included the top adult definitions (see Supplementary Table 3) and the top pediatric definitions (20), one of which was identical in both groups. Final consensus was reached for the combined adult DM/PM and juvenile DM response criteria, with 91% of

Table 3. Final myositis response criteria for minimal, moderate, and major improvement in adult dermatomyositis/polymyositis (DM/PM) and combined adult DM/PM and juvenile DM clinical trials and studies*

Core set measure, level of improvement based on absolute percent change	Improvement score
Physician global activity	
Worsening to 5% improvement	0
>5% to 15% improvement	7.5
>15% to 25% improvement	15
>25% to 40% improvement	17.5
>40% improvement	20
Patient global activity	
Worsening to 5% improvement	0
>5% to 15% improvement	2.5
>15% to 25% improvement	5
>25% to 40% improvement	7.5
>40% improvement	10
Manual muscle testing	
Worsening to 2% improvement	0
>2% to 10% improvement	10
>10% to 20% improvement	20
>20% to 30% improvement	27.5
>30% improvement	32.5
Health Assessment Questionnaire	
Worsening to 5% improvement	0
>5% to 15% improvement	5
>15% to 25% improvement	7.5
>25% to 40% improvement	7.5
>40% improvement	10
Enzyme (most abnormal)	
Worsening to 5% improvement	0
>5% to 15% improvement	2.5
>15% to 25% improvement	5
>25% to 40% improvement	7.5
>40% improvement	7.5
Extramuscular activity	
Worsening to 5% improvement	0
>5% to 15% improvement	7.5
>15% to 25% improvement	12.5
>25% to 40% improvement	15
>40% improvement	20

The **total improvement score** is the sum of all 6 improvement scores associated with the change in each core set measure. A total improvement score of **≥20** represents **minimal improvement**, a score of **≥40** represents **moderate improvement**, and a score of **≥60** represents **major improvement**.

* Note that these response criteria are also proposed for use in combined adult DM/PM and juvenile DM trials (20). For comparison, the thresholds of improvement in the total improvement score for juvenile DM are ≥30 for minimal improvement, ≥45 for moderate improvement, and ≥70 for major improvement. Also note that the criteria for major improvement for adult DM/PM are preliminary.
How to calculate the improvement score: The absolute percent change ([final value – baseline value]/range × 100) is calculated for each core set measure. For muscle enzymes, the most abnormal serum muscle enzyme level at baseline (creatine kinase, aldolase, alanine transaminase, aspartate aminotransferase, lactate dehydrogenase) is used. The enzyme range was calculated based on a 90% range of enzymes from natural history data (34,46), which for creatine kinase is 15 times the upper limit of normal (ULN), for aldolase is 6 times the ULN, and for lactate dehydrogenase, aspartate aminotransferase, and alanine transaminase is 3 times the ULN. The ULN is determined according to the individual laboratories in the participating centers. The ranges for physician global activity, patient global activity, manual muscle testing, Health Assessment Questionnaire, and extramuscular global activity are based on the instrument scale used (3,26). An improvement score is assigned for each core set measure based on the absolute percent change in the core set measure according to the definition. These individual core set measure improvement scores are then totaled among the 6 core set measures to give the total improvement score. The thresholds for minimal, moderate, and major improvement are provided. The total improvement score itself may also be compared among treatment arms in a trial. A total improvement score between 0 and 100 corresponds to the degree of improvement, with higher scores corresponding to a greater degree of improvement.

participants voting for the conjoint analysis–based continuous definition, based on absolute percent change in the core set measure (Table 3). The combined working group agreed that the same final response criteria will be used for clinical trials of both adult DM/PM and juvenile DM, but with different thresholds for improvement in adult versus

pediatric patients as well as different core set measures for adult patients (IMACS) and pediatric patients (IMACS and PRINTO). Participants favored using the same response criteria for adult DM/PM and juvenile DM, because the top definition from each working group was very similar (i.e., both being conjoint analysis–based continuous models, with excellent and similar performance characteristics) and because it would permit comparison of outcomes in separate studies. Although only the IMACS core set measures were used for adult DM/PM, for further congruence with pediatric core set measures, the experts in adult myositis agreed to include the Short Form-36 (33) as a health-related quality-of-life measure to correspond to the PRINTO quality-of-life core set measure, the parent form of the Child Health Questionnaire (34–36). In a post-conference final vote, consensus (74%) was reached on threshold values for minimal, moderate, and major response for adult DM/PM patients, which are ≥20 in the total improvement score for minimal improvement, ≥40 for moderate improvement, and ≥60 for major improvement. In contrast, consensus on the final threshold values for minimal, moderate, and major response for juvenile DM were ≥30, ≥45, and ≥70 points, respectively.

Discussion

After a systematic data- and consensus-driven process, a conjoint analysis–based continuous (i.e., hybrid) definition based on absolute percent change in core set measures was selected as the response criteria for adult DM/PM for minimal and moderate improvement in future clinical trials and studies (Figure 1). Because the total number of cases in the trial data sets and clinical profiles that achieved major improvement was small, it was decided that the thresholds for major improvement would be considered preliminary. The same continuous (or hybrid) definition, but with different thresholds for minimal, moderate, and major improvement in IMACS or PRINTO core set measures, will be used for juvenile DM clinical trials and studies, as well as for combined adult DM/PM and juvenile DM studies and clinical trials in the future (20,24).

The process for developing and validating the candidate definitions for the response criteria was extensive and comprehensive, as we used large prospective clinical cohort data sets to develop patient profiles, and myositis expert consensus was used as the gold standard for clinical response. Consequently, we derived 6 different types of candidate definitions, each with many variations, leading to a total of 287 candidate definitions tested, which were validated using natural history cohorts and data from a randomized clinical trial. Subsequently, a representative number of international myositis experts from various disciplines (rheumatology, neurology, and dermatology) agreed on an innovative continuous (or hybrid) model using absolute percent change in validated core set measures.

These response criteria were developed using a novel conjoint analysis methodology, the 1000Minds software (13). Conjoint analysis, or discrete choice experiment, is a statistical technique used to determine expert group decision-making around various measures (and multiple levels within each measure), providing the ability to develop differential weighting of measures and composite criteria using those measures. The 1000Minds software for conjoint analysis has been used recently to develop rheumatologic classification and/or outcome criteria for rheumatoid arthritis (RA), systemic sclerosis (12,13,37,38), and gout (11,16,17,39).

The criteria developed are continuous in nature and generate a total improvement score (on a scale of 0–100), which can provide a quantitative degree of improvement for each patient rather than a dichotomous or categorical assessment of improvement. The total improvement score is the sum of the improvement reflected in each of the 6 core set measures, but the individual core set measures are weighted, such that those deemed more important provide a greater contribution to the final score. For example, changes in the MMT and physician global disease activity scores are weighted more heavily than changes in the most abnormal enzyme or the HAQ. These weights were consistent with our myositis expert survey (26), which was independent of the process used to develop and validate our response criteria.

There are significant advantages of using continuous response criteria (especially in pilot studies). For example, it might be possible to enroll fewer subjects and still have sufficient statistical power to differentiate between treatment groups by using the mean or median total improvement score. Moreover, continuous measures have the best sensitivity to change, the use of which allows modest treatment differences to be detected as statistically significant, which in turn leads to better clinical trials (10). Moreover, the criteria developed provide thresholds for both minimal and moderate improvement, with a preliminary threshold for major improvement. Therefore, larger, adequately powered clinical trials and studies can use the threshold of minimal clinically significant improvement to differentiate the treatment groups, because this difference will be considered *clinically* significant. Similarly, the proportions of patients achieving minimal or moderate improvement can be determined and compared between treatment arms. The ability of the same response criteria to be used not only as a continuous measure, where a higher score implies greater improvement, but also as a categorical response of minimal and moderate improvement, results in a unique hybrid aspect to these criteria.

Another advantage of continuous response criteria over the previous IMACS response criteria is that inclusion criteria for clinical trials will not require minimal severity in any core set measure, because all levels of improvement in each core set measure contribute more or less to the response. However, for each trial the investigators will have to determine the entry criteria for baseline core set measure abnormality, but those will depend on the effect size, disease or organ target, recruitment, and feasibility rather than on the response criteria alone. This is an improvement over the previous IMACS preliminary response criteria, where the clinical trial inclusion criteria required a baseline deficit of at least 20% in each core set measure to enable reaching the threshold of ≥20% improvement in core set measures after treatment.

Another important aspect of these response criteria is that they are based on an absolute percent change in core set measures rather than relative percent change, as used for scoring other rheumatologic diseases such as RA (40,41) and prior myositis response criteria (9). The panelists strongly believed that absolute percent change rather than relative percent change in core set measures more accurately reflects the degree of change. For example, for a patient in whom disease activity improved from 2 cm to 1 cm on a 10-cm VAS, this was interpreted by experts as more consistent with 10% improvement (absolute percent change) and not as 50% improvement reflected by relative percent change. Also, because many of the myositis core set measures arbitrarily have 0 as the lower limit of normal, using 10-cm VAS, the relative percent change is difficult to calculate if there is a change from 0 to a higher value.

The myositis experts decided to use similar response criteria for adult DM/PM and juvenile DM, to facilitate combined clinical trials, such as the RIM trial (3). Another advantage of the response criteria is that although they are the same for adult DM/PM and juvenile DM, they address the unique differences in the core set measure responsiveness between the 2 disease entities by specifying higher thresholds for juvenile DM than for adult DM/PM, which reflects the fact that more responsiveness is seen in juvenile DM patients in clinical trials (3,5). Additionally, the juvenile DM response criteria allow for the possibility of using the IMACS or PRINTO core set measures and provide a more definitive threshold for major improvement (20).

Some limitations of the new response criteria should be noted. First, most of the core set measures, although proven to have good reliability and validity, are subjective and evaluator dependent. However, similar metrics have been used successfully in RA trials that used a physician global measure similar to that used for myositis.

Second, only one major clinical trial was available for validation, and it failed to meet its primary end point and was not truly placebo controlled. Thus, we validated the results using the treating physician's improvement scores in the clinical trial.

Third, the threshold for major improvement in the response criteria is considered preliminary due to an insufficient number of adult DM/PM cases showing major improvement. We believe that future studies using therapeutic agents that have a greater impact on myositis disease activity will lead to better clinical responses, thus allowing investigators to determine a final threshold for major improvement. We plan to validate major improvement in future studies.

Fourth, given that the criteria are focused on improvement and thus fail to differentiate between no change and worsening, these criteria might not be applicable in studies of worsening disease activity (i.e., disease flare designs) in myositis. However, in the future, it will be necessary to develop criteria for flare in myositis.

Fifth, the response criteria were developed using a PM diagnosis based on the Bohan and Peter classification criteria, but experts now recognize that PM, according to those criteria, may include different syndromes, such as necrotizing myopathy, the antisynthetase syndrome, and others (42,43). We believe that these response criteria will still be applicable to these newer entities given that the data- and consensus-driven processes described herein were inclusive of those syndromes. In the future, with changes in classification criteria terminology (44), the response criteria terminology will need to be modified accordingly.

Sixth, because the criteria are complex and might be difficult to apply in research studies, we are developing a web-based tool as well as a downloadable calculator that will allow easy application of the response criteria. The time required to apply these criteria is estimated to be 25 minutes to complete the core set measures at each visit (6) and 3 minutes to hand-calculate the total improvement score and degree of response, while with a computer-based system the calculation time is negligible. Moreover, although the criteria may appear to be complicated, the core set measures to be collected by any study or investigators are simple and are essentially the same as those in previous myositis studies and trials.

Finally, patient-reported outcomes as core set measures, with the exception of the HAQ and patient global assessment, were not part of the response criteria, perhaps due to the paucity of sensitive and responsive patient-reported outcomes for DM/PM (45).

In conclusion, the development of data- and consensus-driven conjoint analysis–based continuous

response criteria with quantitative assessment of improvement on a scale of 0–100 and with thresholds for minimal, moderate, and major (preliminary threshold) improvement marks a major advancement in assessing response in myositis clinical trials and studies. These response criteria are sensitive and specific and provide a way to determine clinically meaningful change corresponding to degree of clinical improvement. These response criteria were valid in a clinical trial and had excellent face validity and acceptance among myositis experts from various specialties who care for adult DM/PM patients in different parts of the world. A conjoint analysis–based definition with a continuous improvement score using absolute percent change in core set measures with thresholds for minimal, moderate, and major improvement was selected as the response criteria to be used for adult clinical trials.

ACKNOWLEDGMENTS

We thank the following individuals for providing invaluable input and feedback on project development and support: members of the American College of Rheumatology Criteria Committee; Dr. Daniel Aletaha (European League Against Rheumatism), Drs. Suzette Peng and Sarah Yim (US Food and Drug Administration), Drs. Thorsten Vetter and Richard Vesely (European Medicines Agency), Bob Goldberg and Theresa Curry (The Myositis Association), Rhonda McKeever and Patti Lawler (Cure JM Foundation), and Irene Oakley (Myositis UK). We also thank Drs. Michael Ward, Steven Pavletic, and Adam Schiffenbauer for their critical review of the manuscript. Paul Hansen, who with Franz Ombler owns and co-invented the 1000Minds software referred to in the article, provided intellectual and logistic support for this project.

AUTHOR CONTRIBUTIONS

All authors were involved in drafting the article or revising it critically for important intellectual content, and all authors approved the final version to be published. Drs. Aggarwal and Rider had full access to all of the data in the study and take responsibility for the integrity of the data and the accuracy of the data analysis.

Study conception and design. Aggarwal, Rider, Ruperto, Bayat, Erman, Feldman, Oddis, Amato, Chinoy, Cooper, Dastmalchi, Fiorentino, Isenberg, Katz, Mammen, de Visser, Ytterberg, Lundberg, Chung, Danko, Garcia-De la Torre, Song, Villa, Rinaldi, Rockette, Lachenbruch, Miller, Vencovsky.

Acquisition of data. Aggarwal, Rider, Ruperto, Bayat, Erman, Feldman, Oddis, Amato, Chinoy, Cooper, Dastmalchi, Fiorentino, Isenberg, Katz, Mammen, de Visser, Ytterberg, Lundberg, Chung, Danko, Garcia-De la Torre, Song, Villa, Rinaldi, Rockette, Lachenbruch, Miller, Vencovsky.

Analysis and interpretation of data. Aggarwal, Rider, Ruperto, Bayat, Erman, Feldman, Oddis, Amato, Chinoy, Cooper, Dastmalchi, Fiorentino, Isenberg, Katz, Mammen, de Visser, Ytterberg, Lundberg, Chung, Danko, Garcia-De la Torre, Song, Villa, Rinaldi, Rockette, Lachenbruch, Miller, Vencovsky.

REFERENCES

1. Rider LG, Miller FW. Deciphering the clinical presentations, pathogenesis, and treatment of the idiopathic inflammatory myopathies. JAMA 2011;305:183–90.
2. Moghadam-Kia S, Aggarwal R, Oddis CV. Treatment of inflammatory myopathy: emerging therapies and therapeutic targets. Expert Rev Clin Immunol 2015;11:1265–75.
3. Oddis CV, Reed AM, Aggarwal R, Rider LG, Ascherman DP, Levesque MC, et al. Rituximab in the treatment of refractory adult and juvenile dermatomyositis and adult polymyositis: a randomized, placebo-phase trial. Arthritis Rheum 2013;65:314–24.
4. Muscle Study Group. A randomized, pilot trial of etanercept in dermatomyositis. Ann Neurol 2011;70:427–36.
5. Ruperto N, Pistorio A, Oliveira S, Zulian F, Cuttica R, Ravelli A, et al. Prednisone versus prednisone plus ciclosporin versus prednisone plus methotrexate in new-onset juvenile dermatomyositis: a randomised trial. Lancet 2016;387:671–8.
6. Rider LG, Werth VP, Huber AM, Alexanderson H, Rao AP, Ruperto N, et al. Measures of adult and juvenile dermatomyositis, polymyositis, and inclusion body myositis: Physician and Patient/Parent Global Activity, Manual Muscle Testing (MMT), Health Assessment Questionnaire (HAQ)/Childhood Health Assessment Questionnaire (C-HAQ), Childhood Myositis Assessment Scale (CMAS), Myositis Disease Activity Assessment Tool (MDAAT), Disease Activity Score (DAS), Short Form 36 (SF-36), Child Health Questionnaire (CHQ), Physician Global Damage, Myositis Damage Index (MDI), Quantitative Muscle Testing (QMT), Myositis Functional Index-2 (FI-2), Myositis Activities Profile (MAP), Inclusion Body Myositis Functional Rating Scale (IBMFRS), Cutaneous Dermatomyositis Disease Area and Severity Index (CDASI), Cutaneous Assessment Tool (CAT), Dermatomyositis Skin Severity Index (DSSI), Skindex, and Dermatology Life Quality Index (DLQI). Arthritis Care Res (Hoboken) 2011;63 Suppl 11:S118–57.
7. Miller FW, Rider LG, Chung YL, Cooper R, Danko K, Farewell V, et al. Proposed preliminary core set measures for disease outcome assessment in adult and juvenile idiopathic inflammatory myopathies. Rheumatology (Oxford) 2001;40:1262–73.
8. Rider LG, Giannini EH, Harris-Love M, Joe G, Isenberg D, Pilkington C, et al. Defining clinical improvement in adult and juvenile myositis. J Rheumatol 2003;30:603–17.
9. Rider LG, Giannini EH, Brunner HI, Ruperto N, James-Newton L, Reed AM, et al. International consensus on preliminary definitions of improvement in adult and juvenile myositis. Arthritis Rheum 2004;50:2281–90.
10. American College of Rheumatology Committee to Reevaluate Improvement Criteria. A proposed revision to the ACR20: the hybrid measure of American College of Rheumatology response. Arthritis Rheum 2007;57:193–202.
11. De Lautour H, Taylor WJ, Adebajo A, Alten R, Burgos-Vargas R, Chapman P, et al. Development of preliminary remission criteria for gout using Delphi and 1000Minds consensus exercises. Arthritis Care Res (Hoboken) 2016;68:667–72.
12. Johnson SR, Naden RP, Fransen J, van Den Hoogen F, Pope JE, Baron M, et al. Multicriteria decision analysis methods with 1000Minds for developing systemic sclerosis classification criteria. J Clin Epidemiol 2014;67:706–14.
13. Hansen P, Ombler F. A new method for scoring additive multi-attribute value models using pairwise rankings of alternatives. J Multi-Crit Decis Anal 2008;15:87–107.
14. Amaya-Amaya M, Gerard K, Ryan M. Discrete choice experiments in a nutshell. In: Ryan M, Gerard K, Amaya-Amaya M, editors. Using discrete choice experiments to value health and health care. Dordrecht: Springer; 2008.
15. Ruperto N, Martini A. Networking in paediatrics: the example of the Paediatric Rheumatology International Trials Organisation (PRINTO). Arch Dis Child 2011;96:596–601.
16. Taylor WJ, Singh JA, Saag KG, Dalbeth N, MacDonald PA, Edwards NL, et al. Bringing it all together: a novel approach to the development of response criteria for chronic gout clinical trials. J Rheumatol 2011;38:1467–70.
17. Taylor WJ, Brown M, Aati O, Weatherall M, Dalbeth N. Do patient preferences for core outcome domains for chronic gout

studies support the validity of composite response criteria? Arthritis Care Res (Hoboken) 2013;65:1259–64.
18. Utz KS, Hoog J, Wentrup A, Berg S, Lammer A, Jainsch B, et al. Patient preferences for disease-modifying drugs in multiple sclerosis therapy: a choice-based conjoint analysis. Ther Adv Neurol Disord 2014;7:263–75.
19. De Bekker-Grob E, Ryan M, Gerard K. Discrete choice experiments in health economics: a review of the literature. Health Econ 2012;21:145–72.
20. Rider LG, Aggarwal R, Pistorio A, Bayat N, Erman B, Feldman BM, et al. 2016 American College of Rheumatology/European League Against Rheumatism criteria for minimal, moderate and major clinical response for juvenile dermatomyositis: an International Myositis Assessment and Clinical Studies Group/Paediatric Rheumatology International Trials Organisation collaborative initiative. Arthritis Rheumatol 2017;69:911–23.
21. Fries JF, Spitz P, Kraines RG, Holman HR. Measurement of patient outcome in arthritis. Arthritis Rheum 1980;23:137–45.
22. Rider LG. Outcome assessment in the adult and juvenile idiopathic inflammatory myopathies. Rheum Dis Clin North Am 2002;28:935–77.
23. Aggarwal R, Rider LG, Ruperto N, Bayat N, Erman B, Feldman BM, et al. A consensus hybrid definition using a conjoint analysis is the proposed response criteria for minimal and moderate improvement for adult polymyositis and dermatomyositis clinical trials [abstract]. Arthritis Rheumatol 2014;66 Suppl:S404.
24. Rider LG, Ruperto N, Pistorio A, Erman B, Bayat N, Lachenbruch PA, et al. 2016 development of adult dermatomyositis and polymyositis and juvenile dermatomyositis response criteria: methodological aspects: an American College of Rheumatology/European League Against Rheumatism/International Myositis Assessment and Clinical Studies Group/Paediatric Rheumatology International Trials Organisation collaborative initiative. Rheumatology (Oxford). In press.
25. Bohan A, Peter JB. Polymyositis and dermatomyositis. Parts 1 and 2. N Engl J Med 1975;292:344–7, 403–7.
26. Rider LG, Lee J, Jansen A, Ruperto N, Huber AM, Oddis CV, et al. Defining clinically relevant changes in core set activity measures for adult and juvenile idiopathic inflammatory myopathies (IIM) [abstract]. Arthritis Rheum 2011;63 (Suppl):S89.
27. Metz CE. Basic principles of ROC analysis. Semin Nucl Med 1978;8:283–98.
28. Ruperto N, Meiorin S, Iusan SM, Ravelli A, Pistorio A, Martini A. Consensus procedures and their role in pediatric rheumatology. Curr Rheumatol Rep 2008;10:142–6.
29. Delbecq A, van de Ven A, Gustafson D. Group techniques for program planning: a guide to nominal group and Delphi processes. Glenview (IL): Scott, Foresman and Company; 1975.
30. Nair R, Aggarwal R, Khanna D. Methods of formal consensus in classification/diagnostic criteria and guideline development. Semin Arthritis Rheum 2011;41:95–105.
31. Ruperto N, Ozen S, Pistorio A, Dolezalova P, Brogan P, Cabral DA, et al. EULAR/PRINTO/PRES criteria for Henoch-Schonlein purpura, childhood polyarteritis nodosa, childhood Wegener granulomatosis and childhood Takayasu arteritis: Ankara 2008. Part I: overall methodology and clinical characterisation. Ann Rheum Dis 2010;69:790–7.
32. Piram M, Kone-Paut I, Lachmann HJ, Frenkel J, Ozen S, Kuemmerle-Deschner J, et al. Validation of the auto-inflammatory diseases activity index (AIDAI) for hereditary recurrent fever syndromes. Ann Rheum Dis 2014;73:2168–73.
33. Ware JE Jr, Snow KK, Kosinski M, Gandek B. SF-36 health survey: manual and interpretation guide. Boston: The Health Institute, New England Medical Center; 1993.
34. Ruperto N, Ravelli A, Pistorio A, Ferriani V, Calvo I, Ganser G, et al. The provisional Paediatric Rheumatology International Trials Organisation/American College of Rheumatology/European League Against Rheumatism Disease Activity Core Set for the Evaluation of Response to Therapy in Juvenile Dermatomyositis: a prospective validation study. Arthritis Rheum 2008;59:4–13.
35. Ruperto N, Ravelli A, Pistorio A, Malattia C, Cavuto S, Gado-West L, et al. Cross-cultural adaptation and psychometric evaluation of the Childhood Health Assessment Questionnaire (CHAQ) and the Child Health Questionnaire (CHQ) in 32 countries: review of the general methodology. Clin Exp Rheumatol 2001;19 Suppl 23:S1–9.
36. Apaz MT, Saad-Magalhaes C, Pistorio A, Ravelli A, de Oliveira Sato J, Marcantoni MB, et al. Health-related quality of life of patients with juvenile dermatomyositis: results from the Paediatric Rheumatology International Trials Organisation Multinational Quality of Life cohort study. Arthritis Rheum 2009;61:509–17.
37. Van den Hoogen F, Khanna D, Fransen J, Johnson SR, Baron M, Tyndall A, et al. 2013 classification criteria for systemic sclerosis: an American College of Rheumatology/European League Against Rheumatism collaborative initiative. Arthritis Rheum 2013;65:2737–47.
38. Neogi T, Aletaha D, Silman AJ, Naden RL, Felson DT, Aggarwal R, et al. The 2010 American College of Rheumatology/European League Against Rheumatism classification criteria for rheumatoid arthritis: phase 2 methodological report. Arthritis Rheum 2010;62:2582–91.
39. Neogi T, Jansen TL, Dalbeth N, Fransen J, Schumacher HR, Berendsen D, et al. 2015 gout classification criteria: an American College of Rheumatology/European League Against Rheumatism collaborative initiative. Arthritis Rheumatol 2015;67:2557–68.
40. Felson DT, Anderson JJ, Boers M, Bombardier C, Furst D, Goldsmith C, et al. American College of Rheumatology preliminary definition of improvement in rheumatoid arthritis. Arthritis Rheum 1995;38:727–35.
41. Felson DT, Smolen JS, Wells G, Zhang B, van Tuyl LH, Funovits J, et al. American College of Rheumatology/European League Against Rheumatism provisional definition of remission in rheumatoid arthritis for clinical trials. Arthritis Rheum 2011;63:573–86.
42. Aggarwal R, Cassidy E, Fertig N, Koontz DC, Lucas M, Ascherman DP, et al. Patients with non-Jo-1 anti-tRNA-synthetase autoantibodies have worse survival than Jo-1 positive patients. Ann Rheum Dis 2014;73:227–32.
43. Hengstman GJ, ter Laak HJ, Vree Egberts WT, Lundberg IE, Moutsopoulos HM, Vencovsky J, et al. Anti-signal recognition particle autoantibodies: marker of a necrotising myopathy. Ann Rheum Dis 2006;65:1635–8.
44. Tjarnlund A, Bottai M, Rider LG, Werth VP, Pilkington CA, de Visser M, et al. Progress report on development of classification criteria for adult and juvenile idiopathic inflammatory myopathies [abstract]. Arthritis Rheum 2012;64 Suppl:S323–4.
45. Alexanderson H, del Grande M, Bingham CO III, Orbai AM, Sarver C, Clegg-Smith K, et al. Patient-reported outcomes and adult patients' disease experience in the idiopathic inflammatory myopathies: report from the OMERACT 11 Myositis Special Interest Group. J Rheumatol 2014;41:581–92.
46. Volochayev R, Csako G, Wesley R, Rider LG, Miller FW. Laboratory test abnormalities are common in polymyositis and dermatomyositis and differ among clinical and demographic groups. Open Rheumatol J 2012;6:54–63.

APPENDIX A: MEMBERS OF THE INTERNATIONAL MYOSITIS ASSESSMENT AND CLINICAL STUDIES GROUP AND THE PAEDIATRIC RHEUMATOLOGY INTERNATIONAL TRIALS ORGANISATION WHO CONTRIBUTED TO DEVELOPING THE RESPONSE CRITERIA

Steering committee: Lisa G. Rider (co–principal investigator), Nicolino Ruperto (co–principal investigator), Rohit Aggarwal (methodology lead), Frederick W. Miller, Jiri Vencovsky.

Statistical team: Rohit Aggarwal, Brian Erman, Nastaran Bayat, Angela Pistorio, Adam M. Huber, Brian M. Feldman, Paul

Hansen, Howard Rockette, Peter A. Lachenbruch, Nicolino Ruperto, Lisa G. Rider.

Adult core set survey group: Anthony A. Amato, Hector Chinoy, Lisa Christopher-Stine, Lorinda Chung, Robert G. Cooper, Lisa Criscione-Schreiber, Leslie Crofford, Mary E. Cronin, Katalin Dankó, David Fiorentino, Ignacio García-De la Torre, Patrick Gordon, Gerald Hengstman, James D. Katz, Andrew Mammen, Galina Marder, Neil McHugh, Chester V. Oddis, Elena Schiopu, Albert Selva-O'Callaghan, Yeong Wook Song, Jiri Vencovsky, Gil Wolfe, Robert Wortmann.

Clinical trial or natural history study data set contributions: Anthony A. Amato, Hector Chinoy, Lorinda Chung, Robert G. Cooper, Katalin Dankó, David Fiorentino, Ignacio García-De la Torre, Mark Gourley, Ingrid Lundberg, Frederick W. Miller, Chester V. Oddis, Paul Plotz, Lisa G. Rider, Yeong Wook Song, Jiri Vencovsky.

Adult patient profile working group: Rohit Aggarwal, Anthony A. Amato, Dana Ascherman, Richard Barohn, Olivier Benveniste, Jan De Bleecker, Jeffrey Callen, Christina Charles-Schoeman, Hector Chinoy, Lisa Christopher-Stine, Lorinda Chung, Robert G. Cooper, Leslie Crofford, Mary E. Cronin, Katalin Dankó, Sonye Danoff, Maryam Dastmalchi, Marianne de Visser, Mazen Dimachkie, Steve DiMartino, Lyubomir Dourmishev, Floranne Ernste, David Fiorentino, Ignacio García-De la Torre, Takahisa Gono, Patrick Gordon, Mark Gourley, David Isenberg, Yasuhiro Katsumata, James D. Katz, John Kissel, Richard L. Leff, Todd Levine, Ingrid Lundberg, Andrew Mammen, Herman Mann, Galina Marder, Isabelle Marie, Neil McHugh, Joseph Merola, Frederick W. Miller, Chester V. Oddis, Marzena Olesinska, Nancy Olsen, Nicolo Pipitone, Sindhu Ramchandren, Seward Rutkove, Lesley Ann Saketkoo, Adam Schiffenbauer, Albert Selva-O'Callaghan, Samuel Katsuyuki Shinjo, Rachel Shupak, Yeong Wook Song, Katarzyna Swierkocka, Jiri Vencovsky, Julia Wanschitz, Victoria Werth, Irene Whitt, Robert Wortmann, Steven R. Ytterberg.

Conjoint analysis, adult group: Rohit Aggarwal, Anthony A. Amato, Hector Chinoy, Lisa Christopher-Stine, Lorinda Chung, Robert G. Cooper, Mary E. Cronin, Katalin Dankó, Mazen Dimachkie, Steve DiMartino, David Fiorentino, Ignacio García-De la Torre, Patrick Gordon, Ingrid Lundberg, Herman Mann, Frederick W. Miller, Chester V. Oddis, Albert Selva-O'Callaghan, Jiri Vencovsky, Victoria Werth, Robert Wortmann, Steven R. Ytterberg.

Participants in consensus conference, adult working group: Anthony A. Amato, Hector Chinoy, Robert G. Cooper, Maryam Dastmalchi, Marianne de Visser, David Fiorentino, David Isenberg, James D. Katz, Andrew Mammen, Chester V. Oddis, Jiri Vencovsky, Steven R. Ytterberg.

Participants in consensus conference, pediatric working group: Rolando Cimaz, Rubén Cuttica, Sheila Knupp Feitosa de Oliveira, Brian M. Feldman, Adam M. Huber, Carol B. Lindsley, Clarissa Pilkington, Marilynn Punaro, Angelo Ravelli, Ann Reed, Kelly Rouster-Stevens, Annet van Royen-Kerkhof.

ARTHRITIS & RHEUMATOLOGY
Vol. 69, No. 5, May 2017, pp 911–923
DOI 10.1002/art.40060

SPECIAL ARTICLE

2016 American College of Rheumatology/European League Against Rheumatism Criteria for Minimal, Moderate, and Major Clinical Response in Juvenile Dermatomyositis

An International Myositis Assessment and Clinical Studies Group/Paediatric Rheumatology International Trials Organisation Collaborative Initiative

Lisa G. Rider,[1] Rohit Aggarwal,[2] Angela Pistorio,[3] Nastaran Bayat,[1] Brian Erman,[4] Brian M. Feldman,[5] Adam M. Huber,[6] Rolando Cimaz,[7] Rubén J. Cuttica,[8] Sheila Knupp de Oliveira,[9] Carol B. Lindsley,[10] Clarissa A. Pilkington,[11] Marilynn Punaro,[12] Angelo Ravelli,[13] Ann M. Reed,[14] Kelly Rouster-Stevens,[15] Annet van Royen-Kerkhof,[16] Frank Dressler,[17] Claudia Saad Magalhaes,[18] Tamás Constantin,[19] Joyce E. Davidson,[20] Bo Magnusson,[21] Ricardo Russo,[22] Luca Villa,[23] Mariangela Rinaldi,[23] Howard Rockette,[2] Peter A. Lachenbruch,[1] Frederick W. Miller,[1] Jiri Vencovsky,[24] and Nicolino Ruperto,[23] for the International Myositis Assessment and Clinical Studies Group and the Paediatric Rheumatology International Trials Organisation

This criteria set has been approved by the American College of Rheumatology (ACR) Board of Directors and the European League Against Rheumatism (EULAR) Executive Committee. This signifies that the criteria set has been quantitatively validated using patient data, and it has undergone validation based on an independent data set. All ACR/EULAR-approved criteria sets are expected to undergo intermittent updates.

The ACR is an independent, professional, medical and scientific society that does not guarantee, warrant, or endorse any commercial product or service.

This article is published simultaneously in the May 2017 issue of *Annals of the Rheumatic Diseases*.

Supported in part by the American College of Rheumatology, the European League Against Rheumatism, the NIH (Intramural Research Programs of the National Institute of Environmental Health Sciences [NIEHS], National Center for Advancing Translational Sciences, and National Institute of Arthritis and Musculoskeletal and Skin Diseases), Istituto G. Gaslini and the Paediatric Rheumatology International Trials Organisation (PRINTO), Cure JM Foundation, Myositis UK, and the Myositis Association. Dr. Vencovsky's work was supported by the Ministry of Health, Czech Republic (Institute of Rheumatology project for conceptual development of a research organization, 00023728).

[1]Lisa G. Rider, MD, Nastaran Bayat, MD, Peter A. Lachenbruch, PhD, Frederick W. Miller, MD, PhD: NIEHS, NIH, Bethesda, Maryland; [2]Rohit Aggarwal, MD, MSc, Howard Rockette, PhD: University of Pittsburgh, Pittsburgh, Pennsylvania; [3]Angela Pistorio, MD, PhD: Istituto Giannina Gaslini, Servizio di Epidemiologia e Biostatistica, Genoa, Italy; [4]Brian Erman, MS: Social and Scientific Systems, Inc., Durham, North Carolina; [5]Brian M. Feldman, MD, MSc, FRCPC: The Hospital for Sick Children, Toronto, Ontario, Canada; [6]Adam M. Huber, MD: IWK Health Centre, Halifax, Nova Scotia, Canada; [7]Rolando Cimaz, MD: University of Firenze, Florence, Italy; [8]Rubén J. Cuttica, MD: Hospital de Niños Pedro de Elizalde, University of Buenos Aires, Buenos Aires, Argentina; [9]Sheila Knupp de Oliveira, MD: Universidade Federal do Rio de Janeiro, Rio de Janeiro, Brazil; [10]Carol B. Lindsley, MD: University of Kansas City Medical Center, Kansas City, Kansas; [11]Clarissa A. Pilkington, BSc, MBBS, MRCP: Great Ormond Street Hospital for Children NHS Trust, London, UK; [12]Marilynn Punaro, MD: University of Texas Southwestern Medical Center, Dallas; [13]Angelo Ravelli, MD: Istituto Giannina Gaslini, Pediatria II - Reumatologia, and Università degli Studi di Genova, Genoa, Italy; [14]Ann M. Reed, MD: Duke University, Durham, North Carolina; [15]Kelly Rouster-Stevens,

Objective. **To develop response criteria for juvenile dermatomyositis (DM).**

Methods. **We analyzed the performance of 312 definitions that used core set measures from either the International Myositis Assessment and Clinical Studies Group (IMACS) or the Paediatric Rheumatology International Trials Organisation (PRINTO) and were derived from natural history data and a conjoint analysis survey. They were further validated using data from the PRINTO trial of prednisone alone compared to prednisone with methotrexate or cyclosporine and the Rituximab in Myositis (RIM) trial. At a consensus conference, experts considered 14 top candidate criteria based on their performance characteristics and clinical face validity, using nominal group technique.**

Results. **Consensus was reached for a conjoint analysis–based continuous model with a total improvement score of 0–100, using absolute percent change in core set measures of minimal (≥30), moderate (≥45), and major (≥70) improvement. The same criteria were chosen for adult DM/polymyositis, with differing thresholds for improvement. The sensitivity and specificity were 89% and 91–98% for minimal improvement, 92–94% and 94–99% for moderate improvement, and 91–98% and 85–86% for major improvement, respectively, in juvenile DM patient cohorts using the IMACS and PRINTO core set measures. These criteria were validated in the PRINTO trial for differentiating between treatment arms for minimal and moderate improvement ($P = 0.009$–0.057) and in the RIM trial for significantly differentiating the physician's rating for improvement ($P < 0.006$).**

Conclusion. **The response criteria for juvenile DM consisted of a conjoint analysis–based model using a continuous improvement score based on absolute percent change in core set measures, with thresholds for minimal, moderate, and major improvement.**

MD: Emory University School of Medicine, Atlanta, Georgia; [16]Annet van Royen-Kerkhof, MD, PhD: University Medical Centre Utrecht, Wilhelmina Children's Hospital, Utrecht, The Netherlands; [17]Frank Dressler, MD: Hannover Medical School, Hannover, Germany; [18]Claudia Saad Magalhaes, MD: Universidade Estadual Paulista Júlio de Mesquita Filho, Botucatu, Saõ Paulo, Brazil; [19]Tamás Constantin, MD, PhD: Semmelweis University, Budapest, Hungary; [20]Joyce E. Davidson, FRCP, FRCPCH: Royal Hospital for Sick Children, Glasgow, UK, and Royal Hospital for Sick Children, Edinburgh, UK; [21]Bo Magnusson, MD: Karolinska University Hospital, Stockholm, Sweden; [22]Ricardo Russo, MD: Hospital de Pediatría Garrahan, Buenos Aires, Argentina; [23]Luca Villa, MA, Mariangela Rinaldi, MEng, Nicolino Ruperto, MD, MPH: Istituto Giannina Gaslini, Pediatria II - Reumatologia, PRINTO, Genoa, Italy; [24]Jiri Vencovsky, MD, PhD: Charles University, Prague, Czech Republic. See Appendix A for members of the International Myositis Assessment and Clinical Studies Group and the Paediatric Rheumatology International Trials Organisation who contributed to developing the response criteria.

Drs. Rider and Aggarwal contributed equally to this work. Drs. Vencovsky and Ruperto contributed equally to this work.

Address correspondence to Nicolino Ruperto, MD, MPH, Istituto Giannina Gaslini, Pediatria II, PRINTO, Via G. Gaslini 5, 16147 Genoa, Italy. E-mail: nicolaruperto@gaslini.org.

Juvenile dermatomyositis (DM) is a systemic autoimmune disease characterized by chronic skeletal muscle inflammation and weakness. Core set measures to assess juvenile DM disease activity have been established and validated by the International Myositis Assessment and Clinical Studies Group (IMACS) and the Paediatric Rheumatology International Trials Organisation (PRINTO), with provisional endorsement by the American College of Rheumatology and the European League Against Rheumatism (1–6). Both core sets include physician and parent global activity, muscle strength, and physical function. IMACS also includes the most abnormal serum muscle enzyme value and extramuscular global activity, whereas PRINTO includes instead a health-related quality of life measure, the Child Health Questionnaire (7) and a global activity score, the Disease Activity Score (8). IMACS measures muscle strength using manual muscle testing, and PRINTO measures muscle strength using the Childhood Myositis Assessment Scale (1,2,5).

Combinations of these measures to determine clinical improvement were developed to enhance the sensitivity of responses and decrease the sample sizes needed, by using large prospective natural history data sets and expert clinician consensus as the gold standard. For both PRINTO and IMACS, at least 20% improvement in 3 of 6 core set measures with no more than 1 or 2 worsening (which cannot be muscle strength) had been established as preliminary response criteria, and additional combinations of improvement in the core set measures serve as secondary response criteria (9,10). PRINTO adapted its top criteria for minimal clinical improvement to moderate and major improvement by using cutoffs of 50% and 70%, similar to the improvement criteria for juvenile idiopathic arthritis (JIA) (11–13).

Although the preliminary response criteria for juvenile DM advanced the assessment of patients and their responses to treatment, those criteria were limited by differences in the core set measures and final consensus response criteria between IMACS and PRINTO, a lack of randomized controlled trial data for full validation, and inadequate exploration of more sensitive approaches using hybrid or continuous methods (14). The preliminary response criteria also considered each core set measure equally rather than differentially weighting them. However, most myositis experts agree that some core set measures are more important, such as physician global activity and muscle strength (3,15). For PRINTO studies, physician global evaluation of disease activity, muscle strength, and parent global evaluation of the child's overall well-being were weighted as the most important core set measures in a logistic regression analysis (3,10). Moreover, the preliminary response criteria did not validate criteria for moderate

or major improvement. There is, therefore, a clear need to have standardized improvement criteria for all levels of improvement in future clinical trials, similar to the standardized criteria developed for rheumatoid arthritis (RA) and JIA.

For these reasons, IMACS and PRINTO engaged in a joint effort to develop fully validated response criteria for juvenile DM, including criteria for minimal, moderate, and major clinical response. This report focuses on the consensus conference in which the top candidate definitions of response leading to the final juvenile DM response criteria were considered.

Methods

In previous reports (16,17), we described the methodology used a) to create patient profiles using natural history data and obtain expert consensus on minimal, moderate, and major improvement (16), b) to determine differential weights of the core set measures using conjoint analysis, and c) to draft 6 types of candidate definitions for response criteria using the myositis expert survey on thresholds of improvement and data-driven methods, such as logistic regression and conjoint analysis (Table 1).

Conjoint analysis is a choice modeling or discrete choice experiment, which is a valid methodology for developing composite criteria and has been used recently in rheumatology (19–22). In the conjoint analysis surveys administered using 1000Minds online software (23), experts were presented with pairs of hypothetical patient scenarios; each patient had different levels of improvement in the same 2 core set measures, assuming other core set measures remained the same. Experts rated which of the 2 scenarios had greater improvement. Based on the rater's response, the relative weights of core set measures and their levels of improvement were established and used to develop a scoring system by mathematical methods based on linear programming (24) such that when all 6 core set measures are considered together, the maximum score (total improvement score) possible for representing a patient's improvement is 100, and the minimum score is 0.

We then compared the performance characteristics of the drafted definitions in the patient profiles, using expert consensus ratings as a gold standard, and externally validated the candidate response criteria by applying them to clinical trial data. This process led to the development of traditional categorical as well as continuous candidate definitions for response criteria, with thresholds for minimal, moderate, and major improvement (18). Continuous candidate definitions can also be considered hybrid definitions, because the same definition can be used either as a continuous outcome measure by using the total improvement score or as a categorical outcome measure by using the thresholds for minimal, moderate, and major improvement.

Candidate definitions were evaluated using consensus profile ratings as the gold standard, by assessing sensitivity, specificity, and area under the curve (AUC) to compare the performance of these candidate definitions. Those that performed well in the consensus profiles (sensitivity and specificity both $\geq$80%, AUC $\geq$0.9 for minimal, and AUC $\geq$0.8 for moderate and major improvement, using IMACS or PRINTO core set measures [1]) were externally validated. The PRINTO trial randomized patients with new-onset juvenile DM to receive prednisone alone (n = 47) or prednisone combined with methotrexate or cyclosporine (n = 46 patients per treatment arm) (13). Chi-square analysis was used to compare the percentages of patients meeting the candidate definitions for response at the primary end point (6 months) for the combined treatment arms versus the prednisone-alone (placebo) arm. Definitions with a significant difference ($P < 0.05$) between treatment arms for minimal improvement were further considered. Both PRINTO and IMACS core set measures were available in this trial.

A second trial validation data set included 48 juvenile DM patients enrolled in the Rituximab in Myositis (RIM) trial for treatment-refractory patients. It had a randomized placebo-phase design in which patients received either rituximab or placebo at weeks 0 and 1, and at weeks 8 and 9 their treatment assignment was reversed in a blinded manner (25). We used the Mann-Whitney U test to determine whether each candidate definition could differentiate between the treating physician's rating of improvement (score range 1–7) at 6 months, a time point when most patients improved and that was also comparable to that in the PRINTO trial. For the RIM trial, only the IMACS core set measures were available.

We then selected the top candidate definitions, up to 4 top-performing definitions from each of the 6 different types of candidate definitions (Table 1), for consideration at the final consensus conference as a manageable number of definitions to discuss.

Consensus conference. Nominal group technique was used at a consensus conference held in Paris, France on June 9–10, 2014, led by experienced moderators (LGR and NR, for the pediatric working group). The methodologies used to develop the new candidate response criteria and performance characteristics of each type of candidate definition were reviewed with the participants in a general session. The 12 pediatric working group participants first independently and then as a group reviewed the performance characteristics of the 14 top candidate definitions of response criteria for juvenile DM. Data for minimal, moderate, and major clinical response were presented for each definition, including a detailed spreadsheet that included the performance in the patient profiles using the IMACS and PRINTO core set measures, including sensitivity, specificity, AUC, as well as kappa values and odds ratios. AUC was defined as the average of the sensitivity and specificity values for all categorical candidate definitions, as well as for thresholds for minimal, moderate, and major improvement in continuous candidate definitions. In addition, for continuous definitions, an AUC for the total improvement score was determined from the receiver operating characteristic (ROC) curve as a plot of sensitivity versus (1 – specificity) for total improvement scores as well as for thresholds (26–28). Results of the external validation for each candidate definition from the PRINTO and RIM clinical trial data sets were also presented.

Pediatric working group. After reviewing the performance of the 14 top performing candidate definitions, the 12 pediatric working group participants developed consensus response criteria for minimal, moderate, and major improvement in juvenile DM. The participants were informed of the secondary goal of reaching consensus on response criteria for both juvenile DM and adult DM/polymyositis (PM). Participants were first asked to rank their top 5 choices, considering the data presented, based on face validity, feasibility, and

Table 1. Types of candidate definitions for response criteria that were developed and tested*

Type of candidate definitions of response	Description	Example of the candidate definition for the response criteria
Previously published (categorical definition)	Previously published response criteria that were retested	Minimal. Three of any 6 improved by ≥20%, no more than 1 worse by >30% (which cannot be CMAS) (10) Moderate. Three of any 6 improved by ≥50%, no more than 1 worse by >30% (which cannot be CMAS) (11) Major. Three of any 6 improved by ≥70%, no more than 1 worse by >30% (which cannot be CMAS) (11)
Newly drafted (categorical definition)	Drafted relative or absolute percent change in candidate definitions of response, based on recent CSM survey	Minimal. MD global, muscle strength (MMT or CMAS), and 1 other CSM improved by ≥20% Moderate. MD global, muscle strength (MMT or CMAS), and 1 other CSM improved by ≥30% Major. MD global, muscle strength (MMT or CMAS), and 1 other CSM improved by ≥50%
Weighted (categorical definition)	Applied conjoint analysis relative weights to CSM in newly drafted definitions; each CSM receives improvement points (corresponding relative weights) when it reaches the threshold for minimal, moderate, or major improvement; worsening points are applied similarly; improvement is calculated based on a total score of improvement versus worsening	Improvement = at least 3.5 improvement points of 10 total improvement points, and no more than 1.5 worsening points, where MD global = 2 points, parent global = 1 point, MMT/CMAS = 3 points, C-HAQ = 1.5 points, extramusc/DAS = 1.5 points, enzyme/CHQ-PhS = 1 point Minimal. Improvement points given when CSM ≥20%; worsening points given when CSM worse by >30% Moderate. Improvement points given when CSM ≥50%; worsening points given when CSM worse by >30% Major. Improvement points given when CSM ≥75%; worsening points given when CSM worse by >30%
Logistic regression (continuous definition)	Model of improvement using a combination of CSM with different weights, as developed in the logistic regression model; total scores derived, with different cutoffs for minimal, moderate, and major improvement Relative % change	Improvement score = (MD global % change) + 0.5 × (parent global activity % change) + 0.5 × (extramusc activity or DAS % change) Minimal. Improvement score ≥15 Moderate. Improvement score ≥30 Major. Improvement score ≥60
Core set measure–weighted (continuous definition)†	Multiply the % change in each CSM by the weights derived from conjoint analysis, then sum (% change in each CSM × conjoint analysis weights) to get final total improvement score; different thresholds for minimal, moderate, and major improvement established based on consensus profile ratings as gold standard	Improvement score = 2 × (MD global % change) + (parent global % change) + 3 × (MMT or CMAS % change) + 1.5 × (C-HAQ % change) + 1.5 × (extramusc or DAS % change) + (enzyme or CHQ-PhS % change) Minimal. Improvement score ≥100 Moderate. Improvement score ≥250 Major. Improvement score ≥400
Conjoint analysis (continuous definition)	For a given range in the level of improvement in each CSM, a score is assigned, as developed by the survey results and modeling; greater degrees of improvement receive higher scores; a patient is minimally improved if the improvement score is above the cutoff for minimal improvement; similarly for moderate and major improvement	Cut points for the model for juvenile DM are: Minimal. Improvement score ≥30 Moderate. Improvement score ≥45 Major. Improvement score ≥70‡

* CMAS = Childhood Myositis Assessment Scale; CSM = core set measure; MD global = physician global activity score; MMT = manual muscle testing; parent global = parent global activity score; C-HAQ, Childhood Health Assessment Questionnaire; extramusc = extramuscular global activity; DAS = Disease Activity Score; enzyme = most abnormal serum muscle enzyme value among aldolase, alanine aminotransferase, aspartate aminotransferase, lactate dehydrogenase, and creatine kinase; CHQ-PhS = physical summary score of the Child Health Questionnaire–Parent Form 50.

† This type of definition was not brought to the final consensus conference.

‡ The full absolute percent change model is shown in Table 3 and in Supplementary Table 2 (available on the *Arthritis & Rheumatology* web site at http://onlinelibrary.wiley.com/doi/10.1002/art.40060/abstract).

generalizability, and to determine which response criteria were most clinically meaningful. The voting process was conducted in a systematic manner with a predetermined format using nominal group technique (29,30) facilitated by an internet-based system developed by staff at the PRINTO coordinating center (31,32). Voting was done anonymously and independently using the online voting software.

After the initial round of voting, the results were shared with the group. Each participant was then asked to explain his or her top- and bottom-ranked choices to the group. The rounds of voting continued in the same manner until consensus was reached (≥80% of the votes) or until it was clear that consensus would not be reached. Between each round, after the participants were shown the results, the administrators were allowed to remove candidate definitions that decisively received a small proportion of the votes. In the final round, participants were asked to select their final top response criteria. The pediatric working group also voted on additional issues, including use of both IMACS and PRINTO core set measures and response criteria for juvenile DM that would interchange both the IMACS and PRINTO measures. Participants also voted on retesting the performance of the top candidate response criteria in future trials.

Combined pediatric and adult working group. After consensus was attained for juvenile DM response criteria, a combined working group of 22 pediatric and adult experts was formed to determine whether consensus could be reached on final, common response criteria for both juvenile DM and adult DM/PM. Common response criteria that would include both juvenile DM and adult DM/PM were considered for use in clinical trials, which might facilitate drug approvals for myositis treatment. Experienced moderators (LGR, RA, FWM, and NR) led the combined working group. For the first round of votes, the top adult and pediatric definitions from the final round of voting in each working group were considered. The online voting system was utilized again, and each participant discussed his or her top-choice candidate definition, using nominal group technique in a round-robin manner. At each round, participants were asked to select only 1 candidate top response criteria set; discussion was stopped once consensus of ≥80% was reached. For determining the thresholds of improvement for the selected definition, the required consensus was ≥70%, which was done by post-conference voting.

Results

The performance characteristics of 101 of 312 candidate definitions were excellent (sensitivity and specificity of ≥80%, AUC ≥0.90 for minimal improvement), and 30 candidate definitions also performed well in 2 clinical trials, in which they differentiated between treatment arms ($P < 0.05$ for minimal improvement) and differentiated the treating physician's improvement score at week 24 ($P < 0.001$) (15).

Top candidate definitions for response criteria. Fourteen top-performing candidate definitions were brought to the pediatric working group for consideration at the consensus conference (Table 2 and Supplementary Tables 1 and 2, available on the *Arthritis & Rheumatology* web site at http://onlinelibrary.wiley.com/doi/10.1002/art.40060/abstract). These candidate criteria included 9 categorical definitions in which different criteria were set for minimal, moderate, and major improvement and 5 continuous definitions in which improvement points are given on a continuous scale that corresponds to the magnitude of improvement, with different thresholds for minimal, moderate, and major improvement. Among the 9 categorical definitions, 2 were previously published IMACS and PRINTO response criteria (9–11), 4 were newly drafted definitions based on a survey of experts, and 3 were weighted definitions. Among the continuous definitions, 2 were developed by logistic regression, and 3 were developed from the conjoint analysis survey. Among the 14 candidate criteria considered, 11 were based on relative percent change, and 3 were based on absolute percent change in the core set measures.

The performance characteristics of these 14 candidate definitions are shown in Table 2 and Supplementary Table 1 (available on the *Arthritis & Rheumatology* web site at http://onlinelibrary.wiley.com/doi/10.1002/art.40060/abstract). In the patient profiles, with expert consensus as a gold standard, all definitions presented at the conference had sensitivity and specificity of ≥87% (AUC ≥0.90) for minimal improvement (Table 2 and Supplementary Table 1). For moderate improvement, specificity decreased but was ≥80% (AUC ≥0.88), and for major improvement specificity was generally ≥75% (AUC ≥0.84). For continuous definitions, the AUCs (from ROC curves) for the total improvement score were generally better than the AUCs (average of sensitivity and specificity) for the thresholds of minimal, moderate, and major improvement. Performance was similar between the IMACS and PRINTO core set measures for each definition.

Almost all candidate criteria were validated using the PRINTO trial at 6 months, when they could differentiate between treatment arms, with $P < 0.05$ for minimal improvement (Table 2 and Supplementary Table 1). All candidate criteria were also validated in 48 juvenile DM patients in the RIM trial (25). All definitions could differentiate the median treating physician's improvement score at week 24 ($P \leq 0.006$).

Consensus conference voting. Among the 14 candidate definitions, 13 and 11 candidate definitions of response were promoted in the first and second voting rounds, respectively. In round 3, 6 candidate definitions were chosen, each receiving a similar number of votes. These 6 included the 3 conjoint analysis–based continuous definitions, a conjoint analysis–based weighted definition, a logistic regression absolute percent change definition, and the previously published PRINTO preliminary response criteria (8,9). In the fourth round of voting and discussion, participants reached consensus

Table 2. Detailed performance characteristics of patient profiles for the top 5 candidate definitions presented at the consensus conference*

Candidate definition type based on final consensus rank order, improvement category, core set measure	Sensitivity, %	Specificity, %	Threshold AUC†	Total improvement score AUC‡	PRINTO trial§			RIM trial¶			Rank
					Tx (%)	Ctrl (%)	*P*	Response criteria, improved#	Response criteria, not improved#	*P*	
Conjoint analysis, absolute % change (model 3)**											1
Minimal (≥30)											
IMACS	89	91	0.90	0.98	75	53	0.009	2.0	3.0	<0.001	
PRINTO	89	98	0.93	0.99	73	55	0.038				
Moderate (≥45)											
IMACS	92	99	0.95	0.99	70	53	0.057	2.0	3.0	<0.001	
PRINTO	94	94	0.94	0.99	71	51	0.023				
Major (≥70)											
IMACS	91	86	0.89	0.96	51	43	0.341	2.0	3.0	0.006	
PRINTO	98	85	0.91	0.98	58	49	0.331				
Conjoint analysis, relative % change (model 1)††											2
Minimal (≥33)											
IMACS	99	87	0.93	0.98	75	55	0.018	2.0	4.0		
PRINTO	96	98	0.97	1.00	74	55	0.027				
Moderate (≥60)											
IMACS	97	93	0.95	0.99	73	51	0.011	2.0	3.0	<0.001	
PRINTO	97	96	0.96	1.00	70	51	0.032				
Major (≥80)											
IMACS	91	87	0.89	0.96	57	49	0.396	1.5	3.0	<0.001	
PRINTO	98	86	0.92	0.97	61	49	0.179				
Conjoint analysis, relative % change (model 2)††											3
Miminal (≥33)											
IMACS	95	94	0.94	0.98	75	53	0.009	2.0	4.0	<0.001	
PRINTO	94	98	0.96	0.99	74	55	0.027				
Moderate (≥55)											
IMACS	95	95	0.95	1.00	70	51	0.032	2.0	3.0	<0.001	
PRINTO	97	98	0.98	1.00	70	51	0.032				
Major (≥77)											
IMACS	93	86	0.90	0.97	49	47	0.814	1.0	2.0	0.011	
PRINTO	96	90	0.93	0.99	59	49	0.273				
Weighted definition, relative % change‡‡											4
Minimal (improvement points given when CSM ≥20, worsening points given when CSM worse by >30)											
IMACS	95	100	0.97	NA	70	51	0.032	2.0	3.0	<0.001	
PRINTO	92	98	0.95	NA	73	53	0.021				
Moderate (improvement points given when CSM ≥ 50%, worsening points given when CSM worse by >30%)											
IMACS	95	91	0.93	NA	68	51	0.045	2.0	3.0	<0.001	
PRINTO	95	92	0.94	NA	71	51	0.023				
Major (improvement points given when CSM ≥75%, worsening points given when CSM worse by >30%)											
IMACS	100	81	0.91	NA	64	47	0.050	1.5	3.0	<0.001	
PRINTO	98	85	0.91	NA	62	49	0.142				

Table 2. *(Cont'd)*

Candidate definition type based on final consensus rank order, improvement category, core set measure	Sensitivity, %	Specificity, %	Threshold AUC†	Total improvement score AUC‡	PRINTO trial§			RIM trial¶			Rank
					Tx (%)	Ctrl (%)	*P*	Response criteria, improved#	Response criteria, not improved#	*P*	
Previously published definition (10,11), relative % change											5
Minimal (3 of any 6 improved by ≥20%, no more than 1 worse by >30%) (which cannot be MMT/CMAS) (10)											
IMACS	93	100	0.97	NA	70	51	0.032	2.0	3.0	<0.001	
PRINTO	88	100	0.94	NA	71	51	0.023				
Moderate (3 of any 6 improved by ≥50%, no more than 1 worse by > 30%) (which cannot be MMT/CMAS) (11)											
IMACS	90	95	0.93	NA	66	51	0.081	2.0	3.0	<0.001	
PRINTO	90	96	0.93	NA	68	51	0.045				
Major (3 of any 6 improved by ≥70%, no more than 1 worse by >30%) (which cannot be MMT/CMAS) (11)											
IMACS	99	83	0.91	NA	63	49	0.111	2.0	3.0	<0.001	
PRINTO	99	89	0.94	NA	60	49	0.223				

* The performance characteristics of patient profiles for definitions ranked 6–14 are shown in Supplementary Table 1 (available on the *Arthritis & Rheumatology* web site at http://onlinelibrary.wiley.com/doi/10.1002/art.40060/abstract). Note that either International Myositis Assessment and Clinical Studies (IMACS) or Paediatric Rheumatology International Trials Organisation (PRINTO) core set measures (CSMs) may be used in these candidate definitions of response; the candidate definitions were developed in parallel with IMACS or PRINTO CSMs. Tx = treatment arm of prednisone in combination with methotrexate or cyclosporine; Ctrl = control; NA = not applicable.

† Calculated as the area under the curve (AUC) from the receiver operating characteristic (ROC) curve for the total improvement score and the threshold for minimal, moderate, and major improvement.

‡ Calculated as the AUC from the ROC curve, using the total improvement score and the threshold cutoffs for minimal, moderate, and major improvement, which applies only to continuous definitions.

§ PRINTO juvenile dermatomyositis (DM) trial of prednisone alone versus prednisone with methotrexate or cyclosporine (n = 139) (13).

¶ Rituximab in Myositis (RIM) trial juvenile DM arm (n = 48). Comparison of the treating physician's rating of improvement if the improvement criteria are met versus not met at week 24 (25). A 1-point difference in physician's rating of improvement from no improvement to minimal improvement was considered not only statistically significant but also clinically significant.

Median score for physician's rating of improvement.

** The conjoint analysis–based continuous candidate response criteria using absolute percent change in core set measures (absolute percent change model) are shown in Table 3. These criteria are also the top response criteria for adult DM/polymyositis (PM), but with different thresholds for the total improvement score for minimal, moderate, and major improvement (18).

†† The conjoint analysis–based continuous candidate definitions using relative percent change in core set measures are shown in Supplementary Table 3 (available on the *Arthritis & Rheumatology* web site at http://onlinelibrary.wiley.com/doi/10.1002/art.40060/abstract). These criteria are also the second- and third-choice criteria for adult DM/PM, but with different thresholds in the total improvement score for minimal, moderate, and major improvement (18).

‡‡ Improvement = at least 3.5 improvement points of 10 total improvement points, and no more than 1.5 worsening points, where physician global activity = 2 points, parent global activity = 1 point, manual muscle testing (MMT) or Childhood Myositis Assessment Scale (CMAS) = 3 points, Childhood Health Assessment Questionnaire = 1.5 points, extramuscular global activity or Disease Activity Score = 1.5 points, and enzyme or physical summary score of the Child Health Questionnaire–Parent Form 50 = 1 point.

Table 3. Final myositis response criteria for minimal, moderate, and major improvement in juvenile dermatomyositis (DM) and combined adult DM/PM and juvenile DM clinical trials and studies*

Core set measure, level of improvement based on absolute percent change	Improvement score
Physician global activity	
Worsening to 5% improvement	0
>5% to 15% improvement	7.5
>15% to 25% improvement	15
>25% to 40% improvement	17.5
>40% improvement	20
Parent global activity	
Worsening to 5% improvement	0
>5% to 15% improvement	2.5
>15% to 25% improvement	5
>25% to 40% improvement	7.5
>40% improvement	10
Manual muscle testing or CMAS	
Worsening to 2% improvement	0
>2% to 10% improvement	10
>10% to 20% improvement	20
>20% to 30% improvement	27.5
>30% improvement	32.5
Childhood Health Assessment Questionnaire	
Worsening to 5% improvement	0
>5% to 15% improvement	5
>15% to 25% improvement	7.5
>25% to 40% improvement	7.5
>40% improvement	10
Enzyme (most abnormal) or CHQ-PhS	
Worsening to 5% improvement	0
>5% to 15% improvement	2.5
>15% to 25% improvement	5
>25% to 40% improvement	7.5
>40% improvement	7.5
Extramuscular activity or Disease Activity Score	
Worsening to 5% improvement	0
>5% to 15% improvement	7.5
>15% to 25% improvement	12.5
>25% to 40% improvement	15
>40% improvement	20

The **total improvement score** is the sum of all 6 improvement scores associated with the change in each core set measure. A total improvement score of **≥30** represents **minimal improvement**, a score of **≥45** represents **moderate improvement**, and a score of **≥70** represents **major improvement**.

* Either all of the International Myositis Assessment and Clinical Studies Group (IMACS) or all of the Paediatric Rheumatology International Trials Organisation (PRINTO) core set measures may be used. Note that these response criteria are also proposed for use in combined adult DM/polymyositis (DM/PM) and juvenile DM trials (18). For comparison, the thresholds of improvement in the total improvement score for adult DM/PM are ≥20 for minimal improvement, ≥40 for moderate improvement, and ≥60 for major improvement.

How to calculate the improvement score: The absolute percent change ([final value – baseline value]/range × 100) is calculated for each core set measure. For muscle enzymes, the most abnormal serum muscle enzyme level at baseline (creatine kinase, aldolase, alanine transaminase, aspartate aminotransferase, lactate dehydrogenase) is used. The enzyme range was calculated based on a 90% range of enzymes from natural history data (5,38), which for creatine kinase is 15 times the upper limit of normal (ULN), for aldolase is 6 times the ULN, and for lactate dehydrogenase, aspartate aminotransferase, and alanine transaminase is 3 times the ULN. The ULN is determined according to the individual laboratories in the participating centers. The ranges for the other core set activity measures are based on the instrument scale used (13,15,25). An improvement score is assigned for each core set measure based on the absolute percent change. These are totaled among the 6 IMACS or PRINTO core set measures. The thresholds for minimal, moderate, and major improvement are provided. The total improvement score itself may also be compared among treatment arms in a trial. A total improvement score between 0 and 100 corresponds to the degree of improvement, with higher scores corresponding to a greater degree of improvement. CMAS = Childhood Myositis Assessment Scale; CHQ-PhS = Physical Summary Score of the Child Health Questionnaire–Parent Form 50.

on final top response criteria, a conjoint analysis–based continuous model using absolute percent change in the IMACS or PRINTO core set measures (Table 3).

Table 2 and Supplementary Table 1 (available on the *Arthritis & Rheumatology* web site at http://onlinelibrary.wiley.com/doi/10.1002/art.40060/abstract) show the

performance characteristics in the patient profiles and the trial validation for each of the top candidate response criteria presented at the conference. For the top conjoint analysis–based continuous response criteria using absolute percent change in each of the core set measures, the sensitivity and specificity in the patient profiles was generally >90% and the AUC >0.90 for both the IMACS and PRINTO measures. For the PRINTO trial, a difference in the treatment arms was detected for minimal and moderate improvement using the top response criteria, and in the RIM trial a difference in the physician's rating of improvement when the response criteria rated the patient as improved versus not improved was detected for minimal, moderate, and major improvement.

Pediatric experts favored the conjoint analysis–based continuous response criteria because of the continuous improvement score that corresponds to the magnitude of improvement and provides the ability to categorize a patient's degree of change into minimal, moderate, and major improvement. The continuous model definitions also differentially weight the various core set measures, which experts thought were consistent with their assessment of the relative importance of each of the core set measures. The top response criteria were based on absolute percent change in core set measures, which was also favored by the participants because, given the various visual analog scale (VAS) measurements used in the core set measures, the absolute percent changes were more congruent than relative percent changes with actual changes that the myositis experts see in clinical practice.

Final response criteria chosen by the combined pediatric and adult working group. For this round of votes, the top 2 pediatric (Table 2) and adult definitions (18) were considered. Two rounds of voting resulted in final consensus response criteria, with 91% of participants voting for the conjoint analysis–based continuous response criteria based on absolute percent change in the core set measures (Table 3). It was agreed that the top response criteria would be used in future clinical trials that combined juvenile DM and adult DM/PM. Because the final response criteria were similar, participants favored using response criteria that would be common to juvenile DM and adult DM/PM, and they favored combined studies when possible as well as the possibility of comparing outcomes in separate studies using the same final response criteria.

Other votes. In a post-conference final vote using the Delphi method, 74% of the participants agreed to use the following pediatric threshold values for minimal, moderate, and major response in juvenile DM: total improvement score ≥30 (on a scale of 0–100) for minimal, ≥45 for moderate, and ≥70 for major improvement. In contrast, the final thresholds for minimal, moderate, and major response in adult DM/PM were ≥20, ≥40, and ≥60, respectively. The pediatric working group also reached consensus that, given the overall similarity between the IMACS and PRINTO response criteria, joint IMACS/PRINTO response criteria for juvenile DM are being proposed. The current development of the response criteria in parallel between the IMACS and PRINTO core set measures necessitates that either all of the IMACS or all of the PRINTO core set measures be used. The pediatric experts, however, committed to measure both IMACS and PRINTO core set measures in future therapeutic trials, with 92% agreement, and to continue to test the interchangeability of the IMACS and PRINTO core set measures. The group also unanimously agreed to retest the validity of the top 5 candidate definitions for response criteria and to utilize the other 4 definitions as secondary end points in future clinical trials. The top 3 of these criteria, the conjoint analysis definitions, are the same for both juvenile DM and adult DM/PM, with different thresholds of improvement (Table 3 and Supplementary Table 3, available on the *Arthritis & Rheumatology* web site at http://onlinelibrary.wiley.com/doi/10.1002/art.40060/abstract).

Discussion

Conjoint analysis–based continuous response criteria, based on absolute percent change in the core set measures, were developed as the consensus- and data-driven response criteria for minimal, moderate, and major improvement in juvenile DM. For the response criteria, either IMACS or PRINTO core set measures could be used. In addition, it was agreed that the same response criteria, using the IMACS core set measures but with different thresholds for improvement, would be the consensus response criteria for adult DM/PM trials and combined juvenile DM and adult DM/PM trials in the future (18).

The comprehensive process used to develop final response criteria for minimal, moderate, and major improvement in juvenile DM included the use of large, prospective, natural history data sets for juvenile DM and data from 2 randomized controlled trials for validation, which included a wide range of disease activity and different stages of disease, from recently diagnosed to treatment-refractory patients (13,15,25). The involvement of many clinical experts who had experience using the core set measures in juvenile DM patients was also critical. They provided input at several points throughout the process, including determining thresholds for improvement in core set measures by which definitions of response were drafted, achieving gold standard ratings of improvement by evaluating and developing

consensus patient profiles, completing the conjoint analysis surveys to develop differential weights for the core set measures, and participating in the final consensus conference to achieve consensus for common response criteria with the greatest clinical face validity. The current response criteria (Table 3) also resolve the differences between PRINTO and IMACS core set measures by testing candidate definitions of response criteria in parallel using both sets of measures and showing that they are largely interchangeable, and that their performance is comparable. Moreover, this project brought both IMACS and PRINTO consortia to work together for this rare disease.

The combined group of pediatric and adult experts selected the same top-choice definition but with differing thresholds for improvement, which had very similar performance characteristics and were thought to be more appropriate for use in clinical trials that would, in the future, combine adult and pediatric patients.

The final response criteria selected, conjoint analysis–based continuous response criteria using absolute percent change in core set measures, have many advantages. For each measure, improvement points are calculated based on the level of change in that measure, and each core set measure is differentially weighted, such that changes in muscle strength and physician global activity are weighted more heavily than changes in the most abnormal enzyme value or quality of life. A total improvement score can be obtained as a continuous measure, and the means or medians of total improvement scores can be compared between treatment arms (33). A total improvement score between 0 and 100 also corresponds to the degree of improvement, with higher scores corresponding to a greater magnitude of improvement. This score may be more sensitive to change, resulting in smaller trial sample sizes (33,34). Alternatively, thresholds for minimal, moderate, and major improvement have been established that allow dichotomous use of the response criteria as well. Therefore, this is truly a hybrid model that can be used as either a continuous or categorical outcome measure within the same response criteria depending on the trial design and needs of the study.

The response criteria allow input from all the core set measures instead of relying on only a few measures to determine whether a patient has experienced improvement. However, although these response criteria were developed using all 6 core set measures, the response criteria could still be used if fewer core set measures were obtained, allowing for greater flexibility in the types of patients and improvements that can occur, but we caution that the response criteria are most accurate when all 6 core set measures are used. As such, the response criteria signify a major advance in assessing improvement in therapeutic trials and other clinical research studies by providing data-driven response criteria that were developed by consensus of major stakeholders in the field who come from all over the world.

Prior response criteria in rheumatic diseases have included relative percent change (35,36), whereas myositis response criteria are based on absolute percent change. The experts favored the use of absolute percent change for various reasons. In this study, several core set measures used a 10-cm VAS, and the experts thought that absolute percent change better represents the degree of change they see in clinical practice. Moreover, absolute percent changes can be calculated when the baseline core set measure is 0 and give similar results for similar degrees of change at either end of the VAS.

The participants also favored using the same response criteria for juvenile DM and adult DM/PM, but with cut points or thresholds for improvement specific to pediatric or adult patients. Having common response criteria facilitates the potential to conduct combined clinical trials, such as the RIM trial (25), and to compare the outcomes of trials and studies conducted separately. Participants agreed to include other top-performing definitions that were highly rated as secondary end points for future clinical trials. Among these were not only other conjoint analysis–based continuous models but also the published PRINTO preliminary response criteria (10,11). Future work should also evaluate whether a baseline composite score threshold derived from the PRINTO or IMACS core set measures could be used as inclusion criteria for future clinical trials.

Limitations of the present work include the lack of a placebo group in the RIM trial. For this reason, the physician's assessment of improvement at 6 months was used instead. We were fortunate to have another controlled clinical trial for juvenile DM that had 3 treatment arms to use for external validation (13), in which we evaluated the ability of the candidate definitions to differentiate between treatment arms. Although thresholds for major improvement were developed and validated in fewer patients, we believe that it was sufficient given that 29% of patients had major improvement in patient profiles, and 17% had major improvement in the clinical trials used for validation. The final conjoint analysis–based continuous response criteria also do not address worsening in the core set measures; however, this generally does not affect the outcome, because when patients are rated as improved, no more than 1 or 2 measures worsen in our clinical data sets. Also, although we tested the interchange of IMACS and PRINTO core set measures, we tested these variations as

2 parallel core set measures but did not examine intermixing the PRINTO and IMACS core set measures. Further work to examine the interchangeability of the IMACS and PRINTO core set measures will be needed.

The data sets used to develop the new response criteria primarily contained information about patients with a recent diagnosis or those experiencing a disease flare, and further work is needed to determine how the response criteria perform in patients with longstanding disease or those with significant disease-related damage. Finally, although application of the criteria might seem cumbersome, as regularly done for JIA and RA, the evaluation of improvement will be facilitated by appropriate dedicated software or "apps," or in the future, by simplification of the manner in which the core set measures are evaluated (e.g., similar to the Juvenile Arthritis Disease Activity Score for JIA) (37). The time required to apply these criteria is estimated to be 25–35 minutes to complete the core set measures at each visit (1) and 2–3 minutes to hand-calculate the total improvement score and degree of response. Both IMACS and PRINTO are developing a web-based tool as well as a downloadable calculator that will allow easy administration of the response criteria and immediate calculation. The apparent complexity is, however, counterbalanced by the establishment of different validated levels of improvement, which constitute the real novelty of this project and which have never been validated as such for either RA or JIA, despite being regularly reported in clinical trials.

In summary, conjoint analysis–based continuous response criteria that establish different thresholds for minimal, moderate, and major improvement and utilize the absolute percent change in core set measures were chosen as the consensus response criteria for juvenile DM and were validated using both natural history and trial data. These response criteria should be highly acceptable and widely used given that they were developed with consensus among many myositis experts worldwide. They should be sensitive in detecting differences in improvement and in quantitating the degree of improvement, as seen in the 2 clinical trials. Thus, clinical trials that test new therapies for juvenile DM should be easier to design, conduct, and compare.

ACKNOWLEDGMENTS

We thank the following individuals for providing invaluable input and feedback on project development and support: Dr. Daniel Aletaha (European League Against Rheumatism), Drs. Suzette Peng and Sarah Yim (Food and Drug Administration), Drs. Thorsten Vetter and Richard Vesely (European Medicines Agency), Bob Goldberg and Theresa Curry (The Myositis Association), Rhonda McKeever and Patti Lawler (Cure JM Foundation), and Irene Oakley (Myositis UK). We also thank Drs. Michael Ward and Steven Pavletic for their critical review of the manuscript. Paul Hansen, who with Franz Ombler owns and co-invented the 1000Minds software referred to in the article, provided intellectual and logistic support for this project.

AUTHOR CONTRIBUTIONS

All authors were involved in drafting the article or revising it critically for important intellectual content, and all authors approved the final version to be published. Drs. Rider and Ruperto had full access to all of the data in the study and take responsibility for the integrity of the data and the accuracy of the data analysis.

Study conception and design. Rider, Aggarwal, Miller, Vencovsky, Ruperto.

Acquisition of data. Rider, Aggarwal, Pistorio, Bayat, Erman, Feldman, Huber, Cimaz, Cuttica, de Oliveira, Lindsley, Pilkington, Punaro, Ravelli, Reed, Rouster-Stevens, van Royen-Kerkhof, Dressler, Magalhaes, Constantin, Davidson, Magnusson, Russo, Villa, Rinaldi, Rockette, Lachenbruch, Vencovsky, Ruperto.

Analysis and interpretation of data. Rider, Aggarwal, Pistorio, Bayat, Erman, Feldman, Huber, Rockette, Lachenbruch, Miller, Vencovsky, Ruperto.

REFERENCES

1. Rider LG, Werth VP, Huber AM, Alexanderson H, Rao AP, Ruperto N, et al. Measures of adult and juvenile dermatomyositis, polymyositis, and inclusion body myositis: Physician and Patient/Parent Global Activity, Manual Muscle Testing (MMT), Health Assessment Questionnaire (HAQ)/Childhood Health Assessment Questionnaire (C-HAQ), Childhood Myositis Assessment Scale (CMAS), Myositis Disease Activity Assessment Tool (MDAAT), Disease Activity Score (DAS), Short Form 36 (SF-36), Child Health Questionnaire (CHQ), Physician Global Damage, Myositis Damage Index (MDI), Quantitative Muscle Testing (QMT), Myositis Functional Index-2 (FI-2), Myositis Activities Profile (MAP), Inclusion Body Myositis Functional Rating Scale (IBMFRS), Cutaneous Dermatomyositis Disease Area and Severity Index (CDASI), Cutaneous Assessment Tool (CAT), Dermatomyositis Skin Severity Index (DSSI), Skindex, and Dermatology Life Quality Index (DLQI). Arthritis Care Res (Hoboken) 2011;63 Suppl 11:S118–57.
2. Miller FW, Rider LG, Chung YL, Cooper R, Danko K, Farewell V, et al. Proposed preliminary core set measures for disease outcome assessment in adult and juvenile idiopathic inflammatory myopathies. Rheumatology (Oxford) 2001;40:1262–73.
3. Rider LG, Giannini EH, Harris-Love M, Joe G, Isenberg D, Pilkington C, et al. Defining clinical improvement in adult and juvenile myositis. J Rheumatol 2003;30:603–17.
4. Ruperto N, Ravelli A, Murray KJ, Lovell DJ, Andersson-Gare B, Feldman BM, et al. Preliminary core sets of measures for disease activity and damage assessment in juvenile systemic lupus erythematosus and juvenile dermatomyositis. Rheumatology (Oxford) 2003;42:1452–9.
5. Ruperto N, Ravelli A, Pistorio A, Ferriani V, Calvo I, Ganser G, et al. The provisional Paediatric Rheumatology International Trials Organisation/American College of Rheumatology/European League Against Rheumatism Disease Activity Core Set for the Evaluation of Response to Therapy in Juvenile Dermatomyositis: a prospective validation study. Arthritis Rheum 2008;59:4–13.
6. Ruperto N, Martini A. Networking in paediatrics: the example of the Paediatric Rheumatology International Trials Organisation (PRINTO). Arch Dis Child 2011;96:596–601.
7. Singh G, Athreya BH, Fries JF, Goldsmith DP. Measurement of health status in children with juvenile rheumatoid arthritis. Arthritis Rheum 1994;37:1761–9.
8. Bode RK, Klein-Gitelman MS, Miller ML, Lechman TS, Pachman LM. Disease Activity Score for children with juvenile

dermatomyositis: reliability and validity evidence. Arthritis Rheum 2003;49:7–15.
9. Rider LG, Giannini EH, Brunner HI, Ruperto N, James-Newton L, Reed AM, et al. International consensus on preliminary definitions of improvement in adult and juvenile myositis. Arthritis Rheum 2004;50:2281–90.
10. Ruperto N, Pistorio A, Ravelli A, Rider LG, Pilkington C, Oliveira S, et al. The Paediatric Rheumatology International Trials Organization provisional criteria for the evaluation of response to therapy in juvenile dermatomyositis. Arthritis Care Res (Hoboken) 2010;62:1533–41.
11. Hasija R, Pistorio A, Ravelli A, Demirkaya E, Khubchandani R, Guseinova D, et al. Therapeutic approaches in the treatment of juvenile dermatomyositis in patients with recent-onset disease and in those experiencing disease flare: an international multicenter PRINTO study. Arthritis Rheum 2011;63:3142–52.
12. Ruperto N, Pistorio A, Ravelli A, Hasija R, Guseinova D, Filocamo G, et al. Criteria to define response to therapy in paediatric rheumatic diseases. Eur J Clin Pharmacol 2011;67 Suppl 1:125–31.
13. Ruperto N, Pistorio A, Oliveira S, Zulian F, Cuttica R, Ravelli A, et al. Prednisone versus prednisone plus ciclosporin versus prednisone plus methotrexate in new-onset juvenile dermatomyositis: a randomised trial. Lancet 2016;387:671–8.
14. Felson DT, Furst DE, Boers M. Rationale and strategies for reevaluating the ACR20. J Rheumatol 2007;34:1184–7.
15. Rider LG, Ruperto N, Pistorio A, Erman B, Bayat N, Lachenbruch PA, et al. 2016 development of adult dermatomyositis and polymyositis and juvenile dermatomyositis response criteria: methodological aspects: an American College of Rheumatology/European League Against Rheumatism/International Myositis Assessment and Clinical Studies Group/Paediatric Rheumatology International Trials Organisation Collaborative Initiative. Rheumatology (Oxford) 2016. In press.
16. Rider LG, Aggarwal R, Bayat N, Erman B, Feldman BM, Huber AM, et al. A hybrid conjoint analysis model is proposed as the definition of minimal, moderate and major clinical improvement in juvenile dermatomyositis clinical trials [abstract]. Arthritis Rheumatol 2014;66 Suppl:S578.
17. Aggarwal R, Rider LG, Ruperto N, Bayat N, Erman B, Feldman BM, et al. A consensus hybrid definition using a conjoint analysis is the proposed response criteria for minimal and moderate improvement for adult polymyositis and dermatomyositis clinical trials [abstract]. Arthritis Rheumatol 2014;66 Suppl:S404.
18. Aggarwal R, Rider LG, Ruperto N, Bayat N, Erman B, Feldman BM, et al. 2016 American College of Rheumatology/European League Against Rheumatism criteria for minimal, moderate, and major clinical response in adult dermatomyositis and polymyositis: an International Myositis Assessment and Clinical Studies Group/Paediatric Rheumatology International Trials Organisation collaborative initiative. Arthritis Rheumatol 2017;69:898–910.
19. Neogi T, Jansen TL, Dalbeth N, Fransen J, Schumacher HR, Berendsen D, et al. 2015 gout classification criteria: an American College of Rheumatology/European League Against Rheumatism collaborative initiative. Arthritis Rheumatol 2015;67:2557–68.
20. Utz KS, Hoog J, Wentrup A, Berg S, Lammer A, Jainsch B, et al. Patient preferences for disease-modifying drugs in multiple sclerosis therapy: a choice-based conjoint analysis. Ther Adv Neurol Disord 2014;7:263–75.
21. Amaya-Amaya M, Gerard K, Ryan M. Discrete choice experiments in a nutshell. In: Ryan M, Gerard K, Amaya-Amaya M, editors. Using discrete choice experiments to value health and health care. Dordrecht: Springer; 2008.
22. De Bekker-Grob E, Ryan M, Gerard K. Discrete choice experiments in health economics: a review of the literature. Health Econ 2012;21:145–72.
23. De Lautour H, Taylor WJ, Adebajo A, Alten R, Burgos-Vargas R, Chapman P, et al. Development of preliminary remission criteria for gout using Delphi and 1000Minds consensus exercises. Arthritis Care Res (Hoboken) 2016;68:667–72.
24. Hansen P, Ombler F. A new method for scoring additive multi-attribute value models using pairwise rankings of alternatives. J Multi-Crit Decis Anal 2008;15:87–107.
25. Oddis CV, Reed AM, Aggarwal R, Rider LG, Ascherman DP, Levesque MC, et al. Rituximab in the treatment of refractory adult and juvenile dermatomyositis and adult polymyositis: a randomized, placebo-phase trial. Arthritis Rheum 2013;65:314–24.
26. Metz CE. Basic principles of ROC analysis. Semin Nucl Med 1978;8:283–98.
27. Finney DJ. Statistical method in biological assay. 3rd ed. London: Charles Griffin; 1978.
28. Liengme BV. A guide to Microsoft Excel 2002 for scientists and engineers. 3rd ed. Oxford: Butterworth-Heinemann; 2002.
29. Ruperto N, Meiorin S, Iusan SM, Ravelli A, Pistorio A, Martini A. Consensus procedures and their role in pediatric rheumatology. Curr Rheumatol Rep 2008;10:142–6.
30. Delbecq A, van de Ven A, Gustafson D. Group techniques for program planning: a guide to nominal group and Delphi processes. Glenview (IL): Scott, Foresman and Company; 1975.
31. Ruperto N, Ozen S, Pistorio A, Dolezalova P, Brogan P, Cabral DA, et al. EULAR/PRINTO/PRES criteria for Henoch-Schonlein purpura, childhood polyarteritis nodosa, childhood Wegener granulomatosis and childhood Takayasu arteritis: Ankara 2008. Part I: overall methodology and clinical characterisation. Ann Rheum Dis 2010;69:790–7.
32. Piram M, Kone-Paut I, Lachmann HJ, Frenkel J, Ozen S, Kuemmerle-Deschner J, et al. Validation of the auto-inflammatory diseases activity index (AIDAI) for hereditary recurrent fever syndromes. Ann Rheum Dis 2014;73:2168–73.
33. American College of Rheumatology Committee to Reevaluate Improvement Criteria. A proposed revision to the ACR20: the hybrid measure of American College of Rheumatology response. Arthritis Rheum 2007;57:193–202.
34. Streiner DL. Breaking up is hard to do: the heartbreak of dichotomizing continuous data. Can J Psychiatry 2002;47:262–6.
35. Felson DT, Anderson JJ, Boers M, Bombardier C, Furst D, Goldsmith C, et al. American College of Rheumatology preliminary definition of improvement in rheumatoid arthritis. Arthritis Rheum 1995;38:727–35.
36. Giannini EH, Ruperto N, Ravelli A, Lovell DJ, Felson DT, Martini A. Preliminary definition of improvement in juvenile arthritis. Arthritis Rheum 1997;40:1202–9.
37. Consolaro A, Ruperto N, Bazso A, Pistorio A, Magni-Manzoni S, Filocamo G, et al. Development and validation of a composite disease activity score for juvenile idiopathic arthritis. Arthritis Rheum 2009;61:658–66.
38. Volochayev R, Csako G, Wesley R, Rider LG, Miller FW. Laboratory test abnormalities are common in polymyositis and dermatomyositis and differ among clinical and demographic groups. Open Rheumatol J 2012;6:54–63.

APPENDIX A: MEMBERS OF THE INTERNATIONAL MYOSITIS ASSESSMENT AND CLINICAL STUDIES GROUP AND THE PAEDIATRIC RHEUMATOLOGY INTERNATIONAL TRIALS ORGANISATION WHO CONTRIBUTED TO DEVELOPING THE RESPONSE CRITERIA

Steering committee: Lisa G. Rider (co–principal investigator), Nicolino Ruperto (co–principal investigator), Rohit Aggarwal (methodology lead), Frederick W. Miller, Jiri Vencovsky.

Statistical team: Rohit Aggarwal, Brian Erman, Nastaran Bayat, Angela Pistorio, Adam M. Huber, Brian M. Feldman, Paul Hansen, Howard Rockette, Peter A. Lachenbruch, Nicolino Ruperto, Lisa G. Rider.

Pediatric core set survey group: Maria Apaz, Suzanne Bowyer, Rolando Cimaz, Tamás Constantin, Megan Curran, Joyce Davidson, Brian M. Feldman, Thomas Griffin, Adam H. Huber, Olcay Jones, Susan Kim, Bianca Lang, Carol Lindsley, Daniel Lovell, Claudia Saad Magalhaes, Lauren M. Pachman, Clarissa Pilkington, Andrea Ponyi, Marilynn Punaro, Pierre Quartier, Athimalaipet V. Ramanan, Angelo Ravelli, Ann Reed, Robert Rennebohm, David D. Sherry, Clovis A. Silva, Elizabeth Stringer, Annet van Royen-Kerkhof, Carol Wallace.

Clinical trial or natural history study data set contributors: Frederick W. Miller, Chester V. Oddis, Ann Reed, Lisa G. Rider, Nicolino Ruperto, and PRINTO members.

Pediatric patient profile working group: Maria Apaz, Tadej Avcin, Mara Becker, Michael W. Beresford, Rolando Cimaz, Tamás Constantin, Megan Curran, Ruben Cuttica, Joyce Davidson, Frank Dressler, Jeffrey Dvergsten, Sheila Knupp Feitosa de Oliveira, Brian M. Feldman, Virginia Paes Leme Ferriani, Berit Flato, Valeria Gerloni, Thomas Griffin, Michael Henrickson, Claas Hinze, Mark Hoeltzel, Adam M. Huber, Maria Ibarra, Norman Ilowite, Lisa Imundo, Olcay Jones, Susan Kim, Daniel Kingsbury, Bianca Lang, Carol Lindsley, Daniel Lovell, Alberto Martini, Claudia Saad Magalhaes, Bo Magnusson, Sheilagh Maguiness, Susan Maillard, Pernille Mathiesen, Liza McCann, Susan Nielsen, Lauren M. Pachman, Murray Passo, Clarissa Pilkington, Marilynn Punaro, Pierre Quartier, Egla Rabinovich, Athimalaipet V. Ramanan, Angelo Ravelli, Ann Reed, Robert Rennebohm, Lisa G. Rider, Rafael Rivas-Chacon, Angela Byun Robinson, Kelly Rouster-Stevens, Ricardo Russo, Lidia Rutkowska-Sak, Adriana Sallum, Helga Sanner, Heinrike Schmeling, Duygu Selcen, Bracha Shaham, David D. Sherry, Clovis A. Silva, Charles H. Spencer, Robert Sundel, Marc Tardieu, Akaluck Thatayatikom, Janjaap van der Net, Annet van Royen-Kerkhof, Dawn Wahezi, Carol Wallace, Francesco Zulian.

Conjoint analysis, pediatric group: Rolando Cimaz, Tamás Constantin, Ruben Cuttica, Joyce Davidson, Frank Dressler, Sheila Knupp Feitosa de Oliveira, Brian M. Feldman, Thomas Griffin, Michael Henrickson, Adam M. Huber, Lisa Imundo, Bianca Lang, Carol Lindsley, Claudia Saad Magalhaes, Bo Magnusson, Susan Maillard, Lauren M. Pachman, Murray Passo, Clarissa Pilkington, Marilynn Punaro, Angelo Ravelli, Ann Reed, Lisa G. Rider, Kelly Rouster-Stevens, Ricardo Russo, Bracha Shaham, Robert Sundel, Janjaap van der Net, Annet van Royen-Kerkhof.

Participants in consensus conference, pediatric working group: Rolando Cimaz, Rubén Cuttica, Sheila Knupp Feitosa de Oliveira, Brian M. Feldman, Adam M. Huber, Carol B. Lindsley, Clarissa Pilkington, Marilynn Punaro, Angelo Ravelli, Ann Reed, Kelly Rouster-Stevens, Annet van Royen-Kerkhof.

Participants in consensus conference, adult working group: Anthony Amato, Hector Chinoy, Robert G. Cooper, Maryam Dastmalchi, Marianne de Visser, David Fiorentino, David Isenberg, James Katz, Andrew Mammen, Chester V. Oddis, Jiri Vencovsky, Steven R. Ytterberg.

ARTHRITIS & RHEUMATOLOGY
Vol. 69, No. 5, May 2017, pp 924–925
DOI 10.1002/art.40072

SPECIAL ARTICLE

Winners of the 2016 American College of Rheumatology Annual Image Competition

American College of Rheumatology Image Library Subcommittee

The mission of the Image Library Subcommittee is to provide ACR members, as well as the entire medical community, access to a wide variety of clinical images to help educators effectively present the manifestations of the rheumatologic diseases. Additionally, our images have been widely used in peer-reviewed publications and textbooks. Since its inception, the ACR Image Library has become the preeminent collection devoted to the rheumatologic diseases. The collection is a dynamic one, changing yearly because of submissions from the medical community. The Image Library Subcommittee meets annually to review these new images and awards prizes based on the panel's consensus. Additionally, many nonwinners are introduced into the image library; greatly enhancing the collection. For the 2016 competition, more than 100 entries were received. The subcommittee carefully evaluates each entry. Winners, as well as those images selected for inclusion, are chosen based on image quality and educational value.

The 2016 grand prize winner was a series of images showing coronary and other aneurysms in a patient with polyarteritis nodosa (Figure 1). In the still-image category, the winner was a depiction of pachyderma in a patient with hypertrophic osteoarthropathy (Figure 2). The case study category winner was a series of radiographic and histologic images showing nodal and extranodal involvement in a girl with Rosai-Dorfman disease (Figure 3).

Honorable mention was awarded to images of the following: rheumatoid arthritis: elbow erosions (Sandra Chatrand, MD), cardiac sarcoidosis: ventricular enhancement with noncaseating endomyocardial granulomas (Shakaib Hayat, DO), gout: double contour sign (Jawad Bilal, MD), Sjögren's syndrome: parotid pseudolymphoma (Santhanam Lakshminarayanan, MD), idiopathic transient osteoporosis: left hip (Aaradhana Kaul,

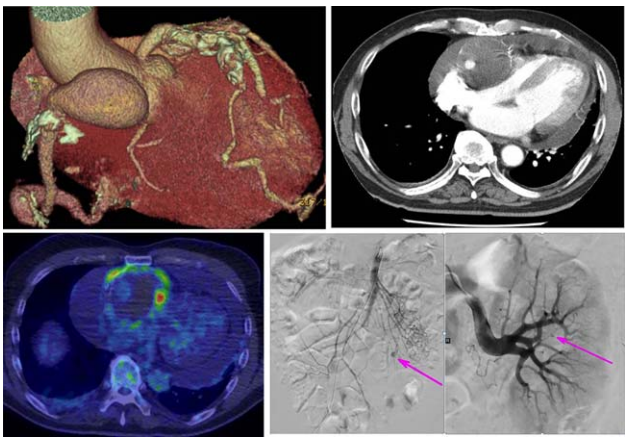

Figure 1. Polyarteritis nodosa: coronary and other aneurysms. The patient, a 64-year-old man with type 2 diabetes mellitus and hypertension, presented with a 2-month history of fever, weight loss, and cough. The C-reactive protein level was 16 mg/dl. Imaging studies revealed a giant coronary aneurysm (top left and right) and pericarditis. Inflammation of the right coronary artery was detected by ^{18}F-fluorodeoxyglucose–based positron emission tomography (bottom left). He had no medical history consistent with Kawasaki disease. Antineutrophil cytoplasmic antibodies (myeloperoxidase and proteinase 3) and antinuclear antibodies were absent. Results of testing for hepatitis B, hepatitis C, tuberculosis, *Chlamydia pneumoniae*, HIV, syphilis, and *Mycoplasma* were all negative, as were cultures from the pericardial effusion. Aneurysms of the superior mesenteric and renal arteries were detected (bottom middle and right) (**arrows**), and polyarteritis nodosa was diagnosed. After a course of glucocorticoid treatment, the pericardial effusion completely subsided and the patient's general condition improved. Submitted by Koji Takasugi, MD, Nagoya, Japan.

Members of the Image Library Subcommittee of the American College of Rheumatology Committee on Education: Brian J. Keroack, MD, Portland, ME (Chair); Alan N. Baer, MD, Baltimore, MD; Brian E. Daikh, MD, Portland, ME; Eric P. Gall, MD, Tucson, AZ; Kristine M. Lohr, MD, Lexington, KY; Janet Maynard, MD, Baltimore, MD; Erika H. Noss, MD, Seattle, WA; Andrea Ramirez, MD, Houston, TX; Mary Christenson, PT, PhD, Berthoud, CO (ARHP representative); Noel Heath, OT, Thunder Bay, Ontario, Canada (ARHP representative); Michael Jennings, RT, CBDT, New Lebanon, NY (ARHP representative).

Submitted for publication February 9, 2017; accepted February 9, 2017.

Figure 2. Hypertrophic osteoarthropathy: pachyderma ("bulldog" appearance). The patient, a 30-year-old man, presented with coarsening of the skin with clubbing of all digits. He had pain and swelling of multiple joints and bones. There was no family history of rheumatologic disease. On further investigation he was found to have cirrhosis of the liver with chronic hepatitis B infection. Submitted by Nibha Jain, MD, Ahmedbad, India.

MD), de Quervain's tenosynovitis: ultrasound (Mario Chavez-Lopez, MD), and rheumatoid arthritis–associated interstitial lung disease: airway-centered cystic disease with bronchiole compression from lymphoplasmacytic inflammation and follicles (Milena Cavalcante, MD).

The winning submissions, as well as several other outstanding images, will be added to the library. The digital format of the library provides the worldwide medical community with 24/7 real-time access. The collection features contributions from all over the world and is critical in advancing rheumatology education. Since its launch in 2009, the Rheumatology Image Library has received over 2.5 million unique visitors worldwide. To view the newest images, visit the Rheumatology Image Library at http://images.rheumatology.org.

As mentioned, the image library is a dynamic enterprise. We need you to consider submitting so this endeavor can continue to provide cutting-edge information for both new and experienced rheumatologists. The Image Library Subcommittee targets not only images that illustrate rheumatologic conditions, but also those that are relevant to rheumatology practice. If you think your image(s) have the "right stuff," please submit them. Go to http://images.rheumatology.org for competition rules and entry/deadline dates. If you have any questions regarding the image competition, please contact education@rheumatology.org.

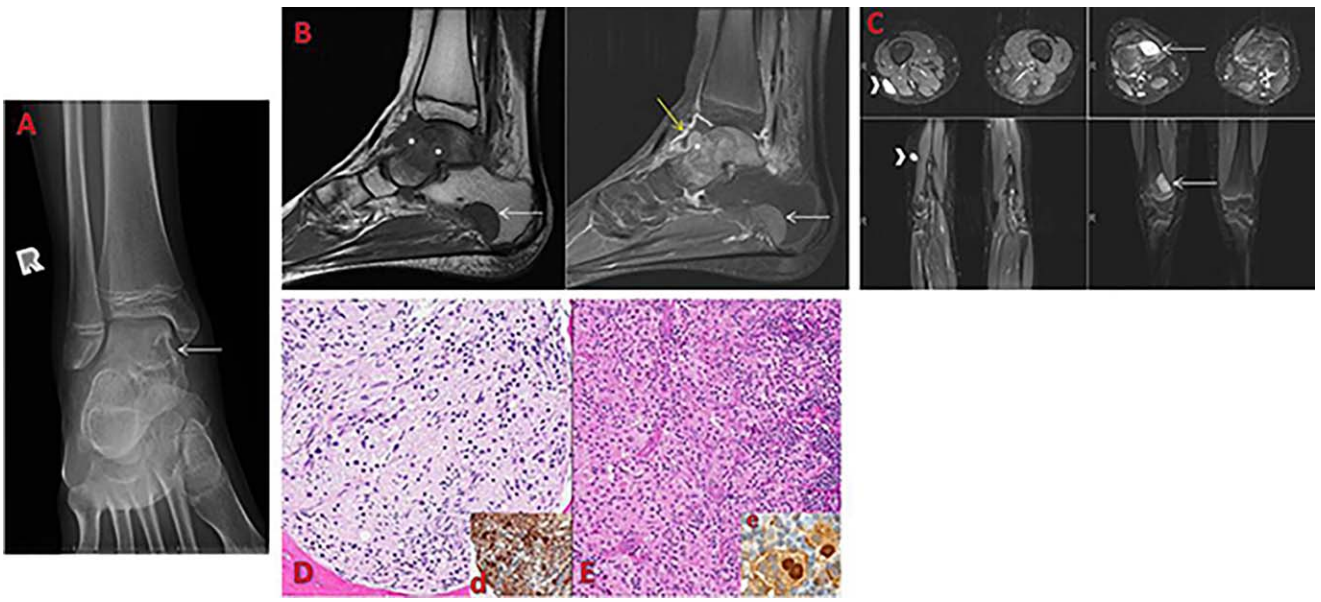

Figure 3. Sinus histiocytosis with massive lymphadenopathy (Rosai-Dorfman disease): nodal and extranodal involvement. The patient, an 11-year-old girl, presented with right ankle and left elbow pain. On physical examination, tibiotalar and elbow synovitis, prominent cervical lymphadenopathy, and a palpable thigh nodule were found. Radiography (**A**) and magnetic resonance imaging (**B** and **C**) demonstrated multifocal bony lesions (**white arrows** and **asterisks**), some resulting in cortical disruption, and massive lymphadenopathy. A tibiotalar effusion with synovial thickening (**yellow arrow**) and subcutaneous nodules (**arrowheads**) were also seen. Initial talar bone biopsy revealed features of chronic osteomyelitis with lymphocytic and histiocytic infiltration (**D**). Excisional biopsy of an enlarged cervical lymph node (**E**) showed diffuse sinusoidal infiltration of S100-immunostaining histiocytes in a sinusoidal pattern (**e**). Further S100 immunostaining of the bone biopsy sample revealed a small cluster of Rosai-Dorfman disease cells at the edge of the specimen (**d**). Emperipolesis (ingestion) of lymphocytes is seen in the cytoplasm of these large histiocytic cells. Some of the lesions resolved after 4 months of treatment with nonsteroidal antiinflammatory drugs and oral corticosteroids. Submitted by Laura Tasan, MD, Pittsburgh, PA. Other contributors: Sameh S. Tadros, Jennifer Picarsic, and Kathryn Torok.

ARTHRITIS & RHEUMATOLOGY
Vol. 69, No. 5, May 2017, pp 926–931
DOI 10.1002/art.40062

BRIEF REPORT

Clinical Trials Aiming to Prevent Rheumatoid Arthritis Cannot Detect Prevention Without Adequate Risk Stratification: A Trial of Methotrexate Versus Placebo in Undifferentiated Arthritis as an Example

Leonie E. Burgers, Cornelia F. Allaart, Tom W. J. Huizinga, and Annette H. M. van der Helm-van Mil

Objective. **Prevention of rheumatoid arthritis (RA) was the aim of several trials in undifferentiated arthritis (UA), with overall negative results. As preparatory work has revealed that only ~30% of UA patients progress to having RA, we hypothesized that inclusion of patients without imminent RA could lead to false-negative results. We undertook this study to evaluate this hypothesis by reinvestigating the Probable Rheumatoid Arthritis: Methotrexate versus Placebo Treatment (PROMPT) trial (a 1-year course of methotrexate [MTX] versus placebo in UA) after excluding patients without a high risk of developing RA.**

Methods. **A validated prediction model was used to determine the risk of RA in all patients included in the PROMPT trial. Patients with a prediction score of ≥8 (positive predictive value of ≥84% for developing RA) were considered to have a high risk of developing RA. The effect of a 1-year course of MTX during 5 years of follow-up was reinvestigated in these patients.**

Results. **Twenty-two of the 110 patients in the PROMPT trial had a high risk of RA at baseline. In the MTX arm, 6 of 11 patients (55%) developed RA, compared to 11 of 11 patients (100%) in the placebo arm ($P = 0.011$). Time to RA development was longer in the MTX arm than in the placebo arm (median 22.5 months versus 3 months; $P < 0.001$). Drug-free remission was achieved by 4 of 11 patients (36%) in the MTX arm compared to 0 of 11 patients (0%) in the placebo arm ($P = 0.031$). These beneficial effects of MTX were observed both in anti–citrullinated protein antibody (ACPA)–positive and in ACPA-negative UA patients with a high risk of RA, but not in UA patients without a high risk of RA. In retrospect, 43 of 110 patients fulfilled the American College of Rheumatology/European League Against Rheumatism 2010 classification criteria for RA at baseline. In addition, beneficial effects were observed only in patients with a high prediction score.**

Conclusion. **A 1-year course of MTX delayed and prevented RA development in high-risk UA patients. This emphasizes the importance of adequate risk prediction in trials that aim to prevent RA.**

Disease outcomes in rheumatoid arthritis (RA) have improved dramatically since the introduction of biologic agents and improved treatment strategies. Nevertheless, the majority of patients still require prolonged, if not lifelong, therapy. Therefore, the ultimate goal would be prevention of RA.

Before RA is diagnosed, many patients present with undifferentiated arthritis (UA) or with arthralgia. Clinical trials in patients presenting with arthralgia are still scarce (1), but several trials have evaluated whether intervention with disease-modifying antirheumatic drugs (DMARDs) in UA is effective in preventing progression to classifiable RA (2–6). The results of these trials were mixed, but none of the trials showed that RA development could be prevented by early intervention with DMARDs (see Supplementary Table 1, available on the *Arthritis & Rheumatology* web site at http://onlinelibrary.wiley.com/doi/10.1002/art.40062/abstract). The finding that there was no improved outcome if disease-modifying treatment was started in the phase of UA is surprising and is in contrast to results of multiple observational studies that clearly showed the benefit of early intervention in RA (7). Altogether, this raises the

Supported by a Vidi grant from the Netherlands Organisation for Scientific Research (NWO). The Probable Rheumatoid Arthritis: Methotrexate versus Placebo Treatment trial was supported by the Dutch Arthritis Foundation (grant NR-02-01-301) and the NWO (grant 920-03-259).

Leonie E. Burgers, MD, Cornelia F. Allaart, MD, PhD, Tom W. J. Huizinga, MD, PhD, Annette H. M. van der Helm-van Mil, MD, PhD: Leiden University Medical Centre, Leiden, The Netherlands.

Address correspondence to Leonie E. Burgers, MD, Leiden University Medical Centre, Department of Rheumatology, C-01-046, PO Box 9600, 2300 RC Leiden, The Netherlands. E-mail: l.e.burgers@lumc.nl.

Submitted for publication August 12, 2016; accepted in revised form January 31, 2017.

question of whether the principle of "the earlier the better" does not apply to the phase of UA.

One of the trials that showed no benefit of DMARD initiation in patients with UA is the Probable Rheumatoid Arthritis: Methotrexate versus Placebo Treatment (PROMPT) trial (6). This study evaluated the effect of a 1-year course of methotrexate (MTX) versus placebo in 110 UA patients. After a follow-up period of 5 years, no preventive effect of MTX on RA development was observed.

Previous studies have investigated the natural course of UA in patients and have shown that ~30% of patients will develop RA (the remaining 70% have other diagnoses or achieve spontaneous remission, or their disease remains unclassified) (8). Ideally, only patients that truly have imminent RA should be included in pre-RA trials, as inclusion of all other UA patients could dilute a possible preventive effect and lead to Type II errors (false-negative results).

The problem of inclusion of uninformative patients has been described previously in other fields of medicine, for example, in trials that aimed to reduce mortality in sepsis (9,10). Although encouraging results were frequently observed in phase I and phase II studies, phase III trials repeatedly failed to demonstrate statistically significant results. This was presumably due to the fact that the inclusion criteria for these trials were broad and heterogeneous groups of patients were included, including patients who were a priori unlikely to benefit from treatment.

A solution to this problem can be postrandomization exclusion of uninformative patients. This method allows exclusion of patient data from analysis in certain cases, without risking bias. However, postrandomization exclusion is only allowed when the excluded uninformative patients can already be identified as being uninformative at the time treatment decisions have to be made in clinical practice. Otherwise, postrandomization exclusion could lead to misleading results (9). Therefore, in the case of the PROMPT trial, postrandomization exclusion is only allowed when uninformative UA patients without a high risk of progression to RA can already be identified at the time of first presentation.

Around the time that the PROMPT trial finished, a model to predict the risk of RA development in UA patients became available (11). This prediction model is now well established and widely replicated and offers the opportunity to identify those UA patients who have a high risk of developing RA (12,13). This model therefore enables postrandomization exclusion of patients without a high risk of RA. Therefore, in the present study, we aimed to analyze the effect of a 1-year course of MTX in high-risk UA patients by reanalyzing the PROMPT study after postrandomization exclusion of patients without a high risk of developing RA.

PATIENTS AND METHODS

Patients. All patients in the current study were included in the PROMPT trial. This trial was a prospective double-blind, randomized, placebo-controlled multicenter study that evaluated the effect of a 1-year course of MTX versus placebo in UA patients. All patients included in this trial fulfilled the diagnostic criteria for probable RA as revised in 1958 (14), were DMARD naive, and had a symptom duration of <2 years. After the first year, the study drug was tapered and discontinued in all patients unless patients had developed RA during the first year. In that case, study medication was switched to open-label MTX. Other DMARDs or steroids were not allowed during the study period unless patients developed RA. Nonsteroidal antiinflammatory drugs were allowed during the entire study period.

Risk stratification. The well-validated Leiden prediction rule was used to predict the risk of RA development in all patients included in the PROMPT trial (11–13). This rule results in a prediction score ranging from 0 to 14. Previous studies revealed that in UA patients with a score of ≥8, the positive predictive value for developing RA was ≥84%. It has been suggested that if treatment decisions are to be made based on this prediction rule, a cutoff score of 8 should be used for initiating treatment (11). Therefore, patients with a prediction score of ≥8 were considered to have a high risk of developing RA and were included in the current study.

Outcome measures. Similar to the main study (6), the main outcome measure was fulfillment of the American College of Rheumatology (ACR) 1987 revised classification criteria for RA (15) after 5 years of follow-up. A secondary outcome measure was the proportion of patients achieving drug-free remission without progression to RA.

Statistical analysis. Chi-square tests and Kaplan-Meier curves with log rank tests were used as described previously (6).

RESULTS

Results without risk stratification. As reported previously, after 5 years of follow-up, 25 of 55 patients (45%) in the MTX arm had developed RA, compared to 29 of 55 patients (53%) in the placebo arm ($P = 0.45$). Also, the time to RA development was not significantly different between the 2 arms ($P = 0.11$) (Figure 1A). However, in anti–citrullinated protein antibody (ACPA)–positive patients, RA development was delayed significantly in the MTX arm compared to the placebo arm (median 18 months versus 6 months; $P < 0.001$) (Figure 1B). This delay was not observed in ACPA-negative patients (Figure 1C). No differences were observed between the 2 arms either in the number of patients who achieved drug-free remission or in the time to achieve drug-free remission (Figure 1D).

Results after risk stratification. By applying the Leiden prediction rule, 22 high-risk UA patients (11 in each arm) were identified in the PROMPT trial. The

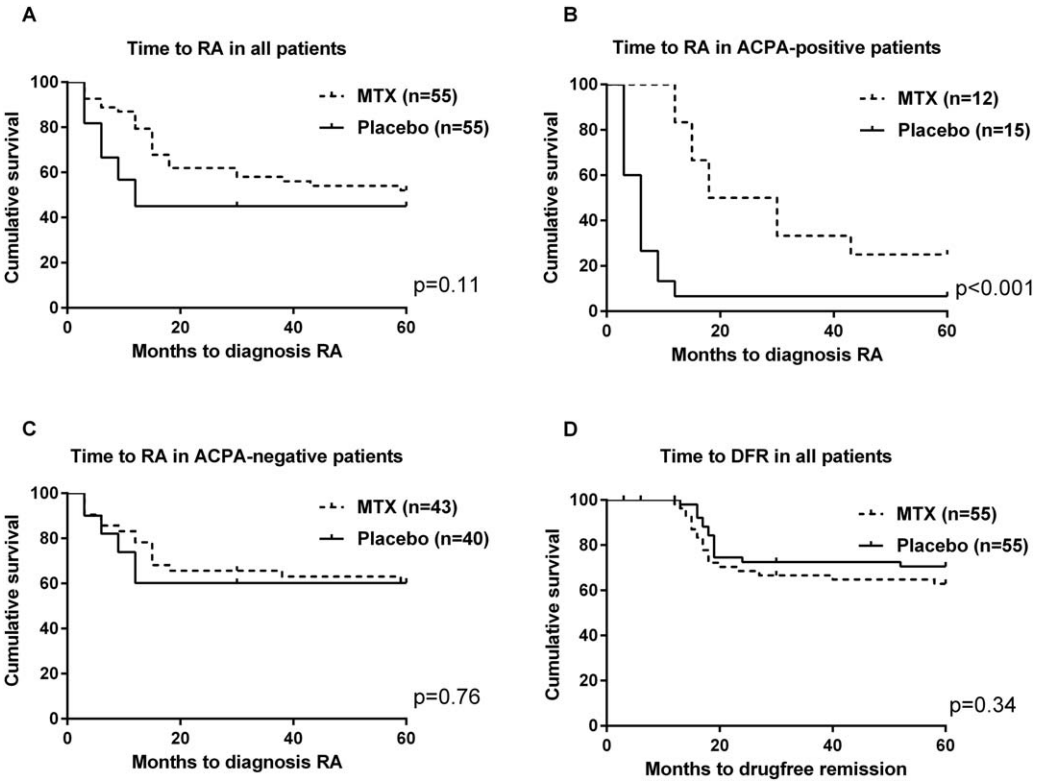

Figure 1. Main outcomes of the Probable Rheumatoid Arthritis: Methotrexate versus Placebo Treatment trial without risk stratification, as reported previously (6), with development of rheumatoid arthritis (RA) and drug-free remission (DFR) as outcome measures. Shown are Kaplan-Meier curves for time to RA development in all patients (**A**), in anti–citrullinated protein antibody (ACPA)–positive patients (**B**), and in ACPA-negative patients (**C**) as well as time to drug-free remission in all patients (**D**). MTX = methotrexate.

fact that the high-risk patients were randomized equally between the 2 treatment arms was based on chance. In the MTX arm, 6 of 11 patients (55%) developed RA, compared to 11 of 11 patients (100%) in the placebo arm ($P = 0.011$). Therefore, a 1-year course of MTX was associated with an absolute risk reduction of 45% in RA development, resulting in a number needed to treat (NNT) of 2.2 (95% confidence interval [95% CI] 1.3–6.2). Furthermore, Kaplan-Meier curves showed that RA development was significantly delayed in the MTX arm compared to the placebo arm (median 22.5 months versus 3 months until the 1987 revised criteria were fulfilled; $P < 0.001$) (Figure 2A). In addition, drug-free remission was achieved significantly more often in the MTX arm than in the placebo arm (36% versus 0%; $P = 0.027$).

As in the main study (6), a post hoc analysis was performed on ACPA-positive and ACPA-negative patients. Eighteen of the 22 high-risk UA patients were ACPA positive and 4 were ACPA negative. Evaluating only high-risk ACPA-positive patients revealed that, as in the main study, MTX delayed progression to RA ($P < 0.001$) (Figure 2B). However, when we evaluated the 4 high-risk ACPA-negative patients, a preventive effect of MTX was suggested as well. None of the 3 MTX-treated patients developed RA, while the placebo-treated patient did develop RA (Figure 2C).

We then evaluated the UA patients without a high risk of developing RA. These patients had a median prediction score of 6.1, and 75% of them had a prediction score of <7, which corresponds to a predicted risk of developing RA of <50% (13). Thus, the predicted risk in these patients was relatively low. In these patients, no significant beneficial effects of MTX were observed (Figure 3). The data therefore suggested a protective effect of MTX treatment for both ACPA-positive and ACPA-negative high-risk UA patients, but not for patients without a high risk of developing RA, regardless of their ACPA status. Finally, we stratified the outcome of drug-free remission by ACPA status and the predicted risk of developing RA, and we observed similar effects, namely, that MTX is beneficial only in high-risk UA patients (see

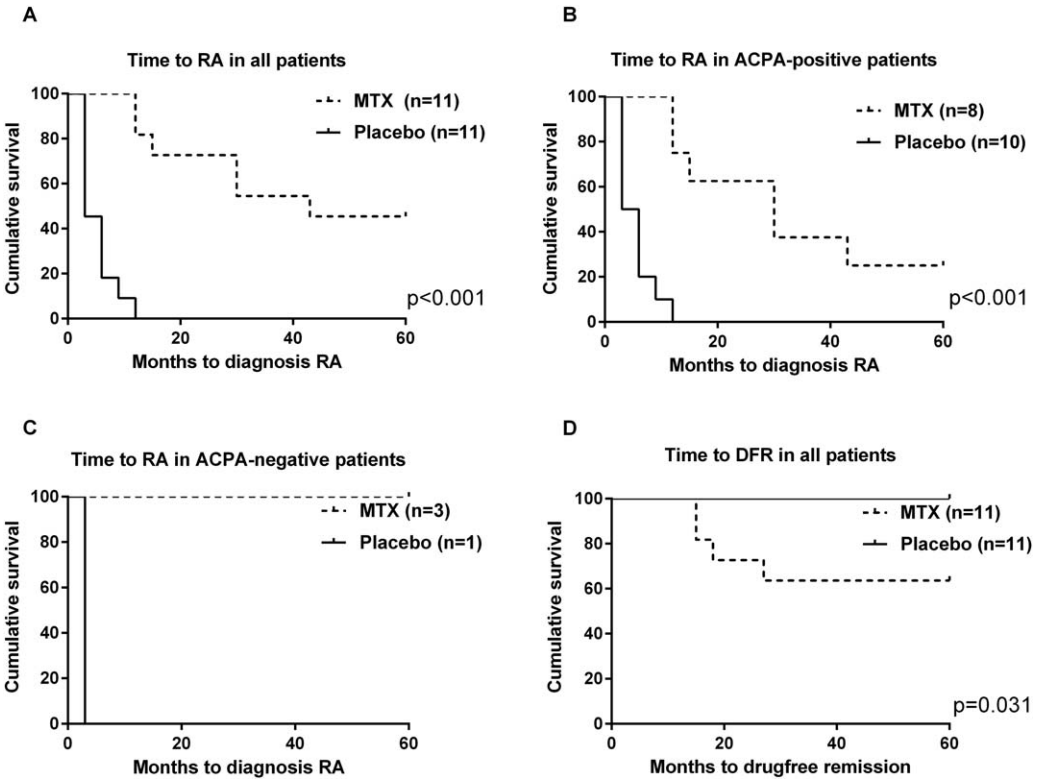

Figure 2. Main outcomes of the Probable Rheumatoid Arthritis: Methotrexate versus Placebo Treatment trial in patients with undifferentiated arthritis at high risk of developing RA, with development of RA and drug-free remission as outcome measures. Shown are Kaplan-Meier curves for time to RA development in all patients (**A**), in ACPA-positive patients (**B**), and in ACPA-negative patients (**C**) as well as time to drug-free remission in all patients (**D**). See Figure 1 for definitions.

Supplementary Figure 1, http://onlinelibrary.wiley.com/doi/10.1002/art.40062/abstract).

DISCUSSION

Evaluation of UA patients with a high risk of developing RA in the PROMPT trial revealed that MTX treatment prevented progression to RA with an estimated NNT of 2.2. The current findings suggest that the PROMPT trial yielded false-negative results due to the inclusion of UA patients without a high risk of developing RA. These data therefore illustrate how inclusion of uninformative patients can blur highly relevant study outcomes, such as prevention of RA.

When using the PROMPT trial as an example, the impact of uninformative patients on study outcome can clearly be observed, not only the impact on the main outcome, but also the impact on the subanalyses. Based on the findings of subanalyses that stratified by ACPA status, investigators in the main study suggested that MTX could delay the development of RA in ACPA-positive UA patients only (6). However, in patients with a high risk of developing RA, a preventive effect of MTX was observed both in ACPA-positive and in ACPA-negative patients, although the numbers of patients in these groups became small. Importantly, no such effect was observed in patients without a high risk of developing RA (Figure 3). The previous finding of a beneficial effect of MTX in ACPA-positive patients was presumably based on the fact that the ACPA-positive group contained more high-risk patients than did the ACPA-negative group. In other words, the interpretation of the results of the PROMPT trial may be, not that MTX is not effective in ACPA-negative patients, but that MTX is not effective in UA patients without a high risk of developing RA.

None of the clinical trials performed in UA used extensive risk stratification. As these trials generally showed negative results (2–6), the present observation led us to speculate whether the results of these trials would change if only patients with a high risk of RA were evaluated. Potentially, some other treatment strategies in UA might seem effective if uninformative patients were excluded.

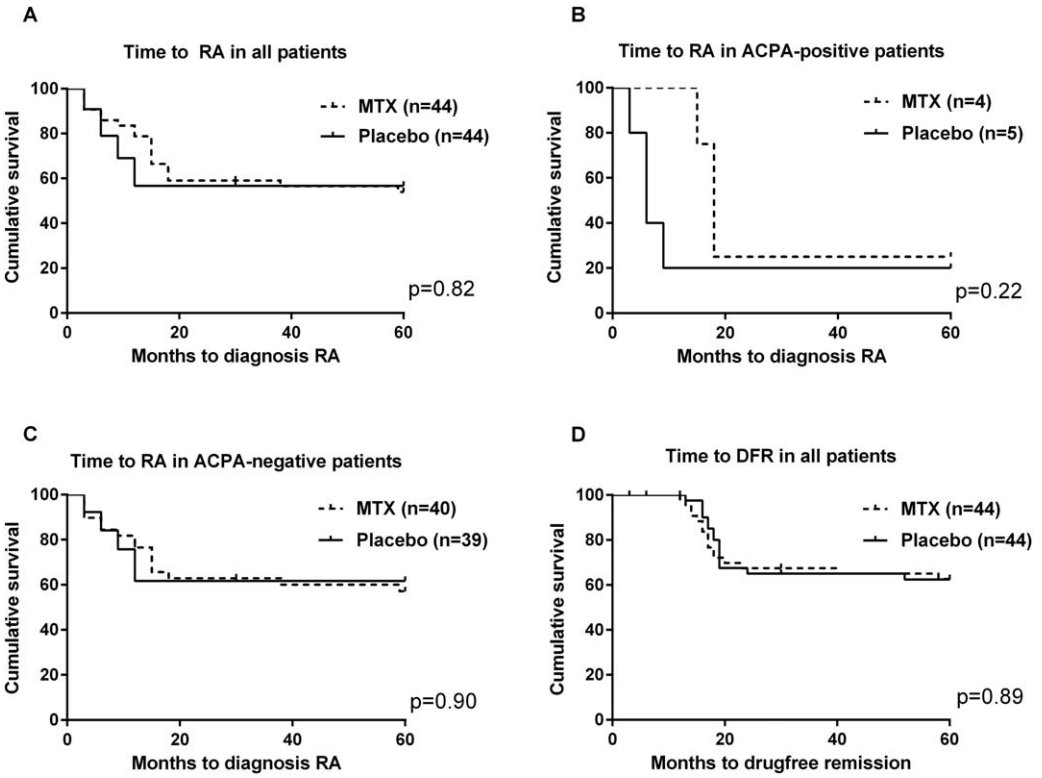

Figure 3. Main outcomes of the Probable Rheumatoid Arthritis: Methotrexate versus Placebo Treatment trial in patients with undifferentiated arthritis not at high risk of developing RA, with development of RA and drug-free remission as outcome measures. Shown are Kaplan-Meier curves for time to RA development in all patients (**A**), in ACPA-positive patients (**B**), and in ACPA-negative patients (**C**) as well as time to drug-free remission in all patients (**D**). See Figure 1 for definitions.

Of similar importance is the fact that the field is currently moving to perform trials in the prearthritis phase of arthralgia, with the ultimate aim of preventing development of RA. This move to even earlier treatment was made because treatment in the phase of clinical arthritis appeared not to be effective and was considered to be initiated "too late." At present we do not have validated models to accurately predict the risk of RA in patients who present with arthralgia. Observational studies in clinically suspected arthralgia or ACPA-positive arthralgia showed a 1-year risk of progression to clinical arthritis or RA of 32–35% (16,17) This bears the risk that two-thirds of the patients included in these trials will also be uninformative. The present data therefore underline the necessity of developing prediction models in patients with arthralgia who are at risk of RA, so that over time the results of these trials can be valued appropriately. Even though selecting only high-risk patients may make the recruitment of patients for pre-RA trials even more difficult, the current data suggest that it may positively affect the power of a study.

The PROMPT trial was performed prior to the development of the ACR/European League Against Rheumatism 2010 classification criteria for RA (18). Similarly, the prediction rule for RA development preceded the development of the 2010 criteria. In retrospect, 43 of 110 patients (39%) included in the PROMPT trial fulfilled the 2010 criteria at baseline. Of these patients, 18 had a high predicted risk of developing RA according to the 1987 revised criteria. Hence, only 4 of all 22 high-risk patients (18%) in the PROMPT trial did not fulfill the 2010 criteria for RA at baseline. Of these patients, 1 of 1 (100%) in the placebo arm developed RA according to the 1987 revised criteria compared to 1 of 3 (33%) in the MTX arm (see Supplementary Figure 2, http://onlinelibrary.wiley.com/doi/10.1002/art.40062/abstract). Because of the small numbers, no conclusions can be drawn about the efficacy of MTX in UA patients, when UA was defined as not fulfilling the 2010 criteria. Interestingly enough, within the group of RA patients who fulfilled the 2010 criteria, a preventive effect was observed in those with a high predicted risk of RA but not in those without a high predicted risk (see Supplementary Figure 3, http://onlinelibrary.wiley.com/doi/10.1002/art.40062/abstract).

Previous studies have shown that the 2010 criteria have lower specificity than the 1987 criteria (19,20), which can explain how patients can fulfill the criteria but

have a low predicted risk of RA. The presence of ACPAs is strongly weighted in the 2010 criteria, but the ACPA-positive patients (or patients meeting the 2010 criteria) without a high predicted risk of RA who were included in this study did not benefit from MTX (Figure 3 and Supplementary Figure 3).

The large drawback of the current post hoc analysis is the small sample size. All comparisons were based on a limited number of patients, and this was even more the case for subgroup analyses, for instance, those of ACPA-positive or ACPA-negative patients. Despite the small numbers large effects were observed, and therefore statistically significant results were obtained for the primary outcome, prevention of RA. Nonetheless, ideally the findings of the current post hoc analysis will be validated in a novel randomized clinical trial including only UA patients with a high risk of developing RA.

In conclusion, as shown in a reassessment of the PROMPT trial, inclusion of uninformative patients can importantly affect the results of trials aimed at preventing RA. As trials are now being conducted to evaluate the efficacy of treatment initiated in the phase of arthralgia, the development of adequate risk prediction models is important for preventing false-negative study results in the future.

AUTHOR CONTRIBUTIONS

All authors were involved in drafting the article or revising it critically for important intellectual content, and all authors approved the final version to be published. Dr. Burgers had full access to all of the data in the study and takes responsibility for the integrity of the data and the accuracy of the data analysis.

Study conception and design. Burgers, Allaart, Huizinga, van der Helm-van Mil.

Acquisition of data. Burgers, Allaart.

Analysis and interpretation of data. Burgers, Huizinga, van der Helm-van Mil.

REFERENCES

1. Bos WH, Dijkmans BA, Boers M, van de Stadt RJ, van Schaardenburg D. Effect of dexamethasone on autoantibody levels and arthritis development in patients with arthralgia: a randomised trial. Ann Rheum Dis 2010;69:571–4.
2. Saleem B, Mackie S, Quinn M, Nizam S, Hensor E, Jarrett S, et al. Does the use of tumour necrosis factor antagonist therapy in poor prognosis, undifferentiated arthritis prevent progression to rheumatoid arthritis? Ann Rheum Dis 2008;67:1178–80.
3. Emery P, Durez P, Dougados M, Legerton CW, Becker JC, Vratsanos G, et al. Impact of T-cell costimulation modulation in patients with undifferentiated inflammatory arthritis or very early rheumatoid arthritis: a clinical and imaging study of abatacept (the ADJUST trial). Ann Rheum Dis 2010;69:510–6.
4. Machold KP, Landewé R, Smolen JS, Stamm TA, van der Heijde DM, Verpoort KN, et al. The Stop Arthritis Very Early (SAVE) trial, an international multicentre, randomised, double-blind, placebo-controlled trial on glucocorticoids in very early arthritis. Ann Rheum Dis 2010;69:495–502.
5. Verstappen SM, McCoy MJ, Roberts C, Dale NE, Hassell AB, Symmons DP. Beneficial effects of a 3-week course of intramuscular glucocorticoid injections in patients with very early inflammatory polyarthritis: results of the STIVEA trial. Ann Rheum Dis 2010;69:503–9.
6. Van Aken J, Heimans L, Gillet-van Dongen H, Visser K, Ronday HK, Speyer I, et al. Five-year outcomes of probable rheumatoid arthritis treated with methotrexate or placebo during the first year (the PROMPT study). Ann Rheum Dis 2014;73:396–400.
7. Van Nies JA, Krabben A, Schoones JW, Huizinga TW, Kloppenburg M, van der Helm-van Mil AH. What is the evidence for the presence of a therapeutic window of opportunity in rheumatoid arthritis? A systematic literature review. Ann Rheum Dis 2014;73:861–70.
8. Van Aken J, van Dongen H, le Cessie S, Allaart CF, Breedveld FC, Huizinga TW. Comparison of long term outcome of patients with rheumatoid arthritis presenting with undifferentiated arthritis or with rheumatoid arthritis: an observational cohort study. Ann Rheum Dis 2006;65:20–5.
9. Fergusson D, Aaron SD, Guyatt G, Hébert P. Post-randomisation exclusions: the intention to treat principle and excluding patients from analysis. BMJ 2002;325:652–4.
10. Cohen J, Guyatt G, Bernard GR, Calandra T, Cook D, Elbourne D, et al. New strategies for clinical trials in patients with sepsis and septic shock. Crit Care Med 2001;29:880–6.
11. Van der Helm-van Mil AH, le Cessie S, van Dongen H, Breedveld FC, Toes RE, Huizinga TW. A prediction rule for disease outcome in patients with recent-onset undifferentiated arthritis: how to guide individual treatment decisions. Arthritis Rheum 2007;56:433–40.
12. McNally E, Keogh C, Galvin R, Fahey T. Diagnostic accuracy of a clinical prediction rule (CPR) for identifying patients with recent-onset undifferentiated arthritis who are at a high risk of developing rheumatoid arthritis: a systematic review and meta-analysis. Semin Arthritis Rheum 2014;43:498–507.
13. Van der Helm-van Mil AH, Detert J, le Cessie S, Filer A, Bastian H, Burmester GR, et al. Validation of a prediction rule for disease outcome in patients with recent-onset undifferentiated arthritis: moving toward individualized treatment decision-making. Arthritis Rheum 2008;58:2241–7.
14. Ropes MW, Bennett GA, Cobb S, Jacox R, Jessar RA. 1958 revision of diagnostic criteria for rheumatoid arthritis. Bull Rheum Dis 1958;9:175–6.
15. Arnett FC, Edworthy SM, Bloch DA, McShane DJ, Fries JF, Cooper NS, et al. The American Rheumatism Association 1987 revised criteria for the classification of rheumatoid arthritis. Arthritis Rheum 1988;31:315–24.
16. Van Steenbergen HW, Mangnus L, Reijnierse M, Huizinga TW, van der Helm-van Mil AH. Clinical factors, anticitrullinated peptide antibodies and MRI-detected subclinical inflammation in relation to progression from clinically suspect arthralgia to arthritis. Ann Rheum Dis 2016;75:1824–30.
17. Bos WH, Wolbink GJ, Boers M, Tijhuis GJ, de Vries N, van der Horst-Bruinsma IE, et al. Arthritis development in patients with arthralgia is strongly associated with anti-citrullinated protein antibody status: a prospective cohort study. Ann Rheum Dis 2010;69:490–4.
18. Aletaha D, Neogi T, Silman AJ, Funovits J, Felson DT, Bingham CO III, et al. 2010 rheumatoid arthritis classification criteria: an American College of Rheumatology/European League Against Rheumatism collaborative initiative. Arthritis Rheum 2010;62:2569–81.
19. Radner H, Neogi T, Smolen JS, Aletaha D. Performance of the 2010 ACR/EULAR classification criteria for rheumatoid arthritis: a systematic literature review. Ann Rheum Dis 2014;73:114–23.
20. Burgers LE, van Nies JA, Ho LY, de Rooy DP, Huizinga TW, van der Helm-van Mil AH. Long-term outcome of rheumatoid arthritis defined according to the 2010-classification criteria. Ann Rheum Dis 2014;73:428–32.

ARTHRITIS & RHEUMATOLOGY
Vol. 69, No. 5, May 2017, pp 932–942
DOI 10.1002/art.40054

Peficitinib, a JAK Inhibitor, in Combination With Limited Conventional Synthetic Disease-Modifying Antirheumatic Drugs in the Treatment of Moderate-to-Severe Rheumatoid Arthritis

Mark C. Genovese,[1] Maria Greenwald,[2] Christine Codding,[3] Anna Zubrzycka-Sienkiewicz,[4] Alan J. Kivitz,[5] Annie Wang,[6] Kathyjo Shay,[6] Xuegong Wang,[6] Jay P. Garg,[6] and Mario H. Cardiel[7]

Objective. **To evaluate the efficacy and safety of orally administered once-daily peficitinib in combination with limited conventional synthetic disease-modifying antirheumatic drugs (csDMARDs) in patients with moderate-to-severe rheumatoid arthritis (RA).**

Methods. **In this randomized, double-blind, phase IIb trial, patients with RA (n = 289) were treated with peficitinib 25 mg, 50 mg, 100 mg, or 150 mg or matching placebo once daily for 12 weeks. The primary end point was the percentage of patients who met the American College of Rheumatology 20% improvement criteria (achieved an ACR20 response) at week 12.**

Results. **ACR20 response rates at week 12 were 22.0%, 36.8%, 48.3% ($P < 0.05$), 56.3% ($P < 0.01$), and 29.4% in the peficitinib 25 mg, 50 mg, 100 mg, 150 mg, and placebo groups, respectively. Patients in the peficitinib 100 mg and 150 mg groups achieved a rapid and statistically significant ACR20 response compared with those in the placebo group ($P < 0.05$), reaching statistical significance by week 2. Overall, the incidence of adverse events (AEs) was similar between patients receiving peficitinib and those receiving placebo. The most common AEs were upper respiratory tract infection (5% [n = 15]), nausea (4% [n = 12]), and urinary tract infection (4% [n = 10]). There was 1 case of herpes zoster in the placebo group, and 1 serious infection (limb abscess) in the peficitinib 25 mg group. There were no incidences of grade 2 or higher neutropenia or lymphopenia.**

Conclusion. **In patients with moderate-to-severe RA, orally administered once-daily peficitinib in combination with limited csDMARDs resulted in a dose-dependent ACR20 response rate over 12 weeks with satisfactory tolerability.**

Targeting intracellular signaling molecules of the JAK family (comprising JAK-1, JAK-2, JAK-3, and Tyk-2) is currently being explored for the treatment of rheumatoid arthritis (RA) (1). Tofacitinib (a pan-JAK inhibitor) is currently the only approved JAK inhibitor for RA (2–7), while others such as baricitinib (JAK-1 and JAK-2 selective) (8–12), filgotinib (JAK-1 selective)

ClinicalTrials.gov identifier: NCT01565655.
Supported by Astellas Pharma Global Development.
[1]Mark C. Genovese, MD: Stanford University, Palo Alto, California; [2]Maria Greenwald, MD: Desert Medical Advances, Palm Desert, California; [3]Christine Codding, MD: Health Research of Oklahoma, Oklahoma City; [4]Anna Zubrzycka-Sienkiewicz, MD: ARS Rheumatica, Warsaw, Poland; [5]Alan J. Kivitz, MD: Altoona Center for Clinical Research, Duncansville, Pennsylvania; [6]Annie Wang, PhD, Kathyjo Shay, BA, Xuegong Wang, MD, Jay P. Garg, MD (current address: Genentech, San Francisco, California): Astellas Pharma Global Development, Northbrook, Illinois; [7]Mario H. Cardiel, MD, MSc: Centro de Investigación Clínica de Morelia SC, Morelia, Mexico.

Dr. Genovese has received consulting fees, speaking fees, and/or honoraria from Galapagos, Pfizer, Vertex, AbbVie, and Lilly (less than $10,000 each), and Gilead (more than $10,000) and grants from Pfizer, Vertex, AbbVie, Lilly, and Gilead. Dr. Codding has received grants from Genentech, AbbVie, Bristol-Myers Squibb, Novartis, Lilly, Astellas Pharma Global Development, Pfizer, Janssen, Gilead, Celgene, Merck, Mesoblast, Sandoz, Coherus, Sanofi, Daiichi Sankyo, and UCB. Dr. Zubrzycka-Sienkiewicz has received grants from Galapagos NV, Merck & Company, Inc., Celltrion, Inc., Roche Holding Ltd, Janssen Biotech Inc., Auven Therapeutics, UCB SA, Mabion, and Astellas Pharma Global Development. Dr. Kivitz has received consulting fees, speaking fees, and/or honoraria from Astellas Pharma Global Development, Eli Lilly and Company, Galapagos NV, and Genentech (less than $10,00 each) and AbbVie, Inc., Johnson & Johnson, Pfizer, and Vertex Pharmaceuticals, Inc. (more than $10,000 each). Dr. Cardiel has received consulting fees, speaking fees, and/or honoraria from Pfizer, AbbVie, Roche, and Lilly (less than $10,000 each) and has provided expert testimony on behalf of Roche and Pfizer.

Address correspondence to Mark Genovese, MD, Division of Immunology and Rheumatology, Stanford University, 1000 Welch Road, #203, Palo Alto, CA 94304. E-mail: Genovese@stanford.edu.

Submitted for publication April 15, 2016; accepted in revised form January 17, 2017.

(13), and ABT-494 (JAK-1 selective) (14) are currently in various stages of development.

Peficitinib (ASP015K) is an orally administered once-daily JAK inhibitor in development for the treatment of RA (15). Peficitinib inhibits JAK-1, JAK-2, JAK-3, and Tyk-2 enzyme activities with 50% inhibition concentration values of 3.9, 5.0, 0.7, and 4.8 nmoles/liter, respectively, and therefore has moderate selectivity for JAK-3 inhibition (15). The efficacy and safety profile of peficitinib for the treatment of RA has been investigated in 2 other phase II trials. In a 12-week, phase IIb, randomized, double-blind, placebo-controlled study of peficitinib monotherapy (25 mg, 50 mg, 100 mg, and 150 mg) in Japanese patients with moderate-to-severe RA (not required to fail to respond to 1 or more conventional synthetic disease-modifying antirheumatic drugs [csDMARDs]; ClinicalTrials.gov identifier NCT01649999), 50 mg, 100 mg, or 150 mg once-daily doses of peficitinib resulted in statistically significant American College of Rheumatology 20% improvement criteria (ACR20) responses (16) compared with placebo, and had satisfactory tolerability (15). In a second 12-week, phase IIb, randomized, double-blind, parallel-group, placebo-controlled, dose-finding (peficitinib 25 mg, 50 mg, 100 mg, and 150 mg), multicenter study, statistically significant improvements in ACR20 response with peficitinib combined with methotrexate (MTX) were only observed in the peficitinib 50 mg group compared with placebo plus MTX ($P < 0.05$) in patients who had an inadequate response to MTX (NCT01554696) (17).

Here, we report the findings of a third randomized phase IIb study to evaluate the efficacy, safety, and dose response of orally administered once-daily peficitinib over 12 weeks in patients with moderate-to-severe RA who had an inadequate response or intolerance to csDMARDs.

PATIENTS AND METHODS

Study design. This phase IIb, randomized, double-blind, parallel-group, placebo-controlled, dose-finding, global, multicenter study of orally administered once-daily peficitinib in patients with moderate-to-severe RA who had an inadequate response or intolerance to csDMARDs (ClinicalTrials.gov identifier NCT01565655) was conducted at 41 sites in 6 countries (the US [20 sites], Poland [6 sites], Hungary [5 sites], Czech Republic [4 sites], Mexico [4 sites], and Bulgaria [3 sites]).

The trial was conducted over 12 weeks, during which patients were seen at baseline and at weeks 1, 2, 4, 8, and 12. Screening visits were performed up to 4 weeks prior to baseline, and patients who completed the 12-week study were given the option to participate in a long-term, open-label extension study. Patients who did not participate in the extension study were included in a 30-day follow-up.

Patients were randomly assigned in a 1:1:1:1:1 ratio to receive either peficitinib 25 mg, 50 mg, 100 mg, 150 mg or matching placebo once a day for 12 weeks. The investigator, patient, clinical staff, and sponsor were blinded with regard to treatment assignments. Patients were stratified by geographic region (Europe [Bulgaria, Czech Republic, Hungary, and Poland], Latin America [Mexico], or North America [US]).

An Institutional Review Board/Independent Ethics Committee–approved written informed consent form was obtained from each patient or from a legally authorized representative prior to the initiation of any study-specific procedures. Changes to the protocol, made after the initiation of study enrollment, are described in the Supplementary Methods, available on the *Arthritis & Rheumatology* web site at http://onlinelibrary.wiley.com/doi/10.1002/art.40054/abstract. This study was conducted in compliance with the Declaration of Helsinki, Good Clinical Practice, International Conference on Harmonisation of Technical Requirements for Registration of Pharmaceuticals for Human Use guidelines, the EU Clinical Trials Directive, and applicable laws and regulations.

Study population. Eligible study participants were patients ages ≥18 years, who had been diagnosed as having RA according to the ACR 1987 revised criteria (18) ≥6 months prior to screening and who had an inadequate response or intolerance to a previous csDMARD. Patients were also required to be classified as having class I, II, or III functional status according to the ACR 1991 revised criteria for global functional status in RA (19) and to have active RA as defined by ≥6 tender/painful joints (tender joint count in 68 joints [TJC68]), ≥6 swollen joints (swollen joint count in 66 joints [SJC66]), and either a C-reactive protein (CRP) level of ≥0.8 mg/dl (normal range <1.0 mg/dl) or an erythrocyte sedimentation rate (ESR) of ≥28 mm/hour at screening and at baseline.

Patients who had taken any of the following csDMARDs or biologic agents within the following periods prior to the first study drug dose were excluded: MTX, gold, azathioprine, minocycline, or penicillamine (28 days); etanercept (28 days); certolizumab, adalimumab, golimumab, infliximab, or tocilizumab (60 days); rituximab or other CD20 inhibitors, or cyclophosphamide (180 days); leflunomide (60 days; if the patient had undergone a cholestyramine washout, the period was reduced to 30 days prior to day 1 dosing); abatacept (90 days); and anakinra (7 days). Exclusion criteria also included abnormal findings on a chest radiograph within 90 days of screening or at screening, indicative of an acute or chronic infectious process or malignancy, virus vaccination within 30 days prior to the first dose of study drug, hepatitis B/C or HIV, any other autoimmune rheumatic disease other than Sjögren's syndrome, clinically significant infections, and any malignancy except for successfully treated basal or squamous cell carcinoma of the skin or in situ carcinoma of the cervix. Additionally, patients who had tuberculosis (TB) who were not taking guideline antimicrobial therapy were excluded. Patients were not required to undergo a TB test at screening if there was documentation of a negative TB test within 90 days of screening or if they had documentation of previously successfully completed treatment for latent TB per the Centers for Disease Control and Prevention or local guidelines. For subjects who had a previous BCG vaccination, QuantiFeron blood testing was conducted to identify latent TB infection within 90 days of screening. Any positive TB test result was considered positive for the purposes of study entry evaluation.

Concomitant medications. The only permitted concomitant medications for RA were nonsteroidal antiinflammatory drugs, csDMARDs (≤400 mg hydroxychloroquine per day, ≤250 mg chloroquine per day, and ≤3 gm sulfasalazine per day), and/or oral corticosteroids (≤10 mg of prednisone or equivalent per day).

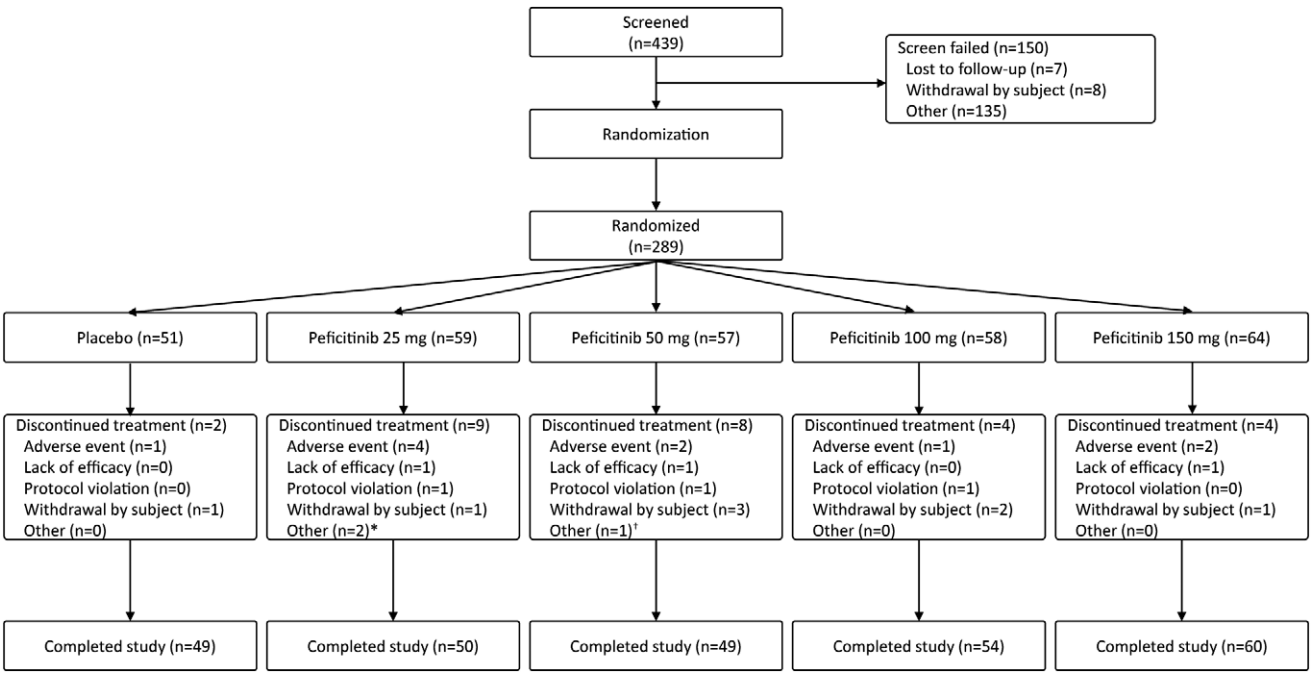

Figure 1. Disposition of the patients. * = Treatment of both patients was interrupted, due to an adverse event in 1 patient, with plans to restart in the open-label study, and due to antibiotic treatment in 1 patient. † = The patient was noncompliant with study drug, did not bring back study medication after multiple reminders, and the patient diary was not accurate.

Prohibited concomitant medications were biologic agents approved for the treatment of RA (including, but not limited to, abatacept, tocilizumab, rituximab, etanercept, certolizumab, adalimumab, golimumab, and infliximab); csDMARDs (including MTX, gold, penicillamine, leflunomide, azathioprine, minocycline, and cyclophosphamide), intraarticular or parenteral corticosteroids, >10 mg oral prednisone (or equivalent) per day, treatment with another investigational drug, and medications that are CYP3A substrates with a narrow therapeutic range (including, but not limited to, cyclosporine, sirolimus, tacrolimus, and terfenadine).

Study end points. The primary end point was the percentage of patients who met the ACR20 criteria using the CRP level at week 12. Secondary and other end points included the percentages of patients achieving an ACR50 or ACR70 response at week 12, the change from baseline in Disease Activity Score in 28 joints (DAS28) (20) using the CRP level (DAS28-CRP) at week 12, the percentage of patients achieving a DAS28 using the ESR (DAS28-ESR) of <2.6, the percentage of patients acheiving a DAS28-CRP of <2.6, and the change from baseline in Simplified Disease Activity Index (SDAI) and Clinical Disease Activity Index (CDAI) at week 12.

Safety and laboratory assessments. Safety was assessed through AE reporting (coded using the Medical Dictionary for Regulatory Activities [MedDRA] version 14.0) (21), vital signs, clinical laboratory evaluations (hematology, chemistry, urinalysis, and fasting lipids profile), 12-lead electrocardiograms, and physical examinations. AE grades were based on National Cancer Institute Common Terminology Criteria for Adverse Events version 4.03.

Sample size determination. The planned sample size for the study was 275 patients. Assuming an ACR20 response of 60% for any peficitinib group and 30% for placebo, 55 patients per treatment group (adjusted for an expected 10% dropout rate) were needed to reach 80% power to detect a difference between any of the peficitinib groups and placebo, using a 2-sided continuity-corrected chi-square test with a significance level of 5%.

Statistical analysis. The full analysis set consisted of all patients who were randomized and received at least 1 dose of peficitinib. This was the primary data set for efficacy analyses. Primary analysis of ACR20/50/70 response rates and the change from baseline in DAS28-CRP at week 12 was based on a logistic regression model with effects for treatment group and geographic region. When all ACR component values were missing, nonresponder imputation was used for the missing ACR responses at week 12. If not all ACR component values were missing at week 12, the last observation carried forward (LOCF) was used to impute missing values and then the ACR response was calculated. In addition, patients who received rescue therapy (defined as patients who initiated any csDMARD medication after day 1 or who received intramuscular or intravenous corticosteroids after day 1) prior to or at week 12 were classified as nonresponders. Additional analyses using normal approximation to the binomial distribution were also conducted.

Analysis of covariance with fixed effects for treatment group, geographic region, and baseline score as a covariate was used on the secondary end point of change from baseline in DAS28-CRP. All DAS28 component values at a time point for any patient receiving rescue therapy prior to or at the time point were set to missing, and missing component values were imputed using the LOCF. A mixed-effects model for repeated measures was used for the analysis of change from baseline in CDAI and SDAI, with the patient as a random effect.

Table 1. Demographic and baseline disease characteristics of the 289 patients with RA (full analysis set)*

	Placebo (n = 51)	Peficitinib 25 mg (n = 59)	Peficitinib 50 mg (n = 57)	Peficitinib 100 mg (n = 58)	Peficitinib 150 mg (n = 64)
Female	42 (82.4)	46 (78.0)	48 (84.2)	51 (87.9)	50 (78.1)
Age, mean ± SD years	52.7 ± 12.2	52.6 ± 10.2	54.8 ± 10.0	54.9 ± 11.3	54.4 ± 12.5
Age <65 years	44 (86.3)	52 (88.1)	52 (91.2)	49 (84.5)	53 (82.8)
Weight, mean ± SD kg	75.7 ± 15.2	79.5 ± 16.9	76.1 ± 18.9	78.4 ± 24.3	76.5 ± 20.9
Hispanic or Latino	10 (19.6)	15 (25.4)	13 (22.8)	9 (15.5)	11 (17.2)
Duration of RA, mean ± SD years	9.8 ± 7.7	10.4 ± 8.6	10.3 ± 9.6	11.0 ± 8.4	10.5 ± 8.2
Prior MTX use	35 (68.6)	41 (69.5)	36 (63.2)	41 (70.7)	49 (76.6)
Prior leflunomide use	8 (15.7)	10 (16.9)	10 (17.5)	9 (15.5)	10 (15.6)
Prior biologic agent use	27 (52.9)	27 (45.8)	28 (49.1)	25 (43.1)	33 (51.6)
No. of previous biologic agents					
1	9 (17.6)	6 (10.2)	6 (10.5)	8 (13.8)	7 (10.9)
2	5 (9.8)	9 (15.3)	10 (17.5)	7 (12.1)	10 (15.6)
≥3	13 (25.5)	12 (20.3)	12 (21.1)	10 (17.2)	16 (25.0)
Prior JAK inhibitor use	0 (0)	0 (0)	0 (0)	0 (0)	0 (0)
Concomitant prednisone	9 (17.6)	12 (20.3)	21 (36.8)	13 (22.4)	12 (18.8)
Concomitant SSZ	10 (19.6)	5 (8.5)	1 (1.8)	5 (8.6)	6 (9.4)
Concomitant antimalarial	4 (7.8)	9 (15.3)	5 (8.8)	7 (12.1)	4 (6.3)
Geographic region					
North America	24 (47.1)	30 (50.8)	28 (49.1)	27 (46.6)	29 (45.3)
US	24 (47.1)	30 (50.8)	28 (49.1)	27 (46.6)	29 (45.3)
Europe	21 (41.2)	22 (37.3)	21 (36.8)	27 (46.6)	28 (43.8)
Bulgaria	2 (3.9)	3 (5.1)	1 (1.8)	4 (6.9)	2 (3.1)
Czech Republic	5 (9.8)	4 (6.8)	5 (8.8)	6 (10.3)	5 (7.8)
Hungary	4 (7.8)	6 (10.2)	5 (8.8)	4 (6.9)	6 (9.4)
Poland	10 (19.6)	9 (15.3)	10 (17.5)	13 (22.4)	15 (23.4)
Latin America	6 (11.8)	7 (11.9)	8 (14.0)	4 (6.9)	7 (10.9)
Mexico	6 (11.8)	7 (11.9)	8 (14.0)	4 (6.9)	7 (10.9)
Baseline disease activity, mean ± SD					
SDAI	42.5 ± 13.2	42.2 ± 14.6	44.0 ± 13.4	41.7 ± 13.3	43.5 ± 15.2
CDAI	40.8 ± 12.1	40.8 ± 14.1	42.0 ± 12.4	40.4 ± 12.9	41.6 ± 14.2
TJC68	24.3 ± 12.2	26.1 ± 14.2	26.2 ± 15.4	25.3 ± 15.9	26.6 ± 16.8
SJC66	14.5 ± 8.1	17.0 ± 10.4	16.9 ± 10.1	15.6 ± 9.8	17.1 ± 11.3
CRP, mg/dl	1.8 ± 2.0	1.4 ± 1.7	2.0 ± 2.4	1.3 ± 2.0	1.9 ± 2.5
ESR, mm/hour	43.2 ± 18.9	43.0 ± 19.7	48.7 ± 21.4	42.2 ± 15.7	44.6 ± 20.3
SGAP (100-mm VAS)	70.0 ± 19.3	66.6 ± 20.1	66.5 ± 21.8	67.0 ± 18.4	68.8 ± 20.4
SGA (100-mm VAS)	68.1 ± 19.3	64.1 ±19.8	64.5 ± 21.0	66.7 ± 18.7	67.7 ± 19.0
PGA (100-mm VAS)	68.5 ± 11.9	64.8 ± 19.0	66.6 ± 17.2	64.4 ± 16.8	66.0 ± 19.9
HAQ DI	1.6 ± 0.6	1.4 ± 0.6	1.6 ± 0.7	1.4 ± 0.7	1.5 ± 0.7
DAS28-ESR	6.6 ± 0.9	6.6 ± 0.9	6.7 ± 0.8	6.6 ± 0.8	6.7 ± 1.0
DAS28-CRP	5.9 ± 0.9	5.8 ± 1.0	5.9 ± 0.9	5.7 ± 0.9	5.9 ± 1.1

* Except where indicated otherwise, values are the number (%). RA = rheumatoid arthritis; MTX = methotrexate; SSZ = sulfasalazine; SDAI = Simplified Disease Activity Index; CDAI = Clinical Disease Activity Index; TJC68 = tender joint count in 68 joints; SJC66 = swollen joint count in 66 joints; CRP = C-reactive protein; ESR = erythrocyte sedimentation rate; SGAP = subject's global assessment of arthritis pain; VAS = visual analog scale; SGA = subject's global assessment; PGA = physician's global assessment; HAQ DI = Health Assessment Questionnaire disability index; DAS28-ESR = Disease Activity Score in 28 joints using the erythrocyte sedimentation rate; DAS28-CRP = DAS28 using the C-reactive protein level.

Treatment stratified by geographic region was excluded from the model if not significant ($P < 0.01$). Within-patient variance–covariance was estimated using an unstructured covariance matrix. No adjustments for multiplicity were performed in these analyses. The safety analysis set was defined as all patients who received at least 1 dose of peficitinib.

RESULTS

Patients. A total of 439 patients were screened for inclusion, of which 289 were randomized and treated (peficitinib 25 mg [n = 59], 50 mg [n = 57], 100 mg [n = 58], 150 mg [n = 64], and placebo [n = 51]). A total of 262 patients (91%) completed the 12-week study (Figure 1). Demographic characteristics and baseline disease activity were similar across the study arms (Table 1).

Efficacy. The primary end point of ACR20 response at week 12 was achieved by 22.0%, 36.8%, 48.3%, 56.3%, and 29.4% of patients in the peficitinib 25 mg, 50 mg, 100 mg, 150 mg, and placebo groups, respectively (Figure 2). Statistically significant differences in the ACR20

response rate versus placebo were reported for the peficitinib 100 mg ($P < 0.05$) and 150 mg ($P < 0.01$) groups at week 12.

ACR50 response rates at week 12 were 15.3%, 24.6%, 27.6%, 28.1%, and 9.8% in the peficitinib 25 mg, 50 mg, 100 mg, 150 mg, and placebo groups, respectively. The peficitinib 50 mg ($P < 0.05$), 100 mg ($P < 0.05$), and 150 mg ($P < 0.01$) groups had a significantly greater number of patients achieving ACR50 response rates at week 12 than the placebo group. ACR70 response rates at week 12 were 6.8%, 15.8%, 19.0%, 10.9%, and 7.8% in the peficitinib 25 mg, 50 mg, 100 mg, 150 mg, and placebo groups, respectively. No peficitinib treatment group reached statistical significance for ACR70 response rate versus placebo at week 12.

ACR20 responses by geographic region are shown in Supplementary Figure 1, available on the *Arthritis & Rheumatology* web site at http://onlinelibrary.wiley.com/doi/10.1002/art.40054/abstract. There was some variability in ACR20/50/70 response rates when patients were stratified by elevated CRP versus ESR at baseline. However, this stratification resulted in small patient numbers in each group (Supplementary Table 1, available on the *Arthritis & Rheumatology* web site at http://onlinelibrary.wiley.com/doi/10.1002/art.40054/abstract).

Overall, ACR20 response rates increased over time (Figure 3A). Patients in the peficitinib 100 mg and 150 mg groups achieved a significantly greater ACR20 response rate at week 2 ($P < 0.05$) compared with placebo, which was maintained to week 12. Throughout the 12-week study, least squares mean (LSM) DAS28-ESR and DAS28-CRP levels decreased from baseline in all study arms (Figures 3B and C). Patients in the peficitinib 100 mg and 150 mg groups achieved a statistically significant decrease in both LSM DAS28-ESR and DAS28-CRP from baseline at week 4, which was maintained to week 12.

Statistically significant differences in LSM SDAI and CDAI at week 12 were observed in the peficitinib 50 mg ($P < 0.05$), 100 mg ($P < 0.001$), and 150 mg ($P < 0.001$) groups versus the placebo group (Table 2). There were no statistically significant differences in LSM Health Assessment Questionnaire (HAQ) disability index (DI) at week 12 between any peficitinib group and placebo. The mean TJC68 and SJC66 decreased further from baseline in the peficitinib groups compared with placebo, and the decreases were dose dependent.

A significantly greater percentage of patients in the peficitinib 100 mg and 150 mg groups achieved a DAS28-ESR of <2.6 at week 12 compared with placebo ($P < 0.05$). No peficitinib group had a significantly greater percentage of patients achieving a DAS28-CRP of <2.6 at week 12 compared with placebo.

Safety. *Adverse events.* A total of 121 patients (42%) reported AEs (Table 3). AEs occurring in ≥2% of patients overall were upper respiratory tract infection (5% [n = 15]), nausea (4% [n = 12]), urinary tract infection (4% [n = 10]), diarrhea (4% [n = 10]), dyspepsia (2% [n = 7]), RA (2% [n = 7]), and headache (2% [n = 7]). The majority of AEs (88%) were mild or moderate in severity, with a total of 15 serious AEs experienced by 12 patients, and no deaths were reported. The serious AEs

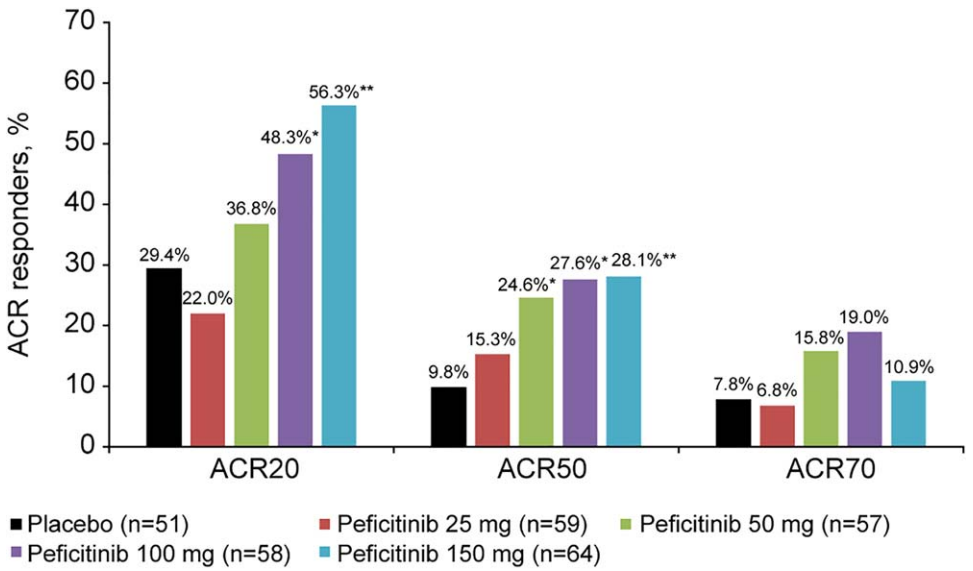

Figure 2. Percentages of patients in each treatment group achieving a response according to the American College of Rheumatology criteria for 20% improvement (ACR20), 50% improvement, and 70% improvement at week 12. * = $P < 0.05$; ** = $P < 0.01$, versus placebo.

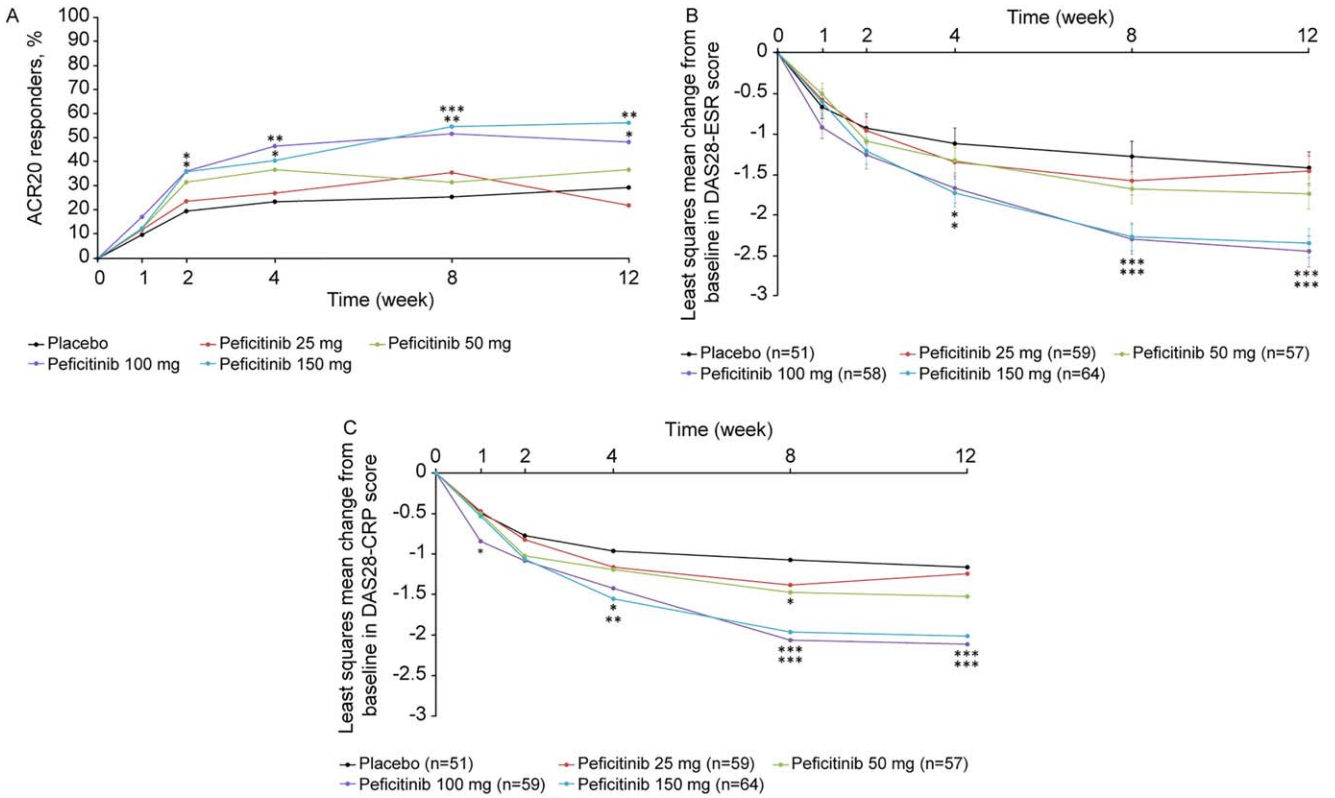

Figure 3. Responses over time in each treatment group. **A,** American College of Rheumatology criteria for 20% improvement (ACR20) response rates. **B,** Least squares mean (LSM) change from baseline in the Disease Activity Score in 28 joints using the erythrocyte sedimentation rate (DAS28-ESR). **C,** LSM change from baseline in the DAS28 using the C-reactive protein level (DAS28-CRP). $* = P < 0.05$; $** = P < 0.01$; $*** = P < 0.001$, versus placebo.

Table 2. Changes in disease activity from baseline to week 12 (full analysis set)*

	Placebo (n = 51)	Peficitinib 25 mg (n = 58)	Peficitinib 50 mg (n = 56)	Peficitinib 100 mg (n = 57)	Peficitinib 150 mg (n = 60)
Patients achieving DAS28-ESR <2.6, no. (%)	2 (3.9)	4 (6.8)	4 (7.1)	10 (17.5)†	11 (17.2)†
Patients achieving DAS28-CRP <2.6, no. (%)	5 (9.8)	4 (6.8)	7 (12.5)	13 (22.8)	13 (20.3)
SDAI, LSM difference versus placebo (95% CI)	–	−1.98 (−7.44, 3.48)	−6.67 (−12.18, −1.16)†	−12.04 (−17.52, −6.57)‡	−9.56 (−14.90, −4.22)‡
CDAI, LSM difference versus placebo (95% CI)	–	−2.40 (−7.81, −3.01)	−6.64 (−12.09, −1.18)†	−12.03 (−17.45, −6.61)‡	−9.15 (−14.43, −3.87)‡
TJC68, median (range)§	−6.0 (−29, 32)	−7.0 (−40, 10)	−10.0 (−61, 15)	−10.5 (−57, 18)¶	−11.0 (−55, 17)¶
SJC66, median (range)§	−5.0 (−21, 32)	−6.0 (−41, 11)	−7.0 (−54, 11)†	−8.0 (−31, 10)¶	−7.0 (−34, 12)¶
HAQ DI, LSM difference versus placebo (95% CI)	–	−0.02 (−0.18, 0.21)	−0.12 (−0.31, 0.07)	−0.11 (−0.30, 0.09)	−0.17 (−0.36, 0.02)

* DAS28-ESR = Disease Activity Score in 28 joints using the erythrocyte sedimentation rate; DAS28-CRP = DAS28 using the C-reactive protein level; SDAI = Simplified Disease Activity Index; LSM = least squares mean; 95% CI = 95% confidence interval; TJC68 = tender joint count in 68 joints; SJC66 = swollen joint count in 66 joints; HAQ DI = Health Assessment Questionnaire disability index.
† $P < 0.05$ versus placebo.
‡ $P < 0.001$ versus placebo.
§ P values are for comparison of medians between each peficitinib group and placebo based on the Wilcoxon rank sum test stratified by geographic region.
¶ $P < 0.01$ versus placebo.

Table 3. Adverse events and laboratory values in the 289 patients with RA*

	Placebo (n = 51)	Peficitinib 25 mg (n = 59)	Peficitinib 50 mg (n = 57)	Peficitinib 100 mg (n = 58)	Peficitinib 150 mg (n = 64)
AEs, no. (%)	22 (43.1)	22 (37.3)	19 (33.3)	30 (51.7)	28 (43.8)
SAEs†	2 (3.9)	2 (3.4)	2 (3.5)	4 (6.9)	2 (3.1)
Cardiac disorders	1 (2.0)	0 (0)	1 (1.8)	0 (0)	1 (1.6)
Serious infections	0 (0)	1 (1.7)	0 (0)	0 (0)	0 (0)
Other‡	1 (2.0)	1 (1.7)	2 (3.5)	5 (8.6)	2 (3.1)
Deaths	0 (0)	0 (0)	0 (0)	0 (0)	0 (0)
Malignancies	0 (0)	0 (0)	0 (0)	0 (0)	0 (0)
Herpes zoster	1 (2.0)	0 (0)	0 (0)	0 (0)	0 (0)
Gastrointestinal perforation	0 (0)	0 (0)	0 (0)	0 (0)	0 (0)
AEs leading to discontinuation	0 (0)	4 (6.8)	2 (3.5)	1 (1.7)	2 (3.1)
SAEs leading to discontinuation	0 (0)	1 (1.7)	0 (0)	0 (0)	1 (1.6)
AEs occurring in ≥2% of patients overall, no. (%)					
URI	2 (3.9)	4 (6.8)	0 (0)	4 (6.9)	5 (7.8)
Nausea	0 (0)	2 (3.4)	1 (1.8)	3 (5.2)	6 (9.4)
UTI	2 (3.9)	1 (1.7)	0 (0)	2 (3.4)	5 (7.8)
Diarrhea	1 (2.0)	4 (6.8)	1 (1.8)	4 (6.9)	0 (0)
Dyspepsia	1 (2.0)	0 (0)	1 (1.8)	2 (3.4)	3 (4.7)
RA	1 (2.0)	1 (1.7)	3 (5.3)	0 (0)	2 (3.1)
Headache	1 (2.0)	1 (1.7)	0 (0)	4 (6.9)	1 (1.6)
Laboratory values at week 12, mean ± SD change from baseline					
Absolute neutrophil count, 10^6/liter	297.7 ± 2,189	97.8 ± 1,480	−10.6 ± 1,338	−212.8 ± 1,449	−142.4 ± 1,470
Hgb, gm/liter	−1.6 ± 8.18	0.1 ± 7.24	1.1 ± 7.63	−1.4 ± 8.17	1.3 ± 8.74
Absolute lymphocyte count, 10^6/liter	132 ± 546	−25 ± 507	−98 ± 590	11 ± 618	4 ± 613
Platelets, 10^9/liter	7.6 ± 42	−4.8 ± 31	−10.1 ± 48	−10.8 ± 36	−19.2 ± 59
WBCs, 10^6/liter	410 ± 2,138	70 ± 1,667	−160 ± 1,345	−260 ± 1,840	−220 ± 1,556
ALT, units/liter	1.7 ± 10.0	−0.4 ± 9.6	−1.1 ± 8.6	−1.3 ± 10.2	3.9 ± 12.2
AST, units/liter	0.4 ± 5.40	0.4 ± 5.20	−0.4 ± 7.10	0.2 ± 7.90	3.5 ± 9.50
CPK, units/liter	−4.0 ± 23.8	8.0 ± 51.4	10.2 ± 74.4	39.1 ± 76.8	37.6 ± 219.3
Creatinine, mg/dl	−0.03 ± 0.09	−0.01 ± 0.88	0.04 ± 0.11	0.05 ± 0.09	0.06 ± 0.14
HDL, mg/dl	1.60 ± 5.80	1.75 ± 3.94	2.27 ± 3.75	3.78 ± 4.72	4.3 ± 4.92
LDL, mg/dl	1.21 ± 7.93	−0.2 ± 9.05	3.87 ± 9.63	1.71 ± 11.52	2.02 ± 9.65
HDL:LDL	0.02 ± 0.16	0.04 ± 0.12	0 ± 0.11	0.06 ± 0.16	0.07 ± 0.15
HDL:total cholesterol	0.01 ± 0.05	0.02 ± 0.04	0 ± 0.04	0.03 ± 0.05	0.02 ± 0.05
Triglycerides, mg/dl	0.45 ± 11.86	−1.40 ± 9.42	0.07 ± 10.43	−2.09 ± 13.94	4.91 ± 11.60
Laboratory values at week 12, no. (%)					
Absolute neutrophil count, cells/μl					
<500	0 (0)	0 (0)	0 (0)	0 (0)	0 (0)
500 to <1,000	0 (0)	0 (0)	0 (0)	0 (0)	0 (0)
1,000 to <1,500	0 (0)	0 (0)	0 (0)	0 (0)	0 (0)
Grade ≥2	0 (0)	0 (0)	0 (0)	0 (0)	0 (0)
Absolute lymphocyte count, cells/μl					
<200	0 (0)	0 (0)	0 (0)	0 (0)	0 (0)
200 to <500	0 (0)	0 (0)	0 (0)	0 (0)	0 (0)
Grade ≥2	0 (0)	0 (0)	0 (0)	0 (0)	0 (0)
Hgb, gm/dl					
<8.0	0 (0)	0 (0)	0 (0)	0 (0)	0 (0)
8.0 to <10.0	2 (3.9)	0 (0)	0 (0)	1 (1.7)	1 (1.6)
Grade ≥2	2 (3.9)	0 (0)	0 (0)	1 (1.7)	1 (1.6)
Platelets, cells/μl					
≤2 × 10^4	0 (0)	0 (0)	0 (0)	0 (0)	0 (0)
≤5 × 10^4	0 (0)	0 (0)	0 (0)	0 (0)	0 (0)
Grade ≥2	0 (0)	0 (0)	0 (0)	0 (0)	0 (0)
CPK					
>2× ULN to ≤5× ULN	0 (0)	1 (1.7)	0 (0)	2 (3.4)	1 (1.6)
>5× ULN to ≤10× ULN	0 (0)	0 (0)	0 (0)	0 (0)	0 (0)
>10× ULN	0 (0)	0 (0)	0 (0)	0 (0)	0 (0)
Grade ≥2	0 (0)	0 (0)	0 (0)	2 (3.4)	0 (0)
ALT					
>2× ULN to ≤3× ULN	0 (0)	1 (1.7)	0 (0)	0 (0)	2 (3.1)
>3× ULN to ≤5× ULN	0 (0)	0 (0)	0 (0)	0 (0)	0 (0)
>5× ULN	0 (0)	0 (0)	0 (0)	0 (0)	0 (0)
Grade ≥2	0 (0)	0 (0)	0 (0)	0 (0)	0 (0)

Table 3. *(Cont'd)*

	Placebo (n = 51)	Peficitinib 25 mg (n = 59)	Peficitinib 50 mg (n = 57)	Peficitinib 100 mg (n = 58)	Peficitinib 150 mg (n = 64)
AST					
>2× ULN to ≤3× ULN	0 (0)	0 (0)	0 (0)	0 (0)	0 (0)
>3× ULN to ≤5× ULN	0 (0)	0 (0)	0 (0)	0 (0)	0 (0)
>5× ULN	0 (0)	0 (0)	0 (0)	0 (0)	0 (0)
Grade ≥2	0 (0)	0 (0)	0 (0)	0 (0)	0 (0)
Creatinine					
>1.5× baseline to ≤3.0× baseline	0 (0)	0 (0)	1 (1.8)	0 (0)	0 (0)
>3.0× baseline	0 (0)	0 (0)	0 (0)	0 (0)	0 (0)
Grade ≥2	0 (0)	0 (0)	0 (0)	0 (0)	0 (0)
WBCs					
$<3.6 \times 10^9$ cells/liter	0 (0)	1 (1.7)	1 (1.8)	0 (0)	1 (1.6)
3.6 to 10×10^9 cells/liter	38 (74.5)	46 (78.0)	43 (75.4)	47 (81.0)	56 (87.5)
$>10 \times 10^9$ cells/liter	13 (25.5)	12 (20.3)	12 (21.1)	11 (19.0)	7 (10.9)
Grade ≥2	0 (0)	0 (0)	0 (0)	0 (0)	0 (0)
LDL					
≤160 mg/dl	45 (88.2)	47 (79.7)	44 (77.2)	42 (72.4)	52 (81.3)
>160 mg/dl	1 (2.0)	3 (5.1)	6 (10.5)	8 (13.8)	4 (6.3)
Grade ≥2	0 (0)	0 (0)	0 (0)	0 (0)	0 (0)
HDL					
<1.06 mmoles/liter	9 (17.6)	7 (11.9)	5 (8.8)	5 (8.6)	4 (6.3)
≥1.06 mmoles/liter	42 (82.4)	52 (88.1)	51 (89.5)	53 (91.4)	60 (93.8)
Grade ≥2	0 (0)	0 (0)	0 (0)	0 (0)	0 (0)
Triglycerides					
0–1.68 mmoles/liter	37 (72.5)	48 (81.4)	36 (63.2)	40 (69.0)	43 (67.2)
>1.68 mmoles/liter	14 (27.5)	11 (18.6)	20 (35.1)	18 (31.0)	21 (32.8)
Grade ≥2	4 (7.8)	2 (3.4)	2 (3.5)	3 (5.2)	4 (6.3)

* URI = upper respiratory tract infection; UTI = urinary tract infection; Hgb = hemoglobin; WBCs = white blood cells; ALT = alanine transaminase; AST = aspartate transaminase; CPK = creatine phosphokinase; HDL = high-density lipoprotein; LDL = low-density lipoprotein; ULN = upper limit of normal.
† Twelve patients experienced 15 serious adverse events (SAEs).
‡ Other adverse events were joint dislocation (n = 1) in the placebo group, rheumatoid arthritis (RA; n = 1) in the peficitinib 25 mg group, asthma (n = 1) and hemoptysis (n = 1) in the peficitinib 50 mg group, synovial cyst (n=1), transient ischemic attack (n = 2), humerus fracture (n = 1), and abnormal electrocardiogram (n = 1) in the peficitinib 100 mg group, and musculoskeletal chest pain (n = 1) and pleuritic pain (n = 1) in the peficitinib 150 mg group.

were myocardial ischemia and joint dislocation in the placebo group; RA and limb abscess in the peficitinib 25 mg group; asthma, hemoptysis, and atrial fibrillation in the peficitinib 50 mg group; synovial cyst, humerus fracture, electrocardiogram abnormality and 2 incidents of transient ischemic attack in the peficitinib 100 mg group; and musculoskeletal chest pain, pleuritic pain, and myocardial infarction in the peficitinib 150 mg group. There was 1 case (<1%) of herpes zoster in the placebo group that was not disseminated, and 1 serious infection (limb abscess) in the peficitinib 25 mg group.

A total of 9 patients discontinued treatment due to an AE (4 in the peficitinib 25 mg group, 2 in the peficitinib 50 mg group, 1 in the peficitinib 100 mg group, and 2 in the peficitinib 150 mg group). Adverse events that led to discontinuation were dyspepsia (in the peficitinib 100 mg and 150 mg groups; n = 2), abdominal hernia (in the peficitinib 50 mg group; n = 1), nausea (in the peficitinib 150 mg group; n = 1), vomiting (in the peficitinib 100 mg group; n = 1), hidradenitis (in the peficitinib 25 mg group; n = 1), skin lesion (in the peficitinib 25 mg group; n = 1), myocardial infarction (in the peficitinib 150 mg group; n = 1), limb abscess (in the peficitinib 25 mg group; n = 1), contusion (in the peficitinib 25 mg group; n = 1), and RA (in the peficitinib 50 mg group; n = 1).

Laboratory values. Decreases in the mean absolute neutrophil count from baseline at week 12 were observed in the peficitinib 50 mg, 100 mg, and 150 mg groups. There were no shifts from baseline to any prespecified ranges for absolute neutrophil count or incidences of grade 2 or higher neutropenia at week 12. Decreases in mean absolute lymphocyte count at week 12 were reported in the peficitinib 25 mg and 50 mg groups

compared with placebo, and there were no shifts from baseline to any prespecified ranges for absolute lymphocyte count or incidences of grade 2 or higher lymphopenia at week 12. There was a dose-dependent decrease in mean platelet count (no patients shifted from baseline to any prespecified ranges for platelet count at week 12), and treatment with peficitinib was associated with a decreased white blood cell (WBC) count, with no decreases of grade 2 or higher in platelet or WBC count at week 12.

At week 12, the mean alanine aminotransferase (ALT) and aspartate aminotransferase (AST) levels remained stable in the placebo and peficitinib 25 mg, 50 mg, and 100 mg groups, but were increased from baseline in the peficitinib 150 mg group. Furthermore, ALT levels in 1 patient in the peficitinib 25 mg group (1.7%) and in 2 patients in the peficitinib 150 mg group (3.1%) shifted from baseline to the prespecified range of >2 times the upper limit of normal (ULN) to ≤ 3 times the ULN at week 12. There were no shifts to any prespecified ranges for AST, and there were no incidences of grade 2 or higher increases in ALT or AST levels at week 12.

There were 2 grade 3 or higher increases in creatine phosphokinase (CPK) level throughout the study, 1 each in the peficitinib 100 mg and 150 mg groups. Neither patient had received concomitant statins. The increase in CPK level did not resolve in either patient, but both patients continued until the end of the study. CPK levels in 4 patients (1 in the peficitinib 25 mg group, 2 in the peficitinib 100 mg group, and 1 in the peficitinib 150 mg group) shifted from baseline to the prespecified range of >2 times the ULN to ≤ 5 times the ULN at week 12. There were 2 grade 2 or higher CPK elevations at week 12 in the peficitinib 100 mg group. Dose-dependent increases in creatinine were observed across the peficitinib groups. In 1 patient in the peficitinib 50 mg group, the creatinine level shifted from baseline to the prespecified range of >1.5 times baseline to ≤ 3.0 times baseline at week 12. There were no grade 2 or higher increases in creatinine at week 12.

The mean change from baseline in high-density lipoprotein (HDL) level was dose dependent, and the change in triglyceride level varied among all groups of patients and was not dose dependent. However, there were 4 incidents of hypertriglyceridemia higher than grade 3 (2 each in the peficitinib 25 mg and 100 mg groups, 3 of which were considered drug related). In a total of 22 patients (1 in the placebo group, 3 in the peficitinib 25 mg group, 6 in the peficitinib 50 mg, 8 in the peficitinib 100 mg group, and 4 in the peficitinib 150 mg group), low-density lipoprotein (LDL) level shifted from baseline to >160 mg/dl at week 12. Overall, in 84 patients (14 in the placebo group, 11 in the peficitinib 25 mg group, 20 in the peficitinib 50 mg group, 18 in the peficitinib 100 mg group, and 21 in the peficitinib 150 mg group) the triglyceride level shifted from baseline to >1.68 mmoles/liter at week 12, and in 30 patients (9 in the placebo group, 7 in the peficitinib 25 mg group, 5 in the peficitinib 50 mg group, 5 in the peficitinib 100 mg group, and 4 in the peficitinib 150 mg group) the HDL level shifted from baseline to <1.06 mmoles/liter at week 12. Lipid ratios (HDL:LDL and HDL:total cholesterol) remained stable in all treatment groups throughout the 12-week study.

DISCUSSION

Patients with RA who had long-term refractory disease and inadequate responses to previous treatment with multiple DMARDs, including biologics, who were treated with peficitinib in combination with limited csDMARDs demonstrated ACR20 dose-dependent response rates at week 12. The peficitinib 100 mg and 150 mg groups showed a statistically significant difference compared with placebo in ACR20 response (starting at week 2 and continuing throughout the study), ACR50 response, and in change from baseline DAS28-CRP. The peficitinib 25 mg and 50 mg groups did not show a statistically significant difference in the percentage of patients achieving an ACR20 response compared with placebo. When ACR20 responses were stratified by geographic region, differences were seen between regions across treatment arms; however, it is difficult to draw any definitive conclusions due to low patient numbers.

In assessment of higher hurdle end points, such as ACR70 response and DAS28-ESR remission at week 12, there was a statistically significant difference in DAS28-ESR remission (but not ACR70 response) with higher doses of peficitinib (100 mg and 150 mg) compared with placebo; however, overall, the proportion of patients achieving these end points with peficitinib was relatively low. Similarly, although there appeared to be a trend toward a dose-dependent improvement in HAQ DI with peficitinib compared with placebo, these differences were small and were not statistically significant. Taking into consideration the small number of patients, limited study duration, and that this study involved a heterogeneous patient group with prior exposure to DMARDs and biologic DMARDs, it is difficult to make conclusions regarding these responses.

Treatment with orally administered once-daily peficitinib in combination with limited csDMARDs demonstrated satisfactory tolerability, with an overall incidence of AEs similar to that in the placebo group. Safety evaluation found no dose-related increases in any AEs during this study, and there were no new safety signals compared with other peficitinib phase II trials (15,17). However, the total number

of AEs of any grade were lower than anticipated based on data from previous trials with peficitinib (17) and other JAK inhibitors (2–8). Dose-dependent decreases in absolute neutrophil count, platelet count, and WBCs, and dose-dependent increases in CPK, HDL, and creatinine levels were seen. Lipid ratios remained stable throughout this study.

This study was limited by its short duration and small patient population, consistent with phase II studies. Further challenges to the interpretation of treatment responses in this study included the global design with a varied patient population, the low number of patients from Latin America, and the inclusion of patients who had previously received biologic agents and were not required to have had an inadequate response or intolerance to a biologic agent. Additionally, the permitted use of hydroxychloroquine, chloroquine, and sulfasalazine may be seen as a limitation because it prevented this study from being a true peficitinib monotherapy study; however, because this was a placebo-controlled study, health authorities requested that patients be permitted csDMARD use. Thus, although this was not a monotherapy study, the design permitted assessment of the safety and efficacy of peficitinib in the setting of no background MTX use.

In addition to other inclusion/exclusion criteria, patients were required to have either an elevated CRP or an elevated ESR to enter the trial. Differences in responses were observed between patients who entered the study with an elevated CRP level and those who entered with an elevated ESR (Table 1). For patients who qualified via an elevated CRP level, a trend was observed toward higher response rates, particularly in the peficitinib 150 mg group, compared with patients who qualified by an elevated ESR. Responses to placebo were also higher in patients who entered with an elevated ESR; this latter group comprised 50% of the enrolled patients. Patients qualifying based on ESR, which is measured locally rather than at a central laboratory, might have been subject to less rigorous laboratory standards and may have influenced the study results.

To fully assess the efficacy and safety of this novel JAK inhibitor, longer-term and larger-scale phase III studies of peficitinib 100 mg and 150 mg are currently ongoing (ClinicalTrials.gov identifiers NCT02308163 and NCT02305849). In conclusion, orally administered once-daily peficitinib without concomitant use of MTX reduced the symptoms of RA, and a dose-dependent response was observed in the ACR20 and ACR50 response rates as well as in the change from baseline DAS28-CRP.

ACKNOWLEDGMENTS

We would like to acknowledge all investigators for their participation in this trial.

AUTHOR CONTRIBUTIONS

All authors were involved in drafting the article or revising it critically for important intellectual content, and all authors approved the final version to be published. Dr. Genovese had full access to all of the data in the study and takes responsibility for the integrity of the data and the accuracy of the data analysis.

Study conception and design. Genovese, A. Wang, Shay, Garg.

Acquisition of data. Genovese, Greenwald, Codding, Zubrzycka-Sienkiewicz, Kivitz, X. Wang, Garg, Cardiel.

Analysis and interpretation of data. Genovese, Greenwald, Zubrzycka-Sienkiewicz, Kivitz, A. Wang, Shay, X. Wang, Garg, Cardiel.

ROLE OF THE STUDY SPONSOR

Astellas Pharma Global Development was involved in the study design and in the collection, analysis, and interpretation of the data. The authors had the final decision to submit the manuscript for publication. Writing assistance was provided by Matthew Reynolds and Leigh Church (Succinct Choice). Publication of the article was not contingent upon approval by Astellas Pharma Global Development.

REFERENCES

1. O'Shea JJ, Kontzias A, Yamaoka K, Tanaka Y, Laurence A. Janus kinase inhibitors in autoimmune diseases. Ann Rheum Dis 2013;72 Suppl 2:ii111–5.
2. Burmester GR, Blanco R, Charles-Schoeman C, Wollenhaupt J, Zerbini C, Benda B, et al. Tofacitinib (CP-690,550) in combination with methotrexate in patients with active rheumatoid arthritis with an inadequate response to tumour necrosis factor inhibitors: a randomised phase 3 trial. Lancet 2013;381:451–60.
3. Fleischmann R, Kremer J, Cush J, Schulze-Koops H, Connell CA, Bradley JD, et al. Placebo-controlled trial of tofacitinib monotherapy in rheumatoid arthritis. N Engl J Med 2012;367:495–507.
4. Van der Heijde D, Tanaka Y, Fleischmann R, Keystone E, Kremer J, Zerbini C, et al. Tofacitinib (CP-690,550) in patients with rheumatoid arthritis receiving methotrexate: twelve-month data from a twenty-four–month phase III randomized radiographic study. Arthritis Rheum 2013;65:559–70.
5. Van Vollenhoven RF, Fleischmann R, Cohen S, Lee EB, Garcia Meijide JA, Wagner S, et al. Tofacitinib or adalimumab versus placebo in rheumatoid arthritis. N Engl J Med 2012;367:508–19.
6. Lee EB, Fleischmann R, Hall S, Wilkinson B, Bradley JD, Gruben D, et al. Tofacitinib versus methotrexate in rheumatoid arthritis. N Engl J Med 2014;370:2377–86.
7. Asahina A, Etoh T, Igarashi A, Imafuku S, Saeki H, Shibasaki Y, et al. Oral tofacitinib efficacy, safety and tolerability in Japanese patients with moderate to severe plaque psoriasis and psoriatic arthritis: a randomized, double-blind, phase 3 study. J Dermatol 2016;43:869–80.
8. Keystone EC, Taylor PC, Drescher E, Schlichting DE, Beattie SD, Berclaz PY, et al. Safety and efficacy of baricitinib at 24 weeks in patients with rheumatoid arthritis who have had an inadequate response to methotrexate. Ann Rheum Dis 2015;74:333–40.
9. Dougados M, van der Heijde D, Chen YC, Greenwald M, Drescher E, Liu J, et al. Baricitinib in patients with inadequate response or intolerance to conventional synthetic DMARDs: results from the RA-BUILD study. Ann Rheum Dis 2017;76:88–95.
10. Genovese MC, Kremer J, Zamani O, Ludivico C, Krogulec M, Xie L, et al. Baricitinib in patients with refractory rheumatoid arthritis. N Engl J Med 2016;374:1243–52.
11. Papp K, Menter MA, Raman M, Disch D, Schlichting DE, Gaich C, et al. A randomized phase 2b trial of baricitinib, an

oral Janus kinase (JAK) 1/JAK2 inhibitor, in patients with moderate-to-severe psoriasis. Br J Dermatol 2016;174:1266–76.
12. Tanaka Y, Emoto K, Cai Z, Aoki T, Schlichting D, Rooney T, et al. Efficacy and safety of baricitinib in Japanese patients with active rheumatoid arthritis receiving background methotrexate therapy: a 12-week, double-blind, randomized placebo-controlled study. J Rheumatol 2016;43:504–11.
13. Westhovens R, Alten R, Pavlova D, Enriquez-Sosa F, Mazur M, Greenwald M, et al. Filgotinib (GLPG0634), an oral JAK1 selective inhibitor is effective in combination with methotrexate in patients with active rheumatoid arthritis: results from a phase 2B dose ranging study [abstract]. Arthritis Rheumatol 2015; 67 Suppl 10. URL: http://acrabstracts.org/abstract/filgotinib-glpg0634-an-oral-jak1-selective-inhibitor-is-effective-in-combination-with-methotrexate-in-patients-with-active-rheumatoid-arthritis-results-from-a-phase-2b-dose-ranging-study/.
14. Mohamed ME, Camp H, Jiang P, Padley R, Asatryan A, Othman AA. THU0176 pharmacokinetics, safety and tolerability of the selective JAK1 inhibitor, ABT-494, in healthy volunteers and subjects with rheumatoid arthritis [poster]. Ann Rheum Dis 2015;74:258.
15. Takeuchi T, Tanaka Y, Iwasaki M, Ishikura H, Saeki S, Kaneko Y. Efficacy and safety of the oral Janus kinase inhibitor peficitinib (ASP015K) monotherapy in patients with moderate to severe rheumatoid arthritis in Japan: a 12-week, randomised, double-blind, placebo-controlled phase IIb study. Ann Rheum Dis 2016;75:1057–64.
16. Felson DT, Anderson JJ, Boers M, Bombardier C, Furst D, Goldsmith C, et al. American College of Rheumatology preliminary definition of improvement in rheumatoid arthritis. Arthritis Rheum 1995;38:727–35.
17. Kivitz AJ, Gutierrez-Urena SR, Poiley J, Genovese MC, Kristy R, Shay K, et al. Peficitinib, a JAK inhibitor, in the treatment of moderate-to-severe rheumatoid arthritis in patients with an inadequate response to methotrexate [abstract]. Arthritis Rheumatol doi: http://onlinelibrary.wiley.com/doi/10.1002/art.39955/abstract). E-pub ahead of print.
18. Arnett FC, Edworthy SM, Bloch DA, McShane DJ, Fries JF, Cooper NS, et al. The American Rheumatism Association 1987 revised criteria for the classification of rheumatoid arthritis. Arthritis Rheum 1988;31:315–24.
19. Hochberg MC, Chang RW, Dwosh I, Lindsey S, Pincus T, Wolfe F. The American College of Rheumatology 1991 revised criteria for the classification of global functional status in rheumatoid arthritis. Arthritis Rheum 1992;35:498–502.
20. Prevoo ML, van 't Hof MA, Kuper HH, van Leeuwen MA, van de Putte LB, van Riel PL. Modified disease activity scores that include twenty-eight–joint counts: development and validation in a prospective longitudinal study of patients with rheumatoid arthritis. Arthritis Rheum 1995;38:44–8.
21. MedDRA v14.0. URL: http://www.meddra.org/.

ARTHRITIS & RHEUMATOLOGY
Vol. 69, No. 5, May 2017, pp 943–952
DOI 10.1002/art.40036

Effects of Baricitinib on Lipid, Apolipoprotein, and Lipoprotein Particle Profiles in a Phase IIb Study of Patients With Active Rheumatoid Arthritis

Joel M. Kremer,[1] Mark C. Genovese,[2] Edward Keystone,[3] Peter C. Taylor,[4] Steven H. Zuckerman,[5] Giacomo Ruotolo,[5] Douglas E. Schlichting,[5] Victoria L. Crotzer,[5] Eric Nantz,[5] Scott D. Beattie,[5] and William L. Macias[5]

Objective. **To assess the effects of baricitinib on lipid profiles in patients with moderate-to-severe rheumatoid arthritis.**

Methods. **Treatment with once-daily doses of baricitinib (1, 2, 4, or 8 mg) or placebo was studied in 301 randomized patients. Changes in lipid profile and lipoprotein particle size and particle number were assessed at weeks 12 and 24, and associations with clinical efficacy were evaluated. Apolipoproteins were assessed at weeks 4 and 12 in the placebo group and the 4-mg and 8-mg baricitinib groups.**

Results. **Treatment with baricitinib resulted in dose-dependent increases in serum lipid levels from baseline to week 12 (low-density lipoprotein [LDL] cholesterol increases of 3.4 mg/dl and 11.8 mg/dl in the 1 mg and 8 mg treatment groups, respectively; high-density lipoprotein [HDL] cholesterol increases of 3.3 mg/dl and 8.1 mg/dl, respectively; triglycerides increases of 6.4 mg/dl and 15.4 mg/dl, respectively). Group-wise mean increases in LDL cholesterol were coincident with mean increases in large LDL particles and mean reductions in small dense LDL particles. Increases from baseline to week 12 in apolipoprotein A-I, apolipoprotein B, and apolipoprotein CIII were observed with 4-mg doses of baricitinib (9.5%, 6.8%, and 23.0%, respectively) and with 8-mg doses (12.2%, 7.1%, and 19.7%, respectively), with no increase in LDL-associated apolipoprotein CIII (–4.5% with 4-mg baricitinib; –9.0% with 8-mg baricitinib). Baricitinib reduced HDL-associated serum amyloid A when administered at 4 mg (−36.0%) and 8 mg (−32.0%); a significant reduction in lipoprotein (a) was observed only with 8-mg doses (−16.6%). Increased HDL cholesterol at week 12 correlated with improved Disease Activity Scores and Simplified Disease Activity Index; changes in total cholesterol, LDL cholesterol, and triglycerides did not reveal a similar relationship.**

Conclusion. **Baricitinib-associated increases in serum lipid levels were observed in this study. Increases in levels of HDL cholesterol correlated with improved clinical outcomes.**

Activation of proinflammatory cytokine pathways contributes to the pathogenesis of rheumatoid arthritis (RA) (1,2). Several of these cytokines, including interleukin-6 (IL-6), granulocyte–macrophage colony-stimulating factor, IL-23, the IL-2 cytokine

Supported by Eli Lilly and Company and Incyte Corporation.

[1]Joel M. Kremer, MD: Albany Medical College, Albany, New York; [2]Mark C. Genovese, MD: Stanford University Medical Center, Palo Alto, California; [3]Edward Keystone, MD: University of Toronto, Toronto, Ontario, Canada; [4]Peter C. Taylor, MD, PhD: University of Oxford, Oxford, UK; [5]Steven H. Zuckerman, PhD, Giacomo Ruotolo, MD, PhD, Douglas E. Schlichting, PhD, Victoria L. Crotzer, PhD, Eric Nantz, PhD, Scott D. Beattie, PhD, William L. Macias, MD, PhD: Eli Lilly and Company, Indianapolis, Indiana.

Dr. Kremer has received consulting fees from Eli Lilly and Company, Pfizer, AbbVie, Genentech, and Novartis (less than $10,000 each) and research grants from these companies. Dr. Genovese has received consulting fees, speaking fees, and/or honoraria from Galapagos, Pfizer, Vertex, AbbVie, and Eli Lilly and Company (less than $10,000 each) and Gilead (more than $10,000) and grants from Pfizer, Vertex, AbbVie, Eli Lilly and Company, and Gilead. Dr. Keystone has received consulting and/or speaking fees from Roche, Pfizer, and Janssen (less than $10,000 each) and honoraria from Eli Lilly and Company, Janssen, and Amgen (more than $10,000 each). Dr. Taylor has received consulting fees, speaking fees, and/or honoraria from Merck, AbbVie, Pfizer, Roche, Bristol-Myers Squibb, Novartis, Biogen, Sanofi, Sandoz, and Janssen (less than $10,000 each) and from UCB and Eli Lilly and Company (more than $10,000 each), and research grants from UCB Pharma, GlaxoSmithKline, Janssen, and Abide Therapeutics. Drs. Zuckerman, Ruotolo, Schlichting, Crotzer, Nantz, Beattie, and Macias own stock or stock options in Eli Lilly and Company.

Address correspondence to Joel M. Kremer, MD, Albany Medical College and the Center for Rheumatology, 4 Tower Place, 8th Floor, Albany, NY 12203. E-mail: jkremer@joint-docs.com.

Submitted for publication April 8, 2016; accepted in revised form December 22, 2016.

family, and type I and type II interferons, utilize the JAK intracellular signaling pathway (3). Accordingly, the development of various inhibitors, each having differing degrees of specificity toward the 4 identified JAKs (JAK-1, JAK-2, JAK-3, Tyk-2), has been intensively investigated for the treatment of RA (4).

Baricitinib, formerly referred to as LY3009104 (INCB028050), is a potent, selective, and reversible orally administered inhibitor of JAK-1 (50% inhibition concentration [IC_{50}] = 5.9 n*M*) and JAK-2 (IC_{50} = 5.7 n*M*), with much less activity against Tyk-2 (IC_{50} = 53 n*M*) and JAK-3 (IC_{50} > 400 n*M*), and it inhibits proinflammatory cytokine signaling implicated in RA (5). In a phase IIb, double-blind, randomized, placebo-controlled study of patients with moderate-to-severe RA (6), despite treatment with methotrexate and other conventional disease-modifying antirheumatic drugs, significantly more patients in the combined baricitinib 4- and 8-mg groups compared to the placebo group had achieved the primary end point of response according to the American College of Rheumatology criteria for 20% improvement (7) at week 12. Baricitinib rapidly improved the signs and symptoms of RA, with an acceptable risk profile consistent with what has previously been described (8).

Increases in total cholesterol, low-density lipoprotein (LDL) cholesterol, and high-density lipoprotein (HDL) cholesterol have been observed in studies of JAK inhibitors (9), the IL-6 receptor monoclonal antibody tocilizumab (10), and less consistently of anti–tumor necrosis factor (anti-TNF) therapies (11). These increases have also been noted in various RA clinical trials of methotrexate (12). An understanding of the basis for increases in LDL cholesterol is important because LDL represents a heterogeneous collection of apolipoprotein B–containing particles that transport cholesterol (13). Additionally, the behavior of these different-sized particles has implications for particle clearance and atherogenicity (14). Increases in LDL particle number, particularly small LDL particles, have been associated with an increased risk of cardiovascular events (15). In the current study, we assessed changes in lipid profile and lipoprotein particle size and number (through 24 weeks) and apolipoprotein content (through 12 weeks) in patients with RA. In addition, the relationships between lipid parameters and measures of clinical efficacy were investigated at 12 weeks.

PATIENTS AND METHODS

Patients and study design. Eligible patients met the inclusion criteria for the phase IIb randomized, double-blind, placebo-controlled study as previously described (6). Qualifying patients (n = 301) were randomly assigned in a 2:1:1:1:1 ratio to once-daily doses of placebo or baricitinib (1, 2, 4, or 8 mg). After 12 weeks of treatment, patients initially assigned to the placebo or baricitinib 1 mg groups were re-randomized to either baricitinib 2 mg twice daily or baricitinib 4 mg once daily for an additional 12 weeks of blinded treatment. Patients initially assigned to 2-, 4-, and 8-mg doses of baricitinib continued to receive the treatment, still in a blinded manner, for an additional 12 weeks.

The study was conducted in accordance with the ethical principles of the Declaration of Helsinki and Good Clinical Practice Guidelines and was approved by the institutional review board or ethics committee at each center. All patients provided written informed consent.

Extended lipid profile. Serum samples were collected at baseline and at weeks 2, 4, 8, 12, 14, 16, 20, and 24, after randomization for conventional lipid profile (total cholesterol, LDL cholesterol, HDL cholesterol, and triglycerides). Fasting serum samples were collected at baseline and at weeks 12 and 24 for determination of lipoprotein particle subfractions by nuclear magnetic resonance (NMR) spectroscopy (LipoScience) (14). Diameter ranges (nm) for LDL cholesterol were 21.2–23 for large LDL and 18–21.2 for small LDL; ranges for HDL cholesterol were 8.8–13 for large HDL, 8.2–8.8 for medium HDL, and 7.3–8.2 for small HDL (14). LDL cholesterol levels were calculated using the Friedewald formula. For apolipoprotein levels, serum samples were analyzed from the placebo and 4- and 8-mg baricitinib groups at baseline and weeks 4 and 12. Apolipoprotein A-I, apolipoprotein B, apolipoprotein CIII (LDL-associated and total), and lipoprotein (a) (Lp[a]), as well as HDL-associated serum amyloid A (SAA) were quantified using conventional enzyme-linked immunosorbent assays (Pacific Biomarkers).

The standard cholesterol panel (LDL, HDL, triglycerides, and total cholesterol) as well as the NMR panel (lipoprotein subfractions) were planned as part of the original study protocol. Assessments at baseline, week 12, and week 24 were planned to evaluate the effects of the various doses of baricitinib, relative to placebo or to each other, at the end of each study period. Patients were in a fasting state at the time of sample collection so the results would not be affected by timing in relation to meals, as patient visits could be scheduled throughout the day. The specialized lipid panel (apolipoprotein B, apolipoprotein A-I, LDL-associated apolipoprotein CIII, and HDL-associated SAA) was analyzed from stored samples collected during the course of the trial. Because the 4-mg and 8-mg doses of baricitinib were carried into the long-term extension of this study, analysis was limited to patients from those dose groups. In addition to baseline and week 12, week 4 was selected in order to understand the kinetics of any observed changes in this apolipoprotein panel.

Statistical analysis. Conventional lipid profile and lipoprotein particle size and number (assessed by NMR) were summarized as mean changes from baseline and compared between each treatment group and the placebo group by Student's unpaired 2-tailed *t*-test. For patients within the same treatment group, changes from baseline values were analyzed by 1-sample *t*-test. For each treatment group, apolipoprotein values were summarized as median percent changes from baseline and compared to placebo using the Wilcoxon-Mann-Whitney test. Changes from baseline values among patients within the same treatment group were analyzed by Wilcoxon's signed rank test. The strengths of linear associations between levels of lipids and inflammatory markers (high-sensitivity C-reactive protein [hsCRP]) and various RA disease improvement and activity

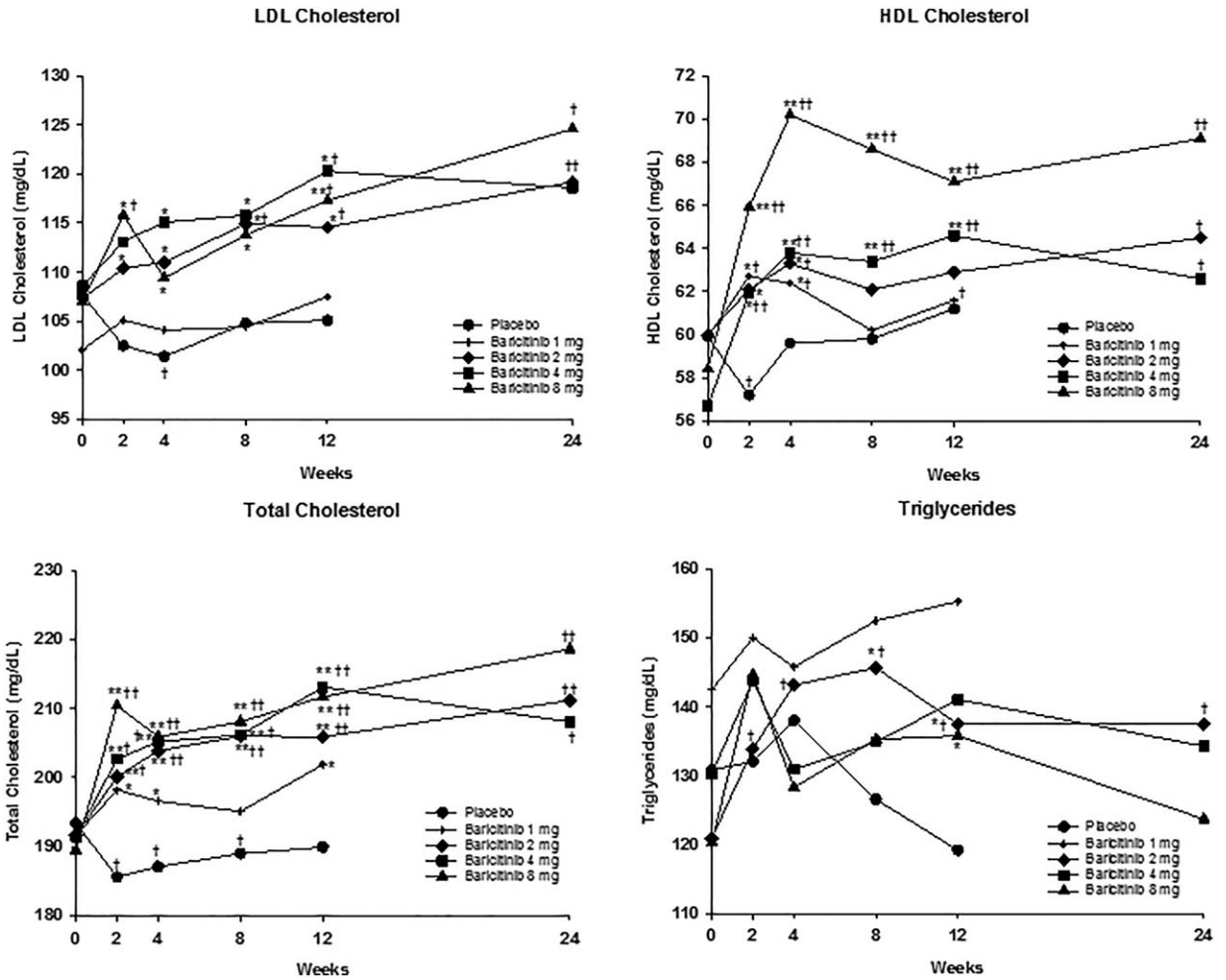

Figure 1. Dose- and time-dependent changes in the levels of low-density lipoprotein (LDL) cholesterol, high-density lipoprotein (HDL) cholesterol, total cholesterol, and triglycerides in the baricitinib treatment groups and the placebo group over 24 weeks. Baseline, week 12, and week 24 values were obtained with patients in a fasting state. Only patients in the 2, 4, and 8 mg baricitinib treatment groups continued treatment beyond week 12. Values are the mean. $* = P < 0.05$ versus placebo; $** = P < 0.001$ versus placebo; $\dagger = P < 0.05$ versus baseline in the same treatment group; $\dagger\dagger = P < 0.001$ versus baseline in the same treatment group.

measures (Disease Activity Score 28-joint assessment [DAS28], Simplified Disease Activity Index [SDAI], and Clinical Disease Activity Index [CDAI]) (16–18) were assessed by correlation analysis. The Pearson correlation coefficient was used for assessing the relationship with hsCRP, and the Pearson and partial correlation coefficients were used within and across treatment groups, respectively, for assessing the relationships with disease activity measures, including tests for increasing or decreasing strength of linear relationship between lipid changes and disease activity measures. For analyses at a given time point, only patients with available data from that time point were included; no missing data imputation was performed.

RESULTS

Demographic and baseline clinical characteristics of the different treatment groups were generally comparable (6). The overall study population was 74% white and 83% female, with a mean age of 51 years and mean disease duration of 5.6 years. Forty-nine percent of the patients were being treated with steroids, at a mean dosage of 6 mg/day. The mean baseline DAS28 using the CRP (DAS28-CRP) was 5.5, with ~70% of patients being seropositive for rheumatoid factor and/or anti–citrullinated protein antibodies. Increases in levels of LDL cholesterol, HDL cholesterol, triglycerides, and total cholesterol were observed as early as week 2 in patients receiving baricitinib treatment, and were dose dependent over time. LDL cholesterol levels in the 1-, 2-, 4-, and 8-mg baricitinib groups increased by 3.4, 8.0, 9.5, and 11.8 mg/dl, respectively, from baseline to week 12. HDL cholesterol levels increased by 3.3, 3.0, 7.3, and 8.1 mg/dl, and triglyceride levels increased by 6.4, 15.3, 8.5, and 15.4 mg/dl

Table 1. Lipoprotein particle subfractions in patients with moderate-to-severe rheumatoid arthritis*

		Baricitinib			
	Placebo (n = 98)	1 mg/day (n = 49)	2 mg/day (n = 52)	4 mg/day (n = 52)	8 mg/day (n = 50)
LDL, nmoles/liter					
Total LDL particles					
Baseline	1,251 ± 385	1,269 ± 474	1,324 ± 504	1,319 ± 373	1,285 ± 397
Week 12	1,191 ± 374	1,243 ± 441	1,275 ± 512	1,306 ± 404	1,248 ± 414
Week 24	–	–	1,309 ± 474	1,233 ± 422	1,270 ± 429
Mean change from baseline					
At week 12	−80 ± 280†	−55 ± 307	−56 ± 294	−4 ± 287	−35 ± 303
At week 24	–	–	−18 ± 344	−69 ± 301	−67 ± 366
Large LDL particles					
Baseline	521 ± 293	463 ± 283	476 ± 207	512 ± 242	490 ± 234
Week 12	507 ± 226	494 ± 293	536 ± 265	564 ± 271	555 ± 284
Week 24	–	–	568 ± 302	544 ± 262	581 ± 251
Mean change from baseline					
At week 12	−29 ± 200	45 ± 193‡	61 ± 168†‡	56 ± 163†‡	61 ± 250‡
At week 24	–	–	88 ± 212†	42 ± 220	69 ± 229
Small LDL particles					
Baseline	693 ± 425	765 ± 552	801 ± 501	771 ± 397	754 ± 451
Week 12	648 ± 416	706 ± 536	690 ± 527	700 ± 514	645 ± 490
Week 24	–	–	697 ± 502	640 ± 507	642 ± 494
Mean change from baseline					
At week 12	−50 ± 257	−99 ± 311†	−119 ± 268†	−64 ± 302	−103 ± 410
At week 24	–	–	−103 ± 397	−123 ± 337†	−139 ± 433†
Medium small LDL particles					
Baseline	146 ± 88	159 ± 114	163 ± 101	158 ± 85	157 ± 93
Week 12	136 ± 85	147 ± 115	143 ± 111	145 ± 102	134 ± 100
Week 24	–	–	146 ± 106	131 ± 99	129 ± 96
Mean change from baseline					
At week 12	−10 ± 56	−20 ± 66	−21 ± 57†	−12 ± 61	−22 ± 82
At week 24	–	–	−17 ± 84	−27 ± 66†	−33 ± 89†
Very small LDL particles					
Baseline	546 ± 339	607 ± 439	638 ± 403	613 ± 314	597 ± 360
Week 12	512 ± 333	559 ± 422	547 ± 418	555 ± 413	511 ± 392
Week 24	–	–	551 ± 396	509 ± 409	512 ± 398
Mean change from baseline					
At week 12	−39 ± 208	−79 ± 250†	−97 ± 217†	−52 ± 244	−81 ± 330
At week 24	–	–	−86 ± 317	−96 ± 275†	−106 ± 348†
HDL, μmoles/liter					
Total HDL particles					
Baseline	32 ± 6	33 ± 7	32 ± 8	33 ± 7	31 ± 8
Week 12	32 ± 7	34 ± 7	33 ± 8	38 ± 8	36 ± 9
Week 24	–	–	35 ± 7	37 ± 8	37 ± 7
Mean change from baseline					
At week 12	1 ± 6	2 ± 6	1 ± 6	4 ± 6‡§	4 ± 6§¶
At week 24	–	–	2 ± 6†	3 ± 5§	5 ± 6§
Large HDL particles					
Baseline	10 ± 4	10 ± 5	10 ± 4	9 ± 3	9 ± 4
Week 12	11 ± 4	10 ± 5	10 ± 5	10 ± 5	11 ± 5
Week 24	–	–	10 ± 4	10 ± 4	11 ± 5
Mean change from baseline					
At week 12	0	1†	0	1†	1†
At week 24	–	–	1†	1	1†
Medium HDL particles					
Baseline	4 ± 4	4 ± 5	4 ± 4	3 ± 3	4 ± 5
Week 12	3 ± 3	4 ± 3	5 ± 7	4 ± 5	5 ± 7
Week 24	–	–	5 ± 5	4 ± 4	6 ± 6
Mean change from baseline					
At week 12	−1 ± 3	−1 ± 4	1 ± 5‡	2 ± 5†‡	1 ± 4‡
At week 24	–	–	1 ± 3†	1 ± 3†	1 ± 5
Small HDL particles					
Baseline	18 ± 7	19 ± 5	19 ± 7	22 ± 6	18 ± 7
Week 12	19 ± 7	21 ± 6	19 ± 6	23 ± 7	20 ± 6
Week 24	–	–	19 ± 7	23 ± 7	20 ± 6
Mean change from baseline					
At week 12	1 ± 5	2 ± 4†	−1 ± 5	1 ± 6	2 ± 5†
At week 24	–	–	0 ± 5	2 ± 6	2 ± 7†

Table 1. *(Cont'd)*

		Baricitinib			
	Placebo (n = 98)	1 mg/day (n = 49)	2 mg/day (n = 52)	4 mg/day (n = 52)	8 mg/day (n = 50)
IDL, nmoles/liter					
IDL particles					
Baseline	37 ± 40	40 ± 52	46 ± 58	37 ± 34	41 ± 50
Week 12	36 ± 42	43 ± 63	48 ± 69	42 ± 45	48 ± 58
Week 24	–	–	43 ± 51	48 ± 53	48 ± 58
Mean change from baseline					
At week 12	−1 ± 39	−1 ± 47	1 ± 53	4 ± 46	7 ± 45
At week 24	–	–	−4 ± 54	12 ± 49	3 ± 55
VLDL, nmoles/liter					
Total VLDL particles					
Baseline	62 ± 40	73 ± 49	63 ± 41	60 ± 28	58 ± 34
Week 12	55 ± 32	81 ± 58	70 ± 48	72 ± 37	69 ± 46
Week 24	–	–	72 ± 36	76 ± 38	73 ± 46
Mean change from baseline					
At week 12	−7 ± 27†	5 ± 31‡	6 ± 33‡	12 ± 28†¶	12 ± 38†‡
At week 24	–	–	8 ± 31	15 ± 35†	13 ± 38†
Medium VLDL particles					
Baseline	25 ± 24	32 ± 28	26 ± 26	20 ± 17	23 ± 22
Week 12	21 ± 16	41 ± 37	31 ± 40	28 ± 23	28 ± 25
Week 24	–	–	29 ± 24	30 ± 24	28 ± 28
Mean change from baseline					
At week 12	−3 ± 19	8 ± 22†‡	5 ± 25‡	8 ± 21†‡	5 ± 26‡
At week 24	–	–	4 ± 20	8 ± 25†	4 ± 24
Small VLDL particles					
Baseline	35 ± 19	38 ± 23	35 ± 18	36 ± 17	32 ± 15
Week 12	32 ± 20	36 ± 23	35 ± 20	39 ± 19	37 ± 22
Week 24	–	–	39 ± 16	43 ± 20	42 ± 23
Mean change from baseline					
At week 12	−4 ± 15†	−3 ± 20	1 ± 20	3 ± 18‡	5 ± 18†‡
At week 24	–	–	4 ± 16	7 ± 18†	9 ± 21†

* Patients were randomized to receive placebo or the indicated doses of once-daily baricitinib. Values are the mean ± SD. LDL = low-density lipoprotein; HDL = high-density lipoprotein; IDL = intermediate-density lipoprotein; VLDL = very low-density lipoprotein.
† $P < 0.05$ versus baseline in the same treatment group.
‡ $P < 0.05$ versus placebo.
§ $P < 0.001$ versus baseline in the same treatment group.
¶ $P < 0.001$ versus placebo.

(Figure 1 and Supplementary Table 1, available on the *Arthritis & Rheumatology* web site at http://onlinelibrary.wiley.com/doi/10.1002/art.40036/abstract). There were no changes in the HDL cholesterol:LDL cholesterol ratio at 12 or 24 weeks in any of the baricitinib dose groups (Supplementary Table 1). With the exception of patients in the 8-mg baricitinib group (at week 12), patients receiving concomitant treatment with a hydroxymethylglutaryl-coenzyme A reductase inhibitor (statin) during the study did not have significant increases in LDL cholesterol levels compared with the placebo group at 12 or 24 weeks (see Supplementary Table 2, http://onlinelibrary.wiley.com/doi/10.1002/art.40036/abstract), although the sample size was small (n = 31).

Lipoprotein profiling on NMR demonstrated that the mean increase in LDL cholesterol levels in patients being treated with baricitinib was coincident with an increase in the total number of large LDL particles and a decrease in the number of small, dense LDL particles (Table 1). The number of large LDL particles was significantly increased at week 12 in all baricitinib treatment groups versus placebo, and at week 24 versus baseline in the 2-mg group (within treatment group). Compared with conditions at baseline, the numbers of very small and medium small LDL particles were significantly reduced at 24 weeks in the 4- and 8-mg baricitinib groups (Table 1). As a result, the total LDL particle number did not change with baricitinib treatment. The mean increase in HDL cholesterol levels among patients being treated with baricitinib was accompanied by a mean increase in total HDL particle number, which was significant in the 4- and 8-mg baricitinib groups at week 12 (versus placebo and within treatment) and week 24 (within treatment only)

Table 2. Percent change from baseline in apolipoprotein results*

		Baricitinib	
	Placebo (n = 96)	4 mg/day (n = 52)	8 mg/day (n = 50)
Apolipoprotein A-I, mg/dl			
Baseline	184.0 ± 5.5	188.0 ± 10	178.5 ± 8.5
Percent change from baseline			
At week 4	−1.9 ± 3.0	5.1 ± 4.1†‡	11.6 ± 3.9§¶
At week 12	1.1 ± 2.5	9.5 ± 3.8†‡	12.2 ± 3.0‡§
Apolipoprotein B, mg/dl			
Baseline	105.0 ± 3	110.5 ± 6.5	100.0 ± 6.5
Percent change from baseline			
At week 4	−4.5 ± 2.6†	3.6 ± 2.44‡	0.85 ± 3‡
At week 12	−4.5 ± 0.93†	6.8 ± 3.55‡	7.14 ± 3.83‡
Apolipoprotein B:apolipoprotein A-I ratio			
Baseline	0.6 ± 0.03	0.6 ± 0.03	0.6 ± 0.03
Percent change from baseline			
At week 4	−3.4 ± 2.5†	−2.69 ± 3.0	−9.8 ± 5.3‡
At week 12	−6.6 ± 2.7†	−5.33 ± 2.7	−4.9 ± 6.2
Apolipoprotein CIII, mg/dl			
Baseline	8.3 ± 0.4	7.6 ± 0.65	7.4 ± 0.6
Percent change from baseline			
At week 4	−4.2 ± 4.3	17.0 ± 13.0	22.3 ± 10.5‡§
At week 12	−8.9 ± 4.3	23.0 ± 6.9†‡	19.7 ± 3.8§¶
LDL-associated apolipoprotein CIII, mg/dl			
Baseline	1.1 ± 0.08	1.2 ± 0.17	1.2 ± 0.12
Percent change from baseline			
At week 4	−20.8 ± 14.8	−4.7 ± 18.7	−1.3 ± 18.1
At week 12	0 ± 8.3	−4.5 ± 10.8	−9.0 ± 18.9
HDL-associated serum amyloid A, mg/liter			
Baseline	5.7 ± 0.6	6.4 ± 0.9	11.1 ± 3.5
Percent change from baseline			
At week 4	12.0 ± 14.3	−51.3 ± 5.3§¶	−50.2 ± 7.5†¶
At week 12	11.3 ± 6.5	−36.0 ± 3.5†‡	−32.0 ± 16.1†‡
Lipoprotein(a), mg/dl			
Baseline	8.4 ± 1.5	10.7 ± 3.0	11.1 ± 2.3
Percent change from baseline			
At week 4	0.7 ± 5.4	2.53 ± 7.4	−8.1 ± 6.5†‡
At week 12	−2.4 ± 3.9	−4.62 ± 4.5	−16.6 ± 2.6†

* Data on 2 of the 98 placebo-treated patients were missing for these analyses. Due to skewed distribution, values are reported as the median ± SEM. LDL = low-density lipoprotein; HDL = high-density lipoprotein.
† $P < 0.05$ versus baseline in the same treatment group.
‡ $P < 0.05$ versus placebo.
§ $P < 0.001$ versus baseline in the same treatment group.
¶ $P < 0.001$ versus placebo.

(Table 1). The increase in total HDL particle number was accounted for by increases in all HDL particles (large, medium, and small). Finally, the observed mean increase in triglyceride levels was also coincident with a mean increase in total very low-density lipoprotein (VLDL) particle number (Table 1).

Consistent with the results regarding LDL and HDL cholesterol, increases in apolipoprotein B and apolipoprotein A-I were observed as early as 4 weeks in patients in the 4- and 8-mg baricitinib groups (Table 2). With the exception of the 8-mg baricitinib group (at week 4), decreases in the apolipoprotein B/apolipoprotein A-I ratio were not significant compared to the placebo group. A significant increase was observed in total apolipoprotein CIII at weeks 4 and 12 in the 8-mg baricitinib group (versus placebo and within treatment) and at 12 weeks in the 4-mg baricitinib group versus placebo and within treatment. However, no changes were observed in the amount of apolipoprotein CIII associated with LDL. There were significant reductions in HDL-associated SAA at weeks 4 and 12

Table 3. Correlation analysis between lipid changes and changes in clinical end points from baseline to week 12*

Clinical end point	HDL cholesterol		LDL cholesterol		Triglycerides		Total cholesterol	
	r†	*P*	r†	*P*	r†	*P*	r†	*P*
DAS28-CRP	−0.23	<0.001	0.02	0.806	0.07	0.234	−0.03	0.572
DAS28-ESR	−0.17	0.004	0.09	0.143	0.07	0.273	0.05	0.419
SDAI	−0.14	0.022	0.00	0.980	0.12	0.059	0.00	0.984
CDAI	−0.08	0.185	0.01	0.921	0.13	0.031	0.03	0.590

* HDL = high-density lipoprotein; LDL = low-density lipoprotein; DAS28-CRP = Disease Activity Score 28-joint assessment using the C-reactive protein level; DAS28-ESR = DAS28 using the erythrocyte sedimentation rate; SDAI = Simplified Disease Activity Index; CDAI = Clinical Disease Activity Index.
† Pearson partial correlation coefficient.

in the baricitinib 4- and 8-mg dose groups (versus placebo and within treatment). Finally, a significant reduction in Lp(a) was observed only in the 8-mg treatment group at week 4 (versus placebo and within treatment) and week 12 (within treatment).

Changes in hsCRP levels (mg/liter) with baricitinib treatment through 12 weeks have been previously reported (−0.4 with placebo, and −3.3, −0.8, −2.0, and −3.0 with treatment at 1 mg, 2 mg, 4 mg, and 8 mg, respectively) (8); in this secondary analysis, changes in HDL cholesterol demonstrated an inverse correlation with changes in hsCRP ($r = -0.37$, $P < 0.0001$) among patients treated with baricitinib. In contrast, changes in LDL cholesterol with baricitinib treatment did not correlate with changes in hsCRP ($r = -0.02$, $P = 0.7291$) (Supplementary Figure 1, available on the *Arthritis & Rheumatology* web site at http://onlinelibrary.wiley.com/doi/10.1002/art.40036/abstract).

Further correlation analyses with disease activity measures revealed a dose-dependent relationship between change from baseline in HDL cholesterol and change from baseline to week 12 in DAS28-CRP ($P < 0.001$ [$P = 0.005$ for the dose-response test]), as well as in DAS28 using the erythrocyte sedimentation rate (DAS28-ESR) ($P = 0.004$ [$P = 0.019$ for the dose-response test]) and SDAI ($P = 0.022$ [$P = 0.003$ for the dose-response test]), with no apparent relationship

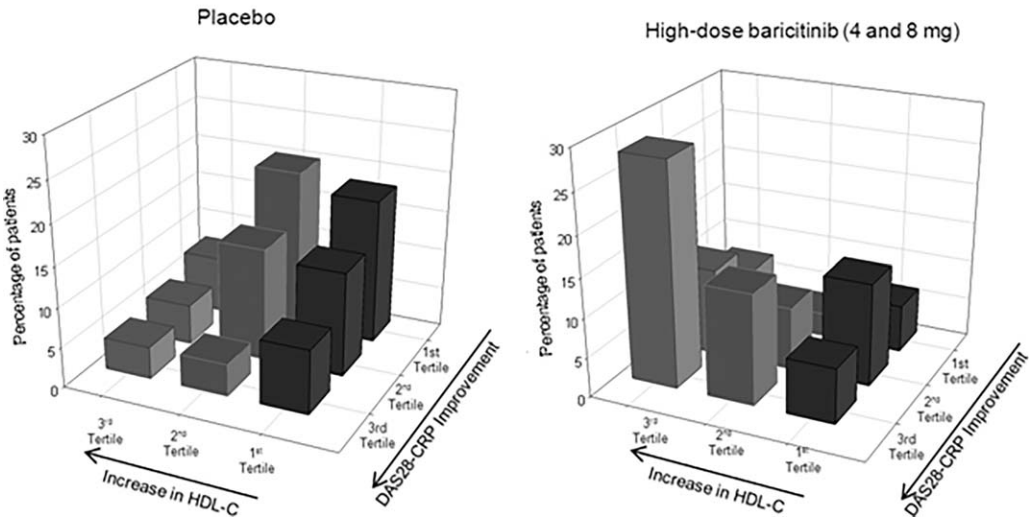

Figure 2. Correlation analysis of the changes in high-density lipoprotein cholesterol (HDL-C) levels from baseline to week 12 versus changes in the Disease Activity Score 28-joint assessment using the C-reactive protein level (DAS28-CRP) from baseline to week 12. Patients were divided into tertiles of change in HDL cholesterol levels (first tertile ≤0.0 mg/dl, second tertile >0.0 but ≤7.7 mg/dl, and third tertile >7.7 mg/dl) and change in the DAS28-CRP from baseline to week 12 (lowest tertile of improvement <1.07, second tertile ≥1.07 but <1.97, highest tertile ≥1.97). Higher peaks along the east–west diagonal represent an increased relationship between changes in HDL cholesterol levels and changes in the DAS28-CRP.

observed for placebo and correlations increasing in magnitude with increasing baricitinib dose levels (Table 3). In patients treated with baricitinib, increases in HDL cholesterol were significantly correlated with an improvement in the DAS28-CRP (for all baricitinib treatment groups combined; $r = -0.28$, $P < 0.001$) (Figure 2 and Supplementary Figure 2, http://onlinelibrary.wiley.com/doi/10.1002/art.40036/abstract). Correlations were −0.05, −0.28, −0.14, and −0.55 following treatment with baricitinib at 1, 2, 4, and 8 mg, respectively. In patients treated with placebo, no relationship between HDL cholesterol and DAS28-CRP was apparent ($r = -0.05$, $P = 0.648$). A similar correlation analysis comparing total cholesterol, LDL cholesterol, and triglyceride levels with disease activity measures revealed no relationships with total cholesterol and LDL cholesterol (Table 3). Triglyceride levels were found to have a positive correlation with the CDAI ($r = 0.13$, $P = 0.031$) (change from baseline to week 12), but not with the DAS28 or SDAI (Table 3).

DISCUSSION

Following 2 weeks of baricitinib treatment, increases in LDL cholesterol, HDL cholesterol, and triglyceride levels were observed and remained elevated through 24 weeks. The increase in LDL cholesterol levels after treatment with baricitinib was associated with a shift in LDL particle distribution, as shown on NMR. It is well established that increases in the total number of LDL and small, dense LDL particles are both directly associated with incident coronary heart disease (CHD) (19,20). In the present study, however, treatment with baricitinib did not increase the number of total LDL particles and in fact decreased the number of small, dense LDL particles. These results would suggest that the shift in LDL particle size to large LDL particles is most likely responsible for the observed increase in LDL cholesterol levels.

In contrast, the increase in HDL cholesterol levels with baricitinib treatment was concurrent with an increase in the total number of HDL particles, which was mostly due to medium HDL particles but also all other (large and small) HDL particles. In addition to the well-established inverse association of HDL cholesterol level with risk of CHD (21), the total number of HDL particles has also been shown to be inversely associated with carotid intima-media thickness and incident CHD, in the Multi-Ethnic Study of Atherosclerosis (22). The inverse association shown in that study was independent of atherogenic lipoproteins (including total number of LDL particles) and HDL cholesterol level. Consistent with the increase in the number of HDL particles, treatment with baricitinib resulted in an increase in apolipoprotein A-I and a reduction in SAA content on the HDL particles. Because SAA negatively impacts HDL function by reducing the ability of these particles to mediate cholesterol efflux (23), a reduction in SAA per HDL particle would likely render these particles more efficient for reverse cholesterol transport (24). Similar results have also been found in studies regarding treatments with anti-TNF (25), tofacitinib (9), and tocilizumab (26).

The NMR lipoprotein profile also showed no change in intermediate-density lipoprotein particles but did reflect an increase in the total number of VLDL particles, which most likely accounts for the increase in triglyceride levels. Increases in apolipoprotein B and apolipoprotein CIII were also observed with baricitinib treatment. Although TNF inhibitors also increase apolipoprotein B in conjunction with increases in LDL cholesterol (25), their use is associated with a decreased incidence of cardiovascular events (27). The increases in apolipoprotein B and apolipoprotein CIII in the present study are consistent with the increases observed in VLDL particle number and serum triglycerides. Additionally, a reduction in Lp(a) was also observed at week 4 (within treatment and compared to placebo) and at week 12 (within treatment only) in patients treated with 8 mg of baricitinib (but not for the 4-mg dosage group).

The present study also demonstrated a correlation between the increase in HDL cholesterol levels and the change from baseline to week 12 in the DAS28-CRP. The increase in HDL cholesterol levels also correlated with change from baseline to week 12 in the DAS28-ESR and the SDAI. This association provides additional support for a potential causal relationship between the increase in HDL cholesterol levels and the reduction in inflammation and disease activity scores. Significant dose-response relationships were identified in the correlation analyses of HDL cholesterol levels, suggesting that the relationship between HDL cholesterol and disease activity measures became greater in magnitude as a result of the baricitinib treatment. The lack of a similar correlation between these disease activity scores and the increases in LDL cholesterol and total cholesterol levels demonstrates the possibility of different mechanisms for explaining the increase in HDL cholesterol versus LDL cholesterol levels. Furthermore, although a positive correlation was observed between triglyceride levels and the CDAI, a similar relationship was not observed with other disease activity scores.

There were some limitations in this study. Enrollment in this study was restricted to the anti-TNF/biologic-naive population being treated with methotrexate, and

thus interpretation was limited to this patient subset. Although the increase noted in LDL cholesterol levels was not observed in a subgroup of patients treated with baricitinib (n = 31) who were receiving a statin at various times during the study, the number of patients receiving statins varied across treatment groups. There was no attempt to evaluate the effects of statin initiation or dosage on the lipid profile of patients being treated with baricitinib. Thus, it is noteworthy to mention that by chance a higher percentage of patients in the 4- and 8-mg baricitinib groups were receiving concomitant statins than those being treated with the lower baricitinib doses. Therefore, it is possible that the increases in total cholesterol levels in these two higher dosage groups would have been higher than in the lower doses, as suggested in the subset analysis of the non–statin users versus statin users (see Supplementary Table 2, available on the *Arthritis & Rheumatology* web site at http://onlinelibrary.wiley.com/doi/10.1002/art.40036/abstract). However, due to the small sample size per treatment arm once non–statin users and statin users are subdivided, interpretation of this subgroup analysis should be undertaken with caution.

Additionally, the use of other lipid-lowering medications was not restricted; however, the initiation of new medications and/or treatments during the course of the study was prohibited unless it was required in order to treat an adverse event or ongoing medical condition. The placebo-controlled period was limited to 12 weeks duration due to ethical concerns of continuing placebo in patients with active RA. Evaluation of the changes in lipid profile and lipoprotein particle size and number was limited to 24 weeks, with a total enrollment of 301 patients based on the phase II dose-ranging study design. Finally, as with any post hoc analyses and especially with evaluations in small subgroups, the number of statistical comparisons performed without control of the Type I error rate may lead to some spurious findings.

The results found in this study are most consistent with those reported in studies of patients treated with tocilizumab, in whom increases in total cholesterol, LDL cholesterol, HDL cholesterol, and triglyceride levels, and reductions in HDL-associated SAA and Lp(a) have been described (10). These similarities suggest that the inhibition of IL-6 signaling may explain, in part, the mechanism by which baricitinib modulates lipoprotein particle distribution and metabolism. Treatment with the JAK inhibitor tofacitinib has resulted in increases in LDL cholesterol, HDL cholesterol, total cholesterol, and triglyceride levels, with increases in HDL particle number and LDL particle size, similarly observed by NMR (9). That study also showed that tofacitinib decreased the fractional catabolic rate for cholesterol esters, which in part may explain the similar qualitative changes in serum lipids observed in our study. The present study demonstrated a series of changes in lipid particle size and apolipoproteins in patients with RA who were receiving treatment with baricitinib. Before the clinical impact of the lipid changes described in this study can be better understood, longer-term observational studies that track actual cardiovascular events and lipid changes of patients being treated with baricitinib are needed.

ACKNOWLEDGMENTS

The authors would like to thank Stephanie Brillhart and Kathy Oneacre of inVentiv Health Clinical for their writing and editorial assistance and draft coordination during manuscript preparation.

AUTHOR CONTRIBUTIONS

All authors were involved in drafting the article or revising it critically for important intellectual content, and all authors approved the final version to be published. Dr. Kremer had full access to all of the data in the study and takes responsibility for the integrity of the data and the accuracy of the data analysis.

Study conception and design. Kremer, Genovese, Keystone, Taylor, Zuckerman, Schlichting, Beattie, Macias.

Acquisition of data. Kremer, Genovese, Keystone, Macias.

Analysis and interpretation of data. Kremer, Genovese, Keystone, Taylor, Zuckerman, Ruotolo, Schlichting, Crotzer, Nantz, Beattie, Macias.

ROLE OF THE STUDY SPONSOR

The study was designed by Eli Lilly and Company in consultation with an academic advisory board and Incyte Corporation. Eli Lilly and Company provided data analysis, laboratory, and site-monitoring services and was involved in data interpretation. All authors and Eli Lilly and Company reviewed and approved the manuscript. The authors maintained control over the final content. Writing and editorial support for the manuscript was provided by Stephanie Brillhart and Kathy Oneacre (inVentiv Health Clinical) and was funded by Eli Lilly and Company.

REFERENCES

1. Smolen JS, Aletaha D, Koeller M, Weisman MH, Emery P. New therapies for treatment of rheumatoid arthritis. Lancet 2007;370:1861–74.
2. Smolen JS, Steiner G. Therapeutic strategies for rheumatoid arthritis. Nat Rev Drug Discov 2003;2:473–88.
3. Leonard WJ, O'Shea JJ. Jaks and STATs: biological implications. Annu Rev Immunol 1998;16:293–322.
4. O'Shea JJ, Kontzias A, Yamaoka K, Tanaka Y, Laurence A. Janus kinase inhibitors in autoimmune diseases. Ann Rheum Dis 2013;72 Suppl 2:ii111–5.
5. Fridman JS, Scherle PA, Collins R, Burn TC, Li Y, Li J, et al. Selective inhibition of JAK1 and JAK2 is efficacious in rodent models of arthritis: preclinical characterization of INCB028050. J Immunol 2010;184:5298–307.

6. Keystone EC, Taylor PC, Drescher E, Schlichting DE, Beattie SD, Berclaz PY, et al. Safety and efficacy of baricitinib at 24 weeks in patients with rheumatoid arthritis who have had an inadequate response to methotrexate. Ann Rheum Dis 2015;74: 333–40.
7. Felson DT, Anderson JJ, Boers M, Bombardier C, Furst D, Goldsmith C, et al. American College of Rheumatology preliminary definition of improvement in rheumatoid arthritis. Arthritis Rheum 1995;38:727–35.
8. Greenwald MW, Fidelus-Gort R, Levy R, Liang J, Vaddi K, Williams WV, et al. A randomized dose-ranging, placebo-controlled study of INCB028050, a selective JAK1 and JAK2 inhibitor in subjects with active rheumatoid arthritis [abstract]. Arthritis Rheum 2010;62 Suppl:S911.
9. Charles-Schoeman C, Fleischmann R, Davignon J, Schwartz H, Turner SM, Beysen C, et al. Potential mechanisms leading to the abnormal lipid profile in patients with rheumatoid arthritis versus healthy volunteers and reversal by tofacitinib. Arthritis Rheumatol 2015;67:616–25.
10. Genovese MC, McKay JD, Nasonov EL, Mysler EF, da Silva NA, Alecock E, et al. Interleukin-6 receptor inhibition with tocilizumab reduces disease activity in rheumatoid arthritis with inadequate response to disease-modifying antirheumatic drugs: the tocilizumab in combination with traditional disease-modifying antirheumatic drug therapy study. Arthritis Rheum 2008;58:2968–80.
11. Tam LS, Tomlinson B, Chu TT, Li TK, Li EK. Impact of TNF inhibition on insulin resistance and lipids levels in patients with rheumatoid arthritis. Clin Rheumatol 2007;26:1495–8.
12. Navarro-Millán I, Charles-Schoeman C, Yang S, Bathon JM, Bridges SL Jr, Chen L, et al. Changes in lipoproteins associated with methotrexate or combination therapy in early rheumatoid arthritis: results from the treatment of early rheumatoid arthritis trial. Arthritis Rheum 2013;65:1430–8.
13. Carmena R, Duriez P, Fruchart JC. Atherogenic lipoprotein particles in atherosclerosis. Circulation 2004;109 Suppl 1:III2–7.
14. Jeyarajah EJ, Cromwell WC, Otvos JD. Lipoprotein particle analysis by nuclear magnetic resonance spectroscopy. Clin Lab Med 2006;26:847–70.
15. Mora S, Otvos JD, Rifai N, Rosenson RS, Buring JE, Ridker PM. Lipoprotein particle profiles by nuclear magnetic resonance compared with standard lipids and apolipoproteins in predicting incident cardiovascular disease in women. Circulation 2009;119: 931–9.
16. Prevoo ML, van 't Hof MA, Kuper HH, van Leeuwen MA, van de Putte LB, van Riel PL. Modified disease activity scores that include twenty-eight–joint counts: development and validation in a prospective longitudinal study of patients with rheumatoid arthritis. Arthritis Rheum 1995;38:44–8.
17. Smolen JS, Breedveld FC, Schiff MH, Kalden JR, Emery P, Eberl G, et al. A Simplified Disease Activity Index for rheumatoid arthritis for use in clinical practice. Rheumatology (Oxford) 2003;42:244–57.
18. Aletaha D, Nell VP, Stamm T, Uffmann M, Pflugbeil S, Machold K, et al. Acute phase reactants add little to composite disease activity indices for rheumatoid arthritis: validation of a clinical activity score. Arthritis Res Ther 2005;7:R796–806.
19. Hoogeveen RC, Gaubatz JW, Sun W, Dodge RC, Crosby JR, Jiang J, et al. Small dense low-density lipoprotein-cholesterol concentrations predict risk for coronary heart disease: the Atherosclerosis Risk In Communities (ARIC) study. Arterioscler Thromb Vasc Biol 2014;34:1069–77.
20. Krauss RM. Lipoprotein subfractions and cardiovascular disease risk. Curr Opin Lipidol 2010;21:305–11.
21. Vergeer M, Holleboom AG, Kastelein JJ, Kuivenhoven JA. The HDL hypothesis: does high-density lipoprotein protect from atherosclerosis? J Lipid Res 2010;51:2058–73.
22. Mackey RH, Greenland P, Goff DC Jr, Lloyd-Jones D, Sibley CT, Mora S. High-density lipoprotein cholesterol and particle concentrations, carotid atherosclerosis, and coronary events: MESA (multi-ethnic study of atherosclerosis). J Am Coll Cardiol 2012;60:508–16.
23. Banka CL, Yuan T, de Beer MC, Kindy M, Curtiss LK, de Beer FC. Serum amyloid A (SAA): influence on HDL-mediated cellular cholesterol efflux. J Lipid Res 1995;36:1058–65.
24. Kontush A, Chapman MJ. Functionally defective high-density lipoprotein: a new therapeutic target at the crossroads of dyslipidemia, inflammation, and atherosclerosis. Pharmacol Rev 2006; 58:342–74.
25. Kirkham BW, Wasko MC, Hsia EC, Fleischmann RM, Genovese MC, Matteson EL, et al. Effects of golimumab, an anti-tumour necrosis factor-α human monoclonal antibody, on lipids and markers of inflammation. Ann Rheum Dis 2014;73:161–9.
26. McInnes IB, Thompson L, Giles JT, Bathon JM, Salmon JE, Beaulieu AD, et al. Effect of interleukin-6 receptor blockade on surrogates of vascular risk in rheumatoid arthritis: MEASURE, a randomised, placebo-controlled study. Ann Rheum Dis 2015; 74:694–702.
27. Greenberg JD, Kremer JM, Curtis JR, Hochberg MC, Reed G, Tsao P, et al. Tumour necrosis factor antagonist use and associated risk reduction of cardiovascular events among patients with rheumatoid arthritis. Ann Rheum Dis 2011;70:576–82.

ARTHRITIS & RHEUMATOLOGY
Vol. 69, No. 5, May 2017, pp 953–963
DOI 10.1002/art.40019

A Multi-Biomarker Disease Activity Score and the Choice of Second-Line Therapy in Early Rheumatoid Arthritis After Methotrexate Failure

Karen Hambardzumyan,[1] Saedis Saevarsdottir,[1] Kristina Forslind,[2] Ingemar F. Petersson,[3] Johan K. Wallman,[3] Sofia Ernestam,[4] Rebecca J. Bolce,[5] and Ronald F. van Vollenhoven[1]

Objective. **To investigate whether the Multi-Biomarker Disease Activity (MBDA) score predicts optimal add-on treatment in patients with early rheumatoid arthritis (RA) who were inadequate responders to MTX (MTX-IRs).**

Methods. **We analyzed data from 157 MTX-IRs (with a Disease Activity Score using the erythrocyte sedimentation rate [DAS28-ESR] >3.2) from the Swedish Pharmacotherapy (SWEFOT) trial who were randomized to receive triple therapy (MTX plus sulfasalazine plus hydroxychloroquine) versus MTX plus infliximab. The MBDA score as a predictor of the subsequent DAS28-based response to each second-line treatment was analyzed at randomization with the Breslow-Day test for 2 × 2 groups, using both validated categories (low [<30], moderate [30–44], and high [>44]) and dichotomized categories (lower [≤38] versus higher [>38]).**

Results. **Among the 157 patients, 12% had a low MBDA score, 32% moderate, and 56% high. Of those with a low MBDA score, 88% responded to subsequent triple therapy, and 18% responded to MTX plus infliximab ($P = 0.006$); for those with a high MBDA score, the response rates were 35% and 58%, respectively ($P = 0.040$). When using 38 as a cutoff for the MBDA score (29% patients with lower scores versus 71% with higher scores), the differential associations with response to triple therapy versus MTX plus infliximab were 79% versus 44% and 36% versus 58%, respectively ($P = 0.001$). Clinical and inflammatory markers had poorer predictive capacity for response to triple therapy or MTX plus infliximab.**

Conclusion. **In patients with RA who had an inadequate response to MTX, the MBDA score categories were differentially associated with response to subsequent therapies. Thus, patients with post-MTX biochemical improvements (lower MBDA scores) were more likely to respond to triple therapy than to MTX plus infliximab. If confirmed, these results may help to improve treatment in RA.**

In the standard care of patients with early rheumatoid arthritis (RA) (1,2), inadequate response to methotrexate (MTX) monotherapy is followed by a further intensification

ClinicalTrials.gov identifier: NCT00764725. World Health Organization database at Karolinska Institute identifier: CT20080004.

Crescendo Bioscience, Inc., a wholly owned subsidiary of Myriad Genetics, Inc., performed the analyses of serum for the Multi-Biomarker Disease Activity scores at no cost to the investigators. The Swedish Pharmacotherapy (SWEFOT) trial (2003–2010) was supported in part by a grant from the Swedish Rheumatism Association, clinical research funds from the Stockholm County Council (ALF Project funds), and an unrestricted grant from Schering-Plough Sweden.

[1]Karen Hambardzumyan, MSc, Saedis Saevarsdottir, MD, PhD, Ronald F. van Vollenhoven, MD, PhD: Karolinska Institutet, Karolinska University Hospital, Stockholm, Sweden; [2]Kristina Forslind, MD, PhD: Lund University and Helsingborg's Lasarett, Helsingborg, Sweden; [3]Ingemar F. Petersson, MD, PhD, Johan K. Wallman, MD, PhD: Lund University, Lund, Sweden; [4]Sofia Ernestam, MD, PhD: Institution LIME Medical Management Centre, Karolinska Institutet, Stockholm, Sweden; [5]Rebecca J. Bolce, MSN: Crescendo Bioscience, Inc., South San Francisco, California.

Dr. Petersson has received honoraria from AbbVie, UCB, and Pfizer (less than $10,000 each) and research support from those companies. Dr. Wallman has received honoraria from Novartis, Celgene, and UCB (less than $10,000 each). Ms Bolce owns stock or stock options in Myriad Genetics, Inc. Dr. van Vollenhoven has received consulting fees from AbbVie, Biotest, Bristol-Myers Squibb, Crescendo Bioscience, GlaxoSmithKline, Janssen, Lilly, Merck, Pfizer, Roche, UCB, and Vertex (less than $10,000 each) and research support from AbbVie, Bristol-Myers Squibb, GlaxoSmithKline, Pfizer, Roche, and UCB.

Address correspondence to Karen Hambardzumyan, MSc, ClinTRID, Karolinska University Hospital, SE-17176 Stockholm, Sweden. E-mail: karen.hambardzumyan@ki.se.

Submitted for publication February 22, 2016; accepted in revised form December 6, 2016.

Table 1. Baseline characteristics and demographic data of the study patients, by clinical response at 1 year in the SWEFOT trial*

Baseline characteristic	All SWEFOT patients (n = 487)†	MTX-IR subset in the present study		
		All MTX-IR patients (n = 157)	Responders (DAS28 ≤3.2) (n = 79)	Nonresponders (DAS28 >3.2) (n = 78)
No. (%) female	344 (70)	125 (79.6)	54 (68.4)	71 (91)‡
Symptom duration, mean ± SD months	6.2 ± 4.6	6.1 ± 3.5	6.2 ± 3. 8	6.0 ± 3.2
Anti-CCP status, no. (%)				
Positive	275 (57)	87 (55)	45 (57)	42 (54)
Negative	157 (32)	62 (40)	30 (38)	32 (41)
Not available	55 (11)	8 (5)	4 (5)	4 (5)
RF status, no. (%)				
Positive	330 (68)	97 (62)	47 (60)	50 (64)
Negative	152 (31)	59 (38)	32 (40)	27 (35)
Not available	5 (1)	1 (1)	0 (0)	1 (1)
Joint counts, mean ± SD of 28 joints				
Swollen joints	10.8 ± 5.3	11.6 ± 5.4	11.3 ± 5.3	11.9 ± 5.4
Tender joints	9.6 ± 6.1	10.6 ± 6.1	9.6 ± 6.4	11.7 ± 5.6§
ESR, mean ± SD mm/hour	39.9 ± 25.9	44.3 ± 27.0	39.7 ± 22.2	48.9 ± 30.6
CRP, mean ± SD mg/liter	33.8 ± 36.8	37.0 ± 38.2	34.5 ± 35.4	39.6 ± 4.1
PGA, mean ± SD mm (0–100-mm VAS)	56.0 ± 23.9	57.6 ± 25.1	55.0 ± 25.5	60.1 ± 24.6
DAS28, mean ± SD	5.7 ± 1.0	6.0 ± 1.0	5.8 ± 0.9	6.2 ± 0.9§
MBDA score, mean ± SD	58.6 ± 15.1	59.2 ± 15.7	58.9 ± 13.8	59.5 ± 17.5

* In the present study, a subset of 157 patients with early rheumatoid arthritis who participated in the Swedish Pharmacotherapy (SWEFOT) trial and were inadequate responders to methotrexate monotherapy (MTX-IRs) at 3 months were evaluated according to the Multi-Biomarker Disease Activity (MBDA) score. Anti-CCP = anti–cyclic citrullinated peptide; RF = rheumatoid factor; VAS = visual analog scale.
† Patients in the main study group were missing data for the following assessments: swollen and tender joint counts (n = 2), erythrocyte sedimentation rate (ESR; n = 5), C-reactive protein (CRP; n = 3), patient's global assessment (PGA; n = 3), Disease Activity Score in 28 joints (DAS28; n = 8), and MBDA score (n = 185).
‡ $P < 0.001$ versus responders, by chi-square test.
§ $P = 0.006$ versus responders, by Mann-Whitney U test (tender joint count) or Student's *t*-test (DAS28).

of treatment by adding conventional, nonbiologic disease-modifying antirheumatic drugs (cDMARDs) such as sulfasalazine and hydroxychloroquine, also known as triple therapy (3–5), or biologic medications, such as anti–tumor necrosis factor (anti-TNF), including infliximab (1,2,6). The relative strengths of these 2 options were compared in several trials. In the open-label randomized Swedish Pharmacotherapy (SWEFOT) trial, the addition of infliximab was significantly more effective after 1 year, but the difference was no longer significant after 2 years (7). Addition of infliximab to triple therapy for 6 months in patients from the New Finnish RA Combination Therapy (NEO-RACo) trial showed a clinically beneficial trend at 2 years as compared with the group of patients who received triple therapy plus placebo (8). Following further yearly examinations, however, the slope between the 2 arms merged closer, resulting in a disappearance of the trend at 5 years. In the randomized double-blind trials Treatment of Early Aggressive RA (TEAR) and RA: Comparison of Active Therapies in Patients With Active Disease Despite Methotrexate Therapy (RACAT), the addition of etanercept to MTX was not more effective than the addition of sulfasalazine plus hydroxychloroquine with regard to the primary end point, establishing formal noninferiority in the latter trial but identifying some 2-year differences in radiographic progression (in only the TEAR trial) that differed between the treatments (9,10). Moreover, even if a true difference might be present between these options, the cost difference between cDMARDs and biologic drugs is so large that use of the latter has not been shown to be cost-effective (11).

Results from all these trials, however, apply on a group level, and it stands to reason that for each patient, the 2 treatment options may have different likelihoods of response (10). Although some clinical and serologic factors have been shown to be associated with response to certain treatment options (12,13), there have yet been no consistent predictors that could identify an individual patient with a higher chance of responding to a particular therapy compared with another (14,15).

The Multi-Biomarker Disease Activity (MBDA) score is a disease activity measure based on the measurement of 12 serum biomarkers that was designed to correlate with the Disease Activity Score in 28 joints using the C-reactive protein level (DAS28-CRP) (16,17). The MBDA score includes measurement of the levels of acute-phase reactants, inflammatory cytokines, cell-adhesion molecules,

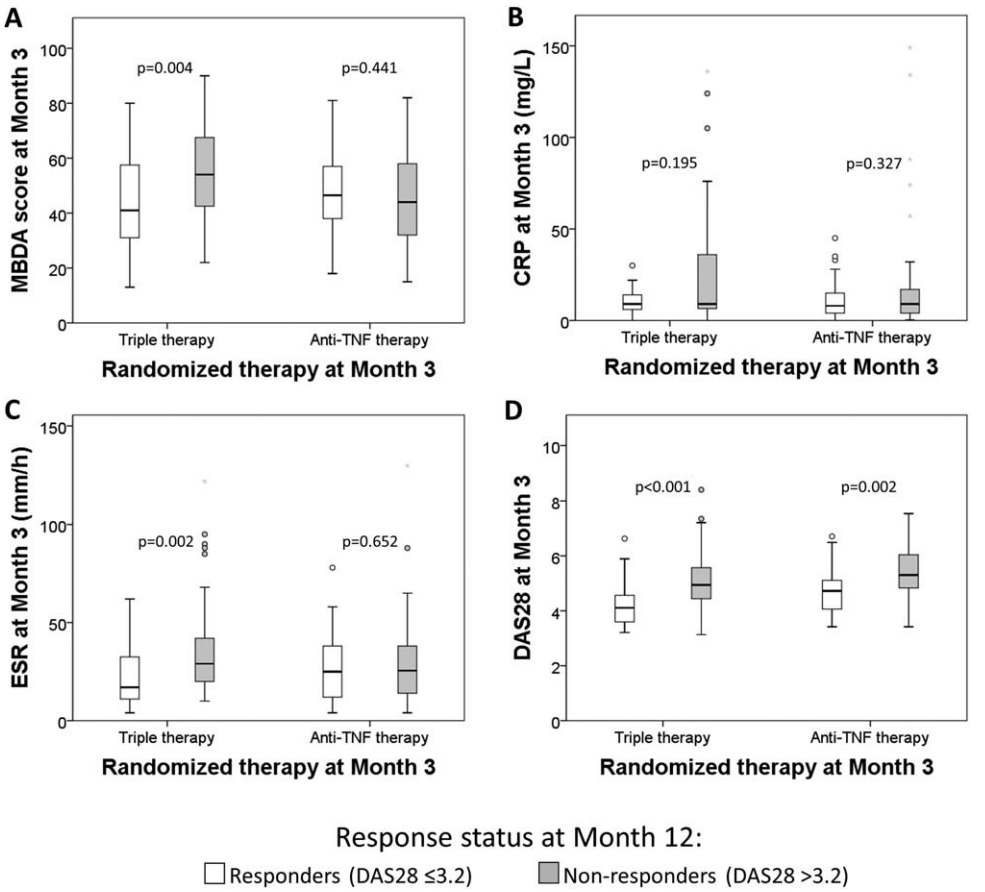

Figure 1. Distribution of disease activity measures at month 3 in responders and nonresponders to second-line therapy at year 1. The Multi-Biomarker Disease Activity (MBDA) score (**A**), C-reactive protein (CRP) level (**B**), erythrocyte sedimentation rate (ESR) (**C**), and Disease Activity Score in 28 joints (DAS28) (**D**) at month 3 (at the time of randomization) among responders and nonresponders to triple therapy or anti–tumor necrosis factor (anti-TNF) therapy are shown. Data are shown as box plots. Each box represents the upper and lower interquartile range (IQR). Lines inside the boxes represent the median. Whiskers represent 1.5 times the upper and lower IQRs. Circles indicate outliers.

adipose tissue products, and matrix metalloproteinases. We previously showed that in the SWEFOT clinical trial (7,18), low and moderate MBDA scores (<30 and 30–44, respectively) were associated with a very low risk of subsequent radiographic joint damage (19). However, baseline MBDA scores did not predict the clinical response to MTX monotherapy or to second-line therapies.

We reasoned that rather than focusing on the baseline score, the MBDA score at month 3 of MTX monotherapy might provide useful clues as to the efficacy of subsequent treatments in inadequate responders to MTX (MTX-IRs). Thus, in the present study, we investigated whether an MBDA score at the time of randomization to second-line therapy might be predictive of subsequent clinical responses to triple therapy versus MTX plus anti-TNF therapies and whether it might guide the optimal choice of treatment strategy.

PATIENTS AND METHODS

Study design. This was a post hoc study done on samples and clinical data from the SWEFOT trial. Patients with early RA (n = 487) diagnosed according to American College of Rheumatology (ACR) criteria were recruited to the SWEFOT trial. Inclusion criteria were active disease (DAS28 using the erythrocyte sedimentation rate [DAS28-ESR] >3.2), age ≥18 years, and symptom duration <1 year (7). Patients started MTX monotherapy for 3 months, and those with a DAS28 of ≤3.2 at month 3 (responders) continued the MTX monotherapy, while those with a DAS28 of >3.2 at month 3 (n = 258) were randomized to receive intensified treatment: either MTX plus sulfasalazine plus hydroxychloroquine (triple therapy) or MTX plus infliximab (anti-TNF). Samples from 157 of the 258 randomized MTX-IR patients were analyzed using the MBDA, based on availability of serum samples and completeness of the available clinical data (data available upon request from RFvV, the senior author and coordinating investigator of the SWEFOT trial).

The SWEFOT trial was registered at the World Health Organization database at Karolinska Institute (CT20080004)

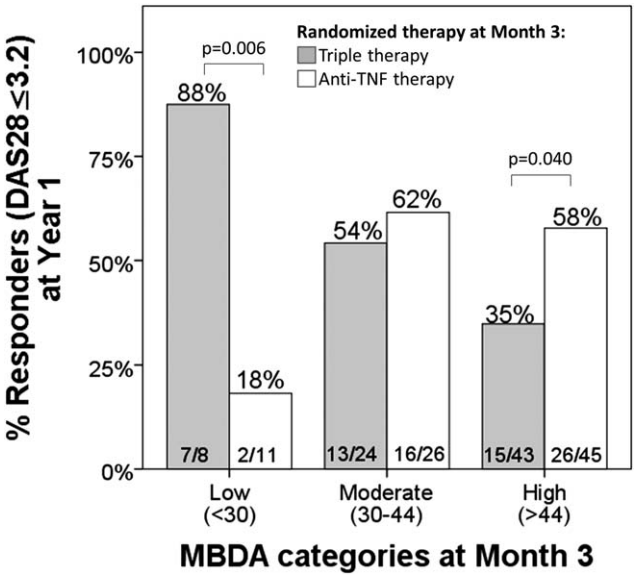

Figure 2. Proportion of patients with a clinical response to second-line therapy at year 1 according to a DAS28 score of ≤3.2, stratified by conventional cutoffs of the MBDA score at the start of treatment intensification. Responders at year 1 were evaluated according to low (<30), moderate (30–44), or high (>44) scores on the MBDA at month 3. See Figure 1 for definitions.

and at the ClinicalTrials.gov database (NCT00764725). All patients gave their written informed consent before the start of the SWEFOT trial. The trial was approved by the regional ethics committees of all participating units. See Appendix A for the names of the principal investigators.

Outcomes measures. The MBDA score at month 3 was measured and related to the likelihood of low disease activity (DAS28 ≤3.2) or good response according to the European League Against Rheumatism (EULAR) criteria (20,21) at year 1 in the 2 separate groups of MTX-IR patients: those receiving triple therapy (n = 75) and those receiving anti-TNF (n = 82). The same analysis was done after stratification of patients according to rheumatoid factor (RF) and anti–cyclic citrullinated peptide (anti-CCP) status. For comparison, we also studied values for the CRP, ESR, and DAS28 at month 3. Two of the 157 MTX-IR patients had missing CRP data (n = 155) and 3 had missing ESR data (n = 154). Categorization of the DAS28 values at month 3 was based on standard cutoffs recommended by EULAR (20,21): >3.2–5.1 for moderate disease activity and >5.1 for high disease activity. For the MBDA score, CRP level, and ESR, receiver operating characteristic (ROC) curve analysis yielded the following cutoffs (based on the largest sum of the sensitivity plus the specificity) for lower versus higher disease activity categories: for the MBDA score, ≤38 versus >38; for the CRP level, ≤32 mg/liter versus >32 mg/liter; and for the ESR, ≤25.5 mm/hour versus >25.5 mm/hour.

MBDA scores. Serum samples from the SWEFOT trial were analyzed for components of the MBDA score by Crescendo Bioscience using electrochemiluminescence-based multiplexed immunoassay on a Meso Scale Discovery Multi-Array platform (22). The MBDA score (Vectra DA disease activity test) is based on serum levels of the following 12 biomarkers: vascular cell adhesion molecule 1, epidermal growth factor, vascular endothelial growth factor, interleukin-6, TNF receptor 1, matrix metalloproteinases 1 and 3, cartilage glycoprotein 39 (YKL-40), leptin, resistin, serum amyloid A, and CRP. The scale of the MBDA score has a range of 1–100, and validated cutoffs for different categories of disease activity are as follows: low = <30, moderate = 30–44, and high = >44 (16,17). In addition to the cutoff based on ROC curve analysis mentioned above, these validated cutoffs were used for further analyses.

Statistical analysis. Baseline characteristics and demographic data were analyzed by *t*-test for normally distributed variables, Mann-Whitney U test for non-normally distributed variables, and chi-square test for categorical variables. For the comparison of continuous values of the MBDA score, the CRP level, and the ESR at month 3 between the responders and the nonresponders to triple therapy or anti-TNF treatment at year 1, the Mann-Whitney U test was used, and for the DAS28, Student's *t*-test was used. Categories of the MBDA score, the CRP level, and the ESR were obtained from ROC curve analysis. Based on this analysis, we selected the cutoff values that corresponded to the highest sum of the sensitivity plus the specificity. For the MBDA score and the DAS28, validated cutoffs were also used. The proportion of clinical responders (DAS28 ≤3.2) to triple therapy or anti-TNF therapy within patient groups with different disease activity categories was compared using chi-square test or Fisher's exact test. The homogeneity of odds ratios for clinical response or a EULAR good response at year 1 to triple therapy or anti-TNF therapy among patients with lower or higher levels of the MBDA score, CRP level, ESR, or DAS28 was determined by Breslow-Day test. All statistical analyses were done using IBM SPSS Statistics 22 software.

RESULTS

Baseline characteristics. The baseline characteristics and demographic data for the entire SWEFOT cohort (n = 487) and for the 157 MTX-IR patients included in the present study were similar (Table 1). Characteristics at month 3 between randomized patients who were included in this study (n = 157) and those who were not (n = 101) were also similar, with the patient's global assessment by visual analog scale being the only significantly different variable (lower among the patients in the present study; data available upon request from the corresponding author).

Relationship between the MBDA score, CRP level, ESR, and DAS28 and a subsequent clinical response to triple therapy or anti-TNF therapy. Overall, there was no significant difference in the proportion of responders at year 1 between the triple therapy (n = 75) and the anti-TNF therapy (n = 82) groups (47% versus 54%; $P = 0.381$). At month 3, the MBDA score, ESR, and DAS28 values were significantly lower in subsequent responders versus nonresponders to triple therapy at year 1 (Figures 1A, C, and D), whereas this was only observed for the DAS28 value in those receiving anti-TNF therapy (Figure 1D). When stratified according to established cutoffs for the MBDA score, 12%

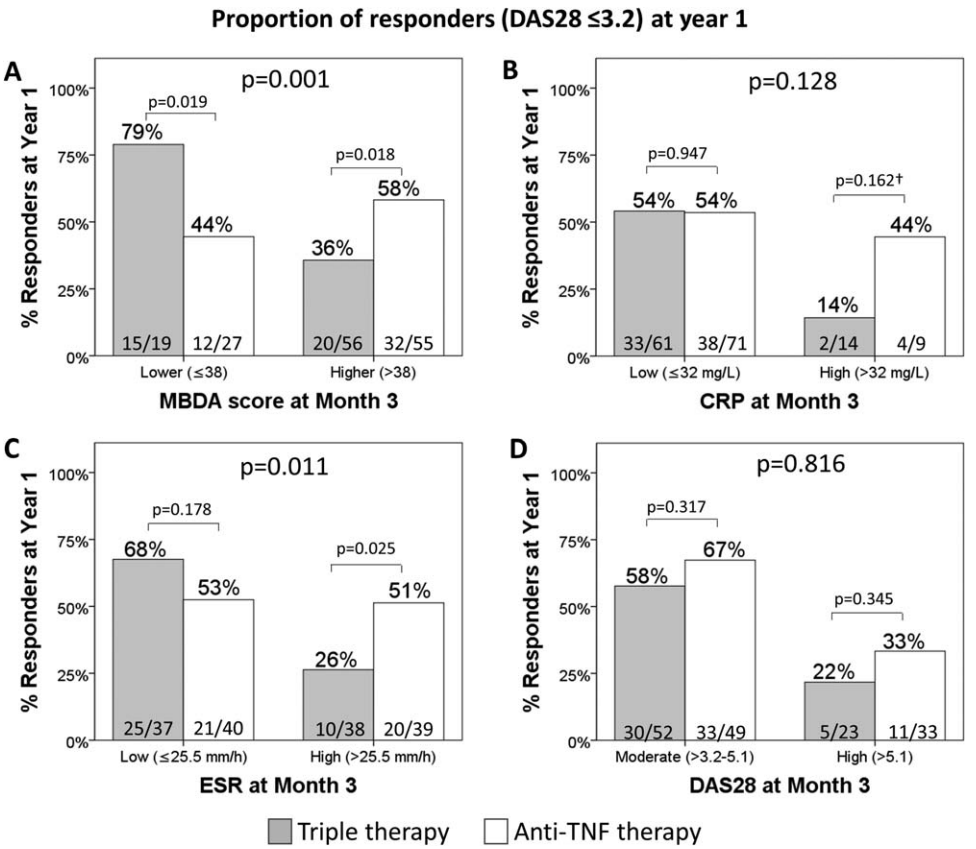

Figure 3. Proportion of patients with a clinical response to second-line therapy at year 1 according to a DAS28 score of ≤3.2, stratified by receiver operating characteristic curve–based cutoffs of disease activity measures at month 3. Responders at year 1 were evaluated according to the MBDA score (**A**), CRP level (**B**), ESR (**C**), and DAS28 (**D**) at month 3. Overall *P* values for the 4 groups were calculated using the Breslow-Day test; *P* values for triple therapy versus anti-TNF therapy were calculated using the chi-square test, except where indicated otherwise. † = *P* value was calculated using Fisher's exact test. See Figure 1 for definitions.

of patients had low (<30), 32% had moderate (30–44), and 56% had high (>44) MBDA scores at treatment escalation.

Patients with low MBDA scores included a significantly greater proportion of subsequent responders at year 1 to triple therapy as compared with anti-TNF therapy (88% versus 18%; $P = 0.006$). Patients with high MBDA scores responded better to anti-TNF (35% versus 58%; $P = 0.040$) (Figure 2).

Similar results were obtained using ROC-based cutoffs; patients with lower MBDA scores (≤38) at month 3 (29% of 157 patients) had a higher likelihood of response at year 1 to triple therapy (79%) as compared with anti-TNF (44%) (Figure 3A). For patients with higher (>38) MBDA scores (71% of 157 patients), the response rates were 36% and 58%, respectively ($P = 0.001$ for comparison across all 4 groups). Using the same approach, we analyzed the CRP, ESR, and DAS28 values (Figures 3B–D). Only the ESR resulted in a similar, although weaker, association, with 68% responding to triple therapy and 53% responding to anti-TNF therapy for patients with lower ESRs and 26% versus 51% responding to the respective therapies among those with higher ESRs ($P = 0.011$ for comparison across all 4 groups) (Figure 3C).

Impact of autoantibodies on the association of the MBDA score with subsequent clinical response to triple therapy or anti-TNF therapy. Of the 157 MTX-IR patients, RF status was missing in 1 and anti-CCP in 8 (Table 1). When grouped according to RF or anti-CCP status, the pattern of associations of the MBDA score at month 3 with the subsequent achievement of a low disease activity score (DAS28 ≤3.2) for each therapeutic group was similar between seropositive and seronegative patients (Figure 4). Thus, among the RF-negative patients with lower MBDA scores (n = 19), the proportions achieving a DAS28 of ≤3.2 at year 1 were 78% of those receiving triple therapy and 50% of those receiving anti-TNF, while for patients with higher MBDA scores (n = 40), the proportions were 37% and 62%, respectively ($P = 0.055$) (Figure 4A). Among RF-positive patients, these proportions were 80% versus 41% and 35% versus 58%, respectively

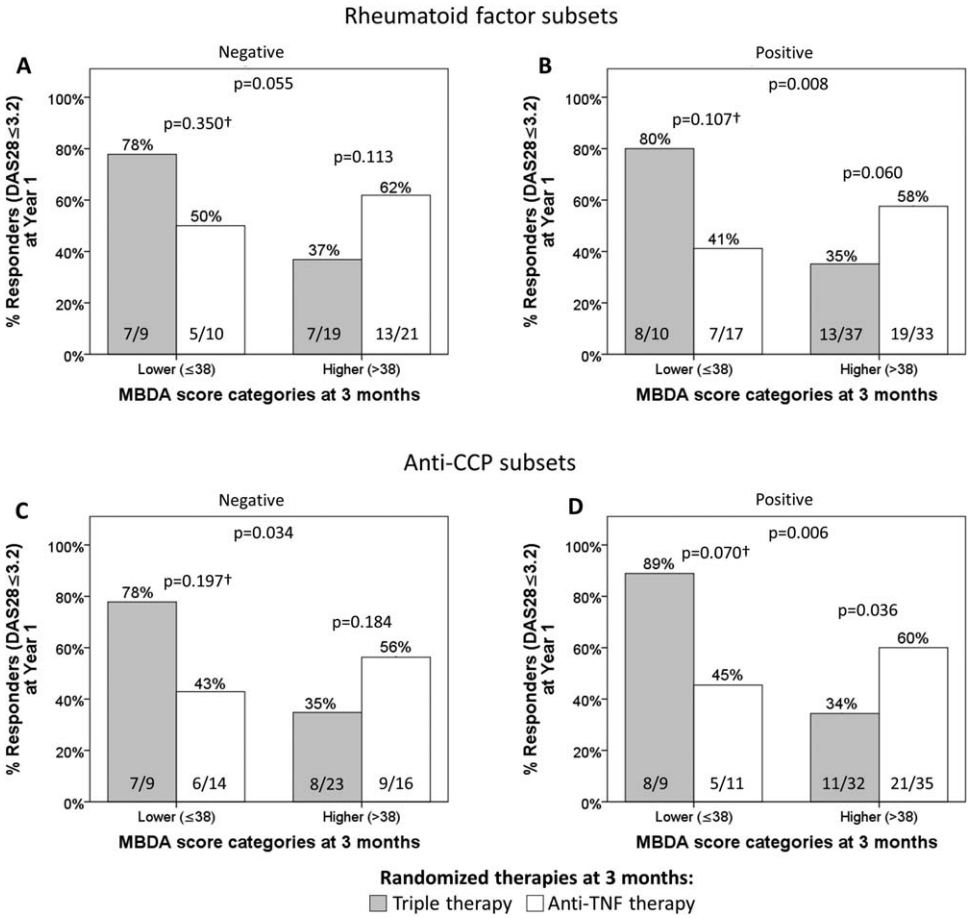

Figure 4. Proportion of patients achieving low levels of disease activity at year 1 according to a DAS28 score of ≤3.2, stratified by the MBDA scores at month 3 in seropositive and seronegative subsets. Responders at year 1 were evaluated according to rheumatoid factor (RF)–negative (**A**), RF-positive (**B**), anti–cyclic citrullinated peptide (anti-CCP)–negative (**C**), and anti-CCP–positive (**D**) status. Overall *P* values for the 4 groups were calculated using the Breslow-Day test, and *P* values for triple therapy versus anti-TNF therapy were calculated using the chi-square test, except where indicated otherwise. † = *P* value was calculated using Fisher's exact test. See Figure 1 for other definitions.

($P = 0.008$) (Figure 4B). When stratified according to anti-CCP status, among the anti-CCP–negative patients with lower MBDA scores (n = 23), the proportion who achieved a DAS28 of ≤3.2 at year 1 was 78% of those receiving triple therapy and 43% of those receiving anti-TNF, while for those with higher MBDA scores (n = 39), the proportions were 35% and 56%, respectively ($P = 0.034$) (Figure 4C). Among anti-CCP–positive patients, these proportions were 89% versus 45% and 34% versus 60%, respectively ($P = 0.006$) (Figure 4D).

Relationship between the MBDA score, CRP level, ESR, and DAS28 and a good clinical response at year 1 according to the EULAR criteria. Among patients with lower (≤38) MBDA scores, the proportions of EULAR good responders at year 1 in the triple therapy and anti-TNF therapy arms were 58% and 30%, respectively, while among those with higher (>38) MBDA scores, the proportions were 34% and 53%, respectively ($P = 0.007$) (Figure 5A). Similar but weaker patterns were obtained from analyses according to the CRP level ($P = 0.034$) (Figure 5B) or the ESR ($P = 0.012$) (Figure 5C). Analyses according to the DAS28 did not reveal a similar pattern (Figure 5D).

DISCUSSION

The aim of this study, which was based on the early RA SWEFOT trial, was to investigate whether the MBDA score is a valuable tool for predicting which of the second-line treatments (anti-TNF or triple therapy) is preferable for the individual patient in whom MTX monotherapy has failed. We have previously shown that smoking, functional impairment, and female sex strongly predict a nonresponse to MTX at 3 months of follow-up (13), whereas those who

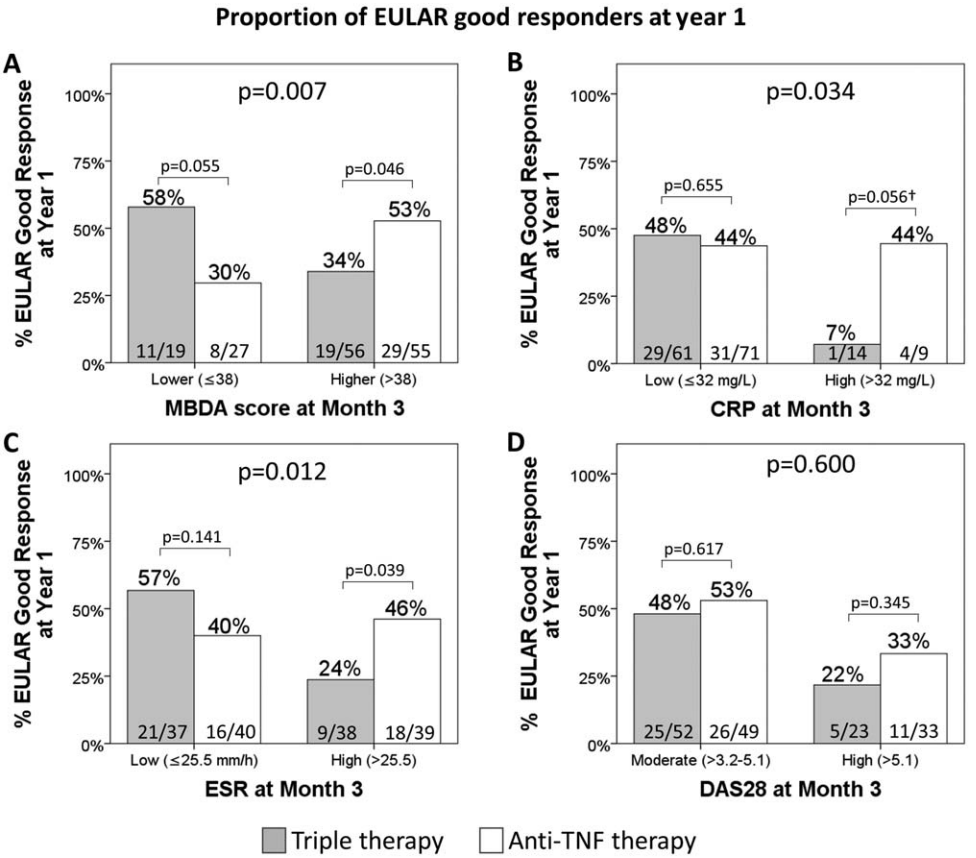

Figure 5. Proportions of patients with a good clinical response to second-line therapy at year 1 according to the European League Against Rheumatism (EULAR) criteria, among those with lower versus higher disease activity at month 3. Responders at year 1 were evaluated according to the MBDA score (**A**), CRP level (**B**), ESR (**C**), and DAS28 (**D**) at month 3. Overall *P* values for the 4 groups were calculated using the Breslow-Day test, and *P* values for triple therapy versus anti-TNF therapy were calculated using the chi-square test, except where indicated otherwise. † = *P* value was calculated using Fisher's exact test. See Figure 1 for other definitions.

responded well to MTX did well during 2 years of follow-up under standard care (23). All clinical guidelines recommend that treatment start with MTX, while there are several options to choose from in cases of nonresponse: cDMARD combinations and different biologic drugs. Predictors of the optimal choice are scarce.

In the present study, we found that a validated score based on a panel of biomarkers could help predict in a differential manner which subsequent therapy would be most effective in early RA patients with an insufficient response to MTX monotherapy. Thus, while overall, second-line therapy with anti-TNF was better in terms of the DAS28 (although perhaps only marginally so) at the group level, we found that for patients with lower MBDA scores (≤38) at treatment escalation, triple therapy was not only equal but was in fact a better therapeutic option than anti-TNF in terms of clinical response. In contrast, in patients with higher MBDA scores (>38), anti-TNF was more efficient in achieving low DAS28 values at year 1.

The conventional markers of inflammation did not show any preferential outcome for triple therapy. Among them, only higher ESRs (>25.5 mm/hour) showed similar, though weaker, associations with response (either a DAS28 of ≤3.2 or a EULAR good response) to therapy with anti-TNF. The observed significance regarding the homogeneity of odds ratios for a EULAR good response to triple therapy or anti-TNF therapy in patients with higher (>32 mg/liter) versus lower (≤32 mg/liter) CRP levels could be explained by the fact that among the 14 patients with higher CRP levels, only 1 responded to triple therapy. However, comparison of the proportion of responders between the triple therapy and anti-TNF therapy groups within each CRP category did not reveal any significant differences (Figure 5B).

Several trials have shown that early and aggressive treatment of RA increases the chances of achieving remission or low levels of disease activity. However, the superiority of biologic drugs versus combination cDMARDs was

observed only for the first few months of treatment, gradually losing their advantage after further follow-up (7–10). Moreover, O'Dell and colleagues (10) showed in the RACAT trial that MTX nonresponders who received triple therapy and failed to respond improved significantly after switching to MTX plus etanercept. Similarly, those who received MTX plus etanercept and did not respond had better clinical outcomes after they were switched to triple therapy.

The results presented herein may, if confirmed, have a major bearing on clinical practice. According to widely accepted guidelines, initial (first-line) therapy for RA is usually MTX, but if this yields an insufficient response, several second-line options are available, including the addition of anti-TNF or escalation to triple therapy (1). While both of these options are superior to placebo, their head-to-head efficacy has been a matter of some debate. The data currently available indicate either that the 2 options are equivalent or that anti-TNF is only marginally better than triple therapy but at a very large cost, and it has therefore been argued that triple therapy should be attempted first. However, as demonstrated in the RACAT trial, where patients failing anti-TNF therapy could respond to triple therapy and vice versa, the equivalence of the 2 options is only true at the group level; individual patients may show different responses to triple therapy versus anti-TNF therapy (10).

Because escalation of therapy in clinical practice is usually from conventional drugs to biologic drugs rather than vice versa, clinicians are often keenly aware of patients who responded much better to anti-TNF than to triple therapy and much less aware of the reverse scenario. This may be a reason that clinicians have been reluctant to adopt triple therapy. The findings in our study allow the identification of a patient subgroup that is much more likely to respond to triple therapy than to anti-TNF, and this may help clinicians choose the better option. The MDBA score cutoff of ≤ 38 and >38, which was defined here based on ROC curve analyses, needs to be confirmed in other patient populations; however, the findings were also striking for the already validated cutoffs and for continuous levels of the MBDA score.

Clinical outcomes do not always reflect radiologic data (23–27). We previously showed in the SWEFOT trial that MTX-IR patients receiving anti-TNF therapy had a significantly lower proportion of radiographic progression at year 2 compared with those receiving triple therapy (18). However, in a later study of the same patients, it was shown that patients with low MBDA scores at the time of randomization did not progress radiographically during 2 years from baseline, regardless of the choice of therapy (28). Neither differed in the proportion of patients with 2-year radiographic progression among those with moderate MBDA scores between the anti-TNF and triple therapy groups (24% and 25%, respectively). The superiority of anti-TNF versus triple therapy was obvious only in patients with high MBDA scores (32% and 57%, respectively; $P = 0.038$). Thus, it may be speculated that giving preference to triple therapy over anti-TNF for patients with lower MBDA scores is not likely to have a negative effect on radiographic outcome.

There have indeed been many studies performed on biomarkers as potential predictors of response to biologic therapies. Trocme and colleagues (29) demonstrated that increased levels of plasma apolipoprotein A-I were an indicator of response to infliximab therapy (according to the ACR criteria for 70% improvement), while platelet factor 4 was associated with nonresponse. Another study on cytokines showed that a simultaneous increase in the levels of monocyte chemoattractant protein 1 and epidermal growth factor (EGF) or in the levels of CRP and EGF was associated with a response to etanercept therapy (30). In a randomized trial, different biomarkers measured at baseline or during the first 4 weeks of treatment correlated with a subsequent clinical response to the anti-TNF agent golimumab (31). Likewise, Hueber et al (32) demonstrated that a panel of 24 biomarkers (13 autoantibodies and 11 cytokines) predicted response to etanercept. However, none of these studies analyzed whether the biomarkers differentially predicted response to triple therapy versus anti-TNF.

Thus, in this study, the MBDA score was differentially associated with the likelihood of response to one or the other second-line treatment. A possible explanation for these findings might lie in the fact that an inadequate response to MTX monotherapy was based on the DAS28, which is mostly based on symptomatic parameters. Some of these patients might have experienced improvements during the 3 months of MTX monotherapy, but of a minor magnitude, making them symptomatically undetectable at the time of the month 3 evaluation (lagging response). The MBDA blood test, on the other hand, shows changes on a molecular level, which can show early improvements that are not yet detectable on physical examination. Therefore, patients who achieved lower MBDA scores by the end of MTX monotherapy but still had moderate/high disease activity based on the DAS28 value were able to accelerate their improvements after addition of other nonbiologic DMARDs. One of the components of the triple therapy, sulfasalazine, has a pharmacokinetic/pharmacodynamic interaction with MTX (33,34), which could further support this theory. If this was indeed the case, for those who responded to triple therapy, taking MTX longer or escalating the dosage might be another option for achieving clinical response.

It is therefore conceivable that patients who show biochemical improvements with MTX treatment, even when they have insufficient clinical responses, are more likely to respond to intensification of treatment with a drug that acts by the same mechanism rather than switching to a drug with a different mechanism of action. In contrast, patients with a lack of biochemical improvements during MTX monotherapy may need a drug with a completely different treatment mechanism (e.g., TNF inhibition) to achieve low levels of disease activity. This hypothesis could also apply to the prediction of responders to anti-TNF according to the ESR, which also detects changes on a molecular/cellular level.

There were some limitations in this study which could affect the results. This was a post hoc analysis, prompted by novel biomarker findings that did not exist when the SWEFOT trial was designed. There is no validated threshold value for defining patients with low or high CRP or ESR values. Therefore, we used ROC curve analysis to define the best cutoffs. Even though the MBDA score had validated categories, those were developed to monitor RA. We therefore also defined new cutoffs using ROC curve analysis for the MBDA scores. This allowed us to create 2 groups (lower and higher) instead of 3 (low, moderate, and high), which led to a more comparable sample size in each group. Another limitation was that we did not have an opportunity to study these relationships for other anti-TNF medications or for biologic drugs other than anti-TNF. Similar studies using other anti-TNF, anti–interleukin-6, T cell–modulating, or anti–B cell therapies would give us further opportunities to explore predictive patterns of the MBDA score. And finally, because of missing data, we were unable to analyze 40% of patients who were randomized to second-line therapy. This fact may generate uncertainty concerning the reliability of the results. We tried to address this challenge by comparing characteristics at the time of randomization between these 40% of patients and the remaining 60% who were included in this study (data available upon request from the corresponding author). The results did not show striking differences, which allowed us to assume that the inclusion of these patients would be less likely to affect the results presented here.

The main strength of this study was that the patient population included in the SWEFOT trial is from standard care with little selection; almost all patients in the areas of the participating centers were referred directly there, and the only inclusion criteria were an age $\geq$18 years, a symptom duration of $<$12 months, a DAS28 of $>$3.2, and a stable low dosage of prednisolone in those who were taking it. Another strength of this study was a reasonable sample size and comparable numbers of patients in each treatment arm (n = 75 for triple therapy versus n = 82 for anti-TNF), which allowed us to obtain reliable statistical results. However, of the entire group of MTX-IR patients randomized to triple therapy or anti-TNF (n = 258), 40% were not included in the analyses because complete data at 3 and 12 months were lacking. The characteristics at 3 months did not differ between the 2 groups, except for global health assessment in the patients who were not analyzed (n = 101) versus those who were (n = 157) (data available upon request from the corresponding author).

In conclusion, in patients with early RA who had an insufficient clinical response to first-line therapy with MTX, the MBDA score was significantly and differentially associated with subsequent response to triple therapy or to anti-TNF therapy. A subset of patients (29% of the study population) had lower MBDA scores and a higher proportion of responders to triple therapy than to anti-TNF. In contrast, patients with higher MBDA scores (71% of the study population) had greater benefit from anti-TNF than triple therapy. We believe this is the first identification of a biomarker test that identifies a group of patients in whom conventional therapy is more optimal than biologic therapy.

ACKNOWLEDGMENTS

We would like to thank all of the patients who participated in the SWEFOT trial, as well as the study nurses, coinvestigators, and colleagues who made the trial possible.

AUTHOR CONTRIBUTIONS

All authors were involved in drafting the article or revising it critically for important intellectual content, and all authors approved the final version to be published. Dr. van Vollenhoven had full access to all of the data in the study and takes responsibility for the integrity of the data and the accuracy of the data analysis.

Study conception and design. Van Vollenhoven.

Acquisition of data. Hambardzumyan, Saevarsdottir, Forslind, Petersson, Wallman, Ernestam, Bolce, van Vollenhoven.

Analysis and interpretation of data. Hambardzumyan, Saevarsdottir, Forslind, Petersson, Wallman, Ernestam, Bolce, van Vollenhoven.

ADDITIONAL DISCLOSURES

Crescendo Bioscience, Inc. performed the serum analyses for the MBDA scores at no cost to the investigators. Author Bolce, an employee of Crescendo Bioscience, Inc., had a role in the analysis and interpretation of the data and the writing of the manuscript, but had no role in collection of the data. Publication of this article was not contingent upon approval by Crescendo Bioscience, Inc. Schering-Plough Sweden provided an unrestricted grant for the original SWEFOT trial (2003–2010).

REFERENCES

1. Smolen JS, Landewé R, Breedveld FC, Buch M, Burmester G, Dougados M, et al. EULAR recommendations for the management of rheumatoid arthritis with synthetic and biological

disease-modifying antirheumatic drugs: 2013 update. Ann Rheum Dis 2014;73:492–509.
2. Singh JA, Saag KG, Bridges SL Jr, Akl EA, Bannuru RR, Sullivan MC, et al. 2015 American College of Rheumatology guideline for the treatment of rheumatoid arthritis. Arthritis Rheumatol 2016;68: 1–26.
3. O'Dell JR, Haire CE, Erikson N, Drymalski W, Palmer W, Eckhoff PJ, et al. Treatment of rheumatoid arthritis with methotrexate alone, sulfasalazine and hydroxychloroquine, or a combination of all three medications. N Engl J Med 1996;334: 1287–91.
4. O'Dell JR, Leff R, Paulsen G, Haire C, Mallek J, Eckhoff PJ, et al. Treatment of rheumatoid arthritis with methotrexate and hydroxychloroquine, methotrexate and sulfasalazine, or a combination of the three medications: results of a two-year, randomized, double-blind, placebo-controlled trial. Arthritis Rheum 2002;46:1164–70.
5. De Jong PH, Hazes JM, Han HK, Huisman M, van Zeben D, van der Lubbe PA, et al. Randomised comparison of initial triple DMARD therapy with methotrexate monotherapy in combination with low-dose glucocorticoid bridging therapy: 1-year data of the tREACH trial. Ann Rheum Dis 2014;73: 1331–9.
6. Maini R, St.Clair EW, Breedveld F, Furst D, Kalden J, Weisman M, et al, for the ATTRACT Study Group. Infliximab (chimeric anti-tumour necrosis factor α monoclonal antibody) versus placebo in rheumatoid arthritis patients receiving concomitant methotrexate: a randomised phase III trial. Lancet 1999; 354:1932–9.
7. Van Vollenhoven RF, Ernestam S, Geborek P, Petersson IF, Coster L, Waltbrand E, et al. Addition of infliximab compared with addition of sulfasalazine and hydroxychloroquine to methotrexate in patients with early rheumatoid arthritis (Swefot trial): 1-year results of a randomised trial. Lancet 2009;374:459–66.
8. Rantalaiho V, Kautiainen H, Korpela M, Hannonen P, Kaipiainen-Seppänen O, Möttönen T, et al. Targeted treatment with a combination of traditional DMARDs produces excellent clinical and radiographic long-term outcomes in early rheumatoid arthritis regardless of initial infliximab: the 5-year follow-up results of a randomised clinical trial, the NEO-RACo trial. Ann Rheum Dis 2014;73:1954–61.
9. Moreland LW, O'Dell JR, Paulus HE, Curtis JR, Bathon JM, St.Clair EW, et al. A randomized comparative effectiveness study of oral triple therapy versus etanercept plus methotrexate in early aggressive rheumatoid arthritis: the Treatment of Early Aggressive Rheumatoid Arthritis trial. Arthritis Rheum 2012;64: 2824–35.
10. O'Dell JR, Mikuls TR, Taylor TH, Ahluwalia V, Brophy M, Warren SR, et al, for the CSP 551 RACAT Investigators. Therapies for active rheumatoid arthritis after methotrexate failure. N Engl J Med 2013;369:307–18.
11. Eriksson JK, Karlsson JA, Bratt J, Petersson IF, van Vollenhoven RF, Ernestam S, et al. Cost-effectiveness of infliximab versus conventional combination treatment in methotrexate-refractory early rheumatoid arthritis: 2-year results of the register-enriched randomised controlled SWEFOT trial. Ann Rheum Dis 2015;74: 1094–101.
12. Ma MH, Scott IC, Dahanayake C, Cope AP, Scott DL. Clinical and serological predictors of remission in rheumatoid arthritis are dependent on treatment regimen. J Rheumatol 2014;41: 1298–303.
13. Saevarsdottir S, Wallin H, Seddighzadeh M, Ernestam S, Geborek P, Petersson IF, et al. Predictors of response to methotrexate in early DMARD naive rheumatoid arthritis: results from the initial open-label phase of the SWEFOT trial. Ann Rheum Dis 2011;70:469–75.
14. Jacobs JW. Lessons for the use of non-biologic anchor treatments for rheumatoid arthritis in the era of biologic therapies. Rheumatology (Oxford) 2012;51 Suppl 4:iv27–33.
15. McWilliams DF, Kiely PD, Young A, Walsh DA. Baseline factors predicting change from the initial DMARD treatment during the first 2 years of rheumatoid arthritis: experience in the ERAN inception cohort. BMC Musculoskelet Disord 2013;14: 153.
16. Centola M, Cavet G, Shen Y, Ramanujan S, Knowlton N, Swan KA, et al. Development of a multi-biomarker disease activity test for rheumatoid arthritis. PloS One 2013;8:e60635.
17. Curtis JR, van der Helm-van Mil AH, Knevel R, Huizinga TW, Haney DJ, Shen Y, et al. Validation of a novel multibiomarker test to assess rheumatoid arthritis disease activity. Arthritis Care Res (Hoboken) 2012;64:1794–803.
18. Van Vollenhoven RF, Geborek P, Forslind K, Albertsson K, Ernestam S, Petersson IF, et al. Conventional combination treatment versus biological treatment in methotrexate-refractory early rheumatoid arthritis: 2 year follow-up of the randomised, non-blinded, parallel-group Swefot trial. Lancet 2012;379:1712–20.
19. Hambardzumyan K, Bolce R, Saevarsdottir S, Cruickshank SE, Sasso EH, Chernoff D, et al. Pretreatment multi-biomarker disease activity score and radiographic progression in early RA: results from the SWEFOT trial. Ann Rheum Dis 2015;74:1102–9.
20. Van Gestel AM, Prevoo ML, van 't Hof MA, van Rijswijk MH, van de Putte LB, van Riel PL. Development and validation of the European League Against Rheumatism response criteria for rheumatoid arthritis: comparison with the preliminary American College of Rheumatology and the World Health Organization/ International League Against Rheumatism criteria. Arthritis Rheum 1996;39:34–40.
21. Van Gestel AM, Haagsma CJ, van Riel PL. Validation of rheumatoid arthritis improvement criteria that include simplified joint counts. Arthritis Rheum 1998;41:1845–50.
22. Eastman PS, Manning WC, Qureshi F, Haney D, Cavet G, Alexander C, et al. Characterization of a multiplex, 12-biomarker test for rheumatoid arthritis. J Pharm Biomed Anal 2012;70:415–24.
23. Rezaei H, Saevarsdottir S, Forslind K, Albertsson K, Wallin H, Bratt J, et al. In early rheumatoid arthritis, patients with a good initial response to methotrexate have excellent 2-year clinical outcomes, but radiological progression is not fully prevented: data from the methotrexate responders population in the SWEFOT trial. Ann Rheum Dis 2012;71:186–91.
24. Molenaar ET, Voskuyl AE, Dinant HJ, Bezemer PD, Boers M, Dijkmans BA. Progression of radiologic damage in patients with rheumatoid arthritis in clinical remission. Arthritis Rheum 2004; 50:36–42.
25. Landewé R, Geusens P, Boers M, van der Heijde D, Lems W, te Koppele J, et al. Markers for type II collagen breakdown predict the effect of disease-modifying treatment on long-term radiographic progression in patients with rheumatoid arthritis. Arthritis Rheum 2004;50:1390–9.
26. Lillegraven S, Prince FH, Shadick NA, Bykerk VP, Lu B, Frits ML, et al. Remission and radiographic outcome in rheumatoid arthritis: application of the 2011 ACR/EULAR remission criteria in an observational cohort. Ann Rheum Dis 2012;71:681–6.
27. Klarenbeek NB, Koevoets R, van der Heijde DM, Gerards AH, Ten Wolde S, Kerstens PJ, et al. Association with joint damage and physical functioning of nine composite indices and the 2011 ACR/EULAR remission criteria in rheumatoid arthritis. Ann Rheum Dis 2011;70:1815–21.
28. Hambardzumyan K, Bolce RJ, Saevarsdottir S, Forslind K, Wallman JK, Cruickshank SE, et al. Association of a multibiomarker disease activity score at multiple time-points with radiographic progression in rheumatoid arthritis: results from the SWEFOT trial. RMD Open 2016;2:e000197.
29. Trocme C, Marotte H, Baillet A, Pallot-Prades B, Garin J, Grange L, et al. Apolipoprotein A-I and platelet factor 4 are biomarkers for infliximab response in rheumatoid arthritis. Ann Rheum Dis 2009;68:1328–33.

30. Fabre S, Dupuy AM, Dossat N, Guisset C, Cohen JD, Cristol JP, et al. Protein biochip array technology for cytokine profiling predicts etanercept responsiveness in rheumatoid arthritis. Clin Exp Immunol 2008;153:188–95.
31. Visvanathan S, Rahman MU, Keystone E, Genovese M, Klareskog L, Hsia E, et al. Association of serum markers with improvement in clinical response measures after treatment with golimumab in patients with active rheumatoid arthritis despite receiving methotrexate: results from the GO-FORWARD study. Arthritis Res Ther 2010;12:R211.
32. Hueber W, Tomooka BH, Batliwalla F, Li W, Monach PA, Tibshirani RJ, et al. Blood autoantibody and cytokine profiles predict response to anti-tumor necrosis factor therapy in rheumatoid arthritis. Arthritis Res Ther 2009;11:R76.
33. Shiroky JB, Watts CS, Neville C. Combination methotrexate and sulfasalazine in the management of rheumatoid arthritis: case observations. Arthritis Rheum 1989;32:1160–4.
34. Schipper LG, Fransen J, Barrera P, van Riel PL. Methotrexate in combination with sulfasalazine is more effective in rheumatoid arthritis patients who failed sulfasalazine than in patients naive to both drugs. Rheumatology (Oxford) 2009;48:828–33.

APPENDIX A: THE SWEFOT TRIAL INVESTIGATORS

Members of the SWEFOT trial investigators group, in addition to the authors, are as follows: Finn Akre (Örebro), Kristina Albertsson (Stockholm), Johan Bratt (Stockholm), Katerina Chatzidionysiou (Stockholm), Lars Cöster (Linköping), Christina Dackhammar (Mölndal), Helena Hellström (Falun), Lotta Ljung (Umeå), Rolf Oding (Västerås), Annika Teleman (Halmstad), Jan Theander (Kristianstad), Åke Thörner (Eskilstuna), Eva Waltbrand (Borås), Margareta Wörnert (Stockholm), and Agneta Zickert (Stockholm).

ARTHRITIS & RHEUMATOLOGY
Vol. 69, No. 5, May 2017, pp 964–975
DOI 10.1002/art.40003

Evidence of the Immune Relevance of *Prevotella copri*, a Gut Microbe, in Patients With Rheumatoid Arthritis

Annalisa Pianta,[1] Sheila Arvikar,[1] Klemen Strle,[1] Elise E. Drouin,[1] Qi Wang,[2] Catherine E. Costello,[2] and Allen C. Steere[1]

Objective. ***Prevotella copri*****, an intestinal microbe, may overexpand in stool samples from patients with new-onset rheumatoid arthritis (RA), but it is not yet clear whether the organism has immune relevance in RA pathogenesis.**

Methods. **HLA–DR–presented peptides (T cell epitopes) from *P copri* were sought directly in the patients' synovial tissue or peripheral blood mononuclear cell (PBMC) samples using tandem mass spectrometry. The antigenicity of peptides or their source proteins was examined in samples from the RA patients or comparison groups. T cell reactivity was determined by enzyme-linked immunospot assay; antibody responses were measured by enzyme-linked immunosorbent assay, and cytokine/chemokine determinations were made by bead-based assays. Serum and synovial fluid samples were examined for 16S ribosomal DNA for *P copri* using nested polymerase chain reaction analysis.**

Results. **In PBMCs, we identified an HLA–DR–presented peptide from a 27-kd protein of *P copri* (*Pc*-p27), which stimulated Th1 responses in 42% of patients with new-onset RA. In both new-onset RA patients and chronic RA patients, 1 subgroup had IgA antibody responses to either *Pc*-p27 or the whole organism, which correlated with Th17 cytokine responses and frequent anti–citrullinated protein antibodies (ACPAs). The other subgroup had IgG *P copri* antibodies, which were associated with *Prevotella* DNA in synovial fluid, *P copri*–specific Th1 responses, and less frequent ACPAs. In contrast, *P copri* antibody responses were rarely found in patients with other rheumatic diseases or in healthy controls.**

Conclusion. **Subgroups of RA patients have differential IgG or IgA immune reactivity with *P copri*, which appears to be specific for this disease. These observations provide evidence that *P copri* is immune-relevant in RA pathogenesis.**

Rheumatoid arthritis (RA) results from a complex interplay between genetic and environmental factors (1,2). Great progress has been made in the identification of genetic factors and inflammatory pathways that influence the disease (1,3), but environmental factors are only now being determined (4). A key hypothesis is that specific organisms in the mouth or microbiota in the gut, the composition of which is strongly influenced by environmental cues, may shape mucosal and systemic immune responses that affect joints in RA patients (4–7).

Using high-throughput sequencing, Scher et al (8) showed that *Prevotella copri* in the gut microbiota was overexpanded in stool samples from patients with new-onset RA compared with patients with chronic RA, patients with psoriatic arthritis, or healthy individuals. In new-onset RA patients, *Prevotella* abundance in the gut was at the expense of *Bacteroides fragilis*, an organism that is important for Treg function (9,10).

Presented in part at the Annual Scientific Meeting of the American College of Rheumatology, San Francisco, CA, November 2015.

Supported by the American College of Rheumatology (Innovative Grant program Within Our Reach: Finding a Cure for Rheumatoid Arthritis), the Ounsworth-Fitzgerald Foundation, the Mathers Foundation, the English-Bonter-Mitchell Foundation, the Littauer Foundation, the Lillian B. Davey Foundation, the Eshe Fund (grant to Dr. Steere), and the NIH (Division of Intramural Research, National Institute of Allergy and Infectious Diseases grants P41-GM-104603, S10-RR-020946, and S10-OD-010724 to Dr. Costello). Dr. Arvikar's work was supported by the Rheumatology Research Foundation (Scientist Development Award).

[1]Annalisa Pianta, PhD, Sheila Arvikar, MD, Klemen Strle, PhD, Elise E. Drouin, PhD (current address: Agenus, Inc., Lexington, Massachusetts), Allen C. Steere, MD: Massachusetts General Hospital and, Harvard Medical School, Boston, Massachusetts; [2]Qi Wang, PhD, Catherine E. Costello, PhD: Boston University School of Medicine, Boston, Massachusetts.

Address correspondence to Annalisa Pianta, PhD, Center for Immunology and Inflammatory Diseases, Massachusetts General Hospital, CNY 149/8301, 55 Fruit Street, Boston, MA 02114. E-mail: apianta@mgh.harvard.edu.

Submitted for publication August 25, 2016; accepted in revised form November 15, 2016.

A second metagenome-wide analysis of fecal samples from RA patients showed dysbiosis in the gut as well as in the mouth and salivary glands (11). Moreover, a recent study in mice showed that dysbiosis contributes to arthritis development via activation of autoreactive T cells in the intestine (12). However, it is unclear whether overexpansion of *P copri* in the human gut has the potential to affect immune cell functions at both mucosal and systemic sites, thereby contributing to RA disease pathogenesis.

Whereas the previous studies used unbiased, discovery-based approaches to assess dysbiosis of microorganisms in the oral or gut microbiome, we developed an unbiased, discovery-based approach to identify novel, immunogenic T cell epitopes in patients with chronic inflammatory arthritis. With this approach, in vivo HLA–DR–presented peptides are identified directly from patients' synovial tissue, synovial fluid mononuclear cells (SFMCs), or peripheral blood mononuclear cells (PBMCs) by liquid chromatography tandem mass spectrometry (LC-MS/MS) (13,14), followed by testing the antigenicity of identified peptides and their source proteins using patients' samples (15–19).

Recently, we used this approach to search for T cell epitopes of proteins derived from microbes implicated in RA. We report here the identification of an HLA–DR–presented peptide (T cell epitope) derived from a *P copri* 27-kd protein (*Pc*-p27), which stimulated Th1 responses in 42% of RA patients. We then found that *P copri* induced differential antibody responses to this protein or the whole organism in a substantial portion of RA patients. These observations provide evidence of the immune relevance of *P copri* in the pathogenesis of RA.

PATIENTS AND METHODS

RA patients and control subjects. The study was approved by the Human Investigations Committee at Massachusetts General Hospital (MGH); all subjects gave written informed consent. All RA patients met the American College of Rheumatology (ACR)/European League Against Rheumatism (EULAR) criteria for the disease (20). All study patients with RA or other rheumatic diseases were recruited from the Rheumatology Clinic at MGH or from suburban MGH clinics.

We obtained synovial tissue, SFMCs, or PBMCs from 5 patients with RA to use for isolation of HLA–DR–presented peptides. To test implicated peptides and their source proteins for immunoreactivity in larger numbers of patients, we used our cohort of patients with new-onset RA from whom systematic clinical information, PBMCs, serum samples, and in some cases, SF samples were available. For comparison, PBMCs and serum samples were available from patients with Lyme arthritis. In addition, we used our cohort of patients with chronic RA from whom serum and sometimes SF samples were collected. Serum samples were obtained from patients with other types of arthritis or connective tissue diseases (CTDs) as well as from healthy control subjects. HLA–DR typing was performed on blood samples from RA patients at the American Red Cross Laboratory in Dedham, MA. Anti–citrullinated protein antibodies (ACPAs) and rheumatoid factor (RF) determinations were made in the clinical laboratories at MGH.

Enzyme-linked immunospot (ELISpot) T cell assay. The detailed methods for isolation and identification of HLA–DR–presented peptides are described in our previous publication (13). In the present study, 1 microbial peptide (^{2}KRIILILTVLLAMLGQVAY^{20}) derived from a 27-kd *P copri* protein (WP_022121928.1) was identified in the PBMCs from 1 RA patient. This *P copri* peptide and 2 additional peptides from the same protein, which were predicted to be promiscuous T cell epitopes (^{52}DYRGYWTMRYQFDSATVS^{69} and ^{118}EKINSLPTSSTGI^{130}), were synthesized and purified by high-performance liquid chromatography in the Core Proteomics Laboratory at MGH. PBMCs from RA patients were then stimulated with the peptides (1 μM) in duplicate along with positive (phytohemagglutinin) and negative (no antigen) controls, and incubated for 5 days in culture at 37°C in a 5% CO_2 incubator. Cells were then transferred to Dual-Color ELISpot plates coated with interferon-γ (IFNγ)/interleukin-17 (IL-17) antibodies (Cellular Technology Limited) and incubated overnight at 37°C. Images of wells were captured using an ImmunoSpot series 3B analyzer, and spots were counted using ImmunoSpot software. A positive T cell response was defined as 3 SD above the mean value in healthy subjects.

Enzyme-linked immunosorbent assay (ELISA) for serum IgG and IgA antibodies to the *P copri* protein *Pc*-p27. ELISA plates were coated overnight at 4°C with 0.25 μg/ml of the *P copri* protein *Pc*-p27 (GenScript). Afterwards, plates were incubated for 1 hour with blocking buffer (5% nonfat dry milk in phosphate buffered saline [PBS]–Tween). Each patient's serum sample (diluted 200-fold) was then added in duplicate wells for 1.5 hours, followed by horseradish peroxidase (HRP)–conjugated goat anti-human IgG (item sc-2453; Santa Cruz Biotechnology) or HRP-conjugated goat anti-human IgA (Bio-Rad) and then tetramethylbenzidine (TMB) substrate (BD). For interplate standardization, 2 control samples were included on each plate. In addition, using HeteroBlock (Omega Biologicals), we tested serum samples from 15 patients who had a range of optical density values on ELISA and confirmed that RF did not alter the ELISA results. Therefore, HeteroBlock was not used in subsequent antibody determinations.

ELISA for serum IgG and IgA antibodies to microbial organisms. The *P copri* type strain (DSM 18205) was obtained from the Leibniz Institute DSMZ, German Collection of Microorganisms and Cell Cultures. *Bacteroides fragilis* (ATCC 25285), *Escherichia coli* (ATCC 25922), and *Porphyromonas gingivalis* (ATCC 33277) isolates were obtained from the American Type Culture Collection. The bacterial cultures were inactivated in 1% formalin for 24 hours, washed twice in PBS, and diluted in PBS at a final concentration of 10^6 cells/ml.

IgG and IgA antibody responses to whole-cell *P copri, B fragilis*, or *E coli* were determined by ELISA. The plates were coated overnight at 4°C with suspensions of inactivated bacterial cells (10^6 cells/ml). Afterwards, plates were incubated for 1 hour with blocking buffer. Patients' serum samples (diluted 1:100) were added in duplicate wells for 1.5 hours, followed by HRP-conjugated goat anti-human IgG or HRP-conjugated goat anti-human IgA and then TMB substrate. For interplate standardization, 2 control samples were included on each plate. The ELISA for *P gingivalis* was performed as previously described (21).

Cytokine and chemokine determinations. The levels of 14 cytokines and chemokines associated with innate immune responses (IFNα, tumor necrosis factor, macrophage inflammatory protein 1α [MIP-1α], and MIP-1β) and with Th1 (IFNγ, IL-12, CXCL9, and CXCL10) or Th17 (IL-1β, IL-17A, IL-17E, IL-17F, IL-22, and IL-23) adaptive immune responses were determined in serum or SF samples from RA patients. Samples were diluted 1:5 in PBS and incubated with HeteroBlock at a concentration of 150 μg/ml to limit the possible confounding effects of RF. Protein levels of all 14 mediators of inflammation in serum or SF were assessed in 1 complete experiment using bead-based Luminex assays (EMD-Millipore) coupled with a Luminex-200 System Analyzer. Data were assessed using xPonent 3.1 software.

Detection of *P copri and B fragilis* 16S ribosomal DNA (rDNA) in patient samples by polymerase chain reaction (PCR). DNA was isolated from 200 μl of serum or SF using a QIAamp DNA Mini kit (Qiagen). Nested PCR primers were designed to detect DNA for *P copri* or *B fragilis* 16S rDNA using Primer3 software (data not shown). DNA was amplified for outer PCR using species-specific forward and reverse primers; 1 μl of the amplified DNA (diluted 1:10 in sterile distilled water) was then used for the nested PCR reaction. All reactions were carried out using 2.5 units of HotStarTaq DNA polymerase (Qiagen). The amplification program included 40 cycles with denaturation at 94°C for 30 seconds, annealing at 59°C for 30 seconds, extension at 72°C for 50 seconds, and a final extension for 10 minutes. For both outer and nested PCR reactions, a positive control (*P copri* or *B fragilis* DNA) and a negative control (sterile distilled water) were included. When sufficient DNA was available, samples were tested in duplicate. Amplified products (10 μl) were visualized by electrophoresis in a 2% agarose gel. The identity of the PCR products was validated by direct DNA sequencing, which was carried out at the Center for Computational and Integrative Biology DNA Core facility at MGH. The sequenced product was aligned with all human and known microbial genomes using Genomic Blast Sequence (NCBI).

Statistical analysis. Categorical data were analyzed by Fisher's exact test, and quantitative data were analyzed using unpaired *t*-test with Welch's correction. Correlations were sought using Pearson's correlation test. All analyses were performed using GraphPad Prism 6 software. All *P* values were two-tailed. *P* values less than or equal to 0.05 were considered statistically significant.

RESULTS

Identification of naturally presented, microbial HLA–DR–presented peptides. Using LC-MS/MS, we identified HLA–DR–presented peptides in synovial tissue (n = 4), SFMCs (n = 3), or PBMCs (n = 2) from 5 patients with new-onset RA or chronic RA (14). From the 17 HLA–DR–presented peptides identified in the PBMCs from 1 patient with chronic RA (patient RA1), 1 *P copri* sequence was found (Figure 1A). In contrast, no sequences from *P gingivalis* or from *Borrelia burgdorferi*, the agent of Lyme disease, were identified in any sample.

At disease onset, patient RA1, who had 2 copies of the RA shared epitope (HLA–DRB1*0401 and 0101), had severe symmetric polyarthritis of the large and small joints. During the course of the disease, tests for ACPAs, but not for RF, became positive. Despite treatment with disease-modifying antirheumatic drugs (DMARDs), she had recurrent episodes of knee swelling, with evidence of destructive changes in cartilage and bone. The HLA–DR–presented peptide derived from *P copri* was identified from PBMCs obtained during 1 such episode 7 years after disease onset.

The peptide sequence of 19 amino acids had 100% sequence homology with part of the signal sequence of a 27-kd protein of *P copri* (*Pc*-p27, WP_022121928.1) (Figure 1A). The peptide had minimal sequence homology with any human peptide, suggesting that it was not a human protein erroneously assigned with a microbial database. Using signalP 4.0 software (22), this HLA–DR–presented *P copri* peptide was predicted to be part of the Sec secretion signal peptide sequence (D score = 0.869), strongly suggesting that the peptide would be cleaved from the source protein. This signal peptide was not predicted to be lipidated (LipoP 1.0 Server). In addition, the algorithm TEPITOPE predicted that the peptide was highly promiscuous, as is typical of signal peptides, and would bind all 25 HLA–DR molecules modeled in the program (23), including the patient's DRB1*0101 and 0401 molecules. When her PBMCs were stimulated with this *P copri* peptide in an IFNγ ELISpot assay, her T cells secreted levels of IFNγ that were >3 times the background levels (insert in Figure 1A), attesting to the immunogenicity of the peptide.

T cell reactivity with *P copri* peptides in patients with new-onset RA. To determine the immunogenicity of HLA–DR–presented peptides of *Pc*-p27 more broadly, we used PBMCs obtained from our cohort of patients with new-onset RA who were seen prior to DMARD therapy, the time when immune responses would be expected to be most robust. All patients met the ACR/EULAR criteria for the disease (20).

When PBMCs from 39 new-onset RA patients and from case patient RA1 (a patient with chronic RA) were stimulated with *Pc*-p27 peptide 1, a total of 17 of these 40 patients (42.5%) secreted levels of IFNγ that were >3 SD above the mean value in healthy control subjects ($P = 0.0002$), as determined with an IFNγ/IL-17 double-color ELISpot assay (Figure 1B). In comparison, patients with Lyme arthritis lacked reactivity with this peptide ($P < 0.0001$). Stimulation of cells with phytohemagglutinin (used as a positive control) verified the viability of cells in all patients. The predominant response to stimulation with *Pc*-p27 in the RA patients was a Th1-type response, whereas PBMCs from only 1 RA patient secreted small amounts of IL-17 (data not shown).

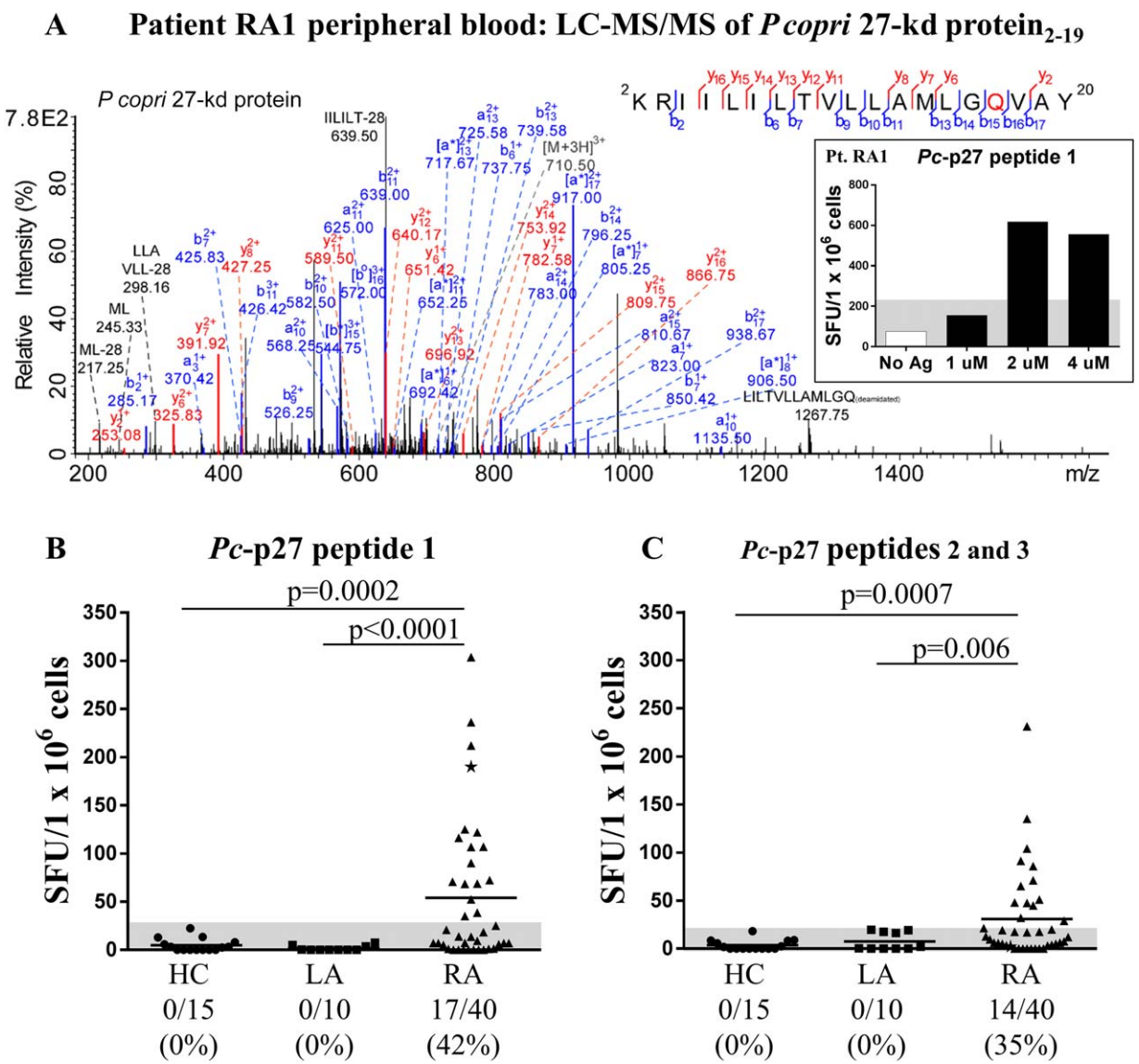

Figure 1. Identification of a broadly immunogenic *Prevotella copri* T cell epitope. **A,** Liquid chromatography tandem mass spectrometry (LC-MS/MS) spectrum of the *P copri* 27-kd protein, *Pc*-p27$_{2–20}$ peptide. Consensus peptide identification as ^{2}KRIILILTVLLAMLGQ(deamidated)VAY^{20} was achieved by OMSSA and X!Tandem analysis. **Inset,** Findings of the interferon-γ (IFNγ) enzyme-linked immunospot (ELISpot) assay using matching peripheral blood mononuclear cells (PBMCs) from a patient with chronic rheumatoid arthritis (patient RA1) stimulated with the peptide (1, 2, and 4 *μM*). Reactivity of >3 times background (no antigen [Ag]) was considered positive. SFU = spot-forming units. **B,** Findings of the IFNγ ELISpot assay using PBMCs from patients with RA, patients with Lyme arthritis (LA), and healthy control (HC) subjects. Cells were incubated with the HLA–DR–presented peptide identified from the PBMCs of patient RA1 (peptide 1; 1 *μM*). **C,** IFNγ secretion of PBMCs from the same groups of patients and controls, incubated with 2 predicted promiscuous HLA–DR–binding peptides from *Pc*-p27 (1 *μM* each). A positive response was defined as a value >3 SD above the mean in healthy controls (area above the shaded region). In **B** and **C,** each symbol represents a single subject; horizontal lines show the mean. **Star** represents patient RA1. Color figure can be viewed in the online issue, which is available at http://onlinelibrary.wiley.com/journal/doi/10.1002/art.40003/abstract.

To determine whether patients had reactivity with other epitopes of the *Pc*-p27 protein, TEPITOPE was used to predict 2 additional promiscuous peptides derived from the same protein (*Pc*-p27 peptides 2 and 3). The 2 peptides together were predicted to be presented by all 25 HLA–DR molecules in the program, and therefore, these peptides were pooled for testing. PBMCs from 14 of the 40 patients (35%) secreted levels of IFNγ to peptides 2 and 3 that were >3 SD above the mean value in healthy controls ($P = 0.0007$) or in patients with Lyme arthritis ($P = 0.006$) (Figure 1C). Altogether, PBMCs from 24 of the 40 patients (60%) had reactivity with 1 or more of the 3 *P copri* peptide sequences, showing that Th1 immune responses to this protein were common in new-onset RA patients.

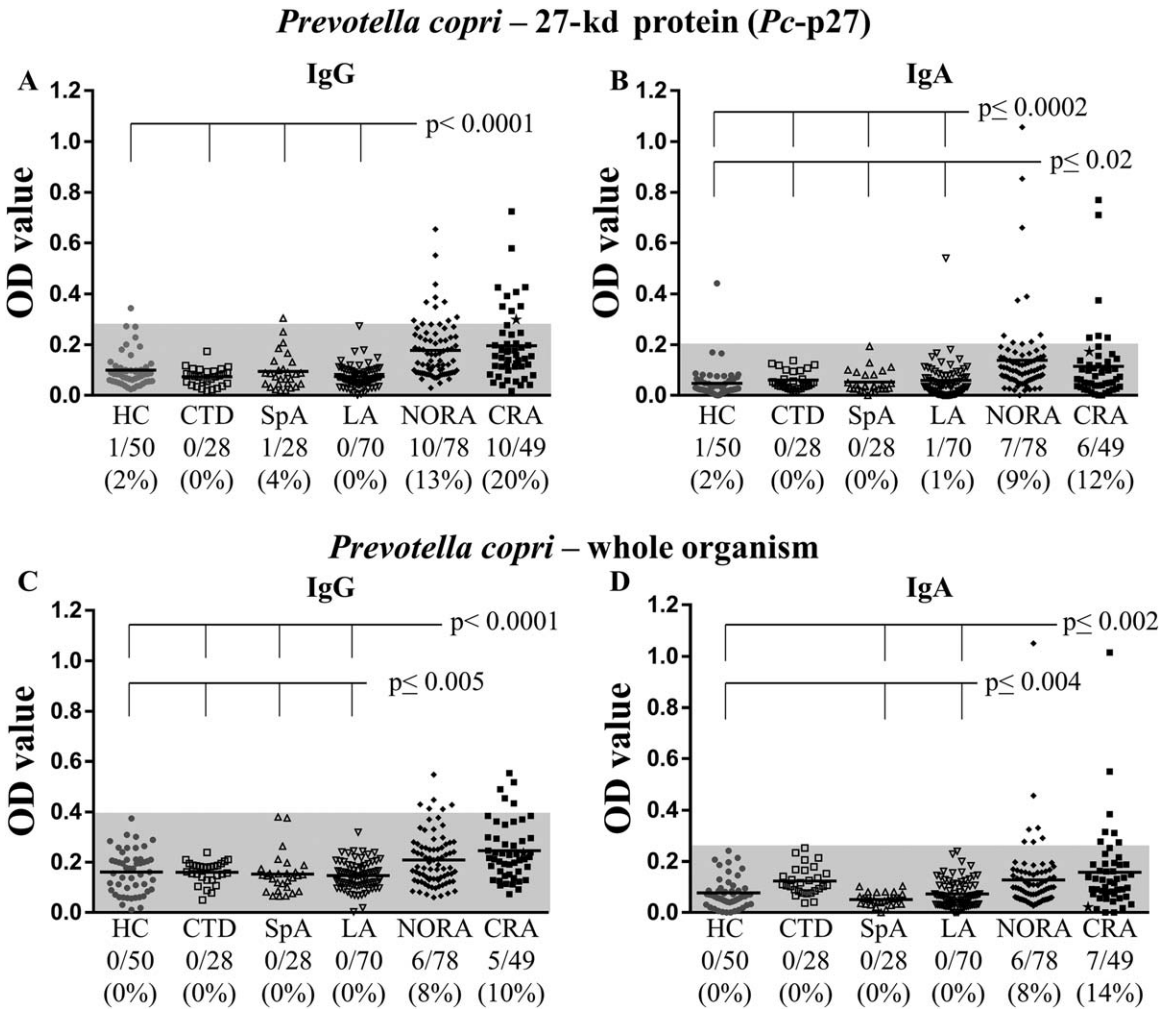

Figure 2. IgG and IgA responses to *Prevotella copri* in rheumatoid arthritis (RA) patients and control subjects. Serum samples from 303 individuals (healthy control [HC] subjects and patients with connective tissue diseases [CTDs], spondyloarthritides [SpA], Lyme arthritis [LA], new-onset RA [NORA], or chronic RA [CRA]) were tested for *P copri* antibodies. Enzyme-linked immunosorbent assays were performed to measure levels of IgG (**A**) and IgA (**B**) against the *P copri* 27-kd protein (*Pc*-p27) as well as levels of IgG (**C**) and IgA (**D**) against 1% formalin–inactivated *P copri* (whole organism). A positive response was defined as a value >3 SD above the mean in healthy controls (area above the shaded region). Each symbol represents a single subject; horizontal lines show the mean. **Star** represents patient RA1. Only significant *P* values relative to healthy controls are shown.

Because of the importance of ACPAs in the diagnosis and pathogenesis of RA (1,24), peptide 1 was resynthesized with a citrulline in place of the only arginine in the peptide, which was predicted to be in the –P1-flanking position of the HLA–DR–binding pocket. However, the results suggested that the *Pc*-p27 signal peptide sequence was probably not citrullinated in vivo (data not shown). This does not preclude citrullination of other parts of the protein, including B cell epitopes.

IgG and IgA antibody responses to *Pc*-p27 and whole *P copri*. We next determined antibody responses to *Pc*-p27 in serum samples from 303 individuals. These included samples from 127 patients with new-onset or chronic RA, 28 patients with CTDs (14 with systemic lupus erythematosus, 4 with mixed CTD, 4 with scleroderma, and 6 with Sjögren's syndrome), 28 patients with spondyloarthritides (SpA) (15 with psoriatic arthritis, 10 with ankylosing spondylitis, and 3 with reactive arthritis), 70 patients with Lyme arthritis, and 50 healthy subjects.

Of the 78 new-onset RA patients, 10 (13%) had IgG antibody responses to *Pc*-p27 that were >3 SD above those in healthy controls ($P < 0.0001$) (Figure 2A). Moreover, 10 of 49 patients with chronic RA (20%) had IgG antibody responses to the protein ($P < 0.0001$), including patient RA1, in whom 4 serial samples obtained 4–9 years

after disease onset yielded positive results. In contrast, only 1 patient with SpA and 1 healthy subject had borderline positive IgG antibody responses to the protein.

Because the first interactions between *P copri* and immune cells would presumably occur in the gut mucosa, we also determined IgA antibody responses to the organism. About 10% of the patients in both the new-onset RA and chronic RA groups had IgA antibody responses to *Pc*-p27 ($P \leq 0.0002$ and $P \leq 0.02$, respectively), and the responses tended to be more robust in those with new-onset RA (Figure 2B). In contrast, only 1 patient with Lyme arthritis and 1 healthy subject had IgA antibody reactivity with the protein. Except for 2 RA patients who had both IgG and IgA responses to *Pc*-p27, the other *Pc*-p27–positive patients had either an IgG or an IgA response, but not both. Altogether, 24% of the 127 RA patients had IgG or IgA antibody responses to *Pc*-p27.

When both T and B cell responses were considered together, 3 of the 24 patients who had T cell reactivity with *Pc*-p27 peptides also had IgG *Pc*-p27 antibody responses, but none had IgA responses to the protein. In comparison, among 16 patients lacking T cell reactivity with *Pc*-p27 peptides, only 1 had an IgG antibody response to the protein, but 5 had IgA responses ($P = 0.05$). The frequencies of shared epitope alleles in patients with *P copri* T cell or B cell responses was not significantly different from those in patients who lacked these responses (data not shown).

In an effort to confirm these findings, we determined IgG and IgA antibody responses to whole *P copri* using the same set of 303 serum samples. Using PCR, we confirmed that this strain expressed *Pc*-p27 (data not shown). Six of the 78 new-onset RA patients (8%) and 5 of the 49 chronic RA patients (10%) had IgG antibody responses to *P copri* (Figure 2C). Similarly, 6 of 78 new-onset RA patients (8%) had IgA antibody responses to *P copri* ($P \leq 0.004$), and 7 of 49 patients with chronic RA (14%) had elevated IgA antibody levels to the organism ($P \leq 0.002$) (Figure 2D). Among the 19 patients who had positive IgG or IgA responses to *P copri*, only 5 (26%) had both responses. No patient with CTD, SpA, or Lyme arthritis had IgG or IgA antibodies to the organism. Altogether, 15% of 127 RA patients had *P copri* IgG or IgA antibody responses.

When the antibody responses to whole *P copri* or recombinant *Pc*-p27 were combined, 41 of the 127 RA patients (32%) had IgG or IgA antibody reactivity with the organism. Thus, antibody responses to *P copri* were common in RA patients, both early and late in the disease, yet they were rarely found in patients with other types of arthritis, implying specificity in RA.

Antibody responses to other oral or commensal bowel flora. To examine the specificity of antibody responses to *P copri* in RA patients, the same serum samples were also tested for reactivity with whole *P gingivalis*, an oral periodontal pathogen implicated in RA (25), and with 2 common gut commensal organisms, *Bacteroides fragilis* and *Escherichia coli*.

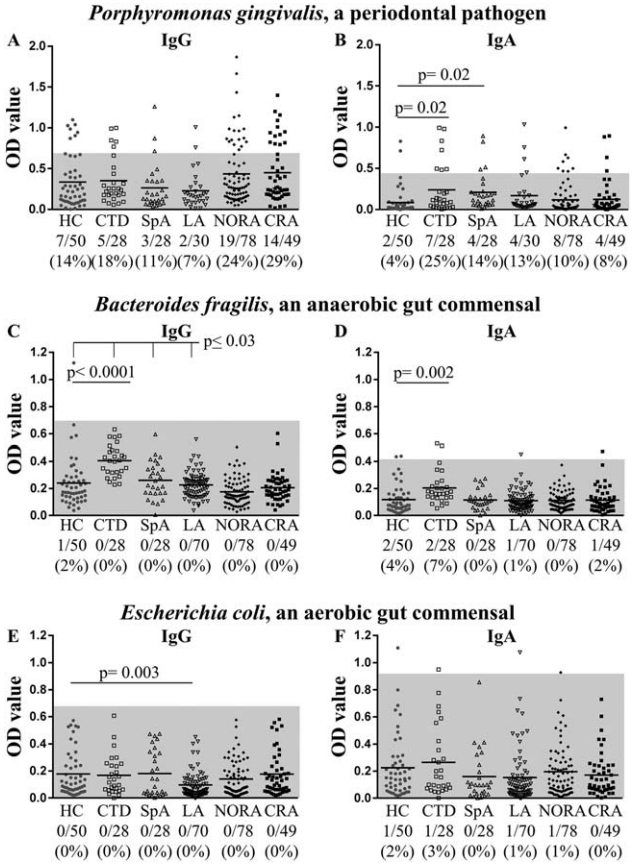

Figure 3. IgG and IgA responses to other organisms in rheumatoid arthritis (RA) patients and control subjects. Serum samples from the same 303 individuals as in Figure 2 (healthy control [HC] subjects and patients with connective tissue diseases [CTDs], spondyloarthritides [SpA], Lyme arthritis [LA], new-onset RA [NORA], or chronic RA [CRA]) were tested for antibody responses to *Porphyromonas gingivalis*, *Bacteroides fragilis*, and *Escherichia coli*. Enzyme-linked immunosorbent assays (ELISAs) were performed to measure levels of IgG (**A**) and IgA (**B**) against *P gingivalis*, levels of IgG (**C**) and IgA (**D**) against *B fragilis*, as well as levels of IgG (**E**) and IgA (**F**) against *E coli*. All ELISAs used 1% formalin–inactivated bacteria. A positive response was defined as a value >2 SD (*P gingivalis*, as previously reported [26]) or >3 SD (*B fragilis* and *E coli*) above the mean in healthy controls (area above the shaded region). Each symbol represents a single subject; horizontal lines show the mean. Only significant *P* values are shown.

Similar to previous studies (26,27), IgG antibody responses to *P gingivalis* were found in ~25% of our new-onset RA and chronic RA patients, and these responses tended to be higher in RA patients than in the other comparison groups (Figure 3A). However, in contrast with *P*

Table 1. Demographic and clinical findings in patients with rheumatoid arthritis, according to the presence of antibodies to *Prevotella copri* and *Prevotella gingivalis**

	P copri antibody response			*P gingivalis* antibody response		
	IgG (n = 27)	IgA (n = 23)	None (n = 86)	IgG (n = 33)	IgA (n = 12)	None (n = 94)
Age, median (range) years	47 (19–85)	53 (19–71)	57 (23–84)	58 (21–84)	62 (41–74)	54 (19–85)
Sex, no. female/male	24/3	21/2	60/26†	23/10	7/5	73/21
Body mass index, median	27	28	27	29	34	27
Smoking history, no. (%)						
Current or former	9 (33)	9 (39)	38 (44)	13 (39)	6 (50)	39 (41)
Never	18 (67)	14 (61)	48 (56)	20 (61)	6 (50)	55 (59)
Autoantibodies, no. (%)						
RF positive	9 (33)	12 (52)	46 (53)	20 (61)	8 (67)	43 (46)
ACPA positive	10 (37)‡	17 (74)	61 (71)	26 (79)	11 (92)§	58 (62)
Markers of inflammation, median (range)						
ESR, mm/hour	12.9 (1–84)	17 (4–34)	16 (1–111)	19.2 (1–67)	36 (10–67)§	15.4 (1–111)
CRP, mg/liter	8.5 (0.2–70)	4.5 (0.1–15)	8.2 (0.1–87)	9.2 (0.1–68)	7.3 (0.1–66)	6.8 (0.1–87)
Disease activity, median						
DAS28-ESR	5.2	4.4	4.2	5.2	5	4.5
DAS28-CRP	4.6	3.8	3.9	4.9	5	4

* Values for the erythrocyte sedimentation rate (ESR), C-reactive protein (CRP) level, and Disease Activity Score in 28 joints (DAS28; using either the ESR or the CRP) were available only in patients with new-onset rheumatoid arthritis. RF = rheumatoid factor; ACPA = anti–citrullinated protein antibody.
† $P = 0.006$ versus the combined group of patients with IgG and patients with IgA *P copri* antibody responses.
‡ $P = 0.003$ versus patients without *P copri* antibody responses (None).
§ $P \leq 0.05$ versus patients without *P gingivalis* antibody responses (None).

copri antibody responses, IgG antibodies to *P gingivalis* were also present in small percentages of patients with other rheumatic diseases or in healthy control subjects, and IgA antibody reactivity with *P gingivalis* was not increased in RA patients compared with the other groups (Figure 3B). Moreover, in contrast with the dichotomy between IgG and IgA antibody responses to *P copri*, all RA patients with IgA antibodies to *P gingivalis* also had IgG responses to this microbe. Importantly, 66 of the 127 RA patients (52%) had antibody responses to either *P copri* or *P gingivalis*, but only 8 of the 66 patients (12%) had antibody responses to both microbes. Thus, minimal overlap was observed in the antibody responses to these 2 organisms, indicating that these responses are largely independent, and only the response to *P copri* was specific for RA.

Very few RA patients or those with other rheumatic diseases had IgG or IgA antibody responses to *B fragilis* or *E coli* that were >3 SD above the mean values in healthy control subjects (Figures 3C–F). However, IgG absorbance values for *B fragilis* were significantly lower in new-onset RA patients than in patients in the other groups ($P \leq 0.03$) (Figure 3C), consistent with the decrease in the abundance of *B fragilis* noted previously in new-onset RA patients (8). Conversely, IgG and IgA absorbance values for *B fragilis* in the CTD group were significantly higher than those in the other groups. Thus, in contrast with *P copri* antibody responses, antibody levels to *B fragilis* and *E coli* were similar or lower in RA patients than in patients with other types of arthritis or in healthy subjects.

Clinical features of patients with *P copri* or *P gingivalis* antibody responses. Because *P copri* and *P gingivalis* have both been implicated in RA, we compared the clinical findings in our cohorts of new-onset and chronic RA patients who did or did not have IgG or IgA antibody responses to these microbes. Because the findings were similar in the 2 groups of RA patients, the groups were combined for presentation here.

Several significant differences between these groups were found (Table 1). First, 45 of the 50 patients (90%) with *P copri* antibody responses were female compared with 60 of the 86 patients (70%) who lacked such responses ($P = 0.006$). In contrast, the percentages of female and male patients were not significantly different in those with *P gingivalis* antibody responses. Second, only 37% of the RA patients with IgG *P copri* antibody responses had ACPAs, compared with 74% of those who had IgA *P copri* antibodies ($P = 0.01$) and 71% who lacked *P copri* antibodies ($P = 0.003$). There was a similar trend with RF ($P = 0.08$). In contrast, patients with *P gingivalis* IgG and IgA antibody responses had higher frequencies of ACPA and RF than did those who lacked these responses. Finally, at study entry, there was a trend toward higher disease activity scores (DAS28) in new-onset RA patients with either *P copri* or *P gingivalis* IgG antibody responses. There

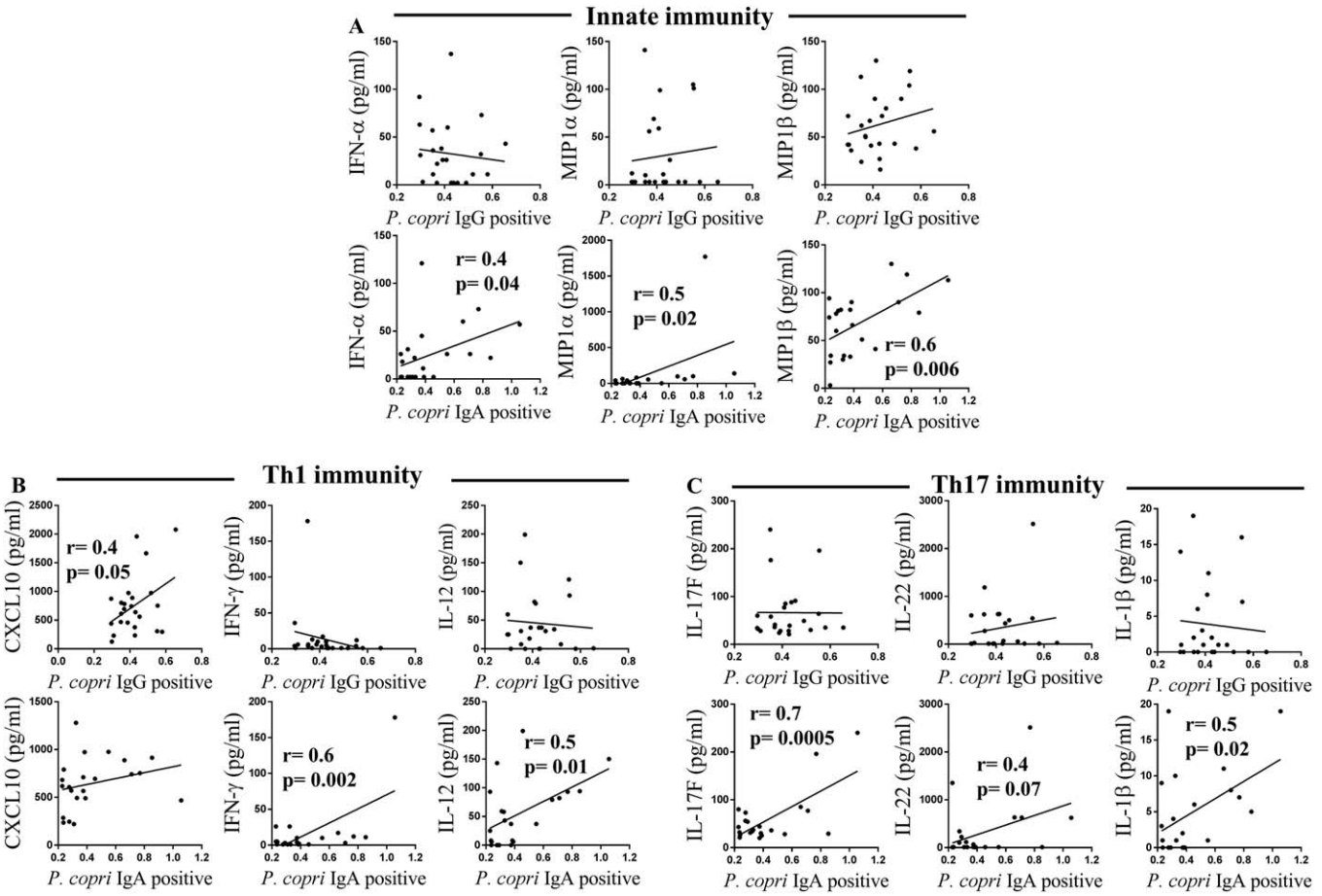

Figure 4. Correlation between cytokine levels and *Prevotella copri* antibody responses in antibody-positive rheumatoid arthritis patients. Pearson's correlation test was used to determine correlations between *P copri*–specific IgG or IgA responses and cytokines associated with innate immunity (**A**) (interferon-α [IFNα], macrophage inflammatory protein 1α [MIP-1α], and MIP-1β), Th1 immunity (**B**) (CXCL10, IFNγ, and interleukin-12 [IL-12]), or Th17 immunity (**C**) (IL-17F, IL-22, and IL-1β).

were no significant differences among the groups in age, body mass index, or smoking history. Thus, *P copri* antibodies were found primarily in women, and ACPAs were less common in patients with IgG *P copri* antibodies, whereas neither of these factors correlated with *P gingivalis* antibody responses, again indicating that these microbes induce distinct responses.

Correlation of *P copri* antibodies with serum cytokine and chemokine levels. In an effort to link *P copri* with inflammatory responses and autoantibody production, IgG and IgA *P copri* antibody values were correlated with serum cytokine levels in 120 of the 127 RA patients in whom sufficient serum samples were still available. The 14 cytokines and chemokines measured were representative of innate, Th1, and Th17 immune responses. The assays were performed with HeteroBlock to limit possible interference by RF. Because the results were similar in new-onset RA and chronic RA patients, they were combined for presentation here.

When the magnitude of *P copri* IgG or IgA antibodies in the 37 antibody-positive patients were correlated with the cytokine levels, strong positive correlations were found between the IgA antibody values and the levels of 3 innate cytokines (IFNα, MIP-1α, and MIP-1β), 2 Th1-associated cytokines (IFNγ and IL-12), and 3 Th17-associated cytokines (IL-17F, IL-22, and IL-1β) (Figures 4A–C). In contrast, IgG *P copri* antibody values correlated only with levels of the Th1 chemoattractant CXCL10 (Figure 4B).

When *P copri* IgA absorbance values in all 120 RA patients, including those with positive and negative results, were correlated with the cytokine levels, even stronger associations were found with innate (MIP-1α and MIP-1β), Th1 (IFNγ and IL-12), and Th17 (IL-23, IL-22, IL-

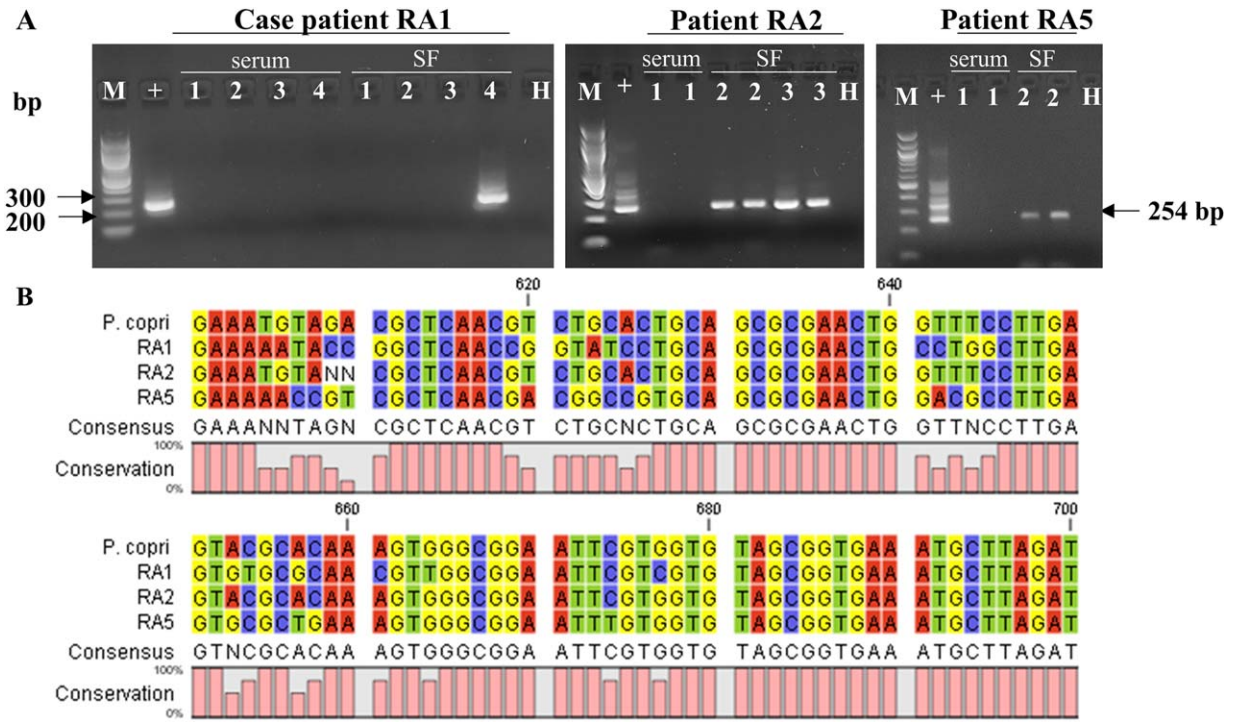

Figure 5. *Prevotella copri* 16S ribosomal DNA (rDNA) in concomitant serum and synovial fluid (SF) samples from rheumatoid arthritis (RA) patients, as determined by polymerase chain reaction (PCR) analysis. **A,** Nested PCR of *P copri* 16S rDNA amplicons (254 bp) analyzed on ethidium bromide–stained 1.5% agarose gels. Results are from the 3 patients who were positive for *P copri*. Patient RA1 had 4 paired serum and SF samples; patient RA2 had 1 serum and 2 SF samples, and patient RA5 had 1 serum and 1 SF sample. In patients RA2 and RA5, enough material was available for testing in duplicate. Lane M contains a 100-bp DNA ladder, lane + contains positive control (*P copri* DSM 18205), and lane H contains water control. **B,** Sequence alignment of the 16S gene amplicons obtained from patients RA1, RA2, and RA5, as determined using CLC Genomic Workbench software. The sequence of the *P copri* 16S gene (DSM 18205) is shown as the reference, and the conservation of all sequence positions is shown below the alignment.

17A, IL-17E, and IL-17F) cytokines (data not shown). In contrast, IgG absorbance values did not correlate with any cytokine or chemokine levels. Similarly, *P gingivalis* IgG and IgA antibodies did not correlate with any cytokine or chemokine level (data available upon request from the corresponding author), further indicating that these microbes induce distinct responses at different mucosal sites.

Detection of *P copri* 16S rDNA in synovial fluid. Because *P copri* IgG antibody responses were suggestive of a systemic immune response to the organism, we investigated whether *P copri* itself may spread to joints. For this purpose, we designed nested PCR primers to detect DNA for the 16S ribosomal RNA gene of *P copri* (16S rDNA) in patients' samples. Of 18 patients in whom paired serum and SF samples were available, 10 were obtained from new-onset RA patients and 8 were from chronic RA patients who were seen 3–50 years after disease onset. Five of the 18 patients had IgG antibody responses to *P copri*, 2 had IgA antibody reactivity with the organism, and 11 did not have *P copri* antibody responses. Although the numbers were small, the clinical correlations in each of these groups, including disease duration, DAS28 scores, and ACPA and RF frequencies, were similar to those in the larger groups of RA patients (data not shown).

Of the 5 patients with IgG *P copri* antibodies (patients RA1–RA5), *P copri* 16S rDNA was detected in SF from 3 of them. In 2 of these 3 patients, 16S rDNA was found in samples obtained prior to DMARD therapy. In the third patient (chronic RA patient RA1), in whom the original HLA–DR–presented *P copri* peptide was identified in PBMCs collected 7 years after disease onset (Figure 1A), *P copri* 16S rDNA was detected in SF obtained 9 years after disease onset (Figure 5A). In contrast, *P copri* DNA was not detected in SF samples from the remaining 13 patients: 2 with IgA *P copri* antibodies and 11 without *P copri* antibodies. Serum samples from all 18 patients had negative PCR results. Thus, 3 of the 5 patients with IgG *P copri* antibodies had positive PCR results for *Prevotella* DNA in SF as compared with none of 13 patients in the other 2 groups ($P = 0.01$).

For comparison, nested PCR primers were designed to detect 16S rDNA from *B fragilis*, another gut commensal. Of the 18 patients, 1 (patient RA15) had *B fragilis* 16S rDNA in SF; the sequence of this amplicon had 98% homology to *B fragilis* 16S rDNA (data not shown). This patient did not have positive findings on tests for *P copri* DNA or *P copri* antibody responses, and none of the 18 patients had IgG or IgA responses to *B fragilis*.

All positive results were confirmed by sequencing. Amplicons from patient RA2 had 100% identity with the sequence for *P copri* 16S rDNA in the NCBI database, which was obtained from a Japanese isolate. Interestingly, patient RA2 grew up in Korea. Amplicons from patient RA1 and from patient RA5 annealed with *P copri* sequences (DSM18205), but they had 86% and 89% sequence homology, respectively (Figure 5B), suggesting that the sequence could be from another *Prevotella* species (Figure 5B). Alternatively, even though cultures of *P copri* from stool samples were not available for analysis, the differences in *P copri* 16S rDNA sequences may be explained by strain variation, since the 3 patients grew up in widely different geographic locations (Korea, the US, or the Caribbean Islands). This is consistent with a study in which *P copri* was ranked as the second most-variable member of the human gut microbiota between continents (28).

DISCUSSION

In this study, using a discovery-based search for HLA–DR–presented peptides derived from *P copri*, 1 spectrum-to-peptide match was identified in PBMCs from 1 RA patient. This peptide sequence was found in the signal domain of a 27-kd protein of *P copri*, which was predicted to be a secreted protein. Signal sequences, which are cleaved prior to secretion, can accumulate in transmembrane locations; they are often highly antigenic, and they typically bind many different HLA–DR molecules (21). In addition, the secreted portion of the protein may become an immunogenic soluble antigen (6,29). We then found that the signal sequence peptide and 2 other peptides from the *Pc*-p27 protein induced Th1 responses in 60% of patients with RA. Although RA shared epitope alleles have been reported to correlate inversely with *P copri* overexpansion in the gut (8), our study showed no significant correlations between these T cell epitopes and shared epitope alleles, which is consistent with the fact that these epitopes are promiscuous HLA–DR binders.

While PBMCs were available only from patients with new-onset RA, we were able to test for antibody responses to *P copri* in both new-onset RA and chronic RA patients. Although overexpansion of *P copri* was previously detected only in the stool of new-onset RA patients (8), we found similar frequencies of *P copri* antibody responses and similar clinical associations in new-onset RA and chronic RA patients, suggesting that once initiated, these antibody responses may persist for years. Importantly, in both patient groups, *P copri* antibody responses were specific for RA. First, *P copri* antibodies were rarely found in patients with other rheumatic diseases or in healthy controls. Second, antibody levels to 2 other gut commensals, *B fragilis* and *E coli*, were similar or lower in RA patients than those in patients with other arthritides or in healthy subjects. Third, there was little overlap between patients with *P gingivalis* antibodies and those with *P copri* antibodies.

P copri antibody responses were found primarily in women, both in those with new-onset RA and in those with chronic RA. When the 2 cohorts of patients were combined, *P copri*–negative patients had a sex ratio of 2.3 to 1 in favor of women, which is close to the ratio of 3 to 1 generally reported in RA cohorts. In contrast, the patients with *P copri* antibody responses had a sex ratio of 9 to 1, implying that this organism may be a substantial contributor to the female predominance in RA.

In mice, gut symbiotic gram-negative bacteria may disseminate systemically to other sites and induce IgG antibody responses (30). These homeostatic IgG responses may help later in protecting against invasion by pathogenic gram-negative bacteria. Our studies showed high background values in *E coli* and *B fragilis* antibody assays, perhaps reflecting positive responses to these bacteria in some individuals. However, antibody responses to these bacteria were not higher in RA patients than in other comparison groups, including healthy controls, whereas *P copri* antibody responses were significantly higher in RA patients and correlated with inflammatory cytokine levels. Thus, our findings could not be explained simply by homeostatic *P copri* antibody responses.

The magnitude of IgA *P copri* antibody responses in RA patients in our study correlated with serum levels of a range of cytokines and chemokines associated with innate, Th1, and Th17 immune responses. Although we did not find *Pc*-p27–specific Th17 cells in PBMCs from these patients, it is likely that such cells were present in their intestinal mucosa. Th17 responses are presumably important initially in containing the organism in the bowel, but with chronic antigenic stimulation, they can promote systemic inflammation and autoimmunity (31). This idea is supported here by strong correlations among IgA antibody values, serum levels of Th17-associated

cytokines, and high frequencies of ACPAs, which could react with citrullinated proteins in joints (32).

Conversely, other RA patients had IgG *P copri* antibody responses associated with *Prevotella* DNA in the joints, inflammatory Th1 responses, and infrequent ACPAs. We postulate that in these patients, *P copri*, a strict anaerobe, may spread systemically within phagocytic cells, including to the joints. In 2 of 3 patients, *Prevotella* DNA was detected in SF obtained early in the disease. However, in the remaining patient, in whom the *Pc*-p27 HLA–DR–presented peptide was identified in PBMCs obtained 7 years after disease onset (patient RA1), *P copri* DNA was detected in SF collected 9 years after disease onset. This suggests that *P copri* may spread from the bowel in repeated waves over a period of years, perhaps explaining the persistence of antibody responses to *P copri* in patients with chronic RA. The finding of 16S rDNA of *B fragilis* in the SF of 1 additional patient suggests that escape of other commensal bacteria from the bowel may occur, but this patient lacked an antibody response to the organism.

There are parallels between the potential role of *P copri* in RA pathogenesis and that of the periodontal pathogen *P gingivalis* (25,33). In patients with periodontitis, the composition of the oral flora shifts in favor of organisms, particularly anaerobes such as *P gingivalis*, that thrive in an inflammatory environment (34). IgG antibody responses to *P gingivalis* in RA patients correlate strongly with systemic inflammation and coexistent periodontal disease (25,27,35). Furthermore, *P gingivalis* may disseminate from the gingiva, presumably via dendritic cells, and lead to infection and inflammation at distant sites (6,36). DNA from periodontal bacteria has been detected by PCR in SF from a few RA patients with periodontal disease (37).

In conclusion, our study provides evidence for the immune relevance of *P copri* in RA and suggests that bowel pathology may be a feature of the disease in this subgroup of patients. These new insights are likely to have implications for both the diagnosis and treatment of RA. For example, *P copri* IgG antibody responses could provide support for the diagnosis in RA patients who lack ACPA or RF. Moreover, dietary interventions or specifically tailored antibiotic regimens targeting *P copri* could play an adjunctive role to DMARDs in the treatment of this disease. Previously, patients with early RA who received tetracycline or its derivatives had significantly better outcomes than patients who received placebo (38,39). These results are often attributed to the antiinflammatory effects of tetracyclines, but recent insights about the microbiota suggest an additional explanation. Importantly, insights about specific immune-relevant commensal organisms in the microbiota promise a new era in the understanding and treatment of RA.

ACKNOWLEDGMENTS

We thank John Branda, Judith M. Holden, and Gail McHugh for help with the microbial cultures, Dan Littman and Hannah Fehlner-Peach for providing *P copri* DNA for cloning the *Pc*-p27 protein, Chunxiang Yao for help with the mass spectrometry analyses, Deborah Collier and Marcy Bolster for help with patient care, Dennis Burke and John Aversa for help with obtaining synovial tissue, Mandakolathur Murali for the RF and ACPA analyses, the American Red Cross HLA laboratory for HLA–DR typing of the patients, Katherine Sulka for help with the preparation of samples for HLA–DR typing, and the Center for Computational and Integrative Biology DNA Core facility at MGH for the sequencing of *P copri* 16S rDNA amplicons.

AUTHOR CONTRIBUTIONS

All authors were involved in drafting the article or revising it critically for important intellectual content, and all authors approved the final version to be published. Dr. Steere had full access to all of the data in the study and takes responsibility for the integrity of the data and the accuracy of the data analysis.

Study conception and design. Pianta, Drouin, Costello, Steere.
Acquisition of data. Pianta, Arvikar, Strle, Wang, Steere.
Analysis and interpretation of data. Pianta, Arvikar, Strle, Drouin, Wang, Costello, Steere.

REFERENCES

1. McInnes IB, Schett G. The pathogenesis of rheumatoid arthritis. N Engl J Med 2011;365:2205–19.
2. Firestein GS. Evolving concepts of rheumatoid arthritis. Nature 2003;423:356–61.
3. Plenge RM. Rheumatoid arthritis genetics: 2009 update. Curr Rheumatol Rep 2009;11:351–6.
4. Catrina AI, Deane KD, Scher JU. Gene, environment, microbiome and mucosal immune tolerance in rheumatoid arthritis. Rheumatology (Oxford) 2016;55:391–402.
5. Longman RS, Littman DR. The functional impact of the intestinal microbiome on mucosal immunity and systemic autoimmunity. Curr Opin Rheumatol 2015;27:381–7.
6. Han YW, Wang X. Mobile microbiome: oral bacteria in extra-oral infections and inflammation. J Dent Res 2013;92:485–91.
7. Scher JU, Abramson SB. The microbiome and rheumatoid arthritis. Nat Rev Rheumatol 2011;7:569–78.
8. Scher JU, Sczesnak A, Longman RS, Segata N, Ubeda C, Bielski C, et al. Expansion of intestinal Prevotella copri correlates with enhanced susceptibility to arthritis. Elife 2013;2: e01202.
9. Atarashi K, Tanoue T, Shima T, Imaoka A, Kuwahara T, Momose Y, et al. Induction of colonic regulatory T cells by indigenous Clostridium species. Science 2011;331:337–41.
10. Round JL, Lee SM, Li J, Tran G, Jabri B, Chatila TA, et al. The Toll-like receptor 2 pathway establishes colonization by a commensal of the human microbiota. Science 2011;332:974–7.
11. Zhang X, Zhang D, Jia H, Feng Q, Wang D, Liang D, et al. The oral and gut microbiomes are perturbed in rheumatoid arthritis and partly normalized after treatment. Nat Med 2015; 21:895–905.
12. Maeda Y, Kurakawa T, Umemoto E, Motooka D, Ito Y, Gotoh K, et al. Dysbiosis contributes to arthritis development via activation of autoreactive T cells in the intestine. Arthritis Rheumatol 2016;68: 2646–61.

13. Seward RJ, Drouin EE, Steere AC, Costello CE. Peptides presented by HLA-DR molecules in synovia of patients with rheumatoid arthritis or antibiotic-refractory Lyme arthritis. Mol Cell Proteomics 2011;10:M110.002477.
14. Wang Q, Drouin EE, Yao C, Zhang J, Huang Y, Leon DR, et al. Immunogenic HLA-DR-presented self-peptides identified directly from clinical samples of synovial tissue, synovial fluid, or peripheral blood in patients with rheumatoid arthritis or Lyme arthritis. J Proteome Res 2016;16:122–36.
15. Crowley JT, Strle K, Drouin EE, Pianta A, Arvikar SL, Wang Q, et al. Matrix metalloproteinase-10 is a target of T and B cell responses that correlate with synovial pathology in patients with antibiotic-refractory Lyme arthritis. J Autoimmun 2016;69:24–37.
16. Crowley JT, Drouin EE, Pianta A, Strle K, Wang Q, Costello CE, et al. A highly expressed human protein, apolipoprotein B-100, serves as an autoantigen in a subgroup of patients with Lyme disease. J Infect Dis 2015;212:1841–50.
17. Drouin EE, Seward RJ, Strle K, McHugh G, Katchar K, Londono D, et al. A novel human autoantigen, endothelial cell growth factor, is a target of T and B cell responses in patients with Lyme disease. Arthritis Rheum 2013;65:186–96.
18. Pianta A, Drouin EE, Crowley JT, Arvikar S, Strle K, Costello CE, et al. Annexin A2 is a target of autoimmune T and B cell responses associated with synovial fibroblast proliferation in patients with antibiotic-refractory Lyme arthritis. Clin Immunol 2015;160:336–41.
19. Pianta A, Drouin EE, Wang Q, Arvikar S, Costello CE, Steere AC. Identification of N-acetylglucosamine-6-sulfatase and filamin A as novel targets of autoimmune T and B cell responses in rheumatoid arthritis [abstract]. Ann Rheum Dis 2015;74 Suppl 2:112.
20. Aletaha D, Neogi T, Silman AJ, Funovits J, Felson DT, Bingham CO III, et al. 2010 rheumatoid arthritis classification criteria: an American College of Rheumatology/European League Against Rheumatism collaborative initiative. Arthritis Rheum 2010;62:2569–81.
21. Kovjazin R, Volovitz I, Daon Y, Vider-Shalit T, Azran R, Tsaban L, et al. Signal peptides and trans-membrane regions are broadly immunogenic and have high CD8+ T cell epitope densities: implications for vaccine development. Mol Immunol 2011;48:1009–18.
22. Petersen TN, Brunak S, von Heijne G, Nielsen H. SignalP 4.0: discriminating signal peptides from transmembrane regions. Nat Methods 2011;8:785–6.
23. Sturniolo T, Bono E, Ding J, Raddrizzani L, Tuereci O, Sahin U, et al. Generation of tissue-specific and promiscuous HLA ligand databases using DNA microarrays and virtual HLA class II matrices. Nat Biotechnol 1999;17:555–61.
24. Brink M, Hansson M, Mathsson L, Jakobsson PJ, Holmdahl R, Hallmans G, et al. Multiplex analyses of antibodies against citrullinated peptides in individuals prior to development of rheumatoid arthritis. Arthritis Rheum 2013;65:899–910.
25. Mikuls TR, Payne JB, Yu F, Thiele GM, Reynolds RJ, Cannon GW, et al. Periodontitis and Porphyromonas gingivalis in patients with rheumatoid arthritis. Arthritis Rheumatol 2014;66:1090–100.
26. De Smit M, Westra J, Vissink A, Doornbos-van der Meer B, Brouwer E, van Winkelhoff AJ. Periodontitis in established rheumatoid arthritis patients: a cross-sectional clinical, microbiological and serological study. Arthritis Res Ther 2012;14:R222.
27. Arvikar SL, Collier DS, Fisher MC, Unizony S, Cohen GL, McHugh G, et al. Clinical correlations with Porphyromonas gingivalis antibody responses in patients with early rheumatoid arthritis. Arthritis Res Ther 2013;15:R109.
28. Schloissnig S, Arumugam M, Sunagawa S, Mitreva M, Tap J, Zhu A, et al. Genomic variation landscape of the human gut microbiome. Nature 2013;493:45–50.
29. Yang Y, Torchinsky MB, Gobert M, Xiong H, Xu M, Linehan JL, et al. Focused specificity of intestinal TH17 cells towards commensal bacterial antigens. Nature 2014;510:152–6.
30. Zeng MY, Cisalpino D, Varadarajan S, Hellman J, Warren HS, Cascalho M, et al. Gut microbiota-induced immunoglobulin G controls systemic infection by symbiotic bacteria and pathogens. Immunity 2016;44:647–58.
31. Ruff WE, Kriegel MA. Autoimmune host-microbiota interactions at barrier sites and beyond. Trends Mol Med 2015;21:233–44.
32. Romero V, Fert-Bober J, Nigrovic PA, Darrah E, Haque UJ, Lee DM, et al. Immune-mediated pore-forming pathways induce cellular hypercitrullination and generate citrullinated autoantigens in rheumatoid arthritis. Sci Transl Med 2013;5:209ra150.
33. Pischon N, Pischon T, Kroger J, Gulmez E, Kleber BM, Bernimoulin JP, et al. Association among rheumatoid arthritis, oral hygiene, and periodontitis. J Periodontol 2008;79:979–86.
34. Hajishengallis G. Periodontitis: from microbial immune subversion to systemic inflammation. Nat Rev Immunol 2015;15:30–44.
35. Scher JU, Abramson SB. Periodontal disease, Porphyromonas gingivalis, and rheumatoid arthritis: what triggers autoimmunity and clinical disease? Arthritis Res Ther 2013;15:122.
36. Carrion J, Scisci E, Miles B, Sabino GJ, Zeituni AE, Gu Y, et al. Microbial carriage state of peripheral blood dendritic cells (DCs) in chronic periodontitis influences DC differentiation, atherogenic potential. J Immunol 2012;189:3178–87.
37. Martinez-Martinez RE, Abud-Mendoza C, Patino-Marin N, Rizo-Rodriguez JC, Little JW, Loyola-Rodriguez JP. Detection of periodontal bacterial DNA in serum and synovial fluid in refractory rheumatoid arthritis patients. J Clin Periodontol 2009;36:1004–10.
38. O'Dell JR, Haire CE, Palmer W, Drymalski W, Wees S, Blakely K, et al. Treatment of early rheumatoid arthritis with minocycline or placebo: results of a randomized, double-blind, placebo-controlled trial. Arthritis Rheum 1997;40:842–8.
39. Stone M, Fortin PR, Pacheco-Tena C, Inman RD. Should tetracycline treatment be used more extensively for rheumatoid arthritis? Metaanalysis demonstrates clinical benefit with reduction in disease activity. J Rheumatol 2003;30:2112–22.

ARTHRITIS & RHEUMATOLOGY
Vol. 69, No. 5, May 2017, pp 976–985
DOI 10.1002/art.40051

A Multinational Arab Genome-Wide Association Study Identifies New Genetic Associations for Rheumatoid Arthritis

Richa Saxena,[1] Robert M. Plenge,[2] Andrew C. Bjonnes,[1] Hassan S. Dashti,[1] Yukinori Okada,[3] Wessam Gad El Haq,[4] Mohammed Hammoudeh,[5] Samar Al Emadi,[5] Basel K. Masri,[6] Hussein Halabi,[7] Humeira Badsha,[8] Imad W. Uthman,[9] Lauren Margolin,[10] Namrata Gupta,[10] Ziyad R. Mahfoud,[4] Marianthi Kapiri,[4] Soha R. Dargham,[4] Grace Aranki,[4] Layla A. Kazkaz,[11] and Thurayya Arayssi[4]

Objective. **Genetic factors underlying susceptibility to rheumatoid arthritis (RA) in Arab populations are largely unknown. This genome-wide association study (GWAS) was undertaken to explore the generalizability of previously reported RA loci to Arab subjects and to discover new Arab-specific genetic loci.**

Methods. **The Genetics of Rheumatoid Arthritis in Some Arab States Study was designed to examine the genetics and clinical features of RA patients from Jordan, the Kingdom of Saudi Arabia, Lebanon, Qatar, and the United Arab Emirates. In total, >7 million single-nucleotide polymorphisms (SNPs) were tested for association with RA overall and with seropositive or seronegative RA in 511 RA cases and 352 healthy controls. In addition, replication of 15 signals was attempted in 283 RA cases and 221 healthy controls. A genetic risk score of 68 known RA SNPs was also examined in this study population.**

Results. **Three loci (*HLA* region, intergenic 5q13, and 17p13 at *SMTNL2*/*GGT6*) reached genome-wide significance in the analyses of association with RA and with seropositive RA, and for all 3 loci, evidence of independent replication was demonstrated. Consistent with the findings in European and East Asian populations, the association of RA with *HLA–DRB1* amino acid position 11 conferred the strongest effect ($P = 4.8 \times 10^{-16}$), and a weighted genetic risk score of previously associated RA loci was found to be associated with RA ($P = 3.41 \times 10^{-5}$) and with seropositive RA ($P = 1.48 \times 10^{-6}$) in this population. In addition, 2 novel associations specific to Arab populations were found at the 5q13 and 17p13 loci.**

Conclusion. **This first RA GWAS in Arab populations confirms that established *HLA*-region and known RA risk alleles contribute strongly to the risk and severity of disease in some Arab groups, suggesting that the genetic architecture of RA is similar across ethnic groups. Moreover, this study identified 2 novel RA risk loci in Arabs, offering further population-specific insights into the pathophysiology of RA.**

The statements made herein are solely the responsibility of the authors.

Supported by the National Priorities Research Program (grant 4-344-3-105 from the Qatar National Research Fund, a member of Qatar Foundation). Drs. Saxena, Plenge, Dashti, Hammoudeh, Al Emadi, Masri, Halabi, Badsha, Uthman, Mahfoud, Kazkaz, and Arayssi are members of the Middle East Rheumatoid Arthritis Consortium.

[1]Richa Saxena, PhD, Andrew C. Bjonnes, MSc, Hassan S. Dashti, PhD, RD: Massachusetts General Hospital, Harvard Medical School, Boston, Massachusetts, and Broad Institute, Cambridge, Massachusetts; [2]Robert M. Plenge, MD, PhD: Broad Institute, Cambridge, Massachusetts, and Merck Research Laboratories and Brigham and Women's Hospital, Harvard Medical School, Boston, Massachusetts; [3]Yukinori Okada, MD, PhD: Tokyo Medical and Dental University Graduate School of Medical and Dental Sciences, Tokyo, Japan, and Riken, Yokohama, Japan; [4]Wessam Gad El Haq, MBBS, Ziyad R. Mahfoud, PhD, Marianthi Kapiri, MSc, Soha R. Dargham, MPH, Grace Aranki, BSc, Thurayya Arayssi, MD: Weill Cornell Medicine–Qatar, Education City, Doha, Qatar; [5]Mohammed Hammoudeh, MD, Samar Al Emadi, MBBS: Hamad Medical Corporation, Doha, Qatar; [6]Basel K. Masri, MD: Jordan Hospital, Amman, Jordan; [7]Hussein Halabi, MBBS: King Faisal Specialist Hospital and Research Center, Jeddah, Saudi Arabia; [8]Humeira Badsha, MD: Dr. Humeira Badsha Medical Center, Dubai, United Arab Emirates; [9]Imad W. Uthman, MD, MPH: American University of Beirut, Beirut, Lebanon; [10]Lauren Margolin, BSc, Namrata Gupta, PhD: Broad Institute, Cambridge, Massachusetts; [11]Layla A. Kazkaz, MD: Tishreen Hospital, Damascus, Syria.

Address correspondence to Thurayya Arayssi, MD, Weill Cornell Medicine–Qatar, Education City, PO Box 24144, Doha, Qatar (e-mail: Tha2002@qatar-med.cornell.edu); or to Richa Saxena, PhD, Center for Human Genetic Research, 185 Cambridge Street, Boston, MA 02114 (e-mail: rsaxena@broadinstitute.org).

Submitted for publication September 2, 2016; accepted in revised form January 17, 2017.

Rheumatoid arthritis (RA) is a chronic systemic inflammatory disorder with an estimated worldwide prevalence of up to ~1% in the adult population (1). The root cause of disease is unknown, although both genetic and environmental factors play a role. The clinical hallmark of RA is an inflammatory arthritis with a predilection for diarthrodial joints (2). Premenopausal women are at greater risk than men for developing RA (at a ratio of ~3:1) (1). While the disease can occur at any age, the peak age at disease onset is in the 40–50-year range, with an increasing incidence with age.

The genetic contribution to RA susceptibility in humans has been demonstrated convincingly through twin and family studies (3,4). It is estimated that ~60% of RA disease variability is inherited (3). Whereas the population risk of RA is ~1%, the monozygotic twin of a patient with RA has a risk of ~15% (5–7). The major histocompatibility complex (MHC) region explains up to one-third of RA risk (8,9). Most of the risk attributable to the MHC region is associated with common alleles within the *HLA–DRB1* gene—these are often referred to as "shared epitope" alleles (10,11)—and the risk is increased only in anti–cyclic citrullinated peptide (anti-CCP)–positive patients with RA (in whom the odds ratio [OR] for RA is >5) (12,13). Genome-wide association studies (GWAS) have identified 100 non-MHC loci, which, together, explain an additional 5.5% of the RA heritability in Europeans and 4.7% of the RA heritability in Asians (14).

Importantly, the genetic studies conducted to date have largely been restricted to patients of European or East Asian ancestry (14). It is therefore unknown whether these same risk alleles contribute to the risk of RA among patients of Arab ancestry in the Middle East, or whether genetic studies in these populations might identify new loci for disease.

The purpose of our study was to investigate the cross-ethnic association of known European RA risk loci and to discover new RA risk loci in a multinational Arab case–control cohort. First, we hypothesized that common alleles identified from genetic studies of subjects of European ancestry will also contribute to the risk of RA among individuals of Arab ancestry, given that recent studies have shown that many risk alleles are shared among individuals of diverse ancestries (14,15). Second, we hypothesized that GWAS in an Arab population may point to novel RA risk loci of strong effect specific to Arab populations, similar to *PADI1* variants in Asians (16), or may indicate risk loci that have a higher allele frequency in Arabs relative to currently studied ethnic groups (as was found for a *PTPN22* missense association in whites [17]). Therefore, we enrolled RA patients and healthy controls in a genetic study of RA in a pan-Arab RA genetics consortium. We obtained measures of autoantibody status and performed genome-wide genotyping and a GWAS of RA, both in the entire population and in analyses stratified by ethnicity or autoantibody status.

PATIENTS AND METHODS

Subjects. A total of 794 RA patients and 573 healthy controls were included in this study. Subjects were enrolled from 5 centers in Jordan, the Kingdom of Saudi Arabia, Lebanon, Qatar, and the United Arab Emirates. To be eligible for the study, patients had to be of Arab ancestry (by self report), have RA diagnosed in accordance with the American College of Rheumatology 1987 criteria (18), be ≥18 years of age, and be able to sign an informed consent. Controls eligible for enrollment in the study were healthy subjects free of autoimmune diseases. The controls were age-, sex-, and ethnicity-matched by frequency to the enrolled patients. Ethnicity was classified as self-reported African, Gulf, or Levant Arab ancestry.

Written informed consent was obtained from all subjects prior to enrollment in the study, in accordance with the Declaration of Helsinki for Human Studies, and the study was approved across all sites by the local Institutional Review Boards. In addition to age, sex, and self-reported ethnicity, we collected additional clinical information on the presence or absence of rheumatoid factor (RF) and anti-CCP antibodies, disease duration, medications used to treat RA, family history of RA, and vascular comorbidities (Table 1).

Sample collection. For sample collection, 15 ml of whole blood was collected from each patient and each control subject in a prelabeled EDTA tube. Whole blood was then transferred into cryovials and stored at −80°C at each Rheumatology Center, and then batched-shipped to the Weill Cornell Medical College-Qatar for DNA extraction and storage. Samples were centrifuged so that buffy coat cells could be separated from plasma. Aliquots consisting of 1 ml buffy coat and 2 aliquots of up to 1 ml of plasma were created and stored at −80°C. DNA was extracted from the blood with a Gentra Puregene DNA extraction kit (Qiagen). An aliquot of the samples was sent to the Broad Institute for quality control and genome-wide genotyping. The DNA concentration was determined with a Quant-IT Picogreen double-stranded DNA reagent kit (Invitrogen). In total, 928 of the 937 samples had a sufficient concentration of DNA (>10 ng/μl) and sufficient yield of DNA for the GWAS. Thus, genome-wide genotyping of 922 samples was attempted. All 513 replication samples had a sufficient concentration of DNA (>10 ng/μl) for replication genotyping.

Genotyping and imputation in the discovery GWAS. In total, 922 samples were genotyped with a panel of ~30 single-nucleotide polymorphisms (SNPs) in the discovery GWAS, to create a molecular barcode for each sample. Genome-wide genotyping was performed at the Broad Institute in 2 batches (n = 166 in batch 1 and n = 756 in batch 2) using an Infinium HumanCoreExome Bead Chip array (Illumina). This array consists of 547,644 markers, with ~50% of the markers being selected to provide a GWAS scaffold for high-quality imputation and the other half being selected to provide coverage of low-frequency, protein-altering variants identified from >12,000 worldwide sequences. Variant bases were called using the default Illumina GenCall algorithm. Subjects were removed from these analyses because of inbreeding (n = 16), discrepancy in sex

Table 1. Clinical characteristics of the Arab rheumatoid arthritis cases and matched controls in the discovery and replication populations*

	Discovery cohort (n = 863)				Replication cohort (n = 513)			
	Overall	Cases (n = 511)	Controls (n = 352)	*P*	Overall	Cases (n = 288)	Controls (n = 225)	*P*
Age, mean ± SD years	45.5 ± 13.9	48.9 ± 13.0	40.5 ± 13.6	<0.001†	48.5 ± 14.2	48.7 ± 13.7	48.2 ± 14.9	0.703
Sex, no. female:no. male	4:1	6:1	2:1	<0.001†	4:1	6:1	3:1	<0.001†
Duration of disease, mean ± SD years	9.4 ± 8.6	9.4 ± 8.6	–	–	9.2 ± 8.3	9.2 ± 8.3	–	–
Ancestry								
Africa	124 (14.4)	79 (15.5)	45 (12.8)	–	102 (19.9)	50 (17.4)	52 (23.1)	–
Gulf	329 (38.1)	226 (44.2)	103 (29.3)	<0.001†	213 (41.5)	129 (44.8)	84 (37.3)	0.143
Levant	410 (47.5)	206 (40.3)	204 (58.0)	–	198 (38.6)	109 (37.8)	89 (39.6)	–
Anti-CCP and RF status								
Anti-CCP+	–	264 (51.7)	–	–	–	170 (59.0)	–	–
RF+	–	311 (60.9)	–	–	–	188 (65.3)	–	–
Anti-CCP+/RF+	–	218 (42.7)	–	–	–	148 (56.1)	–	–
Anti-CCP+/RF−	–	154 (30.1)	–	–	–	54 (20.5)	–	–
Cigarette smoking status								
Ever smoked	199 (21.4)	109 (19.7)	90 (23.8)	–	93 (18.4)	58 (20.4)	35 (16.1)	–
Never smoked	732 (78.6)	444 (80.3)	288 (76.2)	–	410 (81.6)	227 (79.6)	183 (83.9)	–
Shisha smoking status								
Ever smoked	135 (14.5)	61 (11.0)	74 (19.6)	–	54 (10.7)	32 (11.2)	22 (10.1)	–
Never smoked	796 (85.5)	492 (99.0)	304 (80.4)	–	449 (89.3)	253 (88.8)	196 (89.9)	–

* Except where indicated otherwise, values are the number (%) of subjects. Anti-CCP = anti–cyclic citrullinated peptide; RF = rheumatoid factor.
† Significant difference between cases and controls at $P \leq 0.05$.

between the genetic and clinical data (n = 3), duplicate samples (n = 12), and cryptic relatedness (pi-hat >0.125, n = 35), with 7 samples overlapping.

All samples had a genotyping rate of >90%. A total of 863 (93.6%) of the 922 samples passed the quality control review for the GWAS analysis. Only SNPs present at a frequency of ≥1% in the population were included in the GWAS. Of the 541,168 SNPs screened, 532,102 SNPs (98.3%) passed quality control. SNPs removed included 8,788 SNPs that were removed for having a call rate of <95% or unmatched call rates in cases and controls, 450 SNPs that departed from Hardy-Weinberg equilibrium ($P < 1.0 \times 10^{-6}$), and 172 SNPs that failed both tests. Imputation on clean genotypes was performed using the Impute 2 software package (19) and using the 1000 Genomes Phase 3 panel (May 2013). Postimputation quality control analyses filtered out variants with imputation quality information scores of <0.88 and a minor allele frequency (MAF) of <1%. After quality control, 7,000,653 SNPs in 511 cases and 352 controls were successfully tested for our discovery GWAS of Arab RA populations. *HLA* imputation was performed using SNP2HLA and the T1DGC European reference panel (20).

Replication analysis. In total, 513 samples were genotyped for 23 SNPs in the replication analysis, using primer extension of multiplex products. SNPs were detected using matrix-assisted laser desorption ionization–time-of-flight mass spectrometry with a Sequenom platform, as previously described (Broad Institute) (21). Quality control steps excluded samples with a call rate of <60% and SNPs with a call rate of <95%, departure from Hardy-Weinberg equilibrium ($P < 1.0 \times 10^{-6}$), or MAF of <1%. Nineteen SNPs on 504 samples that passed quality control were available for replication association testing.

Assessment of population structure. To evaluate the population structure of this Middle-Eastern cohort relative to global populations, principal components (PCs) in the GWAS sample were calculated, prior to imputation, with the LASER: Locating Ancestry from SEquence Reads technique (22), using 938 reference samples from the Human Genome Diversity Project (HGDP) (23) (Figure 1A). Clusters of individuals based on proximity to known HGDP samples in the PC analysis (PCA) were defined as either African-admixed (n = 153) or non–African-admixed (n = 700) Arab subgroups for secondary analyses (Figure 1B).

Statistical analysis. The GWAS were performed using logistic regression in SNPTEST (19), with SNPs coded in an additive model and with adjustments for age, sex, and self-reported ancestry. Our discovery GWAS analysis comprised the entire case–control Arab population, and additional GWAS were performed in subpopulations stratified by seropositivity (seropositive RA, RF+/anti-CCP+ [n = 357 cases, n = 352 controls]; seronegative RA, RF−/anti-CCP− [n = 154 cases, n = 352 controls]) or by ancestry (African-admixed Arabs, n = 97 cases and n = 56 controls; non–African-admixed Arabs, n = 410 cases and n = 290 controls). Genome-wide significance was considered at the Bonferroni-corrected threshold of $P < 5.0 \times 10^{-8}$ (24).

Replication analysis was performed using logistic regression in Plink (25), with SNPs coded additively and adjustments made for age, sex, and self-reported ancestry (African, Gulf, Levant). The threshold for statistical significance in the replication analysis was $P < 0.003$ (0.05 divided by 15). Association analysis of the imputed *HLA* variants in the MHC region was conducted as described elsewhere (26,27). Results from the discovery GWAS and replication analyses were combined in a fixed-effects meta-analysis with inverse variance weights, using METAL (28).

We further calculated a cumulative aggregate genetic risk score (15) using the sum of the weighted risk allele counts for all previously known RA risk alleles that passed quality control in our current analysis (n = 68 independent SNPs). The

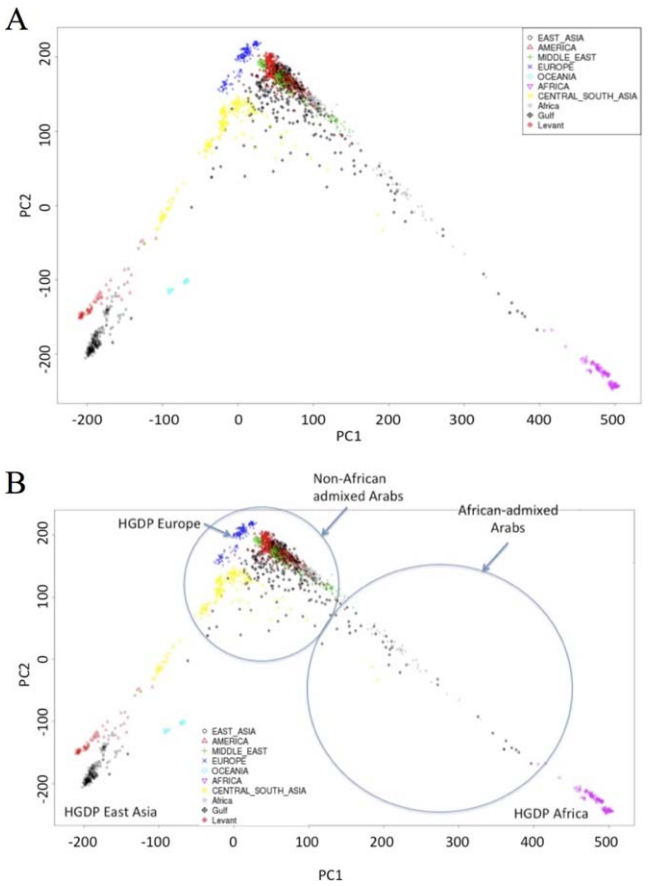

Figure 1. Principal components (PC) analyses of the entire rheumatoid arthritis case–control discovery cohort of Arabs **(A)** and the subgroups of Arab populations (African-admixed and non–African-admixed) defined for secondary analysis **(B)**, relative to Human Genome Diversity Project (HGDP) populations. The first PC (PC1) and second PC (PC2) are shown in the plots.

weights for each SNP were derived from the recently published meta-analysis of RA GWAS (14) and were calculated as the natural log of the OR for each allele. We determined the relationship between the genetic risk score and RA traits (29). The level of statistical significance was considered at the Bonferroni-corrected threshold of $P < 0.0125$ for 4 genetic risk score tests (0.05 divided by 4).

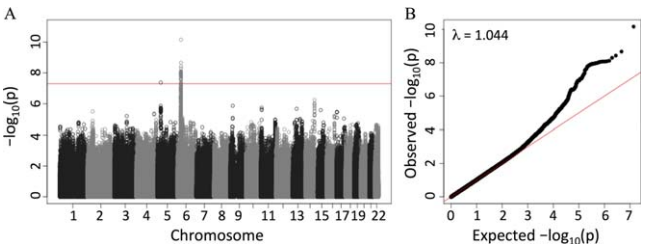

Figure 2. Manhattan plot **(A)** and qq plot **(B)** of the genome-wide association study results in the entire rheumatoid arthritis (RA) case–control discovery cohort of Arab subjects (n = 511 RA cases, n = 352 healthy controls) among single-nucleotide polymorphisms (SNPs) with a frequency of >1%. Values are the $-\log_{10} P$ values for each SNP. The lambda value in **B** represents the inflation factor. In **A**, the red line indicates the genome-wide significance threshold, while in **B**, it represents a flat diagonal line for reference.

RESULTS

Genetic ancestries of the case–control Arab cohort. Results of PCA suggested that the group of individuals with self-reported African ancestry extended along a cline toward the HGDP Africans, while self-reported Gulf ancestry comprised ancestral components from African, Asian, and European populations, and self-reported Levant ancestry localized near the HGDP European populations (Figure 1A). Genetic ancestry allowed us to define 2 major subgroups of Arabs for secondary analyses: African-admixed (n = 153) and non–African-admixed (n = 700) (Figure 1B). Cases with African admixture (based on self-report or genetic ancestry) were more likely than non–African-admixed cases to be seropositive for RF and/or anti-CCP (Table 2).

Results of discovery and replication GWAS. In the discovery GWAS analysis of RA in the entire Arab case–control population, there was little inflation from undetected population structure or relatedness (λ = 1.044) (Figures 2A and B) and the estimated heritability

Table 2. Associations of self-reported and genetic ancestry with seropositive rheumatoid arthritis status in cases with genome-wide genotypes (n = 511)*

Ancestry	No. of subjects	RF positive	Anti-CCP positive	RF positive and anti-CCP positive	RF positive or anti-CCP positive	RF negative and anti-CCP negative
Self-reported						
Africa	79	54 (68.4)	46 (58.2)	41 (51.9)	18 (22.8)	20 (25.3)
Gulf	226	146 (64.6)	113 (50.0)	98 (43.4)	63 (27.8)	65 (28.8)
Levant	206	111 (53.9)	105 (51.0)	79 (38.3)	58 (28.1)	69 (33.5)
P between groups		0.025†	0.438	0.113	0.63	0.336
Genetic						
African-admixed	97	67 (69.1)	57 (58.8)	50 (51.5)	24 (24.7)	23 (23.7)
Non–African admixed	410	241 (58.8)	205 (50.0)	166 (40.5)	114 (27.8)	130 (31.7)
P between groups		0.062	0.12	0.048†	0.542	0.123

* Values are the number (%) of subjects. RF = rheumatoid factor; anti-CCP = anti–cyclic citrullinated peptide.
† Significant difference between ancestral groups at $P \leq 0.05$.

Table 3. Significant and suggestive association signals from the discovery RA GWAS (all RA and seropositive RA), replication analysis, and meta-analysis in Arabs*

					Discovery analysis (n = 511 cases, n = 352 controls)		Replication analysis (n = 283 cases, n = 221 controls)		Meta-analysis (n = 794 cases, n = 573 controls)	
SNP	Chr:Pos†	Nearest gene	Allele‡	AF§	OR (95% CI)	*P*	OR (95% CI)	*P*	OR (95% CI)	*P*
All RA										
rs9269234	6:32451788	*HLA–DRB1*	G/C	0.65	2.05 (1.65–2.55)	7.00×10^{-11}	1.38 (1.07–1.79)	1.4×10^{-2}	1.75 (1.48–2.06)	4.55×10^{-11}
rs12519788	5:30405068	*CDH6*	G/A	0.79	2.02 (1.57–2.59)	4.24×10^{-8}	1.46 (1.05–2.03)	2.4×10^{-2}	1.79 (1.47–2.19)	1.04×10^{-8}
rs12601925	17:4503195	*SMTNL2/GGT6*	G/A	0.86	2.03 (1.50–2.73)	3.60×10^{-6}	1.49 (1.04–2.15)	3.0×10^{-2}	1.79 (1.42–2.26)	7.21×10^{-7}
rs9860428	3:114053609	*CD200R1*	C/A	0.38	1.64 (1.33–2.04)	6.24×10^{-6}	1.51 (1.16–1.97)	2.0×10^{-3}	1.59 (1.35–1.88)	5.46×10^{-8}
Seropositive RA										
rs9269234	6:32451788	*HLA–DRB1*	G/C	0.65	2.51 (1.98–3.19)	4.86×10^{-14}	1.70 (1.27–2.26)	3.13×10^{-4}	2.14 (1.78–2.57)	5.70×10^{-16}
rs12519788	5:30405068	*CDH6*	G/A	0.79	2.06 (1.57–2.70)	1.58×10^{-7}	1.47 (1.03–2.10)	3.56×10^{-2}	1.82 (1.47–2.26)	4.99×10^{-8}
rs12601925	17:4503195	*SMTNL2/GGT6*	G/A	0.86	2.55 (1.83–3.56)	3.76×10^{-8}	1.67 (1.11–2.51)	1.3×10^{-2}	2.15 (1.66–2.78)	5.68×10^{-9}
rs9860428	3:114053609	*CD200R1*	C/A	0.38	1.68 (1.32–2.12)	1.69×10^{-5}	1.50 (1.12–1.99)	5.6×10^{-3}	1.60 (1.33–1.92)	3.75×10^{-7}

* Analyses were conducted in an additive allele model, adjusted for age, sex, and self-reported ancestry. Association coefficients are shown as the odds ratio (OR) and 95% confidence interval (95% CI) for association with rheumatoid arthritis (RA), per each additional copy of the effect allele. GWAS = genome-wide association study; SNP = single nucleotide polymorphism; Chr:Pos = chromosome:position.

† The position was ascertained from NCBI database 37.

‡ The effect allele/noneffect allele is shown.

§ The allele frequency (AF) of the effect allele in the discovery population is shown.

from autosomal SNPs was $H^2 = 0.301$ ($P = 0.091$). A genome-wide significant association with RA was observed at the *HLA* locus (lead SNP, rs9269234 G allele; OR 2.05 [95% confidence interval (95% CI) 1.65–2.55, $P = 7.00 \times 10^{-11}$) and with 43 other correlated *HLA*-region SNPs surpassing the genome-wide significance threshold. Furthermore, a genome-wide significant association was observed at 5q13 (lead SNP, rs12519788 G allele; OR 2.02 [95% CI 1.57–2.59], $P = 4.24 \times 10^{-8}$) in an intergenic region that was 789 kb from the nearest gene, *CDH6* (Table 3 and Figure 3A). A significant association with RA was also seen at rs9860428 on chromosome 3 (OR 1.64 [95% CI 1.33–2.04], $P = 6.24 \times 10^{-6}$) (Figure 3B).

GWAS analysis of subjects with seropositive RA (n = 357 cases, n = 352 controls) identified association signals at the *HLA* locus that were even stronger than those seen for RA overall (lead SNP, rs9269234 G allele; OR 2.51 [95% CI 1.98–3.19], $P = 4.86 \times 10^{-14}$) (Table 3 and Figure 4A). Moreover, a novel signal at 17p13.2 was identified in seropositive RA subjects (lead SNP, rs12601925 G allele; OR 2.55 [95% CI 1.83–3.56], $P = 3.76 \times 10^{-8}$) (Table 3, Figure 4B, and Figures 5A and B; see also Supplementary Tables 1 and 2, available on the *Arthritis & Rheumatology* web site at http://onlinelibrary.wiley.com/doi/10.1002/art.40051/abstract). In the GWAS analysis of seronegative RA subjects (n = 154 cases, n = 352 controls), no signals reached genome-wide significance (see Supplementary Table 2 and Supplementary Figure 1A, http://onlinelibrary.wiley.com/doi/10.1002/art.40051/abstract).

In the GWAS of ancestral subgroups, genomic inflation was only slightly lower than that in the GWAS

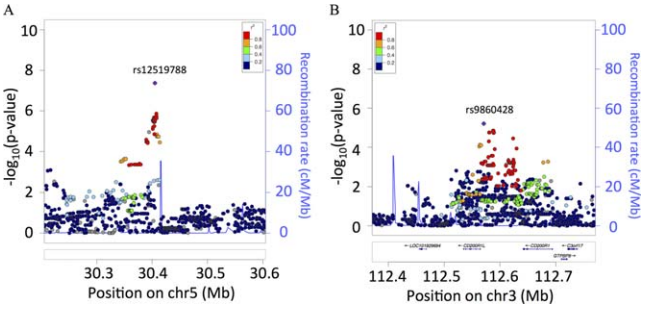

Figure 3. Regional association plots of the genome-wide association study (GWAS) discovery results for the association of rheumatoid arthritis with single-nucleotide polymorphisms (SNPs) at chromosome 5 (Chr5) **(A)** and chromosome 3 **(B)**. Analyses were adjusted for age, sex, and self-reported ancestry. Values are the $-\log_{10} P$ values of SNPs from the case–control GWAS plotted against the chromosomal position encompassing 400 kb around each lead SNP (purple): rs12519788 on chromosome 5 **(A)** and rs9860428 on chromosome 3 **(B)**. The defined r^2 color scheme indicates the linkage disequilibrium (LD) relationship with the lead SNP. LD was calculated based on 1000 Genomes European population data. The recombination rate is shown in blue on the right.

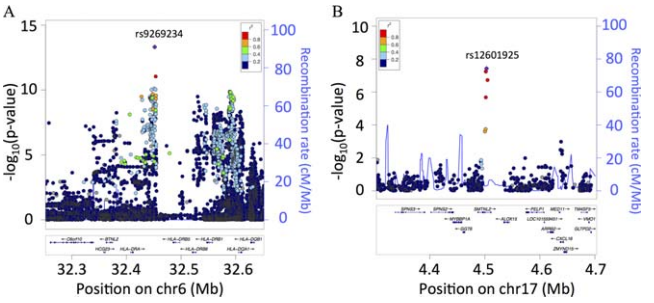

Figure 4. Regional association plots of the genome-wide association study (GWAS) discovery results for the association of seropositive rheumatoid arthritis with single-nucleotide polymorphisms (SNPs) at chromosome 6 (Chr6) **(A)** and chromosome 17 **(B)**. Analyses were adjusted for age, sex, and self-reported ancestry. Values are the $-\log_{10} P$ values of SNPs from the case–control GWAS plotted against the chromosomal position encompassing 400 kb around each lead SNP (purple): rs9269234 on chromosome 6 **(A)** and rs12601925 on chromosome 17 **(B)**. The defined r^2 color scheme indicates the linkage disequilibrium (LD) relationship with the lead SNP. LD was calculated based on 1000 Genomes European population data. The recombination rate is shown in blue on the right.

analysis of RA overall (African-admixed Arabs, $\lambda = 0.973$; non–African-admixed Arabs, $\lambda = 1.04$) (see Supplementary Figures 1B and C, available on the *Arthritis & Rheumatology* web site at http://onlinelibrary.wiley.com/doi/10.1002/art.40051/abstract). In the RA GWAS restricted to the smaller subgroup of subjects of African-admixed ancestry, no SNPs reached significance, whereas in the larger, more homogeneous non–African-admixed subgroup, the *HLA* locus remained significant (lead SNP, rs9269234 G allele; OR 2.00 [95% CI 1.57–2.54], $P = 1.87 \times 10^{-8}$) (see Supplementary Table 3, http://onlinelibrary.wiley.com/doi/10.1002/art.40051/abstract).

Suggestive evidence of replication of significant SNPs at 4 of the 15 lead association signals was observed in an independent sample of 283 RA cases and 221 healthy

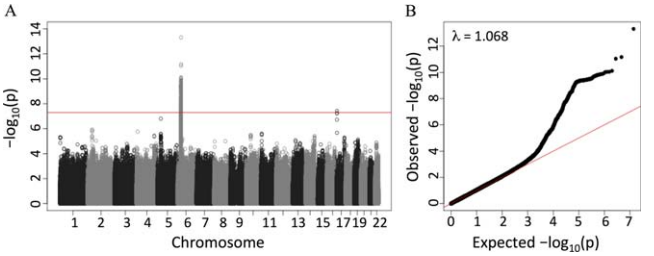

Figure 5. Manhattan plot **(A)** and qq plot **(B)** of the genome-wide association study results in the seropositive rheumatoid arthritis (RA) cohort of Arab subjects (n = 357 RA cases, n = 352 healthy controls) among single-nucleotide polymorphisms (SNPs) with a frequency of >1%. Values are the $-\log_{10} P$ values for each SNP. The lambda value in **B** represents the inflation factor. In **A**, the red line indicates the genome-wide significance threshold, while in **B**, it represents a flat diagonal line for reference.

controls in our replication analysis (Table 3; see also Supplementary Table 1, available on the *Arthritis & Rheumatology* web site at http://onlinelibrary.wiley.com/doi/10.1002/art.40051/abstract). Notably, all 3 signals that reached genome-wide significance in the discovery GWAS (*HLA–DRB1,* 5q13, and 17p13) showed consistent allelic effects and remained genome-wide significant in the meta-analysis. A fourth signal, at 3q13.2, between the genes *CD200R1* and *CD200R1L*, did not reach genome-wide significance in the discovery GWAS but showed evidence of replication after Bonferroni correction ($P < 0.003$). Furthermore, all 4 association signals showed consistent evidence of association in replication analyses restricted to cases with seropositive RA and all controls (Table 3). These signals explained 3.55% of the variability in risk of RA.

We cross-checked our results with regard to the lead SNPs at the 2 novel genome-wide significant signals at 5q13 and 17p13 in our Arab study population against the results of a recently reported transethnic meta-analysis of GWAS comprising subjects of East Asian and European ancestry (n = 19,234 RA cases, n = 61,565 controls) (14). However, little evidence of association of these 2 signals with RA was observed in that study of East Asian and European subjects (for rs12519788 G allele, OR 1.01 [95% CI 0.97–1.04], $P = 0.63$; for rs12601925 G allele, OR 0.99 [95% CI 0.95–1.04], $P = 0.82$).

Genetic risk score of previously established RA loci in Arabs. We tested whether previously reported genome-wide significant RA associations from the transethnic meta-analysis previously conducted in East Asian and European populations (14) could be generalized to our Arab study population. Results for index SNPs at 68 of 101 non-*HLA* loci were available in our GWAS analyses (see Supplementary Table 4, available on the *Arthritis & Rheumatology* web site at http://onlinelibrary.wiley.com/doi/10.1002/art.40051/abstract). In total, 46 of the 68 SNPs demonstrated a concordant direction of effect between the European and Arab populations in the RA GWAS (binomial $P = 2.78 \times 10^{-4}$). A weighted genetic risk score of the 68 SNPs was associated with RA overall (OR 1.85 [95% CI 1.38–2.48] per risk allele, $P = 3.41 \times 10^{-5}$) and with seropositive RA (OR 2.20 [95% CI 1.60–3.04] per risk allele, $P = 1.48 \times 10^{-6}$) but not with seronegative RA (OR 1.37 [95% CI 0.92–2.04] per risk allele, $P = 0.12$). In stratified analyses, the effect of the genetic risk score on RA was stronger and more significant in the non–African-admixed Arab population (OR 1.98 [95% CI 1.43–2.75] per risk allele, $P = 4.01 \times 10^{-5}$), while no significant effect was observed in the smaller population of African-admixed Arabs (OR 1.55 [95% CI 0.77–3.10] per risk allele, $P = 0.22$).

Imputation of *HLA* region amino acids and SNPs. In order to identify the SNPs and amino acids responsible for the *HLA* association signal, we performed *HLA* variant imputation in a manner as previously described (20), using the European T1DGC reference panel, and tested for genetic association of imputed SNPs and amino acids with RA and with seropositive RA. Previous studies have suggested that 5 amino acids in 3 HLA proteins in the MHC account for most of the RA signal observed in individuals of European ancestry, and a common set of amino acid residues also confers risk in individuals of Asian ancestry, despite differences in traditional *HLA* alleles (26,27). Although we could not directly assess the imputation accuracy of the *HLA* variants in our study samples, previous studies have demonstrated the reliable accuracy of *HLA* imputation in multiple populations (26,27). Moreover, considering that *HLA* variants are known to have essential roles in RA according to seropositivity status, we assessed *HLA* variant risks separately in GWAS of subjects with seropositive RA and those with seronegative RA. In seropositive RA GWAS, amino acid position 11 in the gene *HLA–DRB1* could account for the lead association signal (omnibus $P = 4.8 \times 10^{-16}$). In analyses conditioned on *HLA–DRB1* amino acid position 11, no other *HLA* variants remained significant ($P > 6.2 \times 10^{-4}$). We did not observe a significant association of *HLA* variants in the GWAS of subjects with seronegative RA ($P > 3.6 \times 10^{-4}$).

DISCUSSION

Herein we report the first GWAS of RA in Arabs. First, we observed that known *HLA* and non-*HLA* RA risk loci observed in Europeans and East Asians are strongly associated with RA in our multinational Arab cohort. Consistently, we observed significant replication of the association of a specific *HLA* region amino acid with RA and with seropositive RA in this population. Second, we discovered 2 novel genome-wide significant RA risk loci specific to Arab populations, with limited associations in other ethnicities.

In the last decade, genetic association studies in RA and meta-analyses of these associations have been helpful in uncovering novel risk alleles (14). The majority of these studies have been performed in populations of European and East Asian ancestry, revealing some replication across different ethnicities while uncovering novel genetic risk factors (30–33). However, no genetic studies had been conducted in an Arab population to date.

The definition of Arab ancestry was based on self-report, and all subjects studied were nationals of 1 of the 22 countries of the Arab world spanning from North Africa to the Arabian Gulf region, and categorized as 1 of 3 geographic Arab regions: Africa, Gulf, or Levant (as detailed in the League of Arab States web site at http://

www.lasportal.org/ar/Pages/default.aspx). As expected based on the multiple waves of migration that characterize Arab populations, our study population showed continental genetic heterogeneity, with genetic ancestry that distinguished African-admixed Arabs from non–African-admixed Arabs. While these ancestral differences are large, we did not observe a significant effect of population stratification in the primary GWAS, most likely because within each ancestral group, cases and controls were well matched and our analyses included adjustment for ancestry.

Our hypothesis that common alleles identified from genetic studies of subjects of European ancestry also contribute to the risk of RA among individuals of Arab ancestry was validated in this study. GWAS of the entire RA case–control population showed a significant association within the *HLA* locus. This finding validates the importance of this region in RA susceptibility across different ethnic groups and confirms that our study is well powered to identify common alleles with large effect. The association was of larger magnitude and greater significance when the analysis was restricted to seropositive cases, as has been previously described.

Imputation of the *HLA* classic alleles and the *HLA* amino acid polymorphisms showed that *HLA–DRB1* amino acid position 11 is the allele at the *HLA* locus most significantly associated with seropositive RA in Arabs, which is consistent with observations in European, Asian, and African-American populations (26,27,34). In a study of Arab Syrians, *DRB1* was found to be more common in RA patients compared to controls, and *DRB1*0101*, **0404*, and **0405* had a stronger association with joint destruction (35). Similarly, a strong association of a genetic risk score of 68 known RA loci was observed in our Arab population, again confirming that a majority of RA risk loci are consistently associated across multiple ethnic groups.

Second, we hypothesized that GWAS in an Arab population may point to novel RA risk loci of strong effect specific to Arab populations. Two loci that have not been previously reported in European or East Asian RA GWAS reached statistical significance in our study, consistent with the notion of strong population-specific effects, as was also previously seen for the *PADI1* locus in Asians. The locus at 5q13 was detected in the entire case–control study, and the locus at 17p13 was identified in the seropositive RA subgroup. Replication of these findings in independent Arab samples suggests that the causal SNPs underlying these association signals are likely to play an important role in the risk of RA in the Arab population.

The lead SNP at the novel 5q13 signal lies in an intergenic region flanked by the calcium-dependent cell–cell adhesion gene *CDH6* ~789 kb upstream and the gene encoding the 7SK small nuclear RNA controlling transcriptional elongation ~456 kb downstream (36). The *CDH6* gene encodes K-cadherin, which has previously been implicated in adhesion between immune cells (37), has been described as a tumor suppressor (38), and has been found to be significantly down-regulated in a rat model of arthritis (39). The 7SK small nuclear RNA has also been implicated in cancer (40) and HIV latency (41), but not in autoimmunity. The lead SNP at the 17p13 locus lies in an intron of the smoothelin-like gene *SMTNL2*, which is implicated in a region defined by epigenetic marks for promoters and enhancers as well as DNase 1 hypersensitivity sites across many tissues (42). However, whether this regulatory region influences this gene or neighboring genes, e.g., *ALOX15* or *GGT6*, among several, will require future studies. *SMTNL2* is exclusively expressed in skeletal muscle (43), while *ALOX15* and *GGT* have previously been implicated in RA inflammatory processes (44,45).

A fourth association signal at 3q13.2 near *CD200R1,* encoding the CD200 receptor (CD200R), almost reached significance after replication. The *CD200–CD200R* axis has previously been demonstrated to be important in autoimmunity, both in humans and in mice, with a potential role in Th17 cell differentiation, chemotaxis, and osteoclastogenesis in RA (46). A soluble ligand of CD200R has been investigated in preclinical models as a therapeutic agent for RA (47).

Our cross-check investigation of the 2 novel signals (5q13 and 17p13) against a large transethnic meta-analysis of subjects of East Asian and European ancestry suggests that these Arab-specific loci may not be relevant in the other 2 ethnicities, although the alleles themselves are quite common in all ethnic groups. The frequency of the risk allele of the lead SNP at 17p13 varies between studies and was found to be highest in our Arab cohort (frequency of the G allele, 0.86 in Arabs [present study], 0.83 in Europeans, and 0.40 in East Asians), whereas the risk allele frequency at 5q13 was more similar, yet still highest in Arabs (frequency of the G allele, 0.79 in Arabs [present study], 0.66 in Europeans, and 0.78 in East Asians). Thus, we expect that these loci have a population-specific effect in Arabs, and associated SNPs may tag as-yet–undetected novel variations in Arab populations that might have arisen after divergence from other populations. Notably, we did detect consistent effects at these loci in both non–African-admixed and African-admixed Arab populations.

RA risk loci tend to demonstrate pleiotropy with other human phenotypes, including immune-related diseases. However, this was not the case for the novel loci identified in this GWAS (17p13, 5q13, and 3q13.2). It might be that these loci are Arab-specific with limited relevance to other ethnicities, and as a result, have not been associated with other diseases. With that said,

unraveling these ethnicity-specific loci is only possible by conducting these transethnic GWAS for RA.

Earlier investigations have suggested that the genetic architecture of seropositive RA and seronegative RA is different, and also that few genetic markers, including the *HLA* locus, may or may not be associated with seronegative RA (48). Our analyses have not pointed to other loci that predict seronegative RA, likely because of the heterogeneity in phenotype, low heritability, and high polygenicity of the trait, as well as the low statistical power of our study. It is highly possible that multiple undiscovered loci remain to be determined.

Strengths of our study include the large pan-Arab case–control population, implementation of careful technical and analytic quality control measures across our study population, as demonstrated by low inflation values and validation of known associations, and discovery and confirmation of novel associations that may be specific to Arab populations and other related populations. Weaknesses of the study include the lack of a central laboratory to test for RF and anti-CCP status in a standardized manner, possibly resulting in underestimation of the number of seropositive cases. In addition, data on anti-CCP status were missing from 1 of the countries due to financial restrictions, and radiographic data as well as data on disease severity or response to medication were lacking. Finally, there was insufficient power to detect associations with seronegative RA, and a European reference panel was used for *HLA* imputation.

In summary, our study findings establish that the *HLA* region, previous RA risk alleles identified in European and Asian populations, and novel Arab-specific loci play a causal role in RA and in seropositive disease in the Arab population. Larger studies using genome-wide approaches are now needed to validate population-specific alleles and to more fully characterize the genes and pathways involved in RA pathogenesis and severity in Arab populations.

ACKNOWLEDGMENTS

We would like to thank the Middle East Rheumatoid Arthritis Consortium scientific advisory board for reviewing the manuscript, and the following individuals for their help in patient recruitment and data management: Dr. Shymma El Ataway, Dr. Abdurahman Albeity, Ms Eman Bawazeer, Mr. Mohammad Habli, Dr. Saskia Mandy, Dr. Mira Merashli, Ms Marioneke Mook, Ms Rawan Shayboub, and Ms Zeinab Slim. In addition, we thank all of the patients and control subjects, without whom this study would not have been possible.

AUTHOR CONTRIBUTIONS

All authors were involved in drafting the article or revising it critically for important intellectual content, and all authors approved the final version to be published. Drs. Saxena and Arayssi had full access to all of the data in the study and take responsibility for the integrity of the data and the accuracy of the data analysis.

Study conception and design. Saxena, Plenge, Arayssi.

Acquisition of data. El Haq, Hammoudeh, Al Emadi, Masri, Halabi, Badsha, Uthman, Margolin, Gupta, Kapiri, Aranki, Arayssi.

Analysis and interpretation of data. Saxena, Plenge, Bjonnes, Dashti, Okada, El Haq, Hammoudeh, Al Emadi, Masri, Halabi, Badsha, Uthman, Mahfoud, Dargham, Aranki, Kazkaz, Arayssi.

ADDITIONAL DISCLOSURES

Author Plenge is an employee of Merck.

REFERENCES

1. Silman AJ, Pearson JE. Epidemiology and genetics of rheumatoid arthritis. Arthritis Res 2002;4 Suppl 3:S265–72.
2. Lee DM, Weinblatt ME. Rheumatoid arthritis. Lancet 2001;358:903–11.
3. MacGregor AJ, Snieder H, Rigby AS, Koskenvuo M, Kaprio J, Aho K, et al. Characterizing the quantitative genetic contribution to rheumatoid arthritis using data from twins. Arthritis Rheum 2000;43:30–7.
4. Bali D, Gourley S, Kostyu DD, Goel N, Bruce I, Bell A, et al. Genetic analysis of multiplex rheumatoid arthritis families. Genes Immun 1999;1:28–36.
5. Silman AJ, MacGregor AJ, Thomson W, Holligan S, Carthy D, Farhan A, et al. Twin concordance rates for rheumatoid arthritis: results from a nationwide study. Br J Rheumatol 1993;32:903–7.
6. Aho K, Koskenvuo M, Tuominen J, Kaprio J. Occurrence of rheumatoid arthritis in a nationwide series of twins. J Rheumatol 1986;13:899–902.
7. Jarvinen P, Aho K. Twin studies in rheumatic diseases. Semin Arthritis Rheum 1994;24:19–28.
8. Deighton CM, Walker DJ, Griffiths ID, Roberts DF. The contribution of HLA to rheumatoid arthritis. Clin Genet 1989;36:178–82.
9. Rigby AS, Silman AJ, Voelm L, Gregory JC, Ollier WE, Khan MA, et al. Investigating the HLA component in rheumatoid arthritis: an additive (dominant) mode of inheritance is rejected, a recessive mode is preferred. Genet Epidemiol 1991;8:153–75.
10. Gregersen PK, Moriuchi T, Karr RW, Obata F, Moriuchi J, Maccari J, et al. Polymorphism of HLA-DR β chains in DR4, -7, and -9 haplotypes: implications for the mechanisms of allelic variation. Proc Natl Acad Sci U S A 1986;83:9149–53.
11. Gregersen PK, Shen M, Song QL, Merryman P, Degar S, Seki T, et al. Molecular diversity of HLA-DR4 haplotypes. Proc Natl Acad Sci U S A 1986;83:2642–6.
12. Irigoyen P, Lee AT, Wener MH, Li W, Kern M, Batliwalla F, et al. Regulation of anti–cyclic citrullinated peptide antibodies in rheumatoid arthritis: contrasting effects of HLA–DR3 and the shared epitope alleles. Arthritis Rheum 2005;52:3813–8.
13. Huizinga TW, Amos CI, van der Helm-van Mil AH, Chen W, van Gaalen FA, Jawaheer D, et al. Refining the complex rheumatoid arthritis phenotype based on specificity of the HLA–DRB1 shared epitope for antibodies to citrullinated proteins. Arthritis Rheum 2005;52:3433–8.
14. Okada Y, Wu D, Trynka G, Raj T, Terao C, Ikari K, et al. Genetics of rheumatoid arthritis contributes to biology and drug discovery. Nature 2014;506:376–81.
15. Kurreeman F, Liao K, Chibnik L, Hickey B, Stahl E, Gainer V, et al. Genetic basis of autoantibody positive and negative rheumatoid arthritis risk in a multi-ethnic cohort derived from electronic health records. Am J Hum Genet 2011;88:57–69.
16. Too CL, Murad S, Dhaliwal JS, Larsson P, Jiang X, Ding B, et al. Polymorphisms in peptidylarginine deiminase associate with rheumatoid arthritis in diverse Asian populations: evidence from MyEIRA study and meta-analysis. Arthritis Res Ther 2012;14:R250.

17. Begovich AB, Carlton VE, Honigberg LA, Schrodi SJ, Chokkalingam AP, Alexander HC, et al. A missense single-nucleotide polymorphism in a gene encoding a protein tyrosine phosphatase (PTPN22) is associated with rheumatoid arthritis. Am J Hum Genet 2004;75:330–7.
18. Arnett FC, Edworthy SM, Bloch DA, McShane DJ, Fries JF, Cooper NS, et al. The American Rheumatism Association 1987 revised criteria for the classification of rheumatoid arthritis. Arthritis Rheum 1988;31:315–24.
19. Marchini J, Howie B, Myers S, McVean G, Donnelly P. A new multipoint method for genome-wide association studies by imputation of genotypes. Nat Genet 2007;39:906–13.
20. Jia X, Han B, Onengut-Gumuscu S, Chen WM, Concannon PJ, Rich SS, et al. Imputing amino acid polymorphisms in human leukocyte antigens. PLoS One 2013;8:e64683.
21. Tang K, Fu DJ, Julien D, Braun A, Cantor CR, Koster H. Chip-based genotyping by mass spectrometry. Proc Natl Acad Sci U S A 1999;96:10016–20.
22. Wang C, Zhan X, Bragg-Gresham J, Kang HM, Stambolian D, Chew EY, et al. Ancestry estimation and control of population stratification for sequence-based association studies. Nat Genet 2014;46:409–15.
23. Li JZ, Absher DM, Tang H, Southwick AM, Casto AM, Ramachandran S, et al. Worldwide human relationships inferred from genome-wide patterns of variation. Science 2008;319:1100–4.
24. Pe'er I, Yelensky R, Altshuler D, Daly MJ. Estimation of the multiple testing burden for genomewide association studies of nearly all common variants. Genet Epidemiol 2008;32:381–5.
25. Purcell S, Neale B, Todd-Brown K, Thomas L, Ferreira MA, Bender D, et al. PLINK: a tool set for whole-genome association and population-based linkage analyses. Am J Hum Genet 2007;81:559–75.
26. Okada Y, Kim K, Han B, Pillai NE, Ong RT, Saw WY, et al. Risk for ACPA-positive rheumatoid arthritis is driven by shared HLA amino acid polymorphisms in Asian and European populations. Hum Mol Genet 2014;23:6916–26.
27. Raychaudhuri S, Sandor C, Stahl EA, Freudenberg J, Lee HS, Jia X, et al. Five amino acids in three HLA proteins explain most of the association between MHC and seropositive rheumatoid arthritis. Nat Genet 2012;44:291–6.
28. Willer CJ, Li Y, Abecasis GR. METAL: fast and efficient meta-analysis of genomewide association scans. Bioinformatics 2010;26:2190–1.
29. Dastani Z, Hivert MF, Timpson N, Perry JR, Yuan X, Scott RA, et al. Novel loci for adiponectin levels and their influence on type 2 diabetes and metabolic traits: a multi-ethnic meta-analysis of 45,891 individuals. PLoS Genet 2012;8:e1002607.
30. Negi S, Juyal G, Senapati S, Prasad P, Gupta A, Singh S, et al. A genome-wide association study reveals ARL15, a novel non-HLA susceptibility gene for rheumatoid arthritis in North Indians. Arthritis Rheum 2013;65:3026–35.
31. Prasad P, Kumar A, Gupta R, Juyal RC, Thelma BK. Caucasian and Asian specific rheumatoid arthritis risk loci reveal limited replication and apparent allelic heterogeneity in north Indians. PLoS One 2012;7:e31584.
32. Lee HS, Korman BD, Le JM, Kastner DL, Remmers EF, Gregersen PK, et al. Genetic risk factors for rheumatoid arthritis differ in Caucasian and Korean populations. Arthritis Rheum 2009;60:364–71.
33. Jiang L, Yin J, Ye L, Yang J, Hemani G, Liu AJ, et al. Novel risk loci for rheumatoid arthritis in Han Chinese and congruence with risk variants in Europeans [published erratum appears in Arthritis Rheumatol 2014;66:1881]. Arthritis Rheumatol 2014;66:1121–32.
34. Reynolds RJ, Ahmed AF, Danila MI, Hughes LB, Consortium for the Longitudinal Evaluation of African Americans with Early Rheumatoid Arthritis Investigators, Gregersen PK, et al. HLA–DRB1–associated rheumatoid arthritis risk at multiple levels in African Americans: hierarchical classification systems, amino acid positions, and residues. Arthritis Rheumatol 2014;66:3274–82.
35. Kazkaz L, Marotte H, Hamwi M, Angelique Cazalis M, Roy P, Mougin B, et al. Rheumatoid arthritis and genetic markers in Syrian and French populations: different effect of the shared epitope. Ann Rheum Dis 2007;66:195–201.
36. McNamara RP, Bacon CW, D'Orso I. Transcription elongation control by the 7SK snRNP complex: releasing the pause. Cell Cycle 2016;15:2115–23.
37. Munro SB, Duclos AJ, Jackson AR, Baines MG, Blaschuk OW. Characterization of cadherins expressed by murine thymocytes. Cell Immunol 1996;169:309–12.
38. Goeppert B, Ernst C, Baer C, Roessler S, Renner M, Mehrabi A, et al. Cadherin-6 is a putative tumor suppressor and target of epigenetically dysregulated miR-429 in cholangiocarcinoma. Epigenetics 2016;11:780–90.
39. Wester L, Koczan D, Holmberg J, Olofsson P, Thiesen HJ, Holmdahl R, et al. Differential gene expression in pristane-induced arthritis susceptible DA versus resistant E3 rats. Arthritis Res Ther 2003;5:R361–72.
40. Keramati F, Seyedjafari E, Fallah P, Soleimani M, Ghanbarian H. 7SK small nuclear RNA inhibits cancer cell proliferation through apoptosis induction. Tumour Biol 2015;36:2809–14.
41. Cary DC, Fujinaga K, Peterlin BM. Molecular mechanisms of HIV latency. J Clin Invest 2016;126:448–54.
42. Ward LD, Kellis M. HaploReg: a resource for exploring chromatin states, conservation, and regulatory motif alterations within sets of genetically linked variants. Nucleic Acids Res 2012; 40(Database issue):D930–4.
43. Mele M, Ferreira PG, Reverter F, DeLuca DS, Monlong J, Sammeth M, et al. Human genomics: the human transcriptome across tissues and individuals. Science 2015;348:660–5.
44. Gheorghe KR, Korotkova M, Catrina AI, Backman L, af Klint E, Claesson HE, et al. Expression of 5-lipoxygenase and 15-lipoxygenase in rheumatoid arthritis synovium and effects of intraarticular glucocorticoids. Arthritis Res Ther 2009;11:R83.
45. Rambabu K, Ansari AA, Shaafie IA, Chelvam AP, Ziu MM. γ-glutamyl transpeptidase in synovial fluid, serum, and urine of patients with rheumatoid arthritis. Biochem Med Metab Biol 1990;43:183–92.
46. Ren Y, Yang B, Yin Y, Leng X, Jiang Y, Zhang L, et al. Aberrant CD200/CD200R1 expression and its potential role in Th17 cell differentiation, chemotaxis and osteoclastogenesis in rheumatoid arthritis. Rheumatology (Oxford) 2015;54:712–21.
47. Simelyte E, Criado G, Essex D, Uger RA, Feldmann M, Williams RO. CD200-Fc, a novel antiarthritic biologic agent that targets proinflammatory cytokine expression in the joints of mice with collagen-induced arthritis. Arthritis Rheum 2008;58:1038–43.
48. Kim K, Bang SY, Lee HS, Bae SC. Update on the genetic architecture of rheumatoid arthritis. Nat Rev Rheumatol 2017;13:13–24.

ARTHRITIS & RHEUMATOLOGY
Vol. 69, No. 5, May 2017, pp 986–995
DOI 10.1002/art.40035

High-Titer Rheumatoid Arthritis Antibodies Preferentially Bind Fibrinogen Citrullinated by Peptidylarginine Deiminase 4

Nathalie E. Blachère,[1] Salina Parveen,[2] Mayu O. Frank,[3] Brian D. Dill,[2] Henrik Molina,[2] and Dana E. Orange[4]

Objective. **Most patients with rheumatoid arthritis (RA) harbor antibodies to citrullinated autoantigens such as citrullinated fibrinogen. Two isoforms of peptidylarginine deiminase (PAD), PAD type 2 (PAD2) and PAD4, which catalyze citrullination with different substrate specificities, can be detected in the synovium of RA patients. This study was undertaken to determine whether RA antibodies preferentially bind PAD2- or PAD4-citrullinated fibrinogen.**

Methods. **RA patient and normal donor plasma specimens were tested for binding to PAD2- or PAD4-citrullinated fibrinogen, native fibrinogen, or citrullinated fibrinogen peptides in various dilutions by enzyme-linked immunosorbent assay (ELISA) and Western blotting. Bands corresponding to masses demonstrating RA antibody reactivity by Western blotting were excised and analyzed by mass spectrometry.**

Results. **At low antibody titers (1:40 and 1:100), there was no significant difference between RA antibody reactivity to PAD2- and PAD4-citrullinated fibrinogen. When plasma was further diluted to 1:250 and 1:1,000, RA patient plasma bound PAD4-citrullinated fibrinogen significantly more than PAD2-citrullinated fibrinogen, as measured by ELISA and Western blotting. An increased antibody titer was associated with increased avidity for both PAD2- and PAD4-citrullinated fibrinogen. Both enzymes hypercitrullinated fibrinogen, but PAD4 citrullinated arginines more intermittently, generating a mix of citrullinated and noncitrullinated arginines. Peptide ELISA and preadsorption assays confirmed that the region of intermittent citrullination accounts for the majority of RA antibody binding to the β-chain of citrullinated fibrinogen.**

Conclusion. **At high titers, RA antibodies preferentially bind fibrinogen modified by PAD4, because intermittent citrullination offers a more diverse assortment of citrullinated epitopes.**

The majority of patients with rheumatoid arthritis (RA) harbor autoantibodies to citrullinated isoforms of self proteins, called anti–citrullinated protein antibodies (ACPAs), which are highly specific for the disease (1). Citrullinated protein targets of ACPAs include filaggrin, type II collagen, α-enolase, vimentin, aggrecan, histone, and fibrinogen (2–4). Anti–citrullinated fibrinogen antibodies are more sensitive for RA (5) than are other ACPAs, such as antibodies that bind citrullinated type II collagen and α-enolase (2,4), with diagnostic performance similar to that of the clinical version of the ACPA assay, anti–cyclic citrullinated peptide 2 (anti–CCP-2), suggesting citrullinated fibrinogen may be particularly important in RA.

Proteins can become citrullinated as a result of enzymatic modification by peptidylarginine deiminase (PAD) enzymes, which catalyze conversion of the positively charged amino acid arginine to a neutral citrulline. Treatment with a pan-PAD inhibitor reduced the severity of arthritis and was associated with lower autoantibody production in an animal model of arthritis (6). It is hypothesized that PAD inhibitors may alleviate RA via prevention of further activation of the immune system by limiting autoantigen production. There are 5 PAD family members (PAD type 1 [PAD1], PAD2, PAD3, PAD4, and PAD6), each with unique tissue distribution. It is not known which of the PAD family members are most important for generating

Dr. Orange's work was supported by the Arthritis Foundation (Clinical to Research Transition Award), Rockefeller University (Pilot Award), and the NIH (Clinical and Translational Science Award UL1-TR-000043 from the National Center for Advancing Translational Sciences).

[1]Nathalie E. Blachère, PhD: Rockefeller University and Howard Hughes Medical Institute, New York, New York; [2]Salina Parveen, MS, Brian D. Dill, PhD, Henrik Molina, PhD: Rockefeller University, New York, New York; [3]Mayu O. Frank, NP: Rockefeller University and New York Genome Center, New York, New York; [4]Dana E. Orange, MD, MS: Rockefeller University, Hospital for Special Surgery, and New York Genome Center, New York, New York.

Address correspondence to Dana E. Orange, MD, MS, Rockefeller University, 1230 York Avenue, New York, NY 10065. E-mail: dorange@rockefeller.edu.

Submitted for publication June 10, 2016; accepted in revised form December 22, 2016.

the antigens that drive RA immune responses, and therefore, it is not known which PADs to target for this treatment approach to be most effective. PAD2 and PAD4 are expressed in immune cells and are overexpressed in RA synovium (7). PAD2 is broadly expressed in sites including skin, intestine, brain, muscle, and hematopoietic cells, while PAD4 expression is restricted to certain cell types, including neurons and neutrophils. PAD4 is unique among PAD family members, because it harbors a nuclear localization sequence and is required for NETosis (8–11).

Our group recently showed that neutrophils undergoing cell death, induced by either NETosis or necrosis, release both PAD2 and PAD4, and this leads to citrullination of extracellular fibrinogen (12). Surface plasmon resonance imaging of PAD2- and PAD4-citrullinated fibrinogen has demonstrated that the 2 isoforms citrullinate different arginine residues within fibrinogen (13), with PAD2 causing more extensive arginine citrullination than PAD4. Because RA-related autoantibody responses to citrullinated fibrin are closely restricted (14), we hypothesized that immunoreactivity to PAD2- and PAD4-citrullinated fibrinogen may differ. We therefore compared RA antibody levels to PAD2- and PAD4-citrullinated fibrinogen and observed that RA patient plasma harbors increased levels of antibodies to fibrinogen when it is citrullinated by PAD4. Mass spectrometry (MS)–based analysis of our samples revealed that although both enzymes heavily citrullinated arginines in a hot spot region between position 44 and position 74, PAD2 citrullinates more consistently, while PAD4 citrullinates intermittently, and this provides a more diverse collection of target citrullinated epitopes against which antibodies are produced.

PATIENTS AND METHODS

Patients and healthy subjects. Plasma samples were obtained from 12 patients with established anti-CCP antibody–positive RA who met the 2010 American College of Rheumatology (ACR)/European League Against Rheumatism (EULAR) classification criteria for RA (15). Plasma samples were also collected from healthy subjects who were matched with patients for sex and age within 5 years. The ethics review board of Rockefeller University Hospital approved this study, and all study subjects gave written informed consent.

Enzyme-linked immunosorbent assay (ELISA). PAD2 (item no. 10785; Cayman Chemical) or PAD4 (item no. 10500; Cayman Chemical) was autocitrullinated by incubating 10 μg/ml in 100 m*M* Tris buffer (Sigma-Aldrich), 10 m*M* $CaCl_2$, and 5 m*M* dithiothreitol (DTT) (Affymetrix) at 37°C overnight. Effective citrullination was verified using Citrulline-specific Probe (item no. 16172; Cayman Chemical). Microtiter plates (Nunc) were coated for 1 hour at room temperature with fibrinogen, PAD4-citrullinated fibrinogen (item no. 400076; Cayman Chemical), PAD2-citrullinated fibrinogen (item no. 18473; Cayman Chemical), citrullinated PAD4, citrullinated PAD2, or peptide antigens (synthesized by 9-fluorenylmethoxycarbonyl chemistry), at 5 μg/ml in 0.05*M* carbonate–bicarbonate buffer (pH 9.6). Plates were washed with 0.05% Tween 20 (Sigma-Aldrich) in phosphate buffered saline (PBS) (Cellgro), and blocked for 1 hour with 1% bovine serum albumin (BSA) in PBS. Plasma, diluted at various concentrations in 1% BSA/PBS, was added for 1 hour. Horseradish peroxidase (HRP)–conjugated goat anti-human IgG (Jackson ImmunoResearch) was added for detection. Bound antibodies were revealed using the chromogenic substrate 3,3′,5,5′-tetramethylbenzidine (Sigma-Aldrich), and the reaction was stopped with 2*M* H_2SO_4. Plates were read at optical density (OD) 450 nm.

Avidity was measured by adding various concentrations of sodium thiocyanate (Sigma-Aldrich) to ELISA plates. Avidity is presented as the avidity index, which was calculated by dividing the amount of residual antibodies bound to the antigen-coated plate by the amount of antibodies bound in the absence of a chaotropic agent.

Western blotting. Either PAD4-citrullinated fibrinogen or PAD2-citrullinated fibrinogen (1 μg per lane) was resolved by polyacrylamide gel electrophoresis (PAGE) and transferred to PVDF membranes (Millipore). The membranes were blocked in 5% nonfat milk in Tris buffered saline (TBS) containing 0.1% Tween 20 for 1 hour at room temperature. Membranes were probed with the following: monoclonal anti–citrullinated fibrinogen (1:1,000) (Cayman Chemical), monoclonal anti-PAD2 antibody (1:500) (catalog no. H00011240-M01; Abnova) (16), anti-PAD4 antibody (1:1,000) (ab128086; Abcam) (17), monoclonal antifibrinogen (1:500) (ab10066; Abcam), or RA patient plasma diluted 1:1,000 in 5% nonfat milk in TBS containing 0.1% Tween 20. Bound immunoglobulin was detected with HRP-labeled secondary antibodies (Life Technologies) and visualized using an enhanced chemiluminescence system (Western Lightning Plus-ECL, Enhanced Chemiluminescence Substrate; PerkinElmer).

For preadsorption assays, RA patient plasma samples, diluted 1:1,000 in TBS containing 0.1% Tween 20 and 5% nonfat milk, were preincubated with PAD2-citrullinated fibrinogen protein or peptide (10 μg/ml) for 1 hour at 37°C prior to being used to probe membranes for 2 hours at room temperature. The density of the bands was evaluated using ImageJ 1.46r software (National Institutes of Health).

Plasmin cleavage assay. PAD4-citrullinated fibrinogen (0.2 mg/ml) was incubated with 0.006 mg/ml plasmin (Sigma-Aldrich) in 20 m*M* Tris HCl, 2 m*M* $CaCl_2$, and 5 m*M* DTT for 1 hour at 37°C. One microgram of PAD4-citrullinated fibrinogen and 5 μg of plasmin-digested PAD4-citrullinated fibrinogen were resolved using 12% sodium dodecyl sulfate (SDS)–PAGE gels. Proteins were transferred to PVDF membranes and probed with RA patient plasma (1:1,000) as described above.

Liquid chromatography (LC)–MS. One microgram of each sample (unmodified, PAD2-modified, or PAD4-modified fibrinogen) was separated by SDS-PAGE and stained with Coomassie brilliant blue. Gel bands corresponding to masses demonstrating reactivity against patient antiplasma by Western blot analysis were excised for in-gel proteolytic digestion (18). In short, following reduction of cysteines with DTT and alkylation with iodoacetamide (Sigma-Aldrich), digestion was conducted with either trypsin (Promega) and Lys-C (Waco Chemicals) or chymotrypsin (Promega). Samples were processed and analyzed in triplicate to provide additional confidence regarding assignment. Following overnight incubation, peptides were extracted from gel pieces with acetonitrile, dried, and resuspended in 2%

acetonitrile/0.1% trifluoroacetic acid. Each sample was analyzed by nano–LC tandem MS (LC-MS/MS) (Dionex 3000 HPLC coupled to Q Exactive MS system; Thermo Scientific). Peptides were separated at 200 nl/minute using a gradient increasing from 5% to 45% acetonitrile/0.1% acid in 60 minutes. Peptides were loaded onto a Trap column prior to separation on a Packed Emitter C18 column (75 μm $\times$ 12 cm; 3-μm particles) (Nikkyo Technos Co., Ltd).

For data-dependent analysis of peptide modification identification, the mass spectrometer was operated in "preferred mode": fragmentation of up to 20 ions per cycle using an underfill ratio of 1%. For quantitation and specific site assignment of arginine citrullination in the identified hot spot (R44, R47, R53, R60, R72, and R74), parallel reaction monitoring (PRM) (19) was used for quantification, using parent and fragment ions for distinct modification sites. MS spectra (mass/charge [m/z] 300–1,400) were recorded at a resolution of 70,000 (automatic gain control [AGC] 5e5) and MS/MS spectra at 17,500 (AGC 1e5) with a lowest m/z of 100. Generated LC-MS/MS data were queried against the UniProt complete human proteome (March 2016) using the Mascot search engine, with carbamidomethylation of cysteine as a static modification and the following variable modifications: oxidation of methionine, acetylation of N-terminal protein, deamidation of asparagine and glutamine, and citrullination of arginine.

Identifications were filtered to include only precursor masses of $<$5 parts per million and highest peptide-spectrum matches ranking, and false discovery rates of $<$1% were controlled using a Percolator algorithm (20). Deamidation was included to allow consideration of de facto asparagine/glutamine deamidation and the isobaric citrullination modification. Up to 4 missed cleavages were allowed for the chymotrypsin searches, while up to 7 missed cleavages were allowed for the trypsin searches (because citrullination will lead to missed cleavage of modified arginines). For the trypsin-digested samples, peptides identified as citrullinated were required to contain a missed cleavage following a modified arginine. Skyline (an open-source document editor for creating and analyzing targeted proteomics experiments) (21) was used for quantitation of PRM data for the relative modification site comparison, by summing precursor peak areas. In the case of isobaric modification variants, the parent signal was distributed proportionally to the discriminating fragment ion areas. A spectral library generated from the Mascot searches was used to assign peak identity.

Statistical analysis. The unpaired *t*-test was used to compare ELISA-derived OD values between normal donor plasma and RA patient plasma. The paired *t*-test was used to compare ELISA-derived OD values for plasma from individual donors to PAD4-citrullinated fibrinogen and PAD2-citrullinated fibrinogen. Wilcoxon's matched pairs signed rank test was used to compare the normalized band intensities of Western blots. One-way analysis of variance and Tukey's test for multiple comparisons were used to evaluate statistical differences between 3 different titers in the avidity ELISA at a concentration of 3*N* sodium thiocyanate. *P* values less than 0.05 were considered significant. Statistical analysis was performed using GraphPad Prism software.

RESULTS

Higher levels of antibodies to PAD4-citrullinated fibrinogen than to PAD2-citrullinated fibrinogen in RA patient plasma, as measured by ELISA. We tested responses of normal donor and RA patient plasma to fibrinogen as well as PAD2- and PAD4-citrullinated fibrinogen. The characteristics of the RA patients are shown in the Supplementary Table (available on the *Arthritis & Rheumatology* web site at http://onlinelibrary.wiley.com/doi/10.1002/art.40035/abstract). Notable features of this cohort are that 100% of patients harbored high-titer CCP antibodies, and 66% of patients had rheumatoid nodules. Otherwise, the patients had varying disease durations, disease activity levels, and exposures to medications. As expected, at low dilutions, neither normal donors nor RA patients had antibodies to unreacted (native) plasma-derived fibrinogen, while antibody binding to both PAD2- and PAD4-citrullinated fibrinogen was significantly increased in RA patients (Figure 1A).

To determine the relative reactivity of RA patient plasma to PAD4-citrullinated fibrinogen versus PAD2-citrullinated fibrinogen, we tested a range of plasma dilutions. At high dilutions (1:250 and 1:1,000), binding to PAD4-citrullinated fibrinogen was significantly greater than that to PAD2-citrullinated fibrinogen, although binding was similar at low dilutions (1:40 and 1:100), likely due to assay saturation at low dilutions (Figure 1B). The ratio of plasma binding to PAD4- or PAD2-citrullinated fibrinogen in each patient was calculated as the OD of PAD4-citrullinated fibrinogen/OD of PAD2-citrullinated fibrinogen. The mean ratios of PAD4-citrullinated:PAD2-citrullinated fibrinogen at the 1:250 and 1:1,000 dilutions were 1.26 (95% confidence interval [95% CI] 1.18 – 1.35) and 1.39 (95% CI 1.24 – 1.53), respectively (Figure 1C). To test whether the increased recognition of PAD4-citrullinated fibrinogen was attributable to antibodies against PAD4 itself, we also measured reactivity against PAD2 and PAD4. We did not detect reactivity to PAD4 or PAD2 that was greater than reactivity to buffer alone at either 1:250 or 1:1,000 (Figure 1D).

Better binding of RA antibodies to PAD4-citrullinated fibrinogen than to PAD2-citrullinated fibrinogen on Western blotting. One limitation of using ELISA to measure RA antibody responses to citrullinated fibrinogen is that the relative importance of the 3 polypeptide chains (α, β, and γ) cannot be distinguished. To address this question, we resolved equal amounts of PAD4-citrullinated fibrinogen and PAD2-citrullinated fibrinogen in adjacent lanes on multiple Western blots and probed with monoclonal anti–citrullinated fibrinogen β-chain (fibrinogen β) antibody (see Supplementary Figure 1A, available on the *Arthritis & Rheumatology* web site at http://onlinelibrary.wiley.com/doi/10.1002/art.40035/abstract), PAD2 antibody (Supplementary Figure 1B), PAD4 antibody (Supplementary Figure 1C), and antifibrinogen antibody (Supplementary Figure 1D). A monoclonal anti–citrullinated fibrinogen antibody showed binding at the

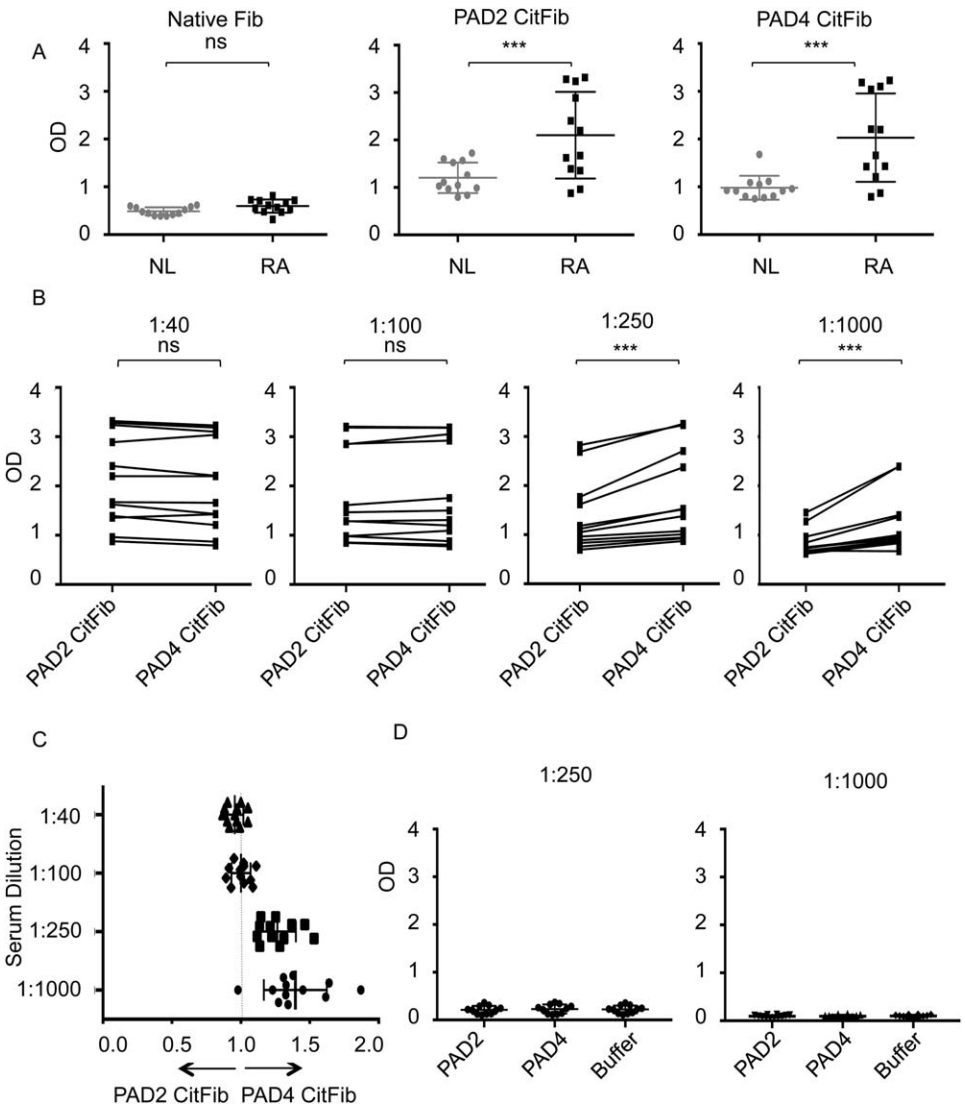

Figure 1. Rheumatoid arthritis (RA) patient plasma preferentially binds peptidylarginine deiminase type 4 (PAD4)–citrullinated fibrinogen (CitFib), as measured by enzyme-linked immunosorbent assay. **A,** Levels of RA and normal (NL) antibodies to unreacted (native) fibrinogen at 1:20 dilution, PAD2-citrullinated fibrinogen at 1:40 dilution, and PAD4-citrullinated fibrinogen at 1:40 dilution. **B,** Levels of antibodies to PAD4-citrullinated fibrinogen and PAD2-citrullinated fibrinogen, at various dilutions, in samples from individual RA patients. Lines connect the data points for each subject. **C,** Ratio of the binding of individual RA patient plasma samples from **B** to PAD4- or PAD2-citrullinated fibrinogen (calculated as the OD of PAD4-citrullinated fibrinogen/OD of PAD2-citrullinated fibrinogen) at various dilutions. **D,** Levels of antibodies to autocitrullinated PAD2 and PAD4, at various dilutions, in samples from individual RA patients. In **A, C,** and **D,** results are representative of 3 independent experiments performed. Symbols represent individual samples; bars show the mean ± SEM. *** = $P < 0.005$. NS = not significant.

predicted molecular weight of fibrinogen β (56 kd), while PAD2 and PAD4 antibodies showed binding at a molecular weight closer to 76 kd, consistent with their established molecular weights of 76 kd and 74 kd, respectively. A polyclonal antifibrinogen antibody recognized several bands, which is consistent with the various molecular weights of the 3 polypeptide chains of fibrinogen: α, β, and γ.

We next compared binding of RA patient plasma to PAD2- or PAD4-citrullinated fibrinogen on adjacent lanes of Western blots (Supplementary Figure 1E). At this dilution, the individual RA patient plasma samples most consistently recognized a band just above 52 kd, consistent with the known molecular weight of fibrinogen β (56 kd). Plasma from some patients also recognized a higher molecular weight band, just above 76 kd, which likely represents recognition of the α-chain of fibrinogen (fibrinogen α), given that there was no recognition of PAD2 or PAD4 itself on ELISA. The band intensity of the 56-kd region was

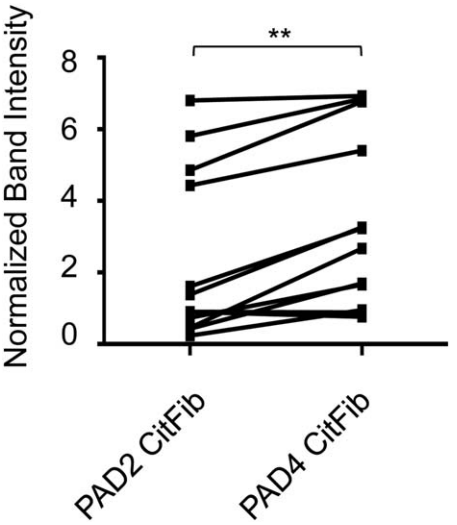

Figure 2. RA patient plasma preferentially recognizes PAD4-citrullinated fibrinogen, as determined by Western blotting. Comparison of the normalized band intensities of the 56-kd region of PAD2-citrullinated fibrinogen and PAD4-citrullinated fibrinogen, resolved by sodium dodecyl sulfate–polyacrylamide gel electrophoresis and probed with individual RA patient plasma samples diluted 1:1,000. The normalized band intensity represents the band intensity of RA patient plasma binding to PAD2- or PAD4-citrullinated fibrinogen divided by loading control antifibrinogen antibody. Lines connect the data points for each individual RA patient sample. Results are representative of 2 independent experiments performed. ** = $P < 0.01$. See Figure 1 for definitions.

quantitated using densitometric analysis. RA patient antibodies generated significantly more intense bands to PAD4-citrullinated fibrinogen compared to PAD2-citrullinated fibrinogen (Figure 2).

There was no difference in RA antibody avidity to PAD4- or PAD2-citrullinated fibrinogen. RA patient antibodies could display increased binding to PAD4-citrullinated fibrinogen on ELISA and Western blotting due to differences in avidity (increased cumulative binding affinity to PAD4-citrullinated fibrinogen) or specificity (more relevant epitopes on PAD4-citrullinated fibrinogen). To compare the avidity of RA antibodies, we compared the ELISA-derived OD values of RA patient plasma incubated with either PAD4- or PAD2-citrullinated fibrinogen and various concentrations of a chaotropic agent, sodium thiocyanate.

Three patient plasma samples that produced 56-kd bands but not 76-kd bands on Western blot were chosen for this assay to specifically measure binding avidity to citrullinated fibrinogen β, since it is more commonly recognized than citrullinated fibrinogen α in our studies of very-high-titer antibodies. Significantly more chaotropic agent was required to inhibit binding at increasing antibody titers, indicating a significant increase in avidity with increased titers (Figure 3). The avidity index and the antibody titer were correlated in both the PAD4- and PAD2-citrullinated fibrinogen samples. There was no difference, however, in the avidity of RA antibodies to PAD4- or PAD2-citrullinated fibrinogen at high titers (1:250 or 1:1,000), which produced a robust difference in both ELISA and Western blot results. Although it is possible that there was a subtle difference in avidity that was below the limit of detection in this assay, this potential difference is less significant than the difference conferred by increasing titers. There was a trend toward an increased avidity index for PAD2-citrullinated fibrinogen relative to PAD4-citrullinated fibrinogen at low titers (1:40), but this was not significant. For the 3 samples tested, differential avidity cannot explain the increased RA antibody binding of PAD4-citrullinated fibrinogen.

More intermittent citrullination at hot spot region of fibrinogen by PAD4, as measured by MS. It is possible that the difference in RA antibody recognition of PAD2- and PAD4-citrullinated fibrinogen is due to a difference in the level of citrullination in the samples. To quantify the extent of citrullination of either noncitrullinated, PAD2-citrullinated, or PAD4-citrullinated fibrinogen, we performed bottom-up MS of the 56-kd band (fibrinogen β) to identify and quantify modified versus unmodified peptides. Fibrinogen β was chosen for this quantitative analysis, because RA patient plasma diluted 1:1,000 bound fibrinogen β more frequently than fibrinogen α. Distal to the signal peptide, starting at position 31, protein sequence coverage was nearly complete (98%). This coverage accounted for all arginines. We identified a "hot spot" of arginine citrullination at positions R44, R47, R53, R60, R72, and R74

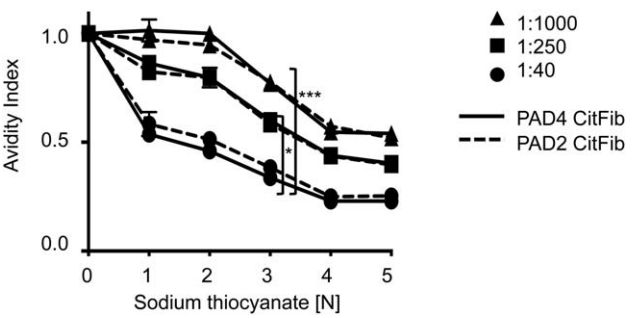

Figure 3. The avidity of RA antibodies to PAD4-citrullinated fibrinogen and to PAD2-citrullinated fibrinogen is not different at high titers. Avidity was measured by adding various concentrations of sodium thiocyanate. The avidity index represents the OD of RA patient plasma for a given concentration of sodium thiocyanate divided by the OD without sodium thiocyanate. Data are from a representative RA patient plasma sample of 3 samples tested. * = $P < 0.05$; *** = $P < 0.001$. See Figure 1 for definitions.

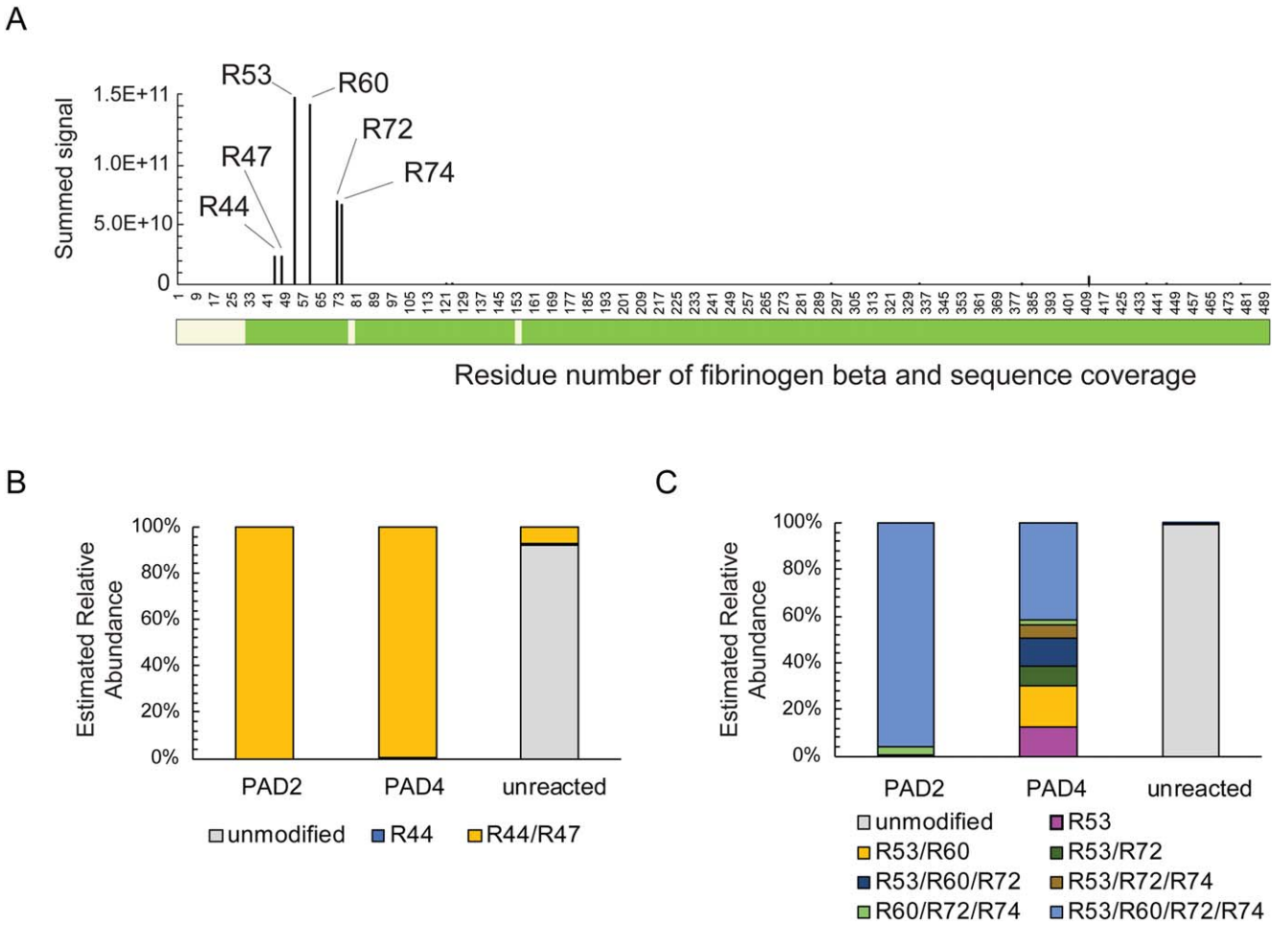

Figure 4. Fibrinogen β-chain (fibrinogen β) arginine sites 44–74 are a hot spot of citrullination that are uniformly modified by peptidylarginine deiminase type 2 (PAD2) and intermittently modified by PAD4. Unmodified, PAD2-citrullinated, or PAD4-citrullinated fibrinogen was enzymatically digested and analyzed by mass spectrometry. **A,** Summed signal (PAD2 and PAD4) of peptides containing a citrullinated arginine, plotted as a function of the amino acid residue number for fibrinogen β. The green bars depict the residues covered based on peptides with a false discovery rate of $<1\%$. **B** and **C,** Relative abundance of identified peptide signals carrying modifications at R44 and R47 (**B**) and R53, R60, R72, and R74 (**C**) in PAD2-citrullinated, PAD4-citrullinated, and unreacted (control) fibrinogen.

in both PAD2- and PAD4-modified fibrinogen β (Figure 4A). At these sites, citrullination was strikingly more abundant than that at other downstream citrullination sites.

The citrullination hot spot region between positions R44 and R74 was analyzed in depth to identify differences in citrullination between PAD2- and PAD4-modified samples. Both PAD2 and PAD4 citrullinated R44 and R47 fully ($>99\%$) (Figure 4B). Interestingly, residues at these positions were also citrullinated, but at a lower level (8%), in unreacted (native) fibrinogen samples. Although PAD2 treatment resulted in 95% citrullination of all 4 remaining hot spot residues (R53, R60, R72, and R74), PAD4 treatment resulted in complete citrullination of all 4 residues in only 42% of peptides identified (Figure 4C). In the majority of peptides, R53, R60, R72, and R74 were citrullinated intermittently. The next most commonly identified combination of PAD4-citrullinated arginines was at positions R53/R60, followed by R53 only, and R53/R60/R72.

In addition to this hot spot region between positions R44 and R74, citrullination was detected at low levels at several sites in the C-terminal region of the fibrinogen β protein. Although the initial analysis detected putative sites of low-level citrullination throughout the fibrinogen β protein, this low level of citrullination can be difficult to discriminate from artifactual deamidation of asparagine and glutamine, because these modifications are isobaric. These sites were manually validated to confirm that fragmentation spectra coverage could differentiate from any adjacent

Table 1. Mass spectrometry–derived signal of PAD2- and PAD4-modified fibrinogen at selected citrullination sites*

Arginine site	PAD2	PAD4
44	1.44×10^{10}	9.39×10^{9}
47	1.44×10^{10}	9.39×10^{9}
53	8.12×10^{10}	7.59×10^{10}
60	8.42×10^{10}	6.65×10^{10}
72	4.55×10^{10}	2.41×10^{10}
74	4.55×10^{10}	2.16×10^{10}
334	0.00	2.76×10^{8}
436	1.40×10^{8}	1.11×10^{8}
445	7.78×10^{7}	8.39×10^{7}
478	0.00	2.22×10^{7}

* Data represent the summed signal from parallel reaction monitoring–based quantification of peptides modified at the indicated citrullinated residues. Quantified citrullinated sites were derived from modified peptides, which were filtered by requiring a missed trypsin cleavage and detection in at least 2 of 3 technical replicates. PAD2 = peptidylarginine deiminase type 2.

asparagine or glutamine residues. A list of validated citrullination sites and their relative quantitation by PRM are shown in Table 1. Taken together, these data indicate that although both PAD2 and PAD4 hypercitrullinate a hot spot region between R44 and R74 on fibrinogen β, PAD4-mediated citrullination is more intermittent at residues R53, R60, R72, and R74.

Better binding of RA antibodies to PAD4-citrullinated fibrinogen hot spot region due to a broader array of epitopes. To determine whether the preferential binding of PAD4-citrullinated fibrinogen was due to recognition of partially citrullinated peptides in the hot spot region (spanning positions 44 to 74) or peptides citrullinated by PAD4 only (positions 334 and 478), we performed an ELISA to compare RA and normal antibody responses to citrullinated peptides. Citrullinated filaggrin peptide 1 (cfc-1) was used as a positive control in this experiment, and cfc-0 (the noncitrullinated isoform) was used as a negative control. Antibodies in half of the RA patient samples tested recognized the positive control peptide cfc-1, while none of these antibodies recognized the negative control peptide cfc-0 (Figure 5A).

We did not identify a single citrullinated fibrinogen β peptide that was consistently more immunogenic when it was only partially citrullinated. Instead, there was a diverse array of peptide recognition. This variability in RA antibody responses to various citrullinated isoforms of the same peptide region is reminiscent of the original article mapping epitopes of citrullinated filaggrin (22). The clinically useful tests for antibodies to citrullinated filaggrin peptides include an array of peptides derived from filaggrin spanning positions 306 to 324. This region includes 5 arginine residues, and while only 36% of RA antibodies bind the peptide when the first arginine residue is citrullinated, the sensitivity of the assay is improved considerably to 76% when it includes a mix of 9 peptides spanning this same region but with different citrullination sites (23). Because PAD4 variably citrullinates arginines in the hot spot region, it stands to reason that the improved RA antibody recognition of PAD4-citrullinated fibrinogen indicates that RA antibodies bind an assortment of citrullinated epitopes, and that citrullination by PAD4 results in a broader array of potential target epitopes.

To confirm that the increased binding of plasma RA antibodies to PAD4-citrullinated fibrinogen was due to the availability of epitopes that are not present in PAD2-citrullinated fibrinogen, we preadsorbed RA patient plasma with PAD2-citrullinated fibrinogen at various concentrations and tested whether there was a remaining antibody capable of binding PAD4-citrullinated fibrinogen. Preadsorption with increasing concentrations of PAD2-citrullinated fibrinogen led to a sharp decrease in recognition of PAD2-citrullinated fibrinogen but relatively preserved binding of PAD4-citrullinated fibrinogen (Figure 5B). Although RA patient antibodies bound both PAD2- and PAD4-citrullinated fibrinogen, this result establishes that PAD4-citrullinated fibrinogen includes additional epitopes that can be recognized by RA patient plasma.

To compare the relative importance of the N-terminal hot spot region and the C-terminal citrullination sites (R334 and R478), we treated PAD4-citrullinated fibrinogen with plasmin, which cleaves fibrinogen β at positions 152 and 163. This results in the generation of 2 main fibrinogen β fragments (23). The C-terminal, 38-kd fragment D spans residues 164–491 and therefore includes the PAD4-specific, low-abundance citrullination sites R334 and R478. The smaller N-terminal (8 kd), fragment E spans positions 30–153, which includes the hot spot region of citrullination. Citrullinated fibrinogen was incubated with plasmin under conditions sufficient to cause partial digestion of the protein and was resolved by SDS-PAGE. A positive control polyclonal anti–fibrinogen β antibody detected intact fibrinogen β (56 kd) and the β-chain fragment D (38 kd) but did not detect the β-chain fragment E (Figure 5C), even when increasing the amount 5-fold and detecting this fragment at its expected molecular weight of 8 kd by Coomassie brilliant blue staining (see Supplementary Figure 2, available on the *Arthritis & Rheumatology* web site at http://onlinelibrary.wiley.com/doi/10.1002/art.40035/abstract).

Loading an increased amount of cleaved fibrinogen revealed the presence of heavy-chain antibodies at 52 kd (fibrinogen was purified from human plasma). All RA antibodies tested in this manner bound intact fibrinogen more than fragment D. The relative band intensity of RA

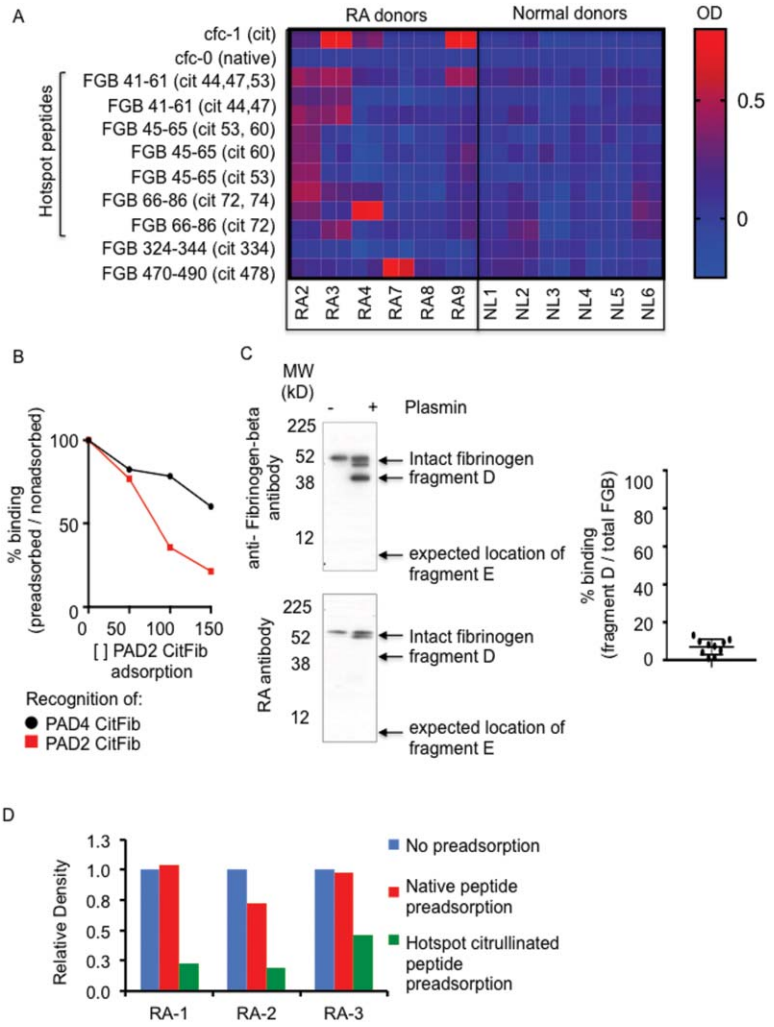

Figure 5. Rheumatoid arthritis antibodies preferentially bind PAD4-citrullinated fibrinogen (CitFib) because it contains a broader array of citrullinated epitopes. **A,** Enzyme-linked immunosorbent assay–derived OD values of RA and normal antibodies to citrullinated peptides at low titers (1:40). Data represent test peptide minus irrelevant β-galactosidase peptide. Technical duplicates are presented. **B,** Band intensity of PAD2- or PAD4-citrullinated fibrinogen on Western blots of RA patient plasma preadsorbed with increasing concentrations of PAD2-citrullinated fibrinogen. Results are representative of 3 independent experiments performed. **C,** Left, Western blots of citrullinated fibrinogen or plasmin-cleaved citrullinated fibrinogen, probed with polyclonal antifibrinogen antibody (top) and RA patient plasma (bottom). Results are representative of 3 independent experiments performed. Right, Summary of Western blot results. Symbols represent individual samples; bars show the mean ± SEM. Data represent the relative band intensity of fragment D divided by the relative band intensity of total fibrinogen β (FGB) in samples from 10 RA patients. **D,** Band intensity of citrullinated fibrinogen β probed with RA patient plasma samples preadsorbed with native peptides or citrullinated peptides from the hot spot region of fibrinogen peptides. Native fibrinogen peptides include 34–54, 41–61, 45–65, 66–86, and 285–305. cfc-1 = citrullinated filaggrin peptide 1; cfc-0 = noncitrullinated filaggrin peptide 1 (see Figure 1 for other definitions).

antibody recognition of fragment D relative to intact fibrinogen ranged from 1% to 13% (Figure 5C). The consistently weaker recognition of fragment D, relative to intact fibrinogen, indicated that RA antibodies likely bind to the N-terminal region, which spans residues 31 to 153. It should be noted that plasmin cleavage could have directly disrupted an important site of antibody recognition; however, there is only 1 arginine residue in proximity to a plasmin cleavage site (R158), and careful re-analysis of MS data failed to detect modification of this arginine in our PAD-modified fibrinogen samples.

To test whether citrullinated peptides from the hot spot region encompass the critical antibody recognition sites, we compared the effect of preadsorbing RA patient plasma with either native or citrullinated isoforms of peptides spanning sites 41–77. Preadsorption of 3 RA patient plasma samples with citrullinated hot spot peptide pools decreased recognition of fibrinogen β by 77%, 53%,

and 80%, while preadsorption with native peptide pools decreased recognition by 0% to 20% (Figure 5D). We therefore conclude that the key site of RA antibody recognition of citrullinated fibrinogen resides in the hot spot region spanning R44 to R74. Taken together, these data demonstrate that RA antibodies bind PAD4-citrullinated fibrinogen more than PAD2-citrullinated fibrinogen, because intermittent citrullination of the hot spot region offers a more diverse assortment of citrullinated epitopes.

DISCUSSION

High-titer CCP ("high-positive ACPA") contributes 3 points to the 2010 ACR/EULAR classification criteria score for RA (15). According to these criteria, "high-positive" refers to values that are >3 times the upper limit of normal (ULN). Because few commercially available assays extend titers beyond 10 times the ULN, relatively little is known about very-high-titer CCP antibodies. The likelihood of undifferentiated arthritis progressing to persistent arthritis further increases in patients with very-high-titer antibodies (>10 times the ULN) relative to those with high-titer antibodies (4–10 times the ULN) (24), suggesting that there may also be a clinically important distinction between high-titer and very-high-titer CCP antibodies. Considering that very-high-titer antibodies are also very-high-avidity antibodies, it is conceivable that they play a more important role in immune targeting and merit further exploration. In this study, we demonstrated that at very high titers, RA antibodies demonstrate preferential binding of PAD4-citrullinated fibrinogen compared to PAD2-citrullinated fibrinogen. Bearing in mind the broad repertoire of citrullinated antigens targeted by RA antibodies, one might have predicted that decreased antibody binding would be attributable to less efficient citrullination in the PAD2-citrullinated fibrinogen samples, but MS analysis of our samples demonstrated less efficient citrullination in PAD4-citrullinated fibrinogen.

An important limitation of this study is that it demonstrates antibody binding to citrullinated fibrinogen generated in vitro, and there may be differences in the activity of PAD2 and PAD4 in vivo. The citrullinated fibrinogen used in this study was generated by adding either PAD2 or PAD4 in buffer containing 10 m*M* $CaCl_2$ and incubated overnight at 37°C (according to the instructions of the manufacturer), which likely represents a higher calcium concentration and longer duration of exposure than occurs in vivo. Interestingly, despite the use of conditions that were optimized to maximize citrullination rather than model conditions in vivo, the validated citrullination sites detected were restricted to 2 domains in the fibrinogen β protein: the N-terminal central domain and the C-terminal globular domain. We could not confirm citrullination at arginine sites in the coiled-coil region.

Although the reaction conditions for citrullinating fibrinogen used in these assays make it difficult to conclude that PAD4 plays a more important role in generating autoantigen targets of RA antibodies, it does not detract from the observation that RA antibodies distinguish fibrinogen β with subtle differences in citrullination profiles. In support of the in vivo relevance of the citrullination hot spot identified here, citrullinated fibrinogen β epitopes derived from the hot spot region have been identified in RA synovial tissue (25) and synovial fluid (26) as well as circulating RA immune complexes (27).

In summary, the current study demonstrates that very-high-titer antibodies bind PAD4-citrullinated fibrinogen more than PAD2-citrullinated fibrinogen, and that this could not be attributed to increased citrullination in PAD4-reacted samples. Instead, while both PAD2 and PAD4 heavily citrullinate a hot spot region between R44 and R74, the PAD4 citrullination profile is more intermittent. Other studies of ACPAs have largely used PAD2-modified target proteins or peptides with citrullination of all possible arginines. Our study indicates that high-titer RA antibodies preferentially bind PAD4-citrullinated fibrinogen, because it produces an assortment of citrullinated isoforms from a hot spot of fibrinogen β citrullination. In the future, it would be useful to compare the relative binding of high-titer RA antibodies to other known citrullinated target antigens modified by PAD2 or PAD4, to evaluate the generalizability of this result.

ACKNOWLEDGMENTS

We are grateful to the study participants and the research staff at Rockefeller University Hospital for facilitating the studies. We thank Michael Moore and Sergio Schwartzman for their helpful discussions and review of the article.

AUTHOR CONTRIBUTIONS

All authors were involved in drafting the article or revising it critically for important intellectual content, and all authors approved the final version to be published. Dr. Orange had full access to all of the data in the study and takes responsibility for the integrity of the data and the accuracy of the data analysis.

Study conception and design. Orange.

Acquisition of data. Blachère, Parveen, Dill, Molina, Orange.

Analysis and interpretation of data. Blachère, Frank, Dill, Molina.

REFERENCES

1. Van Venrooij WJ, Vossenaar ER, Zendman AJ. Anti-CCP antibodies: the new rheumatoid factor in the serology of rheumatoid arthritis. Autoimmun Rev 2004;3 Suppl 1:S17–9.
2. Snir O, Widhe M, von Spee C, Lindberg J, Padyukov L, Lundberg K, et al. Multiple antibody reactivities to citrullinated

antigens in sera from patients with rheumatoid arthritis: association with HLA-DRB1 alleles. Ann Rheum Dis 2009;68:736–43.
3. Ioan-Facsinay A, Willemze A, Robinson DB, Peschken CA, Markland J, van der Woude D, et al. Marked differences in fine specificity and isotype usage of the anti–citrullinated protein antibody in health and disease. Arthritis Rheum 2008;58:3000–8.
4. Snir O, Widhe M, Hermansson M, von Spee C, Lindberg J, Hensen S, et al. Antibodies to several citrullinated antigens are enriched in the joints of rheumatoid arthritis patients. Arthritis Rheum 2010;62:44–52.
5. Vander Cruyssen B, Cantaert T, Nogueira L, Clavel C, de Rycke L, Dendoven A, et al. Diagnostic value of anti-human citrullinated fibrinogen ELISA and comparison with four other anti-citrullinated protein assays. Arthritis Res Ther 2006;8:R122.
6. Willis VC, Gizinski AM, Banda NK, Causey CP, Knuckley B, Cordova KN, et al. N-α-benzoyl-N5-(2-chloro-1-iminoethyl)-L-ornithine amide, a protein arginine deiminase inhibitor, reduces the severity of murine collagen-induced arthritis. J Immunol 2011;186:4396–404.
7. Foulquier C, Sebbag M, Clavel C, Chapuy-Regaud S, Al Badine R, Méchin MC, et al. Peptidyl arginine deiminase type 2 (PAD-2) and PAD-4 but not PAD-1, PAD-3, and PAD-6 are expressed in rheumatoid arthritis synovium in close association with tissue inflammation. Arthritis Rheum 2007;56:3541–53.
8. Khandpur R, Carmona-Rivera C, Vivekanandan-Giri A, Gizinski A, Yalavarthi S, Knight JS, et al. NETs are a source of citrullinated autoantigens and stimulate inflammatory responses in rheumatoid arthritis. Sci Transl Med 2013;5:178ra40.
9. Spengler J, Lugonja B, Ytterberg AJ, Zubarev RA, Creese AJ, Pearson MJ, et al. Release of active peptidyl arginine deiminases by neutrophils can explain production of extracellular citrullinated autoantigens in rheumatoid arthritis synovial fluid. Arthritis Rheumatol 2015;67:3135–45.
10. Li P, Li M, Lindberg MR, Kennett MJ, Xiong N, Wang Y. PAD4 is essential for antibacterial innate immunity mediated by neutrophil extracellular traps. J Exp Med 2010;207:1853–62.
11. Jones JE, Causey CP, Knuckley B, Slack-Noyes JL, Thompson PR. Protein arginine deiminase 4 (PAD4): current understanding and future therapeutic potential. Curr Opin Drug Discov Devel 2009;12:616–27.
12. Blachère NE, Parveen S, Fak J, Frank MO, Orange DE. Inflammatory but not apoptotic death of granulocytes citrullinates fibrinogen. Arthritis Res Ther 2015;17:369.
13. Raijmakers R, van Beers JJ, El-Azzouny M, Visser NF, Božič B, Pruijn GJ, et al. Elevated levels of fibrinogen-derived endogenous citrullinated peptides in synovial fluid of rheumatoid arthritis patients. Arthritis Res Ther 2012;14:R114.
14. Iobagiu C, Magyar A, Nogueira L, Cornillet M, Sebbag M, Arnaud J, et al. The antigen specificity of the rheumatoid arthritis-associated ACPA directed to citrullinated fibrin is very closely restricted. J Autoimmun 2011;37:263–72.
15. Aletaha D, Neogi T, Silman AJ, Funovits J, Felson DT, Bingham CO III, et al. 2010 rheumatoid arthritis classification criteria: an American College of Rheumatology/European League Against Rheumatism collaborative initiative. Arthritis Rheum 2010;62:2569–81.
16. Chumanevich AA, Causey CP, Knuckley BA, Jones JE, Poudyal D, Chumanevich AP, et al. Suppression of colitis in mice by Cl-amidine: a novel peptidylarginine deiminase inhibitor. Am J Physiol Gastrointest Liver Physiol 2011;300:G929–38.
17. Horikoshi N, Tachiwana H, Saito K, Osakabe A, Sato M, Yamada M, et al. Structural and biochemical analyses of the human PAD4 variant encoded by a functional haplotype gene. Acta Crystallogr D Biol Crystallogr 2011;67:112–8.
18. Shevchenko A, Wilm M, Vorm O, Mann M. Mass spectrometric sequencing of proteins silver-stained polyacrylamide gels. Anal Chem 1996;68:850–8.
19. Peterson AC, Russell JD, Bailey DJ, Westphall MS, Coon JJ. Parallel reaction monitoring for high resolution and high mass accuracy quantitative, targeted proteomics. Mol Cell Proteomics 2012;11:1475–88.
20. Käll L, Canterbury JD, Weston J, Noble WS, MacCoss MJ. Semi-supervised learning for peptide identification from shotgun proteomics datasets. Nat Methods 2007;4:923–5.
21. MacLean B, Tomazela DM, Shulman N, Chambers M, Finney GL, Frewen B, et al. Skyline: an open source document editor for creating and analyzing targeted proteomics experiments. Bioinformatics 2010;26:966–8.
22. Schellekens GA, de Jong BA, van den Hoogen FH, van de Putte LB, van Venrooij WJ. Citrulline is an essential constituent of antigenic determinants recognized by rheumatoid arthritis-specific autoantibodies. J Clin Invest 1998;101:273–81.
23. Budzynski AZ, Marder VJ, Shainoff JR. Structure of plasmic degradation products of human fibrinogen. Fibrinopeptide and polypeptide chain analysis. J Biol Chem 1974;249:2294–302.
24. Mjaavatten MD, van der Heijde D, Uhlig T, Haugen AJ, Nygaard H, Sidenvall G, et al. The likelihood of persistent arthritis increases with the level of anti-citrullinated peptide antibody and immunoglobulin M rheumatoid factor: a longitudinal study of 376 patients with very early undifferentiated arthritis. Arthritis Res Ther 2010;12:R76.
25. Hermansson M, Artemenko K, Ossipova E, Eriksson H, Lengqvist J, Makrygiannakis D, et al. MS analysis of rheumatoid arthritic synovial tissue identifies specific citrullination sites on fibrinogen. Proteomics Clin Appl 2010;4:511–8.
26. Wang F, Chen FF, Gao WB, Wang HY, Zhao NW, Xu M, et al. Identification of citrullinated peptides in the synovial fluid of patients with rheumatoid arthritis using LC-MALDI-TOF/TOF. Clin Rheumatol 2016;35:2185–94.
27. Zhao X, Okeke NL, Sharpe O, Batliwalla FM, Lee AT, Ho PP, et al. Circulating immune complexes contain citrullinated fibrinogen in rheumatoid arthritis. Arthritis Res Ther 2008;10:R94.

ARTHRITIS & RHEUMATOLOGY
Vol. 69, No. 5, May 2017, pp 996–1008
DOI 10.1002/art.40001

Targeting the D Series Resolvin Receptor System for the Treatment of Osteoarthritis Pain

Junting Huang, James J. Burston, Li Li, Sadaf Ashraf, Paul I. Mapp, Andrew J. Bennett, Srinivasarao Ravipati, Petros Pousinis, David A. Barrett, Brigitte E. Scammell, and Victoria Chapman

Objective. **Pain is a major symptom of osteoarthritis (OA); currently available analgesics either do not provide adequate pain relief or are associated with serious side effects. The aim of this study was to investigate the therapeutic potential of targeting the resolvin receptor system to modify OA pain and pathology.**

Methods. **Gene expression of 2 resolvin receptors (ALX and ChemR23) was quantified in synovium and medial tibial plateau specimens obtained from patients with OA at the time of joint replacement surgery. Two models of OA joint pain were used for the mechanistic studies. Gene expression in the joint and central nervous system was quantified. The effects of exogenous administration of the D series resolvin precursor 17(R)-hydroxy-docosahexaenoic acid (17[R]-HDoHE) on pain behavior, joint pathology, spinal microglia, and astroglyosis were quantified. Plasma levels of relevant lipids, resolvin D2, 17(R)-HDoHE, and arachidonic acid, were determined in rats, using liquid chromatography tandem mass spectrometry.**

Results. **There was a positive correlation between resolvin receptor and interleukin-6 (IL-6) expression in human OA synovial and medial tibial plateau tissue. In rats, synovial expression of ALX was positively correlated with expression of IL-1β, tumor necrosis factor, and cyclooxygenase 2. Treatment with 17(R)-HDoHE reversed established pain behavior (but not joint pathology) in 2 models of OA pain. This was associated with a significant elevation in the plasma levels of resolvin D2 and a significant reduction in astrogliosis in the spinal cord in the monosodium iodoacetate–induced OA rat model.**

Conclusion. **Our preclinical data demonstrate the robust analgesic effects of activation of the D series resolvin pathways in 2 different animal models of OA. Our data support a predominant central mechanism of action in clinically relevant models of OA pain.**

Osteoarthritis (OA) is a highly prevalent degenerative joint disorder characterized by loss of cartilage, subchondral bone remodeling, and synovial inflammation (1,2). Pain is the predominant symptom of OA, which limits movement and causes disability (3). OA pain is significantly associated with synovial inflammation and changes in the subchondral bone (4), and evidence of central sensitization and the spread of pain has been reported (5). Existing drugs are poorly effective and/or are associated with adverse side effects. Most often, total joint replacement is the only successful therapeutic treatment (6).

Resolvins are endogenous specialized pro-resolution lipid mediators derived from docosahexaenoic acid (DHA [D series resolvins]) and eicosapentaenoic acid (EPA [E series resolvins]), which exhibit potent antiinflammatory and pro-resolution properties (7,8). Four resolvin receptors have been identified: ALX (also known as *N*-formyl peptide receptor 2), G protein–coupled receptor 32 (GPR32) (9–11), chemokine-like receptor 1 (ChemR23) (12), and leukotriene B_4 receptor (BLT-1) (13). Resolvin D1 (RvD1) binds to and activates both ALX and GPR32 in human tissue, while in murine tissue the actions of RvD1 are mediated by ALX (14). ChemR23 and BLT-1 are the receptors through which RvE1 and RvE2 act (14).

In the context of their therapeutic potential for pain management, RvE1 and RvD1 (administered

Supported by Arthritis Research UK (grant 18769).

Junting Huang, PhD (current address: University of Calgary, Calgary, Alberta, Canada), James J. Burston, PhD, Li Li, PhD, Sadaf Ashraf, PhD, Paul I. Mapp, PhD, Andrew J. Bennett, PhD, Srinivasarao Ravipati, PhD, Petros Pousinis, PhD, David A. Barrett, PhD, Brigitte E. Scammell, DM, FRCS(Orth), Victoria Chapman, PhD: University of Nottingham, Nottingham, UK.

Address correspondence to James J. Burston, PhD, Cardiff University School of Medicine, College of Biomedical and Life Sciences, Tenovus Building, Cardiff CF14 4NX, UK. E-mail: BurstonJ3@cardiff.ac.uk; or to Victoria Chapman, PhD, Arthritis Research UK Pain Centre and School of Life Sciences, The University of Nottingham, Queen's Medical Centre, Nottingham NG7 2UH, UK. E-mail: victoria.chapman@nottingham.ac.uk.

Submitted for publication March 8, 2016; accepted in revised form November 10, 2016.

exogenously) attenuate pain behavior in models of acute inflammatory pain (15,16) and a model of chronic adjuvant-induced arthritis (17). RvD1 inhibits the activity of some temperature-sensitive transient receptor potential (TRP) ion channels expressed by the primary afferent sensory fibers TRP ankyrin 1 (TRPA-1) (18) and TRP vanilloid channel 3 (TRPV-3) (19), but not TRPV-1. Due to the rapid degradation of resolvins, local (intraplantar or intrathecal) routes of administration have been studied. Spinal administration of RvE1 reduced capsaicin- and tumor necrosis factor (TNF)–induced spontaneous pain and hypersensitivity in mice and partially attenuated pain behavior in models of neuropathic pain (20). RvD1 and RvE1 can modulate TRPV-1 and TNF responses in the spinal cord (20–22) and inhibit phosphorylation of *N*-methyl-D-aspartate receptors and cytokine expression in the spinal cord in the setting of chronic pancreatitis-induced pain (23). Thus, both peripheral and spinal mechanisms of action contribute to the inhibitory effects of the resolvins in models of inflammatory and neuropathic pain, with predominant peripheral antiinflammatory mechanisms including inhibition of neutrophil infiltration, edema, and proinflammatory cytokine expression (21).

The therapeutic potential of exogenously administered RvD1 and RvE1 may be limited by instability and short durations of action. Treatment with precursors of the active molecules offers an alternative longer-lasting and beneficial approach (17), as does the development of chemically and metabolically stable analogs such as 17R-hydroxy-19-para-fluorophenoxy-resolvin D1 (24). Inhibitory effects of a precursor of RvD1, 17(R)-hydroxy-docosahexaenoic acid (17[R]-HDoHE), on mechanical hyperalgesia in a model of inflammatory joint pain have been reported and associated with reductions in hind paw levels of TNF and interleukin-1β (IL-1β) and spinal cord expression of NF-κB and cyclooxygenase 2 (COX-2) (17). These data suggest that exogenous augmentation of resolvin precursors has therapeutic potential for the treatment of pain states that are underpinned by peripheral and/or central sensitization mechanisms.

The aim of the current study was to provide new clinical and preclinical evidence for the therapeutic potential of the D series resolvin pathway for the treatment of OA pain. Using 2 different clinically relevant models of OA joint pain, we performed mechanistic studies to interrogate the contribution of peripheral joint versus spinal cord sites of action of this novel class of analgesics.

PATIENTS AND METHODS

Subjects. Research using clinical samples was approved by generic ethics committees for the Nottingham University Hospitals NHS Trust Biobank (reference no. RSCH 488). Human synovial tissue and bone from the medial tibial plateau were obtained from 15 patients who underwent total knee replacement (TKR) surgery for OA pain. These tissues were selected on the basis of established associations between inflammation, bone remodeling, and pain (1,2). Fresh tissue samples were collected from the surgical team and snap-frozen and stored in a −80°C freezer at the Biobank, City Hospital, University of Nottingham. Fresh synovial tissue specimens (n = 15) and medial tibial plateau specimens (n = 14) were used to quantify gene expression.

Animals and model induction. Animal experiments were approved by the Nottingham University ethics committee, and all procedures were approved by the UK Home Office in accordance with the Animals (Scientific Procedures) Act 1986 and conform to the guidelines of the International Association for the Study of Pain. Adult male Sprague-Dawley rats (n = 166) were used (Charles River). All procedures and testing were performed in a blinded manner. The model of monosodium iodoacetate (MIA)–induced OA pain was generated as previously described (25). The medial meniscal transection (MNX) induction model of OA pain was based on previously described methods (26) (see also Supplementary Methods, available on the *Arthritis & Rheumatology* web site at http://onlinelibrary.wiley.com/doi/10.1002/art.40001/abstract).

Pharmacologic interventions and assessment of pain behavior. Weight-bearing asymmetry and hind paw mechanical withdrawal thresholds were determined using a Linton incapacitance tester and von Frey monofilaments (Linton Instrumentation; bending force 1–26*g*, respectively) as previously described (27) (see Supplementary Methods). An RvD1 precursor, 17(R)-HDoHE, also known as 17(R)-HDHA, was purchased from Cayman Chemical. This precursor gives rise to the production of 17R RvD1 and 17R RvD2, epimers of endogenous RvD1, RvD2, RvD3, and RvD4 (synthesized from 17[S]-HDoHE), and aspirin-triggered epimers (17R forms), when COX-2 is acetylated (14).

The 17(R)-HDoHE (stock solution 100 μg/ml in ethanol) was diluted in normal sterile saline to provide a concentration of 1 ng/μl. The vehicle solution consisted of 1% ethanol solution in 99% saline. A series of different pharmacologic studies were performed using 300 ng of 17(R)-HDoHE in 300 μl saline administered intraperitoneally. Study 1 determined the effects of a single injection of 17(R)-HDoHE on pain behavior on day 14 after induction of the model. Study 2 determined the effects of repeated administration of 17(R)-HDoHE (300 ng in 300 μl saline, every other day from day 14 until day 28 after induction of the model) on pain behavior in the MIA-induced OA pain model and the MNX induction model of OA pain. Study 3 determined the effects of discontinuous administration of 17(R)-HDoHE (300 ng in 300 μl saline, from day 14 to day 22 after induction of the model) on pain behavior, quantified until day 35 after induction of the model. All of the drug intervention studies were conducted in a blinded manner.

Quantitative real-time polymerase chain reaction. At the end of the behavioral studies, the rats were killed via an overdose of sodium pentobarbital, and fresh-frozen spinal cords and synovial tissue were collected and stored at −80°C. Tissues were homogenized in ice-cold TRI Reagent to extract total RNA from the samples, as previously described (26). Human OA synovial tissue collected at the time of TKR surgery was homogenized in cold TRI Reagent, and RNA was extracted as previously described. Bone from the mid part of the medial tibial plateau

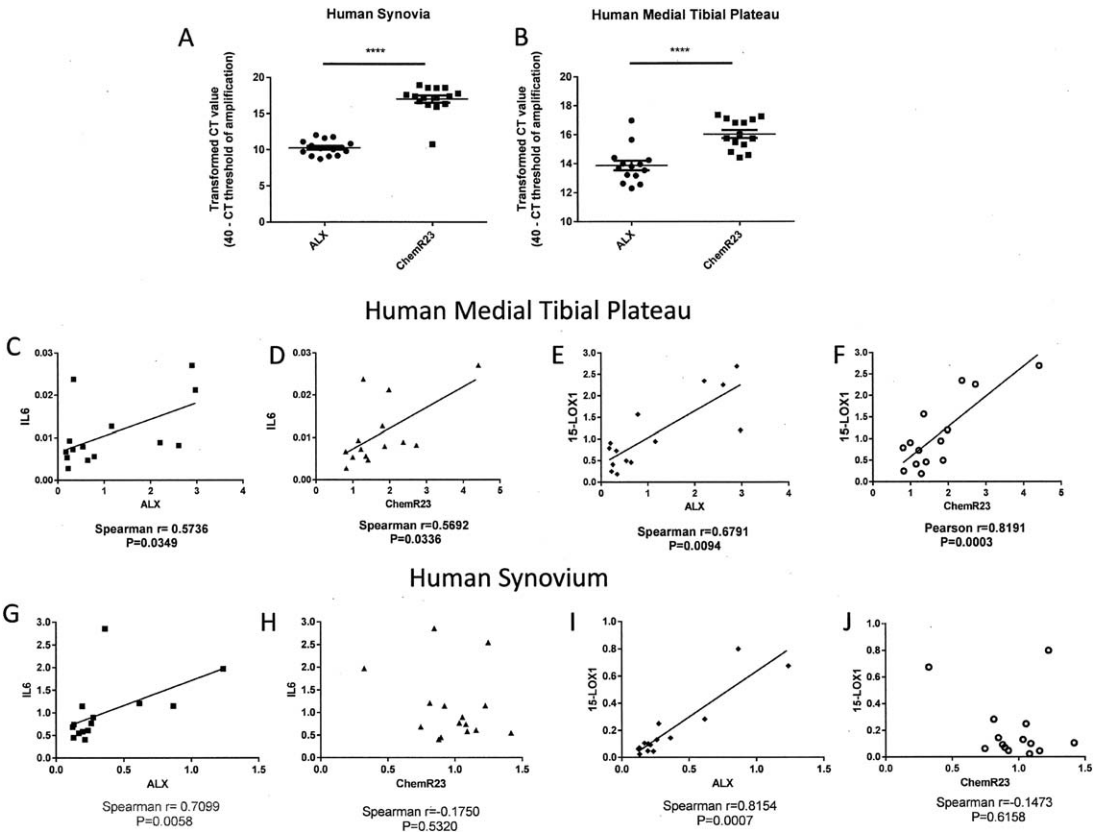

Figure 1. Expression of resolvin receptors ALX and ChemR23 in human osteoarthritis (OA) joint tissue. **A** and **B,** Transformed C_t values for resolvin receptors ALX and ChemR23 mRNA in synovium (**A**) and medial tibial plateau (**B**) specimens obtained from patients with end-stage OA. Expression of ChemR23 was significantly higher than that of ALX in both OA synovium (n = 15 specimens) (**A**) and medial tibial plateau (n = 14 specimens) (**B**), as shown by a larger transformed C_t value (maximum cycle number for run – cycle number at which exponential amplification occurs). Bars show the mean ± SEM. **** = $P < 0.0001$ by unpaired *t*-test. **C–F,** Correlations of ALX and ChemR23 with the cytokine interleukin-6 (IL-6) and the enzyme 15-lipoxygenase 1 (15-LOX-1) in human medial tibial plateau tissue. **G–J,** Correlations of ALX and ChemR23 with IL-6 and 15-LOX-1 in human synovium.

collected at the time of TKR surgery was pulverized in liquid nitrogen, and RNA was extracted in TRI Reagent. RNA samples were kept in a −80°C freezer for future use (see Supplementary Methods, available on the *Arthritis & Rheumatology* web site at http://onlinelibrary.wiley.com/doi/10.1002/art.40001/abstract). Expression of target genes was quantified using previously described methods (26,28). Primers and probes were designed using Primer Express 3.0 software (Applied Biosystems) and synthesized by personnel at MWG Biotech, and minor groove binder probes were biosynthesized by personnel at Applied Biosystems (see Supplementary Methods).

Glial cell immunofluorescence analysis. Rats were killed by sodium pentobarbital overdose and transcardially perfused with saline and then 4% paraformaldehyde, pH 7.4 (Sigma). The lumbar spinal cord was removed, postfixed in 4% paraformaldehyde, and stored in 30% sucrose. The spinal cord was then sectioned, and immunohistochemical analysis was performed using mouse anti–glial fibrillary acidic protein (anti-GFAP) antibodies (1:100) (Fisher Scientific), as previously described (26) (see Supplementary Methods).

Histologic staining and scoring of knee joints. Cartilage histopathology was scored from 0 (normal) to 5 (severe degeneration), and a total joint damage score (range 0–15) was obtained by combining the cartilage score with the score for joint involvement (range 0–3) (29). Synovial inflammation was graded on a scale of 0 (lining layer, 1–2 cells thick) to 3 (lining layer >9 cells thick and/or severe increase in cellularity), as previously described (29). Sections from the posterior half of the knee joints were dewaxed and recalcified with calcium chloride and magnesium chloride before tartrate-resistant acid phosphatase (TRAP) staining was conducted using a commercially available kit (F386A; Sigma-Aldrich). TRAP-positive osteoclasts were quantified as previously described (29) (see also Supplementary Methods, available on the *Arthritis & Rheumatology* web site at http://onlinelibrary.wiley.com/doi/10.1002/art.40001/abstract).

Statistical analysis. Data were analyzed with GraphPad Prism version 5 or 6 and are presented as the mean ± SEM. Behavioral data were analyzed by two-way analysis of variance (ANOVA) with Bonferroni post hoc correction. Histologic scoring was analyzed by one-way ANOVA with Bonferroni post hoc test or by Kruskal-Wallis ANOVA followed by Dunn's post hoc test for nonparametric data. Gene expression levels were analyzed by unpaired *t*-test (parametric data) or Mann-Whitney test (nonparametric data). Correlations between gene expression of resolvin

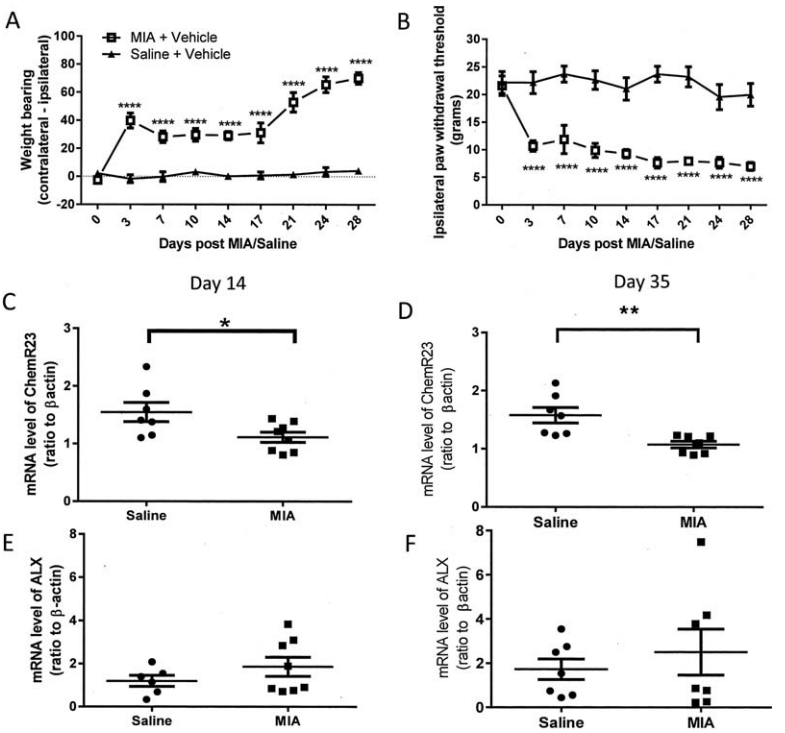

Figure 2. Expression of resolvin receptors ALX and ChemR23 in rat osteoarthritis (OA) joint tissue. **A** and **B,** Significant weight-bearing asymmetry (**A**) and decreased ipsilateral paw withdrawal thresholds (**B**) following intraarticular injection of monosodium iodoacetate (MIA) into the knee joints (MIA-treated rats) compared with saline-treated control rats (n = 8 per group). Values are the mean ± SEM. **** = $P < 0.0001$ versus control, by two-way analysis of variance with Bonferroni's post hoc test. **C** and **D,** Decreased synovial expression of ChemR23 in MIA-treated rats compared with saline-treated control rats on day 14 (**C**) and day 35 (**D**). **E** and **F,** Comparable expression of ALX in the synovium of MIA-treated rats and saline-treated rats on day 14 (**E**) and day 35 (**F**) (n = 7–8 per group). Bars in **C**–**F** show the mean ± SEM. * = $P < 0.05$; ** = $P < 0.01$ by unpaired *t*-test.

receptors and pain behavior or genes of interest were analyzed using Pearson's correlation coefficient (parametric data) or Spearman's correlation coefficient (nonparametric data) analysis. For immunofluorescence analysis, data were analyzed by one-way ANOVA with Bonferroni post hoc test. Correlations between spinal GFAP expression and weight-bearing asymmetry and the ipsilateral paw withdrawal threshold were determined by a Spearman's correlation.

RESULTS

Expression of ChemR23 and ALX messenger RNA (mRNA) in the OA joint. Both ALX and ChemR23 were present in human synovium and medial tibial plateau bone obtained following TKR surgery for OA (Figures 1A and B). For the synovium, there was an approximate 6-C_t difference between ChemR23 and ALX, and for the medial tibial plateau bone there was a 2-C_t difference, indicating higher expression of ChemR23 compared with ALX in both tissues. Given the role of these receptors in regulating inflammatory signaling, it is noteworthy that the expression of both ChemR23 and ALX was positively correlated with mRNA expression of IL-6 in the medial tibial plateau bone (Figures 1C and D). Expression of both ChemR23 and ALX was also positively correlated with expression of the enzyme 15-lipoxygenase 1 (15-LOX-1) in the medial tibial plateau bone (Figures 1E and F). In the synovium, correlations were less robust. Expression of ALX but not ChemR23 was positively correlated with IL-6 expression (Figures 1G and H), and expression of ALX was also positively correlated with 15-LOX-1 expression (Figures 1I and J). There was no correlation between body mass index (BMI) or age with expression of ALX, ChemR23, or any other genes studied in the synovium of OA patients (data not shown). Analysis of the correlation of BMI and age with expression of selected genes in medial tibial plateau bone from OA patients revealed a significant negative correlation between BMI and the expression of TNF. There was a significant negative correlation between age and expression of ChemR23 and 15-LOX-1 (data not shown).

The preclinical MIA model of OA pain was associated with marked weight-bearing asymmetry ($P < 0.0001$ versus saline + vehicle) (Figure 2A). In addition, MIA-induced OA pain was associated with reductions in ipsilateral paw

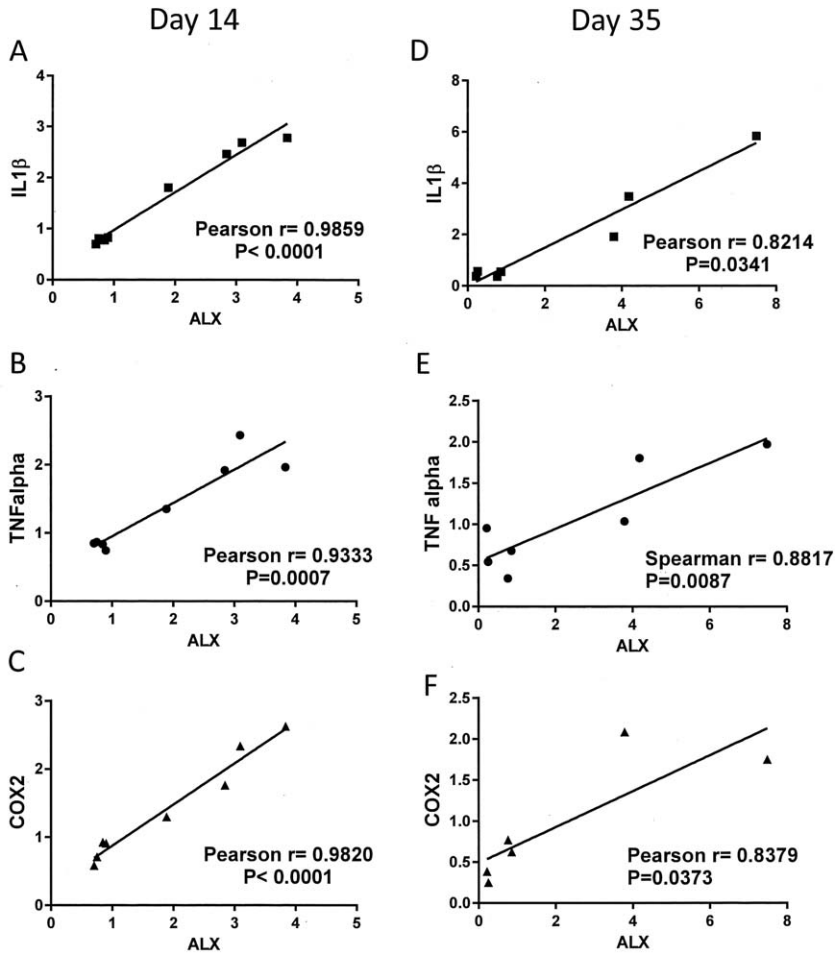

Figure 3. Correlations between synovial expression of ALX and markers of inflammation in rat synovium. Significant correlations between ALX expression and synovial expression of interleukin-1β (IL-1β), tumor necrosis factor (TNF), and cyclooxygenase 2 (COX-2) on day 14 (**A–C**) and day 35 (**D–F**) in monosodium iodoacetate–treated rats (n = 7) were found.

withdrawal thresholds ($P < 0.0001$ versus saline + vehicle) (Figure 2B), as previously described (25). Consistent with the clinical data, synovium from saline-treated (control) rats expressed both ChemR23 and ALX (Figures 2C–F). There was a significant reduction in ChemR23 expression in the synovium at both the earlier (day 14) (Figure 2C) and later (day 35) (Figure 2D) time points in MIA-treated animals compared with saline-treated controls. Synovial expression of ALX was unaltered in MIA-injected rats compared to saline-treated rats at either time point studied (Figures 2E and F).

Consistent with the clinical data, there was a trend toward a correlation between ALX and IL-6 expression (results not shown) at 14 days after induction of the model (r = 0.6826, $P = 0.0621$). At this time point, synovial ALX expression was correlated with IL-1β, TNF, and COX-2 expression (Figures 3A–C). At the later time point, synovial ALX expression was correlated with IL-1β, TNF, and COX-2 expression in the synovium (Figures 3D–F). There were no significant correlations between ALX expression and IL-6, IL-1β, TNF, and COX-2 expression in the synovium of control (saline-treated) rats (data not shown). There were no significant correlations between synovial expression of ChemR23 and IL-1β, TNF, and COX-2 in the MIA-induced model of OA at either time point (data not shown).

The number of ALX-positive and ChemR23-positive cells in the synovium was compared in the MIA-treated rats (day 28 after the MIA injection) and saline-treated controls. The number of DAPI-positive nuclei, ED1/CD68-positive cells, and the number of ALX-positive and ChemR23-positive cells in synovial sections was evaluated. The number of DAPI-positive cells was increased ($P < 0.01$) in the synovium of rats with MIA-induced OA compared with saline-injected control rats (see

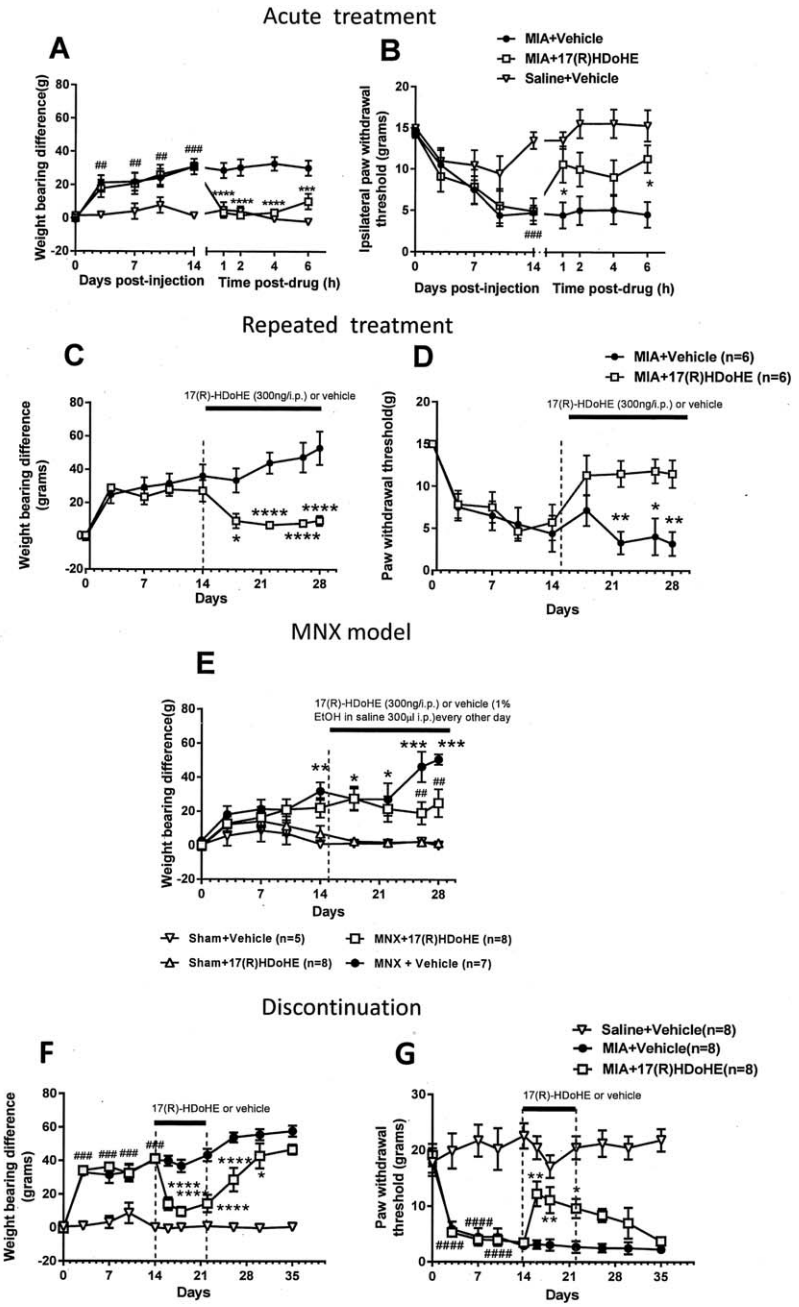

Figure 4. Inhibition of pain behavior by the D series resolvin precursor 17(R)-hydroxy-docosahexaenoic acid (17[R]-HDoHE). **A** and **B,** Attenuated weight-bearing asymmetry (**A**) and decreased ipsilateral hind paw withdrawal thresholds (**B**) 14 days after model induction in rats treated with monosodium iodoacetate (MIA) + 17(R)-HDoHE compared to MIA-injected vehicle-treated rats. Bars show the mean ± SEM (n = 8 per group). ## = $P < 0.01$; ### = $P < 0.001$ versus saline + vehicle. * = $P < 0.05$; *** = $P < 0.001$; **** = $P < 0.0001$ versus MIA + vehicle, by two-way analysis of variance (ANOVA) with Bonferroni's post hoc test. **C** and **D,** Sustained inhibition of weight-bearing asymmetry (**C**) and decreased paw withdrawal thresholds (**D**) from day 14 to day 28 following repeated administration of 17(R)-HDoHE in rats treated with MIA compared with rats treated with MIA+ vehicle. Bars show the mean ± SEM. * = $P < 0.05$; ** = $P < 0.01$; **** = $P < 0.0001$ versus MIA + vehicle, by two-way ANOVA with Bonferroni's post hoc test. **E,** Attenuated weight-bearing asymmetry in rats with medial meniscal transection (MNX)–induced osteoarthritis pain treated with repeated administration of 17(R)-HDoHE compared with those treated with vehicle. Bars show mean ± SEM. * = $P < 0.05$; ** = $P = 0.01$; *** = $P < 0.001$ versus sham + vehicle. ## = $P < 0.01$ versus MNX + vehicle, by two-way ANOVA with Bonferroni's post hoc test. **F** and **G,** Gradual return of weight-bearing asymmetry and decreased hind paw withdrawal thresholds within 7 days following cessation of 7-day treatment with 17(R)-HDoHE. Bars show the mean ± SEM. ### = $P < 0.001$; #### = $P < 0.0001$ versus saline + vehicle. * = $P < 0.05$; ** = $P < 0.01$; **** = $P < 0.0001$ versus MIA + vehicle, by two-way ANOVA with Bonferroni's post hoc test. Values are the mean ± SEM. EtOH = ethanol.

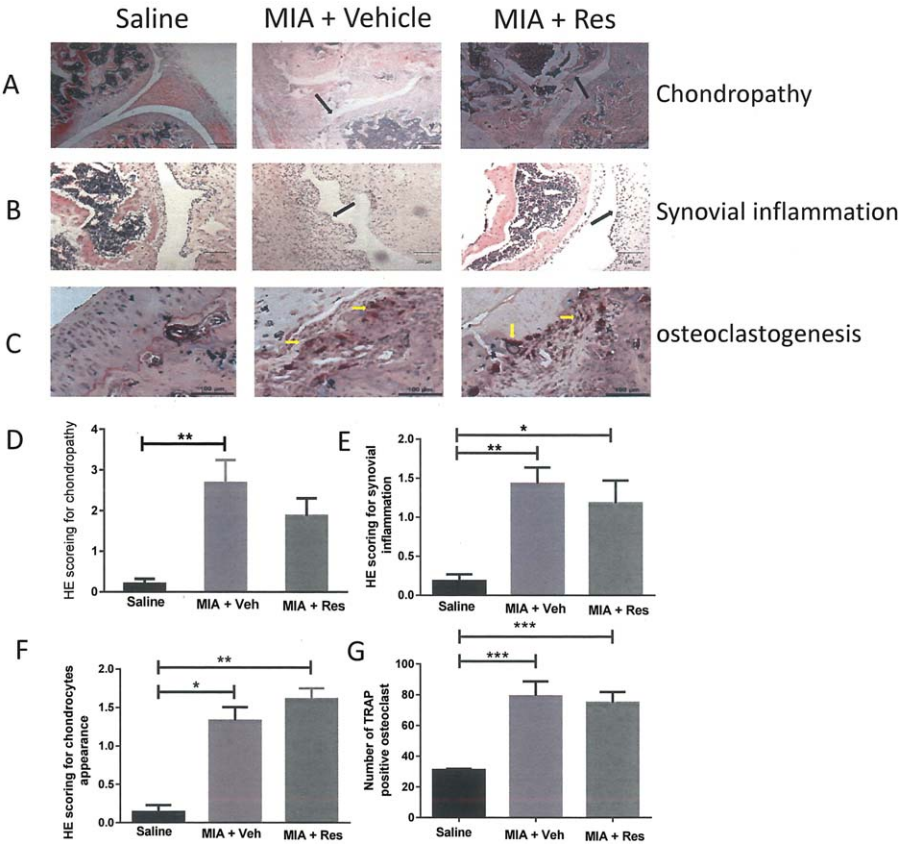

Figure 5. No alteration of osteoarthritis joint pathology by 17(R)-HDoHE (Res). **A–C,** Representative images of hematoxylin and eosin (H&E)–stained knee joint sections from rats treated with saline, MIA + vehicle (Veh), or MIA + 17(R)-HDoHE. A, Chondropathy. Bars = 500 μm. **B,** Synovial inflammation. Bars = 100 μm. **C,** Osteoclastogenesis. Bars = 100 μm. **Black arrows** indicate areas of chondropathy and synovial inflammation; **yellow arrows** indicate osteoclastogenesis. **D–G,** Significant joint pathology at 28 days in rats treated with intraarticular injections of MIA compared with saline-treated rats. Repeated administration of 17(R)-HDoHE from day 14 to day 28 did not alter the chondropathy score (**D**), synovial inflammation (**E**), chondrocyte appearance (**F**), or number of tartrate-resistant acid phosphatase (TRAP)–positive osteoclasts (**G**) in the MIA-treated rats. Bars show the mean ± SEM. $* = P < 0.05$; $** = P < 0.01$; $*** = P < 0.001$ by one-way ANOVA with Bonferroni's post hoc test (parametric data) or Kruskal-Wallis test with Dunn's post hoc test (nonparametric data). See Figure 4 for other definitions.

Supplementary Figures 1A and B, available on the *Arthritis & Rheumatology* web site at http://onlinelibrary.wiley.com/doi/10.1002/art.40001/abstract). In addition, the number of ED1-positive cells (see Supplementary Figures 1A and C) was also increased in the rats with MIA-induced OA ($P < 0.005$), which is indicative of the likely infiltration of ED1-positive macrophages in this model. Despite the increase in the number of macrophages in the synovium of rats with MIA-induced OA pain, the number of ALX-positive and ChemR23-positive cells in the synovium was significantly reduced in MIA-treated rats compared with saline-treated rats (see Supplementary Figures 1A, D, and E) ($P < 0.05$ for both ALX and ChemR23).

In order to confirm that the antibody staining was not attributable to autofluorescence, we conducted negative control experiments with omission of the primary antibodies (see Supplementary Figure 2, available on the *Arthritis & Rheumatology* web site at http://onlinelibrary.wiley.com/doi/10.1002/art.40001/abstract), in which positively labeled cells were not evident either visually or by velocity analysis. We attempted colocalization experiments for ED1-positive cells and ALX and ChemR23, but unfortunately we were unable to obtain sufficient quality of staining when these antibodies were applied to synovial sections for analysis.

Reversal of MIA- and MNX-induced OA pain by the D series precursor 17(R)-HDoHE. In a series of intervention studies, we evaluated the ability of systemic administration of 17(R)-HDoHE to reverse pain behavior in 2 models of OA. Systemic administration produced a pronounced and complete reversal of MIA-induced weight-bearing asymmetry and restored ipsilateral paw withdrawal

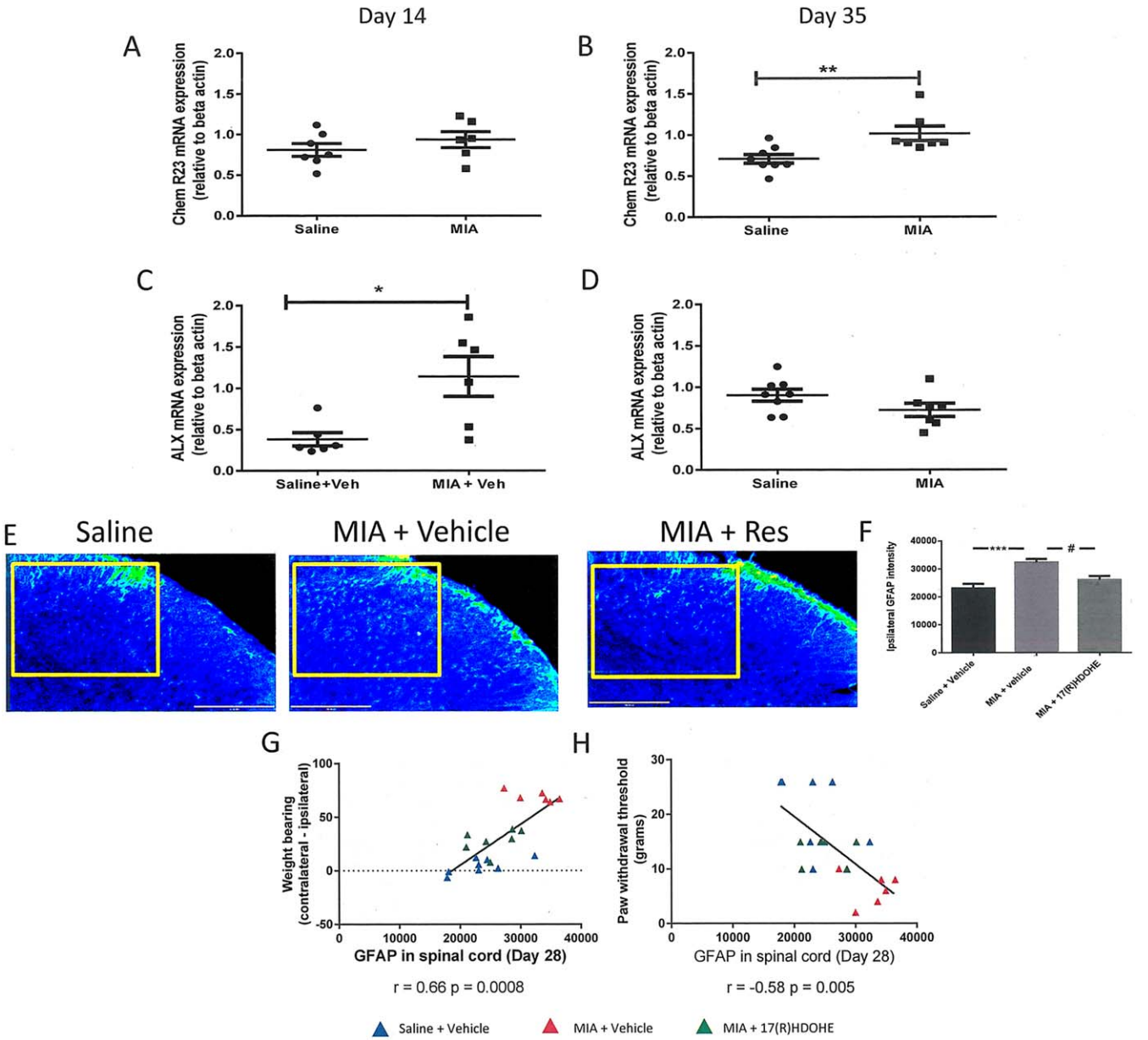

Figure 6. Expression of the resolvin receptors in the spinal cord. **A** and **B,** ChemR23 expression in the ipsilateral dorsal horn of the lumbar spinal cord (L3–L5) on day 14 (**A**) and day 35 (**B**) in MIA-treated rats compared with saline-treated rats. **C** and **D,** ALX expression in the ipsilateral dorsal horn of the lumbar spinal cord (L3–L5) on day 14 (**C**) and day 35 (**D**) in MIA-treated rats compared with saline-treated rats. Bars show the mean ± SEM (n = 5–6 per group). $* = P < 0.05$; $** = P < 0.01$ by unpaired *t*-test. **E,** Anti–glial fibrillary acidic protein (GFAP) immunofluorescence in the ipsilateral L4 dorsal horn of the spinal cord 28 days following induction of the MIA model of OA pain, indicative of increased astrocyte reactivity. Repeated systemic treatment with 17(R)-HDoHE (300 ng every other day from day 14 to day 28 after model induction) resulted in a significant decrease in MIA-induced GFAP immunofluorescence. The boxed area shows the area evaluated for GFAP quantification. **F,** Quantification of GFAP fluorescence. Bars show the mean ± SEM (n = 7–8 rats per group). $*** = P < 0.001$; $\# = P < 0.05$ by one-way ANOVA. **G,** Positive correlation between GFAP expression in the ipsilateral dorsal horn of the spinal cord and weight-bearing asymmetry in all of the treatment groups. **H,** Negative correlation between GFAP expression in the ipsilateral dorsal horn of the spinal cord and the paw withdrawal threshold in all of the treatment groups. See Figure 4 for other definitions.

thresholds toward control values at 1 hour after administration; these effects lasted for 6 hours (Figures 4A and B). Importantly, the inhibitory effects of 17(R)-HDoHE on both weight-bearing asymmetry and hind paw withdrawal thresholds were sustained following repeated administration of 17(R)-HDoHE for 14 days (Figures 4C and D);

there was no evidence of tolerance to this analgesic effect. To consolidate the evidence that these inhibitory effects of the resolvin precursor on MIA-induced pain behavior has translational relevance, the effects of 17(R)-HDoHE on pain behavior were also evaluated in the MNX-induced model of OA. In this analysis, systemic administration of 17(R)-HDoHE (300 ng intraperitoneally every other day from day 14 after model induction) significantly halted further increases in MNX-induced weight-bearing asymmetry (Figure 4E).

The final series of pharmacologic experiments determined the extent to which 17(R)-HDoHE administration altered pain behavior once treatment had ceased. Following a 7-day treatment protocol with 17(R)-HDoHE (days 14–22 after MIA/saline injection), pain behavior was assessed for a further 13 days. It was evident that the analgesic effects of 17(R)-HDoHE were sustained over a short period of time once treatment had ceased, and then pain behavior returned to levels observed in saline-treated rats with MIA-induced OA pain (Figures 4F and G).

To further investigate the potential mechanisms underlying the effects of17(R)-HDoHE on OA-induced pain behavior, the effects of repeated treatment with 17(R)-HDoHE on joint pathology were determined (Figures 5A–C). Intraarticular injection of MIA was associated with a significant increase in chondropathy, synovitis, and chondrocyte appearance and increased numbers of subchondral osteoclasts (Figures 5D–G). Following repeated administration of 17(R)-HDoHE (300 ng in 300 μl every other day from day 14 to day 28) there were no significant changes in any of these features of OA joint pathology (Figures 5D–G). Similarly, repeated treatment with 17(R)-HDoHE did not alter MNX-induced joint pathology (data not shown).

Spinal effects of 17(R)-HDoHE correlated with behavioral analgesia. Given the lack of effect of 17(R)-HDoHE on joint pathology in 2 models of OA pain, we investigated potential spinal mechanisms underlying these effects. ChemR23 expression in the spinal cord on day 14 in MIA-treated rats was comparable with that in saline-treated controls (Figure 6A); however, expression was increased on day 35 in MIA-treated rats compared with saline-treated controls (Figure 6B). The expression of ALX in the ipsilateral dorsal horn of the spinal cord was increased in MIA-treated rats compared with saline-treated rats on day 14 (Figure 6C), while on day 35 there was no difference in spinal ALX expression between MIA-treated and saline-treated rats (Figure 6D).

We previously reported a significant increase in GFAP immunofluorescence, a marker for astrogliosis, in the spinal cord at later time points in the MIA-induced model of OA (25). Consistent with previous findings, GFAP immunofluorescence was significantly increased in the ipsilateral dorsal horn (Figures 6E and F) but not the contralateral dorsal horn (data not shown) of MIA-treated rats that received vehicle, compared with saline-treated controls. Repeated systemic administration of 17(R)-HDoHE (300 ng in 300 μl every other day from day 14 to day 28) significantly inhibited GFAP immunofluorescence in the ipsilateral dorsal horn of the spinal cord in MIA-treated rats, compared with vehicle-treated rats with MIA-induced OA pain (Figures 6E and F). Correlation analysis revealed that spinal GFAP expression was positively correlated with weight-bearing asymmetry (Figure 6G) and negatively correlated with ipsilateral paw withdrawal thresholds (Figure 6H).

Liquid chromatography tandem mass spectrometry (LC-MS/MS) quantitative analysis of resolvins and 17(R)-HdoHE. Plasma levels of 45 oxylipins, including arachidonic acid, RvD1, RvD2, and the precursor 17(R)-HDoHE were quantified 150 minutes following systemic administration of 17(R)-HDoHE in MIA-treated rats, vehicle-treated rats, and saline-treated controls. Levels of arachidonic acid were not altered by systemic administration of 17(R)-HDoHE (see Supplementary Figures 3A and D, available on the *Arthritis & Rheumatology* web site at http://onlinelibrary.wiley.com/doi/10.1002/art.40001/abstract). As expected at the time point studied, plasma levels of 17(R)-HDoHE were not altered following 17(R)-HDoHE pretreatment (see Supplementary Figures 3B and E), but levels of RvD2 were significantly increased in 17(R)-HDoHE–treated rats with MIA-induced OA compared with vehicle-treated rats with MIA-induced OA (see Supplementary Figures 3C and F). Although there were no significant differences in the group data for plasma levels of RvD1, this lipid was detected in a larger number of samples following 17(R)-HDoHE treatment (5 of 8 samples) compared with those that received vehicle (3 of 8). Of the remaining oxylipins quantified, only 9-oxo-10E,12Z-octadecadienoic acid (9-oxoODE) and 13-oxoODE were significantly increased in the group of rats with MIA-induced OA treated with 17(R)-HDoHE compared with the group that received saline plus vehicle (data not shown).

DISCUSSION

Herein we report that the resolvin receptors ALX and ChemR23 are expressed at the mRNA level in both the synovium and tibial plateau of OA patients. ALX expression was positively correlated with expression of IL-6, which is a clinically relevant knee pain biomarker in patients with early OA and those with advanced-stage knee OA (30), and positively correlated with expression of 15-LOX-1, a key enzyme involved in D series resolvin generation, in both OA synovium and medial tibial plateau

bone. Associations between ChemR23, 15-LOX-1, and IL-6 expression were less consistent for both tissues. The enzyme 15-LOX-1 is involved in the biosynthesis of D series resolvins from DHA but not the production of E series resolvins from EPA; therefore, correlations between 15-LOX-1 and ChemR23 may reflect the more general role of 15-LOX-1 in inflammatory pathways. Although correlations between these inflammatory mediators and resolvin receptor expression do not necessarily reflect a causal relationship, they do support the need for further investigation of the role of the resolvin system in OA mechanisms. Due to the lack of availability of fresh non-OA knee synovium and tibial plateau bone, we were unable to evaluate whether expression of ALX and ChemR23 is altered in end-stage OA. To overcome this inevitable hurdle of clinical research, preclinical studies using well-established models of OA pain in the rodent were undertaken.

Both ALX and ChemR23 were present in control rat synovium at the early and late time points in the model of MIA-induced OA pain. The impact of this model of OA on the expression of these receptors differed. Expression of ChemR23 mRNA was reduced in the synovium at both the early and late time points in the MIA model of OA. In contrast, synovial expression of ALX mRNA in MIA-injected rats remained stable and comparable with levels in saline-treated rats at both time points in the model of MIA-induced OA pain. Synovial expression of ALX mRNA in the MIA-induced model of OA pain was positively correlated with key inflammatory genes (TNF, IL-1β, IL-6, and COX-2), which is consistent with the presence of synovial inflammation in this model of OA pain, described herein and in previous studies (31–33), and the expression of ALX by neutrophils, macrophages, and fibroblast-like synoviocytes (34).

In addition to the findings of the gene expression studies, we also demonstrated an increased number of ED1-positive cells in the synovium of rats with MIA-induced pain compared with control rats, reflecting a likely increase in macrophage infiltration. These events were associated with a decrease in the number of ChemR23-positive and ALX-positive cells in the synovium of MIA-treated rats compared with controls. Thus, there was a consistent direction of effect for ChemR23 mRNA and protein. In contrast, ALX mRNA expression was not altered, but the numbers of ALX-positive cells were decreased in the synovium of MIA-treated rats, which may reflect posttranslational changes in this receptor.

Systemic administration of the D series resolvin precursor 17(R)-HDoHE produced robust inhibition of established pain behavior in both the chemically induced and surgically induced OA pain models. Systemic treatment with a single dose of 17(R)-HDoHE rapidly reversed established weight-bearing asymmetry, and this reversal was evident 1 hour posttreatment and was sustained for 6 hours. LC-MS/MS analysis of plasma confirmed that this treatment significantly increased plasma levels of RvD2 and increased the number of samples in which RvD1 was detectable. The dose of 17(R)-HDoHE studied was based on the comprehensive pharmacologic evaluation of 17(R)-HDoHE in a model of inflammatory arthritis (17). Consistent with this previous study, we observed that a very low dose of 17(R)-HDoHE has beneficial effects on pain behavior, and that repeated treatment with 17(R)-HDoHE has a sustained inhibitory effect on pain behavior over a 2-week period in both the chemically induced and surgically induced models of OA pain. Although there were subtle differences in the rapidity of onset and magnitude of the inhibitory effects of 17(R)-HDoHE between the 2 models of OA pain, overall this treatment had a comparable inhibitory effect in the 2 models. Unlike opioid-based analgesics, sustained treatment with 17(R)-HDoHE did not lead to tolerance.

To further investigate the underlying mechanisms leading to the beneficial effects of 17(R)-HDoHE, the effects of repeated treatment on joint pathology were quantified in the model of MIA-induced pain. Consistent with previous studies (26,35–37) and the key clinical features of OA, the model of MIA-induced OA was associated with significant cartilage damage, synovial inflammation, and increased numbers of subchondral osteoclasts. Despite the robust analgesic effects of 17(R)-HDoHE, this treatment did not alter any of the features of knee joint pathology. This was also the case in the model of MNX-induced OA pain and joint pathology. This observation is consistent with our demonstration that the numbers of ALX-positive cells were reduced in the synovium of rats with MIA-induced OA pain compared with saline-treated controls, which is likely to limit/reduce any possible effects of 17(R)-HDoHE at this level. We previously showed that treatments that act to reduce osteoclast function can alter the progression of joint pathology under identical experimental conditions (29). Unlike RvE1, which can inhibit osteoclasts and bone resorption (38) and protects against bone loss (39,40), evidence for a role of RvD1 in bone modulation is sparse. It is feasible, however, that a higher dose of 17(R)-HDoHE may alter pathologic knee changes seen in these models of OA. Overall, our in vivo data demonstrate that 17(R)-HDoHE can robustly block pain behavior in the MIA model of OA in the face of overt joint damage and synovial inflammation.

Once treatment with 17(R)-HDoHE was stopped, pain behavior was blocked for an additional 5–7 days, suggesting that augmentation of the resolvin system has longer-term inhibitory effects on nociceptive signaling, which may

represent alterations in both channel activity and signaling pathways. Chronic pain states are often associated with changes in the spinal signaling pathways and increased excitability of spinal neurones, coupled with increased activation of proinflammatory signaling pathways and changes in the activation state of microglia and astrocytes (41).

RvD1 is known to suppress TRPA-1, TRPV-3, and TRPV-4 channel activity in primary sensory fibers (18,21); therefore, systemic administration of 17(R)-HDoHE may act to reduce sensory nerve activity arising from the damaged knee joint. It is noteworthy that deletion of TRPA-1 attenuates joint pathology and pain behavior in the mouse model of MIA-induced OA (42). It is possible that 17(R)-HDoHE may still have effects at the level of the joint by activating ALX receptors on synovial cells and possibly reducing release of synovium-derived nerve sensitization factors such as NGF (43).

Direct spinal administration of RvD1 inhibited evoked pain behavior in models of acute and chronic pain (18,21,22); similarly, spinal administration of 17(R)-HDoHE attenuated inflammation-induced mechanical hypersensitivity (22). Although the spinal mechanisms underlying the effects of RvD1 are not fully established, common pathways implicated include reductions in TNF release (22) and inhibition of ERK signaling (21). In the current study, immunohistochemical analysis revealed that both ChemR23 and ALX expression in the ipsilateral dorsal horn of the spinal cord is either increased or unaltered in rats with MIA-induced OA pain compared with that in saline-treated controls at the 2 time points studied, providing a putative spinal site of action for the resolvins in this model of OA. It is possible that 17(R)-HDoHE may still have effects at the level of the joint by activating ALX receptors on synovial cells and possibly reducing release of synovium-derived nerve sensitization factors such as NGF (43).

We previously demonstrated a significant increase in GFAP immunofluorescence, indicative of astrogliosis and a marker of central sensitization, in the ipsilateral dorsal horn of the spinal cord at later time points in the model of MIA-induced OA pain (25). In the current study, repeated treatment with 17(R)-HDoHE from day 14 onward resulted in significant blockade of spinal astrogliosis in the model of MIA-induced OA pain at the later time point (day 28 after induction of the model), and spinal GFAP expression at this time was correlated with pain behavior. We previously showed that post mortem knee chondropathy scores are significantly and positively correlated with human spinal GFAP mRNA expression (26), confirming the clinical relevance of these spinal markers of central sensitization.

Astrogliosis is associated with numerous models of chronic pain (for review, see ref. 44) and is a proposed switch in the transition from acute to chronic pain mechanisms (45). The ability of 17(R)-HDoHE to inhibit spinal astrogliosis in preclinical models of OA, along with the clinical associations between joint damage and spinal GFAP expression, supports the need for further investigation of the therapeutic potential of the D series resolvin pathway. The mechanisms by which 17(R)-HDoHE inhibits astrogliosis may arise as a result of direct effects (although there is little evidence to date) or indirect effects on the spinal signaling pathways that lead to astrogliosis. In particular, activated microglia in the spinal cord play a fundamental role in the development of chronic pain mechanisms and are known to be activated 14–28 days following induction of the MIA model of OA (25), coinciding with the increase in expression of ALX in the ipsilateral spinal cord reported herein.

Microglia are known to express ALX (46,47), and activation of microglia in models of chronic pain states, including OA, is associated with increased levels of pERK (48), a known spinal target of 17(R)-HDoHE (21). In addition, the antiinflammatory and pro-resolution molecule lipoxin A_4 also signals through ALX (49), and increases in ALX expression seen in the spinal cord in the MIA model may indicate an enhanced antiinflammatory role of lipoxin A_4.

The results of this series of experiments demonstrate that receptors for both D series and E series resolvins are expressed at multiple sites within the human OA joint, and that the precursor for the D series resolvins reduced OA pain behavior and a key marker of central sensitization (astrocyte activation) associated with chronic pain. These effects, which were not subject to tolerance, at least over a 2-week period of treatment, likely arise from modulation of both nociceptive input arising from the arthritic joint and modulation of central nociceptive processing. Our findings support the need for further investigation of the therapeutic potential of this new class of analgesics for the treatment of OA pain. Future work could address whether combination treatments that use both 17(R)-HDoHE and an E series resolvin precursor such as hydroxy-eicosapentaenoic acid would produce superior analgesic efficacy and potential disease-modifying properties via the modulation of both resolvin signaling systems.

ACKNOWLEDGMENTS

We thank the Nottingham University Hospitals NHS Trust Biobank and all of the individuals who consented to provide synovium and medial tibial plateau tissue samples following total knee replacement surgery.

AUTHOR CONTRIBUTIONS

All authors were involved in drafting the article or revising it critically for important intellectual content, and all authors approved the final version to be published. Drs. Burston and Chapman had full access to all of the data in the study and take responsibility for the integrity of the data and the accuracy of the data analysis.

Study conception and design. Huang, Burston, Mapp, Bennett, Ravipati, Pousinis, Barrett, Scammell, Chapman.

Acquisition of data. Huang, Burston, Li, Ashraf, Mapp, Ravipati.

Analysis and interpretation of data. Huang, Burston, Li, Ashraf, Bennett, Ravipati, Pousinis, Barrett, Scammell, Chapman.

REFERENCES

1. Glyn-Jones S, Palmer AJ, Agricola R, Price AJ, Vincent TL, Weinans H, et al. Osteoarthritis. Lancet 2015;386:376–87.
2. Karsdal MA, Bay-Jensen AC, Lories RJ, Abramson S, Spector T, Pastoureau P, et al. The coupling of bone and cartilage turnover in osteoarthritis: opportunities for bone antiresorptives and anabolics as potential treatments? Ann Rheum Dis 2014;73:336–48.
3. Murray CJ, Vos T, Lozano R, Naghavi M, Flaxman AD, Michaud C, et al. Disability-adjusted life years (DALYs) for 291 diseases and injuries in 21 regions, 1990-2010: a systematic analysis for the Global Burden of Disease Study 2010. Lancet 2012; 380:2197–223.
4. Felson DT, Chaisson CE, Hill CL, Totterman SM, Gale ME, Skinner KM, et al. The association of bone marrow lesions with pain in knee osteoarthritis. Ann Intern Med 2001;134:541–9.
5. Arendt-Nielsen L, Skou ST, Nielsen TA, Petersen KK. Altered central sensitization and pain modulation in the CNS in chronic joint pain. Curr Osteoporos Rep 2015;13:225–34.
6. Dakin H, Gray A, Fitzpatrick R, Maclennan G, Murray D, the KAT Trial Group. Rationing of total knee replacement: a cost-effectiveness analysis on a large trial data set. BMJ Open 2012;2: e000332.
7. Serhan CN, Hong S, Gronert K, Colgan SP, Devchand PR, Mirick G, et al. Resolvins: a family of bioactive products of omega-3 fatty acid transformation circuits initiated by aspirin treatment that counter proinflammation signals. J Exp Med 2002;196:1025–37.
8. Serhan CN, Clish CB, Brannon J, Colgan SP, Chiang N, Gronert K. Novel functional sets of lipid-derived mediators with antiinflammatory actions generated from omega-3 fatty acids via cyclooxygenase 2-nonsteroidal antiinflammatory drugs and transcellular processing. J Exp Med 2000;192:1197–204.
9. Krishnamoorthy S, Recchiuti A, Chiang N, Yacoubian S, Lee CH, Yang R, et al. Resolvin D1 binds human phagocytes with evidence for proresolving receptors. Proc Natl Acad Sci U S A 2010;107:1660–5.
10. Dalli J, Winkler JW, Colas RA, Arnardottir H, Cheng CY, Chiang N, et al. Resolvin D3 and aspirin-triggered resolvin D3 are potent immunoresolvents. Chem Biol 2013;20:188–201.
11. Chiang N, Fredman G, Backhed F, Oh SF, Vickery T, Schmidt BA, et al. Infection regulates pro-resolving mediators that lower antibiotic requirements. Nature 2012;484:524–8.
12. Arita M, Bianchini F, Aliberti J, Sher A, Chiang N, Hong S, et al. Stereochemical assignment, antiinflammatory properties, and receptor for the omega-3 lipid mediator resolvin E1. J Exp Med 2005;201:713–22.
13. Arita M, Ohira T, Sun YP, Elangovan S, Chiang N, Serhan CN. Resolvin E1 selectively interacts with leukotriene B4 receptor BLT1 and ChemR23. J Immunol 2007;178:3912–7.
14. Serhan CN, Petasis NA. Resolvins and protectins in inflammation resolution. Chem Rev 2011;111:5922–43.
15. Ji RR, Xu ZZ, Strichartz G, Serhan CN. Emerging roles of resolvins in the resolution of inflammation and pain. Trends Neurosci 2011;34:599–609.
16. Sungjae Yoo, Lim JY, Hwang SW. Resolvins: endogenously-generated potent painkilling substances and their therapeutic perspectives. Curr Neuropharmacol 2013;11:664–76.
17. Lima-Garcia JF, Dutra RC, da Silva K, Motta EM, Campos MM, Calixto JB. The precursor of resolvin D series and aspirin-triggered resolvin D1 display anti-hyperalgesic properties in adjuvant-induced arthritis in rats. Br J Pharmacol 2011;164:278–93.
18. Bang S, Yoo S, Yang TJ, Cho H, Kim YG, Hwang SW. Resolvin D1 attenuates activation of sensory transient receptor potential channels leading to multiple anti-nociception. Br J Pharmacol 2010;161:707–20.
19. Bang S, Yoo S, Yang TJ, Cho H, Hwang SW. 17(R)-resolvin D1 specifically inhibits transient receptor potential ion channel vanilloid 3 leading to peripheral antinociception. Br J Pharmacol 2012;165:683–92.
20. Xu ZZ, Berta T, Ji RR. Resolvin E1 inhibits neuropathic pain and spinal cord microglial activation following peripheral nerve injury. J Neuroimmune Pharmacol 2012;8:37–41.
21. Xu ZZ, Zhang L, Liu T, Park JY, Berta T, Yang R, et al. Resolvins RvE1 and RvD1 attenuate inflammatory pain via central and peripheral actions. Nat Med 2010;16:592–7.
22. Abdelmoaty S, Wigerblad G, Bas DB, Codeluppi S, Fernandez-Zafra T, El-Awady el-S, et al. Spinal actions of lipoxin A4 and 17(R)-resolvin D1 attenuate inflammation-induced mechanical hypersensitivity and spinal TNF release. PloS One 2013;8:e75543.
23. Feng QX, Feng F, Feng XY, Li SJ, Wang SQ, Liu ZX, et al. Resolvin D1 reverses chronic pancreatitis-induced mechanical allodynia, phosphorylation of NMDA receptors, and cytokines expression in the thoracic spinal dorsal horn. BMC Gastroenterol 2012;12:148.
24. Tang H, Liu Y, Yan C, Petasis NA, Serhan CN, Gao H. Protective actions of aspirin-triggered (17R) resolvin D1 and its analogue, 17R-hydroxy-19-para-fluorophenoxy-resolvin D1 methyl ester, in C5a-dependent IgG immune complex-induced inflammation and lung injury. J Immunol 2014;193:3769–78.
25. Sagar DR, Burston JJ, Hathway GJ, Woodhams SG, Pearson RG, Bennett AJ, et al. The contribution of spinal glial cells to chronic pain behaviour in the monosodium iodoacetate model of osteoarthritic pain. Mol Pain 2011;7:88.
26. Mapp PI, Sagar DR, Ashraf S, Burston JJ, Suri S, Chapman V, et al. Differences in structural and pain phenotypes in the sodium monoiodoacetate and meniscal transection models of osteoarthritis. Osteoarthritis Cartilage 2013;21:1336–45.
27. Sagar DR, Nwosu L, Walsh DA, Chapman V. Dissecting the contribution of knee joint NGF to spinal nociceptive sensitization in a model of OA pain in the rat. Osteoarthritis Cartilage 2015;23:906–13.
28. Erhuma A, Salter AM, Sculley DV, Langley-Evans SC, Bennett A. Prenatal exposure to a low protein diet programmes disordered regulation of lipid metabolism in the ageing rat. Am J Physiol Endocrinol Metab 2007;292:1702–14.
29. Sagar DR, Ashraf S, Xu L, Burston JJ, Menhinick MR, Poulter CL, et al. Osteoprotegerin reduces the development of pain behaviour and joint pathology in a model of osteoarthritis. Ann Rheum Dis 2014;73:1558–65.
30. Shimura Y, Kurosawa H, Sugawara Y, Tsuchiya M, Sawa M, Kaneko H, et al. The factors associated with pain severity in patients with knee osteoarthritis vary according to the radiographic disease severity: a cross-sectional study. Osteoarthritis Cartilage 2013;21:1179–84.
31. Hulejova H, Baresova V, Klezl Z, Polanska M, Adam M, Senolt L. Increased level of cytokines and matrix metalloproteinases in osteoarthritic subchondral bone. Cytokine 2007;38:151–6.
32. Venn G, Nietfeld JJ, Duits AJ, Brennan FM, Arner E, Covington M, et al. Elevated synovial fluid levels of interleukin-6 and tumor necrosis factor associated with early experimental canine osteoarthritis. Arthritis Rheum 1993;36:819–26.
33. Alvarez-Soria MA, Herrero-Beaumont G, Moreno-Rubio J, Calvo E, Santillana J, Egido J, et al. Long-term NSAID

treatment directly decreases COX-2 and mPGES-1 production in the articular cartilage of patients with osteoarthritis. Osteoarthritis Cartilage 2008;16:1484–93.
34. Fiore S, Antico G, Aloman M, Sodin-Semrl S. Lipoxin A4 biology in the human synovium: role of the ALX signaling pathways in modulation of inflammatory arthritis. Prostaglandins Leukot Essent Fatty Acids 2005;73:189–96.
35. Guzman RE, Evans MG, Bove S, Morenko B, Kilgore K. Mono-iodoacetate-induced histologic changes in subchondral bone and articular cartilage of rat femorotibial joints: an animal model of osteoarthritis. Toxicol Pathol 2003;31:619–24.
36. Janusz MJ, Bendele AM, Brown KK, Taiwo YO, Hsieh L, Heitmeyer SA. Induction of osteoarthritis in the rat by surgical tear of the meniscus: inhibition of joint damage by a matrix metalloproteinase inhibitor. Osteoarthritis Cartilage 2002;10:785–91.
37. Beyreuther B, Callizot N, Stohr T. Antinociceptive efficacy of lacosamide in the monosodium iodoacetate rat model for osteoarthritis pain. Arthritis Res Ther 2007;9:R14.
38. Herrera BS, Ohira T, Gao L, Omori K, Yang R, Zhu M, et al. An endogenous regulator of inflammation, resolvin E1, modulates osteoclast differentiation and bone resorption. Br J Pharmacol 2008;155:1214–23.
39. Gao L, Faibish D, Fredman G, Herrera BS, Chiang N, Serhan CN, et al. Resolvin E1 and chemokine-like receptor 1 mediate bone preservation. J Immunol 2013;190:689–94.
40. Hasturk H, Kantarci A, Ohira T, Arita M, Ebrahimi N, Chiang N, et al. RvE1 protects from local inflammation and osteoclast-mediated bone destruction in periodontitis. FASEB J 2006;20:401–3.
41. Scholz J, Woolf CJ. The neuropathic pain triad: neurons, immune cells and glia. Nat Neurosci 2007;10:1361–8.
42. Moilanen LJ, Hamalainen M, Nummenmaa E, Ilmarinen P, Vuolteenaho K, Nieminen RM, et al. Monosodium iodoacetate-induced inflammation and joint pain are reduced in TRPA1 deficient mice: potential role of TRPA1 in osteoarthritis. Osteoarthritis Cartilage 2015;23:2017–26.
43. Shutov LP, Warwick CA, Shi X, Gnanasekaran A, Shepherd AJ, Mohapatra DP, et al. The complement system component C5a produces thermal hyperalgesia via macrophage-to-nociceptor signaling that requires NGF and TRPV1. J Neurosci 2016;36:5055–70.
44. Gao YJ, Ji RR. Targeting astrocyte signaling for chronic pain. Neurotherapeutics 2010;7:482–93.
45. Ji RR, Berta T, Nedergaard M. Glia and pain: is chronic pain a gliopathy? Pain 2013;154 Suppl 1:S10–28.
46. Cui YH, Le Y, Gong W, Proost P, van Damme J, Murphy WJ, et al. Bacterial lipopolysaccharide selectively up-regulates the function of the chemotactic peptide receptor formyl peptide receptor 2 in murine microglial cells. J Immunol 2002;168:434–42.
47. Kong Y, Ruan L, Qian L, Liu X, Le Y. Norepinephrine promotes microglia to uptake and degrade amyloid β peptide through upregulation of mouse formyl peptide receptor 2 and induction of insulin-degrading enzyme. J Neurosci 2010;30:11848–57.
48. Lee Y, Pai M, Brederson JD, Wilcox D, Hsieh G, Jarvis MF, et al. Monosodium iodoacetate-induced joint pain is associated with increased phosphorylation of mitogen activated protein kinases in the rat spinal cord. Mol Pain 2011;7:39.
49. Macdonald LJ, Boddy SC, Denison FC, Sales KJ, Jabbour HN. A role for lipoxin A_4 as an anti-inflammatory mediator in the human endometrium. Reproduction 2011;142:345–52.

ARTHRITIS & RHEUMATOLOGY
Vol. 69, No. 5, May 2017, pp 1009–1015
DOI 10.1002/art.40033

BRIEF REPORT

Functional Interaction of Endoplasmic Reticulum Aminopeptidase 2 and HLA–B27 Activates the Unfolded Protein Response

Zhenbo Zhang,[1] Francesco Ciccia,[2] Fanxing Zeng,[1] Giuliana Guggino,[2] Kirby Yee,[3] Hasan Abdullah,[4] Mark S. Silverberg,[5] Riccardo Alessandro,[2] Giovanni Triolo,[2] and Nigil Haroon[6]

Objective. **The basic mechanisms underlying the pathogenesis of ankylosing spondylitis (AS) remain unresolved. We previously reported an association of the single-nucleotide polymorphism (SNP) rs2549782 in the endoplasmic reticulum aminopeptidase 2 gene (*ERAP2*) with AS. It is known that patients homozygous for the G allele (GG) of another *ERAP2* SNP, rs2248374, lack expression of *ERAP2* (*ERAP2* null). The present study utilized this information to study the impact of *ERAP2* deficiency on HLA–B27 expression in patients with AS, specifically focusing on the functional interaction of *ERAP2* and HLA–B27 in peripheral blood mononuclear cells (PBMCs) from patients with AS and assessing the effects in vitro in specific cell lines.**

Methods. **Expression of intact peptide HLA–B27 (pB27) or the major histocompatibility complex class I free heavy chains (FHCs) was assessed in PBMCs isolated from HLA–B27–positive patients with AS. *ERAP2*-suppressed, stable B27–expressing C1R cells (C1R-B27) were tested for the expression levels of pB27 and FHCs, as well as for markers of the unfolded protein response (UPR). Distribution of the *ERAP2* SNPs rs2549782 and rs2248374 in patients with AS and in patients with Crohn's disease was assessed.**

Results. **PBMCs from AS patients lacking *ERAP2* expressed higher levels of FHCs than did PBMCs from patients positive for *ERAP2*. This finding was replicated in C1R-B27 cells after suppression of *ERAP2*. In addition, *ERAP2* suppression led to increased levels of the UPR markers BiP, CCAAT/enhancer binding protein homologous protein 10, and X-box binding protein 1 [spliced] as compared to that in short hairpin RNA–treated control cells. There was strong linkage disequilibrium in the *ERAP2* locus. All patients with the rs2549782 T allele (which reportedly increases the function of the ERAP-2 protein) were homozygous for the G allele of rs2248374, leading to absence of *ERAP2*.**

Conclusion. ***ERAP2*** **deficiency causes increased FHC expression and up-regulation of the UPR pathway.**

The pathogenic role of HLA–B27 in ankylosing spondylitis (AS) is not clear. The unfolded protein response (UPR) theory proposes that misfolded HLA–B27 can trigger endoplasmic reticulum (ER) stress. Although definitive demonstration of the UPR in AS has been elusive, in specific cell populations, such as macrophages, the UPR appears to be increased (1). In HLA–B27–transgenic rats, the misfolding of HLA–B27 in macrophages precedes the UPR, but UPR activation was not seen in splenocytes, further pointing to cell-specific effects (2). We recently reported an increase in HLA–B27 misfolding in the gut of patients with AS and those with Crohn's disease (CD) compared to healthy control subjects, but no up-regulation of the UPR was demonstrated (3).

Endoplasmic reticulum aminopeptidase 2 (ERAP-2) polymorphisms are associated with both CD and AS (4). ERAP-2 is an enzyme involved in trimming of peptides for major histocompatibility complex (MHC) class I loading. Aberrant ERAP-2 function could influence the stability of peptide HLA–B27 (pB27), the formation of MHC class I free heavy chains (FHCs), and the level of

Supported by the Arthritis Society, Canada. Dr. Haroon's work was supported by the Arthritis Program, Toronto Western Hospital, the Arthritis Research Foundation (CIBC award), the Arthritis Society, and the Canadian Institutes of Health Research.

[1]Zhenbo Zhang, PhD, Fanxing Zeng, PhD: Toronto Western Research Institute, Toronto, Ontario, Canada; [2]Francesco Ciccia, MD, PhD, Giuliana Guggino, MD, Riccardo Alessandro, PhD, Giovanni Triolo, MD: Università degli Studi di Palermo, Palermo, Italy; [3]Kirby Yee, BSc: Toronto Western Research Institute, Toronto, Ontario, Canada, and McMaster University, Hamilton, Ontario, Canada; [4]Hasan Abdullah, MSc: Toronto Western Research Institute and University of Toronto, Toronto, Ontario, Canada; [5]Mark S. Silverberg, MD, PhD: University of Toronto and Mount Sinai Hospital, Toronto, Ontario, Canada; [6]Nigil Haroon, MD, PhD, DM: Toronto Western Research Institute, University of Toronto, and University Health Network, Toronto, Ontario, Canada.

Address correspondence to Nigil Haroon, MD, PhD, DM, 1E-425, Toronto Western Hospital, 399 Bathurst Street, Toronto, Ontario M5T2S8, Canada. E-mail: Nigil.Haroon@uhn.ca.

Submitted for publication September 27, 2016; accepted in revised form December 20, 2016.

ER stress. A structurally and functionally related aminopeptidase, ERAP-1, has also been reported to be associated with AS. We have reported alterations in MHC class I FHC expression in the presence of the *ERAP1* single-nucleotide polymorphism (SNP) rs27044 (5).

Up to 25% of the general population are homozygous for the G allele (GG) of the *ERAP2* SNP rs2248374, which leads to alternate splicing and formation of an aberrant messenger RNA (mRNA) that undergoes nonsense-mediated decay, resulting in absence of *ERAP2* (6). Alternately, in the presence of the T allele of rs2549782, the 392N variant of *ERAP2* is encoded, resulting in increased aminopeptidase activity (7). Herein we studied the influence of *ERAP2* deficiency, resulting from the presence of the rs2248374 SNP, on HLA–B27 misfolding and the UPR in patients with AS. In addition, we studied the linkage disequilibrium (LD) between SNPs rs2248374 and rs2549782 of *ERAP2* in our AS cohort.

PATIENTS AND METHODS

Patients. Study patients comprised sequential HLA–B27–positive patients with AS (diagnosed in accordance with the modified New York criteria [8]) who were not receiving biologic therapy. We previously reported significantly lower levels of FHCs in patients with AS homozygous for the minor allele of the *ERAP1* SNP rs27044 (5). To avoid confounding by *ERAP1*, we included only patients with the major allele C of the rs27044 SNP (CC/CG). We performed a sensitivity analysis in which we included patients who were homozygous for the G allele (GG). Bath AS Disease Activity Index scores (9), the erythrocyte sedimentation rate, and C-reactive protein levels were collected from all patients.

Genotyping. Peripheral blood cell DNA was genotyped by allelic discrimination assays (Applied Biosystems) for the *ERAP1* SNPs rs27044 and rs30187 and the *ERAP2* SNPs rs2248374 and rs2549782. Due to strong LD in the *ERAP2* locus, we studied the distribution of the *ERAP2* SNPs rs2549782 (reported to increase the function of the ERAP-2 protein in vitro) and rs2248374 (reported to lead to absence of ERAP-2 protein expression) in our database of genotyped patients with AS and those with CD. *ERAP2* has been linked to both AS and CD. For this study, we had access to a large cohort of patients with CD who were already genotyped for *ERAP2*. Moreover, by including 2 cohorts of patients, those with AS and those with CD, we were able to increase the sample size and avoid bias from testing just the AS cohort alone. Subsequently, we used the SNP Annotation and Proxy Search (SNAP) tool and the 1000 Genomes Pilot 1 data set (10).

Flow cytometry. Peripheral blood mononuclear cells (PBMCs) were isolated from patients with AS. In sets of one million PBMCs each, the cells were stained with mouse anti-human HC10 antibodies (for assessment of cell surface FHC) or ME1 antibodies (for identification of pB27), followed by allophycocyanin-conjugated goat anti-mouse IgG as a secondary antibody. Antibodies to CD19 (for identification of B cells) and CD14 (for identification of monocytes) were used to identify individual cell populations. The mean fluorescence intensities (MFIs) of FHC and pB27 expression were each assessed by flow cytometry using a FACSCalibur (BD Biosciences). FHC expression was corrected for HLA–B27 expression by calculating the ratio of HC10 MFI to ME1 MFI. Unstained cells and cells stained with secondary antibody alone were used as a control. Although in C1R-B27 cells, staining with the ME1 antibody is likely to reveal the presence of predominantly pB27, staining with this antibody can recognize other HLA–B alleles, such as B7 and B22, that may be present in patients with AS.

Cell lines and culture conditions. C1R-B27 cells, a human B lymphoblastoid cell line that has low endogenous HLA class I expression and that is stably transfected with HLA–B27, were gifted by Dr. José López de Castro (Centro de Biología Molecular Severo Ochoa, Madrid, Spain). The stable, *ERAP2* short hairpin RNA (shRNA)–transfected C1R-B27 cells were maintained in RPMI 1640 medium containing 10% fetal bovine serum, 2 m*M* glutamine, 50 units/ml penicillin, 50 μg/ml streptomycin, 0.55 μg/ml G418, and 0.1 μg/ml puromycin.

Generation of vector-based *ERAP2* RNA–interfering plasmids. Two *ERAP2* shRNA oligomers were designed and commercially generated at The Centre for Applied Genomics (Toronto, Ontario, Canada). These oligonucleotides were added with *Bam* HI and *Eco* RI restriction sites at the 5′ and 3′ ends, respectively (see Supplementary Table 1, available on the *Arthritis & Rheumatology* web site at http://onlinelibrary.wiley.com/doi/10.1002/art.40033/abstract), and annealed and cloned into a pSiHIV-H1 vector. The resulting plasmids containing shRNA sequences for *ERAP2* are hereafter referred to as *ERAP2* shRNA1 and *ERAP2* shRNA2.

Transduction of HLA–B27–expressing C1R cells. Lentivirus supernatants were generated by transiently transfecting 293T cells with constructed Lenti-PacHIV plasmids. C1R-B27 cells were infected with a lentivirus supernatant containing *ERAP2* shRNA plasmids. After infection, the cells were centrifuged and the medium was replaced with 1 ml RPMI 1640. This process was repeated, and after 24 hours, puromycin was added to select stable cells.

Quantitative reverse transcription–polymerase chain reaction (qRT-PCR). Total cellular RNA was isolated with TRIzol reagent and treated with DNase to remove any genomic DNA contamination. Total RNA was quantified in a NanoDrop Bioanalyzer, and complementary DNA was synthesized. Primers used for qRT-PCR analyses are detailed in Supplementary Table 2 (available on the *Arthritis & Rheumatology* web site at http://onlinelibrary.wiley.com/doi/10.1002/art.40033/abstract). The qRT-PCR analyses were performed in a 7900HT Fast Real-Time PCR system using Power SYBR Green Master Mix (both from Life Technologies). The relative gene expression for each sample was determined. Expression values for GAPDH or β-actin were used as internal controls. Each sample was run 3 times.

Semiquantitative RT-PCR for determination of X-box binding protein 1 [spliced] (XBP1[S]) genes. Primers used for elucidating the expression profile of XBP1[S] genes were as follows: forward primer 5′-CTGGAACAGCAAGTGGTAGATTTAG-3′, and reverse primer 5′-AGTCAATACCGCCAGAATCCA-3′. After amplification, 10 μl of each reaction mixture was detected by 2.5% agarose gel electrophoresis, and the bands were visualized with ethidium bromide, followed by analysis with ImageJ software (National Institutes of Health). GAPDH was used as an internal control.

Western blotting. Protein concentrations were determined with a BCA Protein Assay Kit (Fisher Scientific) from clarified cell lysates. Total protein from cell lysates was separated using

10% sodium dodecyl sulfate–polyacrylamide gel electrophoresis mini gels, followed by transfer to nitrocellulose membranes. The antibodies used to probe the membrane were as follows: antibodies to *ERAP2* (1:1,000), antibodies to CCAAT/enhancer binding protein homologous protein 10 (CHOP) (1:2,000), and antibodies to β-actin or GAPDH (1:5,000) (all from BD Biosciences). The membrane was incubated with horseradish peroxidase–conjugated anti-mouse or anti-rabbit antibodies (1:10,000) (Amersham) for 1 hour at room temperature. The membrane was developed using an enhanced chemiluminescence detection system (Fisher Scientific).

Statistical analysis and study approval. All data were analyzed with GraphPad Prism 5 software. The Mann-Whitney U test was used for comparisons between groups. The Research Ethics Board of the University Health Network (Toronto, Ontario, Canada) approved the studies.

RESULTS

Increased MHC class I FHC expression in AS patients with no *ERAP2*. We assessed the effect of loss of *ERAP2* on HLA–B27 expression in patients with AS. Of 39 patients with AS included in the study (10 of whom were female), 13 were *ERAP2* null. The mean ± SD age of the patients was 41.4 ± 13.3 years. There was no significant difference in the baseline characteristics of patients with and those without *ERAP2* expression. The distribution of rs30187 and rs27044 *ERAP1* SNPs in AS patients with and those without *ERAP2* was not significantly different (see Supplementary Tables 3 and 4, available on the *Arthritis & Rheumatology* web site at http://onlinelibrary.wiley.com/doi/10.1002/art.40033/abstract).

Compared to AS patients with *ERAP2*, there was significantly higher FHC expression on PBMCs from *ERAP2*-null patients with AS ($P = 0.009$) (Figure 1A), specifically the expression of FHCs on monocytes ($P = 0.045$) (Figure 1B). When corrected for pB27 expression, there was a significantly higher FHC:pB27 ratio in all PBMCs ($P = 0.002$) (Figure 1C) as well as monocytes ($P = 0.01$) (Figure 1D) from *ERAP2*-null patients with AS. There was a trend toward higher FHC expression on the surface of B cells (significantly different by *t*-test, but not by Mann-Whitney test) (data not shown). There was no significant difference in pB27 expression between patients with and those without *ERAP2* or between those with and those without the *ERAP1* SNP rs30187 (data not shown). In 2 patients, only pB27 expression was assessed, because HC10 antibodies did not stain the cells.

An additional sensitivity analysis, which included the 2 previously excluded patients homozygous for the G allele of *ERAP1* rs27044, showed that FHC expression was significantly higher with loss of *ERAP2* in PBMCs, and that the FHC:pB27 ratio was significantly higher in both PBMCs and monocytes from *ERAP2*-null patients with AS (see Supplementary Figures 1A–D, available on the *Arthritis & Rheumatology* web site at http://onlinelibrary.wiley.com/doi/10.1002/art.40033/abstract). Moreover, the results of this sensitivity analysis showed that the intensity of staining with HC10 in the monocytes was no longer significantly different between those with and those without *ERAP2*. Furthermore, FHC expression did not significantly change in the presence or absence of the *ERAP1* rs30187 SNP (see Supplementary Figures 1E and F, http://onlinelibrary.wiley.com/doi/10.1002/art.40033/abstract).

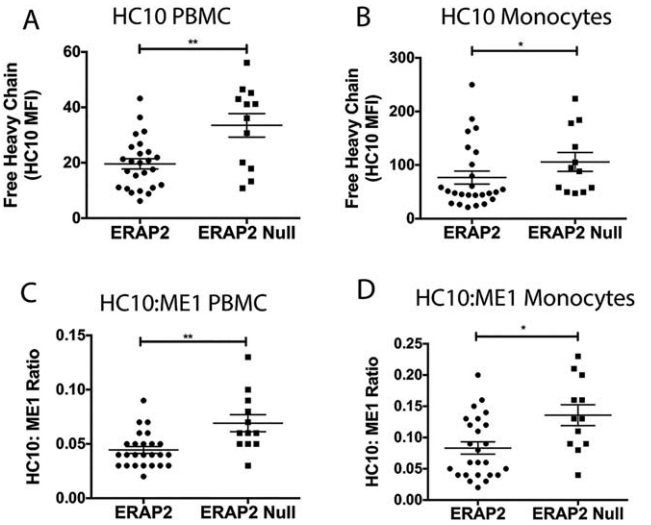

Figure 1. *ERAP2* deficiency increases major histocompatibility complex (MHC) class I free heavy chains (FHCs) in peripheral blood mononuclear cells (PBMCs) and monocytes from patients with ankylosing spondylitis (AS). **A** and **B,** MHC class I FHC expression was assessed by staining with the HC10 antibody in PBMCs **(A)** and monocytes **(B)** from patients with AS. **C** and **D,** To correct for HLA–B27 expression, the ratio of mean fluorescence intensity (MFI) of FHC expression to that of intact peptide HLA–B27 (pB27) expression (ratio of HC10 to ME1 antibody staining) on the surface of PBMCs **(C)** and monocytes **(D)** was compared between AS patients with *ERAP2* expression and those without *ERAP2* expression (*ERAP2* Null). Symbols represent individual patients; horizontal lines with bars show the mean ± SD. * = $P < 0.05$; ** = $P < 0.01$.

Association of *ERAP2* suppression with increased FHC expression. Detection of *ERAP2* mRNA and ERAP-2 protein in C1R-B2705 stable cells was carried out by qRT-PCR and Western blotting. At the mRNA level, there was a 70% reduction in *ERAP2* mRNA in C1R-B2705 stable cells transfected with *ERAP2* shRNA (Figure 2A). ERAP-2 protein levels decreased by 90% and 70% in the presence of shRNA1 and shRNA2, respectively (Figures 2B–D).

Similar to the findings in *ERAP2*-null patients with AS, the expression of FHC was higher in C1R-B27 cells after *ERAP2* suppression (Figures 2E and F). *ERAP2* suppression did not significantly change the intensity of ME1 staining of the B27 heterodimer in the presence of

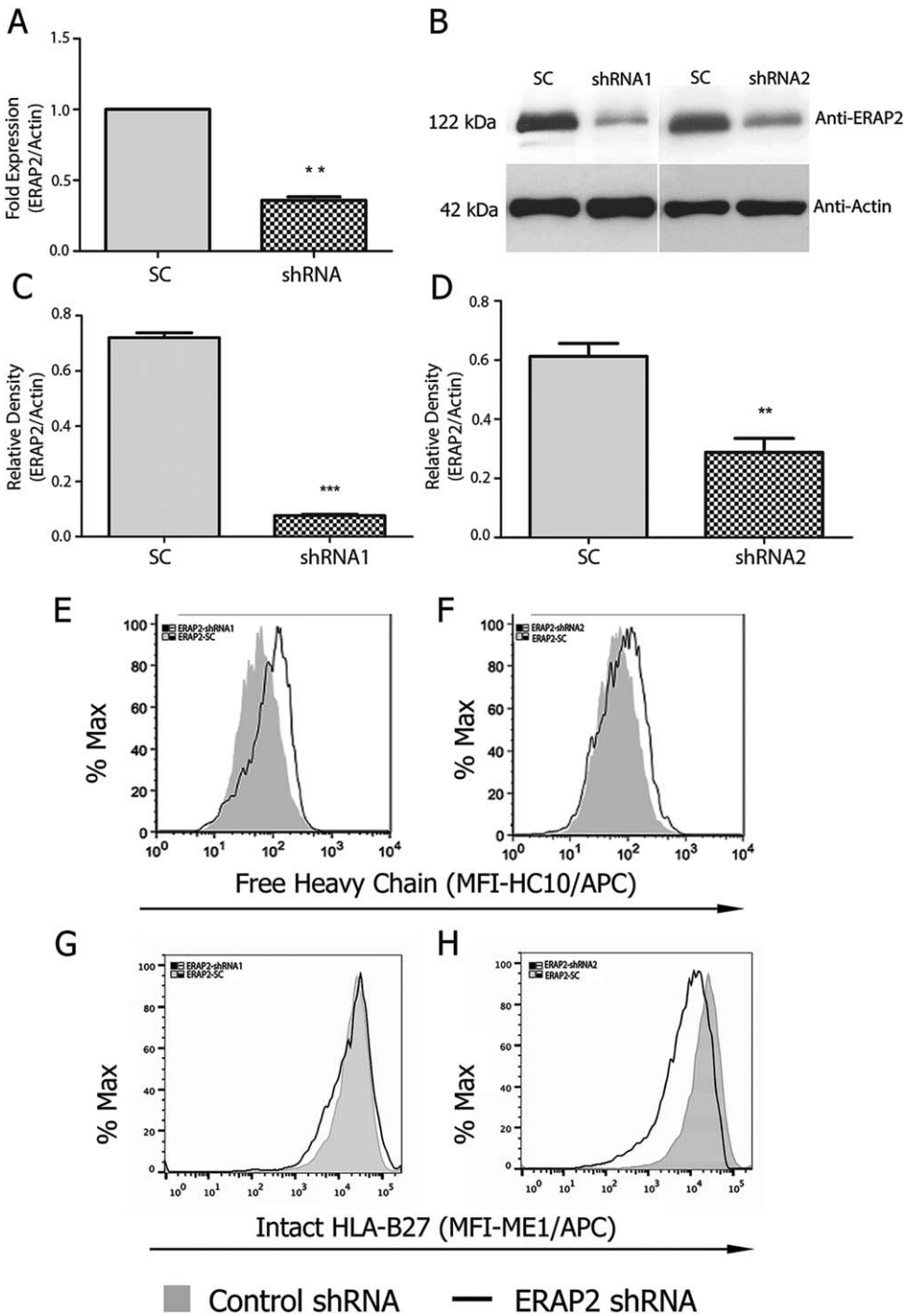

Figure 2. *ERAP2* suppression in C1R-B27 cells increases MHC class I FHC expression. *ERAP2* was suppressed in C1R-B27 cells using 2 separate short hairpin RNAs (shRNA1 and shRNA2); a scrambled sequence shRNA (SC) was used as a control. **A** and **B,** *ERAP2* suppression by the 2 shRNAs was measured by quantitative reverse transcription–polymerase chain reaction **(A)** and Western blotting **(B)**. **C** and **D,** Quantitation of *ERAP2* suppression shows a reduction in endoplasmic reticulum aminopeptidase 2 protein by 90% with shRNA1 **(C)** and 70% with shRNA2 **(D)** compared to scrambled control shRNA. **E** and **F,** HC10 antibodies and flow cytometry were used to detect changes in FHC expression in C1R-B27 cells following suppression of *ERAP2* by shRNA1 **(C)** and shRNA2 **(D)** compared to scrambled control shRNA. **G** and **H,** ME1 staining of the B27 heterodimer did not change with the addition of *ERAP2* shRNA1 **(G)** and slightly decreased with *ERAP2* shRNA2 **(H)** as compared to scrambled control shRNA. In **A, C,** and **D,** bars show the mean and SD of triplicate experiments. ** = $P < 0.01$; *** = $P < 0.001$. APC = allophycocyanin (see Figure 1 for other definitions).

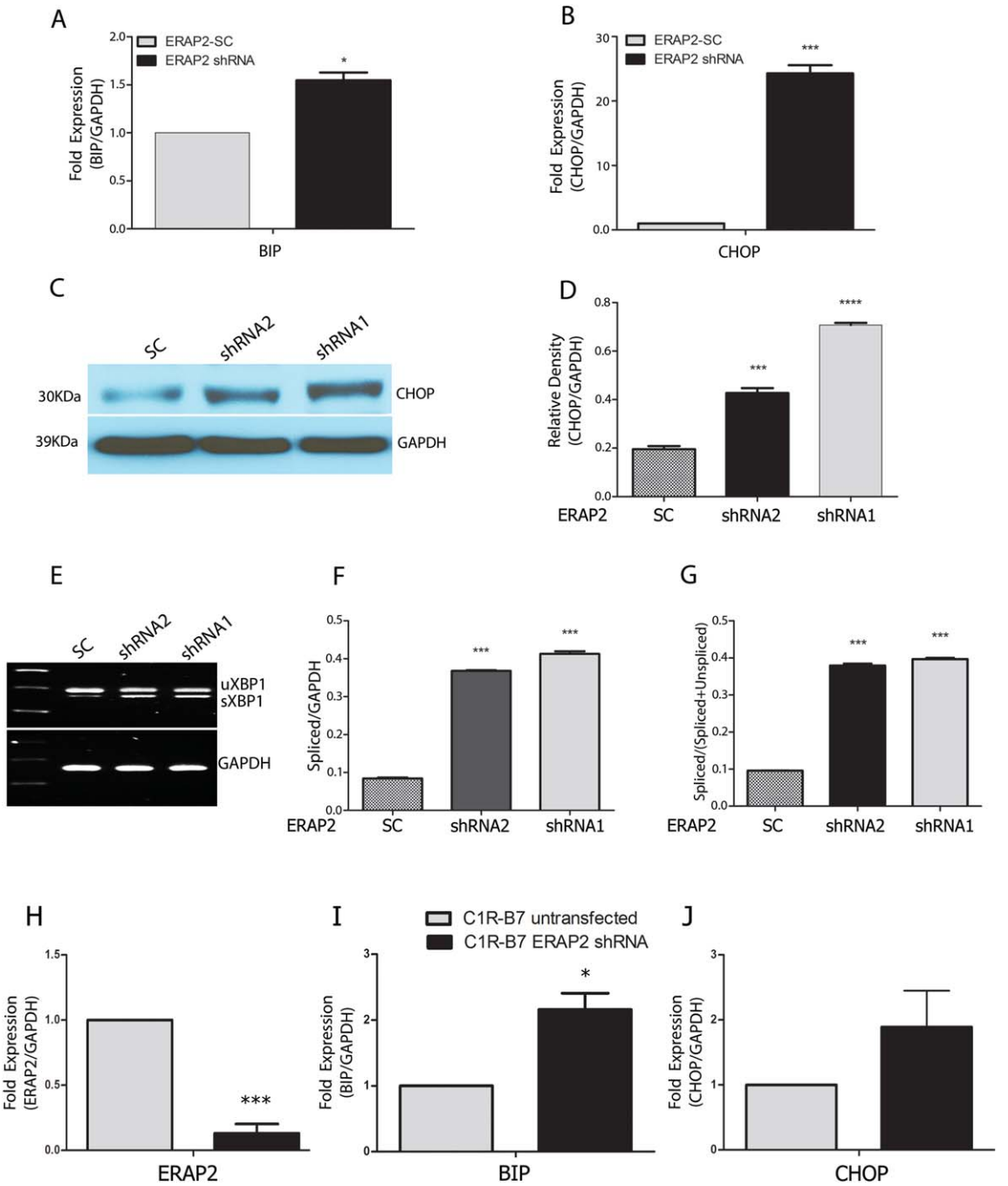

Figure 3. *ERAP2* suppression increases the unfolded protein response (UPR) in C1R-B27 cells. **A** and **B,** Following *ERAP2* suppression in C1R-B27 cells by *ERAP2* short hairpin RNA (shRNA), the UPR was assessed by real-time reverse transcription–polymerase chain reaction (PCR) for the fold change in mRNA expression levels of BiP (**A**) and CCAAT/enhancer binding protein homologous protein 10 (CHOP) (**B**), relative to scrambled control shRNA (SC). **C** and **D,** CHOP protein expression was assessed by Western blotting (**C**) and quantified as the relative density of expression (**D**). **E,** Semiquantitative PCR was used for the X-box binding protein 1 [spliced] (sXBP1) assay. Increased splicing, relative to unspliced XPB1 (uXBP1), indicates UPR activation. GAPDH was used as a loading control. **F** and **G,** The density of the XBP1 spliced bands was normalized to the values for GAPDH (**F**) and total XBP1 (**G**). **H,** *ERAP2* expression was suppressed with transfection of C1R-B7 cells with *ERAP2* shRNA as compared to that in untransfected cells. **I** and **J,** Real-time PCR analysis shows an increase in BiP expression (**I**) but not CHOP expression (**J**) after *ERAP2* suppression in C1R-B7 cells. Bars show the mean and SD of triplicate experiments. $* = P < 0.05$; $*** = P < 0.001$; $**** = P < 0.0001$.

shRNA1 (Figure 2G) and it slightly decreased with *ERAP2* shRNA2 (Figure 2H), as compared to the effects of control shRNA. There was no significant reduction in *ERAP1* levels in the presence of either of the *ERAP2* shRNAs, ruling out the possibility of nonspecific *ERAP1* inhibition (see Supplementary Figure 2, available on the *Arthritis & Rheumatology* web site at http://onlinelibrary.wiley.com/doi/10.1002/art.40033/abstract).

Association of *ERAP2* suppression with activation of the UPR. Silencing of *ERAP2* led to increased expression of BiP (1.42-fold) and CHOP (20-fold), which are key UPR genes (Figures 3A and B). At the protein level, CHOP increased 4.1-fold and 2.5-fold, respectively, in the presence of each *ERAP2* shRNA as compared to a control, scrambled sequence shRNA (Figures 3C and D).

XBP1[S] gene expression was higher after *ERAP2* suppression with both of the *ERAP2* shRNAs compared to the control shRNA (Figure 3E). Moreover, compared to the effects of control shRNA, in the presence of the *ERAP2* shRNAs, XBP1[S] expression was 4.7-fold higher and 4.3-fold higher for values normalized to the expression of GAPDH and total XBP1, respectively (Figures 3F and G).

ERAP2 deficiency differentially affected cells expressing HLA–B7. Unlike the findings in untransfected C1R-B27 cells, there was an increase in the levels of BiP, but no significant increase in the levels of CHOP following 90% suppression of *ERAP2* in C1R-B7 cells (Figures 3H–J).

Strong LD between *ERAP2* SNPs. There is known LD between the *ERAP2* SNPs (11). The rs2549782 polymorphism, which leads to a K392N change in *ERAP2*, results in altered aminopeptidase activity (7). We studied the prevalence of the SNPs rs2549782 and rs2248374 in our research database. *ERAP2* is associated with both CD and AS, and in our database, 145 patients with AS and 406 Caucasian patients with inflammatory bowel disease were genotyped for both rs2549782 and rs2248374. There were 141 patients who were homozygous for the rs2549782 T allele of *ERAP2* (see Supplementary Table 5, available on the *Arthritis & Rheumatology* web site at http://onlinelibrary.wiley.com/doi/10.1002/art.40033/abstract). However, all patients who were homozygous for the rs2549782 T allele (rs2248374 GG) were *ERAP2* null. Thus, the gain-of-function *ERAP2* variant 392N is likely not expressed, due to the strong LD with the *ERAP2*-null allele.

Subsequently, using the SNAP tool and the 1000 Genomes Pilot 1 data set (10), we found strong LD between the 2 AS-associated *ERAP2* SNPs rs2549782 and rs2248374 ($D' = 1$, $r^2 = 0.90$). There are no strong recombination hotspots in the *ERAP2*-LNPEP area of chromosome 5 that would explain the strong LD in this region (see Supplementary Figure 3, available on the *Arthritis & Rheumatology* web site at http://onlinelibrary.wiley.com/doi/10.1002/art.40033/abstract). Thus, in the 1000 Genomes database, there is strong LD in the region of *ERAP2*, and in our analyses of the AS and CD data sets, all patients homozygous for the gain-of-function *ERAP2* variant actually have no *ERAP2* expression.

DISCUSSION

Herein we have shown a link between decreased *ERAP2* levels, increased surface FHC levels, and UPR activation. We found that HLA–B27–positive patients with AS lacking *ERAP2* had higher FHC expression on the surface of PBMCs. In addition, *ERAP2* suppression in a B27 cell line led to increased FHC levels and activation of the UPR. Most importantly, although the observed data indicated that changes to surface FHC expression had occurred with decreases in the *ERAP2* levels, potentially decreased stability of the pB27 complex could lead to changes in HLA–B27 FHC expression in the ER as well. We studied the major UPR pathways by testing for the expression of BiP, XBP1[S] (the inositol-requiring protein 1 pathway), and CHOP (downstream of both the activating transcription factor 4 and RNA-dependent protein kinase–like endoplasmic reticulum kinase pathways). Our results in C1R-B7 and C1R-B27 cells indicated that UPR activation is more prominent but not exclusive to HLA–B27.

In HLA–B27–transgenic rats, high expression of HLA–B27 correlated with the UPR and preceded the onset of disease. Demonstration of the UPR has been difficult in humans. Up-regulation of the UPR was demonstrated in synovial macrophages from patients with AS and correlated with disease activity (1,12). A recent study, which was not corrected for treatment effects, showed no link between the UPR and AS (13). Our study in lamina propria mononuclear cells derived from the gut of patients with AS and those with CD did not show significant UPR activation (3). However, the observed autophagy activation could mask the UPR by clearing misfolded proteins for cell survival (14). Studies on the pathogenesis of AS in humans are plagued by the difficulty in obtaining biopsy specimens from affected axial joints. Human UPR studies in these target joints have not been performed.

Strong LD in the region of *ERAP2* has been reported before (11). Two large studies demonstrated that the G allele of rs2248374 is protective in AS (11,15). In light of these reports, the possibility remains that it might be feasible to consider the notion that loss of *ERAP2* leading to UPR changes has pathogenic significance. Loss of *ERAP2* is seen only when patients are homozygous for the G allele of rs2248374 (GG). A large proportion of heterozygous individuals in the control group could tip the analysis toward a higher frequency of the G allele in controls. To date, there

is no report comparing the prevalence of *ERAP2*-null individuals between AS cohorts and controls. It is important to remember that a significant proportion of patients with AS will have *ERAP2* deficiency. As we showed in our study, 142 patients with AS or CD (25.7%) were homozygous for the *ERAP2*-null allele. It is possible that in this subset of patients, *ERAP2* deficiency could modify the immune-inflammatory response. In our previous family study, the *ERAP2* rs2549782 T allele (conveying increased activity of ERAP-2) in a haplotype with *ERAP1* was associated with AS (4). Although we did not test the rs2248374 G allele frequency, due to LD between the *ERAP2* rs2549782 T allele and rs2248374 G allele, it is likely that all patients who were homozygous for the rs2549782 risk allele were *ERAP2* null.

Extensive *ERAP1* genotyping of patients was not done, as this study was designed on the basis of 2 major SNPs (rs27044 and rs30187) with functional consequences that were initially reported to be associated with AS and replicated in multiple cohorts. We have previously shown that patients with AS who have the *ERAP1* rs27044 SNP but not the rs30187 SNP have significant alterations in the expression of FHC on monocytes (5). Based on this information, we analyzed only patients with the nonrisk allele of *ERAP1* rs27044. However, we cannot rule out the possibility that additional *ERAP1* SNPs might have influenced our results. We confirmed that *ERAP2* shRNA caused no reduction in *ERAP1* levels. Hence, the results seen in the present study are likely to be specific to *ERAP2*.

Our results differ from those in a recent study by Robinson et al (16), but our study had important differences, including the use of freshly isolated PBMCs in a larger cohort of patients. We selected patients who were not receiving any biologic drugs. Moreover, in our study, the UPR was tested in vitro to directly establish the impact of *ERAP2* suppression with appropriate controls.

In conclusion, the results of this study demonstrate a functional interaction of *ERAP2* and HLA–B27. *ERAP2* suppression was associated with increased FHC expression and activation of the UPR. Alterations in the fine balance of the *ERAP2*–HLA–B27–UPR functional interaction could play a role in the pathogenesis of AS.

ACKNOWLEDGMENT

The authors thank Dr. Robert D. Inman (Toronto Western Hospital) for his help with recruitment of patients for this study.

AUTHOR CONTRIBUTIONS

All authors were involved in drafting the article or revising it critically for important intellectual content, and all authors approved the final version to be published. Dr. Haroon had full access to all of the data in the study and takes responsibility for the integrity of the data and the accuracy of the data analysis.

Study conception and design. Zhang, Haroon.
Acquisition of data. Zhang, Ciccia, Zeng, Guggino, Yee, Abdullah, Silverberg, Alessandro, Triolo, Haroon.
Analysis and interpretation of data. Zhang, Ciccia, Zeng, Guggino, Yee, Abdullah, Silverberg, Alessandro, Triolo, Haroon.

REFERENCES

1. Dong W, Zhang Y, Yan M, Liu H, Chen Z, Zhu P. Upregulation of 78-kDa glucose-regulated protein in macrophages in peripheral joints of active ankylosing spondylitis. Scand J Rheumatol 2008;37:427–34.
2. Turner MJ, Delay ML, Bai S, Klenk E, Colbert RA. HLA–B27 up-regulation causes accumulation of misfolded heavy chains and correlates with the magnitude of the unfolded protein response in transgenic rats: implications for the pathogenesis of spondylarthritis-like disease. Arthritis Rheum 2007;56:215–23.
3. Ciccia F, Accardo-Palumbo A, Rizzo A, Guggino G, Raimondo S, Giardina A, et al. Evidence that autophagy, but not the unfolded protein response, regulates the expression of IL-23 in the gut of patients with ankylosing spondylitis and subclinical gut inflammation. Ann Rheum Dis 2014;73:1566–74.
4. Tsui FW, Haroon N, Reveille JD, Rahman P, Chiu B, Tsui HW, et al. Association of an ERAP1 ERAP2 haplotype with familial ankylosing spondylitis. Ann Rheum Dis 2010;69:733–6.
5. Haroon N, Tsui FW, Uchanska-Ziegler B, Ziegler A, Inman RD. Endoplasmic reticulum aminopeptidase 1 (ERAP1) exhibits functionally significant interaction with HLA-B27 and relates to subtype specificity in ankylosing spondylitis. Ann Rheum Dis 2012;71:589–95.
6. Andres AM, Dennis MY, Kretzschmar WW, Cannons JL, Lee-Lin SQ, Hurle B, et al. Balancing selection maintains a form of ERAP2 that undergoes nonsense-mediated decay and affects antigen presentation. PLoS Genet 2010;6:e1001157.
7. Evnouchidou I, Birtley J, Seregin S, Papakyriakou A, Zervoudi E, Samiotaki M, et al. A common single nucleotide polymorphism in endoplasmic reticulum aminopeptidase 2 induces a specificity switch that leads to altered antigen processing. J Immunol 2012;189:2383–92.
8. Van der Linden S, Valkenburg HA, Cats A. Evaluation of diagnostic criteria for ankylosing spondylitis: a proposal for modification of the New York criteria. Arthritis Rheum 1984;27:361–8.
9. Garrett S, Jenkinson T, Kennedy LG, Whitelock H, Gaisford P, Calin A. A new approach to defining disease status in ankylosing spondylitis: the Bath Ankylosing Spondylitis Disease Activity Index. J Rheumatol 1994;21:2286–91.
10. Johnson AD, Handsaker RE, Pulit SL, Nizzari MM, O'Donnell CJ, de Bakker PI. SNAP: a web-based tool for identification and annotation of proxy SNPs using HapMap. Bioinformatics 2008;24:2938–9.
11. Robinson PC, Costello ME, Leo P, Bradbury LA, Hollis K, Cortes A, et al. ERAP2 is associated with ankylosing spondylitis in HLA-B27-positive and HLA-B27-negative patients. Ann Rheum Dis 2015;74:1627–9.
12. Feng Y, Ding J, Fan CM, Zhu P. Interferon-γ contributes to HLA-B27-associated unfolded protein response in spondyloarthropathies. J Rheumatol 2012;39:574–82.
13. Neerinckx B, Carter S, Lories RJ. No evidence for a critical role of the unfolded protein response in synovium and blood of patients with ankylosing spondylitis. Ann Rheum Dis 2014;73:629–30.
14. Bernales S, Schuck S, Walter P. ER-phagy: selective autophagy of the endoplasmic reticulum. Autophagy 2007;3:285–7.
15. International Genetics of Ankylosing Spondylitis Consortium (IGAS), Cortes A, Hadler J, Pointon JP, Robinson PC, Karaderi T, et al. Identification of multiple risk variants for ankylosing spondylitis through high-density genotyping of immune-related loci. Nat Genet 2013;45:730–8.
16. Robinson PC, Lau E, Keith P, Lau MC, Thomas GP, Bradbury LA, et al. ERAP2 functional knockout in humans does not alter surface heavy chains or HLA-B27, inflammatory cytokines or endoplasmic reticulum stress markers. Ann Rheum Dis 2015;74:2092–5.

ARTHRITIS & RHEUMATOLOGY
Vol. 69, No. 5, May 2017, pp 1016–1027
DOI 10.1002/art.40049

Efficacy and Safety of Subcutaneous Belimumab in Systemic Lupus Erythematosus

A Fifty-Two–Week Randomized, Double-Blind, Placebo-Controlled Study

William Stohl,[1] Andreas Schwarting,[2] Masato Okada,[3] Morton Scheinberg,[4] Andrea Doria,[5] Anne E. Hammer,[6] Christi Kleoudis,[7] James Groark,[8] Damon Bass,[8] Norma Lynn Fox,[9] David Roth,[8] and David Gordon[8]

Objective. **To assess the efficacy and safety of subcutaneous (SC) belimumab in patients with systemic lupus erythematosus (SLE).**

Methods. **Patients with moderate-to-severe SLE (score of ≥8 on the Safety of Estrogens in Lupus Erythematosus National Assessment [SELENA] version of the SLE Disease Activity Index [SLEDAI]) were randomized 2:1 to receive weekly SC belimumab 200 mg or placebo by prefilled syringe in addition to standard SLE therapy for 52 weeks. The primary end point was the SLE Responder Index (SRI4) at week 52. Secondary end points were reduction in the corticosteroid dosage and time to severe flare. Safety was assessed according to the adverse events (AEs) reported and the laboratory test results.**

Results. **Of 839 patients randomized, 836 (556 in the belimumab group and 280 in the placebo group) received treatment. A total of 159 patients withdrew before the end of the study. At entry, mean SELENA–SLEDAI scores were 10.5 in the belimumab group and 10.3 in the placebo group. More patients who received belimumab were SRI4 responders than those who received placebo (61.4% versus 48.4%; odds ratio [OR] 1.68 [95% confidence interval (95% CI) 1.25–2.25]; $P = 0.0006$). In the belimumab group, both time to and risk of severe flare were improved (median 171.0 days versus 118.0 days; hazard ratio 0.51 [95% CI 0.35–0.74]; $P = 0.0004$), and more patients were able to reduce their corticosteroid dosage by ≥25% (to ≤7.5 mg/day) during weeks 40–52 (18.2% versus 11.9%; OR 1.65 [95% CI 0.95–2.84]; $P = 0.0732$), compared with placebo. AE incidence was comparable between treatment groups; serious AEs were reported by 10.8% of patients taking belimumab and 15.7% of those taking placebo. A worsening of IgG hypoglobulinemia by ≥2 grades occurred in 0.9% of patients taking belimumab and 1.4% of those taking placebo.**

ClinicalTrials.gov identifier: NCT01484496.

Supported by GlaxoSmithKline (BLISS-SC identifier: BEL112341) and Human Genome Sciences, Inc., a subsidiary of GlaxoSmithKline.

[1]William Stohl, MD, PhD: University of Southern California, Los Angeles; [2]Andreas Schwarting, MD: Acura Kliniken Rheinland-Pfalz AG, Bad Kreuznach, Germany; [3]Masato Okada, MD: St. Luke's International Hospital, Tokyo, Japan; [4]Morton Scheinberg, MD: Rheumatology Hospital Abreu Sodre, São Paulo, Brazil; [5]Andrea Doria, MD: University of Padua, Padua, Italy; [6]Anne E. Hammer: GlaxoSmithKline, Research Triangle Park, North Carolina; [7]Christi Kleoudis, MPH: Parexel, Raleigh-Durham, North Carolina; [8]James Groark, MD, Damon Bass, DO, David Roth, MD, David Gordon, MB, ChB: GlaxoSmithKline, Philadelphia, Pennsylvania; [9]Norma Lynn Fox, PhD, MPH: GlaxoSmithKline, Rockville, Maryland.

Dr. Stohl has received consulting fees and/or honoraria from Akros Pharma, Jansen, Sanofi, GlaxoSmithKline, and Pfizer (less than $10,000 each). Dr. Schwarting has received speaking fees (less than $10,000) and research grants from GlaxoSmithKline. Dr. Okada has received speaking fees and/or honoraria from Santen Pharmaceutical, Mitsubishi Tanabe Pharma, Pfizer, and Abbott Japan (less than $10,000 each). Dr. Scheinberg has received consulting fees from Pfizer, GlaxoSmithKline, Epirus, Samsung Bioepis, and Janssen (less than $10,000 each). Dr. Doria has received speaking fees and/or honoraria from GlaxoSmithKline and Eli Lilly (less than $10,000 each). Ms Hammer, Ms Kleoudis, and Mr. Gordon, and Drs. Groark, Bass, Fox, and Roth own stock or stock options in GlaxoSmithKline.

Address correspondence to William Stohl, MD, PhD, University of Southern California Keck School of Medicine, 2011 Zonal Avenue, HMR 711, Los Angeles, CA 90033. E-mail: stohl@usc.edu.

Submitted for publication May 23, 2016; accepted in revised form January 12, 2017.

Conclusion. **In patients with moderate-to-severe SLE, weekly SC doses of belimumab 200 mg plus standard SLE therapy significantly improved their SRI4 response, decreased severe disease flares as compared with placebo, and had a safety profile similar to placebo plus standard SLE therapy.**

B lymphocyte stimulator (BLyS), also known as B cell–activating factor, is a potent B cell survival and differentiation factor (1–5). Its overexpression drives systemic lupus erythematosus (SLE)–like disease in mice (6–8). BLyS is also associated with SLE in humans (9–11) and correlates with disease activity (12,13). Pharmacologic neutralization or genetic elimination of BLyS successfully treats and/or prevents murine SLE (6,14,15).

Intravenous (IV) administration of belimumab, a recombinant human monoclonal antibody that binds to and inhibits the biologic activity of BLyS (16), was shown in 2 large, multicenter, randomized, double-blind, placebo-controlled trials in patients with SLE (the Study of Belimumab in Subjects with SLE 52-week trial [BLISS-52] and the BLISS 76-week trial [BLISS-76]) to be safe and efficacious at a dose of 10 mg/kg in combination with standard SLE therapy (17,18). IV administration of belimumab was subsequently approved by the US Food and Drug Administration and the European Medicines Agency for the treatment of patients with active, autoantibody-positive SLE who are receiving standard SLE therapy, including corticosteroids, antimalarials, immunosuppressants, and nonsteroidal antiinflammatory drugs (19,20).

The approval of a drug for SLE was a breakthrough; however, the IV route of administration poses challenges for some patients. Patients must visit a clinic or infusion center every 2 weeks for the first 3 doses and then every 4 weeks thereafter (21), thereby incurring substantial costs in time for travel to/from the drug-administering site, time for the infusion itself, and time for postinfusion monitoring. In addition, substantial financial expenses related to clinic personnel and supplies are incurred.

The ability to administer subcutaneous (SC) belimumab away from the clinic would largely eliminate these costs and thereby enhance treatment options for patients with SLE. Indeed, more patients chose SC treatment over IV treatment in a study of patients with rheumatoid arthritis, with a decreased need to travel to receive an infusion being an influential factor (22).

A liquid formulation of belimumab has been developed, along with a prefilled syringe and an autoinjector device for administering belimumab SC. In a single-dose study, healthy volunteers self-administered belimumab 200 mg SC using the prefilled syringe or the autoinjector device; both injection devices demonstrated good usability, reliability, and safety (23). The 200 mg SC dose was selected in order to achieve a target belimumab steady-state area under the curve exposure following SC administration similar to that obtained with 10 mg/kg IV every 4 weeks (24,25).

The objectives of the present study were to evaluate the efficacy, safety, and tolerability of belimumab SC administered via prefilled syringe in patients with active, autoantibody-positive SLE. Our findings are presented below.

PATIENTS AND METHODS

Study design and patient population. This was a 52-week randomized, double-blind, placebo-controlled study (BLISS-SC ID BEL112341; ClinicalTrials.gov ID NCT01484496) carried out at 177 sites in 30 countries in North, Central, and South America, Eastern and Western Europe, Australia, and Asia between November 2011 and February 2015. All study patients provided written informed consent prior to enrollment. The study and all protocols were institutional review board–approved and were conducted in accordance with the Declaration of Helsinki, 2008 (26).

Patients ≥18 years of age were required to have a diagnosis of SLE according to the American College of Rheumatology criteria (27), with antinuclear antibodies and/or anti–double-stranded DNA (anti-dsDNA) antibodies and a score of ≥8 on the Safety of Estrogens in Lupus Erythematosus National Assessment (SELENA) version of the SLE Disease Activity Index (SLEDAI) at screening (range 0–105) (28). Those with severe lupus kidney disease (proteinuria >6 gm/24 hours or equivalent according to a spot urinary protein-to-creatinine ratio or a serum creatinine level >2.5 mg/dl) or severe central nervous system (CNS) lupus were excluded.

Patients were randomized 2:1 to receive weekly doses of belimumab 200 mg or placebo administered SC with a prefilled syringe in addition to stable doses of standard SLE therapy. No loading dose was used. Randomization was stratified by a screening SELENA–SLEDAI score (≤9 versus ≥10), complement level (those with versus those without low C3 and/or C4), and race (black versus non-black). Patients must have received a stable SLE medication regimen for at least 30 days prior to enrollment. Background SLE medications were restricted, such that patients who received a protocol-prohibited medication or a dosage that exceeded the protocol-defined limits were deemed to have failed treatment and were analyzed as nonresponders from the date of treatment failure through week 52. The first and second SC doses of study drug were carried out at the study site under supervision; at the investigator's discretion, patients or caregivers could then administer subsequent doses at home. The injection site was rotated weekly between the abdomen and the thigh. Patients recorded in a logbook the date, injection site, and amount of dose administered.

End points and assessments. The primary end point was the SLE Responder Index (SRI4) response rate at week 52 (29). The SRI4 is a composite index requiring a ≥4-point reduction in the SELENA–SLEDAI score, no worsening (increase of <0.3 from baseline) in the physician's global assessment (on a 0–10-cm visual analog scale), and no new British Isles Lupus Assessment Group (BILAG) A organ domain score or 2 new BILAG B organ domain scores at week 52 compared with baseline. On

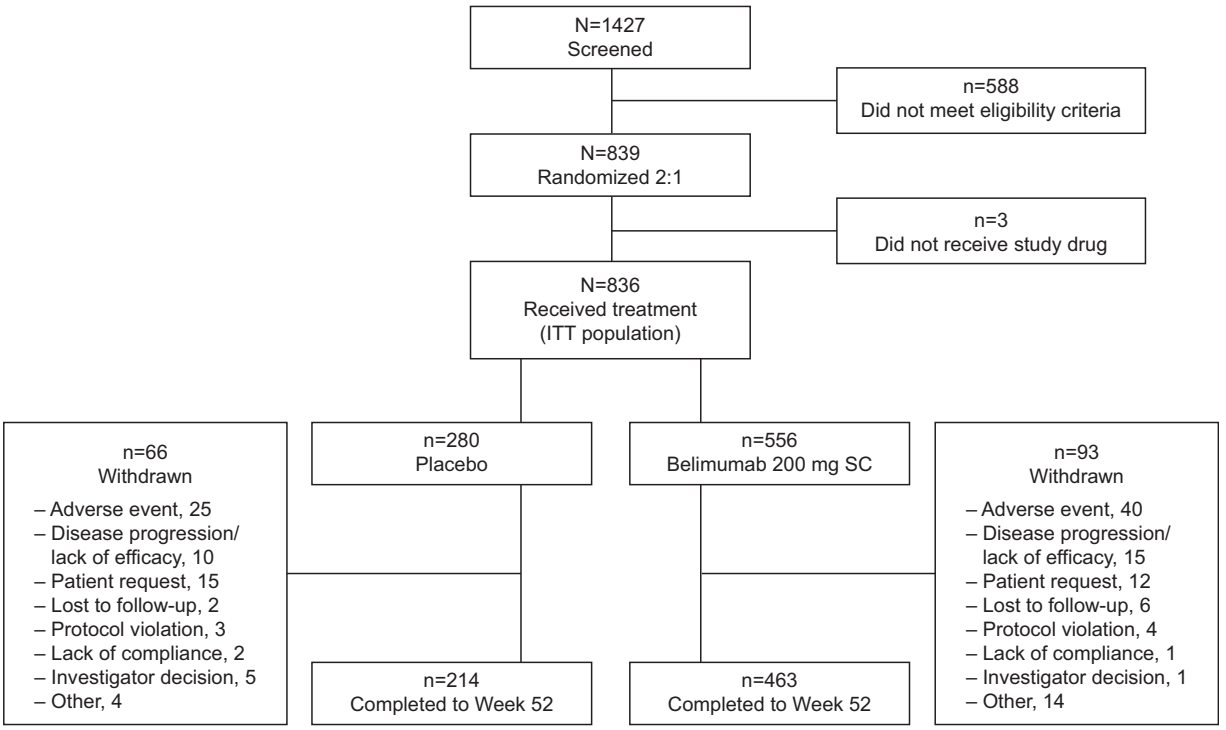

Figure 1. Flow chart showing the disposition of the study patients from initial screening to the end of week 52. ITT = intent-to-treat; SC = subcutaneous.

sensitivity analyses, the primary end point at week 52 was also repeated for the completer and per-protocol populations.

The end points that supported the primary end point included the SRI4 by visit, SRI4 components by visit, and the SRI5–8 by visit. The definition of SRI5–8 was the same as that of SRI4, except with increasingly higher thresholds for SELENA–SLEDAI score reduction of 5–8 points. The time to first SRI4 that was maintained through week 52 was also assessed. The SRI4 response and change from baseline in SELENA–SLEDAI score, excluding the anti-dsDNA and complement components, were analyzed post hoc.

Key secondary end points were time to first severe flare (as measured by the SLE flare index, modified to exclude the single criterion of increased SELENA–SLEDAI score to >12) (30–32) and reduction in corticosteroid dosage (percentage of patients among those receiving >7.5 mg/day at baseline who experienced a mean dosage reduction of ≥25% from baseline to ≤7.5 mg/day during weeks 40–52).

Other prespecified corticosteroid use end points included the percentage of patients with any increase in corticosteroid use, the percentage of patients whose dosage was reduced from >7.5 mg/day at baseline to ≤7.5 mg/day, and cumulative corticosteroid dose.

The SRI4 was analyzed across subgroups, including the baseline SELENA–SLEDAI score (≤9 and ≥10), race (black and non-black), baseline corticosteroid use (receiving and not receiving corticosteroids), and body weight quartiles (<55.05 kg, ≥55.05 kg to <65.15 kg, ≥65.15 kg to <78.25 kg, and ≥78.25 kg). Subgroup analyses were also completed post hoc for Hispanic or Latino patients. Mean change from baseline in the Functional Assessment of Chronic Illness Therapy–Fatigue (FACIT-Fatigue) score (range 0–52) (33) and the percentage of patients with an improvement in the FACIT-Fatigue score of ≥4 (minimal clinically important difference) were analyzed by visit (weeks 4, 8, 12, 24, 36, and 52).

The time to first renal flare over 52 weeks was analyzed among patients with baseline proteinuria >0.5 gm/24 hours. Renal flare was defined as the reproducible development (i.e., confirmed at the subsequent clinical visit) of 1 or more of the following 3 features: 1) an increase in 24-hour urinary protein to >1,000 mg if baseline was <200 mg or to >2,000 mg if baseline was 200–1,000 mg or to more than twice a baseline value of >1,000 mg; 2) a decrease in the glomerular filtration rate of >20%, accompanied by proteinuria (>1,000 mg/24 hours), hematuria (≥4 red blood cells [RBCs]/high-power field [hpf]), and/or cellular (RBC and white blood cell) casts; and 3) new hematuria (≥11–20 RBCs/hpf) or a 2-grade increase in hematuria compared with baseline, associated with >25% dysmorphic RBCs, glomerular in origin, and accompanied by an 800-mg increase in 24-hour urinary protein level or new RBC casts (34).

Safety was evaluated by adverse event (AE) reporting, laboratory parameters, and immunogenicity testing. AEs were coded according to the Medical Dictionary for Regulatory Activities system organ class and preferred term. A serious AE (SAE) was defined as an AE that resulted in any of the following outcomes: death, was life-threatening (i.e., an immediate threat to life), inpatient hospitalization, prolongation of an existing hospitalization, persistent or significant disability/

Table 1. Demographic and clinical characteristics of the study patients at baseline, by treatment group*

	Placebo (n = 280)	Belimumab 200 mg SC (n = 556)
Female, no. (%)	268 (95.7)	521 (93.7)
Age, mean ± SD years	39.6 ± 12.61	38.1 ± 12.10
Weight, mean ± SD kg	69.5 ± 19.76	68.6 ± 18.15
Enrollment by region, no. (%)		
US	84 (30.0)	153 (27.5)
Americas, excluding US	57 (20.4)	115 (20.7)
Western Europe/Australia/Israel	19 (6.8)	48 (8.6)
Eastern Europe	59 (21.1)	129 (23.2)
Asia	61 (21.8)	111 (20.0)
Race/ethnicity		
Hispanic or Latino	80 (28.6)	160 (28.8)
Not Hispanic or Latino	200 (71.4)	396 (71.2)
Disease duration, median (range) years	4.6 (0–38)	4.3 (0–35)
SELENA–SLEDAI (range 0–105)†		
Mean ± SD	10.3 ± 3.04	10.5 ± 3.19
Median (range)	10.0 (4–22)	10.0 (2–24)
Score of ≤9, no. (%)	112 (40.0)	204 (36.7)
Score of ≥10, no. (%)	168 (60.0)	352 (63.3)
Organ system involvement, no. (%)		
Mucocutaneous	248 (88.6)	487 (87.6)
Musculoskeletal	218 (77.9)	438 (78.8)
Immunologic	210 (75.0)	423 (76.1)
Renal	41 (14.6)	58 (10.4)
Hematologic	23 (8.2)	40 (7.2)
Vascular	18 (6.4)	46 (8.3)
Cardiovascular and respiratory	18 (6.4)	29 (5.2)
Constitutional	3 (1.1)	7 (1.3)
Central nervous system	2 (0.7)	7 (1.3)
Disease flare, no. (%)‡		
At least 1 flare	57 (20.4)	92 (16.5)
At least 1 severe flare	4 (1.4)	8 (1.4)
Physician's global assessment, mean ± SD (0–10-cm VAS)	1.5 ± 0.45	1.6 ± 0.43
FACIT-Fatigue, mean ± SD (range 0–52)	32.1 ± 11.35	31.9 ± 12.17
Medications, no. (%)		
Corticosteroids only	31 (11.1)	59 (10.6)
Immunosuppressants only	7 (2.5)	10 (1.8)
Antimalarials only	16 (5.7)	44 (7.9)
Corticosteroids and immunosuppressants only	50 (17.9)	88 (15.8)
Corticosteroids and antimalarials only	93 (33.2)	201 (36.2)
Immunosuppressants and antimalarials only	13 (4.6)	13 (2.3)
Corticosteroids, immunosuppressants, and antimalarials	67 (23.9)	133 (23.9)
Immunosuppressants		
Azathioprine	58 (20.7)	107 (19.2)
Methotrexate	39 (13.9)	52 (9.4)
Mycophenolate mofetil	34 (12.1)	70 (12.6)

* SC = subcutaneous; VAS = visual analog scale; FACIT-Fatigue = Functional Assessment of Chronic Illness Therapy–Fatigue subscale.
† Patients had a score of ≥8 on the Safety of Estrogens in Lupus Erythematosus National Assessment version of the Systemic Lupus Erythematosus Disease Activity Index (SELENA–SLEDAI) at screening (occurring within 35 days prior to baseline). A total of 39 belimumab-treated patients and 24 placebo-treated patients had scores that were <8 at baseline (lowest score was 2).
‡ Occurring during the screening period (day −35 to day 0).

incapacity, congenital anomaly/birth defect, or was medically important (i.e., required treatment to prevent one of the medical outcomes above).

Blood samples for pharmacokinetic analyses were obtained from all randomized patients before the injection at weeks 0, 4, 8, 16, 24, and 52 and at the 8-week follow-up visit.

Statistical analysis. A sample size of 816 (544 taking belimumab and 272 taking placebo) was calculated to provide at least 90% power at a $P = 0.05$ significance level, assuming the true treatment difference was 12% improvement (belimumab versus placebo) at week 52; the treatment difference was based on the response in the phase III belimumab IV studies (17,18).

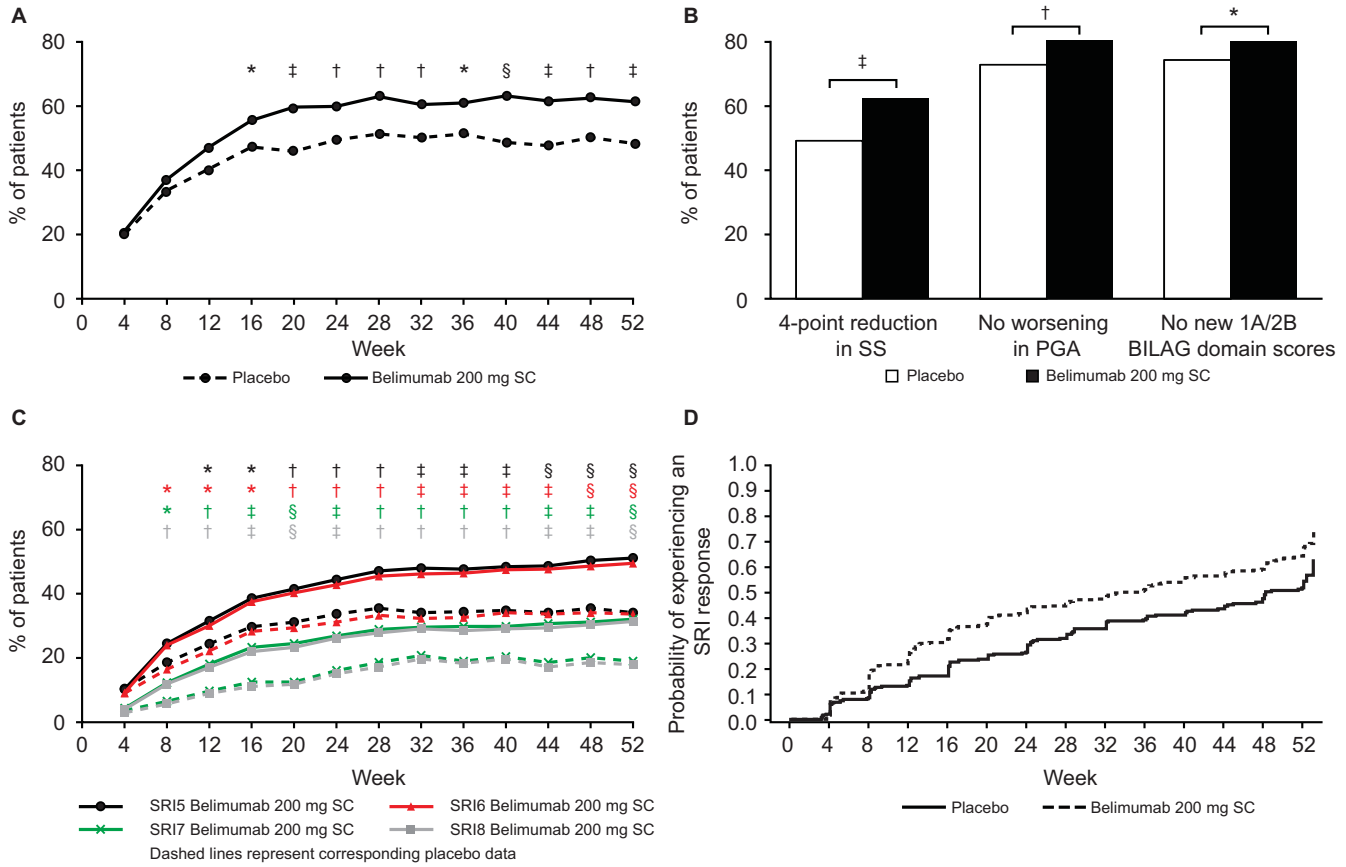

Figure 2. A, Systemic Lupus Erythematosus Responder Index (SRI4) responses over time in patients randomized to receive placebo or belimumab 200 mg subcutaneously (SC). **B,** Percentage of patients with responses on the individual components of the SRI4 at week 52: the Safety of Estrogens in Lupus Erythematosus National Assessment version of the Systemic Lupus Erythematosus Disease Activity Index (SS), the physician's global assessment (PGA), and the British Isles Lupus Assessment Group (BILAG) domain, by treatment group. **C,** SRI5, 6, 7, and 8 responses over time in the 2 treatment groups. **D,** Time to first SRI4 response that was maintained through week 52 in the intent-to-treat population, by treatment group. $* = P \leq 0.05$; $\dagger = P \leq 0.01$; $\ddagger = P \leq 0.001$; $\S = P \leq 0.0001$.

The intent-to-treat (ITT) population was defined as all patients who were randomized and received at least 1 dose of study medication. A completer population (patients who completed 52 weeks of treatment) and a per-protocol population (patients in the ITT who did not have a major protocol deviation) were included in the sensitivity analyses. The pharmacokinetic population included all patients who received at least 1 dose of study medication and who contributed at least 1 post-belimumab pharmacokinetic sample.

A step-down sequential testing procedure was used for the primary and 2 key secondary end points to control the overall Type I error rate (the incorrect rejection of a true null hypothesis). The prespecified sequence for assessing statistical significance (2-sided $\alpha = 0.05$) was as follows: 1) SRI4 response rate at 52 weeks; 2) time to first severe SLE flare; and 3) percentage of patients with a reduction in corticosteroid dosage. End points in this sequence could only be interpreted as being statistically significant if statistical significance was achieved by all prior tests. The proportion of patients with an SRI4 response at week 52 was compared between treatment groups using a logistic regression model. Analyses of other efficacy end points (all 2-sided with a significance level of 0.05) were not subjected to a multiple comparison procedure. Patients who withdrew or were deemed to have failed treatment were analyzed as nonresponders in the primary analysis.

RESULTS

Patient population. There were 836 patients in the ITT population, and 159 withdrew overall. The most common reasons for withdrawal were AEs, patient request, and disease progression/lack of efficacy (Figure 1). The majority of patients were female (93.7% receiving belimumab, 95.7% receiving placebo), with a mean age of 38.6 years (38.1 years in the belimumab group, 39.6 years in the placebo group) and a mean/median baseline SELENA–SLEDAI score of 10.4/10.0 (10.5/10.0 in the belimumab group, 10.3/10.0 in the placebo group) (Table 1). The majority of patients received corticosteroids at baseline (86.5%

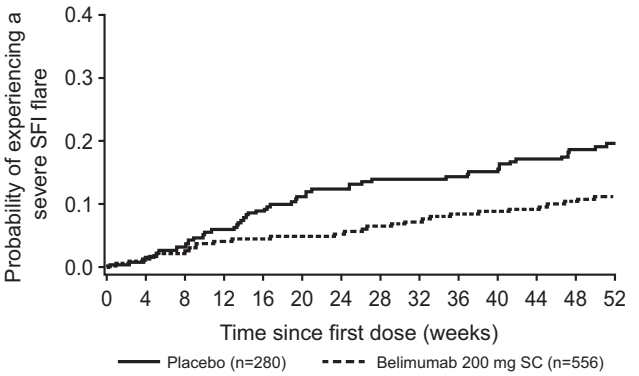

Figure 3. Time to severe flare in patients randomized to receive placebo or belimumab 200 mg subcutaneously (SC). The probability of experiencing a severe flare, according to the Systemic Lupus Erythematosus Flair Index (SFI), is plotted against the time since the first dose of study drug.

belimumab, 86.1% placebo), and approximately one-third of patients received corticosteroids in combination with antimalarials. Almost half of the patients received immunosuppressants (43.9% belimumab, 48.9% placebo), with azathioprine being the one most commonly received (Table 1). The mean ± SD self-reported compliance with the SC injections was 96.4 ± 9.37% for belimumab and 96.4 ± 9.75% for placebo.

SRI4 response. At week 52, 61.4% of belimumab patients were SRI4 responders compared with 48.4% for placebo (odds ratio [OR] 1.68 [95% confidence interval (95% CI) 1.25–2.25]; $P = 0.0006$) (Figure 2A). The SRI4 response was significantly greater in the belimumab group as compared with the placebo group as early as week 16, and the significant difference was sustained up to week 52 (Figure 2A). At week 52, more patients who received belimumab were SRI4 responders compared with placebo in both the completer population (n = 677) (72.9% versus 63.1%; OR 1.54 [95% CI 1.07–2.20]; $P = 0.0185$) and the per-protocol population (n = 789) (61.9% versus 48.3%; OR 1.75 [95% CI 1.29–2.37]; $P = 0.0003$).

All components of the SRI4 showed statistical significance at week 52 (Figure 2B). The immunologic, musculoskeletal, mucocutaneous, and vascular SELENA–SLEDAI organ systems improved significantly more in the belimumab group than in the placebo group at week 52 (data not shown). Improvement in the other organ systems (including renal) favored belimumab numerically, but the analyses in these other organ systems were limited by small sample sizes. Among patients with a BILAG A or B organ domain score at baseline, a significantly greater improvement was observed at week 52 in the belimumab group compared with the placebo group for the vasculitis, mucocutaneous, and musculoskeletal organ domains, but not the other organ domains.

Compared with the placebo group, the SRI5 response was significantly greater in the belimumab group from week 12 through week 52 (Figure 2C). The SRI6, SRI7, and SRI8 responses were significantly greater from week 8 through week 52 ($P \leq 0.0001$ for each comparison at week 52). The median time to first SRI4 response that was maintained through week 52 was 235.0 days (interquartile range [IQR] 85.0–not calculable) for belimumab and 338.0 days (IQR 141.0–386.0) for placebo (hazard ratio [HR] 1.48 [95% CI 1.21–1.81]; $P = 0.0001$) (Figure 2D).

When the anti-dsDNA and complement components of the SELENA–SLEDAI were excluded from the composite score (post hoc analysis), the SRI4 response rate was significantly greater in the belimumab group as compared with placebo (59.6% versus 48.0%; OR 1.58 [95% CI 1.18–2.13]; $P = 0.0023$). The least squares mean ± SEM change from baseline in the SELENA–SLEDAI score (excluding anti-dsDNA and complement components) at week 52 was not significantly different between treatment groups (-3.96 ± 0.246 for belimumab, -3.47 ± 0.295 for placebo; $P = 0.0997$).

Time to severe flare. Patients who received belimumab were 49% less likely to experience severe flare as compared with placebo across the 52 weeks of study (HR 0.51 [95% CI 0.35–0.74]; $P = 0.0004$). Among patients experiencing a severe flare, the median time to severe flare was 171.0 days (IQR 57.0–257.0) for belimumab (n = 59 [10.6%]) versus 118.0 days (IQR 62.0–259.0) for placebo (n = 51 [18.2%]) (Figure 3). The risk of any flare was also significantly lower in the belimumab group compared with placebo (60.6% versus 68.6%; HR 0.78 [95% CI 0.65–0.93]; $P = 0.0061$).

Changes in corticosteroid dosage. At baseline, 335 patients in the belimumab group and 168 in the placebo group were receiving corticosteroids at a dosage of >7.5 mg/day (60.2% of patients overall) and were eligible for this analysis. More patients who received belimumab were able to reduce their corticosteroid dosage by ≥25%, to ≤7.5 mg/day, during weeks 40–52 as compared with placebo (18.2% versus 11.9%), although this difference did not achieve statistical significance (OR 1.65 [95% CI 0.95–2.84]; $P = 0.0732$). Fewer patients in the belimumab group (8.1% [45 of 556]) than in the placebo group (13.2% [37 of 280]) had an increase in corticosteroid dosage through to week 52 (OR 0.55 [95% CI 0.34–0.87]; $P = 0.0117$); the differences were significant from week 20 to week 52, with the exception of week 32. The proportion of patients who had a corticosteroid dosage reduction from >7.5 mg/day at baseline to ≤7.5 mg/day at week 52 was 20.0% (67 of 335) in the belimumab group and 14.3% (24 of 168) in the placebo

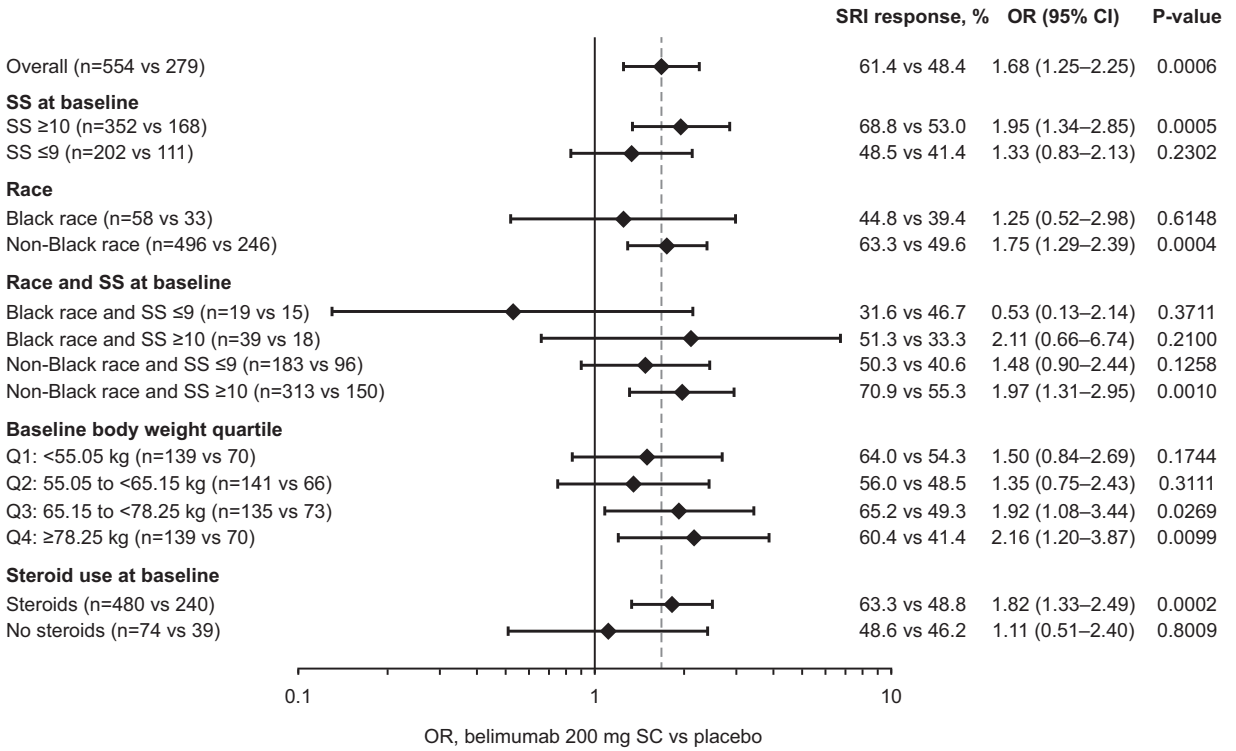

Figure 4. Systemic Lupus Erythematosus Responder Index (SRI4) subgroup responses at week 52 in patients randomized to receive belimumab 200 mg subcutaneously (SC) versus placebo. Bars illustrate the odds ratios (ORs) and 95% confidence intervals (95% CIs) that are given at the right. Broken vertical line indicates the overall OR. SRI = Systemic Lupus Erythematosus Responder index; SS = the Safety of Estrogens in Lupus Erythematosus National Assessment version of the Systemic Lupus Erythematosus Disease Activity Index.

group ($P = 0.1181$). There was a difference of 633.50 mg in the mean ± SD cumulative dose of corticosteroids over 52 weeks (3,933.8 ± 3,660.76 for belimumab and 4,567.3 ± 5,981.53 for placebo; $P = 0.4299$).

Subgroup responses at week 52. Results of the subgroup analyses are summarized in Figure 4, which includes the number of patients in each subgroup. At week 52, significantly more patients with baseline SELENA–SLEDAI scores of ≥10 who received belimumab were SRI4 responders compared with those who received placebo. There was a trend toward an increase in SRI4 responders for belimumab versus placebo among patients with baseline SELENA–SLEDAI scores of ≤9, although this did not reach statistical significance (Figure 4).

The SRI4 response among non-black patients who received belimumab was statistically significantly higher than that among non-black patients who received placebo (OR 1.75 [95% CI 1.29–2.39]; $P = 0.0004$) (Figure 4). Among the black patients, the week 52 SRI4 response was numerically higher for belimumab than for placebo, but the difference did not achieve statistical significance. Post hoc analyses showed that 73.8% (118 of 160) of Hispanic or Latino patients receiving belimumab experienced an SRI4 response at week 52, compared with 50.0% (40 of 80) of those receiving placebo ($P = 0.0003$). Among patients of non-Hispanic or Latino ethnicity, 56.3% (belimumab) and 47.7% (placebo) of patients were responders ($P = 0.0407$). While those receiving belimumab in both ethnic groups reported statistically significant improvements at week 52 (compared with placebo), the numerical difference was greater in the Hispanic or Latino group.

In the third and fourth quartiles for baseline body weight, significantly more patients who received belimumab were SRI4 responders than patients who received placebo (Figure 4). For the first and second quartiles, the differences between treatment arms did not achieve statistical significance.

The SRI4 response at week 52 was significantly greater in belimumab-treated patients who were receiving corticosteroids at baseline compared with placebo-treated patients receiving corticosteroids at baseline (Figure 4). There was no significant difference in SRI4 response at week 52 between belimumab and placebo among patients who were not taking corticosteroids at baseline.

FACIT-Fatigue scores. Scores on the FACIT-Fatigue scale improved over time in both treatment

groups. The mean change from baseline was significantly greater in the belimumab group as compared with the placebo group at weeks 8, 36, and 52 (adjusted mean change at week 52 was 4.4 versus 2.7; $P = 0.0130$) but not at weeks 4, 12, and 24. The percentage of patients with an improvement in the FACIT-Fatigue score of ≥4 also generally increased over time. At week 52, more patients who received belimumab had an improvement of ≥4 compared with placebo (44.4% versus 36.1%; OR 1.42 [95% CI 1.05–1.94]; $P = 0.0245$).

Time to first renal flare. Fewer patients with baseline proteinuria >0.5 gm/24 hours in the belimumab group (11 of 99) had a renal flare compared with those in the placebo group (13 of 48) (11.1% versus 27.1%; HR 0.40 [95% CI 0.18–0.90]; $P = 0.0272$). The median time to first renal flare for patients with baseline proteinuria >0.5 gm/24 hours who experienced a flare was 83.0 days (IQR 33.0–192.0) for belimumab versus 113.0 days (IQR 85.0–229.0) for placebo. In the overall population, fewer patients in the belimumab group had a renal flare as compared with placebo, although this difference was not statistically significant (4.7% versus 7.5%; HR 0.57 [95% CI 0.32–1.01]; $P = 0.0532$). All first renal flares had occurred by week 40 and week 48 in the belimumab and placebo groups, respectively.

Safety. Overall, 449 patients in the belimumab group (80.8%) and 236 patients in the placebo group (84.3%) experienced at least 1 AE (Table 2). The most common types were infections and infestations. SAEs were reported for 10.8% and 15.7% of patients, respectively. The most common types were infections and infestations, renal and urinary disorders, and nervous system disorders. Treatment-related AEs were reported for 31.1% of the belimumab group and 26.1% of the placebo group. For further details, see Supplementary Tables S1 and S2 (available on the *Arthritis & Rheumatology* web site at http://onlinelibrary.wiley.com/doi/10.1002/art.40049/abstract).

Local injection site reactions occurred in 34 patients in the belimumab group (6.1%) and 7 patients in the placebo group (2.5%). All were mild or moderate in severity, and no serious or severe injection site reactions were reported. The incidence of hypersensitivity reactions was similar between treatment groups. Three deaths were reported in the belimumab group (0.5%; 3 infections [bacterial sepsis, urosepsis, and tuberculosis of the CNS]) and 2 were reported in the placebo group (0.7%; 1 vascular [cardiac death] and 1 SLE-related [thrombocytopenia]). Herpes zoster was reported in 18 patients in the belimumab group (3.2%) and 13 patients in the placebo group (4.6%); 1 case was serious (belimumab group). Fifteen patients in the belimumab group (2.7%) and 10 patients in the placebo group (3.6%) experienced depression; none of these episodes were serious. Two cases of serious suicidal ideation (0.4% taking belimumab, as adjudicated by GlaxoSmithKline physicians) and no cases of suicidal behavior were reported.

Table 2. Summary of AEs reported during the study*

	Placebo (n = 280)	Belimumab 200 mg SC (n = 556)
All AEs by system organ class		
AEs†	236 (84.3)	449 (80.8)
Infections and infestations	159 (56.8)	308 (55.4)
Gastrointestinal disorders	68 (24.3)	125 (22.5)
Musculoskeletal and connective tissue disorders	66 (23.6)	124 (22.3)
Nervous system disorders	53 (18.9)	111 (20.0)
Skin and subcutaneous tissue disorders	60 (21.4)	80 (14.4)
SAEs‡	44 (15.7)	60 (10.8)
Infections and infestations	15 (5.4)	23 (4.1)
Renal and urinary disorders	7 (2.5)	8 (1.4)
Nervous system disorders	6 (2.1)	8 (1.4)
Treatment-related AEs	73 (26.1)	173 (31.1)
AEs resulting in study discontinuation	25 (8.9)	40 (7.2)
AEs of special interest		
Malignancies	1 (0.4)	2 (0.4)
Postinjection systemic reactions§	25 (8.9)	38 (6.8)
Serious	0	0
Serious delayed nonacute hypersensitivity reactions§	1 (0.4)	0
All infections	21 (7.5)	30 (5.4)
Serious	3 (1.1)	8 (1.4)
Opportunistic infections§	1 (0.4)	2 (0.4)
Serious	0	1 (0.2)
Herpes zoster	13 (4.6)	18 (3.2)
Serious	0	1 (0.2)
Sepsis	3 (1.1)	6 (1.1)
Serious	2 (0.7)	4 (0.7)
Depression	10 (3.6)	15 (2.7)
Serious	0	0
Serious suicidal ideation§	0	2 (0.4)
Suicidal behavior§	0	0
Deaths	2 (0.7)	3 (0.5)

* Values are the number (%) of patients reporting the event. SC = subcutaneous.
† Adverse events (AEs) that occurred in ≥20% of patients in either treatment group are listed.
‡ Serious adverse events (SAEs) that occurred in >2% of patients in either treatment group are listed.
§ As adjudicated by GlaxoSmithKline physicians.

Four patients experienced worsening of IgG hypoglobulinemia from grade 0 to grade 2 in each treatment group (0.7% receiving belimumab and 1.4% receiving placebo). An additional case of worsening from grade 0 to grade 4 occurred in the belimumab group (0.2%).

The incidence of AEs was higher in both groups among patients in the highest body weight quartile (≥78.25 kg; 86.3% of the belimumab group and 90.0% of the placebo group) as compared with those in the lowest body weight quartile (<55.05 kg; 76.3% of the belimumab group and 77.1% of the placebo group).

Pharmacokinetics. The median plasma concentration in the group taking belimumab increased from week 4 (65.0 μg/ml) to week 24 (104.8 μg/ml), and decreased slightly at week 52 (86.8 μg/ml) (Supplementary Figure 1, available on the *Arthritis & Rheumatology* web site at http://onlinelibrary.wiley.com/doi/10.1002/art.40049/abstract).

DISCUSSION

This was the first phase III randomized, double-blind, placebo-controlled study to investigate the safety and efficacy of belimumab 200 mg SC plus standard SLE therapy in patients with SLE. The results demonstrate that weekly SC doses of belimumab 200 mg plus standard SLE therapy significantly reduced SLE disease activity as early as week 16. The treatment effect for belimumab SC is consistent with that observed with belimumab 10 mg/kg IV in the phase III, randomized, double-blind, placebo-controlled BLISS-52 and BLISS-76 studies (17,18). The present study was designed to test the efficacy of belimumab SC rather than its equivalence (or lack of same) to belimumab IV, so no conclusion can be drawn with regard to equivalence. Nevertheless, the 2 previous belimumab IV trials and the present belimumab SC trial each met their respective primary end points and demonstrated consistent and significant clinical benefits of belimumab plus standard SLE therapy in patients with SLE.

The inclusion criteria for this study required a SELENA–SLEDAI score of ≥8 at screening, whereas the IV BLISS-52 and BLISS-76 studies required a SELENA–SLEDAI score of ≥6 (17,18). This requirement for a higher SELENA–SLEDAI was driven by data from the IV studies that highlighted that patients needed a higher level of disease activity at baseline in order to have the opportunity to achieve the 4-point reduction in SELENA–SLEDAI that was needed to meet the SRI4 end point. Despite that requirement, the mean baseline SELENA–SLEDAI scores in the present study were similar to those in the IV studies (10.0 and 9.5 for belimumab 10 mg/kg, 9.7 and 9.8 for placebo in the BLISS-52 and BLISS-76 studies, respectively). A greater proportion of patients in the present study had SELENA–SLEDAI scores of ≥10 (62%), as compared with those in the BLISS-52 (53%) and BLISS-76 (51%) studies (17,18).

A post hoc analysis of the present (BLISS-SC) study and the pooled BLISS-52 and BLISS-76 studies was undertaken to compare only patients with SELENA–SLEDAI scores of ≥8 at baseline. In this analysis, the SRI4 responses at week 52 were 63.2% for belimumab 200 mg SC versus 50.0% for placebo and 57.4% for belimumab 10 mg/kg IV versus 41.7% for placebo (data on file; GlaxoSmithKline). While no head-to-head comparison between SC and IV belimumab was done, the results of the present study and of this post hoc analysis suggest consistency across the IV and SC studies.

Belimumab SC demonstrated further efficacy benefits, such as reduction of severe flare by 49% over 52 weeks, onset of action as early as week 16, and a shorter time to first SRI4 response that was maintained through week 52 compared with placebo. Significant reductions in severe flare were observed with belimumab 10 mg/kg IV over 52 weeks in the BLISS-52 study (18) and with belimumab 1 mg/kg IV over 76 weeks in the BLISS-76 study (17). Onset of action was also comparable to that in the BLISS-52 and BLISS-76 studies (17,18). In addition, more patients in the belimumab SC group were able to reduce their corticosteroid dosage as compared with those in the placebo group, although this reduction did not achieve statistical significance. The decrease in corticosteroid dosage occurred in parallel with the reduction in risk of flare among those who received belimumab treatment compared with placebo. Since only patients receiving a baseline corticosteroid dosage >7.5 mg/day were eligible for analysis, the absence of statistical significance may reflect insufficient power to detect such a difference in a subgroup of this size. It should be noted that the study design did not mandate or encourage corticosteroid taper, and treatment blinding may have limited the proactive reduction of corticosteroids due to concerns that a patient may have been receiving placebo. The observed reduction in corticosteroid use may therefore not faithfully reflect clinical practice, where a more aggressive approach to corticosteroid tapering might be taken.

In subgroup analyses, patients with SELENA–SLEDAI scores of ≥10 at baseline had significant treatment responses (SRI4) with belimumab, whereas those with scores of ≤9 did not. The difference in response rates in the subgroup with scores ≥10 appeared to be greater than in the overall population, suggesting that belimumab SC may be especially beneficial in patients with high levels of disease activity. Similarly, belimumab-treated patients who were receiving corticosteroids at baseline had a significant treatment response relative to placebo-treated patients, consistent with the findings of a post hoc analysis of the BLISS-IV studies (35). In the present study, the treatment effect on the SRI4 response in black patients indicated a positive trend, but statistical significance was not achieved. The number of patients in this subgroup was low, and the power was insufficient to draw firm conclusions. A separate study is underway to specifically assess the benefits of belimumab in black patients.

In baseline body weight subgroup analyses, the treatment effect did not appear to vary greatly between body weight subgroups. The effect achieved statistical

significance for the third and fourth quartiles, but not for the first and second quartiles. As with other subgroup analyses, the patient numbers were low.

Fatigue is one of the most commonly reported symptoms among patients with SLE and has considerable impact on their lives (36). Patient-reported fatigue was significantly reduced with belimumab SC at weeks 8, 36, and 52 in the present study. Although the time to first renal flare was reduced in patients receiving belimumab 200 mg SC, few renal flares occurred later in the study in this group, resulting in a shorter median time to flare. Patients receiving belimumab experienced fewer renal flares overall, and fewer patients with baseline proteinuria >0.5 gm/24 hours who were receiving belimumab experienced a renal flare as compared with those receiving placebo. Renal involvement is associated with increased morbidity in SLE (37), and a post hoc analysis of BLISS-52 and BLISS-76 study data suggested that belimumab may have beneficial effects in patients with renal involvement (38). However, while these data are encouraging, they offer no insight into efficacy in patients with severe active lupus nephritis, a subgroup that was excluded from the BLISS IV and SC studies (17,18).

The safety profile of belimumab 200 mg SC plus standard SLE therapy was similar to that of placebo SC plus standard SLE therapy and was consistent with the known safety profile of belimumab IV (21). The overall incidences of AEs and SAEs were numerically lower in the belimumab group compared with the placebo group. The increase in AEs with increasing body weight was similar among patients receiving placebo and belimumab, suggesting that body weight did not affect the safety of belimumab.

The incidence of treatment-emergent suicidality was low. Two patients in the belimumab group and none in the placebo group experienced serious suicidal ideation, and there were no cases of suicidal behavior. In prior studies of IV belimumab (phase II and 2 phase III studies), there were 2 completed suicides in the belimumab groups (2 of 1,458 [0.1%]) and none in the placebo groups (0 of 675), and serious depression was reported in 0.4% (6 of 1,458) of patients receiving belimumab and 0.1% (1 of 675) of patients receiving placebo (17,18,29,39). In a phase III trial of SC tabalumab, another BLyS antagonist, in SLE, cases of depression and suicidal ideation were more common in the tabalumab groups (120 mg every 2 or 4 weeks) compared with placebo, although the overall incidence was low (depression, 4.0% and 4.5% versus 0.8%; suicide attempts, 0.3% and 0.5% versus 0%; suicidal ideation, 3.0% and 5.3% versus 0.4%; and suicidal behavior, 0.9% and 1.3% versus 0.4%) (40). Other studies of tabalumab did not report such an imbalance (41). Similarly, no cases of suicidal ideation or behavior were reported in patients with SLE taking other BLyS antagonists blisibimod (42,43) or atacicept (44–46).

The efficacy and safety results in this study support fixed dosing with the SC dose selection of 200 mg (as opposed to the weight-based dosing used for the IV infusion) (24). The pharmacokinetic profile is consistent with the simulated steady-state concentrations for weekly belimumab 200 mg SC (104 μg/ml) and monthly belimumab 10 mg/kg IV (110 μg/ml) (25).

Some aspects of this study may limit interpretation. Not all patients were included in the corticosteroid reduction analyses, as only 503 of 836 (60.2%) patients were receiving corticosteroids at a dosage of >7.5 mg/day at baseline. The inclusion criteria did not permit inclusion of patients with SELENA–SLEDAI scores of <8 at screening, nor did they permit entry of patients with active nephritis or active CNS disease, so no conclusions can be made about these subsets of patients. Sample sizes in some subgroups were small, which limits the conclusions that can be drawn.

In summary, fixed-dose weekly belimumab 200 mg SC in patients with SLE reduced SLE disease activity in the overall population, and patient-reported levels of fatigue were improved. Safety results were consistent with the known safety profile of belimumab. The ability of patients with SLE to administer their medication away from the clinic will provide a more convenient treatment regimen for belimumab, which may make it a more viable treatment option for some patients.

AUTHOR CONTRIBUTIONS

All authors were involved in drafting the article or revising it critically for important intellectual content, and all authors approved the final version to be published. Dr. Stohl had full access to all of the data in the study and takes responsibility for the integrity of the data and the accuracy of the data analysis.

Study conception and design. Stohl, Kleoudis, Bass, Fox, Roth, Gordon.
Acquisition of data. Stohl, Schwarting, Okada, Scheinberg, Doria, Hammer, Kleoudis, Groark, Bass, Fox, Roth, Gordon.
Analysis and interpretation of data. Stohl, Schwarting, Okada, Scheinberg, Doria, Hammer, Kleoudis, Groark, Bass, Fox, Roth, Gordon.

ROLE OF THE STUDY SPONSORS

GlaxoSmithKline plc (GSK) designed, conducted, and funded the study, contributed to the collection, analysis, and interpretation of the data, and supported the authors in the development of the manuscript. All authors, including those employed by GSK, approved the content of the submitted manuscript. GSK is committed to publicly disclosing the results of GSK-sponsored clinical research that evaluates GSK medicines and, as such, was involved in the decision and to submit the manuscript for publication. Medical writing and editorial assistance was funded by GSK and was provided by Louisa Pettinger, PhD (Fishawack Indicia Ltd).

ADDITIONAL DISCLOSURES

Author Kleoudis is an employee of Parexel.

REFERENCES

1. Schneider P, MacKay F, Steiner V, Hofmann K, Bodmer JL, Holler N, et al. BAFF, a novel ligand of the tumor necrosis factor family, stimulates B cell growth. J Exp Med 1999;189:1747–56.
2. Moore PA, Belvedere O, Orr A, Pieri K, LaFleur DW, Feng P, et al. BLyS: member of the tumor necrosis factor family and B lymphocyte stimulator. Science 1999;285:260–3.
3. Thompson JS, Schneider P, Kalled SL, Wang L, Lefevre EA, Cachero TG, et al. BAFF binds to the tumor necrosis factor receptor–like molecule B cell maturation antigen and is important for maintaining the peripheral B cell population. J Exp Med 2000;192:129–36.
4. Do RK, Hatada E, Lee H, Tourigny MR, Hilbert D, Chen-Kiang S. Attenuation of apoptosis underlies B lymphocyte stimulator enhancement of humoral immune response. J Exp Med 2000;192: 953–64.
5. Batten M, Groom J, Cachero TG, Qian F, Schneider P, Tschopp J, et al. BAFF mediates survival of peripheral immature B lymphocytes. J Exp Med 2000;192:1453–66.
6. Gross JA, Johnston J, Mudri S, Enselman R, Dillon SR, Madden K, et al. TACI and BCMA are receptors for a TNF homologue implicated in B-cell autoimmune disease. Nature 2000;404:995–9.
7. Khare SD, Sarosi I, Xia XZ, McCabe S, Miner K, Solovyev I, et al. Severe B cell hyperplasia and autoimmune disease in TALL-1 transgenic mice. Proc Natl Acad Sci U S A 2000;97:3370–5.
8. Mackay F, Woodcock SA, Lawton P, Ambrose C, Baetscher M, Schneider P, et al. Mice transgenic for BAFF develop lymphocytic disorders along with autoimmune manifestations. J Exp Med 1999;190:1697–710.
9. Cheema GS, Roschke V, Hilbert DM, Stohl W. Elevated serum B lymphocyte stimulator levels in patients with systemic immune–based rheumatic diseases. Arthritis Rheum 2001;44:1313–9.
10. Stohl W, Metyas S, Tan SM, Cheema GS, Oamar B, Xu D, et al. B lymphocyte stimulator overexpression in patients with systemic lupus erythematosus: longitudinal observations. Arthritis Rheum 2003;48:3475–86.
11. Zhang J, Roschke V, Baker KP, Wang Z, Alarcón GS, Fessler BJ, et al. Cutting edge: a role for B lymphocyte stimulator in systemic lupus erythematosus. J Immunol 2001;166:6–10.
12. Hong SD, Reiff A, Yang HT, Migone TS, Ward CD, Marzan K, et al. B lymphocyte stimulator expression in pediatric systemic lupus erythematosus and juvenile idiopathic arthritis patients. Arthritis Rheum 2009;60:3400–9.
13. Petri M, Stohl W, Chatham W, McCune WJ, Chevrier M, Ryel J, et al. Association of plasma B lymphocyte stimulator levels and disease activity in systemic lupus erythematosus. Arthritis Rheum 2008;58:2453–9.
14. Jacob CO, Pricop L, Putterman C, Koss MN, Liu Y, Kollaros M, et al. Paucity of clinical disease despite serological autoimmunity and kidney pathology in lupus-prone New Zealand mixed 2328 mice deficient in BAFF. J Immunol 2006;177:2671–80.
15. Ramanujam M, Wang X, Huang W, Liu Z, Schiffer L, Tao H, et al. Similarities and differences between selective and nonselective BAFF blockade in murine SLE. J Clin Invest 2006;116:724–34.
16. Baker KP, Edwards BM, Main SH, Choi GH, Wager RE, Halpern WG, et al. Generation and characterization of LymphoStat-B, a human monoclonal antibody that antagonizes the bioactivities of B lymphocyte stimulator. Arthritis Rheum 2003;48:3253–65.
17. Furie R, Petri M, Zamani O, Cervera R, Wallace DJ, Tegzova D, et al. A phase III, randomized, placebo-controlled study of belimumab, a monoclonal antibody that inhibits B lymphocyte stimulator, in patients with systemic lupus erythematosus. Arthritis Rheum 2011;63:3918–30.
18. Navarra SV, Guzman RM, Gallacher AE, Hall S, Levy RA, Jimenez RE, et al. Efficacy and safety of belimumab in patients with active systemic lupus erythematosus: a randomised, placebo-controlled, phase 3 trial. Lancet 2011;377:721–31.
19. US Food and Drug Administration. FDA approves Benlysta to treat lupus. March 9, 2011. URL: http://www.fda.gov/NewsEvents/Newsroom/PressAnnouncements/ucm246489.htm.
20. European Medicines Agency. Summary of product characteristics: Benlysta (belimumab). September 2011. URL: http://www.ema.europa.eu/ema/index.jsp?curl=pages/medicines/human/medicines/002015/human_med_001466.jsp&mid=WC0b01ac058001d124.
21. Benlysta (belimumab) prescribing information. Rockville (MD): GlaxoSmithKline; 2014. URL: http://www.accessdata.fda.gov/drugsatfda_docs/label/2012/125370s016lbl.pdf.
22. Chilton F, Collett RA. Treatment choices, preferences and decision-making by patients with rheumatoid arthritis. Musculoskeletal Care 2008;6:1–14.
23. Struemper H, Murtaugh T, Gilbert J, Barton ME, Fire J, Groark J, et al. Relative bioavailability of a single dose of belimumab administered subcutaneously by prefilled syringe or autoinjector in healthy subjects. Clin Pharmacol Drug Dev 2016;5:208–15.
24. Cai WW, Fiscella M, Chen C, Zhong ZJ, Freimuth WW, Subich DC. Bioavailability, pharmacokinetics, and safety of belimumab administered subcutaneously in healthy subjects. Clin Pharmacol Drug Dev 2013;2:349–57.
25. Yapa SW, Roth D, Gordon D, Struemper H. Comparison of intravenous and subcutaneous exposure supporting dose selection of subcutaneous belimumab systemic lupus erythematosus phase 3 program. Lupus 2016;25:1448–55.
26. World Medical Association. WMA declaration of Helsinki: ethical principles for medical research involving human subjects. URL: http://www.wma.net/en/30publications/10policies/b3/index.html.
27. Hochberg MC. Updating the American College of Rheumatology revised criteria for the classification of systemic lupus erythematosus [letter]. Arthritis Rheum 1997;40:1725.
28. Petri M, Kim MY, Kalunian KC, Grossman J, Hahn BH, Sammaritano LR, et al, for the OC-SELENA Trial. Combined oral contraceptives in women with systemic lupus erythematosus. N Engl J Med 2005;353:2550–8.
29. Furie RA, Petri MA, Wallace DJ, Ginzler EM, Merrill JT, Stohl W, et al. Novel evidence-based systemic lupus erythematosus responder index. Arthritis Rheum 2009;61:1143–51.
30. Petri M, Buyon J, Kim M. Classification and definition of major flares in SLE clinical trials. Lupus 1999;8:685–91.
31. Petri M, Kim MY, Kalunian KC, Grossman J, Hahn BH, Sammaritano LR, et al. Combined oral contraceptives in women with systemic lupus erythematosus. N Engl J Med 2005;353:2550–8.
32. Buyon JP, Petri MA, Kim MY, Kalunian KC, Grossman J, Hahn BH, et al. The effect of combined estrogen and progesterone hormone replacement therapy on disease activity in systemic lupus erythematosus: a randomized trial. Ann Intern Med 2005;142:953–62.
33. Cella D, Yount S, Sorensen M, Chartash E, Sengupta N, Grober J. Validation of the Functional Assessment of Chronic Illness Therapy Fatigue Scale relative to other instrumentation in patients with rheumatoid arthritis. J Rheumatol 2005;32:811–9.
34. Alarcon-Segovia D, Tumlin JA, Furie RA, McKay JD, Cardiel MH, Strand V, et al. LJP 394 for the prevention of renal flare in patients with systemic lupus erythematosus: results from a randomized, double-blind, placebo-controlled study. Arthritis Rheum 2003;48:442–54.
35. Van Vollenhoven RF, Petri MA, Cervera R, Roth DA, Ji BN, Kleoudis CS, et al. Belimumab in the treatment of systemic lupus erythematosus: high disease activity predictors of response. Ann Rheum Dis 2012;71:1343–9.
36. Tench CM, McCurdie I, White PD, D'Cruz DP. The prevalence and associations of fatigue in systemic lupus erythematosus. Rheumatology (Oxford) 2000;39:1249–54.

37. Ward MM. Changes in the incidence of end-stage renal disease due to lupus nephritis, 1982-1995. Arch Intern Med 2000;160:3136–40.
38. Dooley MA, Houssiau F, Aranow C, D'Cruz DP, Askanase A, Roth DA, et al. Effect of belimumab treatment on renal outcomes: results from the phase 3 belimumab clinical trials in patients with SLE. Lupus 2013;22:63–72.
39. Wallace D, Navarra S, Petri M, Gallacher A, Thomas M, Furie R, et al. Safety profile of belimumab: pooled data from placebo-controlled phase 2 and 3 studies in patients with systemic lupus erythematosus. Lupus 2013;22:144–54.
40. Merrill JT, van Vollenhoven RF, Buyon JP, Furie RA, Stohl W, Morgan-Cox M, et al. Efficacy and safety of subcutaneous tabalumab, a monoclonal antibody to B-cell activating factor, in patients with systemic lupus erythematosus: results from illuminate-2, a 52-week, phase III, multicentre, randomised, double-blind, placebo-controlled study. Ann Rheum Dis 2016;75:332–40.
41. Isenberg DA, Petri M, Kalunian K, Tanaka Y, Urowitz MB, Hoffman RW, et al. Efficacy and safety of subcutaneous tabalumab in patients with systemic lupus erythematosus: results from ILLUMINATE-1, a 52-week, phase III, multicentre, randomised, double-blind, placebo-controlled study. Ann Rheum Dis 2016;75:323–31.
42. Furie RA, Leon G, Thomas M, Petri MA, Chu AD, Hislop C, et al. A phase 2, randomised, placebo-controlled clinical trial of blisibimod, an inhibitor of B cell activating factor, in patients with moderate-to-severe systemic lupus erythematosus, the PEARL-SC study. Ann Rheum Dis 2015;74:1667–75.
43. Stohl W, Merrill J, Looney R, Buyon J, Wallace D, Weisman M, et al. Treatment of systemic lupus erythematosus patients with the BAFF antagonist "peptibody" blisibimod (AMG 623/A-623): results from randomized, double-blind phase 1a and phase 1b trials. Arthritis Res Ther 2015;17:215.
44. Isenberg D, Gordon C, Licu D, Copt S, Rossi CP, Wofsy D. Efficacy and safety of atacicept for prevention of flares in patients with moderate-to-severe systemic lupus erythematosus (SLE): 52-week data (April-SLE randomised trial). Ann Rheum Dis 2015;74:2006–15.
45. Pena-Rossi C, Nasonov E, Stanislav M, Yakusevich V, Ershova O, Lomareva N, et al. An exploratory dose-escalating study investigating the safety, tolerability, pharmacokinetics and pharmacodynamics of intravenous atacicept in patients with systemic lupus erythematosus. Lupus 2009;18:547–55.
46. Dall'Era M, Chakravarty E, Wallace D, Genovese M, Weisman M, Kavanaugh A, et al. Reduced B lymphocyte and immunoglobulin levels after atacicept treatment in patients with systemic lupus erythematosus: results of a multicenter, phase Ib, double-blind, placebo-controlled, dose-escalating trial. Arthritis Rheum 2007;56:4142–50.

ARTHRITIS & RHEUMATOLOGY
Vol. 69, No. 5, May 2017, pp 1028–1034
DOI 10.1002/art.40052

BRIEF REPORT

Pharmacodynamics, Safety, and Clinical Efficacy of AMG 811, a Human Anti–Interferon-γ Antibody, in Patients With Discoid Lupus Erythematosus

Victoria P. Werth,[1] David Fiorentino,[2] Barbara A. Sullivan,[3] Michael J. Boedigheimer,[3] Kit Chiu,[3] Christine Wang,[3] Gregory E. Arnold,[3] Michael A. Damore,[3] Jeannette Bigler,[4] Andrew A. Welcher,[3] Chris B. Russell,[4] David A. Martin,[4] and James B. Chung[3]

Objective. **Interferon-γ (IFNγ) is implicated in the pathogenesis of discoid lupus erythematosus (DLE). This study sought to evaluate a single dose of AMG 811, an anti-IFNγ antibody, in patients with DLE.**

Methods. **The study was designed as a phase I randomized, double-blind, placebo-controlled crossover study of the pharmacodynamics, safety, and clinical efficacy of AMG 811 in patients with DLE. Patients received a single subcutaneous dose of AMG 811 (180 mg) or placebo. The patients in sequence 1 received AMG 811 followed by placebo, while those in sequence 2 received placebo followed by AMG 811. Pharmacodynamic end points included global transcriptional analyses of lesional and nonlesional skin, IFNγ blockade signature (IGBS) transcriptional scores in the skin and blood, keratinocyte IFNγ RNA scores, and serum levels of CXCL10 protein. Additional end points were efficacy outcome measures, including the Cutaneous Lupus Erythematosus Disease Area and Severity Index, and safety outcome measures.**

Results. **Sixteen patients with DLE were enrolled in the study (9 in sequence 1 and 7 in sequence 2). AMG 811 treatment reduced the IGBS score (which was elevated in DLE patients at baseline) in both the blood and lesional skin. The keratinocyte IFNγ RNA score was not affected by administration of AMG 811. Serum CXCL10 protein levels (which were elevated in the blood of DLE patients) were reduced with AMG 811 treatment. The AMG 811 treatment was well tolerated but did not lead to statistically significant improvements in any of the efficacy outcome measures.**

Conclusion. **AMG 811 treatment led to changes in IFNγ-associated biomarkers and was well tolerated, but no significant clinical benefit was observed in patients with DLE.**

Skin involvement (cutaneous lupus) occurs in 70–85% of patients with systemic lupus erythematosus (SLE) and is classified according to the morphologic characteristics of the lesions and the histopathologic appearance of the skin (1). Discoid lesions, the most common manifestation of chronic cutaneous lupus erythematosus, are well-defined lesions, characterized by disk-shaped, erythematous, scaly patches that can cause atrophy and scarring. Biopsy samples of lesional skin from patients with discoid lupus erythematosus (DLE) show deposition of immunoglobulins, complement, and mononuclear cell infiltrates, indicating that this disease may have an antigen-driven immunologic pathogenesis (2).

Members of the interferon (IFN) family have been implicated in the pathogenesis of DLE (3), and analyses of skin samples have shown strong evidence of

ClinicalTrials.gov identifier: NCT01164917.

Supported by Amgen Inc. Dr. Werth's work was supported by the Department of Veterans Affairs Veterans Health Administration, Office of Research and Development, Biomedical Laboratory Research and Development.

[1]Victoria P. Werth, MD: University of Pennsylvania and Corporal Michael J. Crescenz Veterans Administration Medical Center, Philadelphia, Pennsylvania; [2]David Fiorentino, MD, PhD: Stanford University, Palo Alto, California; [3]Barbara A. Sullivan, PhD, Michael J. Boedigheimer, PhD, Kit Chiu, PhD, Christine Wang, MS, Gregory E. Arnold, PhD, Michael A. Damore, PhD, Andrew A. Welcher, PhD, James B. Chung, MD, PhD: Amgen Inc., Thousand Oaks, California; [4]Jeannette Bigler, PhD, Chris B. Russell, PhD, David A. Martin, MD: Amgen, Inc., Seattle, Washington.

Dr. Werth holds a patent for the Cutaneous Lupus Erythematosus Disease Area and Severity Index (owned by the University of Pennsylvania) used in this study. Drs. Sullivan, Boedigheimer, Arnold, and Chung and Ms Wang own stock or stock options in Amgen Inc. Drs. Welcher, Russell, Chiu, Damore, Bigler, and Martin are former employees of Amgen Inc. and own stock or stock options in Amgen Inc.

Address correspondence to James B. Chung, MD, PhD, Amgen Inc., One Amgen Center Drive, Thousand Oaks, CA 91320. E-mail: chung@amgen.com.

Submitted for publication March 10, 2016; accepted in revised form January 17, 2017.

activation of IFN signaling. Elevated levels of IFNγ messenger RNA have been described in DLE skin specimens relative to normal skin, and immunohistochemical analyses have shown a selective staining of IFNγ receptors in DLE skin samples compared to normal skin samples (4). IFNγ modulates the function of several populations of immune system cells, including B cells, T cells, and macrophages. In skin, IFNγ is an inhibitor of keratinocyte growth (5). Elevated levels of IFNγ-inducible 10-kd protein (CXCL10) and infiltrates of CXCR3-expressing T cells have also been found in DLE skin biopsy specimens (6).

AMG 811 is a human anti-IFNγ antibody (IgG1 isotype) that selectively targets human IFNγ (7). Previous trials of AMG 811 in SLE patients with and those without nephritis showed an acceptable safety and tolerability profile (8–10). The objective of the present study was to evaluate the safety, tolerability, pharmacodynamics, and efficacy of a single dose of AMG 811 in patients with DLE.

SUBJECTS AND METHODS

Study design. This study was a phase I multicenter, randomized, double-blind, placebo-controlled, 2-period crossover study that was designed to evaluate a single dose of AMG 811 in comparison to placebo. The treatment was administered in 1 of 2 sequences: in sequence 1, patients received AMG 811 followed by placebo, while in sequence 2, patients received placebo followed by AMG 811. Twenty patients with DLE (with or without SLE) were planned for the study (12 for sequence 1 and 8 for sequence 2).

A single dose of AMG 811 (180 mg) or placebo was administered subcutaneously on day 1 (start of period 1) and on day 85 (start of period 2). Biopsy specimens of lesional and nonlesional skin were collected at baseline, and biopsy specimens of lesional skin were collected on days 15 and 57 postdosing. The presence of lesions was predetermined by each of the investigators before dosing was initiated. In most patients, the lesions were identified in a similar anatomic region. Nonlesional skin specimens were obtained from regions with similar light exposure as selected lesional sites. Blood samples for pharmacodynamic biomarker testing were collected at the following time points: in period 1, at baseline, predose, 6 hours postdose, and days 2, 15, 29, and 57; in period 2, predose, 6 hours postdose, and days 99, 113, 141, and 197 (end of study). Efficacy outcomes were evaluated at screening, baseline, and days 15, 29, and 57 (period 1) and days 85, 99, 113, 141, 169, and 197 (period 2). This study was conducted in accordance with the Declaration of Helsinki.

Patients. Eligible patients were ages 18–70 years at randomization, had a body mass index of 18–40 kg/m^2, and were diagnosed as having DLE with or without SLE based on the Gilliam and Sontheimer classification (1). All eligible patients had a skin biopsy sample that exhibited features consistent with the diagnosis of DLE, and all had previously demonstrated intolerance to antimalarial therapy or had received ≥3 months of antimalarial therapy and had continued to display residual disease activity. Moreover, all eligible patients had stable disease for 4 weeks prior to screening, had received a stable dose of topical steroids no stronger than medium potency (class I, II, or III) for ≥2 weeks and/or systemic immunosuppressive therapy at a stable dose for ≥8 weeks before randomization, had received oral prednisone at a dosage of ≤20 mg/day (or equivalent), and had a current vaccination history. Exclusion criteria included a history of malignancy, signs or symptoms of viral, bacterial, or fungal infection within 30 days of randomization or recent history of repeated infections, an underlying significant medical condition other than SLE, a history of receiving immunosuppressant drugs that predispose to infection, or having received a live vaccine within 3 months of randomization.

Study outcome measures. *Gene expression profiling in the skin and blood.* Transcriptional differences between lesional and nonlesional skin were assessed using microarray analysis. Frozen skin samples were disrupted with a Multi-Sample Bio Pulverizer (Research Products International) and homogenized with a TissueRuptor (Qiagen). Total RNA was isolated using the mirVana Micro-RNA Isolation kit (Applied Biosystems), modified to include on-column DNase treatment with RNase-free DNase (Qiagen). The integrity of the RNA samples was assessed using a Bioanalyzer 2100 (Bio-Rad). The total RNA concentration was measured on an ND-1000 Spectrophotometer (NanoDrop). Labeled complementary DNA was generated using a NuGEN Ovation kit (NuGEN Technologies) and hybridized to GeneChip HT_HG-U133+PM microarrays using a GeneTitan instrument (Affymetrix). Analyses were conducted with $\log_2$-transformed intensities that had been normalized at the array level to have comparable intensity spectrum. Only samples with an RNA integrity number (RIN) of >7 were used. Whole blood PAXgene samples were processed and assayed by microarray as previously described (8), except that the samples were Cy3-labeled and hybridized once to a custom 180k Agilent array with the content of the Human Gene Expression 44K (AMADID #026822; Agilent Technologies), replicated 4 times.

Pharmacodynamic outcome measures. Pharmacodynamic outcome measures included changes in the IFNγ blockade signature (IGBS) RNA score in the serum and skin, changes in the keratinocyte IFNγ RNA score in the skin, and changes in the levels of CXCL10 protein in the serum. The IGBS was derived from 2 microarray experiments. First, whole blood from healthy volunteers was stimulated in vitro with IFNγ and used to identify genes that were up-regulated by IFNγ. Second, whole blood from patients in a phase Ia study (8) was used to identify genes that showed reduced expression following AMG 811 treatment. The IGBS score is a weighted average of the top 10 genes identified in those experiments, as previously described (8).

The keratinocyte IFNγ RNA score is based on a set of genes that are preferentially expressed in keratinocytes stimulated with IFNγ, but not those stimulated with interleukin-17A (IL-17A), IL-22, or tumor necrosis factor (11). For reference, the keratinocyte IFNγ RNA score was measured in a set of 30 skin samples from healthy volunteers, as was the covariance of the expression of each gene. The numeric score for each disease skin sample from DLE patients was the Mahalanobis skin, which is similar to a multidimensional Z score and increases with changes in the expression of each gene in the signature set. The scores for each gene's contribution in the inverse covariance matrix were adjusted for the gene set in the reference normal samples.

Serum CXCL10 protein concentrations were determined using a commercially available enzyme-linked immunosorbent assay in accordance with the manufacturer's instructions (R&D

Systems). Whole blood from healthy volunteers was obtained from the Amgen Research Blood Donor program.

Clinical outcome measures. The study clinical outcome measures included the Cutaneous Lupus Erythematosus Disease Area and Severity Index (CLASI) score for disease activity (CLASI-A; score range 0–70) (12). Additional exploratory clinical outcome measures included the CLASI score for damage (CLASI-D; score range 0–56), the physician's assessment of skin disease, the patient's self-assessment of skin disease, and the SLE Disease Activity Index 2000 (13) (for patients with underlying SLE). In period 1 (baseline to day 84), baseline was defined as day 1 predose, while in period 2 (day 85 to day 197), baseline was defined as day 85 predose. The sole placebo group was the sequence 2, period 1 group (having first received placebo during period 1), since the sequence 1, period 2 group may have had potential confounding by exposure to AMG 811 (having received AMG 811 first).

Statistical analysis. The primary goal of CLASI-A and keratinocyte IFNγ RNA analyses was to provide estimates of effect size (with uncertainty), and statistical significance, although the study lacked sufficient power to achieve statistical significance. Percentage changes from baseline in CLASI-A scores did not follow normal distribution; therefore, Hodges-Lehmann estimates of the median values with associated 90% confidence intervals (90% CIs) were provided. Corresponding *P* values were based on exact Wilcoxon–Mann-Whitney tests.

Global transcriptional analyses were performed on $\log_2$-transformed and normalized fluorescence intensity values of gene expression. Differentially expressed genes and gene signatures were identified by determining the contrast in mean baseline expression values within lesional skin compared to nonlesional skin, which was estimated from a linear model that included factors for skin diagnosis (lesional or nonlesional), RIN, and patient.

IGBS scores were analyzed in a mixed-effects linear model that included time on active treatment as a fixed effect and patient as a random factor. IGBS score plots are shown with simultaneous 95% CIs, using pooled estimates of standard error corrected for small sample sizes.

Serum CXCL10 protein levels were analyzed using a mixed-effects regression model, including factors for treatment, serum CXCL10 protein concentrations before treatment, time after treatment, and a treatment × time interaction term. Time and treatment were fixed factors, and patient was a random factor.

RESULTS

Characteristics of the patients. Of the 20 patients planned for the study, only 16 were enrolled, because enrollment was slow. Of the 16 enrolled patients, 9 were assigned to sequence 1 and 7 were assigned to sequence 2. Two patients (1 from each sequence) discontinued treatment during period 1 (1 withdrew consent and 1 discontinued for other reasons). Fifteen patients received treatment with AMG 811 (9 in period 1 and 6 in period 2). These patients were therefore included in the AMG 811 analysis group, and 7 patients were included in the placebo group. The mean age was 49.2 years, and most of the patients (75%) were female. The majority of patients (88%) had comorbid SLE (Table 1).

Changes in pharmacodynamic outcome measures. The IGBS score was elevated in lesional skin compared to nonlesional skin. In lesional skin, treatment with AMG 811 significantly reduced the mean IGBS score on day 57 compared to the mean value at baseline ($P < 0.05$) (Figure 1A), although the mean IGBS score in lesional skin was not reduced to the level observed at baseline in nonlesional skin, and was significantly higher than the baseline nonlesional skin IGBS score ($P < 0.05$) (Figure 1A). A significant reduction in the IGBS score was also observed in the peripheral blood (data not shown).

The keratinocyte IFNγ RNA score was increased at baseline in both the lesional and nonlesional skin of patients with DLE compared to the normal skin of reference healthy patients. In DLE patients, the keratinocyte IFNγ score was higher in lesional skin than in nonlesional

Table 1. Demographic and clinical characteristics of the study subjects at baseline*

	Sequence 1 (n = 9)	Sequence 2 (n = 7)	All patients (n = 16)
Sex, no. (%) female	8 (89)	4 (57)	12 (75)
Age, mean ± SD years	47.1 ± 10.7	51.9 ± 7.5	49.2 ± 9.4
Race, no. (%)			
White	6 (67)	4 (57)	10 (63)
Black/African American	2 (22)	3 (43)	5 (31)
Asian	1 (11)	0	1 (6)
Comorbid SLE, no. (%)	8 (89)	6 (86)	14 (88)
Receiving prednisone, no. (%)	3 (33)	4 (57)	7 (44)
Prednisone dose, mean ± SD mg/day	9.67 ± 8.96	6.88 ± 3.75	8.07 ± 6.00
Receiving antimalarial drug, no. (%)	6 (67)	5 (71)	11 (69)
CLASI-A score, mean ± SD	19.00 ± 6.18	21.86 ± 10.16	20.25 ± 7.99
CLASI-D score, mean ± SD	14.56 ± 9.13	19.14 ± 3.34	16.56 ± 7.38

* SLE = systemic lupus erythematosus; CLASI-A = Cutaneous Lupus Erythematosus Disease Area and Severity Index for disease activity; CLASI-D = Cutaneous Lupus Erythematosus Disease Area and Severity Index for damage.

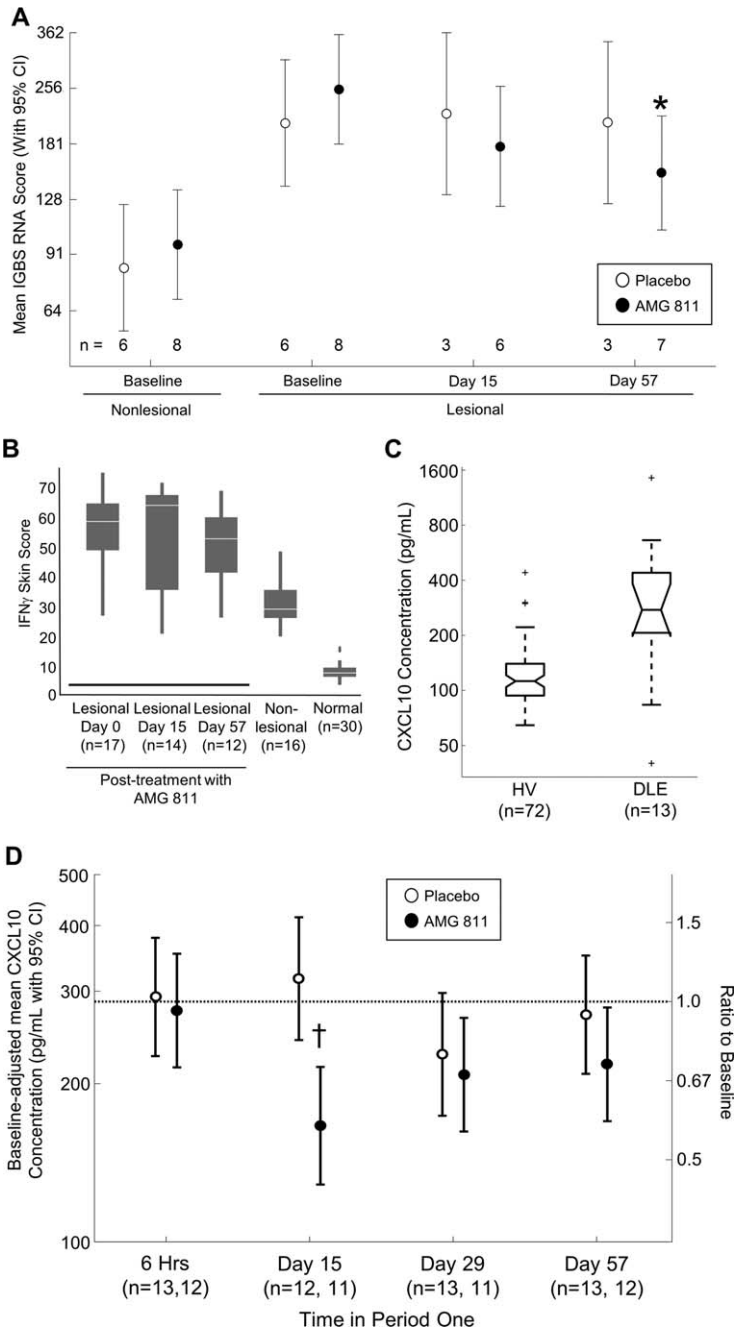

Figure 1. Changes in biomarker expression with AMG 811 treatment. **A,** Interferon-γ (IFNγ) blockade signature (IGBS) scores in nonlesional skin at baseline and in lesional skin of patients with discoid lupus erythematosus (DLE) at baseline and on days 15 and 57 after treatment with AMG 811 or placebo (in period 1). * = $P = 0.0063$ versus AMG 811–treated lesional samples at baseline. **B,** Keratinocyte IFNγ RNA score in lesional skin of DLE patients at baseline and on days 15 and 57 after AMG 811 treatment compared with nonlesional DLE skin and normal healthy control skin. Results are shown as box plots, where the horizontal line within the boxes represents the median, the boxes represent the first and third quartiles, and the bars outside the boxes represent the minimum and maximum values. **C,** Serum CXCL10 protein concentrations in healthy volunteers (HV) and untreated patients with DLE. Results are shown as irregular box plots, where the horizontal line within the boxes represents the median, the notches represent an estimate of the uncertainty about the median, the boxes represent the first and third quartiles, and the dashed bars represent the lower and upper ends of the farthest observed data point within 1.5 times the interquartile range; the plus signs represent outliers. **D,** Baseline-adjusted mean serum CXCL10 protein concentrations in DLE patients treated with AMG 811 or placebo. The dashed horizontal line represents the mean baseline value. † = $P_{\text{adjusted}} = 0.0038$ for the intraday (day 15) comparison between AMG 811 and placebo. 95% CI = 95% confidence interval.

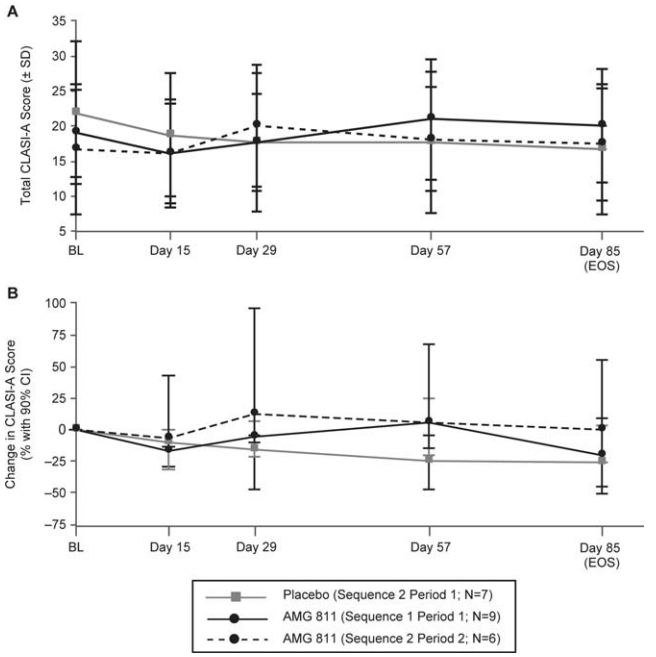

Figure 2. Clinical efficacy as measured by the Cutaneous Lupus Erythematosus Disease Area and Severity Index disease activity (CLASI-A) score. The mean total CLASI-A scores **(A)** and median percentage change in CLASI-A scores **(B)** at baseline (BL) predose and on postdose days 15, 29, 57, and 85 (end of study [EOS]) are shown for patients who received placebo followed by AMG 811 (sequence 2) in period 1, patients who received AMG 811 followed by placebo (sequence 1) in period 1, and patients who received AMG 811 followed by placebo (sequence 2) in period 2. 90% CI = 90% confidence interval.

skin (Figure 1B). In lesional skin, treatment with AMG 811 did not have a significant impact on the keratinocyte IFNγ RNA score on days 15 or 57 postdosing as compared to that at baseline (Figure 1B).

The baseline levels of serum CXCL10 protein were elevated in patients with DLE compared to the levels in reference healthy volunteers (Figure 1C). The serum CXCL10 protein levels were significantly reduced in patients treated with AMG 811 compared to those receiving placebo ($P < 0.05$), with a maximal reduction of −1.7-fold (95% CI −2.2, −1.3) from baseline to day 15 (Figure 1D).

Safety outcomes. Fourteen (93.3%) of 15 patients in the AMG 811 group and 4 (57.1%) of 7 patients in the placebo group had a treatment-emergent adverse event (AE). Arthralgia, headache, hypertriglyceridemia, and upper respiratory tract infections were the only AEs reported in >1 patient (n = 2 patients each [13.3%]) in the AMG 811 group. Two of these events were also reported in the placebo group: hypertriglyceridemia in 1 patient (14.3%) and headache in 2 patients (28.6%). No AEs of grade ≥2 occurred in more than 1 patient in either group. No deaths or withdrawals due to AEs were reported.

Three patients (20.0%) in the AMG 811 group reported experiencing a serious AE (SAE) during the study, whereas no SAEs were reported in the placebo group. SAEs reported within the first 12 weeks following AMG 811 administration included 1 case of *Legionella* pneumonia (deemed to be treatment related), while another patient experienced 4 different SAEs, including gastroenteritis, migraine (deemed to be treatment related), splenic infarction, and viral gastroenteritis. The SAE of *Legionella* pneumonia occurred on study day 47; the patient received levofloxacin and the pneumonia resolved 16 days later. One patient reported the development of a subdural hematoma (deemed to be unrelated to treatment) that occurred ~182 days after the patient had received AMG 811; the event resolved in ~2 weeks.

Changes in clinical outcome measures. Overall, the median changes in the CLASI-A score were not statistically significantly different between patients who received AMG 811 and those who received placebo over the first 85 days (Figures 2A and B). No significant clinical benefits were seen in patients with DLE after AMG 811 treatment in terms of improvements in the CLASI-D score, physician's assessment of skin disease, or patient's self-assessed skin disease (data not shown).

DISCUSSION

Cutaneous lupus, including DLE, is the result of aberrant autoimmune activation in the skin (14). Patients with DLE have an elevated IFN signature in the blood, suggesting that the pathogenic mechanisms are similar in patients with SLE and those with cutaneous lupus (15). AMG 811 is a monoclonal antibody that blocks IFNγ. In this study of patients with DLE, treatment with AMG 811 demonstrated clear pharmacologic activity in both the blood and lesional skin, as measured using the IGBS score. Notably, after treatment, the IGBS score did not reach the levels seen in nonlesional skin, suggesting that either incomplete blockade of the pathway or partial activation by other cytokines may occur.

When IFNγ activity was measured using the keratinocyte IFNγ RNA score, DLE lesional skin, DLE nonlesional skin, and normal skin from healthy volunteers were shown to have correspondingly varying levels of IFNγ activity, with the scores in DLE nonlesional skin being intermediate to those in lesional and normal skin. Treatment with AMG 811 did not significantly impact the keratinocyte IFNγ RNA score in the skin.

Given the pharmacologic responses to AMG 811 in both the blood and skin as measured by the IGBS and keratinocyte IFNγ RNA scores, the single dose of AMG 811 administered to patients with DLE possibly did not provide sufficient coverage to elicit a clinical response that could be measured by the CLASI-A. The 180-mg subcutaneous dose of AMG 811 covered the target adequately as assessed on the basis of changes in the serum CXCL10 levels over $\geq$56 days—a duration of treatment consistent with the measurement of efficacy in other DLE studies (8,16,17)—but the dose level of AMG 811 required to penetrate the skin and overcome local production of IFNγ may be higher. Alternatively, despite coverage of the IFNγ pathway, possibly other pathways, including the type I IFN pathways, may need to be inhibited concurrently to impact clinical disease. Furthermore, the heterogeneity of this population and the role of several interdependent and independent pathways may preclude the use of blockade of a single IFN pathway as an effective treatment for the majority of patients with SLE and DLE. Overall, these results do not provide a clear answer to the role of IFNγ in the pathogenesis of DLE. While differences in gene expression profiles in the blood and skin indicate dysregulation of the IFNγ pathway, conclusions about causality cannot be drawn given the possible incomplete blockade of the pathway in the tissue and the lack of discernible clinical impact.

Conduct of proof-of-concept SLE trials is challenging in terms of enrollment and trial design. Given the large number of patients required, duration of treatment, and the complex composite disease outcome measures needed, small clinical trials (particularly organ-specific trials) that maximize data collection and provide evidence of pharmacodynamic and clinical impact are valuable in the early development of novel agents for SLE. The crossover design utilized in this study allowed us to obtain both placebo- and treatment-related data in the overall analysis and helped us to minimize patient-to-patient variability. This design addressed one of the concerns postulated by patients who are considering participation in a clinical trial, that of potentially receiving placebo treatment. Enrollment of patients with DLE, most of whom also had SLE, enabled the collection of data from the skin in addition to blood and serum, which collectively enabled a rich set of data from which to conduct robust pharmacodynamic analyses. Despite the unclear results, we would encourage the consideration of such a study design, when appropriate, in the future development of agents for SLE.

In conclusion, treatment with AMG 811 led to changes in biomarkers associated with IFNγ in the blood and skin of patients with DLE. The treatment was well tolerated, but there was no significant clinical improvement observed with the single dose (180 mg) of AMG 811 administered in this study.

ACKNOWLEDGMENTS

We thank Dikran Toroser (Amgen Inc.) and Julia R. Gage (on behalf of Amgen Inc.) for assistance with the writing of the manuscript.

AUTHOR CONTRIBUTIONS

All authors were involved in drafting the article or revising it critically for important intellectual content, and all authors approved the final version to be published. Dr. Chung had full access to all of the data in the study and takes responsibility for the integrity of the data and the accuracy of the data analysis.

Study conception and design. Werth, Fiorentino, Boedigheimer, Chiu, Wang, Welcher, Russell, Martin, Chung.

Acquisition of data. Werth, Fiorentino, Sullivan, Chiu, Wang, Damore, Bigler, Welcher, Russell, Martin, Chung.

Analysis and interpretation of data. Werth, Fiorentino, Sullivan, Boedigheimer, Chiu, Wang, Arnold, Welcher, Russell, Martin, Chung.

ROLE OF THE STUDY SPONSOR

Amgen Inc., facilitated the study design, provided writing assistance for the manuscript, and reviewed and approved the manuscript prior to submission. The authors independently collected the data, interpreted the results, and had the final decision to submit the manuscript for publication. Publication of this article was not contingent upon approval by Amgen Inc.

REFERENCES

1. Gilliam JN, Sontheimer RD. Distinctive cutaneous subsets in the spectrum of lupus erythematosus. J Am Acad Dermatol 1981;4:471–5.
2. Fabbri P, Cardinali C, Giomi B, Caproni M. Cutaneous lupus erythematosus: diagnosis and management. Am J Clin Dermatol 2003;4:449–65.
3. Achtman JC, Werth VP. Pathophysiology of cutaneous lupus erythematosus. Arthritis Res Ther 2015;17:182.
4. Toro JR, Finlay D, Dou X, Zheng SC, LeBoit PE, Connolly MK. Detection of type 1 cytokines in discoid lupus erythematosus. Arch Dermatol 2000;136:1497–501.
5. Shirakata Y. Regulation of epidermal keratinocytes by growth factors. J Dermatol Sci 2010;59:73–80.
6. Wenzel J, Uerlich M, Worrenkamper E, Freutel S, Bieber T, Tuting T. Scarring skin lesions of discoid lupus erythematosus are characterized by high numbers of skin-homing cytotoxic lymphocytes associated with strong expression of the type I interferon-induced protein MxA. Br J Dermatol 2005;153:1011–5.
7. Chen P, Vu T, Narayanan A, Sohn W, Wang J, Boedigheimer M, et al. Pharmacokinetic and pharmacodynamic relationship of AMG 811, an anti-IFN-γ IgG1 monoclonal antibody, in patients with systemic lupus erythematosus. Pharm Res 2015;32:640–53.
8. Welcher AA, Boedigheimer M, Kivitz AJ, Amoura Z, Buyon J, Rudinskaya A, et al. Blockade of interferon-γ normalizes interferon-regulated gene expression and serum CXCL10 levels in patients with systemic lupus erythematosus. Arthritis Rheumatol 2015;67:2713–22.
9. Werth VP, Fiorentino D, Cohen SB, Fivenson D, Hansen C, Zoog S, et al. A phase I single-dose crossover study to evaluate the safety, tolerability, pharmacokinetics, pharmacodynamics, and clinical efficacy

of AMG 811 (anti-IFN-gamma) in patients with discoid lupus erythematosus [abstract]. Arthritis Rheum 2013;65 Suppl:S682.
10. Martin DA, Amoura Z, Romero-Diaz J, Chong YB, Sanchez-Guerrero J, Chan T, et al. A multiple dose study of AMG 811 (anti-IFN-gamma) in patients with systemic lupus erythematosus and active nephtiris [abstract]. Ann Rheum Dis 2015;74:337.
11. Nograles KE, Zaba LC, Guttman-Yassky E, Fuentes-Duculan J, Suarez-Farinas M, Cardinale I, et al. Th17 cytokines interleukin (IL)–17 and IL-22 modulate distinct inflammatory and keratinocyte-response pathways. Br J Dermatol 2008;159:1092–102.
12. Albrecht J, Taylor L, Berlin JA, Dulay S, Ang G, Fakharzadeh S, et al. The CLASI (Cutaneous Lupus Erythematosus Disease Area and Severity Index): an outcome instrument for cutaneous lupus erythematosus. J Invest Dermatol 2005;125:889–94.
13. Gladman DD, Ibanez D, Urowitz MB. Systemic Lupus Erythematosus Disease Activity Index 2000. J Rheumatol 2002;29:288–91.
14. Dey-Rao R, Sinha AA. Genome-wide transcriptional profiling of chronic cutaneous lupus erythematosus (CCLE) peripheral blood identifies systemic alterations relevant to the skin manifestation. Genomics 2015;105:90–100.
15. Braunstein I, Klein R, Okawa J, Werth VP. The interferon-regulated gene signature is elevated in subacute cutaneous lupus erythematosus and discoid lupus erythematosus and correlates with the cutaneous lupus area and severity index score. Br J Dermatol 2012;166:971–5.
16. Kreuter A, Tomi NS, Weiner SM, Huger M, Altmeyer P, Gambichler T. Mycophenolate sodium for subacute cutaneous lupus erythematosus resistant to standard therapy. Br J Dermatol 2007;156:1321–7.
17. Shah A, Albrecht J, Bonilla-Martinez Z, Okawa J, Rose M, Rosenbach M, et al. Lenalidomide for the treatment of resistant discoid lupus erythematosus. Arch Dermatol 2009;145:303–6.

ARTHRITIS & RHEUMATOLOGY
Vol. 69, No. 5, May 2017, pp 1035–1044
DOI 10.1002/art.40038

Signaling Lymphocytic Activation Molecule Family Member 7 Engagement Restores Defective Effector CD8+ T Cell Function in Systemic Lupus Erythematosus

Denis Comte,[1] Maria P. Karampetsou,[2] Nobuya Yoshida,[2] Katalin Kis-Toth,[2] Vasileios C. Kyttaris,[2] and George C. Tsokos[2]

Objective. **Effector CD8+ T cell function is impaired in systemic lupus erythematosus (SLE) and is associated with a compromised ability to fight infections. Signaling lymphocytic activation molecule family member 7 (SLAMF7) engagement has been shown to enhance natural killer cell degranulation. This study was undertaken to characterize the expression and function of SLAMF7 on CD8+ T cell subsets isolated from the peripheral blood of SLE patients and healthy subjects.**

Methods. **CD8+ T cell subset distribution, SLAMF7 expression, and expression of cytolytic enzymes (perforin, granzyme A [GzmA], and GzmB) on cells isolated from SLE patients and healthy controls were analyzed by flow cytometry. CD107a expression and interferon-γ (IFNγ) production in response to viral antigenic stimulation in the presence or absence of an anti-SLAMF7 antibody were assessed by flow cytometry. Antiviral cytotoxic activity in response to SLAMF7 engagement was determined using a flow cytometry–based assay.**

Results. **The distribution of CD8+ T cell subsets was altered in the peripheral blood of SLE patients, with a decreased effector cell subpopulation. Memory CD8+ T cells from SLE patients displayed decreased amounts of SLAMF7, a surface receptor that characterizes effector CD8+ T cells. Ligation of SLAMF7 increased CD8+ T cell degranulation capacity and the percentage of IFNγ-producing cells in response to antigen challenge in SLE patients and healthy controls. Moreover, SLAMF7 engagement promoted cytotoxic lysis of target cells in response to stimulation with viral antigens.**

Conclusion. **CD8+ T cell activation in response to viral antigens is defective in SLE patients. Activation of SLAMF7 through a specific monoclonal antibody restores CD8+ T cell antiviral effector function to normal levels and thus represents a potential therapeutic option in SLE.**

Profound abnormalities characterize T cells from patients with systemic lupus erythematosus (SLE) (1,2). Even though CD4+ T cells have been extensively studied, the role of CD8+ T cells in SLE is less well understood. Studies suggest a defect in cytotoxic CD8+ T cell activity in SLE and an accelerated disease in lupus-prone mice in which the major killing pathways of cytotoxic CD8+ T cells have been deleted (3–5). Additionally, SLE has been associated with defective cytotoxic responses against foreign antigens, an abnormality considered to contribute to the increased rate of infections, the leading cause of mortality in SLE (6–8).

Signaling lymphocytic activation molecule (SLAM) family members are type I transmembrane glycoprotein cell surface receptors that deliver downstream signals upon their engagement and modulate the magnitude of the immune response (9). SLAM family member 7 (SLAMF7; CS1, CRACC, CD319) is expressed on natural killer (NK) cells, NK T cells, CD8+ T cells, and subsets of B cells (10). SLAMF7 acts as a self-ligand through the binding of the N-terminal Ig domain of SLAMF7 (10). In NK cells, SLAMF7 uses the adaptor protein Ewing's sarcoma/FLI1-activated transcript 2 (EAT-2) to promote

Supported by the NIH (grants P01-AI-065687, R01-AI-42269, and R37-AI-49954 to Dr. Tsokos) and the SICPA Foundation (grant to Dr. Comte).

[1]Denis Comte, MD: Beth Israel Deaconess Medical Center, Harvard Medical School, Boston, Massachusetts, and Centre Hospitalier Universitaire Vaudois, Lausanne, Switzerland; [2]Maria P. Karampetsou, MD, PhD, Nobuya Yoshida, MD, PhD, Katalin Kis-Toth, PhD, Vasileios C. Kyttaris, MD, George C. Tsokos, MD: Beth Israel Deaconess Medical Center, Harvard Medical School, Boston, Massachusetts.

Address correspondence to George C. Tsokos, MD, Beth Israel Deaconess Medical Center, Harvard Medical School, 330 Brookline Avenue, CLS-937, Boston, MA 02115. E-mail: gtsokos@bidmc.harvard.edu.

Submitted for publication October 3, 2016; accepted in revised form January 5, 2017.

downstream signaling, while other SLAMF molecules preferentially bind to SLAMF-associated protein (11).

SLAMF7 has been extensively studied in patients with multiple myeloma, a malignant disorder of plasma cells. A monoclonal antibody (mAb) directed against SLAMF7 has been shown to eliminate myeloma cells by activating NK cells and by stimulating antibody-dependent cellular cytotoxicity (12–14). SLAMF molecules, and their downstream adaptor protein SLAMF-associated protein, have been suggested to play a role in SLE pathogenesis and to represent a potential therapeutic target (15–17). However, limited data are available concerning the role of SLAMF7 in SLE, and some studies have proposed that SLAMF7 can play a role in the pathogenesis of the disease (18,19). The gene encoding SLAMF7 is located on chromosome 1 within the 1q23 locus, a region known to be associated with an increased susceptibility to SLE (20). SLAMF7 expression has been reported to be altered in NK cells, plasmacytoid dendritic cells, and a subset of B cells in SLE patients (18,19), but the role and function of SLAMF7 in SLE CD8+ T cells has not been established.

In the present study, we show that the frequency of effector CD8+ T cells is decreased in the peripheral blood of SLE patients compared to healthy controls. In addition, we demonstrate that the expression of SLAMF7 is decreased in SLE CD8+ T cells and that the presence of SLAMF7 characterizes cytotoxic CD8+ T cells. More importantly, engagement of SLAMF7 with a specific mAb enhances the degranulation and cytotoxicity of CD8+ T cells in response to viral peptides. Despite the reduced SLAMF7 expression on SLE CD8+ effector T cells, activation of SLAMF7 via an anti-SLAMF7 mAb restores CD8+ T cell antiviral effector function to normal levels and, therefore, represents a potential therapeutic option to enhance immune response against foreign antigens.

MATERIALS AND METHODS

Patients and controls. SLE patients (n = 79) were diagnosed according to the American College of Rheumatology classification criteria (21) and were recruited from the Division of Rheumatology at Beth Israel Deaconess Medical Center. Age-, sex-, and ethnicity-matched healthy individuals were chosen as controls. Disease activity was measured using the SLE Disease Activity Index (SLEDAI) (22) (Table 1). Informed consent was obtained as approved by the Institutional Review Board after the nature and possible consequences of the studies were explained, in compliance with the Declaration of Helsinki.

Cell isolation. Peripheral blood mononuclear cells (PBMCs) were enriched by density-gradient centrifugation (Lymphocyte Separation Medium; Corning Life Sciences). T cells were isolated by negative selection (RosetteSep; StemCell Technologies).

Flow cytometric analysis. Cells were stained to distinguish live and dead cells (Zombie Aqua or Zombie NIR Fixable Viability Kit; BioLegend), and then labeled for surface antibodies. Cells were permeabilized using a Cytofix/Cytoperm kit (BD Biosciences) and stained for cytokines and/or cytotoxic enzymes. Data were acquired with a SORP LSR II flow cytometer (BD Biosciences) and analyzed using FlowJo software (version 10.1r5; Tree Star).

Table 1. Characteristics of the 79 SLE patients*

Age, median (range) years	41.3 (21–72)
Sex, no. (%) female/male	72 (91.1)/7 (8.9)
Ethnicity, no. (%)	
African American	22 (27.8)
Asian	5 (6.3)
Hispanic	7 (8.9)
White	40 (50.6)
Other	5 (6.3)
SLEDAI score, median (range)	3.6 (0–21)
Treatment, no. (%)	
Prednisone	50 (63.3)
Hydroxychloroquine	59 (74.7)
Mycophenolate mofetil	30 (38.0)
Azathioprine	10 (12.7)
Methotrexate	5 (6.3)
Belimumab	2 (2.5)
Tacrolimus	1 (1.3)
IVIG	1 (1.3)

* SLE = systemic lupus erythematosus; SLEDAI = SLE Disease Activity Index; IVIG = intravenous immunoglobulin.

Degranulation assay. Cryopreserved PBMCs (2×10^6) were stimulated for 6 hours in 1 ml of complete RPMI (RPMI 1640 supplemented with 10% fetal bovine serum, 100 mg/ml streptomycin, and 100 units/ml penicillin) in the presence of GolgiPlug (1 μl/ml; BD Biosciences) and GolgiStop (1 μl/ml; BD Biosciences), CD107a (4 μl/ml; BioLegend), and CEF (cytomegalovirus [CMV], Epstein-Barr virus [EBV], and influenza virus) peptide mix (3 μg/ml) or staphylococcal enterotoxin B (SEB; 1 μg/ml) as a positive control. When indicated, cells were also stimulated with anti-SLAMF7 mAb or a mouse IgG2b isotype control antibody (5 μg/ml; BioLegend), in the presence of a goat anti-mouse IgG crosslinker (EMD Millipore). At the end of the stimulation, cells were stained to distinguish live and dead cells (Zombie Aqua or Zombie NIR Fixable Viability Kit), then stained for surface antibodies with CD3 (BD Horizon BUV395 anti-human CD3), CD4 (PerCP eFluor 710–conjugated anti-human CD4; eBioscience), and CD8 (PerCP-conjugated anti-human CD8; BioLegend), fixed/permeabilized (Cytofix/Cytoperm kit), and stained for interferon-γ (IFNγ) (Alexa Fluor 647–conjugated anti-human IFNγ; BioLegend). Cells were then analyzed using a SORP LSR II flow cytometer and FlowJo software (version 10.1r5).

Flow cytometry–based assay for measuring CD8+ T cell cytotoxic activity in response to anti-SLAMF7 mAb treatment. Freshly isolated PBMCs were cultured in the presence of CEF peptide mix (5 μg/ml) and interleukin-2 (IL-2) (20 IU/ml; PeproTech) for 6 days in complete RPMI. On day 3, half of the cell culture medium was replaced with fresh complete RPMI. On day 6, effector CD8+ T cells were isolated by negative selection using magnetic sorting (human CD8+ T cell isolation kit; Miltenyi Biotec). Cells were resuspended at a concentration of 10^6/ml. Six serial dilutions were performed. From each dilution, half of the cells were treated with anti-SLAMF7 mAb (5 μg/ml) and a goat anti-mouse IgG crosslinker, while the other half were

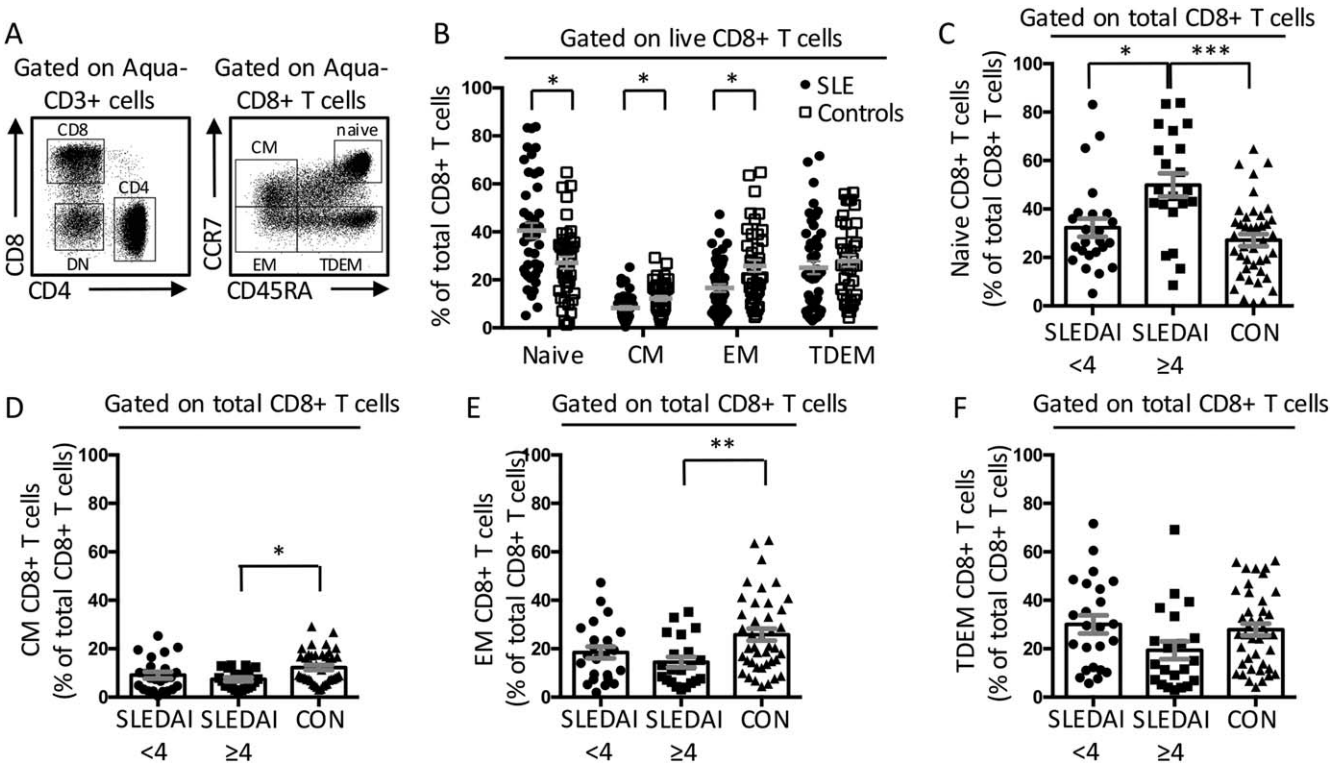

Figure 1. Distribution of differentiated CD8+ T cell subsets in peripheral blood from patients with systemic lupus erythematosus (SLE) and controls. **A,** Staining of peripheral blood mononuclear cells isolated from SLE patients for differentiated subsets of CD8+ T cells. Cells were classified according to the expression of CCR7 and CD45RA. CCR7+CD45RA+ cells were considered naive, CCR7+CD45RA− cells were considered central memory (CM), CCR7−CD45RA− cells were considered effector memory (EM), and CCR7−CD45RA+ cells were considered terminally differentiated effector memory (TDEM) CD8+ T cells. CD3+CD4−CD8− cells were considered double-negative (DN) T cells. **B,** Distribution of differentiated CD8+ T cell subsets in SLE patients compared to healthy controls. Symbols represent individual subjects; horizontal lines with bars show the mean ± SEM (n = 45 patients with SLE and 41 controls). **C–F,** Frequency of naive CD8+ T cells (**C**), central memory CD8+ T cells (**D**), effector memory CD8+ T cells (**E**), and terminally differentiated effector memory CD8+ T cells (**F**) in patients with inactive SLE (SLE Disease Activity Index [SLEDAI] score of <4), patients with active SLE (SLEDAI score of ≥4), and healthy controls. Symbols represent individual subjects; bars show the mean ± SEM. $* = P < 0.05$; $** = P < 0.01$; $*** = P < 0.001$.

treated with an IgG isotype control and a goat anti-mouse IgG crosslinker. One hundred microliters of each CD8+ T cell preparation was seeded in duplicate in a 96-well U-bottomed plate.

Freshly isolated autologous CD4+ T cells sorted by magnetic negative selection (human CD4+ T cell isolation kit; Miltenyi Biotec) were used as a target. Half of the CD4+ T cells were labeled with 5,6-carboxyfluorescein succinimidyl ester (CFSE) 0.2 μM (CFSE high) and were pulsed with CEF peptide (5 μg/ml) for 45 minutes at 37°C in complete RPMI. The other half of the CD4+ T cells were labeled with CFSE 0.02 μM (CFSE low) and were used as a control to determine nonspecific background cell death. CFSE-high and -low CD4+ T cells were mixed at a 1:1 ratio and resuspended at a concentration of 2×10^5 cells/ml. One hundred microliters of target CD4+ T cells was added to each dilution of CD8+ T cells. Cell mixtures were incubated for 6 hours at 37°C.

After incubation, cells were stained to distinguish live and dead cells (Zombie Aqua Fixable Viability Kit), stained for CD4 (allophycocyanin [APC]–conjugated anti-human CD4 antibody; BioLegend) and CD8 (APC/Cy7-conjugated anti-human CD8 antibody; BioLegend), and analyzed by flow cytometry. Aqua-positive staining indicated dead cells. The percentage of target cell lysis in response to effector CD8+ T cells was expressed as (% of Aqua+ pulsed CD4+ T cells) − (% of Aqua+ unpulsed CD4+ T cells).

Real-time quantitative reverse transcriptase–polymerase chain reaction (RT-PCR). Total RNA was extracted using an RNeasy Mini kit (Qiagen). Reverse transcription was performed from 500 ng of total RNA using a High-Capacity cDNA Archive Kit (Applied Biosystems). Quantitative RT-PCR was performed with 40 cycles at 94°C (for 12 seconds) and 60°C (for 60 seconds) using SYBR Green (LightCycler 4800 SYBR Green I Master kit; Roche). The comparative C_t method was used to quantify transcripts relative to the endogenous control gene β-actin. Primer sequences were as follows: for EAT-2, forward 5′-TGTGCCTCTGTGTCTCGTTTA-3′ and reverse 5′-ACCACCATCCCCTGATTTGG-3′; and for β-actin, forward 5′-AGAGCTACGAGCTGCCTGAC-3′ and reverse 5′-AGCACTGTGTTGGCGTACAG-3′.

Statistical analysis. Statistical analysis was performed using Student's *t*-test, corrected with the Holm-Sidak method. For multiple comparisons, statistical analysis was performed using one-way analysis of variance, followed by post hoc analysis

with Tukey's test. Statistical analyses and illustrations were performed using FlowJo software (version 10.1r5) and GraphPad Prism software (version 6).

RESULTS

Skewed distribution of CD8+ T cell subsets in the peripheral blood of SLE patients. We analyzed the distribution of CD8+ T cell subsets in the peripheral blood of 45 SLE patients with varying levels of disease activity and 41 healthy controls by assessing the cell surface expression of CCR7 and CD45RA. This allowed us to distinguish 4 differentiated CD8+ T cell subsets, i.e., naive (CCR7+ CD45RA+), central memory (CCR7+CD45RA−), effector memory (CCR7−CD45RA−), and terminally differentiated effector memory (CCR7−CD45RA+) cells (23) (Figure 1A). The frequency of effector memory CD8+ T cells was reduced in SLE patients compared to healthy controls, while naive CD8+ T cells were enriched (Figure 1B). Moreover, the skewed distribution of CD8+ T cells correlated with disease activity. Patients with active disease (defined as a SLEDAI score of ≥4) displayed a significant increase in naive CD8+ T cells compared to patients with inactive disease (defined as a SLEDAI score of <4) and compared to healthy controls (Figure 1C). In contrast, the frequency of central memory and effector memory CD8+ T cells was significantly decreased in patients with active disease compared to healthy controls (Figures 1D and E).

We observed a significant linear correlation between decreased number of terminally differentiated effector memory CD8+ T cells and the SLEDAI score, which is associated with an increased frequency of CD8+ T cells expressing naive markers (see Supplementary Figure 1, available on the *Arthritis & Rheumatology* web site at http://onlinelibrary.wiley.com/doi/10.1002/art.40038/abstract). Of note, there was no difference in the percentage of total CD8+ T cells between SLE patients and controls (see Supplementary Figure 2, available on the *Arthritis & Rheumatology* web site at http://onlinelibrary.wiley.com/doi/10.1002/art.40038/abstract).

Decreased SLAMF7 expression in CD8+ T cells from SLE patients. Expression of SLAMF7 was examined in T cells isolated from SLE patients (n = 16–27) and healthy controls (n = 13–22). SLAMF7 was mostly expressed by CD8+ T cells, as well as double-negative T cells, a T cell subset that expresses CD3 but has lost CD4 and CD8 expression (Figure 2A and Supplementary Figure 3A, available on the *Arthritis & Rheumatology* web site at http://onlinelibrary.wiley.com/doi/10.1002/art.40038/abstract). In contrast, expression of SLAMF7 on CD4+ T cells was very low. Expression of SLAMF7 was reduced in CD8+ T cells and double-negative cells isolated from SLE patients compared to healthy controls (Figure 2A). Reduced SLAMF7 expression correlated with disease activity. SLE patients with active disease displayed less SLAMF7 expression than patients with inactive disease (Figure 2B and Supplementary Figure 4, available on the *Arthritis & Rheumatology* web site at http://onlinelibrary.wiley.com/doi/10.1002/art.40038/abstract).

Because the distribution of CD8+ T cell subsets was altered in SLE patients, we examined the expression of SLAMF7 in each differentiated CD8+ T cell subset (naive, central memory, effector memory, and terminally differentiated effector memory cells). We observed that SLAMF7 expression increased during cell differentiation. Its expression was low in naive CD8+ T cells, whereas most effector memory and terminally differentiated effector memory cells expressed SLAMF7 (Figure 2C and Supplementary Figure 3B). Importantly, each of the CD8+ T cell subsets from SLE patients displayed decreased amounts of SLAMF7 compared to controls (Figure 2C). SLAMF7 expression was decreased among CD8+ T cells isolated from SLE patients with active disease compared to those from patients with inactive disease (Figure 2D and Supplementary Figure 3C and Supplementary Figure 4).

Because it has previously been reported that SLAMF7 binds to EAT-2 in NK cells to transmit downstream signaling (11), we assessed the expression of EAT-2 in SLAMF7− CD8+ and SLAMF7+ CD8+ T cells by quantitative PCR. We did not detect any EAT-2 gene expression in CD8+ T cells (see Supplementary Figure 5, available on the *Arthritis & Rheumatology* web site at http://onlinelibrary.wiley.com/doi/10.1002/art.40038/abstract).

In summary, SLAMF7 expression increases during the differentiation of CD8+ T cells and is mostly expressed by effector memory and terminally differentiated effector memory CD8+ T cells. Moreover, SLAMF7 expression is decreased in SLE CD8+ T cells compared to healthy controls.

Expression of SLAMF7 by effector CD8+ cytotoxic T cells. To further examine the properties of SLAMF7+ CD8+ T cells, we assessed the coexpression of SLAMF7 and cytolytic enzymes (perforin, granzyme A [GzmA], and GzmB) in CD8+ T cells isolated from the peripheral blood of SLE patients (n = 18) and controls (n = 15). Expression of the cytolytic enzymes perforin, GzmA, and GzmB was found to be restricted to SLAMF7+ CD8+ T cells (Figure 3). As previously described (7), an altered expression of cytolytic enzymes was found in SLE patients compared to healthy controls. Perforin and GzmB expression was reduced in SLE patients, while GzmA expression was slightly increased.

In summary, SLAMF7 expression defines cytotoxic effector CD8+ T cells, and its expression is decreased in SLE and is associated with an altered expression of cytotoxic

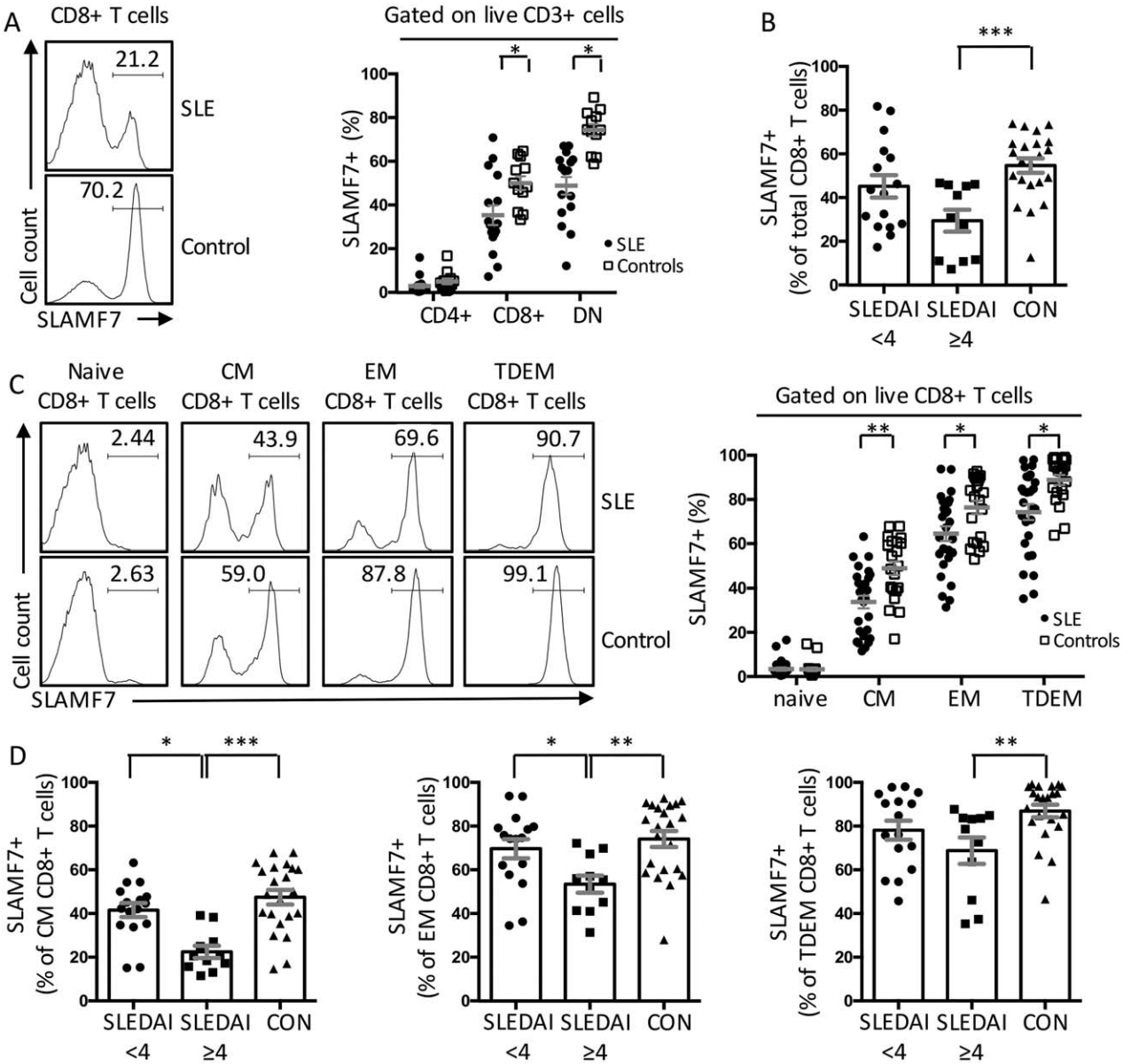

Figure 2. Reduction in signaling lymphocytic activation molecule family member 7 (SLAMF7) expression on CD8+ T cells from SLE patients compared to those from healthy controls. SLAMF7 expression was assessed by flow cytometry on T cells isolated from peripheral blood. **A,** Frequency of SLAMF7 expression on CD4+, CD8+, and double-negative T cells isolated from SLE patients and controls. **B,** Correlation of SLAMF7 expression with disease activity. SLAMF7 expression in patients with inactive SLE (SLEDAI score of <4), patients with active SLE (SLEDAI score of ≥4), and healthy controls is shown. **C,** Frequency of SLAMF7 expression on naive, central memory, effector memory, and terminally differentiated effector memory CD8+ T cells in SLE patients and healthy controls. **D,** SLAMF7 expression on central memory, effector memory, and terminally differentiated effector memory CD8+ T cells in patients with inactive SLE, patients with active SLE, and healthy controls. Symbols represent individual subjects (n = 16–27 SLE patients and 13–22 controls). In **A** and **C,** horizontal lines with bars show the mean ± SEM. In **B** and **D,** bars show the mean ± SEM. * = $P < 0.05$; ** = $P < 0.01$; *** = $P < 0.001$. See Figure 1 for other definitions.

CD8+ T cell enzymes. Expression of cytolytic enzymes was also examined in differentiated subsets of CD8+ T cells. As expected, expression of cytolytic enzymes was higher in effector cells (especially effector memory and terminally differentiated effector memory CD8+ T cells) than in naive CD8+ T cells. When SLE patients and controls were compared, we observed the same alteration in total CD8+ T cells. There was a trend toward decreased expression of perforin and GzmB, while expression of GzmA was increased in SLE effector memory and terminally differentiated

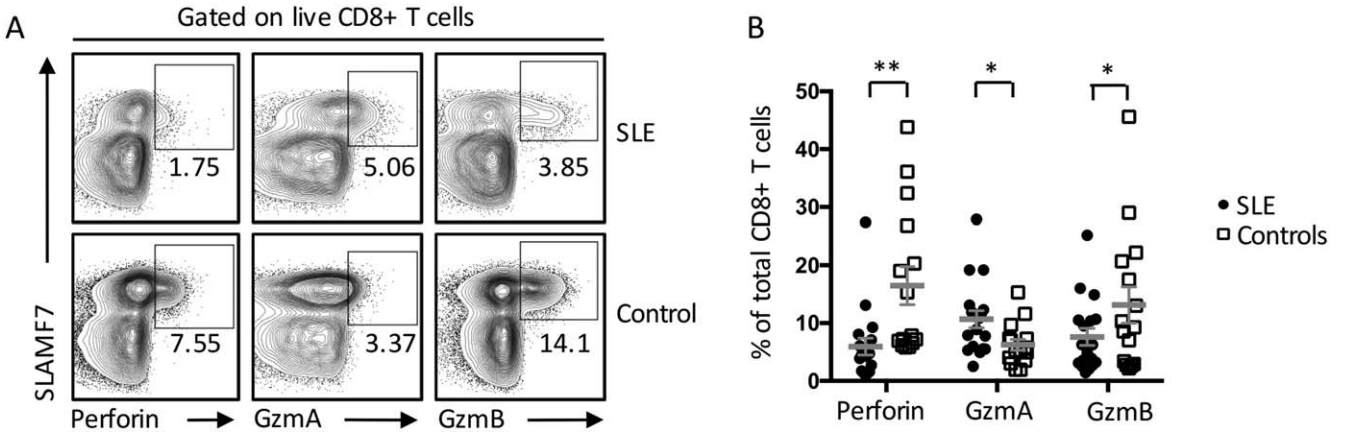

Figure 3. Restriction of the expression of perforin, granzyme A (GzmA), and GzmB to the SLAMF7+ CD8+ T cell population. The frequencies of CD8+ T cells expressing perforin, GzmA, and GzmB were assessed by flow cytometry. **A,** Representative flow cytometry profile of SLAMF7 versus perforin, GzmA, and GzmB in cells from systemic lupus erythematosus (SLE) patients and healthy controls. Values are the percentage of cells. **B,** Percentage of SLE and healthy control CD8+ T cells expressing perforin, GzmA, and GzmB. Symbols represent individual subjects; horizontal lines with bars show the mean ± SEM (n = 18 SLE patients and 15 controls). $* = P < 0.05$; $** = P < 0.01$.

effector memory CD8+ T cell subsets (see Supplementary Figure 6, available on the *Arthritis & Rheumatology* web site at http://onlinelibrary.wiley.com/doi/10.1002/art.40038/abstract).

SLAMF7 engagement restores the antiviral CD8+ T cell response that is impaired in SLE patients. To examine the degranulation capacity of CD8+ T cells in response to viral antigens, we stimulated PBMCs isolated from SLE patients (n = 8) or healthy individuals (n = 8) with a mixture of major histocompatibility complex class I–restricted T cell epitopes from human CMV, EBV, and influenza virus (CEF) (7,24,25). PBMCs were stimulated with or without anti-SLAMF7 mAb. Cells were stained for CD3, CD8, CD107a (lysosome-associated membrane protein 1, a marker of degranulation), and IFNγ, and examined for the proportion of CD8+ T cells that were CD107a/

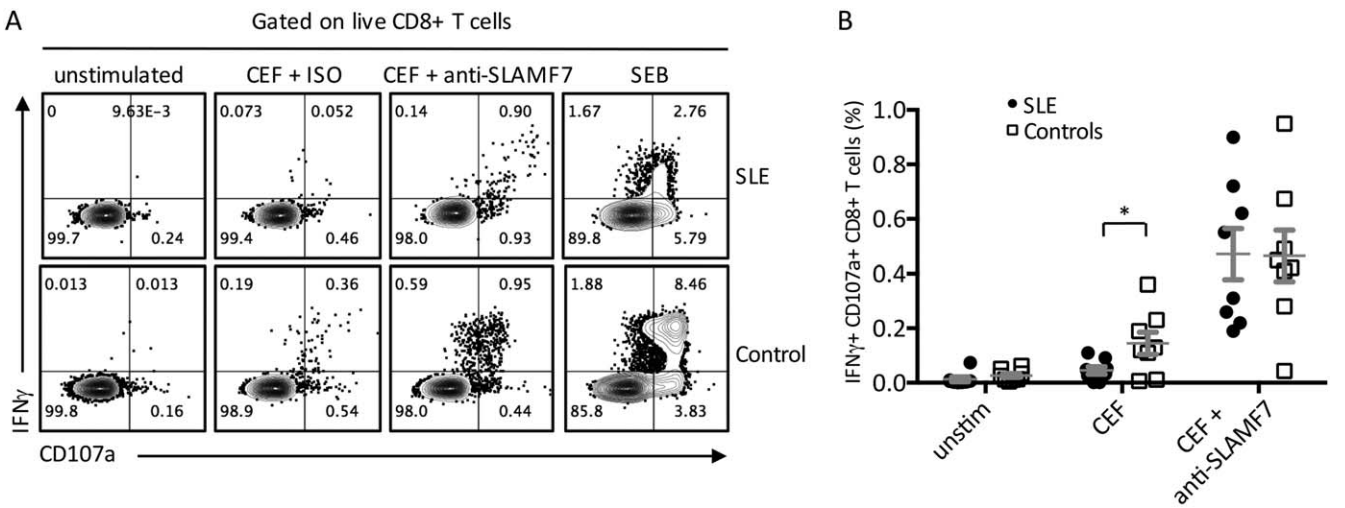

Figure 4. Restoration of the effector function of systemic lupus erythematosus (SLE) CD8+ T cells after signaling lymphocytic activation molecule family member 7 (SLAMF7) engagement. Peripheral blood mononuclear cells (PBMCs) from SLE patients and controls were stimulated with a cytomegalovirus, Epstein-Barr virus, and influenza virus (CEF) peptide mix for 6 hours in the presence of an isotype (ISO) control or an anti-SLAMF7 monoclonal antibody. CD107a expression and interferon-γ (IFNγ) production were assessed by flow cytometry at the end of the stimulation. Staphylococcal enterotoxin B (SEB) was used as a positive control. **A,** Representative flow cytometry plots. Values are the percentage of cells. **B,** Percentage of CD107a/IFNγ double-positive CD8+ T cells in SLE and control PBMCs that were left unstimulated or were stimulated with CEF or with CEF and anti-SLAMF7. Symbols represent individual subjects; horizontal lines with bars show the mean ± SEM (n = 8 SLE patients and 8 controls). $* = P < 0.05$.

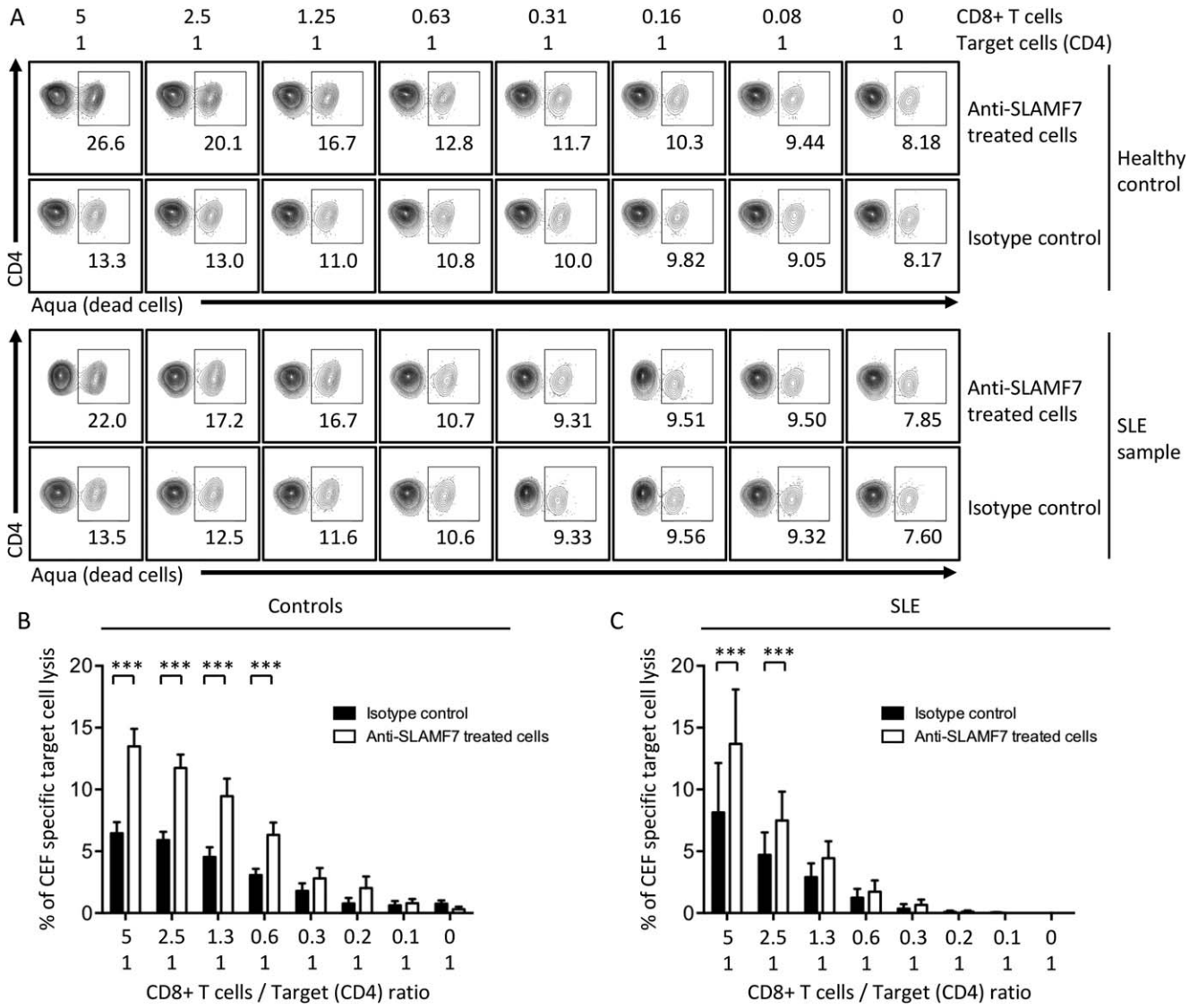

Figure 5. Signaling lymphocytic activation molecule family member 7 (SLAMF7) ligation enhances the viral antigen–induced cytotoxic activity of CD8+ T cells from healthy controls and systemic lupus erythematosus (SLE) patients. Peripheral blood mononuclear cells (PBMCs) stimulated with a cytomegalovirus, Epstein-Barr virus, and influenza virus (CEF) peptide mix were enriched for CD8+ T cells. CD8+ T cells were treated with an isotype control or an anti-SLAMF7 monoclonal antibody and cocultured for 6 hours with autologous CEF pulsed CD4+ T cells and unpulsed CD4+ T cells. CEF-specific killing of target CD4+ T cells was expressed as the percentage of Aqua-positive cells (marker of dead cells) in response to different ratios of CD8+ T cells. Unpulsed CD4+ T cells were used as a control to determine background target cell death. **A,** Representative dot plots showing the percentage of CD4+ T cells killed in response to SLAMF7-treated or isotype control–treated CD8+ T cells. **B** and **C,** Percentage of CEF-specific target cell lysis in PBMCs from healthy controls (**B**) and SLE patients (**C**). Results are expressed as (Aqua+ pulsed CD4+ T cells) − (Aqua+ unpulsed CD4+ T cells). Bars show the mean ± SEM (n = 4 controls and 5 SLE patients). *** = $P < 0.001$.

IFNγ double positive, a population that has been associated with antiviral protective immunity (26,27). SEB was used as a positive control.

SLAMF7 engagement with a specific mAb increased the response of CD8+ T cells to CEF stimulation by enhancing the frequency of CD8+ CD107a/IFNγ double-positive T cells (Figure 4). Compared to healthy controls, SLE patients had fewer CD8+ CD107a/IFNγ double-positive T cells in response to CEF (Figure 4). In the presence of anti-SLAMF7 mAb, the frequency of SLE CD8+ CD107a/IFNγ double-positive T cells in response to CEF stimulation was restored to levels comparable to those observed in healthy controls (Figure 4).

SLAMF7 engagement enhances the cytolytic activity of CD8+ T cells in response to viral antigens. Because SLAMF7 engagement favors CD8+ T cell degranulation

upon viral antigenic stimulation, we investigated whether SLAMF7 activation can trigger CD8+ T cell–mediated lysis of target cells. We performed a flow cytometry–based assay to measure the capacity of CEF-multispecific CD8+ T cells to kill autologous target CD4+ T cells loaded with cognate CEF peptide (modified from ref. 28). Nonloaded autologous CD4+ T cells were used as a control to determine background target cell death. Expanded effector CD8+ T cells were cocultured at different ratios with target cells. Lysis of CEF-loaded target CD4+ cells was augmented in the presence of increasing numbers of CEF antigen–multispecific effector CD8+ T cells (Figure 5 and Supplementary Figure 7, available on the *Arthritis & Rheumatology* web site at http://onlinelibrary.wiley.com/doi/10.1002/art.40038/abstract).

When CEF-expanded CD8+ T cells were activated with anti-SLAMF7 mAb instead of an isotype control prior to coculture with target CD4+ T cells, lysis of CEF-loaded autologous target CD4+ T cells was significantly increased (Figure 5). In samples from SLE patients, treatment with anti-SLAMF7 mAb, compared to treatment with an isotype control, also enhanced effector CD8+ T cell lysis of target cells in response to CEF peptide (Figure 5C). SLAMF7-mediated enhancement of target cell lysis in response to CEF peptides was similar in SLE patients and controls (Figures 5B and C). In summary, SLAMF7 engagement enhanced CD8+ T cell cytotoxicity in response to viral antigenic peptides.

DISCUSSION

In this study, we showed that the distribution of differentiated CD8+ T cell subsets was altered in peripheral blood from SLE patients. This skewed CD8+ T cell distribution was mainly characterized by a decreased number of effector memory CD8+ T cells, a subset of CD8+ cells that produce effector cytokines, such as IFNγ, and rapidly become cytotoxic upon antigenic challenge (29). This subset is poised for a rapid response at the onset of a microbial infection (30). Central memory CD8+ T cells are also decreased in the peripheral blood of patients with active SLE. Central memory cells primarily home to lymph nodes, and their main role is to proliferate and generate effector cells upon antigen stimulation (29). The reason CD8+ T cell distribution is altered in SLE remains unknown. One explanation could be that effector CD8+ T cells tend to become double-negative (CD3+CD4−CD8−) T cells, a subset that has been linked to SLE immunopathogenesis, in the context of continuous antigenic stimulation and chronic inflammation (31).

The reduced frequency of effector memory and central memory CD8+ T cells in patients with SLE may contribute to the increased infection rates seen in lupus patients (6–8). Furthermore, the effector function of CD8+ T cells (cytotoxic activity and cytokine production), which is considered a hallmark of antiviral protective immunity, is compromised in SLE (7,26). Expression of the cytolytic enzymes perforin, GzmA, and GzmB is dysregulated in CD8+ T cells from SLE patients compared with CD8+ T cells isolated from healthy individuals. CD8+ T cells from patients with SLE display significantly decreased levels of perforin and GzmB, whereas levels of GzmA appear to be slightly elevated. Perforin and GzmB are associated with the cytotoxic activity of effector CD8+ T cells (32). GzmA is much less cytotoxic than GzmB and is more likely involved in the proinflammatory process, since it activates monocytes to secrete inflammatory mediators and cleaves IL-1β from a propeptide to its activated form (33,34). Elevated levels of GzmA have been observed in the plasma and synovial fluid of rheumatoid arthritis patients, and in the blood of patients with chronic viral infection or allergic diseases (35). Increased levels of GzmA in SLE patients may represent a response to the underlying inflammation.

Moreover, the proportion of CD8+ T cells that are positive for both CD107a and IFNγ is reduced following stimulation of SLE PBMCs with viral antigens, thus further underscoring the defective effector function of SLE CD8+ T cells. This is consistent with our previous study showing that degranulation of CD8+ T cells in response to anti-CD3 stimulation is decreased in SLE (7).

In both healthy controls and SLE patients, the presence of SLAMF7 defines cytotoxic effector CD8+ T cells. The cytolytic enzymes perforin, GzmA, and GzmB are restricted to the SLAMF7+ CD8+ T cell population. Compared to CD8+ T cells isolated from healthy controls, expression of SLAMF7 is decreased in SLE CD8+ T cells. Reduced SLAMF7 expression was observed in each CD8+ memory cell subset (central memory, effector memory, and terminally differentiated effector memory cells). This difference of expression was more prominent in patients with active SLE.

The role of SLAMF7 has been extensively studied in patients with multiple myeloma, where ligation of SLAMF7 has been suggested to promote NK cytotoxicity and antibody-dependent cell-mediated cytotoxicity followed by a significant clinical benefit. In this study, we demonstrated that engagement of SLAMF7 with a specific anti-SLAMF7 antibody promotes CD8+ T cell degranulation, cytokine production, and cytotoxicity in response to viral peptides. Interestingly, even though SLAMF7 expression is decreased in SLE patients, its engagement enabled the restoration of degranulation, IFNγ production, and cytotoxic activity to levels comparable to those in controls.

Our data also suggest that enhancement of CD8+ T cell effector function in response to antigen may be a part of the mechanism leading to a favorable antitumor response in patients treated with anti-SLAMF7 mAb (36). It would be of interest to assess whether SLAMF7 ligation can expand the CD8+ T cell response against tumor antigens in patients with multiple myeloma or other tumors. Moreover, in NK cells, SLAMF7 has been shown to recruit the SH2 adaptor protein EAT-2 to initiate the cytotoxic signaling cascade (11,37). We did not detect EAT-2 expression in CD8+ SLAMF7+ T cells, suggesting that NK cells and CD8+ T cells use different pathways to promote cytotoxic response to SLAMF7 engagement. Whether SLAMF7-initiated responses in CD8+ T cells are mediated via SLAMF-associated protein or via other adaptor molecules remains to be determined.

The reason SLAMF7 expression is decreased in CD8+ T cells from SLE patients is not clear. In this study, we did not address the molecular mechanisms responsible for the decrease in SLAMF7 expression in SLE CD8+ T cells. An important question regarding this abnormality is whether the decrease in SLAMF7 expression is a primary defect related to the disease itself or an alteration that occurs at the onset of chronic inflammation, which may limit SLAMF7 protein formation or accelerate protein degradation. In this context, persistent antigen stimulation or chronic exposure to proinflammatory cytokines may contribute to SLAMF7 down-regulation. A genetic predisposition contributing to decreased SLAMF7 expression on SLE CD8+ T cells cannot be excluded either, since the SLAMF-containing locus 1q23 has been associated with lupus in both humans and mice (38,39).

Overall, our data suggest that SLAMF7 engagement restores to normal levels the defective effector function of CD8+ T cells in SLE. Correction of the CD8+ T cell antiviral responses in SLE patients should decrease the rate of infections and reduce morbidity and mortality.

ACKNOWLEDGMENT

We thank Dan Barouch for providing the CEF control peptide pool (from the NIH AIDS Reagent Program).

AUTHOR CONTRIBUTIONS

All authors were involved in drafting the article or revising it critically for important intellectual content, and all authors approved the final version to be published. Dr. Tsokos had full access to all of the data in the study and takes responsibility for the integrity of the data and the accuracy of the data analysis.

Study conception and design. Comte, Karampetsou, Tsokos.
Acquisition of data. Comte, Karampetsou, Yoshida, Kis-Toth.
Analysis and interpretation of data. Comte, Karampetsou, Kyttaris.

REFERENCES

1. Tsokos GC. Systemic lupus erythematosus. N Engl J Med 2011; 365:2110–21.
2. Comte D, Karampetsou MP, Tsokos GC. T cells as a therapeutic target in SLE. Lupus 2015;24:351–63.
3. Stohl W. Impaired polyclonal T cell cytolytic activity: a possible risk factor for systemic lupus erythematosus. Arthritis Rheum 1995;38:506–16.
4. Cohen PL, Eisenberg RA. Lpr and gld: single gene models of systemic autoimmunity and lymphoproliferative disease. Annu Rev Immunol 1991;9:243–69.
5. Peng SL, Moslehi J, Robert ME, Craft J. Perforin protects against autoimmunity in lupus-prone mice. J Immunol 1998;160:652–60.
6. Tsokos GC, Magrath IT, Balow JE. Epstein-Barr virus induces normal B cell responses but defective suppressor T cell responses in patients with systemic lupus erythematosus. J Immunol 1983;131:1797–801.
7. Kis-Toth K, Comte D, Karampetsou MP, Kyttaris VC, Kannan L, Terhorst C, et al. Selective loss of signaling lymphocytic activation molecule family member 4–positive CD8+ T cells contributes to the decreased cytotoxic cell activity in systemic lupus erythematosus. Arthritis Rheumatol 2016;68:164–73.
8. Puliaeva I, Puliaev R, Via CS. Therapeutic potential of CD8+ cytotoxic T lymphocytes in SLE. Autoimmun Rev 2009;8:219–23.
9. Cannons JL, Tangye SG, Schwartzberg PL. SLAM family receptors and SAP adaptors in immunity. Annu Rev Immunol 2011; 29:665–705.
10. Romero X, Sintes J, Engel P. Role of SLAM family receptors and specific adapter SAP in innate-like lymphocytes. Crit Rev Immunol 2014;34:263–99.
11. Wu N, Veillette A. SLAM family receptors in normal immunity and immune pathologies. Curr Opin Immunol 2016;38:45–51.
12. Lonial S, Dimopoulos M, Palumbo A, White D, Grosicki S, Spicka I, et al. Elotuzumab therapy for relapsed or refractory multiple myeloma. N Engl J Med 2015;373:621–31.
13. Hsi ED, Steinle R, Balasa B, Szmania S, Draksharapu A, Shum BP, et al. CS1, a potential new therapeutic antibody target for the treatment of multiple myeloma. Clin Cancer Res 2008;14:2775–84.
14. Collins SM, Bakan CE, Swartzel GD, Hofmeister CC, Efebera YA, Kwon H, et al. Elotuzumab directly enhances NK cell cytotoxicity against myeloma via CS1 ligation: evidence for augmented NK cell function complementing ADCC. Cancer Immunol Immunother 2013;62:1841–9.
15. Detre C, Keszei M, Romero X, Tsokos GC, Terhorst C. SLAM family receptors and the SLAM-associated protein (SAP) modulate T cell functions. Semin Immunopathol 2010;32:157–71.
16. Karampetsou MP, Comte D, Kis-Toth K, Terhorst C, Kyttaris VC, Tsokos GC. Decreased SAP expression in T cells from patients with systemic lupus erythematosus contributes to early signaling abnormalities and reduced IL-2 production. J Immunol 2016;196: 4915–24.
17. Comte D, Karampetsou MP, Kis-Toth K, Yoshida N, Bradley SJ, Mizui M, et al. Engagement of SLAMF3 enhances CD4+ T-cell sensitivity to IL-2 and favors regulatory T-cell polarization in systemic lupus erythematosus. Proc Natl Acad Sci U S A 2016;113:9321–6.
18. Hagberg N, Theorell J, Schlums H, Eloranta ML, Bryceson YT, Rönnblom L. Systemic lupus erythematosus immune complexes increase the expression of SLAM family members CD319 (CRACC) and CD229 (LY-9) on plasmacytoid dendritic cells and CD319 on $CD56^{dim}$ NK cells. J Immunol 2013;191:2989–98.
19. Kim JR, Mathew SO, Patel RK, Pertusi RM, Mathew PA. Altered expression of signalling lymphocyte activation molecule (SLAM) family receptors CS1 (CD319) and 2B4 (CD244) in patients with systemic lupus erythematosus. Clin Exp Immunol 2010;160:348–58.
20. Deng Y, Tsao BP. Genetic susceptibility to systemic lupus erythematosus in the genomic era. Nat Rev Rheumatol 2010;6:683–92.

21. Tan EM, Cohen AS, Fries JF, Masi AT, McShane DJ, Rothfield NF, et al. The 1982 revised criteria for the classification of systemic lupus erythematosus. Arthritis Rheum 1982;25:1271–7.
22. Bombardier C, Gladman DD, Urowitz MB, Caron D, Chang DH, and the Committee on Prognosis Studies in SLE. Derivation of the SLEDAI: a disease activity index for lupus patients. Arthritis Rheum 1992;35:630–40.
23. Sallusto F, Lenig D, Förster R, Lipp M, Lanzavecchia A. Two subsets of memory T lymphocytes with distinct homing potentials and effector functions. Nature 1999;401:708–12.
24. Currier JR, Kuta EG, Turk E, Earhart LB, Loomis-Price L, Janetzki S, et al. A panel of MHC class I restricted viral peptides for use as a quality control for vaccine trial ELISPOT assays. J Immunol Methods 2002;260:157–72.
25. Mwau M, McMichael AJ, Hanke T. Design and validation of an enzyme-linked immunospot assay for use in clinical trials of candidate HIV vaccines. AIDS Res Hum Retroviruses 2002;18: 611–8.
26. Seder RA, Darrah PA, Roederer M. T-cell quality in memory and protection: implications for vaccine design. Nat Rev Immunol 2008;8:247–58.
27. Cellerai C, Perreau M, Rozot V, Bellutti Enders F, Pantaleo G, Harari A. Proliferation capacity and cytotoxic activity are mediated by functionally and phenotypically distinct virus-specific CD8 T cells defined by interleukin-7Rα (CD127) and perforin expression. J Virol 2010;84:3868–78.
28. Noto A, Ngauv P, Trautmann L. Cell-based flow cytometry assay to measure cytotoxic activity. J Vis Exp 2013:e51105.
29. Sallusto F, Geginat J, Lanzavecchia A. Central memory and effector memory T cell subsets: function, generation, and maintenance. Annu Rev Immunol 2004;22:745–63.
30. Harari A, Dutoit V, Cellerai C, Bart PA, du Pasquier RA, Pantaleo G. Functional signatures of protective antiviral T-cell immunity in human virus infections. Immunol Rev 2006;211: 236–54.
31. Crispín JC, Tsokos GC. Human TCR-$\alpha\beta^+$ $CD4^-$ $CD8^-$ T cells can derive from $CD8^+$ T cells and display an inflammatory effector phenotype. J Immunol 2009;183:4675–81.
32. Joeckel LT, Bird PI. Are all granzymes cytotoxic in vivo? Biol Chem 2014;395:181–202.
33. Irmler M, Hertig S, MacDonald HR, Sadoul R, Becherer JD, Proudfoot A, et al. Granzyme A is an interleukin 1 β-converting enzyme. J Exp Med 1995;181:1917–22.
34. Metkar SS, Menaa C, Pardo J, Wang B, Wallich R, Freudenberg M, et al. Human and mouse granzyme A induce a proinflammatory cytokine response. Immunity 2008;29:720–33.
35. Lieberman J. Granzyme A activates another way to die. Immunol Rev 2010;235:93–104.
36. Wen YJ, Min R, Tricot G, Barlogie B, Yi Q. Tumor lysate-specific cytotoxic T lymphocytes in multiple myeloma: promising effector cells for immunotherapy. Blood 2002;99:3280–5.
37. Tassi I, Colonna M. The cytotoxicity receptor CRACC (CS-1) recruits EAT-2 and activates the PI3K and phospholipase Cγ signaling pathways in human NK cells. J Immunol 2005;175: 7996–8002.
38. Tsao BP, Cantor RM, Grossman JM, Kim SK, Strong N, Lau CS, et al. Linkage and interaction of loci on 1q23 and 16q12 may contribute to susceptibility to systemic lupus erythematosus. Arthritis Rheum 2002;46:2928–36.
39. Hogarth MB, Slingsby JH, Allen PJ, Thompson EM, Chandler P, Davies KA, et al. Multiple lupus susceptibility loci map to chromosome 1 in BXSB mice. J Immunol 1998;161:2753–61.

ARTHRITIS & RHEUMATOLOGY
Vol. 69, No. 5, May 2017, pp 1045–1053
DOI 10.1002/art.40032

Effect of Continuous B Cell Depletion With Rituximab on Pathogenic Autoantibodies and Total IgG Levels in Antineutrophil Cytoplasmic Antibody–Associated Vasculitis

Frank B. Cortazar,[1] William F. Pendergraft III,[2] Julia Wenger,[2] Charles T. Owens,[3] Karen Laliberte,[1] and John L. Niles[1]

Objective. **To evaluate the effect of rituximab on pathogenic autoantibodies and total Ig levels, and to identify serious adverse events in patients with antineutrophil cytoplasmic antibody (ANCA)–associated vasculitis (AAV) treated with continuous B cell depletion.**

Methods. **We conducted a retrospective analysis of 239 patients with AAV treated with rituximab-induced continuous B cell depletion. Two treatment cohorts were analyzed: an induction group (n = 52) and a maintenance group (n = 237). Changes in ANCA titers and total Ig levels over time were evaluated using mixed-effects models. Risk factors for serious infections during maintenance treatment were evaluated using Poisson regression.**

Results. **During induction, IgG levels fell at a mean rate of 6% per month (95% confidence interval [95% CI] 4, 8%), while ANCA levels declined at a mean rate of 47% per month (95% CI 42, 52%) and 48% per month (95% CI 42, 54%) for patients with antimyeloperoxidase (anti-MPO) antibodies and those with anti–proteinase 3 (anti-PR3) antibodies, respectively. During maintenance treatment, with a median duration of 2.4 years (interquartile range 1.5, 4.0 years), IgG levels declined a mean of 0.6% per year (95% CI −0.2, 1.4%). New significant hypogammaglobulinemia (IgG level of <400 mg/dl) during maintenance treatment occurred in 4.6% of the patients, all of whom were in the lowest baseline IgG quartile. Serious infections during maintenance therapy occurred at a rate of 0.85 per 10 patient-years (95% CI 0.66, 1.1) and were independently associated with an IgG level of <400 mg/dl.**

Conclusion. **B cell–targeted therapy causes a preferential decline in ANCA titers relative to total IgG levels. Despite prolonged maintenance therapy with rituximab, IgG levels remain essentially constant. Serious infections were rare.**

The anti-CD20 monoclonal antibody rituximab has emerged as a useful immunosuppressive agent for the treatment of several antibody-mediated autoimmune diseases (1,2). An important immunosuppressive mechanism of rituximab is the attenuation of the production of pathogenic autoantibodies (3–5). The potential downside of this therapy is suppression of the protective benefits of the humoral immune system, thus predisposing to infectious complications (6,7). The degree to which treatments with rituximab can suppress pathogenic autoantibodies, compared to suppression of protective antibodies, may be a major determinant of the clinical value of these treatments. Characteristics of the disease, variations in the treatment regimen, and patient characteristics may heavily influence this balance.

Rituximab has become an important component of the treatment of antineutrophil cytoplasmic antibody (ANCA)–associated vasculitis (AAV) (2,8,9). The Rituximab in ANCA-Associated Vasculitis (RAVE) trial suggested that a regimen with rituximab and glucocorticoids was equivalent to the standard regimen of cyclophosphamide

Dr. Cortazar's work was supported by the National Institute of Diabetes and Digestive and Kidney Diseases (NIDDK) grant 5T32-DK-007540 from the NIH. Dr. Pendergraft's work was supported by NIDDK grants P01-DK-058335, 1UM1-DK-100845, and F32-DK-097891 from the NIH and by translational research funding from The Broad Institute.

[1]Frank B. Cortazar, MD, Karen Laliberte, RN, John L. Niles, MD: Massachusetts General Hospital, Boston; [2]William F. Pendergraft III, MD, PhD, Julia Wenger, MPH: University of North Carolina Kidney Center, Chapel Hill; [3]Charles T. Owens, MD: Baylor University Medical Center at Dallas, Dallas, Texas.

Dr. Cortazar has received a research grant from Genentech. Dr. Niles has received consulting fees, speaking fees, and/or honoraria from Genentech (less than $10,000).

Address correspondence to Frank B. Cortazar, MD, Vasculitis and Glomerulonephritis Center, Division of Nephrology, Massachusetts General Hospital, 101 Merrimac Street, Boston, MA 02114. E-mail: fcortazar@partners.org.

Submitted for publication April 28, 2016; accepted in revised form December 15, 2016.

with glucocorticoids for induction of remission (2). More recently, the Maintenance of Remission using Rituximab in Systemic ANCA-Associated Vasculitis (MAINRITSAN) trial suggested that rituximab with low-dose prednisone is superior to azathioprine with low-dose prednisone as maintenance therapy to prevent disease relapse (9). An additional randomized controlled trial evaluating rituximab for maintenance of remission is ongoing (10).

Unfortunately, relapse is common in AAV following cessation of rituximab, and is often heralded by B cell reconstitution (11,12). With the aim of preventing disease relapse, our practice has evolved to treat patients for extended periods of time with scheduled rituximab dosing to maintain B cell depletion (13). Data on the complications of such a treatment regimen, however, are sparse. One particular concern is the development of hypogammaglobulinemia and predisposition to serious infections.

In this study, we retrospectively evaluate the impact of continuous B cell depletion with rituximab on Ig levels during induction and maintenance of remission therapy for AAV. In particular, we compare the relative effect of treatment on the levels of pathogenic auto antibodies versus the effect on total Ig levels. In addition, we describe serious adverse events and identify predictive factors for the development of hypogammaglobulinemia and serious infections.

PATIENTS AND METHODS

Study population and treatment groups. We performed a single-center retrospective analysis of 239 patients with AAV treated with rituximab-induced continuous B cell depletion at the Massachusetts General Hospital Vasculitis and Glomerulonephritis Center from April 2006 to August 2015. Patients were considered to have AAV if they had a positive test result for antibodies to proteinase 3 (PR3) or myeloperoxidase (MPO) together with clinical and laboratory features consistent with granulomatosis with polyangiitis (Wegener's), microscopic polyangiitis, or one of the other related forms of vasculitis (14).

Starting in 2006, our practice evolved into following a consistent treatment regimen for induction and maintenance of remission in the majority of patients. For induction therapy, patients receive combination therapy with rituximab, a 2-month course of low-dose oral cyclophosphamide, and a short course of high-dose steroids with a rapid taper to low dose. The rationale for combining rituximab with cyclophosphamide is to allow for rapid tapering of high-dose glucocorticoids, such that the prednisone dosage is reduced to 15 mg daily by the fifth week of treatment.

For maintenance therapy, patients receive scheduled rituximab treatments with or without low-dose prednisone ($\leq$7.5 mg/day). Prednisone is slowly tapered to discontinuation except as limited by adrenal insufficiency. Rituximab is initially administered as two 1-gm doses intravenously (IV) separated by $\sim$2 weeks. Thereafter, rituximab is administered as a 1-gm dose IV every 4 months for 2 years, followed by a 1-gm dose IV every 6 months. B cell depletion, defined as $<$10 CD20+ cells/mm^3, is confirmed using peripheral flow cytometry prior to each rituximab infusion. In the rare event that B cell return is detected, the dosing interval for that patient is shortened.

During induction of remission therapy, all patients receive trimethoprim/sulfamethoxazole as prophylaxis for *Pneumocystis jiroveci* pneumonia (PCP). Patients with an allergy to sulfonamides are administered atovaquone as an alternative. During maintenance therapy, prophylaxis for PCP is continued until prednisone is completely discontinued and patients are receiving rituximab monotherapy. Patients with a positive hepatitis B core antibody are given either entecavir or lamivudine as prophylaxis for hepatitis B reactivation.

Two treatment groups were analyzed in this study: an induction group and a maintenance group (Figure 1). Patients

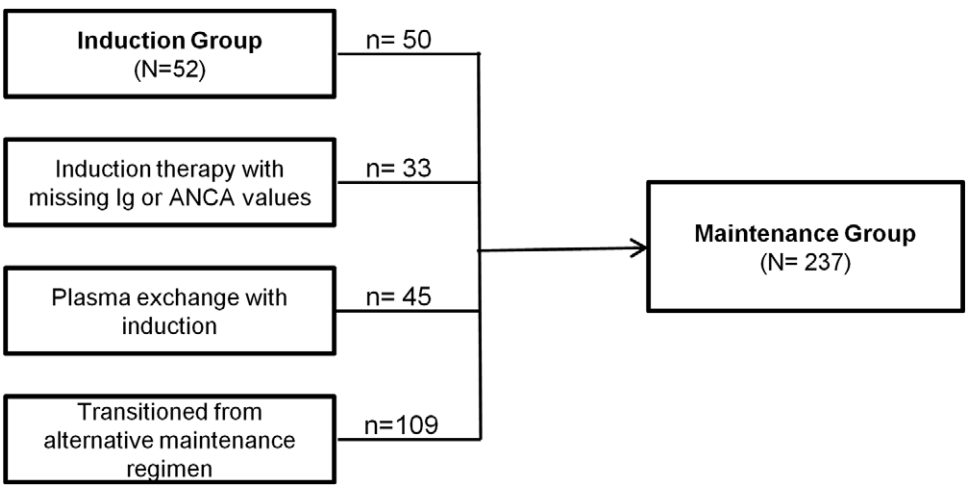

Figure 1. Composition of the induction and maintenance groups. The induction group comprised 52 patients who received treatment with combination rituximab, cyclophosphamide, and prednisone and had data on baseline and follow-up antineutrophil cytoplasmic antibody (ANCA) titers and IgG levels available. The maintenance group comprised 237 patients in whom remission was achieved after induction therapy or who were transitioned from an alternative maintenance regimen.

were included in the induction group if they had newly diagnosed and active AAV (Birmingham Vasculitis Activity Score for Wegener's Granulomatosis [BVAS/WG] ≥3) (15), were treated with the induction regimen described above, and had baseline and follow-up IgG and ANCA levels recorded during the induction period. Patients with relapsing disease and patients treated with plasma exchange were excluded. The induction phase began with the first dose of rituximab during induction therapy and ended when complete remission was achieved (defined as a BVAS/WG of 0, a prednisone dosage of ≤7.5 mg/day, and the absence of immunosuppressants other than rituximab and prednisone).

Patients were included in the maintenance group if they were in complete remission, were being treated with rituximab maintenance therapy as described above, and had baseline and follow-up IgG and ANCA levels recorded during the maintenance period. For patients who had received plasma exchange, inclusion started 180 days after initiation of therapy or after complete remission was attained, whichever was later. Patients who received alternative maintenance regimens were excluded from this analysis. In the event of a disease relapse, patients remained in the maintenance cohort provided they continued to receive scheduled rituximab treatments. Patients who ultimately had rituximab withdrawn were censored at the time of B cell return.

Cases of AAV associated with levamisole were excluded. Likewise, patients with simultaneous membranous nephropathy or anti–glomerular basement membrane disease were excluded. The study was approved by the Partners HealthCare Human Research Committee.

Measurement of Ig and ANCA levels. Ig and ANCA levels were typically measured approximately every 4–6 months in patients receiving continuous B cell depletion as part of clinical care. ANCA titers were measured by enzyme-linked immunosorbent assay as previously described (16,17). Briefly, all samples were tested in comparison to a standard reference serum by creation of a standard curve generated from serial 1:2 dilutions. Test samples were diluted 1:16 followed by serial 1:8 dilutions. Concentrations were read off the standard curve and multiplied by the relative dilution to determine the relative concentration. Only dilutions with reactivity falling on the steep part of the reference curve were used for determining the concentration.

For the induction of remission analysis, changes in levels were determined using values from the first measurements closest to the time of initiation of induction treatment (values obtained >2 months before the first dose were excluded) up to 150 days after the first dose of rituximab. In the maintenance of remission analysis, changes in levels were determined using values from the first measurement on or after the date of full remission until the last measurement with documented B cell depletion (<10 B cells/mm^3).

Serious adverse events and hypogammaglobulinemia. Serious adverse events were defined as events that were life-threatening, led to a hospitalization, caused persistent disability or permanent damage, or resulted in death. Serious adverse events were determined by review of our electronic medical records and flow sheets maintained as part of patient management. Significant hypogammaglobulinemia was defined as an IgG level of <400 mg/dl. This level was chosen based on prior studies that demonstrated a higher risk of infection below this threshold (18,19).

Statistical analysis. All analyses were carried out using Stata version 14. Patient baseline characteristics were stratified by treatment group. Continuous variables are presented as the mean ± SD or median (interquartile range [IQR]) as appropriate, and categorical variables are presented as percentages. *P* values for baseline characteristics are not provided because many patients were included in both the induction and maintenance groups, and the observations were not independent.

Mean population changes in Ig levels and ANCA titers were evaluated using linear mixed-effects modeling by regressing log(ANCA titer or Ig level) against time. In the maintenance group, the model was constructed with a random patient-specific intercept and random time effect. Given the limited number of observations per patient in the induction group, models were constructed with a random patient-specific intercept only.

Time to hypogammaglobulinemia during maintenance treatment stratified by baseline IgG level was described using Kaplan-Meier curves. Predictors of hypogammaglobulinemia were evaluated using Cox proportional hazards models. The 95% confidence intervals (95% CIs) and predictors of serious adverse events/infections were evaluated using Poisson regression, treating serious events as a count outcome. For both Cox and Poisson regression, the following covariates were prespecified based on scientific relevance: age, sex, ANCA serotype, baseline IgG level, history of plasma exchange, time from diagnosis of AAV to initiation of rituximab, and duration of continuous B cell depletion prior to remission. Due to the limited number of patients who developed hypogammaglobulinemia, only univariable Cox models were assessed. For Poisson regression, both univariable and multivariable models were constructed. The multivariable model was adjusted for all prespecified covariates listed above.

RESULTS

Baseline characteristics of the patients. Between April 2006 and April 2015, 52 and 237 patients met inclusion criteria for the induction and maintenance groups, respectively. Fifty patients from the induction group were included in the maintenance group. The induction group comprised patients with newly diagnosed and active AAV (BVAS/WG ≥3) who received a standardized induction regimen. The maintenance group consisted of patients in complete remission (with a BVAS/WG of 0 and a prednisone dosage of ≤7.5 mg/day) treated with rituximab-induced continuous B cell depletion. Patients in the maintenance group included those treated with a standardized induction regimen in whom complete remission was achieved and those who were already receiving maintenance therapy with an alternative agent and were transitioned to rituximab (Figure 1). Patients who transitioned from an alternative maintenance regimen were diagnosed as having AAV a median of 4.3 years (IQR 1.1, 8.1 years) before entering the maintenance cohort. At entry into the maintenance cohort, 92% of the patients were receiving prednisone (median 7.5 mg/day [IQR 5, 7.5]). Thereafter, prednisone was tapered to discontinuation as possible

Table 1. Baseline characteristics of the AAV patients*

Characteristic	Induction therapy (n = 52)	Maintenance therapy (n = 237)
Age, mean ± SD years	62 ± 14	61 ± 16
Sex, no. (%) female	30 (57)	140 (59)
Anti-MPO positive at diagnosis, no. (%)	36 (69)	142 (60)
IgG, mg/dl	797 (643, 1,052)	678 (534, 811)
IgG <400 mg/dl, no. (%)	0 (0)	21 (9)
IgA, mg/dl	170 (134, 224)†	129 (82, 191)‡
IgM, mg/dl	94 (68, 139)†	40 (23, 67)‡
ANCA positive, no. (%)	52 (100)	139 (59)
Estimated GFR, ml/minute§	45 (28, 71)	50 (28, 65)
Estimated GFR, no. (%)		
>60 ml/minute	18 (35)	79 (33)
30–60 ml/minute	20 (38)	90 (38)
<30 ml/minute	14 (27)	68 (29)
Plasma exchange, no. (%)	0 (0)	45 (19)
BVAS/WG	6 (4, 8)	0 (0, 0)
Time from AAV diagnosis, months	0.7 (0.4, 1.3)	14 (4.4, 68)
Cumulative rituximab, gm	2 (2, 2)	7 (5, 10)

* Except where indicated otherwise, values are the median (interquartile range). Fifty patients from the induction group entered the maintenance group. *P* values are not provided since a large subset of observations are not independent. AAV = antineutrophil cytoplasmic antibody–associated vasculitis; anti-MPO = antimyeloperoxidase; ANCA = antineutrophil cytoplasmic antibody; GFR = glomerular filtration rate; BVAS/WG = Birmingham Vasculitis Activity Score for Wegener's Granulomatosis.
† Data were available for 38 patients.
‡ Data were available for 216 patients.
§ Determined using the 4-variable Modification of Diet in Renal Disease equation (28).

such that by the eighth month of maintenance therapy the median prednisone dosage was 0 mg/day (IQR 0, 4).

Baseline characteristics stratified by treatment group are presented in Table 1. The median BVAS/WG in the induction group was 6 (IQR 4, 8) and, by definition, was 0 at entry into the maintenance group. The median IgG level at initiation of induction therapy was 797 mg/dl (IQR 643, 1,052) compared with 678 mg/dl (IQR 534, 811) at entry into the maintenance group. Median baseline IgG levels in the maintenance group were lower in patients who received plasma exchange with the standardized induction regimen (559 mg/dl [IQR 445, 642]) compared with those who received the induction regimen alone (665 mg/dl [IQR 554, 792]) or were transitioned from an alternative maintenance regimen (738 mg/dl [IQR 570, 880]) ($P < 0.01$ for both comparisons).

Among the 50 patients who were included in both groups, the mean within-person decrease in IgG levels from the beginning of induction therapy to the beginning of maintenance therapy was 226 mg/dl (95% CI 155, 298) ($P < 0.001$). None of the patients in the induction group had significant baseline hypogammaglobulinemia (IgG level of <400 mg/dl), compared with 9% of the patients in the maintenance group.

Change in Ig levels and ANCA titers with treatment. The population mean change in total Ig levels and ANCA titers during induction therapy is shown in Table 2 and Figure 2. IgG levels declined at a mean rate of 6% per month (95% CI 4, 8%). ANCA titers showed a more precipitous decline at 47% per month (95% CI 42, 52%) and 48% per month (95% CI 42, 54%) for anti-MPO and anti-PR3 titers, respectively.

Patients in the maintenance therapy group were in a state of continuous B cell depletion for a median of 2.4 years (IQR 1.5, 4.0 years), with the longest duration being 7.6 years. At entry into the maintenance group, 139 patients (59%) continued to have an ANCA titer greater than the cutoff for the assay. The change in ANCA titers in this subset of patients was compared with the change in IgG levels across the entire maintenance group (Table 2 and Figure 2). During maintenance therapy with rituximab-induced continuous B cell depletion, IgG levels fell by a mean of 0.6% per year (95% CI −0.2, 1.4%). Conversely, in patients with a positive ANCA titer at the initiation of maintenance treatment, anti-MPO and anti-PR3 titers fell by a mean of 42% per year (95% CI 32, 50%) and 73% per year (95% CI 58, 83%), respectively.

Ig levels and ANCA titers fell more rapidly in induction than in maintenance. When standardized to a common time unit, IgG levels fell 52% per year (95% CI 39, 61%) during induction and 0.6% per year (95% CI −0.2, 1.4%) during maintenance. Likewise, anti-MPO titers decreased by 47% per month (95% CI 42, 52%) during induction compared with 4% per month (95% CI 3, 6%) during maintenance among patients who still had a positive ANCA titer. A similar trend was seen for anti-PR3 titers.

Table 2. Decline in Ig levels and ANCA titers in the AAV patients receiving rituximab*

Antibody	Induction therapy (n = 52)†	Maintenance therapy (n = 237)‡
IgG	6 (4, 8)	0.6 (−0.2, 1.4)
IgA	5 (2, 9)	5 (3, 6)
IgM	16 (13, 19)	9 (8, 11)
Anti-MPO	47 (42, 52)	42 (32, 50)§
Anti-PR3	48 (42, 54)	73 (58, 83)§

* Values are the mean percent decline (95% confidence interval) estimated from linear mixed-effects models. ANCA = antineutrophil cytoplasmic antibody; AAV = ANCA-associated vasculitis; anti-MPO = antimyeloperoxidase; anti-PR3 = anti–proteinase 3.
† Monthly percent decline.
‡ Yearly percent decline.
§ Data were analyzed for the 139 patients who had positive titers at entry into the maintenance group.

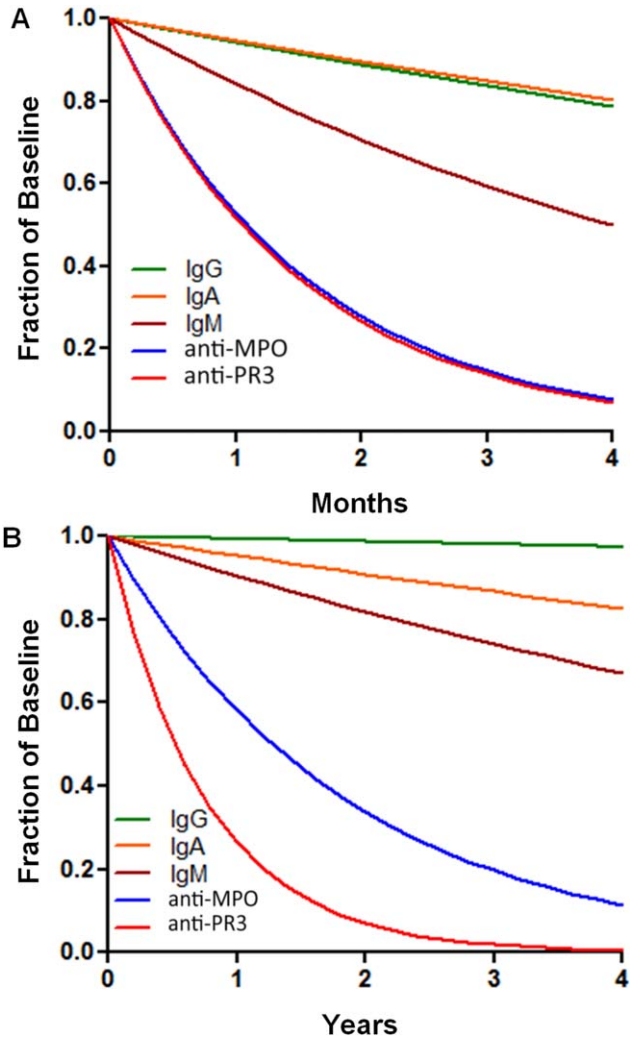

Figure 2. Change in Ig levels and antineutrophil cytoplasmic antibody (ANCA) titers in patients treated with rituximab. The percent change in ANCA titers and Ig levels over time during induction therapy (**A**) and maintenance therapy (**B**) with rituximab, determined using linear mixed-effects models, is shown. Slopes with accompanying 95% confidence intervals are shown in Table 2. anti-MPO = antimyeloperoxidase; anti-PR3 = anti–proteinase 3.

In the maintenance group, 13 of 237 patients (5.5%) experienced a major relapse (BVAS/WG >2). All patients were treated with prednisone and continued rituximab, except for 1 patient who also received 2 months of oral cyclophosphamide. A sensitivity analysis demonstrated that continued inclusion of these patients in the maintenance cohort did not influence the results.

Predictors of hypogammaglobulinemia. At entry into the maintenance group, 21 patients (9%) had significant hypogammaglobulinemia (IgG level of <400 mg/dl). Of the remaining 216 patients with a baseline maintenance IgG level of >400 mg/dl, 10 patients (4.6%) developed significant hypogammaglobulinemia over a median duration of rituximab-induced continuous B cell depletion of 2.4 years (IQR 1.5, 4.0 years). There was no difference in the proportion of patients developing hypogammaglobulinemia among patients treated for disease relapse compared with those who were not ($P = 0.44$).

In univariate Cox proportional hazard models, the baseline IgG level at entry into the maintenance group was the only factor associated with subsequently developing significant hypogammaglobulinemia during maintenance therapy with rituximab (HR 0.25 per 50 mg/dl increase in IgG level [95% CI 0.11, 0.56]; $P = 0.001$). Duration of continuous B cell depletion prior to entry in the maintenance group was not associated with future significant hypogammaglobulinemia. Likewise, time since the initial diagnosis of AAV, which should serve as a rough surrogate for cumulative non-rituximab immunosuppression, lacked a significant association with developing an IgG level of <400 mg/dl.

Only patients with a baseline maintenance IgG level in the lowest quartile (408–559 mg/dl) developed significant hypogammaglobulinemia (Figure 3). The median baseline IgG level in patients who subsequently developed an IgG level of <400 mg/dl was 448 mg/dl (IQR 428, 503). Despite being in the lowest baseline IgG quartile, 82% of patients maintained an IgG level of >400 mg/dl during continuous maintenance rituximab therapy.

Serious adverse events. Cumulative immunosuppressive exposures were 23.8 and 725.4 patient-years for the induction and maintenance groups, respectively.

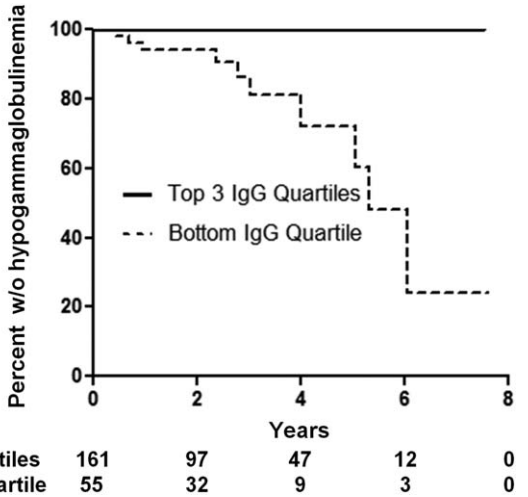

Figure 3. Percent of patients without significant hypogammaglobulinemia over time during maintenance therapy with rituximab. Kaplan-Meier curves for the top 3 IgG quartiles (range 560–1,657 mg/dl) compared to the lowest IgG quartile (range 408–559 mg/dl) in patients who began maintenance therapy with an IgG level of >400 mg/dl are shown. Significant hypogammaglobulinemia was defined as an IgG level of <400 mg/dl. Values below the graph are the number of patients at risk.

Table 3. Risk factors for serious infections in the AAV patients receiving rituximab maintenance therapy*

	Univariable IRR (95% CI)	*P*	Adjusted IRR (95% CI)	*P*
Age (per 10 years)	1.49 (1.24, 1.80)	<0.001	1.46 (1.19, 1.78)	<0.001
Male sex	0.78 (0.46, 1.32)	0.34	0.83 (0.50, 1.42)	0.51
Anti-MPO	1.76 (1.03, 3.02)	0.04	1.32 (0.73, 2.37)	0.36
Time from diagnosis to rituximab treatment (per year)	0.97 (0.92, 1.03)	0.30	0.97 (0.91, 1.04)	0.41
Duration of continuous rituximab treatment before remission (per month)	0.79 (0.53, 1.17)	0.24	0.99 (0.69, 1.41)	0.94
Plasma exchange	0.64 (0.29, 1.41)	0.27	0.42 (0.19, 0.96)	0.04
IgG <400 mg/dl	2.40 (1.22, 4.72)	0.01	2.13 (1.04, 4.36)	0.04

* Values were obtained using univariable and multivariable Poisson regression. IRR = incidence rate ratio; 95% CI = 95% confidence interval; anti-MPO = antimyeloperoxidase.

During induction therapy, there were 5.9 serious adverse events per 10 patient-years (95% CI 3.2, 9.6) compared with 1.8 serious adverse events per 10 patient-years (95% CI 1.5, 2.2) during maintenance. Serious infections occurred at a greater rate during induction (2.9 per 10 patient-years [95% CI 1.2, 6.0]) than during maintenance therapy (0.85 per 10 patient-years [95% CI 0.66, 1.1]). Pulmonary infections accounted for the majority of serious infections in both groups.

During maintenance therapy, 5 patients (2.1%) received treatment with intravenous Ig (IVIG) for recurrent infections: 1 patient had recurrent sinus infections, 3 patients developed bronchiectasis with recurrent pulmonary infections, and 1 had recurrent pulmonary infections without bronchiectasis. The median IgG level at initiation of IVIG was 408 mg/dl (IQR 196, 586).

There were no deaths during induction therapy. However, the induction group inclusion criteria could result in an underreporting of mortality. To address this issue, we analyzed all patients treated with the standardized induction regimen regardless of whether they met criteria for inclusion in the induction group (n = 89). The majority of the additional 37 patients were not included in the induction group due to the absence of ANCA and IgG levels required for analysis. Among these 89 patients, 2 deaths occurred during the induction period (0.6 deaths per 10 patient-years [95% CI 0.1, 2.4]). One patient died of septic shock in the setting of pneumonia and the other died of a myocardial infarction. During maintenance, there were 0.17 deaths per 10 patient-years (95% CI 0.09, 0.29). Two of the 12 deaths in the maintenance group were attributed to an infectious complication, and none were attributed to a vasculitis flare.

In multivariable models, increasing age and a baseline maintenance IgG level of <400 mg/dl were associated with developing a serious infection during maintenance therapy with rituximab-induced continuous B cell depletion (Table 3). There was no association of serious infection with the duration of AAV prior to rituximab treatment or the duration of rituximab-induced continuous B cell depletion prior to entering the maintenance group. In the 216 patients who entered maintenance with an IgG level of >400 mg/dl, there was no association with IgG level and risk of subsequent serious infections in a univariate and adjusted model (incidence rate ratio 1.02 [95% CI 0.95, 1.09]; $P = 0.65$ for the adjusted model).

DISCUSSION

This retrospective analysis of patients with AAV treated with rituximab provides insight into several interesting features of the effect of B cell–targeted therapy on antibody-mediated autoimmune diseases. During induction therapy with combination glucocorticoids, cyclophosphamide, and rituximab, the levels of both pathogenic ANCA and total Ig decline. The decline in ANCA titer, however, occurs at a more rapid rate. There was a 6% (95% CI 4, 8%) per month decline in IgG levels compared with a 47% (95% CI 42, 52%) and 48% (95% CI 42, 54%) per month decline in anti-MPO and anti-PR3 antibodies, respectively. During maintenance therapy with prolonged rituximab-induced continuous B cell depletion, total IgG levels remained essentially constant with a mean decline of 0.6% per year (95% CI −0.2, 1.4%). Furthermore, the rate of serious infections during maintenance therapy was relatively low at 0.85 [95% CI 0.66, 1.1] per 10 patient-years.

A preferential decline in pathogenic ANCA titers allows for a therapeutic window to treat disease while preserving protective humoral immunity. A similar paradigm has been observed in rheumatoid arthritis, whereby

treatment with rituximab leads to a sharper decline in rheumatoid factor and antibodies to cyclic citrullinated peptide compared to total Ig levels (3). Given that plasma cells do not express CD20, it is possible that certain disease-associated autoantibodies are produced by plasmablasts and plasma cells that are inherently short lived. Alternatively, autoantibody-producing cells may be more sensitive to cyclophosphamide, prednisone, or other induction agents used in conjunction with rituximab. Regardless of which mechanism predominates, the autoantibody-producing plasmablasts and plasma cells are unable to be replenished following B cell depletion. Conversely, disease states in which rituximab fails to induce a preferential decline in disease-associated autoantibodies may be relatively resistant to B cell depletion treatments. For example, treatment of the antiphospholipid syndrome with rituximab has little effect on the levels of autoantibodies and appears to be of limited efficacy in most cases (20).

Given the long-term, relapsing nature of many antibody-mediated autoimmune diseases, the development of hypogammaglobulinemia is a particular concern with repeated courses of rituximab (6,7). While prior studies evaluating the effect of B cell–targeted therapy on Ig levels have included heterogeneous populations with varying cumulative rituximab exposure and dosing frequency, our analysis was restricted to patients undergoing continuous B cell depletion. During maintenance treatment, patients receiving scheduled doses of rituximab at 4–6-month intervals showed essentially no change in the mean IgG level despite 25% of patients receiving scheduled rituximab treatments for longer than 4 years. Furthermore, our results suggest that developing hypogammaglobulinemia during maintenance therapy with rituximab is unlikely unless the baseline IgG level is low. Indeed, among patients who entered maintenance therapy in the top 3 IgG quartiles, no patients developed an IgG level of $<$400 mg/dl. Therefore, declines in IgG levels are seen primarily during induction therapy, with little change thereafter. We attribute the stability of IgG levels during maintenance to a long-lived plasma cell population that is resistant to immunosuppressive agents and is able to maintain the IgG pool. In agreement with prior reports, the rate of IgM decline we observed was significantly greater than that of IgG (21,22). IgA levels fell at a rate similar to that of IgG during induction therapy, but at a rate slightly greater than that of IgG during maintenance therapy.

This stability of IgG levels independent of repeated rituximab doses is consistent with prior reports in the literature. In a large analysis of 2,578 patients with rheumatoid arthritis treated with rituximab in clinical trials (1,043 of whom received $\geq$3 rounds of rituximab treatment), 5% of patients developed an IgG level less than the lower limit for the laboratory, and $<$1% developed an IgG level of $<$300 mg/dl (21). Importantly, the rate of hypogammaglobulinemia was similar despite the number of rituximab treatments received. In contrast, low IgM levels were observed more commonly, with 23% of patients developing an IgM level below the lower limit of normal for the assay. In another analysis of 243 patients comprised predominantly of patients with AAV, ~16% developed moderate hypogammaglobulinemia (IgG level 300–500 mg/dl) following treatment with rituximab (22). The pre-rituximab IgG concentration correlated with the development of hypogammaglobulinemia, but the total number of rituximab doses did not. Low IgM levels were significantly more common, with 58% of the patients developing a level of $<$30 mg/dl.

The immunosuppressive effects of rituximab extend beyond a potential reduction in total IgG levels. Despite the relative stability of total IgG levels, the ability to manufacture antibodies against new antigens may be impaired. Indeed, patients undergoing treatment with rituximab have an impaired ability to respond to vaccination with pneumococcal polysaccharide or novel antigens (23). B cell depletion has also been demonstrated to modulate T cell response to infections, which would impair immunity independent of the IgG concentration (24).

To evaluate the safety of long-term continuous B cell depletion, we reviewed all serious adverse events in our cohort. The rate of serious infections observed in our induction cohort (2.9 per 10 patient-years [95% CI 1.2, 6.0]) is comparable to the rate of grade 3 or 4 infections that occurred in patients receiving induction therapy in the RAVE trial (1.4 per 10 patient-years) (2). In our maintenance cohort, serious infections occurred at a rate of 0.85 per 10 patient-years (95% CI 0.66, 1.1), the vast majority of which were pneumonia. Our results are similar to the rate of grade 3 or 4 infections observed in patients receiving rituximab maintenance therapy in the MAINRITSAN trial (0.82 per 10 patient-years) (9).

A baseline IgG level of $<$400 mg/dl and increasing patient age were associated with an increased risk of serious infections in our maintenance cohort. The association of infectious complications with an IgG level of $<$400 mg/dl has been observed in other patient populations. For example, a serum IgG level of $<$400 mg/dl was associated with a higher rate of infections compared with more mild reductions in both patients with solid organ transplantation and those with stem cell transplantation (18,19). Therefore, particular caution should be exercised in using rituximab in patients with IgG levels approaching this level. Of note, low IgM levels following rituximab treatment were not associated with an increased risk of infections in a prior investigation (21). Likewise, IgA levels do not appear to be significantly associated with infectious events (25). The association of prior plasma exchange with a lower risk of

serious infections does not have a plausible scientific explanation. Furthermore, other studies evaluating the role of plasma exchange in AAV have not demonstrated this association (26).

Our study has several strengths and weaknesses. The greatest strengths are the large size for an AAV cohort, long duration of follow-up, and uniformity of treatment. To our knowledge, this cohort provides data on the longest duration of continuous B cell depletion published to date. The main weaknesses are inherent to data collection in retrospective studies. We were only able to accurately record serious adverse events and were not able to provide data on infections that did not require hospitalization. In addition, the exact cumulative dose of cyclophosphamide was unknown for a large percentage of patients transitioned to rituximab from an alternative maintenance regimen, thus precluding a detailed analysis of the effect of cyclophosphamide exposure on IgG levels. Some insight, however, can be derived from the baseline IgG levels of different groups at entry into the maintenance cohort. The 109 patients transitioned to rituximab from an alternative maintenance regimen were diagnosed as having AAV at a median of 4.3 years (IQR 1.1, 8.1 years) before entry into the maintenance cohort and received a minimum of 3–6 months of oral cyclophosphamide for induction of remission. Conversely, those patients who received our standard induction regimen received 2 months of oral cyclophosphamide. There was no difference in baseline maintenance IgG levels or significant hypogammaglobulinemia between these groups, suggesting that cumulative cyclophosphamide exposure alone was not the primary driver of declining IgG levels. Additional investigation is needed to more accurately define the importance of cumulative cyclophosphamide exposure on hypogammaglobulinemia in this setting.

Rituximab has become an important therapy for maintenance of remission in AAV. The results of the MAINRITSAN trial show superior disease control with continuous rituximab compared to maintenance azathioprine. These results await confirmation by the ongoing Rituximab Vasculitis Maintenance (RITAZAREM) trial (10). In addition, the MAINRITSAN 2 trial is currently underway to compare fixed dosing of rituximab versus dosing contingent upon B cell reconstitution (27). A previous analysis of our cohort demonstrated that maintenance therapy with rituximab-induced continuous B cell depletion was extremely effective at preventing relapse, with a major disease flare rate of 5% over a median of 2 years (13).

Since the use of extended courses of rituximab is likely to increase, it is essential to understand the long-term implications of this treatment. This retrospective analysis of 239 patients with AAV undergoing treatment with scheduled doses of rituximab provides several salient insights. While both ANCA and IgG levels decline during induction, pathogenic ANCA levels fall at a more rapid rate. During maintenance therapy, IgG levels remain essentially constant despite prolonged continuous B cell depletion. Serious infections are relatively rare with long-term rituximab therapy and are associated with patient age and significant hypogammaglobulinemia. Further studies are required to help balance the risk of prolonged maintenance therapy against the risk of disease relapse.

AUTHOR CONTRIBUTIONS

All authors were involved in drafting the article or revising it critically for important intellectual content, and all authors approved the final version to be published. Dr. Cortazar had full access to all of the data in the study and takes responsibility for the integrity of the data and the accuracy of the data analysis.

Study conception and design. Cortazar, Pendergraft, Owens, Laliberte, Niles.

Acquisition of data. Cortazar, Owens, Laliberte, Niles.

Analysis and interpretation of data. Cortazar, Pendergraft, Wenger, Niles.

REFERENCES

1. Edwards JC, Szczepanski L, Szechinski J, Filipowicz-Sosnowska A, Emery P, Close DR, et al. Efficacy of B-cell-targeted therapy with rituximab in patients with rheumatoid arthritis. N Engl J Med 2004;350:2572–81.
2. Stone JH, Merkel PA, Spiera R, Seo P, Langford CA, Hoffman GS, et al. Rituximab versus cyclophosphamide for ANCA-associated vasculitis. N Engl J Med 2010;363:221–32.
3. Cambridge G, Leandro MJ, Edwards JC, Ehrenstein MR, Salden M, Bodman-Smith M, et al. Serologic changes following B lymphocyte depletion therapy for rheumatoid arthritis. Arthritis Rheum 2003;48:2146–54.
4. Smith KG, Jones RB, Burns SM, Jayne DR. Long-term comparison of rituximab treatment for refractory systemic lupus erythematosus and vasculitis: remission, relapse, and re-treatment. Arthritis Rheum 2006;54:2970–82.
5. Cambridge G, Leandro MJ, Teodorescu M, Manson J, Rahman A, Isenberg DA, et al. B cell depletion therapy in systemic lupus erythematosus: effect on autoantibody and antimicrobial antibody profiles. Arthritis Rheum 2006;54:3612–22.
6. Besada E, Koldingsnes W, Nossent JC. Long-term efficacy and safety of pre-emptive maintenance therapy with rituximab in granulomatosis with polyangiitis: results from a single centre. Rheumatology (Oxford) 2013;52:2041–7.
7. Venhoff N, Effelsberg NM, Salzer U, Warnatz K, Peter HH, Lebrecht D, et al. Impact of rituximab on immunoglobulin concentrations and B cell numbers after cyclophosphamide treatment in patients with ANCA-associated vasculitides. PLoS One 2012;7:e37626.
8. Specks U, Merkel PA, Seo P, Spiera R, Langford CA, Hoffman GS, et al. Efficacy of remission-induction regimens for ANCA-associated vasculitis. N Engl J Med 2013;369:417–27.
9. Guillevin L, Pagnoux C, Karras A, Khouatra C, Aumaitre O, Cohen P, et al. Rituximab versus azathioprine for maintenance in ANCA-associated vasculitis. N Engl J Med 2014;371:1771–80.
10. Jones RB. Rituximab in the treatment of anti-neutrophil cytoplasm antibody-associated vasculitis. Nephron Clin Pract 2014;128:243–9.
11. Cartin-Ceba R, Golbin JM, Keogh KA, Peikert T, Sanchez-Menendez M, Ytterberg SR, et al. Rituximab for remission induction and maintenance in refractory granulomatosis with polyangiitis (Wegener's): ten-year experience at a single center. Arthritis Rheum 2012;64:3770–8.

12. Smith RM, Jones RB, Guerry MJ, Laurino S, Catapano F, Chaudhry A, et al. Rituximab for remission maintenance in relapsing antineutrophil cytoplasmic antibody–associated vasculitis. Arthritis Rheum 2012;64:3760–9.
13. Pendergraft WF III, Cortazar FB, Wenger J, Murphy AP, Rhee EP, Laliberte KA, et al. Long-term maintenance therapy using rituximab-induced continuous B-cell depletion in patients with ANCA vasculitis. Clin J Am Soc Nephrol 2014;9:736–44.
14. Jennette JC, Falk RJ, Bacon PA, Basu N, Cid MC, Ferrario F, et al. 2012 revised International Chapel Hill Consensus Conference nomenclature of vasculitides. Arthritis Rheum 2013;65:1–11.
15. Stone JH, Hoffman GS, Merkel PA, Min YI, Uhlfelder ML, Hellmann DB, et al. for the International Network for the Study of the Systemic Vasculitides (INSSYS). A disease-specific activity index for Wegener's granulomatosis: modification of the Birmingham Vasculitis Activity Score. Arthritis Rheum 2001;44:912–20.
16. Han WK, Choi HK, Roth RM, McCluskey RT, Niles JL. Serial ANCA titers: useful tool for prevention of relapses in ANCA-associated vasculitis. Kidney Int 2003;63:1079–85.
17. Hellmark T, Niles JL, Collins AB, McCluskey RT, Brunmark C. Comparison of anti-GBM antibodies in sera with or without ANCA. J Am Soc Nephrol 1997;8:376–85.
18. Florescu DF, Kalil AC, Qiu F, Schmidt CM, Sandkovsky U. What is the impact of hypogammaglobulinemia on the rate of infections and survival in solid organ transplantation? A meta-analysis. Am J Transplant 2013;13:2601–10.
19. Norlin AC, Sairafi D, Mattsson J, Ljungman P, Ringden O, Remberger M. Allogeneic stem cell transplantation: low immunoglobulin levels associated with decreased survival. Bone Marrow Transplant 2008;41:267–73.
20. Erkan D, Vega J, Ramon G, Kozora E, Lockshin MD. A pilot open-label phase II trial of rituximab for non-criteria manifestations of antiphospholipid syndrome. Arthritis Rheum 2013;65:464–71.
21. Van Vollenhoven RF, Emery P, Bingham CO III, Keystone EC, Fleischmann R, Furst DE, et al. Longterm safety of patients receiving rituximab in rheumatoid arthritis clinical trials. J Rheumatol 2010;37:558–67.
22. Roberts DM, Jones RB, Smith RM, Alberici F, Kumaratne DS, Burns S, et al. Rituximab-associated hypogammaglobulinemia: incidence, predictors and outcomes in patients with multi-system autoimmune disease. J Autoimmun 2015;57:60–5.
23. Bingham CO III, Looney RJ, Deodhar A, Halsey N, Greenwald M, Codding C, et al. Immunization responses in rheumatoid arthritis patients treated with rituximab: results from a controlled clinical trial. Arthritis Rheum 2010;62:64–74.
24. Lund FE, Randall TD. Effector and regulatory B cells: modulators of $CD4^+$ T cell immunity. Nat Rev Immunol 2010;10:236–47.
25. Furst DE. Serum immunoglobulins and risk of infection: how low can you go? Semin Arthritis Rheum 2009;39:18–29.
26. Walsh M, Casian A, Flossmann O, Westman K, Hoglund P, Pusey C, et al. Long-term follow-up of patients with severe ANCA-associated vasculitis comparing plasma exchange to intravenous methylprednisolone treatment is unclear. Kidney Int 2013;84:397–402.
27. Tanna A, Pusey C. Clinical trials: rituximab for maintenance of remission in AAV. Nat Rev Nephrol 2015;11:131–2.
28. Levey AS, Bosch JP, Lewis JB, Greene T, Rogers N, Roth D, for the Modification of Diet in Renal Disease Study Group. A more accurate method to estimate glomerular filtration rate from serum creatinine: a new prediction equation. Ann Intern Med 1999;130:461–70.

ARTHRITIS & RHEUMATOLOGY
Vol. 69, No. 5, May 2017, pp 1054–1066
DOI 10.1002/art.40034

Identification of Functional and Expression Polymorphisms Associated With Risk for Antineutrophil Cytoplasmic Autoantibody–Associated Vasculitis

Peter A. Merkel,[1] Gang Xie,[2] Paul A. Monach,[3] Xuemei Ji,[4] Dominic J. Ciavatta,[5] Jinyoung Byun,[4] Benjamin D. Pinder,[2] Ai Zhao,[2] Jinyi Zhang,[6] Yohannes Tadesse,[2] David Qian,[4] Matthew Weirauch,[7] Rajan Nair,[8] Alex Tsoi,[8] Christian Pagnoux,[9] Simon Carette,[9] Sharon Chung,[10] David Cuthbertson,[11] John C. Davis Jr.,[12] Paul F. Dellaripa,[13] Lindsy Forbess,[14] Ora Gewurz-Singer,[8] Gary S. Hoffman,[15] Nader Khalidi,[16] Curry Koening,[17] Carol A. Langford,[15] Alfred D. Mahr,[18] Carol McAlear,[1] Larry Moreland,[19] E. Philip Seo,[20] Ulrich Specks,[21] Robert F. Spiera,[22] Antoine Sreih,[1] E. William St.Clair,[23] John H. Stone,[24] Steven R. Ytterberg,[21] James T. Elder,[25] Jia Qu,[26] Toshiki Ochi,[27] Naoto Hirano,[27] Jeffrey C. Edberg,[28] Ronald J. Falk,[5] Christopher I. Amos,[4] and Katherine A. Siminovitch,[6] for the Vasculitis Clinical Research Consortium

Supported by the Erna Baird Memorial Grant, the Vasculitis Foundation, the Ontario Research Fund (grant RE-05075), the University of Toronto Department of Medicine Challenge Grant, and the National Natural Science Foundation of China (grant 31270930). Dr. Siminovitch holds a tier 1 Canada Research Chair and the Sherman Family Chair in Genomic Medicine. The Vasculitis Clinical Research Consortium (VCRC) has received support from the NIH (National Institute of Arthritis and Musculoskeletal and Skin Diseases grants U54-AR-057319 and R01-AR-047799, National Center for Research Resources grant U54-RR-019497, the Office of Rare Diseases Research, and the National Center for Advancing Translational Sciences). The VCRC is part of the Rare Diseases Clinical Research Network.

[1]Peter A. Merkel, MD, MPH, Carol McAlear, MA, Antoine Sreih, MD: University of Pennsylvania, Philadelphia; [2]Gang Xie, MD, PhD, Benjamin D. Pinder, PhD, Ai Zhao, PhD, Yohannes Tadesse, PhD: Mount Sinai Hospital, Lunenfeld-Tanenbaum Research Institute and Toronto General Research Institute, Toronto, Ontario, Canada; [3]Paul A. Monach, MD, PhD: Boston University and VA Boston Healthcare System, Boston, Massachusetts; [4]Xuemei Ji, MD, PhD, Jinyoung Byun, PhD, David Qian, PhD, Christopher I. Amos, PhD: Dartmouth College, Lebanon, New Hampshire; [5]Dominic J. Ciavatta, PhD, Ronald J. Falk, MD: University of North Carolina, Chapel Hill; [6]Jinyi Zhang, MD, PhD, Katherine A. Siminovitch, MD: Mount Sinai Hospital, Lunenfeld-Tanenbaum Research Institute, Toronto General Research Institute and University of Toronto, Toronto, Ontario, Canada; [7]Matthew Weirauch, PhD: Cincinnati Children's Hospital Medical Center, Cincinnati, Ohio; [8]Rajan Nair, PhD, Alex Tsoi, MS, PhD, Ora Gewurz-Singer, MD: University of Michigan, Ann Arbor; [9]Christian Pagnoux, MD, MPH, Simon Carette, MD: Mount Sinai Hospital and University of Toronto, Toronto, Ontario, Canada; [10]Sharon Chung, MD: University of California, San Francisco; [11]David Cuthbertson, MS: University of South Florida, Tampa; [12]John C. Davis Jr., MD: University of California, San Francisco; [13]Paul F. Dellaripa, MD: Brigham and Women's Hospital, Boston, Massachusetts; [14]Lindsy Forbess, MD: Cedars-Sinai Medical Center, West Hollywood, California; [15]Gary S. Hoffman, MD, Carol A. Langford, MD, MHS: Cleveland Clinic, Cleveland, Ohio; [16]Nader Khalidi, MD: McMaster University, Hamilton, Ontario, Canada; [17]Curry Koening, MD: University of Utah, Salt Lake City; [18]Alfred D. Mahr, MD, PhD: Hôpital Saint-Louis, Paris, France; [19]Larry Moreland, MD: University of Pittsburgh, Pittsburgh, Pennsylvania; [20]E. Philip Seo, MD, MHS: Johns Hopkins University, Baltimore, Maryland; [21]Ulrich Specks, MD, Steven R. Ytterberg, MD: Mayo Clinic, Rochester, Minnesota; [22]Robert F. Spiera, MD: Hospital for Special Surgery, New York, New York; [23]E. William St.Clair, MD: Duke University Medical Center, Durham, North Carolina; [24]John H. Stone, MD, MPH: Massachusetts General Hospital, Boston; [25]James T. Elder, MD, PhD: University of Michigan and Ann Arbor VA Hospital, Ann Arbor, Michigan; [26]Jia Qu, MD: Wenzhou Medical University, Wenzhou, China; [27]Toshiki Ochi, PhD, Naoto Hirano, MD, PhD: University of Toronto and Princess Margaret Cancer Centre, Toronto, Ontario, Canada; [28]Jeffrey C. Edberg, PhD: University of Alabama at Birmingham.

Drs. Amos and Siminovitch contributed equally to this work.

Address correspondence to Katherine A. Siminovitch, MD, Mount Sinai Hospital, LTRI, Room 778D, 600 University Avenue, Toronto, Ontario M5G 1X5, Canada. E-mail: ksimin@mshri.on.ca.

Submitted for publication September 8, 2016; accepted in revised form December 20, 2016.

Objective. **To identify risk alleles relevant to the causal and biologic mechanisms of antineutrophil cytoplasmic antibody (ANCA)–associated vasculitis (AAV).**

Methods. **A genome-wide association study and subsequent replication study were conducted in a total cohort of 1,986 cases of AAV (patients with granulomatosis with polyangiitis [Wegener's] [GPA] or microscopic polyangiitis [MPA]) and 4,723 healthy controls. Meta-analysis of these data sets and functional annotation of identified risk loci were performed, and candidate disease variants with unknown functional effects were investigated for their impact on gene expression and/or protein function.**

Results. **Among the genome-wide significant associations identified, the largest effect on risk of AAV came from the single-nucleotide polymorphism variants rs141530233 and rs1042169 at the *HLA–DPB1* locus (odds ratio [OR] 2.99 and OR 2.82, respectively) which, together with a third variant, rs386699872, constitute a triallelic risk haplotype associated with reduced expression of the *HLA–DPB1* gene and HLA–DP protein in B cells and monocytes and with increased frequency of complementary proteinase 3 (PR3)–reactive T cells relative to that in carriers of the protective haplotype. Significant associations were also observed at the *SERPINA1* and *PTPN22* loci, the peak signals arising from functionally relevant missense variants, and at *PRTN3*, in which the top-scoring variant correlated with increased *PRTN3* expression in neutrophils. Effects of individual loci on AAV risk differed between patients with GPA and those with MPA or between patients with PR3-ANCAs and those with myeloperoxidase-ANCAs, but the collective population attributable fraction for these variants was substantive, at 77%.**

Conclusion. **This study reveals the association of susceptibility to GPA and MPA with functional gene variants that explain much of the genetic etiology of AAV, could influence and possibly be predictors of the clinical presentation, and appear to alter immune cell proteins and responses likely to be key factors in the pathogenesis of AAV.**

Granulomatosis with polyangiitis (Wegener's) (GPA) and microscopic polyangiitis (MPA) are life-threatening necrotizing vasculitides that are strongly associated with the presence of antineutrophil cytoplasmic antibodies (ANCAs) reactive to proteinase 3 (PR3) or myeloperoxidase (MPO). Although often considered a single disease, GPA and MPA diverge in important respects, such as in the extent of their association with PR3-reactive ANCAs compared to MPO-reactive ANCAs, the risk of relapsing disease, and the association of GPA with granulomatous inflammation. The etiology of AAV remains unknown; however, genome-wide association studies (GWAS) performed in a North American GPA cohort and a European GPA/MPA cohort confirmed the findings from candidate gene analyses identifying strong associations of these diseases with major histocompatibility complex (MHC) class II region alleles (1,2). A genome-wide significant association at the *SERPINA1* locus was also identified in the European cohort study, with both this and several associations with MHC alleles being differentially detected between patient subsets defined by the presence of PR3-ANCAs or MPO-ANCAs (2).

These findings have not yet been replicated, and knowledge remains rudimentary regarding the non-MHC loci and specific disease-causal variants predisposing to GPA and/or to MPA. Therefore, we sought to further define the genetic variation underpinning the susceptibility to GPA and MPA by conducting a new GWAS and a validation study of a larger, independently ascertained North American–based cohort of GPA/MPA patients and healthy controls, involving functional annotation of the risk loci to identify candidate disease-causal alleles.

PATIENTS AND METHODS

Subjects. All study subjects were of self-reported European ancestry, with the diagnosis of AAV, and specifically of GPA or MPA, being based on the American College of Rheumatology modified criteria for the classification of vasculitis (3). The discovery cohort included the following subjects: 779 AAV cases recruited via 13 centers from the Vasculitis Clinical Research Consortium (VCRC), which conducts studies involving vasculitis patients in the US, Canada, and elsewhere; 438 AAV cases recruited via the Wegener's Granulomatosis Genetic Repository (WGGER), a study conducted at 8 centers in the US from 2001 to 2005; and 378 AAV cases from the University of North Carolina Kidney Center (key clinical and serologic features are provided in Supplementary Table 1, available on the *Arthritis & Rheumatology* web site at http://onlinelibrary.wiley.com/doi/10.1002/art.40034/abstract). The controls included 202 healthy subjects recruited from the WGGER, and 3,121 historic controls whose genotype data were obtained from the Resource for Genetic Epidemiology Research on Aging study (4,5). The replication cohort included 505 AAV cases and 1,477 healthy controls recruited independently from Canada and the US via a Toronto-based AAV study, and 114 independent cases recruited via the VCRC. Demographic data and samples of peripheral blood cells and/or saliva were obtained from all subjects after their provision of written informed consent. The local institutional review boards approved the study.

Genotyping methods. For the GWAS, 1,615 AAV cases and 202 healthy controls were genotyped at the Mount Sinai Hospital Clinical Genomics Centre, and 3,121 historic controls were genotyped at Affymetrix (Santa Cruz, CA) using the Axiom Biobank 1 Genotyping array. This array tests 628,679 single-nucleotide polymorphisms (SNPs), including 246,000 genome-wide association markers (36.5%), 265,000 nonsynonymous coding SNPs (39.3%), 70,000 loss-of-function SNPs (10.4%), 23,000 expression quantitative trait loci (eQTL) SNPs (3.4%), 2,000 pharmacogenetic markers (0.3%), and 27,679 "custom" markers. Genotypes were

called and processed using Affymetrix Genotyping Console version 4.2 and SNPolisher software. Quality control filtering was performed using Golden Helix SVS software (version 8.3.4) and with a genotype call rate of >95%, individual sample call rate of >97%, and exclusion of SNPs with a Hardy-Weinberg equilibrium (HWE) P value of $<10^{-5}$. After filtering, genotypes derived from SNP markers common to both data sets were merged in a single file containing 1,528 cases, 3,309 controls, and 333,040 SNPs. A set of linkage disequilibrium (LD)–pruned SNPs with a minor allele frequency (MAF) of >5% was used to estimate identity by descent (ibd) and ancestry. For each pair of individuals with an estimated ibd of >0.25, the sample with the lower call rate was removed. Principal components analysis was used to exclude samples from subjects with non-European ancestry (6). In total, 1,371 cases, 3,258 controls, and 333,035 SNPs passed quality control filters (see Supplementary Figure 1, available on the *Arthritis & Rheumatology* web site at http://onlinelibrary.wiley.com/doi/10.1002/art.40034/abstract).

For the replication study, 8 SNPs in 6 gene loci were genotyped in 619 AAV cases and 1,477 controls using Sequenom iPLEX assays. One other SNP (rs62132293) at the *PRTN3* locus was genotyped using TaqMan (Applied Biosystems). After quality control filtering, 615 cases, 1,465 controls, and 9 SNPs were retained for analysis. For the replication study of the patients with MPO-ANCAs/perinuclear ANCAs (designated herein as MPO-ANCAs), 3 additional SNPs (rs3998159, rs7454108, and rs1049072) at the *HLA–DQA2* and *DQB1* loci were genotyped on the same platform. The GWAS and replication data sets were then combined for meta-analysis.

Statistical analysis. *Association tests and meta-analyses.* For the discovery data set, case–control association tests were conducted using logistic regression, with the principal components differing between cases and controls included as covariates, to adjust for population stratification. Calculation of the genomic control factor using EigenStrat showed a minimal inflation value of 1.012 and 0.991 before and after adjustment for the top 3 eigenvectors, respectively (see Supplementary Figure 2, http://onlinelibrary.wiley.com/doi/10.1002/art.40034/abstract). An analysis of all of the nonzero eigenvalues established that 221,341 independent tests were conducted from 280,677 autosomal markers, which, with Bonferroni correction, established the P value for genome-wide significance as $<2.2 \times 10^{-7}$.

Meta-analysis of the data from the GWAS and replication logistic regression analyses was conducted using the basic meta-analysis function in Plink version 1.9 (6,7). Differences between patients with GPA and patients with MPA and between patients with PR3-ANCAs/cytoplasmic ANCAs (designated herein as PR3-ANCAs) and those with MPO-ANCAs were studied using this approach. Between-study heterogeneity was tested by the chi-square–based Cochrane's Q statistic. Heritability was estimated using genome-wide complex trait analysis, as described by Lee et al (8), and assuming an AAV prevalence of 1/10,000. Prior to this analysis, we excluded sex chromosome data, SNPs with MAFs of <0.05 and missing rates of >0.01, individuals whose missing SNP rates were >0.01, SNPs with an HWE P value of <0.05, or markers with a significant difference in missingness between cases and controls.

Imputation. Genome-wide imputation for the 4,629 samples in the discovery cohort was performed using 1000 Genomes Project Phase 3 data as the reference (release date October 2014) for the autosomes, and Phase 1 data (release date August 2012) as the reference for the X chromosome. Following removal of SNPs with call rates of <95%, MAFs of <0.001, and HWE P values of $<10^{-5}$, SHAPEIT (http://shapeit.v2.r790.Ubuntu_12.04.4.static) was used to derive phased genotypes, and the phased data were imputed using IMPUTE version 2 (http://impute_v2.3.2_x86_64_static) to assess ~5-Mb nonoverlapping intervals (9). Imputation within defined regions was performed using IMPUTE version 2 without prephasing.

Conditional analysis. To test for multiple independent effects within the HLA region, a logistic regression framework was used to assess individual HLA alleles for association, including the top 3 principal components as covariates to account for population stratification. After we had identified the most significant marker, we tested for additional independent effects by including the dose of the top markers in a joint model. Conditional analysis was performed using the proc logistic module of SAS (version 9.2) to obtain odds ratios (ORs) when all top markers were jointly analyzed.

Population attributable fraction (PAF). The PAF was estimated using ORs from a multivariate logistic regression model incorporating SNPs from multiple loci, so that each OR is adjusted for the effects of the other SNPs. The PAF for effects from an allele at a single locus was determined as follows:

$$\mathrm{PAF} = \frac{\mathrm{RAF}(\mathrm{OR}-1)}{1+\mathrm{RAF}(\mathrm{OR}-1)}$$

where OR is the odds ratio associated with the allele genotype, and RAF is the allele frequency of the risk variant. For computation over multiple loci, the following formula was used:

$$\mathrm{PAF}_{\mathrm{combined}} = 1 - \left(\prod_{1=1}^{nloci} 1 - (\mathrm{PAF_i})\right)$$

Random forest analysis. The potential role of combinations of alleles in the risk of AAV was evaluated by random forest analysis using classification and regression tree (CART) methodology (10). Data from 11 risk-associated variants were subjected to analyses in which CARTs were repetitively built using two-thirds of the samples and variables. The CARTs were then used to classify the remaining one-third of the data. Eight variants that improved the model fit by ≥3% were retained to build a CART. The rpart program in R and the Gini index measure were used to identify optimal splits of the data, with the complexity parameter set to 0.001 and the data then pruned to include only those nodes containing at least 20 observations. This final model had a classification accuracy of 73%. ORs were calculated with the following formula:

$$\mathrm{OR} = \frac{\text{cases in node i/controls in node i}}{\text{cases in node 1/controls in node 1}}$$

The Woolf approximation was used to compute standard errors and confidence intervals.

Functional annotation. The online Probabilistic Identification of Causal SNPs (PICS) algorithm (http://www.broadinstitute.org/pubs/finemapping/?q=pics) was used to identify variants at each risk locus with a PICS probability of >0.0275, consistent with that used by Farh et al (11). We then used the Ensembl Variant Effect Predictor web tool to annotate these variants for predicted functional consequences (http://www.ensembl.org/info/

docs/tools/vep/index.html) and used Genevar (12), seeQTL (http://www.bios.unc.edu/research/genomic_software/seeQTL/) (13), and the University of Chicago eQTL browser (http://eqtl.uchicago.edu/cgi-bin/gbrowse/eqtl/) to identify eQTLs.

Cellular assays. Peripheral blood mononuclear cells (PBMCs) and polymorphonuclear leukocytes (obtained from patients at Mount Sinai Hospital) were isolated over Ficoll-Hypaque. For quantitative polymerase chain reaction (qPCR), RNA (500 ng) was reverse transcribed using random hexamer primers and SuperScript III reverse transcriptase (Invitrogen), and qPCR was performed using SYBR Green and the gene-appropriate primer pairs (listed in Supplementary Table 2, http://onlinelibrary.wiley.com/doi/10.1002/art.40034/abstract). Samples were run on an ABI Prism 7900HT system (Applied Biosystems), and the fold change in expression of the specific gene relative to the internal control gene (*COX5B* for *PRTN3*; *GAPDH* for *HLA–DPB1*) was calculated using the $2^{-\Delta\Delta C_t}$ method (14).

For flow cytometry, PMBCs were stained with phycoerythrin-conjugated anti-CD19 antibodies, allophycocyanin–Cy7–conjugated anti-CD14 antibodies (BD Biosciences), and/or fluorescein isothiocyanate (FITC)–conjugated HLA–DP antibodies (Leinco) or FITC-conjugated murine IgG (BD Biosciences). The cells were then analyzed using a FACSCanto cytometer (BD Biosciences) and FlowJo software.

For ELISpot experiments, 20-mer peptides, which were selected using published data or the NetMHCII version 2.2 prediction algorithm (http://www.cbs.dtu.dk), were synthesized and purified by the manufacturer (Genscript) (for details, see Supplementary Table 3, http://onlinelibrary.wiley.com/doi/10.1002/art.40034/abstract).

PBMCs (2×10^{-5}) from PR3-ANCA–positive vasculitis patients and healthy controls were suspended in 20% fetal bovine serum–supplemented RPMI and incubated in 96-well ELISpot plates (Millipore) precoated with an anti-human interferon-γ (IFNγ) monoclonal antibody (eBioscience). Cells were stimulated for 24 hours at 37°C with 10 μg/ml peptide or 1 μg/ml concanavalin A (Sigma) and incubated with a biotinylated mouse anti-human IFNγ antibody (eBioscience), avidin–horseradish peroxidase (eBioscience), and aminoethylcarbazole solution (BD ELISpot), and an ImmunoSpot reader and software (Cellular Technology) were used to detect IFNγ-releasing cells.

RESULTS

GPA/MPA susceptibility loci. After filtering and correction for population substructure, our GWAS discovery data set included 333,035 SNPs genotyped in 1,371 subject with AAV (GPA or MPA) and 3,258 healthy controls, with no evidence of inflation of the test statistic ($\lambda_{GC} = 0.991$) (see Supplementary Figures 1 and 2 and Supplementary Table 1, http://onlinelibrary.wiley.com/doi/10.1002/art.40034/abstract).

Association analysis of this cohort identified 120 SNPs across the MHC class II locus achieving genome-wide significance levels, with the strongest signals emanating from the *DPB1*, *DPA1*, *DQA1*, and *DQB1* genes (Table 1 and Supplementary Table 4 [http://onlinelibrary.wiley.com/doi/10.1002/art.40034/abstract]). Four other SNPs across 3 non-MHC gene loci also achieved genome-wide significance levels and were taken forward, together with 5 top-scoring SNPs from the MHC region, for a replication study in an independent cohort of 615 cases and 1,465 controls (Table 1; details also shown in Supplementary Figure 1 and Supplementary Table 1 [http://onlinelibrary.wiley.com/doi/10.1002/art.40034/abstract]). Because all of the associations tested were replicated (at a threshold of $P \leq 0.05$), the GWAS and replication data sets were combined for a meta-analysis, and the 9 associations were also explored in patient subgroups defined by GPA or MPA phenotypes or by ANCA specificities and/or immunofluorescence patterns (PR3-ANCAs or MPO-ANCAs).

Results of the meta-analysis confirmed the MHC class II region as the locus most strongly associated with AAV susceptibility (Table 1). The peak association signals arose from 2 *HLA–DPB1* gene variants, rs141530233 ($P = 1.13 \times 10^{-89}$) and rs1042169 ($P = 1.12 \times 10^{-84}$), with other significant associations observed in the *HLA–DPA1*, *DQA1*, and *DQB1* genes (Table 1; see also Supplementary Figures 3 and 4 [http://onlinelibrary.wiley.com/doi/10.1002/art.40034/abstract]). Associations with *DPA1* and *DPB1* remained strong in the GPA and PR3-ANCA subgroups, but not in the MPA or MPO-ANCA subgroups. Conversely, the *DQB1* association was much stronger in patients with MPO-ANCAs compared to those with PR3-ANCAs (Table 2). In view of this divergence, a GWAS, replication analysis, and meta-analysis were also performed de novo to compare patients with either PR3-ANCAs or MPO-ANCAs to healthy controls. These analyses revealed significant associations of the MPO-ANCA phenotype with the variants rs3998159 ($P = 5.24 \times 10^{-25}$) and rs7454108 ($P = 5.03 \times 10^{-25}$) at the *HLA–DQA2* locus (Table 3). Neither this association nor any other significant associations beyond those detected in the AAV total cohort GWAS were detected in the subset GWAS analysis of PR3-ANCA–positive AAV cases and healthy controls (results available in Supplementary Tables 5 and 6, http://onlinelibrary.wiley.com/doi/10.1002/art.40034/abstract).

Among the non-MHC associations identified in the total AAV GWAS, the strongest signal arose from a SNP (rs28929474) in the *SERPINA1* gene ($P = 3.09 \times 10^{-12}$) encoding an α1 anti-trypsin null ("Z") allele that was previously implicated in GPA by candidate gene analysis (Table 1; see also Supplementary Figures 3 and 4 [http://onlinelibrary.wiley.com/doi/10.1002/art.40034/abstract]) (15). This association was limited to the GPA and PR3-ANCA subsets (Table 2) and is consistent with prior GWAS data showing that a significant association with another *SERPINA1* SNP, rs7151526, depended entirely on the concomitant presence of the Z allele (2).

A significant association of AAV with rs62132293, a SNP located 2.6 kb upstream of the *PRTN3* transcription start site, was also observed ($P = 8.60 \times 10^{-11}$); this finding is in keeping with previously observed associations at this locus (albeit with different SNPs) in AAV candidate gene and GWAS analyses (Table 1 and Supplementary Figures 3 and 4 [http://onlinelibrary.wiley.com/doi/10.1002/art.40034/abstract]) (2,16). This association was limited to the GPA and PR3-ANCA subsets (Table 2), consistent with the pathophysiologic relevance of the *PRTN3*-encoded PR3 serine protease to these phenotypes (17).

Significant associations with AAV were observed at the *PTPN22* rs6679677 and rs2476601 loci ($P = 1.88 \times 10^{-8}$ and $P = 1.86 \times 10^{-7}$, respectively) (Table 1 and Supplementary Figures 3 and 4 [http://onlinelibrary.wiley.com/doi/10.1002/art.40034/abstract]). Consistent with their equivalent effect sizes, these variants are in almost complete LD ($r^2 = 0.99$). However, the rs2476601 variant encodes an Arg620Trp substitution in the Lyp phosphatase associated with risk of multiple autoimmune diseases, including giant cell arteritis (18,19). Although not consistently observed in candidate gene studies (20,21), the association of rs2476601 with GPA/MPA is strongly supported by our data, and unlike most of the other significant associations observed, this allele's strength of association did not differ between the subgroups (Table 2).

The discovery GWAS of either the entire cohort or the PR3-ANCA subgroup revealed no reliable associations at the *SEMA6A* gene locus, possibly because those analyses involved a different case–control cohort. In the current discovery GWAS, there were 189 SNPs identified in the 1-MB region around *SEMA6A*, of which the most significant variant, rs12521259, was located ~100 kb upstream of *SEMA6A* (P for association $= 9.11 \times 10^{-3}$ in the full cohort and $P = 4.87 \times 10^{-3}$ in the PR3-ANCA subgroup).

Analyses of the associations in patient subgroups defined by the presence or absence of lung or kidney disease revealed a modest association with AAV risk at the *HLA–DPA1* locus in patients with kidney involvement ($P = 8.15 \times 10^{-3}$), whereas no significant subgroup differences were apparent at the other risk loci (results in Supplementary Table 7, http://onlinelibrary.wiley.com/doi/10.1002/art.40034/abstract). Modest associations with *HLA–DPB1* and *HLA–DPA1* were observed but restricted to the patients with ANCA-positive AAV; this finding may be a reflection of the relatively low numbers of ANCA-negative cases analyzed.

Contribution of risk alleles jointly to disease susceptibility. As the strongest associations in all subgroups were with MHC gene SNPs, independence of the individual allele associations was explored by forward logistic regression selection analysis. Beginning with the most significant SNP identified in the total cohort or in the PR3-ANCA or MPO-ANCA subgroups, additional significant variants were incorporated into the analysis until no variants significant at the $P < 5 \times 10^{-8}$ level remained. This analysis revealed that variants in several of the class II genes studied in each group were jointly significantly associated with AAV risk (results in Supplementary Table 8, http://onlinelibrary.wiley.com/doi/10.1002/art.40034/abstract).

These analyses showed that the array heritability of AAV was a mean ± SD 0.2197 ± 0.0204, while in analyses with the HLA region removed, the array heritability was 0.138 ± 0.022. The PAF for the risk loci to disease was also assessed, and the collective contribution of these loci to risk of AAV was found to be substantive (PAF of 77%), albeit variable (PAFs between 30% and 87%) across different the subgroups (Table 4).

The extent to which the risk variants/variant combinations might be predictive of disease was also evaluated using random forest and CART methods. These analyses confirmed the strong association of HLA class II alleles with AAV risk (details in Supplementary Figure 5, http://onlinelibrary.wiley.com/doi/10.1002/art.40034/abstract). Furthermore, homozygosity for the relatively common *DPB1* risk allele rs141530233 and *DPA1* risk allele rs9277341, together with homozygosity or heterozygosity for the rare *SERPINA1* risk variant rs2829474, identified a subgroup of individuals with an OR of >10 for developing AAV.

For HLA alleles, no subsets were defined by heterozygotes, and further modeling comparing the goodness-of-fit of additive, dominant, and recessive models showed that the risk imbued by the *HLA–DPB1, DPA1*, and *DQA1* disease-associated variants is recessively inherited, i.e., conferred by carriage of the common homozygous genotypes (see Supplementary Table 9, http://onlinelibrary.wiley.com/doi/10.1002/art.40034/abstract). Associations of the homozygous risk genotypes with AAV were as follows: OR of 3.58 for rs141530233, OR of 2.69 for rs9277341, and OR of 1.80 for rs352425282. Similar results were found for the subgroups defined by carriage of PR3-ANCAs or MPO-ANCAs, with recessive models fitting best. These observations suggest a potential for genetic data to inform the distinction of patient subsets within the AAV population and identify an unusual recessive effect for the HLA region loci studied.

Disease-associated *PRTN3* polymorphism identified as a novel eQTL. To identify candidate causal variants, additional genotypes were imputed and the PICS algorithm was applied across each risk locus (11). Although peak association signals at a few loci were stronger for imputed SNPs than for observed SNPs (details in Supplementary Table 10, http://onlinelibrary.wiley.com/doi/10.1002/art.40034/abstract), among all variants with a PICS probability of >0.0275, the

Table 1. Results of GWAS, replication, and combined analyses of associations with antineutrophil cytoplasmic autoantibody–associated vasculitis*

					GWAS (n = 1,371 cases, n = 3,258 controls)				Replication analysis (n = 615 cases, n = 1,465 controls)				Combined analysis (n = 1,986 cases, n = 4,723 controls)	
					RAF				RAF					
SNP	Locus	Position	Gene	Risk allele	Cases	Controls	*P*†	OR (95% CI)‡	Cases	Controls	*P*§	OR (95% CI)	*P*‡	OR (95% CI)
rs141530233	6p21.32	33048688	*HLA–DPB1*	A del¶	0.86	0.70	5.93×10^{-56}	2.76 (2.44–3.13)	0.90	0.69	2.45×10^{-39}	4.00 (3.23–5.00)	1.13×10^{-89}	2.99 (2.69–3.33)
rs1042169	6p21.32	33048686	*HLA–DPB1*	G	0.86	0.70	4.41×10^{-52}	2.57 (2.27–2.94)	0.90	0.68	1.94×10^{-39}	4.00 (3.23–5.00)	1.12×10^{-84}	2.82 (2.54–3.13)
rs9277341	6p21.32	33039625	*HLA–DPA1*	T	0.84	0.70	1.62×10^{-40}	2.21 (1.96–2.50)	0.87	0.66	3.58×10^{-34}	3.13 (2.63–3.70)	6.09×10^{-71}	2.44 (2.21–2.69)
rs35242582	6p21.32	32600057	*HLA–DQA1*	A	0.82	0.74	3.34×10^{-16}	1.61 (1.43–1.79)	0.82	0.74	3.59×10^{-8}	1.59 (1.35–1.89)	6.34×10^{-23}	1.60 (1.46–1.76)
rs1049072	6p21.32	32634355	*HLA–DQB1*	A	0.23	0.17	4.23×10^{-10}	1.43 (1.28–1.59)	0.21	0.17	1.69×10^{-3}	1.30 (1.10–1.54)	6.46×10^{-13}	1.40 (1.28–1.53)
rs6679677	1p13.2	114303808	*PTPN22*	A	0.13	0.09	2.40×10^{-8}	1.49 (1.30–1.72)	0.11	0.09	4.57×10^{-2}	1.25 (1.00–1.55)	1.88×10^{-8}	1.40 (1.25–1.57)
rs62132293	19p13.3	838178	*PRTN3*	G	0.37	0.31	5.55×10^{-8}	1.30 (1.18–1.43)	0.37	0.31	6.81×10^{-5}	1.33 (1.15–1.52)	8.60×10^{-11}	1.29 (1.19–1.39)
rs28929474	14q32.13	94844947	*SERPINA1*	T	0.04	0.02	8.26×10^{-8}	2.09 (1.59–2.73)	0.04	0.02	6.72×10^{-5}	2.18 (1.49–3.20)	3.09×10^{-12}	2.18 (1.75–2.71)
rs2476601	1p13.2	114377568	*PTPN22* (*R620W*)	A	0.13	0.10	3.03×10^{-7}	1.45 (1.26–1.66)	0.11	0.09	5.38×10^{-2}	1.24 (1.00–1.53)	1.86×10^{-7}	1.36 (1.21–1.53)

* RAF = risk allele frequency; OR = odds ratio; 95% CI = 95% confidence interval.
† EigenStrat *P* value.
‡ *P* values for the replication analysis and combined genome-wide association study (GWAS) data sets were calculated using the Cochran-Mantel-Haenszel method, which combines allele frequency counts.
§ Plink *P* value.
¶ The single-nucleotide polymorphism (SNP) rs141530233 is an insertion/deletion polymorphism, with the risk genotype lacking an adenosine residue at nucleotide position 33048688 (adenosine deletion [A del]) and the nonrisk genotype containing this adenosine residue.

Table 2. MHC and non-MHC associations with ANCA-associated vasculitis according to clinically and serologically defined subgroups of patients*

						Clinical syndrome						ANCA specificity					
				Overall analysis of combined cohort (n = 1,986 cases, n = 4,723 controls)		GPA (n = 1,556) vs. controls (n = 4,723)		MPA (n = 236) vs. controls (n = 4,723)		GPA (n = 1,556) vs. MPA (n = 236)		PR3-cANCA (n = 1,361) vs. controls (n = 4,723)		MPO-pANCA (n = 378) vs. controls (n = 4,723)		PR3-cANCA (n = 1,361) vs. MPO-pANCA (n = 378)	
SNP	Locus	Gene	Risk allele	*P*†	OR	*P*†	OR	*P*†	OR	*P*†	OR	*P*†	OR	*P*†	OR	*P*†	OR
rs141530233	6p21.32	*HLA–DPB1*	A del	1.13×10^{-89}	2.99	3.80×10^{-93}	3.82	9.45×10^{-5}	1.58	1.45×10^{-9}	2.04	1.33×10^{-106}	6.19	1.50×10^{-2}	1.24	3.53×10^{-32}	3.93
rs1042169	6p21.32	*HLA–DPB1*	G	1.12×10^{-84}	2.82	1.09×10^{-90}	3.66	2.22×10^{-3}	1.40	9.50×10^{-12}	2.18	6.53×10^{-106}	6.09	1.27×10^{-1}	1.14	3.44×10^{-36}	4.27
rs9277341	6p21.32	*HLA–DPA1*	T	6.09×10^{-71}	2.44	2.78×10^{-73}	2.86	9.40×10^{-4}	1.45	4.96×10^{-7}	1.79	4.52×10^{-84}	3.69	3.61×10^{-3}	1.29	4.55×10^{-20}	2.61
rs35242582	6p21.32	*HLA–DQA1*	A	6.34×10^{-23}	1.60	1.60×10^{-20}	1.63	8.91×10^{-3}	1.36	1.36×10^{-1}	1.20	5.78×10^{-18}	1.62	2.34×10^{-7}	1.68	7.67×10^{-1}	1.03
rs1049072	6p21.32	*HLA–DQB1*	A	6.46×10^{-13}	1.40	1.40×10^{-7}	1.31	4.16×10^{-9}	1.89	2.99×10^{-3}	1.39	3.82×10^{-3}	1.17	2.13×10^{-24}	2.37	7.53×10^{-13}	1.94
rs6679677	1p13.2	*PTPN22*	A	1.88×10^{-8}	1.40	2.38×10^{-7}	1.40	8.96×10^{-4}	1.58	5.48×10^{-1}	1.09	7.89×10^{-6}	1.36	8.83×10^{-7}	1.71	1.08×10^{-1}	1.21
rs62132293	19p13.3	*PRTN3*	G	8.60×10^{-11}	1.29	7.06×10^{-11}	1.32	1.12×10^{-1}	1.17	2.70×10^{-1}	1.12	3.59×10^{-13}	1.39	5.66×10^{-1}	1.05	3.22×10^{-5}	1.45
rs28929474	14q32.13	*SERPINA1*	T	3.09×10^{-12}	2.18	3.53×10^{-13}	2.35	2.06×10^{-2}	1.88	3.86×10^{-1}	1.26	1.29×10^{-13}	2.43	4.96×10^{-3}	1.87	1.92×10^{-1}	1.34
rs2476601	1p13.2	*PTPN22* (*R620W*)	A	1.86×10^{-7}	1.36	1.77×10^{-6}	1.36	1.31×10^{-3}	1.56	4.95×10^{-1}	1.10	3.19×10^{-5}	1.33	5.85×10^{-6}	1.64	1.40×10^{-1}	1.19

* MHC = major histocompatibility complex; ANCA = antineutrophil cytoplasmic autoantibody; GPA = granulomatosis with polyangiitis (Wegener's); MPA = microscopic polyangiitis; PR3 = proteinase 3; cANCA = cytoplasmic ANCA; MPO = myeloperoxidase; pANCA = perinuclear ANCA; SNP = single-nucleotide polymorphism; OR = odds ratio; A del = adenosine deletion.
† EigenStrat *P* value.

Table 3. MHC and non-MHC associations with ANCA-associated vasculitis in the MPO-pANCA subgroup (assessed in GWAS, replication, and combined analyses) compared to the PR3-cANCA subgroup (in combined analysis)*

					Patients with MPO-pANCAs										Patients with PR3-cANCAs in combined association analysis (n = 1,361 patients, n = 4,723 controls)	
					GWAS (n = 324 patients, n = 3,258 controls)				Replication analysis (n = 54 patients, n = 1,465 controls)				Combined association analysis (n = 378 patients, n = 4,723 controls)			
					RAF				RAF							
SNP	Locus	Position	Gene	Risk allele	Cases	Controls	*P*†	OR (95% CI)	Cases	Controls	*P*†	OR (95% CI)	*P*†	OR (95% CI)	*P*†	OR (95% CI)
rs3998159	6p21.32	32682019	*HLA–DQA2*	C	0.23	0.10	3.47×10^{-19}	2.61 (2.12–3.22)	0.25	0.09	7.11×10^{-7}	3.25 (2.04–5.18)	5.24×10^{-25}	2.72 (2.24–3.22)	5.18×10^{-1}	1.05 (0.91–1.20)
rs7454108	6p21.32	32681483	*HLA–DQA2*	C	0.23	0.10	3.90×10^{-19}	2.61 (2.12–3.23)	0.25	0.09	4.78×10^{-7}	3.34 (2.09–5.33)	5.03×10^{-25}	2.73 (2.25–3.24)	5.48×10^{-1}	1.04 (0.90–1.20)
rs1049072	6p21.32	32634355	*HLA–DQB1*	A	0.32	0.17	1.63×10^{-18}	2.27 (1.89–2.72)	0.35	0.17	3.16×10^{-6}	2.60 (1.74–3.88)	2.13×10^{-24}	2.37 (2.01–2.78)	3.82×10^{-3}	1.17 (1.06–1.31)

* MHC = major histocompatibility complex; ANCA = antineutrophil cytoplasmic autoantibody; MPO = myeloperoxidase; pANCA = perinuclear ANCA; GWAS = genome-wide association study; PR3 = proteinase 3; cANCA = cytoplasmic ANCA; RAF = risk allele frequency; SNP = single-nucleotide polymorphism; OR = odds ratio; 95% CI = 95% confidence interval.
† EigenStrat *P* value.

Table 4. Population risk estimates for disease-associated SNPs at the MHC and non-MHC loci in all patients with AAV and in clinically and serologically defined subgroups of patients*

					Clinical syndrome				ANCA specificity			
			Combined AAV cohort		GPA		MPA		PR3-cANCAs		MPO-pANCAs	
Gene	SNP	RAF	OR	PAF	OR	PAF	OR	PAF	OR	PAF	OR	PAF
HLA–DPB1	rs141530233	0.70	2.36	0.49	3.01	0.58	1.64	0.31	3.98	0.68	1.01	0.00
HLA–DPA1	rs9277341	0.70	1.62	0.30	1.81	0.36	1.26	0.00	1.84	0.37	1.03	0.00
HLA–DQA1	rs35242582	0.74	1.39	0.22	1.46	0.26	1.06	0.00	1.27	0.17	1.02	0.00
HLA–DQB1	rs1049072	0.17	1.33	0.05	1.19	0.00	1.91	0.13	1.16	0.00	2.64	0.22
PRTN3	rs62132293	0.31	1.27	0.08	1.30	0.09	1.18	0.00	1.59	0.16	1.10	0.00
SERPINA1	rs28929474	0.02	2.13	0.02	2.43	0.02	1.98	0.00	3.64	0.04	2.98	0.00
PTPN22 (*R620W*)	rs2476601	0.10	1.45	0.04	1.47	0.04	1.62	0.06	1.71	0.06	2.18	0.10
Total	–	–	–	0.77	–	0.83	–	0.43	–	0.87	–	0.30

* Population risk estimates included the risk allele frequency (RAF), odds ratio (OR), and population attributable fraction (PAF) calculated in the overall combined cohort of patients with antineutrophil cytoplasmic autoantibody (ANCA)–associated vasculitis (AAV), in the clinical subgroups of patients with granulomatosis with polyangiitis (Wegener's) (GPA) and those with microscopic polyangiitis (MPA), and in the serologically defined subgroups of patients with proteinase 3 (PR3)–cytoplasmic ANCAs (cANCAs) and those with myeloperoxidase (MPO) perinuclear ANCAs. SNPs = single-nucleotide polymorphisms; MHC = major histocompatibility complex.

index SNPs derived from direct genotyping were consistently associated with the highest PICS values (see Supplementary Table 11, http://onlinelibrary.wiley.com/doi/10.1002/art.40034/abstract). PICS values were particularly high for the index SNPs at the *HLA–DPB1, SERPINA1,* and *PTPN22* loci, all of which are functional missense variants (15,22,23). The candidate causal variants at the other HLA gene loci were either synonymous, intronic, or upstream gene variants, but the majority of these noncoding variants, and even several *HLA–DPB1* coding variants, have been annotated as eQTLs that influence gene expression in immune cell lineages (24).

None of the candidate variants at the *PRTN3* locus were coding or reported eQTL SNPs. Increases in *PRTN3* expression levels have, however, been observed in neutrophils from patients with AAV and implicated in the pathogenicity of AAV (17,25). Because knowledge of neutrophil-specific eQTLs remains limited, we evaluated the lead SNP at this locus (rs62132293) for allelic effects on *PRTN3* expression in neutrophils. Results of qPCR analyses revealed cellular *PRTN3* transcript levels to be significantly higher in those homozygous for the risk (G) allele than in donors with CC or CG genotypes (Figure 1). These results identify the rs62132293 SNP as an eQTL for *PRTN3* and suggest that the causal variant at this locus engenders risk by its association with increased *PRTN3* expression.

Association of the rs141530233 risk variant with altered *HLA–DPB1* expression and T cell responses. Among the candidate causal variants, the *HLA–DPB1* rs141530233 and rs1042169 SNPs had the largest effects on risk, with respective ORs of 2.99 and 2.82 in the primary cohort and respective ORs of 6.19 and 6.09 in the PR3-ANCA subset (Tables 1 and 2). These SNPs are, respectively, insertion/deletion (–/A) and missense (G/A) polymorphisms that map only 2 basepairs apart in exon 2 of the *HLA–DPB1* gene, with their risk alleles in complete LD in the control cohort and the reference 1000 Genomes Project data sets. In the latter population, these alleles correlate perfectly with another insertion/deletion polymorphic variant, rs386699872 CA/G, 3 basepairs downstream of rs141530233, suggesting that these variants comprise a triallelic risk and nonrisk *HLA–DPB1* haplotype (see Supplementary Figure 6, http://onlinelibrary.wiley.com/doi/10.1002/

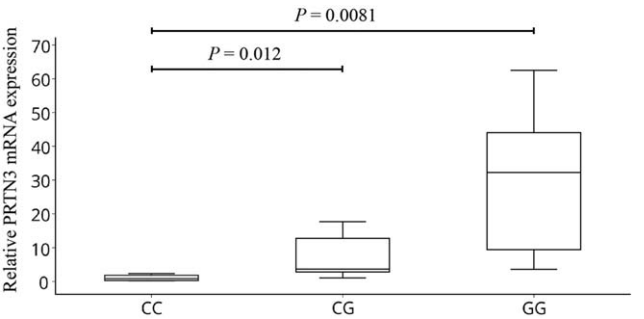

Figure 1. Association between the antineutrophil cytoplasmic autoantibody–associated vasculitis variant rs62132293 and increased expression of *PRTN3*. Levels of mRNA for *PRTN3* were measured using quantititative polymerase chain reaction amplification of cDNA from peripheral blood polymorphonuclear leukocytes obtained from healthy donors with the rs62132293 CC genotype (n = 7), rs62132293 CG genotype (n = 9), or rs62132293 GG genotype (n = 6). *PRTN3* expression levels, relative to the values for the calibrator reference gene *COX5B*, are presented as box plots, in which the boxes represent the 25th to 75th percentiles, the horizontal line within the boxes indicates the median, and the bars outside the boxes indicate the lowest and highest values. Data are representative of 3 independent experiments. *P* values were determined by unpaired *t*-test.

art.40034/abstract). To confirm the haplotypic relatedness of the 3 variants, we sequenced this region in 100 study subjects who were homozygous for the rs141530233 and rs1042169 markers. Our findings confirmed the organization of the 3 variants in 2 haplotype blocks (as shown in Supplementary Figure 6), which is consistent with the findings in prior studies of a dimorphic polymorphism (GGPM versus DEAV) at the corresponding amino acid positions 84–87 of the HLA–DPB chain (22,26,27).

Effects of the rs141530233 SNP on gene expression have not been reported, but the linked missense rs1042169 G/A SNP has been catalogued as an eQTL, with presence of the homozygous GG genotype being correlated with increased expression of *HLA–DPB1* in PBMCs (24). These variants are in LD with a SNP variant (rs9277534) in the downstream *HLA–DPB1* 3′-untranslated region, for which the homozygous genotype is associated with lower levels of *HLA–DPB1* and HLA–DP expression in immune cells compared to those in subjects with the alternate homozygous genotype (28,29). We therefore assessed the relationship between the triallelic AAV risk haplotype and *HLA–DPB1*/HLA–DP expression using PBMCs from healthy subjects carrying either risk or protective rs1042169 alleles. Results of qPCR analysis revealed *HLA–DPB1* messenger RNA levels to be significantly lower in rs1042169 GG risk allele homozygotes than in subjects with the AA or GA genotypes (Figure 2A).

Furthermore, flow cytometric analyses revealed significantly lower HLA–DP expression on CD19+ B cells and CD14+ monocytes from donors with the GG risk allele than on cells from donors with the GA or AA genotype (Figures 2B and C). Thus, the triallelic risk haplotype defined by the rs1042169 G variant is associated with reduced *HLA–DPB1* transcript levels and HLA–DP surface expression in immune cells.

The finding that a triallelic haplotype was correlated with reduced expression of *HLA–DPB1*/HLA–DP and encoded a putative functionally important HLA–DP polymorphism that is highly associated with risk of AAV, and particularly PR3-ANCA vasculitis, strongly suggests that this genetic variation influences HLA–DP–modulated immune responses that could be relevant to susceptibility.

Because T cells that respond to PR3 protein or peptides have been identified in patients with PR3-ANCA–positive AAV, and because the frequency of T cells responding to a "complementary" peptide encoding anti-sense PR3 codons (cPR3) has been correlated with the presence and activity of disease (30–35), we stimulated PBMCs from patients carrying rs1042169 G and/or A alleles with putatively immunogenic cPR3 and PR3 peptides and used an IFNγ ELISpot assay to identify responding T cells. Whereas the PR3 peptides elicited

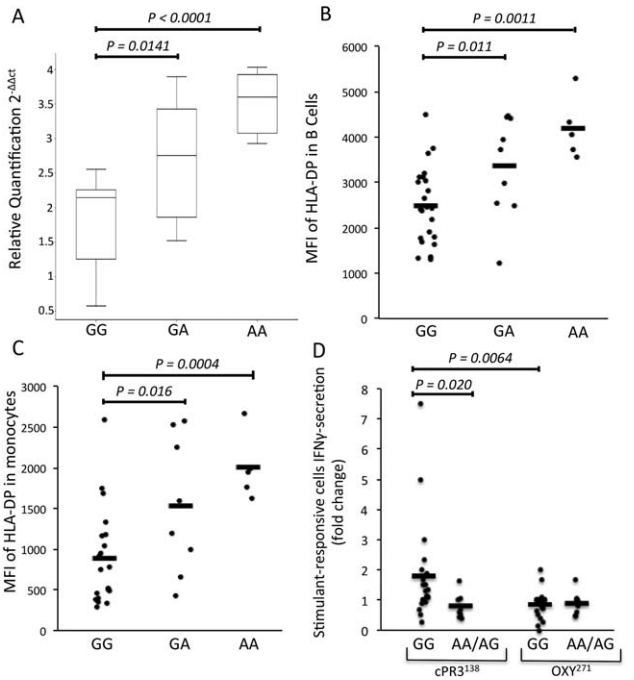

Figure 2. Association of the rs1042169 allele with differential *HLA–DPB1* expression and T cell responses. **A,** *HLA–DPB1* mRNA levels were detected by quantititative polymerase chain reaction amplification of cDNA from peripheral blood mononuclear cells (PBMCs) obtained from healthy donors with the rs1042169 GG genotype (n = 13), rs1042169 GA genotype (n = 8), or rs1042169 AA genotype (n = 7). *HLA–DPB1* mRNA levels, relative to the values for the calibrator reference gene *GAPDH*, are shown as box plots, in which the boxes represent the 25th to 75th percentiles, the horizontal line within the boxes indicates the median, and the bars outside the boxes indicate the lowest and highest values. Data are representative of 3 independent experiments. **B** and **C,** Surface HLA–DP levels were evaluated by flow cytometric assay of B cells **(B)** and monocytes **(C)** in anti-DP and anti-CD19 or anti-CD14 antibody–stained PBMCs obtained from donors with the rs1042169 GG genotype (n = 24), rs1042169 GA genotype (n = 9), or rs1042169 AA genotype (n = 5). **D,** PBMCs from patients positive for proteinase 3 (PR3)–specific antineutrophil cytoplasmic autoantibodies who were carriers of the rs10421699 GG genotype (n = 21) or the AA/AG genotype (n = 8) were stimulated with anti-sense PR3 codons (cPR3) or an OXY control peptide and analyzed by ELISpot for interferon-γ (IFNγ)–secreting T cells. Results are the mean fold change in stimulated cells relative to unstimulated cells. Symbols in **B–D** represent individual donors; horizontal bars indicate the mean. In **A–C,** *P* values were determined by unpaired *t*-test. In **D,** *P* values were determined by Mann-Whitney U test (GG versus AA/AG + $cPR3^{138}$) or Wilcoxon's signed rank test (GG $cPR3^{138}$ versus GG OXY^{271}). MFI = mean fluorescence intensity.

either no response or minimal responses (data not shown), the cPR3 peptide, in most patients, evoked clear reactivity that was completely absent in cells stimulated with an irrelevant (OXY) peptide (Figure 2D) and in cells from healthy controls (data not shown). Frequencies of IFNγ-producing cells differed strikingly among patients

according to their rs1042169 allele status, with the numbers of responding T cells being significantly higher ($P < 0.02$) in risk allele homozygotes than in individuals having 1 or 2 copies of the protective A allele, and significantly higher in risk allele homozygotes following stimulation with cPR3 compared to stimulation with OXY ($P < 0.0064$). These findings are consistent with the presence of cPR3-reactive T cells in PR3-ANCA–positive vasculitis patients and suggest the possibility that the altered HLA–DP expression, and possibly function, associated with the *HLA–DPB1* homozygous risk haplotype is correlated with increased numbers of autoreactive cells.

DISCUSSION

This study identifies MHC and non-MHC gene variants that are associated with GPA/MPA susceptibility and with altered gene expression and/or function of proteins integral to immune responses. Our data reveal that the largest effect on risk emanates from a triallelic *HLA–DPB1* haplotype underpinning a previously reported HLA–DPB amino acid polymorphism across positions 84–87 (22–27). Our data also support major roles for the *PRTN3*, *SERPINA1*, and *PTPN22* genes in AAV susceptibility, providing the first evidence of a genome-wide significant association with the *PTPN22* rs2476601 functional variant, and identifying a correlation of the top-scoring variant at *SERPINA1* as a null allele and at *PRTN3* as an eQTL allele with increased *PRTN3* expression in neutrophils. Results of the CART analysis revealed the potential for these functional variants to be used to identify population subsets of individuals who would be at highly elevated risk of developing GPA or MPA, as indicated by the observed collective PAF of 77%. The estimated array heritability of 21% is comparable to previous estimates of the heritability of inflammatory bowel disease (36).

Among the MHC associations, the *HLA–DPB1* risk haplotype alleles appear particularly significant, having a very strong effect on risk and underpinning a β-chain polymorphism in the HLA–DP antigen-binding pocket that modulates the protein's peptide-binding properties and possibly its effects on T cell allorecognition (22). The physiologic significance of this haplotype can also be inferred on the basis of our data linking these risk alleles to decreased expression of *HLA–DPB1* and HLA–DP and an increased frequency of cPR3 peptide–reactive T cells in patients with anti-PR3 autoantibodies. Although understanding of the autoantigenic epitopes driving T cell responses in AAV is limited, our findings are consistent with prior data correlating alleles at linked *HLA–DPB1* SNP loci to differential *HLA–DPB1*/HLA–DP expression and with the association of such expression changes, as well as the HLA–DP GGPM/DEAV variance, with differential outcomes of specific immune challenges (28,29). Further investigation is required to define the extent to which the risk haplotype–associated increase in levels of autoreactive T cells reflects the failure to eliminate such cells during thymic selection and/or whether another mechanistic aberrancy may be involved.

Among the non-MHC associations identified, direct causal effects of the *PTPN22* risk variant are strongly suggested by previous data linking the associated Lyp variant to aberrant increases in lymphocyte antigen receptor signaling and dendritic cell activation (23). Direct contribution of the *SERPINA1* rs28929474 risk variant to AAV pathogenesis has also been implied in a study that established a role for α_1-antitrypsin in inhibiting PR3 protease activity and, by extension, PR3-induced inflammatory responses (37). Similarly, the most strongly associated *PRTN3* variant has been found to increase the neutrophil expression of *PRTN3*, an aberrancy found often in PR3-ANCA–positive patients, and this is correlated with pathogenic neutrophil activation, suggesting that altered *PRTN3* expression mediated via this or another tightly linked variant functionally underpins the *PRTN3* association with AAV (17,38).

Our analyses revealed that the risk associated with the various AAV phenotypes was linked to joint effects of different genes across the HLA class II region. Consistent with a prior study that demonstrated genetic distinctions between PR3-ANCA–positive vasculitis and MPO-ANCA–positive vasculitis (2), we detected peak associations of the *HLA–DPB1* and *HLA–DPA1* variants with positivity for PR3-ANCAs, whereas in those with MPO-ANCAs, the *HLA–DQA2* and *HLA–DQB1* variants showed the strongest associations. Differential effects of these variants also distinguished patients with GPA from those with MPA, suggesting that GPA and PR3-ANCA–positive AAV share a composite set of MHC class II risk alleles that is largely distinct from those conferring risk of MPA and MPO-ANCA–positive AAV. Stronger associations at the *PRTN3* and *SERPINA1* loci appear to distinguish the GPA and PR3-ANCA subsets from their counterpart subgroups. In contrast, effects of the *PTPN22* locus on AAV risk seem equivalent across the different subsets, suggesting that the genetic disparities between subgroups do not reflect insufficient statistical power and are important determinants of phenotypic heterogeneity in AAV.

In summary, our study has illuminated MHC and non-MHC gene variants that are strongly associated with AAV and that are differentially associated with key clinical

and serologic disease subsets. The identified variants could potentially directly influence the pathogenesis of AAV. The extent to which, and the mechanisms whereby, these variants directly cause disease requires more investigation, and our data do not directly preclude the potential biologic relevance of other alleles in LD with these variants, particularly at the *HLA–DPB1* and *PRTN3* loci. Whether the sample size constrained our analysis of important subsets (such as patients with IgG-ANCAs versus those with IgA-ANCAs) or confounded detection of some important associations remains to be determined (39). Nonetheless, our findings identify a set of risk variants that explain much of the genetic risk of GPA/MPA, that appear to influence the clinical presentation of the disease, and that represent biologically important alleles with high potential to drive the aberrant immune responses contributing to the development of AAV.

AUTHOR CONTRIBUTIONS

All authors were involved in drafting the article or revising it critically for important intellectual content, and all authors approved the final version to be published. Dr. Siminovitch had full access to all of the data in the study and takes responsibility for the integrity of the data and the accuracy of the data analysis.

Study conception and design. Merkel, Xie, Monach, Ciavatta, Pinder, Zhang, Hirano, Edberg, Falk, Amos, Siminovitch.

Acquisition of data. Merkel, Xie, Monach, Ji, Ciavatta, Byun, Pinder, Zhao, Zhang, Tadesse, Qian, Weirauch, Nair, Tsoi, Pagnoux, Carette, Chung, Cuthbertson, Davis Jr., Dellaripa, Forbess, Gewurz-Singer, Hoffman, Khalidi, Koening, Langford, Mahr, McAlear, Moreland, Seo, Specks, Spiera, Sreih, St.Clair, Stone, Ytterberg, Elder, Qu, Ochi, Hirano, Edberg, Falk, Amos, Siminovitch.

Analysis and interpretation of data. Merkel, Xie, Monach, Ji, Byun, Pinder, Zhao, Zhang, Tadesse, Weirauch, Chung, Elder, Qu, Ochi, Hirano, Edberg, Amos, Siminovitch.

ADDITIONAL DISCLOSURE

Dr. Davis is currently an employee of Pfizer Inc.

REFERENCES

1. Xie G, Roshandel D, Sherva R, Monach PA, Lu EY, Kung T, et al. Association of granulomatosis with polyangiitis (Wegener's) with HLA–DPB1*04 and SEMA6A gene variants: evidence from genome-wide analysis. Arthritis Rheum 2013;65:2457–68.
2. Lyons PA, Rayner TF, Trivedi S, Holle JU, Watts RA, Jayne DR, et al. Genetically distinct subsets within ANCA-associated vasculitis. N Engl J Med 2012;367:214–23.
3. Fries JF, Hunder GG, Bloch DA, Michel BA, Arend WP, Calabrese LH, et al. The American College of Rheumatology 1990 criteria for the classification of vasculitis: summary. Arthritis Rheum 1990;33:1135–6.
4. Hoffmann TJ, Zhan Y, Kvale MN, Hesselson SE, Gollub J, Iribarren C, et al. Design and coverage of high throughput genotyping arrays optimized for individuals of East Asian, African American, and Latino race/ethnicity using imputation and a novel hybrid SNP selection algorithm. Genomics 2011;98:422–30.
5. Banda Y, Kvale MN, Hoffmann TJ, Hesselson SE, Ranatunga D, Tang H, et al. Characterizing race/ethnicity and genetic ancestry for 100,000 subjects in the Genetic Epidemiology Research on Adult Health and Aging (GERA) cohort. Genetics 2015;200:1285–95.
6. Purcell S, Neale B, Todd-Brown K, Thomas L, Ferreira MA, Bender D, et al. PLINK: a tool set for whole-genome association and population-based linkage analyses. Am J Hum Genet 2007;81:559–75.
7. Willer CJ, Li Y, Abecasis GR. METAL: fast and efficient meta-analysis of genomewide association scans. Bioinformatics 2010;26:2190–1.
8. Lee SH, Wray NR, Goddard ME, Visscher PM. Estimating missing heritability for disease from genome-wide association studies. Am J Hum Genet 2011;88:294–305.
9. Howie BN, Donnelly P, Marchini J. A flexible and accurate genotype imputation method for the next generation of genome-wide association studies. PLoS Genet 2009;5:e1000529.
10. Breiman L, Friedman J, Olshen RA, Stone CJ. Classification and Regression Trees. Belmont, California: Chapman and Hall/CRC; 1984.
11. Farh KK, Marson A, Zhu J, Kleinewietfeld M, Housley WJ, Beik S, et al. Genetic and epigenetic fine mapping of causal autoimmune disease variants. Nature 2015;518:337–43.
12. Yang TP, Beazley C, Montgomery SB, Dimas AS, Gutierrez-Arcelus M, Stranger BE, et al. Genevar: a database and Java application for the analysis and visualization of SNP-gene associations in eQTL studies. Bioinformatics 2010;26:2474–6.
13. Xia K, Shabalin AA, Huang S, Madar V, Zhou YH, Wang W, et al. seeQTL: a searchable database for human eQTLs. Bioinformatics 2012;28:451–2.
14. Livak KJ, Schmittgen TD. Analysis of relative gene expression data using real-time quantitative PCR and the $2^{-\Delta\Delta C_t}$ method. Methods 2001;25:402–8.
15. Mahr AD, Edberg JC, Stone JH, Hoffman GS, St.Clair EW, Specks U, et al. $Alpha_1$-antitrypsin deficiency–related alleles Z and S and the risk of Wegener's granulomatosis. Arthritis Rheum 2010;62:3760–7.
16. Gencik M, Meller S, Borgmann S, Fricke H. Proteinase 3 gene polymorphisms and Wegener's granulomatosis. Kidney Int 2000;58:2473–7.
17. Rarok AA, Stegeman CA, Limburg PC, Kallenberg CG. Neutrophil membrane expression of proteinase 3 (PR3) is related to relapse in PR3-ANCA-associated vasculitis. J Am Soc Nephrol 2002;13:2232–8.
18. Cho JH, Feldman M. Heterogeneity of autoimmune diseases: pathophysiologic insights from genetics and implications for new therapies. Nat Med 2015;21:730–8.
19. Carmona FD, Mackie SL, Martin JE, Taylor JC, Vaglio A, Eyre S, et al. A large-scale genetic analysis reveals a strong contribution of the HLA class II region to giant cell arteritis susceptibility. Am J Hum Genet 2015;96:565–80.
20. Jagiello P, Aries P, Arning L, Wagenleiter SE, Csernok E, Hellmich B, et al. The PTPN22 620W allele is a risk factor for Wegener's granulomatosis. Arthritis Rheum 2005;52:4039–43.
21. Chung SA, Xie G, Roshandel D, Sherva R, Edberg JC, Kravitz M, et al. Meta-analysis of genetic polymorphisms in granulomatosis with polyangiitis (Wegener's) reveals shared susceptibility loci with rheumatoid arthritis. Arthritis Rheum 2012;64:3463–71.
22. Diaz G, Amicosante M, Jaraquemada D, Butler RH, Guillen MV, Sanchez M, et al. Functional analysis of HLA-DP polymorphism: a crucial role for DPβ residues 9, 11, 35, 55, 56, 69 and 84-87 in T cell allorecognition and peptide binding. Int Immunol 2003;15:565–76.
23. Zhang J, Zahir N, Jiang Q, Miliotis H, Heyraud S, Meng X, et al. The autoimmune disease-associated PTPN22 variant promotes calpain-mediated Lyp/Pep degradation associated with lymphocyte and dendritic cell hyperresponsiveness. Nat Genet 2011;43:902–7.
24. The GTEx Consortium. The Genotype-Tissue Expression (GTEx) project. Nat Genet 2013;45:580–5.

25. Yang JJ, Pendergraft WF, Alcorta DA, Nachman PH, Hogan SL, Thomas RP, et al. Circumvention of normal constraints on granule protein gene expression in peripheral blood neutrophils and monocytes of patients with antineutrophil cytoplasmic autoantibody-associated glomerulonephritis. J Am Soc Nephrol 2004;15:2103–14.
26. Doytchinova IA, Flower DR. In silico identification of supertypes for class II MHCs. J Immunol 2005;174:7085–95.
27. Silveira LJ, McCanlies EC, Fingerlin TE, van Dyke MV, Mroz MM, Strand M, et al. Chronic beryllium disease, HLA-DPB1, and the DP peptide binding groove. J Immunol 2012;189:4014–23.
28. Thomas R, Thio CL, Apps R, Qi Y, Gao X, Marti D, et al. A novel variant marking HLA-DP expression levels predicts recovery from hepatitis B virus infection. J Virol 2012;86:6979–85.
29. Petersdorf EW, Malkki M, O'hUigin C, Carrington M, Gooley T, Haagenson MD, et al. High HLA-DP expression and graft-versus-host disease. N Engl J Med 2015;373:599–609.
30. Van der Geld YM, Huitema MG, Franssen CF, van der Zee R, Limburg PC, Kallenberg CG. In vitro T lymphocyte responses to proteinase 3 (PR3) and linear peptides of PR3 in patients with Wegener's granulomatosis (WG). Clin Exp Immunol 2000;122:504–13.
31. Winek J, Mueller A, Csernok E, Gross WL, Lamprecht P. Frequency of proteinase 3 (PR3)-specific autoreactive T cells determined by cytokine flow cytometry in Wegener's granulomatosis. J Autoimmun 2004;22:79–85.
32. Popa ER, Franssen CF, Limburg PC, Huitema MG, Kallenberg CG, Tervaert JW. In vitro cytokine production and proliferation of T cells from patients with anti–proteinase 3– and antimyeloperoxidase-associated vasculitis, in response to proteinase 3 and myeloperoxidase. Arthritis Rheum 2002;46:1894–904.
33. Pendergraft WF III, Preston GA, Shah RR, Tropsha A, Carter CW Jr, Jennette JC, et al. Autoimmunity is triggered by cPR-3(105–201), a protein complementary to human autoantigen proteinase-3. Nat Med 2004;10:72–9.
34. Csernok E, Ai M, Gross WL, Wicklein D, Petersen A, Lindner B, et al. Wegener autoantigen induces maturation of dendritic cells and licenses them for Th1 priming via the protease-activated receptor-2 pathway. Blood 2006;107:4440–8.
35. Yang J, Bautz DJ, Lionaki S, Hogan SL, Chin H, Tisch RM, et al. ANCA patients have T cells responsive to complementary PR-3 antigen. Kidney Int 2008;74:1159–69.
36. Chen GB, Lee SH, Brion MJ, Montgomery GW, Wray NR, Radford-Smith GL, et al. Estimation and partitioning of (co)heritability of inflammatory bowel disease from GWAS and immunochip data. Hum Mol Genet 2014;23:4710–20.
37. Duranton J, Bieth JG. Inhibition of proteinase 3 by α1-antitrypsin in vitro predicts very fast inhibition in vivo. Am J Respir Cell Mol Biol 2003;29:57–61.
38. Ciavatta DJ, Yang J, Preston GA, Badhwar AK, Xiao H, Hewins P, et al. Epigenetic basis for aberrant upregulation of autoantigen genes in humans with ANCA vasculitis. J Clin Invest 2010;120:3209–19.
39. Kelley JM, Monach PA, Ji C, Zhou Y, Wu J, Tanaka S, et al. IgA and IgG antineutrophil cytoplasmic antibody engagement of Fc receptor genetic variants influences granulomatosis with polyangiitis. Proc Natl Acad Sci U S A 2011;108:20736–41.

ARTHRITIS & RHEUMATOLOGY
Vol. 69, No. 5, May 2017, pp 1067–1077
DOI 10.1002/art.40027

Early Mortality in a Multinational Systemic Sclerosis Inception Cohort

Yanjie Hao,[1] Marie Hudson,[2] Murray Baron,[2] Patricia Carreira,[3] Wendy Stevens,[4] Candice Rabusa,[4] Solene Tatibouet,[5] Loreto Carmona,[6] Beatriz E. Joven,[3] Molla Huq,[7] Susanna Proudman,[8] Mandana Nikpour,[7] the Canadian Scleroderma Research Group, and the Australian Scleroderma Interest Group

Objective. **To determine mortality and causes of death in a multinational inception cohort of subjects with systemic sclerosis (SSc).**

Methods. **We quantified mortality as standardized mortality ratio (SMR), years of life lost, and percentage mortality in the first decade of disease. The inception cohort comprised subjects recruited within 4 years of disease onset. For comparison, we used a prevalent cohort, which included all subjects irrespective of disease duration at recruitment. We determined a single primary cause of death (SSc related or non–SSc related) using a standardized case report form, and we evaluated predictors of mortality using multivariable Cox regression.**

Results. **In the inception cohort of 1,070 subjects, there were 140 deaths (13%) over a median follow-up of 3.0 years (interquartile range 1.0–5.1 years), with a pooled SMR of 4.06 (95% confidence interval [95% CI] 3.39–4.85), up to 22.4 years of life lost in women and up to 26.0 years of life lost in men, and mortality in the diffuse disease subtype of 24.2% at 8 years. In the prevalent cohort of 3,218 subjects, the pooled SMR was lower at 3.39 (95% CI 3.06–3.71). In the inception cohort, 62.1% of the primary causes of death were SSc related. Malignancy, sepsis, cerebrovascular disease, and ischemic heart disease were the most common non–SSc-related causes of death. Predictors of early mortality included male sex, older age at disease onset, diffuse disease subtype, pulmonary arterial hypertension, and renal crisis.**

Conclusion. **Early mortality in SSc is substantial, and prevalent cohorts underestimate mortality in SSc by failing to capture early deaths, particularly in men and those with diffuse disease.**

Systemic sclerosis (SSc) is characterized by immunologic abnormalities, microvascular dysfunction, and tissue fibrosis (1–4), with potential involvement of vital organs including the heart and lungs, resulting in substantial morbidity and mortality. Earlier studies showed a 10-year survival rate as low as 50% (5), while more recent studies, including a study from the European League Against Rheumatism Scleroderma Trial and Research (EUSTAR) registry (6), have shown survival rates of 90% at 5 years and 84% at 10 years.

Supported by Scleroderma Australia, Arthritis Australia, Actelion Australia, Bayer, CSL Biotherapies, GlaxoSmithKline Australia, and Pfizer. The Canadian Scleroderma Research Group (CSRG) is supported by the Canadian Institutes of Health Research (grant FRN 83518), the Scleroderma Society of Canada and its provincial chapters, Scleroderma Society of Ontario, Scleroderma Society of Saskatchewan, Sclérodermie Québec, Cure Scleroderma Foundation, INOVA Diagnostics, Inc., Dr. Fooke Laboratorien GmbH, Euroimmun, Mikrogen GmbH, Fonds de la recherche en santé du Québec, the Canadian Arthritis Network, and Jewish General Hospital and Lady Davis Research Institute, Montreal, Quebec, Canada. The CSRG has also received educational grants from Pfizer and Actelion Pharmaceuticals. The Madrid University Hospital 12 de Octubre Scleroderma Cohort Study was supported by the Instituto de Salud Carlos III, Spanish Ministry of Science and Innovation (FIS grant PI11/0156). Dr. Nikpour's work was supported by the National Health and Medical Research Council of Australia (fellowship APP1071735).

[1]Yanjie Hao, MD: St. Vincent's Hospital Melbourne, Melbourne, Victoria, Australia, and Peking University First Hospital, Beijing, China; [2]Marie Hudson, MD, MPH, Murray Baron, MD: Jewish General Hospital and Lady Davis Research Institute, Montreal, Quebec, Canada; [3]Patricia Carreira, MD, Beatriz E. Joven, MD: Hospital Universitario 12 de Octubre, Madrid, Spain; [4]Wendy Stevens, MBBS, Candice Rabusa, BSc: St. Vincent's Hospital Melbourne, Melbourne, Victoria, Australia; [5]Solene Tatibouet, MSc: Jewish General Hospital, Montreal, Quebec, Canada; [6]Loreto Carmona, MD, PhD: Instituto de Salud Musculoesqueletica, Madrid, Spain; [7]Molla Huq, BSc, MSc, Mandana Nikpour, MBBS, PhD: St. Vincent's Hospital Melbourne and The University of Melbourne, Melbourne, Victoria, Australia; [8]Susanna Proudman, MBBS: Royal Adelaide Hospital and University of Adelaide, Adelaide, South Australia, Australia.

Address correspondence to Mandana Nikpour, MBBS, PhD, Departments of Rheumatology and Medicine, The University of Melbourne, St. Vincent's Hospital, 41 Victoria Parade, Fitzroy, Victoria 3065, Australia. E-mail: m.nikpour@unimelb.edu.au.

Submitted for publication June 12, 2016; accepted in revised form December 13, 2016.

Two major methodologic concerns in these studies of "prevalent" cohorts, including the EUSTAR registry, are underestimation of mortality due to left truncation, which occurs when early deaths are not captured, and survivor bias, which occurs from oversampling of individuals who have survived initial disease and who are therefore likely to have better overall outcomes. Studies of "inception" cohorts, in which subjects are recruited at the time of disease onset, have the potential to overcome these sources of bias. However, to date there have been no reported studies of mortality in SSc in inception cohorts. Furthermore, little has been reported on risk factors for, and causes of death in, incident SSc.

In order to address these issues, we undertook a large multinational study of subjects with SSc recruited from Australia, Canada, and Spain for the purpose of estimating mortality rates and determining causes of death in those recruited within 4 years of disease onset (the "inception cohort"). We then compared our findings in the inception cohort with those in a "prevalent cohort" of subjects for whom there were no restrictions regarding disease duration at recruitment.

SUBJECTS AND METHODS

Subjects and cohorts. We included subjects from the Australian Scleroderma Cohort Study (ASCS), the Canadian Scleroderma Research Group (CSRG) cohort study, and the Madrid University Hospital 12 de Octubre Scleroderma Cohort Study. The Australian Scleroderma Cohort and CSRG cohort are multicenter cohorts, while the Madrid cohort is a single-center cohort. A list of investigators in the CSRG and the Australian Scleroderma Interest Group is provided in Appendix A.

Ethics approval was obtained from the human research ethics committees of each of the participating sites. Subjects in these cohorts fulfilled the American College of Rheumatology preliminary criteria for SSc (7) and provided written informed consent to participate at recruitment. No specific treatment algorithm was used in the 3 cohorts, and subjects were followed up at least once a year. We included adult (age ≥18 years) SSc subjects who had at least 1 follow-up visit in the ASCS between January 2007 and March 2014, in the CSRG cohort study between January 2005 and March 2014, and in the Madrid cohort between January 2000 and March 2014.

The inception cohort was defined as a subset of subjects recruited within 4 years of onset of their first non–Raynaud's phenomenon symptom attributable to SSc. This inception cohort is referred to hereafter as the "4-year inception cohort." The prevalent cohort included all registered subjects, regardless of disease duration at cohort entry. Accordingly, the prevalent cohort included all subjects in the inception cohort. However, we undertook extra analyses in which we removed inception cohort subjects from the prevalent cohort; the remaining subjects in the prevalent cohort are referred to hereafter as the "noninception cohort." We also undertook extra analyses using the definition of subjects recruited for the inception cohort within 1 year of onset of the first non–Raynaud's phenomenon symptom, referred to hereafter as the "1-year inception cohort."

Mortality data. Survival status was ascertained up until the end of April 2014 based on the records in the databases and telephone tracing of subjects for whom no data had been entered in the database for ≥24 months. A subject was determined to be lost to follow-up when no data had been entered for ≥24 months and at least 2 attempts to contact the subject had failed.

Calculation of standardized mortality ratio (SMR). The SMR was used to compare the mortality of subjects with SSc with that of the general populations of Australia, Canada, and Spain. The SMR and its 95% confidence interval (95% CI) were calculated as follows (8,9):

$$\mathrm{SMR} = \frac{\mathrm{O}}{\mathrm{E}}$$

$$95\%\ \mathrm{CI} = \left(\mathrm{SMR} - 1.96 \times \frac{\sqrt{\mathrm{O}}}{\mathrm{E}},\ \ \mathrm{SMR} + 1.96 \times \frac{\sqrt{\mathrm{O}}}{\mathrm{E}}\right)$$

where O is the observed number of deaths in the study population and E is the expected number of deaths. The expected number of deaths is the product of the total number of person-years contributed by the study population of each cohort multiplied by the mortality rate of the general population. The age- and sex-adjusted SMRs were calculated in a similar manner; the expected number of deaths was stratified by 10-year age groups and sex. The mortality rates of the general population were obtained from the Australian Bureau of Statistics, Statistics Canada, and the Spanish National Statistics Institute, and the most recent available data at the time of data analysis were from December 2012. We calculated the SMRs of the 3 national cohorts from the start date of each cohort (January 2007 for Australia, January 2005 for Canada, and January 2000 for Spain) to December 2012. The SMRs of the inception and prevalent cohorts of each country were calculated and compared. We undertook extra SMR analyses for the noninception cohort and the 1-year inception cohort; in these analyses, the noninception cohort included only subjects with disease duration of >4 years at recruitment. In relation to subjects lost to follow-up, we performed 2 sensitivity analyses to recalculate SMR, one of which assumed that all such subjects were alive at the end of the study and the other of which assumed that all such subjects were dead at the end of the study.

Calculation of life expectancy and years of life lost. Life expectancy for the study population as well as for the general population of each country was calculated according to sex using a period-abridged life table as described by Chiang (10) and Newell (11) with 5-year age intervals up to the interval of ≥85 years. The calculations used the same data as those used above for SMR calculations. Years of life lost was calculated as life expectancy at the time of birth in the general population minus life expectancy at the time of birth in the study population.

Causes of death. A standardized death case report form (see Supplementary Forms, available on the *Arthritis & Rheumatology* web site at http://onlinelibrary.wiley.com/doi/10.1002/art.40027/abstract) was completed by the treating doctor for all deaths in every center. Cause of death was then verified against source documents. The causes of death were categorized as a single primary cause (either SSc related or non–SSc related) and all other SSc organ involvement that contributed to death. SSc involvement of each organ was defined using standard uniform

Table 1. Baseline characteristics of the subjects in the study*

Characteristic	Australian cohort		Canadian cohort		Spanish cohort		Combined cohorts	
	Inception (n = 389)	Prevalent (n = 1,411)	Inception (n = 484)	Prevalent (n = 1,465)	Inception (n = 197)	Prevalent (n = 342)	Inception (n = 1,070)	Prevalent (n = 3,218)
Female sex, no. (%)	318 (81.7)	1,277 (90.5)	391 (80.8)	1,258 (85.9)	173 (87.8)	295 (86.3)	882 (82.4)	2,780 (86.4)
Age at disease onset, years†	52.1 ± 13.3	46.2 ± 14.2	52.0 ± 12.7	45.6 ± 13.7	50.2 ± 17.1	46.0 ± 16.6	51.7 ± 13.8	45.9 ± 14.2
Age at recruitment, years	54.1 ± 13.2	57.6 ± 12.5	53.5 ± 12.6	55.5 ± 12.2	51.4 ± 17.1	52.3 ± 15.7	53.3 ± 13.8	56.1 ± 12.8
Disease duration at recruitment, median (IQR) years	1.8 (0.9–2.8)	10.9 (4.1–21.7)	1.9 (1.1–2.9)	7.4 (2.9–15.3)	1.1 (0.4–2.4)	3.3 (0.9–9.6)	1.7 (0.9–2.8)	7.0 (2.7–15.2)
Duration of follow-up, median (IQR) years	2.9 (1.0–4.5)	3.0 (1.0–5.0)	3.0 (0.9–5.0)	3.1 (1.0–5.2)	4.4 (1.3–8.2)	4 (1.4–7.7)	3.0 (1.0–5.1)	3.1 (1.0–5.2)
Number of deaths	36	157	67	213	37	70	140	440
Age at death, years	65.6 ± 11.7	68.0 ± 10.4	60.4 ± 13.8	63.8 ± 12.3	65.8 ± 13.5	63.7 ± 13.4	63.1 ± 13.4	65.2 ± 12.0
Disease duration at death, years	3.5 ± 1.9	16.0 ± 12.1	4.4 ± 2.6	14.1 ± 10.5	4.7 ± 3.7	11.2 ± 9.8	4.2 ± 2.8	14.3 ± 11.0
Disease subtype, no. (%)								
Limited	232 (59.6)	993 (70.4)	255 (52.7)‡	856 (58.4)‡	135 (68.5)	237 (69.3)	622 (58.1)	2,086 (64.8)
Diffuse	156 (40.1)	371 (26.3)	213 (44.0)‡	531 (36.2)‡	62 (42.3)	104 (30.4)	431 (40.3)	1,006 (31.3)
Autoantibodies, no./total no. (%)§								
Anticentromere	136/364 (37.4)	593/1,278 (46.4)	104/352 (29.6)	401/1,164 (34.5)	83/196 (42.3)	140/334 (41.9)	323/912 (35.4)	1,134/2,776 (40.9)
Anti–Scl-70	67/358 (18.7)	181/1,252 (14.5)	64/352 (18.2)	177/1,164 (15.2)	53/196 (27.0)	90/335 (26.9)	184/906 (20.3)	448/2,751 (16.3)
Anti–RNAP III	40/211 (19.0)	89/698 (12.8)	62/236 (26.3)	143/811 (17.6)	–	–	102/447 (22.8)	232/1,509 (15.4)
SSc-associated disease manifestations, no. (%)¶								
PAH	34 (8.7)	152 (10.8)	17 (3.5)	61 (4.2)	7 (3.6)	27 (7.9)	58 (5.4)	240 (7.5)
ILD	96 (24.7)	311 (22.0)	110 (22.7)	301 (20.5)	58 (29.4)	107 (31.3)	264 (24.7)	719 (22.3)
PAH and ILD	10 (2.6)	48 (3.4)	3 (0.6)	19 (1.3)	2 (1.0)	11 (3.2)	15 (1.4)	78 (2.4)
Myocardial involvement	25 (6.4)	96 (6.8)	7 (1.4)	69 (4.7)	13 (6.6)	19 (5.6)	45 (4.2)	184 (5.7)
Pericardial effusion	16 (4.1)	83 (5.9)	189 (39.0)	640 (43.7)	16 (8.1)	36 (10.5)	221 (20.7)	759 (23.6)
Renal crisis	15 (3.9)	37 (2.6)	35 (7.2)	72 (4.9)	12 (6.1)	19 (5.6)	62 (5.8)	128 (4.0)
Gut involvement	213 (54.8)	766 (54.3)	338 (69.8)	1,139 (77.7)	133 (67.5)	252 (73.7)	684 (63.9)	2,157 (67.0)
Digital ulcer	156 (40.1)	639 (45.3)	225 (46.5)	834 (56.9)	74 (37.6)	159 (46.5)	455 (42.5)	1,632 (50.7)
Comorbidities, no. (%)¶								
IHD	21 (5.4)	128 (9.1)	19 (3.9)	75 (5.1)	–	–	40 (3.7)	203 (6.3)
CVD	11 (2.8)	62 (4.4)	22 (4.5)	75 (5.1)	–	–	33 (3.1)	137 (4.3)
Diabetes mellitus	28 (7.2)	94 (6.7)	34 (7.0)	110 (7.5)	11 (5.6)	19 (5.6)	73 (6.8)	223 (6.9)
Malignancy	46 (11.8)	242 (17.2)	40 (8.3)	143 (9.8)	22 (11.2)	32 (9.4)	108 (10.1)	417 (13.0)

* Except where indicated otherwise, values are the mean ± SD. IQR = interquartile range; anti–RNAP III = anti–RNA polymerase III; SSc = systemic sclerosis; PAH = pulmonary arterial hypertension; ILD = interstitial lung disease; IHD = ischemic heart disease; CVD = cerebrovascular disease.
† Defined as the date of the first non–Raynaud's phenomenon symptom.
‡ Disease subtype data were missing for 3.3% of subjects in the Canadian inception cohort and for 4.2% of subjects in the Canadian prevalent cohort.
§ Total number represents all subjects for whom autoantibody records were available and who were tested for the presence of a particular autoantibody.
¶ Ever present during follow-up.

definitions (see Supplementary Forms, http://onlinelibrary.wiley.com/doi/10.1002/art.40027/abstract).

Statistical analysis. Data are presented as the mean ± SD for continuous variables, the median and interquartile range for non-normally distributed continuous variables, and the number and percent for categorical variables. Baseline characteristics were compared between subjects who were alive and those who had died. Normally distributed continuous variables were compared using Student's *t*-test with unequal variances, and non-normally distributed continuous variables were compared using Kruskal-Wallis and Mann-Whitney U tests. Differences in frequency were determined using a chi-square test and Fisher's exact test.

Meta-analysis was performed to pool the incident and prevalent SMRs of the 3 national cohorts; the "weight" of each cohort was calculated based on sample size. Pooling was conducted on the ln(SMR), and statistical heterogeneity was assessed using the I^2 statistic. Since there was heterogeneity, we used a random-effects model to estimate a pooled ln(SMR), which we then back-transformed.

Survival analysis in the first decade was performed using the Kaplan-Meier method with comparisons performed using the log rank test. The primary end point was death from any cause or data censoring. The follow-up period ended in March 2014. The duration of follow-up was defined as the time from onset of the first non–Raynaud's phenomenon symptom until death or the last follow-up visit. We also performed extra Kaplan-Meier survival analysis for the 1-year inception cohort.

Univariable and multivariable Cox proportional hazards models were used to determine variables associated with mortality. Age, sex, disease duration, disease subtypes, antibody positivity, organ involvement, and comorbidities were included in the univariable Cox proportional hazards model. Variables with significance in the univariable analysis were then included in the multivariable Cox proportional hazards regression analysis, in which we ensured that the assumption of proportional hazards was valid.

Two-tailed *P* values less than or equal to 0.05 were considered significant. All statistical analyses were performed using Stata statistical software, release 13.1 (StataCorp).

RESULTS

Characteristics of the subjects. A total of 1,070 subjects (389 Australian, 484 Canadian, and 197 Spanish) were in the combined inception cohort. A total of 3,218 subjects (1,411 Australian, 1,465 Canadian, and 342 Spanish) were in the combined prevalent cohort. Baseline demographics, clinical characteristics, organ involvement, and major comorbidities in the 3 individual national cohorts and the combined cohorts are summarized in Table 1.

There were 140 deaths (36 Australian, 67 Canadian, and 37 Spanish) in the combined inception cohort and 440 deaths (157 Australian, 213 Canadian, and 70 Spanish) in the combined prevalent cohort. In the combined inception cohort, compared with subjects who were alive until the end of follow-up, those who died were significantly older at disease onset (mean ± SD 58.8 ± 13.5 years versus 50.8 ± 13.6 years; $P < 0.0001$) and recruitment and were more likely to be men (30.0% versus 15.4%; $P < 0.0001$). More of those who died had diffuse disease (54.3% versus 38.1%; $P < 0.0001$) and anti–RNA polymerase III (anti–RNAP III) antibodies (36.5% versus 20.2%; $P = 0.005$), while more who were alive had limited disease (60.8% versus 42.9%; $P < 0.0001$) and anticentromere antibodies (36.8% versus 25.8%; $P = 0.018$). In the combined inception cohort, subjects who died had more organ complications, including pulmonary arterial hypertension (PAH), interstitial lung disease (ILD), myocardial involvement, pericardial effusion, and renal crisis, while the frequency of gut involvement in the 2 groups was similar. There were also significant differences between the 2 groups in frequency of comorbidities, including ischemic heart disease (see Supplementary Table 1, http://onlinelibrary.wiley.com/doi/10.1002/art.40027/abstract). In the combined prevalent cohort, the characteristics of subjects who had died and of those who were alive at the end of the study were similar to those of the corresponding subjects in the combined inception cohort, with the notable exception that in the combined prevalent cohort, those who died also had more frequent digital ulcers, cerebrovascular disease, and malignancy (see Supplementary Table 1).

SMR, life expectancy, and years of life lost. Because of the time limitation of matched general population data, in the analyses of SMR and years of life lost we included 942 subjects (339 Australian, 420 Canadian, and 183 Spanish) in the combined inception cohorts and 2,872 subjects (1,252 Australian, 1,325 Canadian, and 295 Spanish) in the combined prevalent cohorts. Among them, 113 subjects (42 Australian, 62 Canadian, and 9 Spanish) in the combined inception cohorts and 430 subjects (196 Australian, 214 Canadian, and 20 Spanish) in the combined prevalent cohorts were lost to follow-up.

SMR. The age- and sex-adjusted SMRs of inception cohorts from Australia (3.4 [95% CI 2.3–4.5]) and Canada (5.1 [95% CI 4.0–6.2]) were higher than those in the corresponding prevalent cohorts, while the age- and sex-adjusted SMR in the inception cohort from Spain (3.2 [95% CI 2.3–4.2]) was lower than that in the corresponding prevalent cohort. Regardless of cohort type (inception versus prevalent), the crude (unadjusted for age) and age-adjusted SMRs for men were higher than for women in all nations. In men, SMRs in inception cohorts were consistently higher than in prevalent cohorts in all nations (Table 2).

Pooled SMR. The pooled age- and sex-adjusted SMR of the 3 inception cohorts was higher at 4.06 (95% CI 3.39–4.85; $I^2 = 76.4\%$; *P* for heterogeneity between studies = 0.014) than that of the 3 prevalent cohorts, which was 3.39 (95% CI 3.06–3.71; $I^2 = 84.9\%$; *P* for heterogeneity between studies = 0.001) (Figure 1). In

Table 2. Measures of mortality in each of the Australian, Canadian, and Spanish inception and prevalent cohorts*

	Australian cohort (01/2007–12/2012)		Canadian cohort (01/2005–12/2012)		Spanish cohort (01/2000–12/2012)	
	Inception (n = 339)	Prevalent (n = 1,252)	Inception (n = 420)	Prevalent (n = 1,325)	Inception (n = 183)	Prevalent (n = 295)
Number of deaths	27	110	58	182	30	58
Number of subjects lost to follow-up	42	196	62	214	9	20
Age- and sex-adjusted SMR (95% CI)	3.4 (2.3–4.5)	2.8 (2.4–3.3)	5.1 (4.0–6.2)	3.8 (3.3–4.2)	3.2 (2.3–4.2)	4.2 (3.3–5.0)
Crude SMR						
Women	2.9	3.8	4.4	4.2	3.7	4.6
Men	9.6	6.5	7.9	7.7	27.1	22.8
Age-adjusted SMR (95% CI)						
Women	2.4 (1.2–3.5)	2.6 (2.1–3.1)	4.4 (3.1–5.7)	3.4 (2.9–4.0)	2.8 (1.7–3.9)	3.8 (2.7–4.9)
Men	9.1 (3.7–14.5)	4.2 (2.4–5.9)	8.6 (4.4–12.9)	5.9 (4.1–7.8)	9.3 (1.9–16.8)	7.9 (3.0–12.8)
Years of life lost						
Women	11.3	11.9	22.4	19.4	15.2	20.9
Men	25.8	17.2	19.2	16.7	26.0	23.9
Survival in the first decade of disease, %						
Overall	84	95	80	94	77	86
Women	87	97	85	96	80	88
Men	74	88	65	88	50	75

* SMR = standardized mortality ratio; 95% CI = 95% confidence interval.

extra SMR analyses, the pooled SMR of the noninception cohorts was even lower at 3.20 (95% CI 2.86–3.58; $I^2 = 90.2\%$; P for heterogeneity between studies < 0.0001).

SMR sensitivity analyses. In SMR sensitivity analyses, assuming that all subjects lost to follow-up were alive or assuming that they were dead, the pooled SMR for the inception cohorts was higher than the pooled SMR for the prevalent cohorts (see Supplementary Table 2, http://onlinelibrary.wiley.com/doi/10.1002/art.40027/abstract).

Extra SMR analysis for 1-year inception cohorts. . The age- and sex-adjusted SMRs of the 1-year inception cohorts were even higher than the corresponding 4-year inception cohort SMRs from all 3 nations and were much higher than the corresponding prevalent cohort SMRs from Australia and Canada. While the age- and sex-adjusted SMR of the 1-year inception cohort from Spain was still lower than that of the corresponding prevalent cohort, the crude SMR in either men or women was higher in all 3 national 1-year inception cohorts than in the

Figure 1. Pooled standardized mortality ratio (SMR) of the Australian, Canadian, and Spanish inception and prevalent cohorts. Each square represents an individual SMR estimate, the size of the square being proportional to the weight given to the SMR. The horizontal lines represent the 95% confidence intervals (95% CIs) for the point estimates in each cohort. The diamond represents the pooled SMR. The pooled SMR of inception cohorts was higher than that of prevalent cohorts.

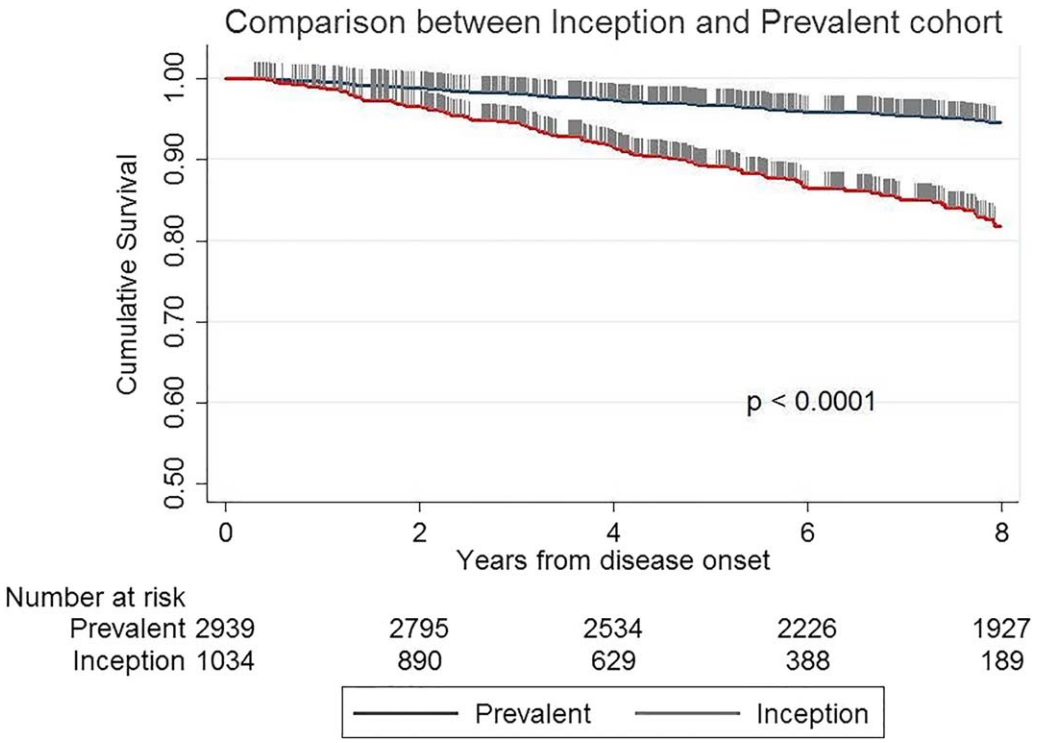

Figure 2. Kaplan-Meier analysis of overall survival in the first decade following disease onset in the combined inception cohort and combined prevalent cohort. The survival of the combined inception cohort was significantly lower than that of the combined prevalent cohort (99.0%, 94.8%, 88.9%, and 81.3% versus 99.5%, 98.0%, 96.7%, and 94.6% at 1, 3, 5, and 8 years, respectively; $P < 0.0001$ by log rank test).

corresponding prevalent cohorts (see Supplementary Table 3, http://onlinelibrary.wiley.com/doi/10.1002/art.40027/abstract).

Life expectancy and years of life lost. The life expectancy at birth of the Australian general population from 2007 to 2012 was 84.4 years for women and 79.9 years for men. The life expectancy of the Australian SSc study population within the same time period was 73.1 and 72.5 years in the inception and prevalent cohorts, respectively, for women and 54.1 and 62.7 years in the inception and prevalent cohorts, respectively, for men. There were 11.3 years of life lost in the inception cohort and 11.9 years of life lost in the prevalent cohort for women, and there were 25.8 years of life lost in the inception cohort and 17.2 years of life lost in the prevalent cohort for men. The findings were similar for the Canadian cohort and for men in the Spanish cohort (Table 2). For women in the Spanish cohort, years of life lost in the inception cohort were much lower than in the prevalent cohort (15.2 years of life lost versus 20.9 years of life lost).

Survival analysis. Overall survival in the first decade of disease in the combined inception cohort was lower than that in the combined prevalent cohort at 1, 3, 5, and 8 years (99.0%, 94.8%, 88.9%, and 81.3%, respectively, versus 99.5%, 98.0%, 96.7%, and 94.6%, respectively; $P < 0.0001$) (Figure 2) and lower than that in the combined noninception cohort (100%, 100%, 99.8%, and 98.8%, respectively; $P < 0.0001$) (see Supplementary Figure 1, http://onlinelibrary.wiley.com/doi/10.1002/art.40027/abstract), and this difference was greater for men than for women (see Supplementary Figure 2, http://onlinelibrary.wiley.com/doi/10.1002/art.40027/abstract) and for diffuse disease subtype than for limited disease subtype (see Supplementary Figure 3, http://onlinelibrary.wiley.com/doi/10.1002/art.40027/abstract). Kaplan-Meier analysis revealed lower survival in men than in women and lower survival in those with the diffuse disease subtype than in those with the limited disease subtype (both $P < 0.0001$), regardless of cohort type (combined inception cohort or combined prevalent cohort) (see Supplementary Figures 2 and 3).

We performed an extra survival analysis for the 1-year combined inception cohort. Survival of subjects in the 1-year combined inception cohort at 1, 3, 5, and 8 years (95.2%, 85.2%, 78.0%, and 70.8%, respectively) decreased further compared with survival of subjects in the 4-year combined inception cohort and combined prevalent cohort. Kaplan-Meier analysis

Table 3. Causes of SSc-related deaths in the combined inception cohort and combined prevalent cohort*

Organ system/ etiology	Combined inception cohort		Combined prevalent cohort	
	Principal cause (n = 87)	Contributing cause (n = 140)	Principal cause (n = 244)	Contributing cause (n = 440)
Heart and lung	48 (55.2)	25 (17.9)	173 (70.9)	111 (25.2)
PAH	22 (25.3)	9 (6.4)	88 (36.1)	49 (11.1)
ILD	18 (20.7)	16 (11.4)	53 (21.7)	62 (14.1)
PAH and ILD	8 (9.2)	–	32 (13.1)	–
Myocardial involvement	13 (14.9)	8 (5.7)	22 (9.0)	15 (3.4)
Gut involvement	12 (13.8)	16 (11.4)	24 (9.8)	44 (10.0)
Renal crisis	12 (13.8)	6 (4.3)	17 (7.0)	10 (2.3)
Pericardial effusion	1 (1.1)	4 (2.9)	4 (1.6)	11 (2.5)
Sepsis	1 (1.1)	11 (7.9)	4 (1.6)	41 (9.3)

* Each combined cohort included the corresponding Australian, Canadian, and Spanish cohorts. Values are the number (%) of subjects. SSc = systemic sclerosis; PAH = pulmonary arterial hypertension; ILD = interstitial lung disease.

revealed that the survival of subjects in the 1-year combined inception cohort was significantly lower than that in the corresponding combined noninception cohort (100%, 99.4%, 98.1%, and 96.1%, respectively) ($P < 0.0001$) (see Supplementary Figure 4, http://onlinelibrary.wiley.com/doi/10.1002/art.40027/abstract).

Causes of death. Among the 140 deaths in the combined inception cohort, 62.1% of the principal causes were SSc related and 24.3% were non–SSc related. We were unable to determine causes of death for 13.6% of subjects. The most common principal cause of SSc-related death (55.2%) was heart–lung disease, including PAH (25.3%), ILD (20.7%), and PAH combined with ILD (9.2%), while other SSc-related principal causes in descending order of frequency were myocardial involvement (14.9%), gut involvement (13.8%), renal crisis (13.8%), pericardial effusion (1.1%), and sepsis due to ischemic digit or decubitus ulcer (1.1%) (Table 3). Malignancy (38.2%), sepsis (14.7%), cerebrovascular disease (11.8%), and ischemic heart disease (8.8%) were the most common non–SSc-related primary causes (Table 4). Regardless of the primary cause, SSc organ involvement contributed to 50.1% of deaths (Table 3). Causes of death in the 3 individual national inception cohorts were similar (see Supplementary Tables 4 and 5, http://onlinelibrary.wiley.com/doi/10.1002/art.40027/abstract).

Among the 440 deaths in the combined prevalent cohort, proportionally fewer principal causes were SSc related (55.5%), and more were non–SSc related (33.6%), compared with principal causes of death in the combined inception cohort. We were unable to determine causes of death for 10.9% of subjects. The most common principal cause of SSc-related death was also heart–lung involvement, accounting for proportionally more deaths than in the combined inception cohort (70.9% versus 55.2%), including PAH (36.1% versus 25.3%), ILD (21.7% versus 20.7%), and PAH combined with ILD (13.1% versus 9.2%). Other major SSc-related principal causes were gut involvement (9.8%), myocardial involvement (9.0%), and renal crisis (7.0%), which were less frequent than in the combined inception cohort. As with the combined inception cohort, malignancy was the most common non–SSc-related primary cause in the combined prevalent cohort (37.1%), with ischemic heart disease and sepsis accounting for 12.2% and 9.5%, respectively, of non–SSc-related deaths (Table 4). Causes of death in the 3 individual national prevalent cohorts were similar (see

Table 4. Principal causes of non-SSc-related deaths in the combined inception cohort and combined prevalent cohort*

Organ system/etiology	Combined inception cohort (n = 34)	Combined prevalent cohort (n = 148)
Malignancy	13 (38.2)	55 (37.2)
Sepsis	5 (14.7)	14 (9.5)
CVD	4 (11.8)	7 (4.7)
IHD	3 (8.8)	18 (12.2)
Liver disease	2 (5.9)	3 (2.0)
Postoperative complications	1 (2.9)	9 (6.1)
Trauma	1 (2.9)	8 (5.4)
Sudden death	1 (2.9)	4 (2.7)
Renal failure	1 (2.9)	1 (0.7)
Asthma/COPD/emphysema	0 (0)	6 (4.1)
Peripheral vascular disease	0 (0)	2 (1.4)
Pulmonary embolism	0 (0)	1 (0.7)
Arrhythmia	0 (0)	1 (0.7)
Drug related	0 (0)	1 (0.7)
Other	3 (8.8)	18 (18.2)

* Each combined cohort included the corresponding Australian, Canadian, and Spanish cohorts. Values are the number (%) of subjects. SSc = systemic sclerosis; CVD = cerebrovascular disease; IHD = ischemic heart disease; COPD = chronic obstructive pulmonary disease.

Table 5. Multivariable predictors of mortality in the combined inception cohort and combined prevalent cohort*

Variable	Combined inception cohort		Combined prevalent cohort	
	HR (95% CI)	*P*	HR (95% CI)	*P*
Male sex	2.28 (1.42–3.65)	0.001	1.72 (1.27–2.33)	0.001
Age at disease onset, years†	1.05 (1.03–1.07)	0.000	1.05 (1.04–1.06)	<0.0001
Diffuse disease subtype	1.83 (1.14–2.92)	0.002	1.40 (1.07–1.83)	0.013
Disease duration at recruitment, years	0.59 (0.47–0.74)	<0.0001	0.71 (0.68–0.74)	<0.0001
Anticentromere antibody‡	–	–	0.71 (0.53–0.94)	0.019
Anti–Scl-70 antibody‡	–	–	0.95 (0.67–1.35)	0.774
PAH	2.35 (1.29–4.29)	0.006	2.50 (1.83–3.42)	<0.0001
ILD‡	–	–	1.31 (1.01–1.70)	0.040
Myocardial involvement	0.99 (0.44–2.23)	0.977	1.18 (0.83–1.69)	0.363
Renal crisis	1.87 (1.01–3.48)	0.048	1.33 (0.86–2.07)	0.205
IHD and/or CVD	1.54 (0.86–2.76)	0.145	1.28 (0.96–1.72)	0.094
Malignancy‡	–	–	0.97 (0.72–1.30)	0.832

* Each combined cohort included the corresponding Australian, Canadian, and Spanish cohorts. HR = hazard ratio; 95% CI = 95% confidence interval; PAH = pulmonary arterial hypertension; ILD = interstitial lung disease; IHD = ischemic heart disease; CVD = cerebrovascular disease.
† Defined as the date of the first non–Raynaud's phenomenon symptom.
‡ Not included in the multivariable model in the inception cohort because not statistically significant in univariable hazards regression analyses.

Supplementary Tables 5 and 6, http://onlinelibrary.wiley.com/doi/10.1002/art.40027/abstract).

Predictors of mortality. In the combined inception cohort, univariable hazards analyses showed that subjects with male sex, older age at disease onset, diffuse disease subtype, PAH, renal crisis, myocardial involvement, and ischemic heart disease/cerebrovascular disease had a higher risk of death (all $P < 0.05$), while subjects with longer disease duration at recruitment had a lower risk of death ($P = 0.001$). Anticentromere positivity, anti–Scl-70 positivity, ILD, gut involvement, and malignancy were not found to be significant predictors of mortality (see Supplementary Table 7, http://onlinelibrary.wiley.com/doi/10.1002/art.40027/abstract). Multivariable hazards regression analysis showed that male sex, older age at disease onset, diffuse disease subtype, PAH, and renal crisis were independent predictors of risk, and longer disease duration at recruitment was an independent protective factor. PAH conferred the highest risk (hazard ratio [HR] 2.35 [95% CI 1.29–4.29]; $P = 0.006$) (Table 5).

In the combined prevalent cohort, univariable hazards analyses showed that subjects with male sex, older age at disease onset, diffuse disease subtype, anti–Scl-70 positivity, PAH, ILD, myocardial involvement, renal crisis, ischemic heart disease/cerebrovascular disease, and malignancy had a higher risk of death, while subjects with longer disease duration at recruitment and anticentromere positivity had a lower risk of death (see Supplementary Table 7, http://onlinelibrary.wiley.com/doi/10.1002/art.40027/abstract). Finally, multivariable hazards regression analysis showed that male sex, older age at disease onset, diffuse disease subtype, PAH, and ILD were independent predictors of death, and longer disease duration at recruitment and anticentromere positivity were independent protective factors. PAH conferred the highest risk (HR 2.50 [95% CI 1.83–3.42]; $P < 0.0001$) (Table 5).

DISCUSSION

In this largest study to date of mortality and causes of death in an inception cohort of subjects with SSc, we have reported a very high pooled SMR of 4.06 (95% CI 3.39–4.85), up to 22.4 years of life lost in women and up to 26.0 years of life lost in men, and mortality in men of 34.2% and in the diffuse disease subtype of 24.2% at 8 years. When we limited the definition of the inception cohort to those recruited within 1 year of disease onset, the SMRs were even higher, at 8.1 (95% CI 4.3–12.0) for the Australian cohort, 9.4 (95% CI 6.1–12.8) for the Canadian cohort, and 3.9 (95% CI 2.4–5.4) for the Spanish cohort. The values for Australian and Canadian 1-year inception cohorts are much higher than those for the corresponding prevalent cohorts and higher than those reported from some previous studies (12–16), and they highlight the phenomenon of survivor bias, which leads to underestimation of the true burden of mortality in prevalent cohorts of subjects with SSc. This bias arises in large part because SSc has a substantial burden of early mortality with many deaths occurring within 5 years of disease onset, particularly in men and in the diffuse disease subtype. The protective effect against mortality of longer disease duration at recruitment that we found in our multivariable hazards regression analyses

further highlights the burden of mortality in the early stage of disease.

In our study, the pooled SMR for the prevalent cohort (3.39) is similar to that reported from a meta-analysis of 9 prevalent cohort studies from the 1960s to the 2000s (3.53) (17). Therefore, although the proportion of deaths attributable to each cause may have changed over time, SSc still carries a large burden of mortality. Although there are several small mortality studies in incident SSc showing 5-year survival ranging from 68% to 88% (18–22), the major strength of the present study is the large sample size achieved by pooling 3 cohorts, which enabled us to compare the mortality of a combined inception cohort with that of a combined prevalent cohort.

As hypothesized, our results showed that the age- and sex-adjusted SMRs of Australian and Canadian inception cohorts were higher than those of the respective prevalent cohorts. In Spanish subjects, the age- and sex-adjusted SMR of the prevalent cohort was higher than that of the inception cohort, but this may have been due to the overall short duration of disease at recruitment in both of the Spanish cohorts as well as the difference in the age structure of the Spanish cohort compared with the Australian and Canadian cohorts as demonstrated by crude SMRs (see Supplementary Table 3, http://onlinelibrary.wiley.com/doi/10.1002/art.40027/abstract).

The SMRs for men were higher than for women in each of the cohorts. The difference in mortality for men in inception cohorts versus prevalent cohorts was more substantial than that for women, which suggests faster disease progression and more deaths in the early stages of disease in men. The hazards regression analysis also revealed that male sex was a strong independent predictor of death in the combined inception cohort. Our univariable comparisons showed more diffuse disease, myocardial involvement, renal crisis, digital ulcers, and ischemic heart disease in men than in women (see Supplementary Table 8, http://onlinelibrary.wiley.com/doi/10.1002/art.40027/abstract), and most of these factors were associated with risk of death according to our univariable hazards regression analyses. A recent published model by Domsic et al also showed that male sex was an independent predictor of mortality in incident disease in patients with the diffuse subtype of SSc (23). Therefore, for male patients, especially those with diffuse disease, close monitoring and active treatment are important (24,25).

Organ involvement is another important factor associated with prognosis. In our combined inception cohort, SSc-related causes of death accounted for 62.1% of all deaths, which was higher than that in the combined prevalent cohort (55.5%) and published EUSTAR data (55%) (6). Although the proportion of SSc-related deaths has been reported to be decreasing from 1972 to 2002 (26), our results suggest that SSc-related causes remain the major contributors to early mortality in this disease.

PAH was the leading SSc-related cause of death, accounting for 34.5% of deaths in the combined inception cohort (25.3% from PAH only and 9.2% from the combination of PAH and ILD). Although advanced PAH therapies have been used more widely in recent years, and the survival of subjects with SSc-associated PAH has improved compared with historical control data, the mortality of subjects with PAH is still high (27,28). In our analyses, the survival of subjects with PAH at 1, 3, 5, and 8 years was 100%, 88.0%, 71.0%, and 53.1%, respectively, in the combined inception cohort, which was significantly lower than that of subjects without PAH (98.0%, 95.0%, 90.5%, and 83.1%, respectively) (see Supplementary Figure 5, http://onlinelibrary.wiley.com/doi/10.1002/art.40027/abstract). In addition to being the leading cause of death, PAH was also identified as the strongest independent risk factor for mortality in both our combined inception cohort and combined prevalent cohort, as some other models showed (14,28). These results confirm that PAH is still the SSc-related complication with the greatest impact on survival.

ILD accounted for a higher proportion of deaths in the combined prevalent cohort than in the combined inception cohort (34.8% versus 29.9% for principal cause of death, and 14.1% versus 11.4% for contributing cause of death, when deaths due to ILD and PAH together with ILD were included). Hazards regression analyses showed that ILD was an independent risk factor for mortality in the combined prevalent cohort but not in the combined inception cohort. Collectively, these results point to ILD as a risk factor for poor long-term survival rather than early death.

In our combined inception cohort, 24.3% of deaths were non–SSc related. A higher proportion of deaths were non–SSc related in the combined prevalent cohort (33.6%), which reminds us that these long-term complications become particularly important later in the disease course. Ischemic heart disease and cerebrovascular disease were major causes of non–SSc-related deaths both in the inception cohort and in the prevalent cohort. A study from the ASCS showed that after adjusting for age, sex, and traditional risk factors for atherosclerosis, SSc patients were 3.2 times more likely to have coronary heart disease than were general population controls (29), which suggests that the high prevalence of ischemic heart disease may be partly related to SSc itself rather than just to traditional atherosclerosis risk factors. Furthermore, a study by Dave et al has shown that SSc patients with ischemic heart disease have higher in-hospital mortality than do controls, systemic lupus erythematosus patients with ischemic heart

disease, and rheumatoid arthritis patients with ischemic heart disease (30). Although not all studies have shown a similarly increased frequency of ischemic heart disease and in-hospital mortality, there is need for better understanding, prevention, and management of atherosclerosis in SSc patients, especially those with longer disease duration.

Malignancy was one of the most common non–SSc-related causes of death both in the combined inception cohort and in the combined prevalent cohort. While a close temporal association has been reported between the onset of SSc and diagnosis of malignancy in patients with anti–RNAP III (31), further studies are needed to determine whether there is an increased risk of malignancy in SSc overall, and, if so, whether this is attributable to the disease itself, to immunosuppressive therapy, or to other factors.

Sepsis was also one of the major non–SSc-related causes of death, which is consistent with mortality data from the EUSTAR registry and several other studies (6,9,24). Sepsis accounted for a higher proportion of deaths in the combined inception cohort (14.7%) than in the combined prevalent cohort (9.5%), possibly due to more use of immunosuppressive therapy early in the disease course, when there is greater inflammatory disease activity.

The present study has some limitations. It is possible that some subjects who died within 1 year of recruitment and whose death was not known to the treating doctors were incorrectly classified as "alive" because the criterion we used for tracing was "lost to follow-up for ≥2 years." Despite considerable efforts to determine the cause of death in all subjects, we were unable to confirm this in 10.9% of the deceased in the whole combined prevalent cohort. Furthermore, while most data regarding cause of death were collected prospectively in each cohort, in order to standardize results, our death case report form was completed retrospectively (although verified against source documents) for all subjects who had died.

Another limitation is that we have refrained from including treatment in our analyses due to the potential bias in observational studies evaluating treatment effects and due to the lack of accurate data on the indication for, and duration of, treatment. Also, anti–RNAP III positivity was not included in the hazards regression model as this variable was not available for all subjects. A large-scale prospective inception cohort study will more accurately quantify early mortality and evaluate the impact of treatment on mortality in SSc, through collection of all relevant data. Among its other goals, the International Systemic Sclerosis Inception Cohort study, initiated in 2012, aims to quantify early mortality in SSc and the potential effect of treatment.

In conclusion, mortality is substantial in Australian, Canadian, and Spanish SSc subjects. Cardiopulmonary disease is still the most common cause of SSc-related death. Malignancy, sepsis, and atherosclerotic disease are the most common non–SSc-related causes. Our results suggest that prevalent cohorts underestimate mortality in SSc by failing to capture early deaths, particularly in men and those with diffuse disease. Collectively, these findings provide a compelling rationale for establishing a large prospective multinational inception cohort of patients with SSc to more accurately quantify early mortality in this disease.

AUTHOR CONTRIBUTIONS

All authors were involved in drafting the article or revising it critically for important intellectual content, and all authors approved the final version to be published. Dr. Nikpour had full access to all of the data in the study and takes responsibility for the integrity of the data and the accuracy of the data analysis.

Study conception and design. Hao, Hudson, Baron, Carreira, Stevens, Proudman, Nikpour.

Acquisition of data. Hao, Hudson, Baron, Carreira, Stevens, Rabusa, Tatibouet, Carmona, Joven, Huq, Proudman, Nikpour.

Analysis and interpretation of data. Hao, Rabusa, Tatibouet, Carmona, Joven, Huq, Nikpour.

ROLE OF THE STUDY SPONSORS

Actelion Australia, Bayer, CSL Biotherapies, GlaxoSmithKline Australia, and Pfizer had no role in the study design or in the collection, analysis, or interpretation of the data, the writing of the manuscript, or the decision to submit the manuscript for publication. Publication of this article was not contingent upon approval by Actelion Australia, Bayer, CSL Biotherapies, GlaxoSmithKline Australia, and Pfizer.

REFERENCES

1. Denton CP. Systemic sclerosis: from pathogenesis to targeted therapy. Clin Exp Rheumatol 2015;33 Suppl 92:S3–7.
2. Stern EP, Denton CP. The pathogenesis of systemic sclerosis. Rheum Dis Clin North Am 2015;41:367–82.
3. Gu YS, Kong J, Cheema GS, Keen CL, Wick G, Gershwin ME. The immunobiology of systemic sclerosis. Semin Arthritis Rheum 2008;38:132–60.
4. Asano Y, Sato S. Vasculopathy in scleroderma. Semin Immunopathol 2015;37:489–500.
5. Bennett R, Bluestone R, Holt PJ, Bywaters EG. Survival in scleroderma. Ann Rheum Dis 1971;30:581–8.
6. Tyndall AJ, Bannert B, Vonk M, Airò P, Cozzi F, Carreira PE, et al. Causes and risk factors for death in systemic sclerosis: a study from the EULAR Scleroderma Trials and Research (EUSTAR) database. Ann Rheum Dis 2010;69:1809–15.
7. Subcommittee for Scleroderma Criteria of the American Rheumatism Association Diagnostic and Therapeutic Criteria Committee. Preliminary criteria for the classification of systemic sclerosis (scleroderma). Arthritis Rheum 1980;23:581–90.
8. Andersen PK, Borgan O, Gill RD, Keiding N. Statistical models based on counting processes. New York: Springer-Verlag; 1993. p. 322.
9. Mok CC, Kwok CL, Ho LY, Chan PT, Yip SF. Life expectancy, standardized mortality ratios, and causes of death in six rheumatic diseases in Hong Kong, China. Arthritis Rheum 2011;63:1182–9.

10. Chiang CL. The life table and its construction. In: Introduction to stochastic processes in biostatistics. New York: John Wiley & Sons; 1968. p. 189–214.
11. Newell C. Methods and models in demography. Chichester (UK): John Wiley & Sons; 1994. p. 63–81.
12. Sampaio-Barros PD, Bortoluzzo AB, Marangoni RG, Rocha LF, del Rio AP, Samara AM, et al. Survival, causes of death, and prognostic factors in systemic sclerosis: analysis of 947 Brazilian patients. J Rheumatol 2012;39:1971–8.
13. Nihtyanova SI, Schreiber BE, Ong VH, Rosenberg D, Moinzadeh P, Coghlan JG, et al. Prediction of pulmonary complications and long-term survival in systemic sclerosis. Arthritis Rheumatol 2014;66:1625–35.
14. Joven BE, Almodovar R, Carmona L, Carreira PE. Survival, causes of death, and risk factors associated with mortality in Spanish systemic sclerosis patients: results from a single university hospital. Semin Arthritis Rheum 2010;39:285–93.
15. Hoffmann-Vold AM, Molberg Ø, Midtvedt Ø, Garen T, Gran JT. Survival and causes of death in an unselected and complete cohort of Norwegian patients with systemic sclerosis. J Rheumatol 2013;40:1127–33.
16. Vettori S, Cuomo G, Abignano G, Iudici M, Valentini G. Survival and death causes in 251 systemic sclerosis patients from a single Italian center. Reumatismo 2010;62:202–9. In Italian.
17. Elhai M, Meune C, Avouac J, Kahan A, Allanore Y. Trends in mortality in patients with systemic sclerosis over 40 years: a systematic review and meta-analysis of cohort studies. Rheumatology (Oxford) 2012;51:1017–26.
18. Jacobsen S, Halberg P, Ullman S. Mortality and causes of death of 344 Danish patients with systemic sclerosis (scleroderma). Br J Rheumatol 1998;37:750–5.
19. Bulpitt KJ, Clements PJ, Lachenbruch PA, Paulus HE, Peter JB, Agopian MS, et al. Early undifferentiated connective tissue disease. Part III. Outcome and prognostic indicators in early scleroderma (systemic sclerosis). Ann Intern Med 1993;118:602–9.
20. Jacobsen S, Ullman S, Shen GQ, Wiik A, Halberg P. Influence of clinical features, serum antinuclear antibodies, and lung function on survival of patients with systemic sclerosis. J Rheumatol 2001;28:2454–9.
21. Bryan C, Knight C, Black CM, Silman AJ. Prediction of five-year survival following presentation with scleroderma: development of a simple model using three disease factors at first visit. Arthritis Rheum 1999;42:2660–5.
22. Bryan C, Howard Y, Brennan P, Black C, Silman A. Survival following the onset of scleroderma: results from a retrospective inception cohort study of the UK patient population. Br J Rheumatol 1996;35:1122–6.
23. Domsic RT, Nihtyanova SI, Wisniewski SR, Fine MJ, Lucas M, Kwoh CK, et al. Derivation and external validation of a prediction rule for five-year mortality in patients with early diffuse cutaneous systemic sclerosis. Arthritis Rheumatol 2016;68:993–1003.
24. Strickland G, Pauling J, Cavill C, Shaddick G, McHugh N. Mortality in systemic sclerosis: a single centre study from the UK. Clin Rheumatol 2013;32:1533–9.
25. Fransen J, Popa-Diaconu D, Hesselstrand R, Carreira P, Valentini G, Beretta L, et al. Clinical prediction of 5-year survival in systemic sclerosis: validation of a simple prognostic model in EUSTAR centres. Ann Rheum Dis 2011;70:1788–92.
26. Steen VD, Medsger TA. Changes in causes of death in systemic sclerosis, 1972–2002. Ann Rheum Dis 2007;66:940–4.
27. Williams MH, Das C, Handler CE, Akram MR, Davar J, Denton CP, et al. Systemic sclerosis associated pulmonary hypertension: improved survival in the current era. Heart 2006;92:926–32.
28. Lefevre G, Dauchet L, Hachulla E, Montani D, Sobanski V, Lambert M, et al. Survival and prognostic factors in systemic sclerosis–associated pulmonary hypertension: a systematic review and meta-analysis. Arthritis Rheum 2013;65:2412–23.
29. Ngian GS, Sahhar J, Proudman SM, Stevens W, Wicks IP, van Doornum S. Prevalence of coronary heart disease and cardiovascular risk factors in a national cross-sectional cohort study of systemic sclerosis. Ann Rheum Dis 2012;71:1980–3.
30. Dave AJ, Fiorentino D, Lingala B, Krishnan E, Chung L. Atherosclerotic cardiovascular disease in hospitalized patients with systemic sclerosis: higher mortality than patients with lupus and rheumatoid arthritis. Arthritis Care Res (Hoboken) 2014;66:323–7.
31. Nikpour M, Hissaria P, Byron J, Sahhar J, Micallef M, Paspaliaris W, et al. Prevalence, correlates and clinical usefulness of antibodies to RNA polymerase III in systemic sclerosis: a cross-sectional analysis of data from an Australian cohort. Arthritis Res Ther 2011;13:R211.

APPENDIX A: CANADIAN SCLERODERMA RESEARCH GROUP AND AUSTRALIAN SCLERODERMA INTEREST GROUP INVESTIGATORS

Canadian Scleroderma Research Group investigators are as follows (in Canada except where indicated otherwise): M. Abu-Hakima (Calgary, Alberta), M. Baron (Montreal, Quebec), A. R. Cabral (Mexico City, Mexico), P. Docherty (Moncton, New Brunswick), P. R. Fortin (Quebec, Quebec), M. Fritzler (Calgary, Alberta), T. Grodzicky (Montreal, Quebec), G. Gyger (Montreal, Quebec), M. Hudson (Montreal, Quebec), N. Jones (Edmonton, Alberta), E. Kaminska (Calgary, Alberta), N. Khalidi (Hamilton, Ontario), M. Larché (Hamilton, Ontario), S. LeClercq (Calgary, Alberta), S. Ligier (Montreal, Quebec), J. Markland (deceased) (Saskatoon, Saskatchewan), A. Masetto (Sherbrooke, Quebec), J.-P. Mathieu (Montreal, Quebec), J. Pope (London, Ontario), D. Robinson (Winnipeg, Manitoba), T. S. Rodriguez-Reyna (Mexico City, Mexico), D. Smith (Ottawa, Ontario), E. Sutton (Halifax, Nova Scotia), C. Thorne (Newmarket, Ontario).

Australian Scleroderma Interest Group investigators are as follows (all in Australia): M. Nikpour (Melbourne, Victoria), S. Proudman (Adelaide, South Australia), J. Roddy (Perth, Western Australia), J. Sahhar (Melbourne, Victoria), W. Stevens (Melbourne, Victoria), J. Walker (Adelaide, South Australia), P. Youssef (Sydney, New South Wales), J. Zochling (Hobart, Tasmania).

ARTHRITIS & RHEUMATOLOGY
Vol. 69, No. 5, May 2017, pp 1078–1089
DOI 10.1002/art.40016

Scleroderma Peripheral B Lymphocytes Secrete Interleukin-6 and Transforming Growth Factor β and Activate Fibroblasts

Nicolas Dumoitier,[1] Benjamin Chaigne,[2] Alexis Régent,[2] Sébastien Lofek,[3] Maissa Mhibik,[4] Peter Dorfmüller,[5] Benjamin Terrier,[2] Jonathan London,[6] Alice Bérezné,[7] Nicolas Tamas,[3] Nadine Varin-Blank,[8] and Luc Mouthon[9]

Objective. **To study the role of B lymphocytes in systemic sclerosis (SSc).**

Methods. **Peripheral B cell subpopulations and the production of interleukin-6 (IL-6) and transforming growth factor β (TGFβ) were analyzed using flow cytometry and multiplex assay. The fibroblast proliferation rate upon incubation with supernatants from B cells isolated from SSc patients or healthy controls was assessed using XTT, bromodeoxyuridine, and Ki-67. Collagen production was assessed using a collagen assay.**

Results. **Ninety untreated patients (12 males) fulfilling the American College of Rheumatology/European League Against Rheumatism criteria for SSc (23 with diffuse cutaneous SSc [dcSSc] and 67 with limited cutaneous SSc [lcSSc]) and 30 healthy controls were recruited. Increased proportions of B cells expressing CD69 and CD95 were identified among the patients with SSc. B lymphocytes from dcSSc patients versus lcSSc patients and healthy controls expressed increased proportion of cells positive for CD5 (mean ± SD 24.12 ± 7.93% versus 14.09 ± 6.58% [$P = 0.03$] and 14.21 ± 5.34% [$P = 0.01$]), CD86 (39.89 ± 22.11% versus 17.72 ± 13.98% [$P = 0.0007$] and 11.68 ± 11.09% [$P < 0.001$]), IL-6 receptor (IL-6R; 33.64 ± 23.12% versus 17.91 ± 13.62% [$P < 0.0001$] and 12.08 ± 8.68% [$P = 0.0009$]), or IL-21R (32.55 ± 20.19% versus 5.76 ± 4.40% [$P < 0.0001$] and 5.93 ± 3.29% [$P < 0.0001$]). In addition, the levels of IL-6 (mean ± SD 314.3 ± 317.8 pg/ml versus 6.10 ± 2.58 pg/ml; $P = 0.0007$) and TGFβ (mean ± SD 1,020 ± 569 pg/ml versus 163.8 ± 98.69 pg/ml; $P = 0.001$) secreted by B lymphocytes from patients with SSc were increased compared to healthy controls. Fibroblast proliferation and collagen production were also significantly increased in the presence of B cell supernatant from SSc patients as compared to healthy controls.**

Conclusion. **The numbers of activated B cells were increased in SSc patients, and the up-regulation of CD5, CD86, IL-6R, and IL-21R discriminated between**

Mr. Dumoitier's work was supported by the Centre of Excellence, LabEx Inflamex, Université Paris-Diderot, Paris, France (ANR-11-IDEX-0005-02).

[1]Nicolas Dumoitier, MSc: INSERM U1016, Institut Cochin, CNRS UMR 8104, Université Paris Descartes, Sorbonne Paris Cité, LabEx Inflamex, Université Sorbonne Paris Cité and Université Paris Diderot, Paris, France; [2]Benjamin Chaigne, MD, Alexis Régent, MD, PhD, Benjamin Terrier, MD, PhD: INSERM U1016, Institut Cochin, CNRS UMR 8104, Université Paris Descartes, Sorbonne Paris Cité and Service de Médecine Interne, Centre de Référence Maladies Systémiques Autoimmunes Rares, Vascularites Nécrosantes et Sclérodermie Systémique, Hôpital Cochin, AP-HP, Paris, France; [3]Sébastien Lofek, MSc, Nicolas Tamas: INSERM U1016, Institut Cochin, CNRS UMR 8104 and Université Paris Descartes, Sorbonne Paris Cité, Paris, France; [4]Maissa Mhibik, MSc: Université Paris XIII, UFR Santé Médecine Biologie Humaine and INSERM U978, Bobigny, France; [5]Peter Dorfmüller, MD, PhD: Service d'Anatomie Pathologique, Hôpital Marie Lannelongue, INSERM UMR-S 999, LabEx LERMIT, Le Plessis-Robinson, France; [6]Jonathan London, MD: Université Paris Descartes, Sorbonne Paris Cité and Service de Médecine Interne, Centre de Référence Maladies Systémiques Autoimmunes Rares, Vascularites Nécrosantes et Sclérodermie Systémique, Hôpital Cochin, AP-HP, Paris, France; [7]Alice Bérezné, MD: Service de Médecine Interne, Centre de Référence Maladies Systémiques Autoimmunes Rares, Vascularites Nécrosantes et Sclérodermie Systémique, Hôpital Cochin, AP-HP, Paris, France; [8]Nadine Varin-Blank, PhD: LabEx Inflamex, Université Sorbonne Paris Cité, Paris, and Université Paris XIII, UFR Santé Médecine Biologie Humaine and INSERM U978, Bobigny, France; [9]Luc Mouthon, MD, PhD: INSERM U1016, Institut Cochin, CNRS UMR 8104, Université Paris Descartes, Sorbonne Paris Cité, LabEx Inflamex, Université Sorbonne Paris Cité and Service de Médecine Interne, Centre de Référence Maladies Systémiques Autoimmunes Rares, Vascularites Nécrosantes et Sclérodermie Systémique, Hôpital Cochin, AP-HP, Paris, France.

Drs. Chaigne and Régent contributed equally to this work.

Dr. Terrier has received consulting fees and honoraria from Roche (less than $10,000). Dr. Mouthon has received consulting fees (less than $10,000) and grants from Roche.

Address correspondence to Luc Mouthon, MD, PhD, INSERM U1016, CNRS UMR 8104, 8 Rue Mechain, 75014 Paris, France (e-mail: luc.mouthon@aphp.fr); or to Nadine Varin-Blank, PhD, UFR SMBH, INSERM U978, 74 Rue Marcel Cachin, 93000 Bobigny, France (e-mail: nadine.varin@inserm.fr).

Submitted for publication January 18, 2016; accepted in revised form November 29, 2016.

patients with dcSSc and those with lcSSc. Peripheral B lymphocytes from SSc patients secreted both IL-6 and TGFβ, and they activated fibroblasts in vitro.

Systemic sclerosis (SSc) is a connective tissue disease characterized by fibroblast activation, increased extracellular matrix synthesis, and vascular remodeling (1). Activation of fibroblasts and endothelial cells, together with increased oxidative stress, represent the hallmarks of SSc pathogenesis. SSc is classified according to the extent of skin involvement as either limited cutaneous SSc (lcSSc), with skin lesions essentially limited to the hands and face, or diffuse cutaneous SSc (dcSSc), with skin lesions occurring proximal to the elbows and knees and with frequent visceral involvement. Although autoantibodies have been detected in the serum of patients with SSc and are helpful in the diagnosis and evaluation of the prognosis, the role of B lymphocytes in the pathogenesis of SSc is still poorly defined (2,3).

Circulating B lymphocytes from SSc patients differ from those from healthy controls by the presence of increased proportions of naive B cells and decreased numbers of memory B cells and plasma cells (4). In addition, signaling alterations, including overexpression of both CD19 and CD21, two activating coreceptors of the B cell antigen receptor, have been detected both in the TSK-1 mouse model of SSc and in naive and memory B lymphocytes from patients with SSc. Moreover, the activation receptors CD80, CD86, and CD95 are up-regulated in memory B cells from SSc patients, suggesting their participation in the pathogenic process (4).

High levels of BAFF have been measured in the serum of SSc patients, as well as overexpression of BAFF receptor at the surface of peripheral B cells from the same patients (5). BAFF acting through the NF-κB pathway promotes B cell survival and participates in autoreactive B cell differentiation (6). B cell infiltrates have also been detected in the dermis of SSc patients (7,8), and serum levels of interleukin-6 (IL-6) have been shown to be increased and to correlate with the extent of skin fibrosis both in humans with SSc and in the TSK-1 mouse model (9,10). IL-6 stimulates collagen secretion by fibroblasts and might therefore be an intermediate for fibroblast activation (11).

Recent studies in which a chimeric anti-CD20 monoclonal antibody was used to deplete B cells, showed that this treatment allowed for the improvement of skin fibrosis and prevented the loss of pulmonary function in patients with SSc (12). In a prospective randomized trial in which the IL-6 receptor (IL-6R) was targeted with tocilizumab, there was a promising effect of this treatment on skin involvement (13,14).

In the present study, we found abnormal phenotype patterns of peripheral B lymphocytes in patients with SSc, notably between those with lcSSc and those with dcSSc. We also identified increased cytokine production leading to fibroblast activation.

PATIENTS AND METHODS

Patients. Peripheral blood was obtained from 90 patients with SSc who fulfilled the American College of Rheumatism (ACR)/European League Against Rheumatism (EULAR) criteria for the diagnosis of SSc (15) and whose cases were followed at Cochin Hospital in the Department of Internal Medicine. The clinical characteristics of the study patients are available upon request from the corresponding author. Skin thickening in areas solely distal to the elbows and knees, with or without facial involvement, was defined as lcSSc. Skin thickening proximal as well as distal to the elbows and knees, with or without facial or truncal involvement, was defined as dcSSc (16). Patients evaluated during the first 12 months after the first non–Raynaud's phenomenon symptom of SSc were defined as having early SSc. Peripheral blood was obtained from 30 healthy blood donors (controls) whose samples were included at the Etablissement Français du Sang (St. Antoine Hospital, Paris, France).

All patients and healthy controls gave written informed consent. Sera and peripheral blood mononuclear cells were collected with the approval of the ethics committee of the Groupe Hospitalier Pitié-Salpêtrière. The study conforms to the principles outlined in the Declaration of Helsinki. The work was performed within the Département Hospitalo-Universitaire, Autoimmune and Hormonal Diseases.

Fibroblast culture and functional studies. Biopsies of involved skin of 4 patients with SSc were performed. Normal human dermal fibroblasts were cultured from skin biopsy samples obtained from 4 healthy controls. Biopsy specimens were cut into small pieces and seeded into petri dishes and then into 175-cm^2 plastic flasks. Patients and healthy control fibroblasts were grown at 37°C in Dulbecco's modified Eagle's medium (DMEM; Gibco) with 10% heat-inactivated fetal calf serum (FCS; Eurobio) in an atmosphere containing in 5% CO_2.

At the third passage, fibroblasts from healthy controls or SSc patients were plated in 96-well plates at a concentration of 5×10^4 cells/ml. After 24 hours, fibroblasts were synchronized by replacing the FCS-supplemented DMEM with DMEM without FCS. After 24 hours of synchronization, media were replaced with FCS-supplemented DMEM with or without 8 representative supernatants of B lymphocytes obtained from 4 healthy controls or 4 patients with dcSSc (performed in triplicate). After 3 days of culture, the viability of fibroblasts was measured using a Colorimetric Cell Viability Kit III (XTT) from (PromoKine), proliferation was quantified using a bromodeoxyuridine cell proliferation enzyme-linked immunosorbent assay (Roche), and indirect immunofluorescence of Ki-67 was evaluated using anti–Ki-67 antibody (Abcam) and fluorescein isothiocyanate–coupled anti-rabbit secondary antibody (Jackson ImmunoResearch). Collagen content was quantified after 5 days of culture using a Sircol assay kit (Biocolor) according to the manufacturer's protocol.

Real-time polymerase chain reaction (PCR) was performed using 2.5×10^4 fibroblasts cultured in a 24-well plate at the same concentration as described above. RNA was extracted

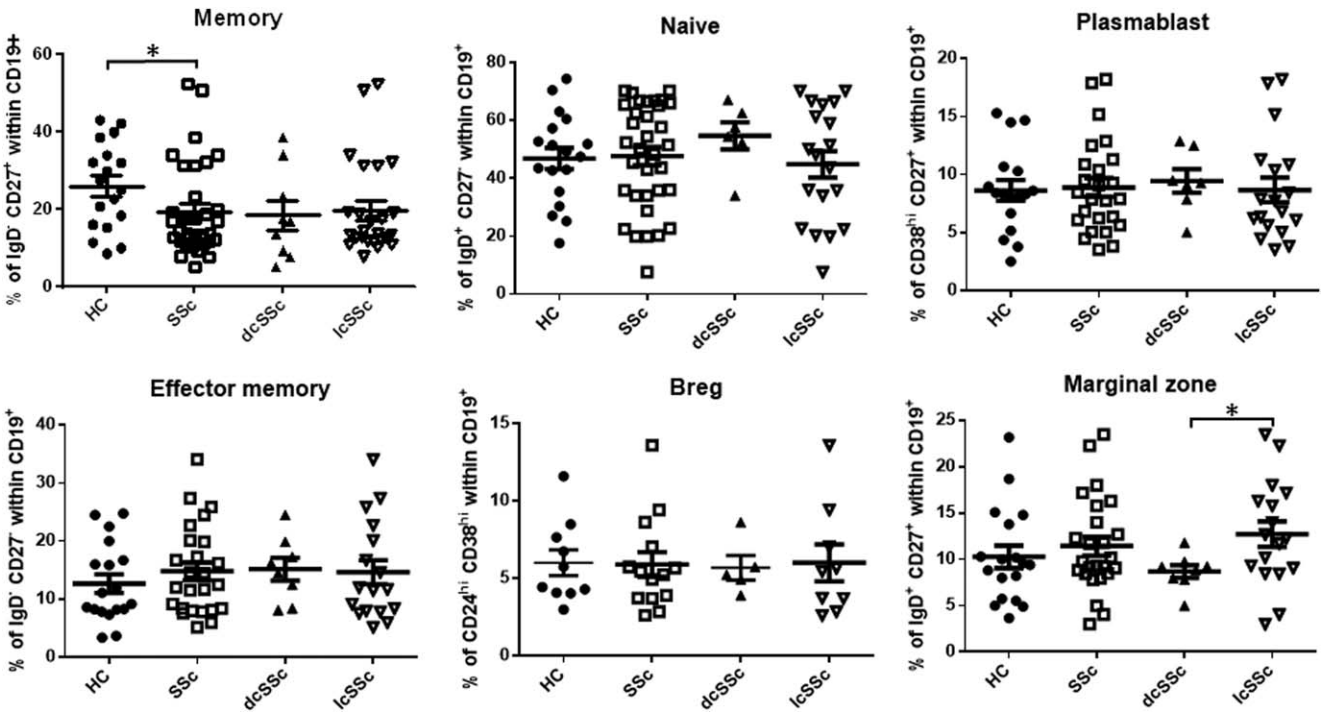

Figure 1. Maturation status of B lymphocyte populations derived from healthy controls (HC) and patients with systemic sclerosis (SSc). B lymphocyte subsets were analyzed in 21 healthy controls (HC) and 34 patients with SSc, including 9 with diffuse cutaneous (dcSSc) and 25 with limited cutaneous (lcSSc) disease. The percentages of the following B lymphocyte subpopulations were quantified: memory/plasmablasts (IgD–CD19+CD27+ cells), naive B lymphocytes (IgD+CD19+CD27– cells), plasmablasts (CD19+CD38^{high}CD27++ cells), effector memory B cells (IgD–CD19+CD27– cells), Breg cells (CD19+CD24^{high}CD38^{high} cells), and marginal-zone B cells (IgD+CD19+CD27+ cells). Each symbol represents an individual subject; horizontal lines with bars show the mean ± SD. * = $P < 0.05$, by Mann-Whitney U test.

using an RNeasy Mini kit (Qiagen) according to the manufacturer's protocol and then quantified using NanoVue (GE Healthcare Life Science). Four hundred nanograms of total RNA was retrotranscripted in complementary DNA (cDNA) using an iScript cDNA synthesis kit (Bio-Rad) and following the manufacturer's protocol. Expression of mRNA for α-smooth muscle actin (α-SMA), type I collagen, Snail, and vimentin was quantified in comparison to β_2-microglobulin as the housekeeping gene. Real-time PCR was performed using a Power SYBR Green quantitative PCR (qPCR) kit on a StepOnePlus Real-Time PCR system (Applied Biosystems). Primers were obtained from Eurogentec (list of primers available upon request from the corresponding author).

Immunohistochemical study. Immunohistochemistry was performed on paraffin-embedded lung samples: 4-μm sections were dewaxed and rehydrated progressively. EDTA buffer (pH 9.0) or citrate buffer (pH 6.0) was used for antigen retrieval; endogenous peroxidase was quenched with hydrogen peroxide. Sections were blocked with 5% bovine serum albumin and incubated for 32 minutes with polyclonal antibody against CD20 (reference BSB5195; Bio SB) or CD69 (reference ab202909; Abcam), as recommended by the manufacturer. After incubation with a biotinylated secondary antibody, detection was performed with horseradish peroxidase–streptavidin and diaminobenzidine solution.

Statistical analysis. All analyses were carried out using GraphPad Prism 6 software, with 4 levels of statistical significance: $P < 0.05$, $P < 0.01$, $P < 0.001$, and $P < 0.0001$. Nonparametric tests, including the Mann-Whitney U test, were used for 2-group independent comparisons. Correlations of protein expression were performed using Spearman's correlation coefficient. Comparisons between fibroblast responses to B lymphocyte stimulation were analyzed using paired *t*-tests.

RESULTS

Differential peripheral B lymphocyte maturation in patients with SSc. The overall number of B cells and T cells was similar between healthy controls and SSc patients, despite a larger dispersal of T cells, which was mainly observed in patients with lcSSc (data available upon request from the corresponding author). Similarly, B lymphocyte subpopulation counts, including naive cells, effector memory cells, Breg cells, and plasmablasts, were equivalent among the healthy control, total SSc, dcSSc, and lcSSc patient groups (Figure 1). In contrast, the proportion of IgD–CD27+ memory B lymphocytes was significantly decreased in patients with SSc as compared to healthy controls ($P = 0.04$) (Figure 1), with a similar distribution between SSc subsets. An additional differential proportion of marginal zone B cells was found between

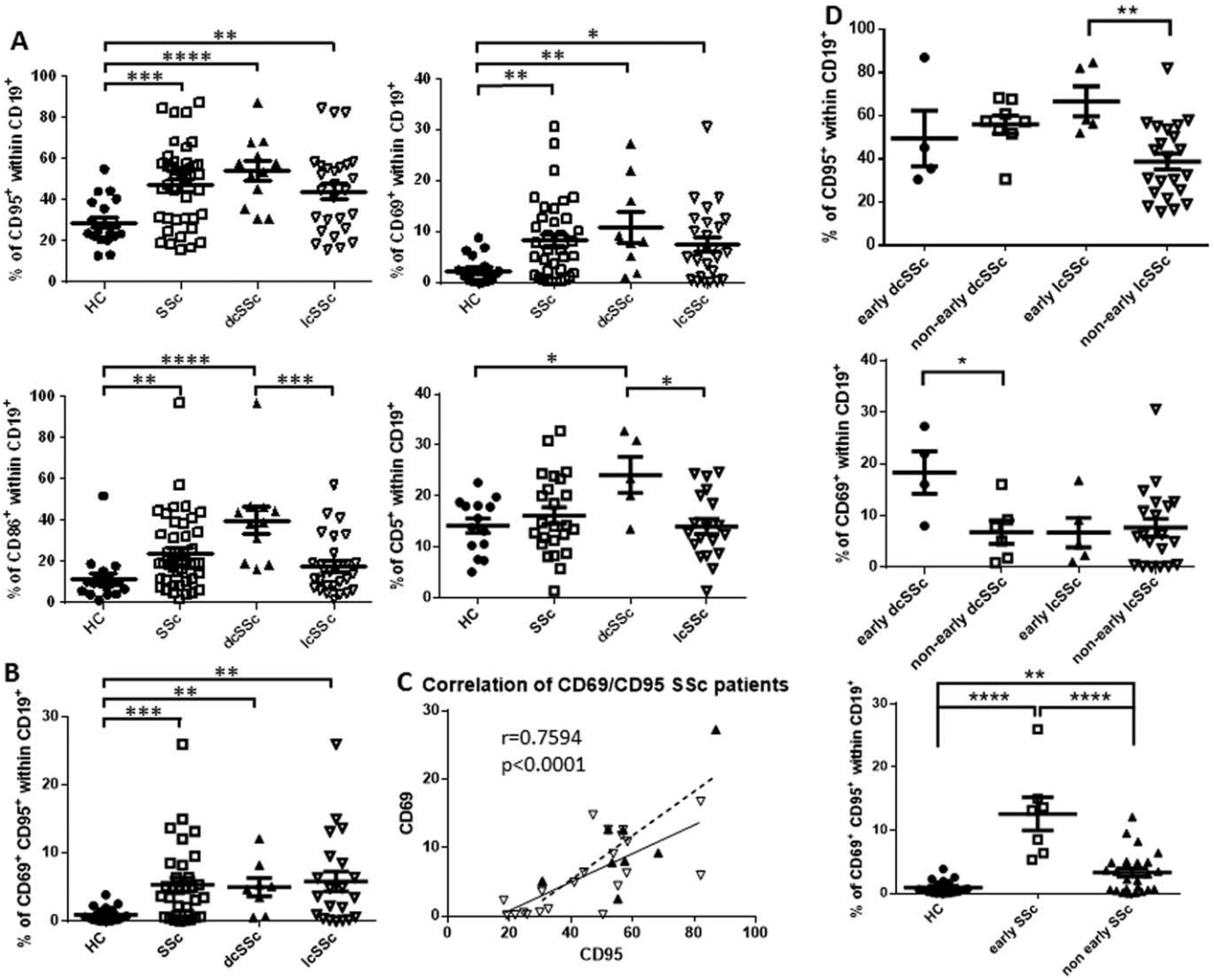

Figure 2. Activation markers of peripheral B lymphocytes from healthy controls (HC) and patients with systemic sclerosis (SSc). B lymphocyte activation markers were analyzed in 21 healthy controls and 43 patients with SSc, 11 with diffuse cutaneous (dcSSc) and 32 with limited cutaneous (lcSSc) disease. **A,** Percentages of CD95+, CD69+, CD86+, and CD5+ cells in total CD19+ B lymphocytes. **B,** Percentages of CD69+CD95+ double-positive cells in total CD19+ B lymphocytes. **C,** Correlation between CD69 and CD95 expression on peripheral CD19+ B lymphocytes from patients with dcSSc (broken line) and patients with lcSSc (solid line), as determined by Spearman's correlation coefficient. **D,** Percentages of CD95+ and CD69+ B cells in patients with early-onset SSc (<1 year after the first non–Raynaud's phenomenon symptom of SSc) versus those without early-onset SSc, by SSc subtype (CD95+ and CD69+ cells), as well as percentages of CD69+CD95+ double-positive B cells in patients with or without early SSc versus healthy controls. Each symbol represents an individual subject; horizontal lines with bars show the mean ± SD. * = $P < 0.05$; ** = $P < 0.01$; *** = $P < 0.001$; **** = $P < 0.0001$, by Mann-Whitney U test.

the dcSSc and lcSSc subgroups, but not between the total SSc group versus healthy controls. Specific analysis of mature B (Bm) cells showed the IgD–CD38+ early Bm5 subpopulation as a predominantly decreased memory B cell subset, irrespective of SSc subset origin ($P = 0.001$) (data available upon request from the corresponding author).

Activated peripheral B lymphocytes from SSc patients. Patients with SSc exhibited increased proportions of B lymphocytes expressing activation markers CD95 ($P = 0.0004$), CD69 ($P = 0.002$), and CD86 ($P = 0.001$) as compared to healthy controls (Figure 2A). Similar results were obtained when the mean fluorescence intensity was quantified (data available upon request from the corresponding author). We also identified a B cell subpopulation expressing both CD69 and CD95 in SSc patients that was absent in healthy controls ($P = 0.0002$) (Figure 2B). Interestingly, subpopulations expressing CD69 were correlated with those expressing CD95 in SSc

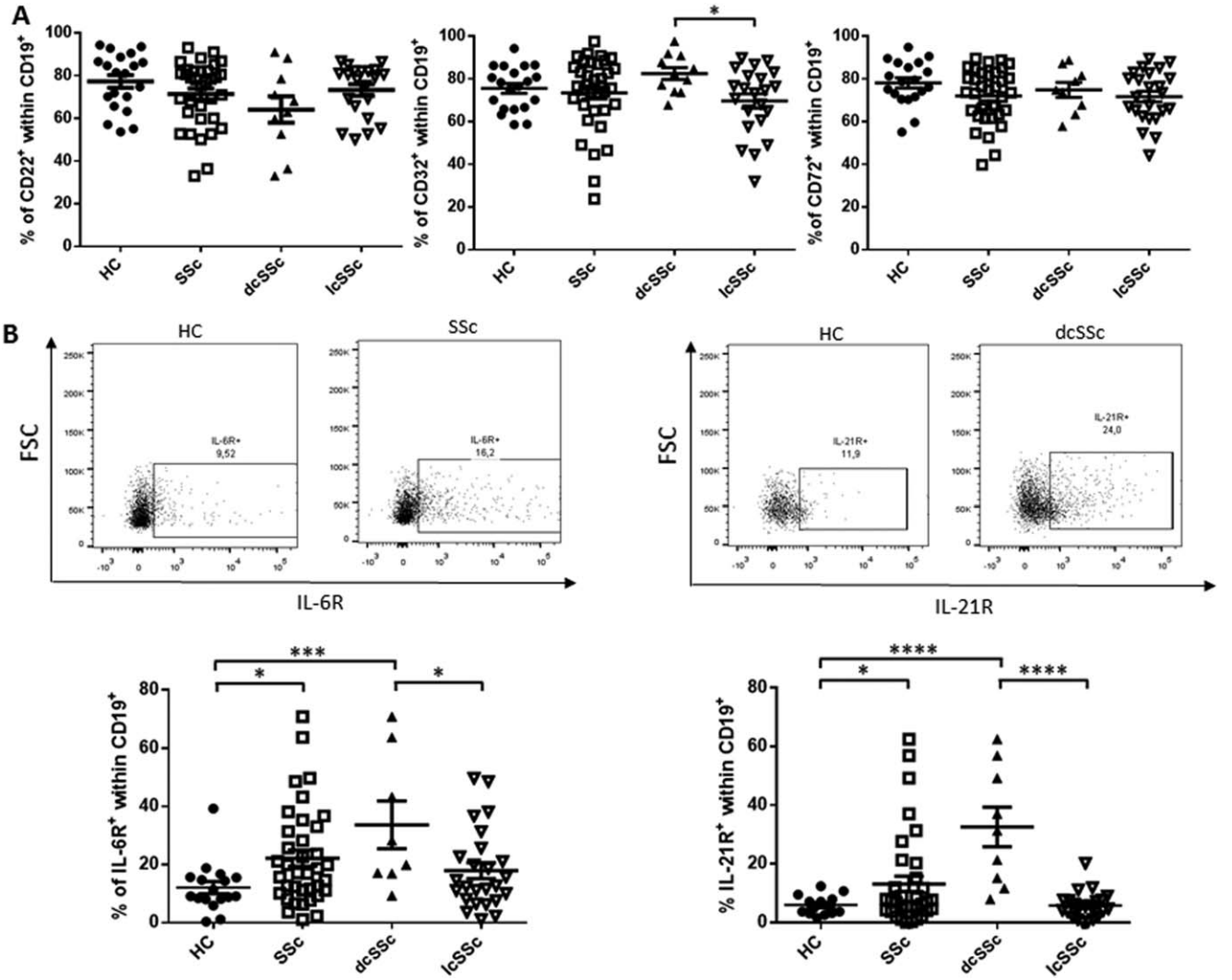

Figure 3. Receptor expression at the membrane of peripheral CD19+ B lymphocytes from healthy controls (HC) and patients with systemic sclerosis (SSc). **A** and **B,** Percentages of CD22+ (inhibitory), CD32+, and CD72+ receptors (**A**), as well as interleukin-6 receptor (IL-6R)–positive and IL-21R+ receptors (**B**) at the surface of CD19+ B lymphocytes from 20 healthy controls and 43 patients with SSc, including 11 with diffuse cutaneous (dcSSc) and 32 with limited cutaneous (lcSSc) disease. Typical dot plots of IL-6R and IL-21R expression are shown. Each symbol represents an individual subject; horizontal lines with bars show the mean ± SD. $* = P < 0.05$; $*** = P < 0.001$; $**** = P < 0.0001$, by Mann-Whitney U test.

patients, both in those with dcSSc and those with lcSSc ($r = 0.76$, $P < 0.0001$) (Figure 2C).

The percentages of CD95+ B cells were higher in patients with early lcSSc as compared to patients without early lcSSc ($P = 0.0027$) (Figure 2D). In contrast, the proportion of peripheral CD69+ B lymphocytes was higher in patients with early dcSSc as compared to those without early dcSSc ($P = 0.048$). Furthermore, when we analyzed these 2 activation markers in combination, the percentage of CD69+CD95+ B cells was higher in early SSc patients than in those without early SSc ($P < 0.0001$). No associations between other activation markers were found for the SSc patients and the healthy controls.

The proportions of cells expressing CD86 differed significantly between dcSSc and lcSSc patients ($P = 0.0007$) as well as for cells expressing CD5 ($P = 0.03$) (Figure 2A). CD86 and CD5 B cell subsets were not associated with autoantibody status (data not shown). Since these 2 receptors play a critical role in the B lymphocyte/T lymphocyte synapse, we investigated potential correlations between the proportions of CD5+ and CD86+ B lymphocytes and the proportions of Th1 (CD3+CD4+IFNγ+), Th2 (CD3+CD4+IL-4+), Th9 (CD3+CD4+IL-9+), and Th17 (CD3+CD4+IL-17A+) cells (data available upon request from the corresponding author). No correlation of the percentage of CD5+ or CD86+ cells with these

T cell subsets was found, except for a correlation between CD86 and the percentage of Th2 cells. Similar results were obtained when patients with dcSSc and lcSSc were analyzed separately.

In contrast, the proportions of cells expressing the inhibitory receptors CD22, CD32, and CD72 did not differ significantly between healthy controls and SSc patients, except for the comparison of CD32+ cells between dcSSc and lcSSc subsets ($P = 0.02$) (Figure 3A). Regarding membrane expression, B lymphocytes from SSc patients showed increased levels of the constitutively expressed activating coreceptor CD20 as compared to those from healthy controls ($P = 0.001$), whereas no significant variation was found for the expression of the inhibitory receptors CD22, CD32, or CD72 or of HLA–DR (data available upon request from the corresponding author). Concerning the crosstalk of B cells with the microenvironment, a slight decrease in BAFF receptor (BR3)–expressing cells was detected in SSc patients as compared to healthy controls ($P = 0.04$); however, this difference was not significant at the cellular level (data available upon request from the corresponding author). It is noteworthy that a remarkable increase in the populations expressing either IL-6R ($P = 0.01$) or IL-21R ($P = 0.02$) was observed in SSc patients versus controls, with major differences for IL-21R expression between dcSSc and lcSSc patients ($P < 0.0001$) regarding both subpopulation percentages (Figure 3B) and mean fluorescence intensity (data available upon request from the corresponding author).

In order to identify clinical manifestations of SSc that could be associated with B cell subsets, expression of activation markers and receptors were evaluated in the presence or absence of pulmonary arterial hypertension (PAH), interstitial lung disease (ILD), arthralgia (joint), and digital ulcers (data available upon request from the corresponding author). There was an increased proportion of B cells expressing CD86, which showed a slight association with PAH and digital ulcers in patients with SSc, while an increased subpopulation of CD95+ B cells was associated with arthralgias. More interestingly, patients with either arthralgias or PAH with or without ILD had increased proportions of B cells expressing the IL-6R. For these 2 late manifestations of SSc, similar proportions of B lymphocytes expressing IL-6R were observed, which allowed us to discriminate between patients with PAH and/or ILD and those without documented pulmonary involvement, who had a lower proportion of peripheral IL-6R+ B cells (data available upon request from the corresponding author).

Overall, we found no significant difference in B cell phenotypes based on autoantibody specificity (data not shown).

Detection of B lymphocytes in the lungs of patients with SSc-associated PAH. We performed immunostaining in lung samples from 3 patients with SSc-associated PAH and 3 healthy controls (normal lung tissue from patients with non–small cell lung carcinoma). In patients with SSc, a number of lymphoid follicles (mostly near bronchioles/small airways) were observed, whereas only scattered B lymphocytes were seen in the lung parenchyma of the control subjects, as assessed by anti-CD20 immunostaining. In lymphocyte-rich areas, scattered CD69+ cells were observed, whereas only faint staining of sparse cells was seen in control subjects (data available upon request from the corresponding author).

Consistency between phenotype characteristics of peripheral B cells and higher production of IL-6 and TGFβ in SSc patients. A major increase in IL-6–producing cells was seen in SSc patients as compared to healthy controls ($P < 0.0001$) (Figure 4A). This difference was also found for both IgD+IL-6+CD27– naive B cells (1:2 ratio; $P < 0.0001$) and IgD–IL-6+CD27+ memory B cells (1:1.8 ratio; $P = 0.0003$) but not for marginal-zone or double-negative effector B cells (data not shown). We further analyzed the intracellular staining of IL-6 in both T lymphocytes (defined as CD27+CD19– cells) and monocytes (using forward scatter/side scatter parameters in CD19–CD27– cells) (data available upon request from the corresponding author). No difference in the percentages of IL-6+ T cells was observed in patients with SSc versus healthy controls, whereas a decreased proportion of monocytes expressed IL-6 in SSc patients as compared to healthy controls (data available upon request from the corresponding author). Thus, in patients with SSc, we identified B cells as the main source of IL-6 as compared to T lymphocytes and monocytes, which was not the case in healthy controls (data available upon request from the corresponding author).

We also investigated IL-10 and TGFβ (Figures 4B and C) production by purified B lymphocytes after 3 days of culture with or without CpG stimulation. The number of IL-10–producing B cells did not differ significantly between the various samples under these conditions, and their phenotype corresponded to CD19+ $CD24^{high}CD27^{+/-}CD38^{high}$, predominantly CD5– (data available upon request from the corresponding author). More interestingly, peripheral B cells isolated from patients with SSc expressed increased proportion of TGFβ+CD19+ B lymphocytes as compared to healthy controls, even in the absence of further stimulation of Toll-like receptor 9 through incubation with CpG ($P = 0.0002$) (Figure 4C). TGFβ-expressing B lymphocytes were CD19+CD5–$CD24^{low}$CD27+$CD38^{high}$ both in healthy controls and in patients with SSc, and did not

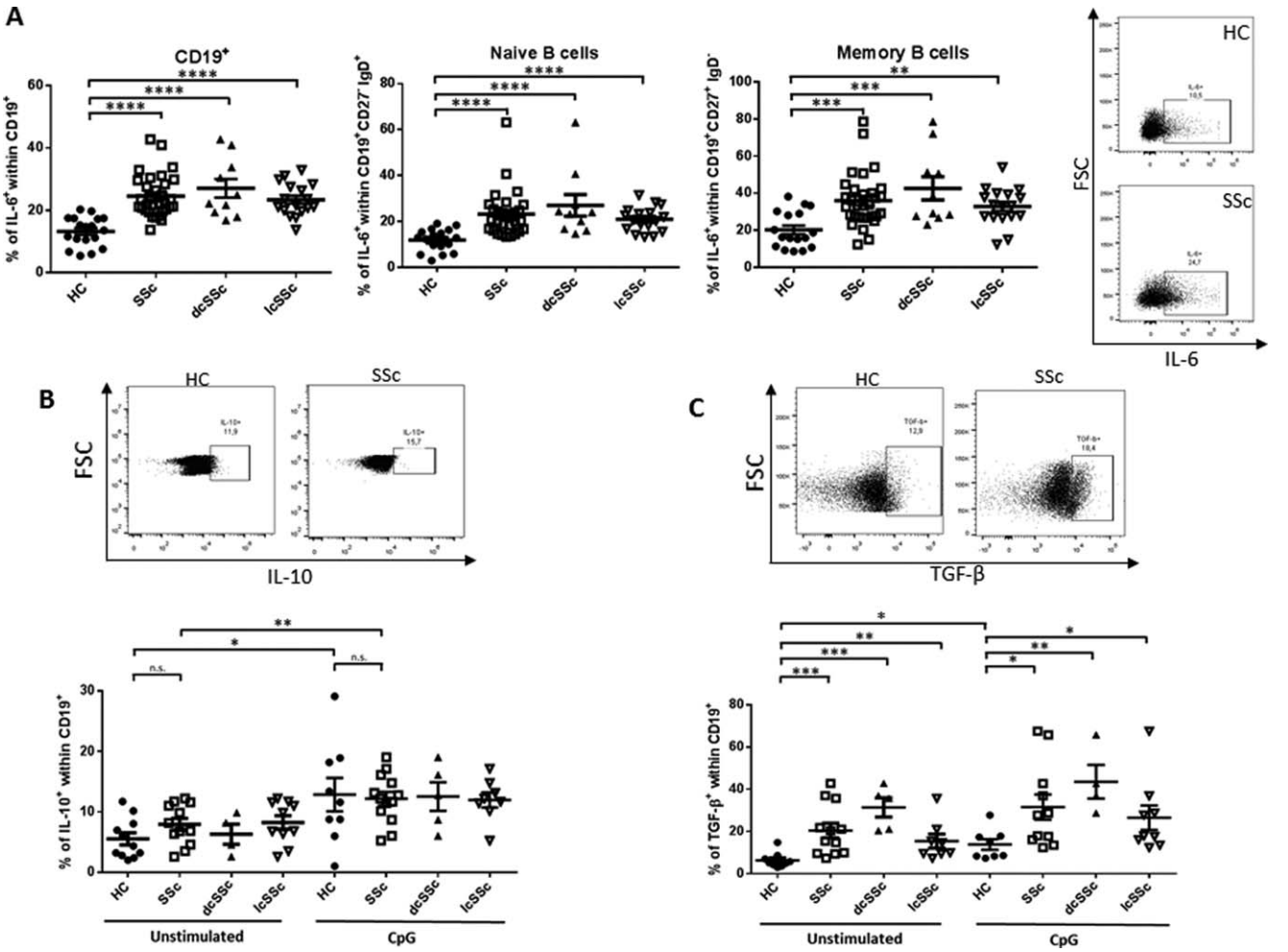

Figure 4. Intracellular cytokine staining of peripheral B lymphocytes from healthy controls (HC) and patients with systemic sclerosis (SSc). **A,** Intracellular interleukin-6 (IL-6) was analyzed in 18 healthy controls and 32 patients with SSc, including 10 with diffuse cutaneous (dcSSc) and 22 with limited cutaneous (lcSSc) disease. Percentages of IL-6+ cells were quantified in total B lymphocytes (CD19+), naive B cells (IgD+CD19+CD27–), and memory B cells (IgD–CD19+CD27+). A typical dot plot of IL-6 expression is shown at the right. **B** and **C,** Intracellular IL-10 (**B**) and transforming growth factor β (TGFβ) (**C**) were analyzed in 11 healthy controls and 12 patients with SSc, including 4 with dcSSc and 8 with lcSSc. Percentages of IL-10+ cells were quantified in unstimulated total B lymphocytes or in CpG-containing oligonucleotide–stimulated B cells. Typical dot plots of IL-10 (**B**) and TGFβ (**C**) staining are shown. Each symbol represents an individual subject; horizontal lines with bars show the mean ± SD. $* = P < 0.05$; $** = P < 0.01$; $*** = P < 0.001$; $**** = P < 0.0001$, by Mann-Whitney U test. NS = not significant.

overlap with IL-10+ B lymphocytes (data available upon request from the corresponding author).

Secretion of higher amounts of IL-6 and TGFβ and lower amounts of IL-10 by stimulated B cells from SSc patients. We detected higher levels of IL-6 in the serum of SSc patients as compared to healthy controls ($P = 0.01$) (Figure 5A). No significant differences in the levels of IL-10 or TGFβ were found (Figure 5A). Interestingly, purified B cells obtained from SSc patients and incubated for 3 days with CpG or for 4 hours with a mix of phorbol myristate acetate (PMA)/ionomycin secreted increased amounts of IL-6, whereas those from healthy controls remained low ($P = 0.0007$) (Figure 5B). We also detected slightly increased concentrations of IL-10 in B cell supernatants from the SSc patients as compared to the healthy controls after cell stimulation with PMA/ionomycin ($P = 0.01$) (Figure 5C). Unexpectedly, while CpG stimulation promoted a weak increase in IL-10 secretion in SSc patients, a strong increase was observed in healthy control cells under these conditions. According to the increased proportion of TGFβ-producing cells, we noted increased amounts of TGFβ in the supernatants of CpG-stimulated B cells from SSc patients as compared to healthy controls ($P = 0.001$) (Figure 5D), while PMA/ionomycin treatment did not significantly affect the

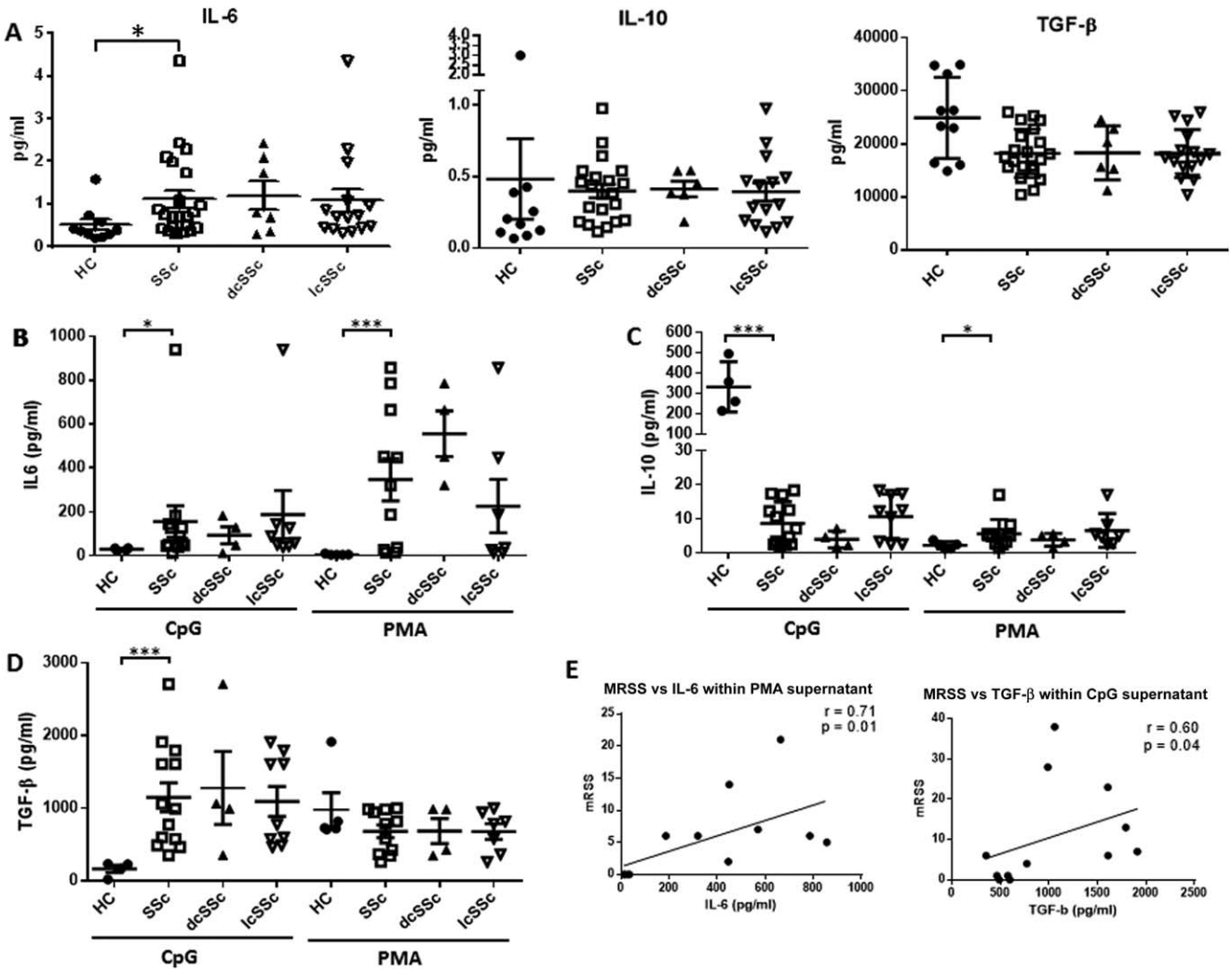

Figure 5. Cytokine concentrations in sera and supernatants of stimulated B cells from the peripheral blood of healthy controls (HC) and systemic sclerosis (SSc) patients. **A,** Levels of interleukin-6 (IL-6), IL-10, and transforming growth factor β (TGFβ) in sera from 10 healthy controls and 22 SSc patients, 7 with diffuse cutaneous (dcSSc) and 15 with limited cutaneous (lcSSc) disease. **B–D,** Levels of IL-6 (**B**), IL-10 (**C**), and TGFβ (**D**) in supernatants of purified B cells after 4 hours of stimulation with either CpG (4 healthy controls and 12 SSc patients, 4 with dcSSc and 8 with lcSSc) or phorbol myristate acetate (PMA)/ionomycin (6 healthy controls and 11 SSc patients, 4 with dcSSc and 7 with lcSSc). Each symbol represents an individual subject; horizontal lines with bars show the mean ± SD. $* = P < 0.05$; $*** = P < 0.001$, by Mann-Whitney U test. **E,** Correlations between the modified Rodnan skin thickness score (MRSS) and concentrations of IL-6 in purified PMA–stimulated B lymphocyte supernatants (left) and concentrations of TGFβ in purified CpG–stimulated B lymphocyte supernatants (right) from 11 patients with SSc, as determined by Spearman's correlation coefficient.

release as compared to unstimulated cells (data available upon request from the corresponding author).

We found a correlation between the modified Rodnan skin thickness score and the concentration of TGFβ in culture supernatants from B cells stimulated with CpG (r = 0.60, $P = 0.04$) (Figure 5E). A similar correlation between the modified Rodnan skin thickness score and the concentration of IL-6 in supernatants from B cells stimulated for 4 hours with PMA/ionomycin (r = 0.71, $P = 0.01$) was also noted, suggesting a potential profibrotic role of B lymphocytes in SSc patients.

Increased proliferative and fibrotic phenotype after in vitro stimulation of B lymphocytes derived from the dermal fibroblasts of healthy controls and SSc patients. Fibroblasts from healthy control subjects or from the involved skin of SSc patients were cultured for 3 days in the presence of supernatants from B cells obtained from healthy controls. We found no significant influence of culture on the metabolic activity (Figure 6A) or the proliferation rate of the fibroblasts, as assessed by immunofluorescence using Ki-67 labeling (data available upon request from the corresponding author). A random increase in

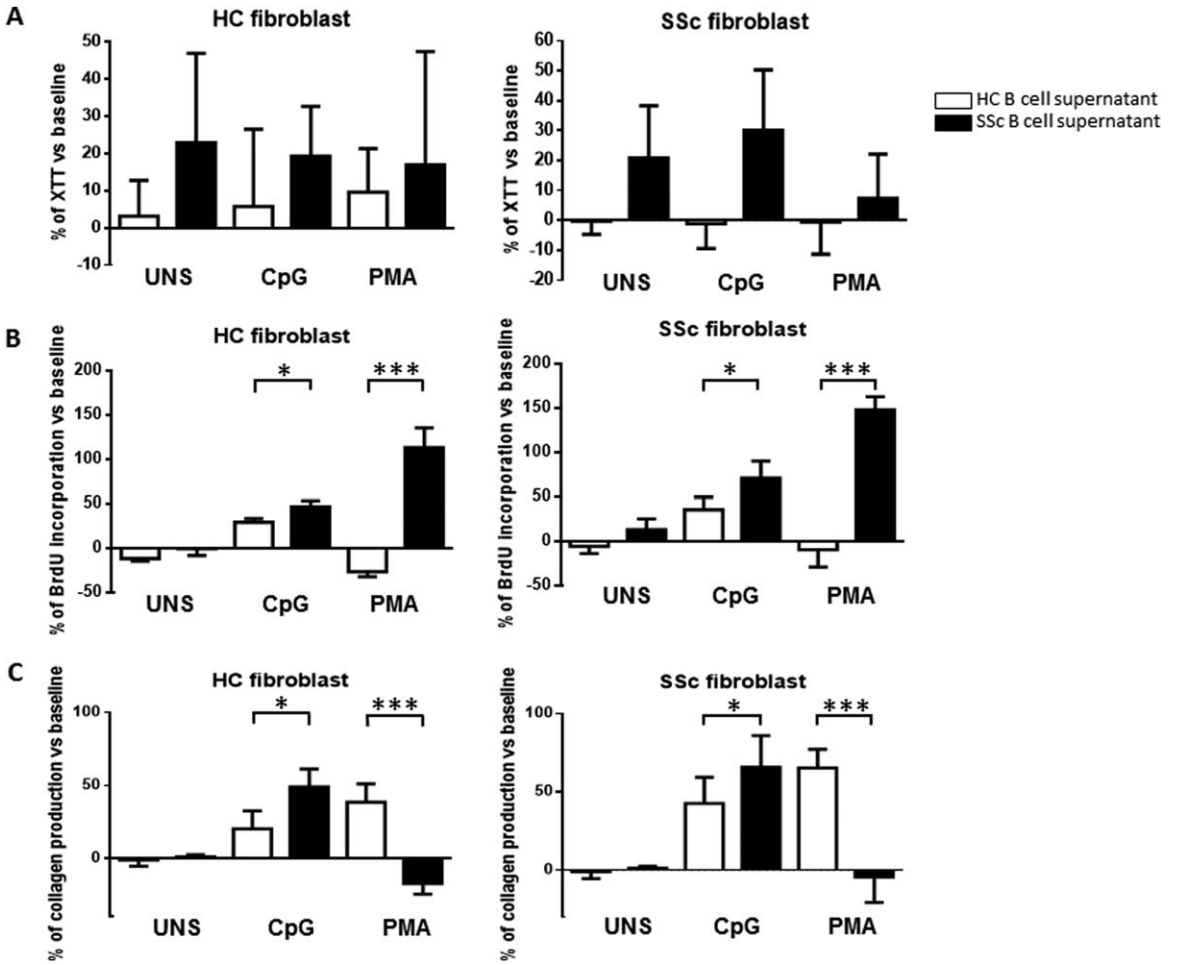

Figure 6. Effect of purified B lymphocyte supernatants from healthy controls (HC) and patients with systemic sclerosis (SSc) on fibroblast proliferation and collagen production. Fibroblasts from 4 healthy controls and 4 patients with SSc were cultured for 3 days in the presence of supernatants from 3-day cultures of unstimulated (UNS) purified B lymphocytes, 3-day cultures of CpG-stimulated purified B lymphocytes, or 4-hour cultures of phorbol myristate acetate (PMA)/ionomycin–stimulated purified B lymphocytes from 4 healthy controls and 4 patients with diffuse SSc (nonautologous). **A,** Viability of fibroblasts was quantified using an XTT reduction assay kit, and the results were expressed as the percentage of XTT reduction in stimulated versus unstimulated fibroblasts. **B,** Proliferation of fibroblasts was quantified using a bromodeoxyuridine (BrdU) incorporation assay. Results were expressed as the percentage of BrdU incorporation by stimulated versus unstimulated fibroblasts. **C,** Collagen production by fibroblasts was quantified using a Sircol assay. Results were expressed as the percentage of collagen production by stimulated versus unstimulated fibroblasts. All experiments were performed twice, and the results were similar. Values are the mean ± SD. $* = P < 0.05$; $*** = P < 0.001$, by paired *t*-test.

viability was observed in all fibroblasts cultured in the presence of supernatants of B cells isolated from SSc patients, but the difference did not reach statistical significance (Figure 6A). Prior stimulation of B cells from healthy controls or SSc patients did not provide any additional effect on viability. However, supernatants from CpG- or PMA-stimulated SSc B cells significantly enhanced to various extents the proliferation of both healthy and SSc fibroblasts (Figure 6B). Consistent with their increased proliferation rate, fibroblasts from both healthy controls and SSc patients showed poor production of collagen in the presence of PMA-stimulated B cell supernatants from SSc patients as compared to those from healthy controls (Figure 6C). When supernatants of CpG-stimulated purified B cells from healthy controls and SSc patients were used to stimulate fibroblasts in culture, collagen production was differentially increased in fibroblasts from both healthy controls and SSc patients (Figure 6C).

The expression of mRNA for α-SMA, type I collagen, Snail, and vimentin in stimulated fibroblasts from healthy controls and SSc patients was analyzed by qPCR and immunofluorescence. There was no consistent detection of α-SMA in fibroblasts from either healthy controls or SSc patients with either technique (data not shown).

However, when fibroblasts from each group were stimulated with either CpG- or PMA/ionomycin-stimulated purified B cell supernatants from SSc patients, we observed increased expression of vimentin. Increased expression of mRNA for the transcription factor Snail and for type I collagen was also detected when fibroblasts from either healthy controls or SSc patients were stimulated with CpG-stimulated B cell supernatants from SSc patients. These increases were abrogated when supernatants were preincubated with anti-TGFβ antibody (for CpG supernatants) or anti–IL-6R antibody (for PMA supernatants). Incubation with anti-TGFβ antibody or anti–IL-6R antibody induced a drastic decrease in fibroblast proliferation without any difference in cell viability, thus reinforcing the potential pathophysiologic role of B lymphocytes in SSc (data available upon request from the corresponding author).

DISCUSSION

In the present work, we found evidence of an increased peripheral B cell subpopulation in SSc patients as compared to healthy controls that expresses both activation markers and cytokine receptors as well as high levels of intracellular IL-6 and TGFβ. We also established that supernatants of B lymphocytes from SSc patients activate both normal and scleroderma fibroblasts at higher levels than do those from healthy controls.

In the SSc patients, we observed increased expression of CD86 and CD95 on B cells, together with a lower proportion of peripheral memory B cells, which is consistent with the results reported by Sato et al (4). This decrease was found to be restricted to the early Bm5 memory peripheral B cell subpopulation, as previously noted in the peripheral blood of patients with Sjögren's syndrome (17). Interestingly, we found increased expression of CD69, IL-6R, and IL-21R on peripheral B lymphocytes from SSc patients, and we further correlated the increased proportions of CD69+ cells with a decreased proportion of CD95+ B lymphocytes. We also showed a major differential proportion of CD5+, CD86+, IL-6R+, or IL-21R+ B cells in the subgroups of patients with dcSSc and lcSSc. Indeed, patients with dcSSc had a higher proportion of these B cells as compared to both lcSSc patients and healthy controls. In contrast, both lcSSc and dcSSc patients showed increased proportions of CD69+ and CD95+ B cells as compared to healthy controls.

We found several correlations between B lymphocyte activation and disease duration in SSc patients, with higher expression of CD95 in the subgroup of patients with early lcSSc and an increased percentage of CD69+ cells in patients with early dcSSc. In addition, we detected a double-positive subpopulation of CD69+CD95+ peripheral B cells in patients with early SSc, suggesting a possible link between B cell activation at an early stage of the disease and disease severity.

Of note, IL-6R expression was strongly associated with arthralgia, PAH, and/or ILD. There were similar proportions of B lymphocytes expressing IL-6R in patients with PAH and ILD. This finding allowed the discrimination of patients with versus those without lung involvement, the latter group exhibiting lower proportions of peripheral IL-6R+ B cells. In lung tissue from patients with SSc-associated PAH, we observed important numbers of B cells, with a number of lymphoid follicles, mostly in the vicinity of bronchioles/small airways, whereas only scattered B lymphocytes were seen in the lung parenchyma of control subjects, which provides further evidence implicating B cells in the lung involvement in SSc.

Taken together, our data support an activation profile of B lymphocytes in SSc patients, probably due to B cell receptor engagement via autoantigens, both for lcSSc and for dcSSc (18,19). Our data also suggest differential activation between dcSSc and lcSSc B lymphocytes, as was found for patients with PAH and/or ILD versus those without lung involvement. This differential activation could potentially occur through cytokine modulation, as suggested in a recent clinical study (20). We found no correlation between B lymphocyte activation and autoantibody status, probably because they represent additional markers of disease activity/severity. Since B cells from dcSSc patients with PAH and/or ILD are activated, these cells could be proposed as biomarkers.

Our findings also provide novel evidence of the production and secretion of cytokines. We identified both naive and memory B lymphocytes derived from SSc patients as major IL-6–secreting cells. However, a direct correlation between IL-6 levels in culture supernatants and IL-6R expression at the membrane of B lymphocytes was not observed. This result does not support an autocrine activating loop in SSc B lymphocytes, similar to the autostimulatory IL-6–driven B cell differentiation in patients with systemic lupus erythematosus (21). The mechanisms leading to B lymphocyte overactivation might instead be due to the increased concentration of IL-6 in the serum of SSc patients versus healthy controls, as previously reported by Needleman et al (22). Moreover, we showed that IL-6 levels in supernatants of purified B cells from SSc patients also correlate with the modified Rodnan skin thickness score, suggesting a critical role of B lymphocytes in the induction of fibrosis. Monocytes have been proposed as the unique immune cells producing IL-6 in patients with SSc (23,24). We provide herein new evidence of the characterization of IL-6–producing B lymphocytes

in patients with SSc. These B lymphocytes might represent interesting treatment targets in these patients, since elevated levels of IL-6 in SSc patient sera have been shown to correlate with disease severity (9).

In contrast to the results of a previous study, we found elevated TGFβ production and release by peripheral B lymphocytes from SSc patients as compared to healthy controls, both under steady-state conditions and upon specific TLR stimulation (25). These high levels of TGFβ in supernatants of sorted B cells also correlated with the modified Rodnan skin thickness score, suggesting a role of B cells in the development of fibrosis. Indeed, Hasegawa et al (25) reported a lack of substantial increase in the release of TGFβ by regulatory B cells, as well as activated T cells (26) or monocytes (27) in SSc patients, consistent with a nonimmune production of TGFβ in those patients. In the present study, we identified a specific B lymphocyte subpopulation that secretes high levels of TGFβ and exhibits a phenotype similar to those recently described in patients with graft-versus-host disease (28). The absence of IL-10 secretion by SSc B lymphocytes might also contribute to the loss of immunoregulation observed in SSc (29,30). Unfortunately, because of the limited amount of biologic samples available, we were not able to perform coculture experiments using B cells and T cells in order to evaluate these immunomodulatory roles or their potential interplay with T cells.

The pathogenic effects of the B lymphocytes in SSc remain poorly understood (2). Recent reports have addressed interesting therapeutic targeting, both in mouse models and in open studies of limited populations of patients with SSc (31–34). Notably, François and colleagues (35) reported a direct implication of normal B cells in increased proliferation and extracellular matrix production by fibroblasts from healthy controls and SSc patients. In the present study, we demonstrated that supernatants of B lymphocytes purified from SSc patients induce fibroblast activation even in absence of direct cell-to-cell interaction or autoantibody secretion, but more as a consequence of an increased secretion of IL-6 and TGFβ. We also found that supernatants of purified B lymphocytes with the higher level of TGFβ (CpG supernatant) induced an increased expression of vimentin and the transcription factor Snail, 2 proteins that have been associated with the differentiation of fibroblasts into myofibroblasts (36–38). Moreover, incubation with either anti-TGFβ or anti–IL-6R antibodies induced a dramatic decrease in fibroblast proliferation without any difference in viability, which suggests an implication of these pathways in B cell/fibroblast cross-talk in SSc.

These data further underscore a possible interplay between B lymphocytes and fibroblasts through new secretory pathways that need to be further investigated in the pathogenesis of SSc. Furthermore, the recent results obtained with IL-6–targeted therapy in the mouse model of bleomycin-induced scleroderma and in patients with SSc highlight the prevalent role of this cytokine in the pathophysiology of SSc and reinforce interest in evaluating the IL-6 secretion capacity of peripheral B cells (22,34,39,40). Finally, these data also support interest in investigating the effects of IL-6–targeted therapy in patient with SSc, as the faSScinate study has shown interesting results using a monoclonal anti–IL-6R antibody (tocilizumab) (41). Our study, based on a consistent number of phenotypically characterized SSc patients who did not receive treatment with glucocorticoid or immunosuppressive drugs, provides new insights into the functional implication of B lymphocytes in SSc.

In conclusion, clinical studies have shown promising results for anti-CD20– and anti–IL-6R–based therapies in patients with SSc (22,40,41). We observed an increased activation of peripheral B cells in patients with dcSSc as compared to those with lcSSc. In vitro, B lymphocytes from SSc patients secreted high amounts of IL-6 and TGFβ, which induced fibroblast proliferation, collagen secretion, and differentiation into myofibroblasts in fibroblasts from both healthy individuals and SSc patients. Our findings are the first to highlight differential B lymphocyte subpopulations in the two different SSc subtypes.

ACKNOWLEDGMENTS

The authors are grateful to staff at the Cochin Cytometry and Immunobiology Facility. We thank Lionel Guitat for designing the primers.

AUTHOR CONTRIBUTIONS

All authors were involved in drafting the article or revising it critically for important intellectual content, and all authors approved the final version to be published. Dr. Mouthon had full access to all of the data in the study and takes responsibility for the integrity of the data and the accuracy of the data analysis.

Study conception and design. Terrier, Varin-Blank, Mouthon.

Acquisition of data. Dumoitier, Chaigne, Régent, Lofek, Mhibik, Dorfmüller, Terrier, London, Bérezné, Tamas.

Analysis and interpretation of data. Dumoitier, Chaigne, Lofek.

REFERENCES

1. Dumoitier N, Lofek S, Mouthon L. Pathophysiology of systemic sclerosis: state of the art in 2014. Presse Med 2014;43:e267–78.
2. Arnett FC. Is scleroderma an autoantibody mediated disease? Curr Opin Rheumatol 2006;18:579–81.
3. Tyndall A, Fistarol S. The differential diagnosis of systemic sclerosis. Curr Opin Rheumatol 2013;25:692–9.
4. Sato S, Fujimoto M, Hasegawa M, Takehara K, Tedder TF. Altered B lymphocyte function induces systemic autoimmunity in systemic sclerosis. Mol Immunol 2004;41:1123–33.
5. Matsushita T, Sato S. The role of BAFF in autoimmune diseases. Nihon Rinsho Meneki Gakkai Kaishi 2005;28:333–42. In Japanese.

6. Liu Z, Davidson A. BAFF and selection of autoreactive B cells. Trends Immunol 2011;32:388–94.
7. Bosello S, Pers JO, Rochas C, Devauchelle V, de Santis M, Daridon C, et al. BAFF and rheumatic autoimmune disorders: implications for disease management and therapy. Int J Immunopathol Pharmacol 2007;20:1–8.
8. Kraaij MD, van Laar JM. The role of B cells in systemic sclerosis. Biologics 2008;2:389–95.
9. Sato S, Hasegawa M, Takehara K. Serum levels of interleukin-6 and interleukin-10 correlate with total skin thickness score in patients with systemic sclerosis. J Dermatol Sci 2001;27:140–6.
10. Hasegawa M, Hamaguchi Y, Yanaba K, Bouaziz JD, Uchida J, Fujimoto M, et al. B-lymphocyte depletion reduces skin fibrosis and autoimmunity in the tight-skin mouse model for systemic sclerosis. Am J Pathol 2006;169:954–66.
11. Chizzolini C. T cells, B cells, and polarized immune response in the pathogenesis of fibrosis and systemic sclerosis. Curr Opin Rheumatol 2008;20:707–12.
12. Bosello SL, de Luca G, Rucco M, Berardi G, Falcione M, Danza FM, et al. Long-term efficacy of B cell depletion therapy on lung and skin involvement in diffuse systemic sclerosis. Semin Arthritis Rheum 2015;44:428–36.
13. Elhai M, Meunier M, Matucci-Cerinic M, Maurer B, Riemekasten G, Leturcq T, et al. Outcomes of patients with systemic sclerosis-associated polyarthritis and myopathy treated with tocilizumab or abatacept: a EUSTAR observational study. Ann Rheum Dis 2013; 72:1217–20.
14. Shima Y, Kuwahara Y, Murota H, Kitaba S, Kawai M, Hirano T, et al. The skin of patients with systemic sclerosis softened during the treatment with anti-IL-6 receptor antibody tocilizumab. Rheumatology (Oxford) 2010;49:2408–12.
15. Van den Hoogen F, Khanna D, Fransen J, Johnson SR, Baron M, Tyndall A, et al. 2013 classification criteria for systemic sclerosis: an American College of Rheumatology/European League Against Rheumatism collaborative initiative. Arthritis Rheum 2013;65:2737–47.
16. LeRoy EC, Black C, Fleischmajer R, Jablonska S, Krieg T, Medsger TA Jr, et al. Scleroderma (systemic sclerosis): classification, subsets, and pathogenesis. J Rheumatol 1988;15:202–5.
17. Bohnhorst JØ, Bjørgan MB, Thoen JE, Natvig JB, Thompson KM. Bm1-Bm5 classification of peripheral blood B cells reveals circulating germinal center founder cells in healthy individuals and disturbance in the B cell subpopulations in patients with primary Sjögren's syndrome. J Immunol 2001;167:3610–8.
18. Koncz G, Hueber AO. The Fas/CD95 receptor regulates the death of autoreactive B cells and the selection of antigen-specific B cells. Front Immunol 2012;3:207.
19. Petterson T, Jendholm J, Månsson A, Bjartell A, Riesbeck K, Cardell LO. Effects of NOD-like receptors in human B lymphocytes and crosstalk between NOD1/NOD2 and Toll-like receptors. J Leukoc Biol 2011;89:177–87.
20. Bosello S, de Santis M, Lama G, Spanò C, Angelucci C, Tolusso B, et al. B cell depletion in diffuse progressive systemic sclerosis: safety, skin score modification and IL-6 modulation in an up to thirty-six months follow-up open-label trial. Arthritis Res Ther 2010;12:R54.
21. Kitani A, Hara M, Hirose T, Harigai M, Suzuki K, Kawakami M, et al. Autostimulatory effects of IL-6 on excessive B cell differentiation in patients with systemic lupus erythematosus: analysis of IL-6 production and IL-6R expression. Clin Exp Immunol 1992;88:75–83.
22. Needleman BW, Wigley FM, Stair RW. Interleukin-1, interleukin-2, interleukin-4, interleukin-6, tumor necrosis factor α, and interferon-γ levels in sera from patients with scleroderma. Arthritis Rheum 1992;35:67–72.
23. Crestani B, Seta N, de Bandt M, Soler P, Rolland C, Dehoux M, et al. Interleukin 6 secretion by monocytes and alveolar macrophages in systemic sclerosis with lung involvement. Am J Respir Crit Care Med 1994;149:1260–5.
24. Giacomelli R, Cipriani P, Danese C, Pizzuto F, Lattanzio R, Parzanese I, et al. Peripheral blood mononuclear cells of patients with systemic sclerosis produce increased amounts of interleukin 6, but not transforming growth factor β 1. J Rheumatol 1996;23:291–6.
25. Hasegawa M, Sato S, Takehara K. Augmented production of transforming growth factor-β by cultured peripheral blood mononuclear cells from patients with systemic sclerosis. Arch Dermatol Res 2004;296:89–93.
26. Radstake TR, van Bon L, Broen J, Wenink M, Santegoets K, Deng Y, et al. Increased frequency and compromised function of T regulatory cells in systemic sclerosis (SSc) is related to a diminished CD69 and TGFβ expression. PLoS One 2009;4:e5981.
27. Baraut J, Grigore EI, Jean-Louis F, Khelifa SH, Durand C, Verrecchia F, et al. Peripheral blood regulatory T cells in patients with diffuse systemic sclerosis (SSc) before and after autologous hematopoietic SCT: a pilot study. Bone Marrow Transplant 2014;49: 349–54.
28. De Masson A, Bouaziz JD, le Buanec H, Robin M, O'Meara A, Parquet N, et al. $CD24^{hi}CD27^{+}$ and plasmablast-like regulatory B cells in human chronic graft-versus-host disease. Blood 2015;125:1830–9.
29. Blair PA, Noreña LY, Flores-Borja F, Rawlings DJ, Isenberg DA, Ehrenstein MR, et al. $CD19^{+}CD24^{hi}CD38^{hi}$ B cells exhibit regulatory capacity in healthy individuals but are functionally impaired in systemic lupus erythematosus patients. Immunity 2010;32:129–40.
30. Yao Y, Simard AR, Shi FD, Hao J. IL-10-producing lymphocytes in inflammatory disease. Int Rev Immunol 2013;32:324–36.
31. Saito E, Fujimoto M, Hasegawa M, Komura K, Hamaguchi Y, Kaburagi Y, et al. CD19-dependent B lymphocyte signaling thresholds influence skin fibrosis and autoimmunity in the tight-skin mouse. J Clin Invest 2002;109:1453–62.
32. Smith V, van Praet JT, Vandooren B, van der Cruyssen B, Naeyaert JM, Decuman S, et al. Rituximab in diffuse cutaneous systemic sclerosis: an open-label clinical and histopathological study. Ann Rheum Dis 2010;69:193–7.
33. Jordan S, Distler JH, Maurer B, Huscher D, van Laar JM, Allanore Y, et al. Effects and safety of rituximab in systemic sclerosis: an analysis from the European Scleroderma Trial and Research (EUSTAR) group. Ann Rheum Dis 2015;74:1188–94.
34. Giuggioli D, Lumetti F, Colaci M, Fallahi P, Antonelli A, Ferri C. Rituximab in the treatment of patients with systemic sclerosis: our experience and review of the literature. Autoimmun Rev 2015;14:1072–8.
35. François A, Chatelus E, Wachsmann D, Sibilia J, Bahram S, Alsaleh G, et al. B lymphocytes and B-cell activating factor promote collagen and profibrotic markers expression by dermal fibroblasts in systemic sclerosis. Arthritis Res Ther 2013;15:R168.
36. Gabbiani G. The myofibroblast in wound healing and fibrocontractive diseases. J Pathol 2003;200:500–3.
37. Franz M, Spiegel K, Umbreit C, Richter P, Codina-Canet C, Berndt A, et al. Expression of Snail is associated with myofibroblast phenotype development in oral squamous cell carcinoma. Histochem Cell Biol 2009;131:651–60.
38. Park HY, Kim JH, Park CK. VEGF induces TGF-β1 expression and myofibroblast transformation after glaucoma surgery. Am J Pathol 2013;182:2147–54.
39. Desallais L, Avouac J, Fréchet M, Elhai M, Ratsimandresey R, Montes M, et al. Targeting IL-6 by both passive or active immunization strategies prevents bleomycin-induced skin fibrosis. Arthritis Res Ther 2014;16:R157.
40. Fernandes das Neves M, Oliveira S, Amaral MC, Delgado Alves J. Treatment of systemic sclerosis with tocilizumab. Rheumatology (Oxford) 2015;54:371–2.
41. Khanna D, Denton CP, Jahreis A, van Laar JM, Frech TM, Anderson ME, et al. Safety and efficacy of subcutaneous tocilizumab in adults with systemic sclerosis (faSScinate): a phase 2, randomised, controlled trial. Lancet 2016;387:2630–40.

ARTHRITIS & RHEUMATOLOGY
Vol. 69, No. 5, May 2017, pp 1090–1099
DOI 10.1002/art.40045

Immune-Array Analysis in Sporadic Inclusion Body Myositis Reveals HLA–DRB1 Amino Acid Heterogeneity Across the Myositis Spectrum

Simon Rothwell,[1] Robert G. Cooper,[2] Ingrid E. Lundberg,[3] Peter K. Gregersen,[4] Michael G. Hanna,[5] Pedro M. Machado,[5] Megan K. Herbert,[6] Ger J. M. Pruijn,[7] James B. Lilleker,[8] Mark Roberts,[9] John Bowes,[1] Michael F. Seldin,[10] Jiri Vencovsky,[11] Katalin Danko,[12] Vidya Limaye,[13] Albert Selva-O'Callaghan,[14] Hazel Platt,[1] Øyvind Molberg,[15] Olivier Benveniste,[16] Timothy R. D. J. Radstake,[17] Andrea Doria,[18] Jan De Bleecker,[19] Boel De Paepe,[19] Christian Gieger,[20] Thomas Meitinger,[21] Juliane Winkelmann,[21] Christopher I. Amos,[22] William E. Ollier,[1] Leonid Padyukov,[23] Annette T. Lee,[4] Janine A. Lamb,[1] and Hector Chinoy,[24] for the Myositis Genetics Consortium

Objective. **Inclusion body myositis (IBM) is characterized by a combination of inflammatory and degenerative changes affecting muscle. While the primary cause of IBM is unknown, genetic factors may influence disease susceptibility. To determine genetic factors contributing to the etiology of IBM, we conducted the largest genetic association study of the disease to date, investigating immune-related genes using the Immunochip.**

The views expressed herein are those of the authors and not necessarily those of the (UK) National Health Service (NHS), the NIHR, or the (UK) Department of Health.

Supported by the NIHR (Biomedical Research Unit Funding Scheme) and the University College London Hospitals Biomedical Research Centre. Supported in part by the Association Francaise Contre Les Myopathies, the European Science Foundation (Research Networking Programme European Myositis Network), the Swedish Research Council, the regional agreement on medical training and clinical research between Stockholm County Council and Karolinska Institutet, the Swedish Research Council, Myositis UK, Arthritis Research UK (grant 18474), and Prinses Beatrix Spierfonds (project W.OR12-15). Dr. Rothwell's work was supported by the Wellcome Trust (grant 105610/Z/14/Z). Dr. Machado's work was supported by the NIHR (Rare Diseases Translational Research Collaboration Post-Doctoral Fellowship). The Czech cohort was supported by the Ministry of Health, Czech Republic (Project for Conceptual Development of Research Organization grant 00023728).

[1]Simon Rothwell, PhD, John Bowes, PhD, Hazel Platt, BSc, William E. Ollier, PhD, Janine A. Lamb, PhD: University of Manchester, Manchester, UK; [2]Robert G. Cooper, MD: University of Liverpool, Liverpool, UK; [3]Ingrid E. Lundberg, MD: Karolinska University Hospital, Karolinska Institutet, Stockholm, Sweden; [4]Peter K. Gregersen, MD, Annette T. Lee, PhD: Feinstein Institute for Medical Research, Manhasset, New York; [5]Michael G. Hanna, MD, Pedro M. Machado, MD, PhD: University College London, London, UK; [6]Megan K. Herbert, PhD: Beth Israel Deaconess Medical Center, Boston, Massachusetts, and Radboud University Nijmegen, Nijmegen, The Netherlands; [7]Ger J. M. Pruijn, PhD: Radboud University Nijmegen, Nijmegen, The Netherlands; [8]James B. Lilleker, MD: University of Manchester, Manchester, UK, and Salford Royal NHS Foundation Trust, Salford, UK; [9]Mark Roberts, MD: Salford Royal NHS Foundation Trust, Salford, UK; [10]Michael F. Seldin, MD: University of California, Davis; [11]Jiri Vencovsky, MD: Charles University, Prague, Czech Republic; [12]Katalin Danko, MD: University of Debrecen, Debrecen, Hungary; [13]Vidya Limaye, PhD, FRACP: Royal Adelaide Hospital, Adelaide, South Australia, Australia; [14]Albert Selva-O'Callaghan, MD: Vall d'Hebron General Hospital, Barcelona, Spain; [15]Øyvind Molberg, MD: University of Oslo, Oslo, Norway; [16]Olivier Benveniste, MD: Hôpital Pitié-Salpêtrière, UPMC, Paris, France; [17]Timothy R. D. J. Radstake, MD: University Medical Center Utrecht, Utrecht, The Netherlands; [18]Andrea Doria, MD: University of Padova, Padua, Italy; [19]Jan De Bleecker, MD, Boel De Paepe, PhD: Ghent University Hospital, Ghent, Belgium; [20]Christian Gieger, PhD: Helmholtz Zentrum München, Neuherberg, Germany; [21]Thomas Meitinger, MD, Juliane Winkelmann, MD: Technische Universität München, Munich, Germany, and Helmholtz Zentrum München, Neuherberg, Germany; [22]Christopher I. Amos, PhD: Dartmouth College, Hanover, New Hampshire; [23]Leonid Padyukov, MD: Karolinska Institutet, Stockholm, Sweden; [24]Hector Chinoy, MD: Central Manchester University Hospitals NHS Foundation Trust, University of Manchester, Manchester, UK.

Drs. Lamb and Chinoy contributed equally to this work.

Address correspondence to Simon Rothwell, PhD, Centre for Musculoskeletal Research, University of Manchester, 2.808 Stopford Building, Oxford Road, Manchester M13 9PT, UK. E-mail: s.rothwell@manchester.ac.uk.

Submitted for publication September 12, 2016; accepted in revised form January 10, 2017.

Methods. **A total of 252 Caucasian patients with IBM were recruited from 11 countries through the Myositis Genetics Consortium and compared with 1,008 ethnically matched controls. Classic HLA alleles and amino acids were imputed using SNP2HLA.**

Results. **The HLA region was confirmed as the most strongly associated region in IBM ($P = 3.58 \times 10^{-33}$). HLA imputation identified 3 independent associations (with HLA–DRB1*03:01, DRB1*01:01, and DRB1*13:01), although the strongest association was with amino acid positions 26 and 11 of the HLA–DRB1 molecule. No association with anti–cytosolic 5′-nucleotidase 1A–positive status was found independent of HLA–DRB1*03:01. There was no association of HLA genotypes with age at onset of IBM. Three non-HLA regions reached suggestive significance, including the chromosome 3 p21.31 region, an established risk locus for autoimmune disease, where a frameshift mutation in *CCR5* is thought to be the causal variant.**

Conclusion. **This is the largest, most comprehensive genetic association study to date in IBM. The data confirm that HLA is the most strongly associated region and identifies novel amino acid associations that may explain the risk in this locus. These amino acid associations differentiate IBM from polymyositis and dermatomyositis and may determine properties of the peptide-binding groove, allowing it to preferentially bind autoantigenic peptides. A novel suggestive association within the chromosome 3 p21.31 region suggests a role for *CCR5*.**

Sporadic inclusion body myositis (IBM) is an acquired muscle disease characterized clinically by weakness and muscle wasting, predominantly of the quadriceps and long finger flexor muscles. While degenerative changes are recognized, there are also immune-mediated mechanisms at play, characterized by inflammatory features in muscle biopsy specimens and the presence of circulating autoantibodies. These autoantibodies include anti-Ro and a recently identified autoantibody directed against cytosolic 5′-nucleotidase 1A (anti-cN1A), which is present in approximately one-third of patients (1,2). While the primary cause of the disease remains unknown, genetic factors may influence disease susceptibility. A group of hereditary diseases that includes the hereditary inclusion body myopathies and other muscular dystrophies such as the myofibrillary myopathies may mimic clinical features of IBM (3). These diseases may also exhibit similar pathologic features, such as rimmed vacuoles and protein accumulations; clinical and histopathologic suspicion of these diseases should prompt appropriate genetic testing.

To date, the strongest genetic risk identified for IBM lies within the major histocompatibility complex (MHC), in particular with HLA–DRB1*03:01, an allele present on the 8.1 ancestral haplotype that is a risk factor for many autoimmune diseases, including the idiopathic inflammatory myopathies (IIMs) (4). Other HLA–DRB1 alleles such as HLA–DRB1*01:01 and HLA–DRB1*13:01 have also been implicated in IBM, and genotypic combinations of these alleles have been reported to correlate with clinical phenotype (5).

Candidate gene studies in IBM have focused mainly on the MHC, and there are few validated associations outside of this region. Genes associated with neurodegenerative diseases such as Alzheimer's Disease have been examined in IBM, for example, the genes for β/A4-amyloid precursor protein and apolipoprotein E, although these studies frequently have shown negative or conflicting results (6–8). Other candidate gene approaches have focused on autoantibody targets (1) and genes previously implicated in hereditary inclusion body myopathies (9,10). However, those studies also have failed to find significant common associations.

We recently reported a genetic association study in polymyositis (PM) and dermatomyositis (DM) using the Immunochip array, a custom-designed, high-density genotyping chip that covers genes known to be associated with a variety of autoimmune diseases (11). Samples from patients with IBM were genotyped concurrently and were analyzed separately in this analysis using a previously described method of case–control matching to control for population differences. Using the Immunochip, we have conducted the largest genetic study to date in IBM to investigate potential associations with immune-related genes, and we have used imputation to refine associations within the MHC.

PATIENTS AND METHODS

Study populations. A total of 252 patients with IBM from 11 countries were recruited through the Myositis Genetics Consortium (MYOGEN). A list of MYOGEN study investigators in addition to the authors of this article is provided in Appendix A. Written informed consent was obtained from all patients with approval from research ethics boards at each participating center. Patients with IBM were included if they fulfilled the following criteria: Griggs ("definite" or "possible") (12), Medical Research Council ("pathologically defined," "clinically defined," or "possible") (13), or European Neuromuscular Centre ("clinico-pathologically defined," "clinically defined," or "probable") (14). Age at onset for UK patients with IBM was the age at onset of first symptoms as recorded in the clinical record.

Shared control samples from Sweden (the Epidemiological Investigation of Rheumatoid Arthritis study), Spain, and The Netherlands were provided by the Rheumatoid Arthritis Consortium International (15), with control samples from the UK provided by the Wellcome Trust Case Control Consortium (16). Control samples from Italy, Norway, Belgium, and France were provided by the International Multiple Sclerosis Genetics Consortium (17). Polish and Hungarian control samples were provided by the Celiac Consortium (18), and German control samples were provided by the KORAgen consortium (19).

Table 1. Numbers of samples from patients with inclusion body myositis and ethnically matched controls included in the analysis after quality control, by country of origin*

	Patients	Controls
Australia	44	–
Belgium	6	23
Czech Republic	2	–
France	19	35
Germany	–	29
Hungary	2	7
Italy	2	44
The Netherlands	9	69
Norway	1	30
Poland	–	8
Sweden	31	97
Spain	8	28
UK	128	485
US	–	153
Total	252	1,008

* Control samples were shared from Immunochip consortia. Four controls for each patient were matched based on nearest neighbor by principal components analysis coordinates.

Genotyping and quality control. Genotyping was performed in accordance with Illumina's protocols in the UK (Centre for Genetics and Genomics Arthritis Research UK, University of Manchester, Manchester, UK) and the US (Feinstein Institute for Medical Research, Manhasset, NY). Standard quality control was performed as described previously (11). Four controls for each case were matched for ethnicity using principal components analysis coordinates using a method described previously (20).

Statistical analysis. Statistical analyses were performed in Plink version 1.7 (http://zzz.bwh.harvard.edu/plink/index.shtml) using a logistic regression applying an additive model. Sex and population differences were controlled for by including sex and the top 10 principal components as covariates. Significance was defined as $P < 5 \times 10^{-8}$. We also reported variants reaching a second tier of significance of $P < 2.25 \times 10^{-5}$, calculated using the genetic Type I Error Calculator (21). Odds ratios (ORs) are provided with 95% confidence intervals (95% CIs).

To investigate associations with HLA and age at onset, linear regressions were used, with P values less than 0.05 considered significant. Analyses were carried out using Stata statistical software version 13.1 (StataCorp).

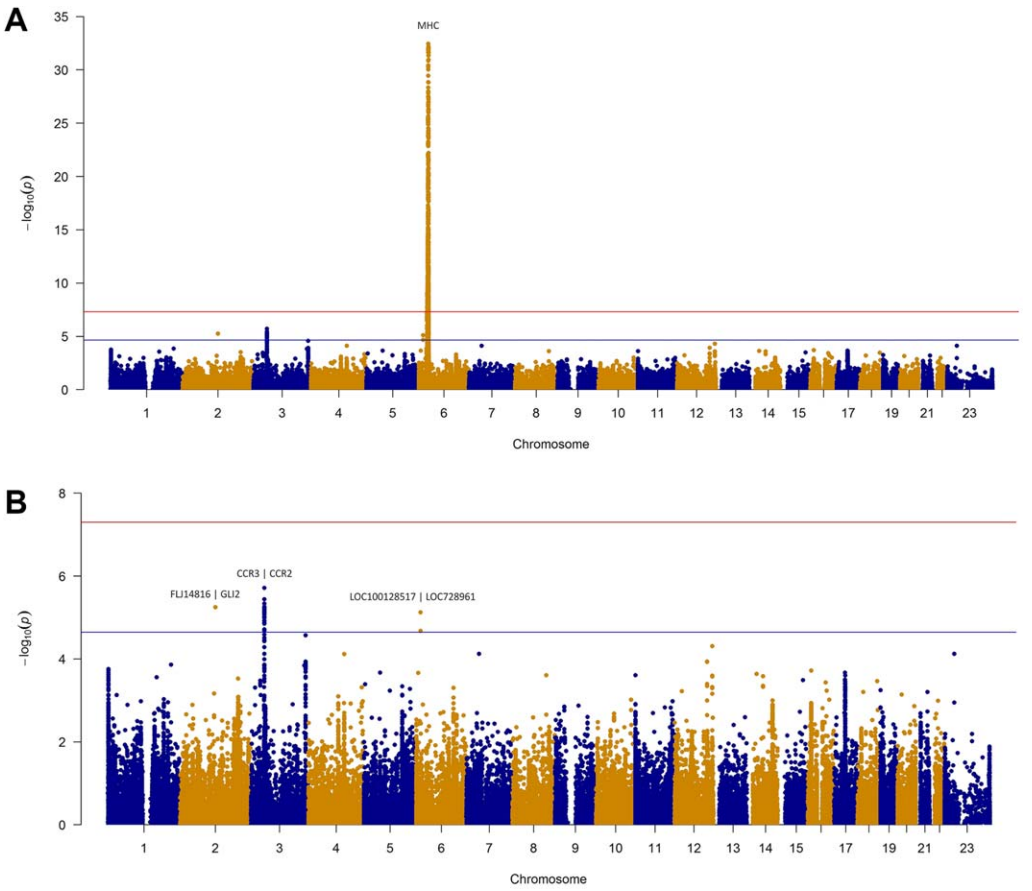

Figure 1. Manhattan plots of the inclusion body myositis (IBM) analysis. Red line represents genome-wide level of significance ($P < 5 \times 10^{-8}$); blue line represents suggestive significance ($P < 2.25 \times 10^{-5}$). Shown is the analysis of 252 patients with IBM and 1,008 matched controls. **A,** Manhattan plot of the total Immunochip analysis. **B,** Manhattan plot of the IBM analysis with the major histocompatibility complex (MHC) region (chromosome 6 25–35) removed for visualization purposes. Color figure can be viewed in the online issue, which is available at http://onlinelibrary.wiley.com/journal/doi/10.1002/art.40045/abstract.

Functional annotation. Evidence for functional effects and expression quantitative trait loci (eQTLs) were investigated for the lead single-nucleotide polymorphisms (SNPs) in each region, and SNPs in high linkage disequilibrium (LD) ($r^2 \geq 0.8$) were obtained from Phase 3 1000 Genomes data using LDlink (22).

MHC imputation and association analysis. Classic HLA alleles and corresponding amino acid sequences were imputed from Immunochip SNP data using the SNP2HLA program as described previously (11). Significance was defined as $P < 6.8 \times 10^{-6}$ based on a Bonferroni correction of the 7,323 markers imputed by SNP2HLA (23). For consistency, the most associated variant was used in the stepwise conditional analysis. Molecular graphics were generated and analyses were performed with the University of California, San Francisco (UCSF) Chimera package version 1.10.2 (Resource for Biocomputing, Visualization, and Informatics at UCSF).

Anti-cN1A detection. Enzyme-linked immunosorbent assay detection of anti-cN1A antibodies was performed using the optimized protocol as described previously (24). Briefly, biotinylated peptides were incubated on Streptawell High Bind microplates (Roche) for 1 hour at 37°C to immobilize the peptides. Unbound peptides were removed by washing the microplates 3 times. Diluted patient serum was then added to the microplate followed by incubation at 37°C for 1 hour. Unbound antigen was removed by further washing the microplate 5 times. Diluted rabbit anti-human Ig was then added, and the plate was incubated for 1 hour at 37°C followed by a further 5 washes. Finally, the bound antibodies were visualized by adding substrate solution, and the reaction was stopped after 5 minutes by adding a stop solution. Signals were quantified by determining optical densities at 450 nm ($OD_{450\ nm}$). The $OD_{450\ nm}$ value corresponding to the highest Youden Index [calculated as: ([sensitivity/100] + [specificity/100] − 1)] (25) at which ≥98% specificity was achieved was chosen for each peptide. Sera were assessed as reactive if they were above the established cutoff value for at least one of the peptide antigens (24).

RESULTS

Genotyping quality control. After stringent SNP and sample quality control, we analyzed 104,636 genetic variants in 252 patients with IBM and 1,008 ethnically matched controls (Table 1). Including the top 10 principal components as covariates and calculating the genomic inflation on a set of null SNPs gave a λ_{gc} of 1.04, indicating that patients and controls were well matched for ethnicity (see Supplementary Figure 1, available on the *Arthritis & Rheumatology* web site at http://onlinelibrary.wiley.com/doi/10.1002/art.40045/abstract).

HLA is the most strongly associated region in IBM. SNPs within the MHC region were the only variants reaching genome-wide significance of $P < 5 \times 10^{-8}$ (Figure 1A). The strongest association was with rs3129950 ($P = 3.58 \times 10^{-33}$), a SNP intronic of *LOC101929163* and 3′ of *BTNL2* (Table 2). As the Immunochip contains high-density SNP coverage across the MHC, this region was subsequently analyzed separately using HLA imputation in an attempt to refine this association to a functional gene. Initially, genes independent of the MHC were investigated that reached a suggestive level of significance.

Suggestive significance of 3 non-HLA associations. Three non-HLA regions reached our second tier of significance (defined as $P < 2.25 \times 10^{-5}$) calculated using the genetic Type I Error Calculator (21). Figure 1B shows the Manhattan plot with the MHC region removed for visualization purposes. The most convincing associations were in the chromosome 3 p21.31 region, where 49 SNPs reached the suggestive level of significance (Figure 2). The strongest association was upstream of *CCR2* (rs112088397, $P = 1.93 \times 10^{-6}$, OR 0.42 [95% CI 0.29–0.60]); however, this haplotype contains many genes including *CCR3*, *CCR2*, *CCR5*, and *CCRL2*.

Potentially functional variants were investigated for all non-HLA SNPs reaching suggestive significance and those tagged by the lead SNP ($r^2 \geq 0.8$) (see Supplementary

Table 2. Analysis of the 252 patients with inclusion body myositis compared to 1,008 ethnically matched controls*

Gene region	Chr.	Position	SNP	Minor allele	MAF in patients	MAF in controls	*P*	OR (95% CI)	Localization of LD to nearest genes ($r^2 \geq 0.9$)
MHC	6	32358201	rs3129950	C	0.34	0.11	3.58×10^{-33}†	5.69 (4.28–7.55)	*MHC*
CCR3/CCR2	3	46389462	rs112088397	T	0.08	0.16	1.93×10^{-6}‡	0.42 (0.29–0.60)	Downstream of *CCR3* to intron 2 of *LTF*; incorporating *CCR2*, *CCR5*, and *CCRL2*
FLJ14816/GLI2	2	121338584	rs1880542	T	0.56	0.45	5.66×10^{-6}‡	1.60 (1.31–1.96)	Intergenic of *FLJ14816* and *GLI2*
LOC100128517/ LOC728961	6	14560180	rs9396510	T	0.11	0.05	7.52×10^{-6}‡	2.23 (1.57–3.17)	Intergenic of *LOC100128517* and *LOC728961*

* Coordinates are based on the human assembly GRCh37. Chr. = chromosome; SNP = single-nucleotide polymorphism; MAF = minor allele frequency; OR = odds ratio; 95% CI = 95% confidence interval; LD = linkage disequilibrium.
† Reported at genome-wide significance ($P < 5 \times 10^{-8}$).
‡ Reported at second tier of significance ($P < 2.25 \times 10^{-5}$).

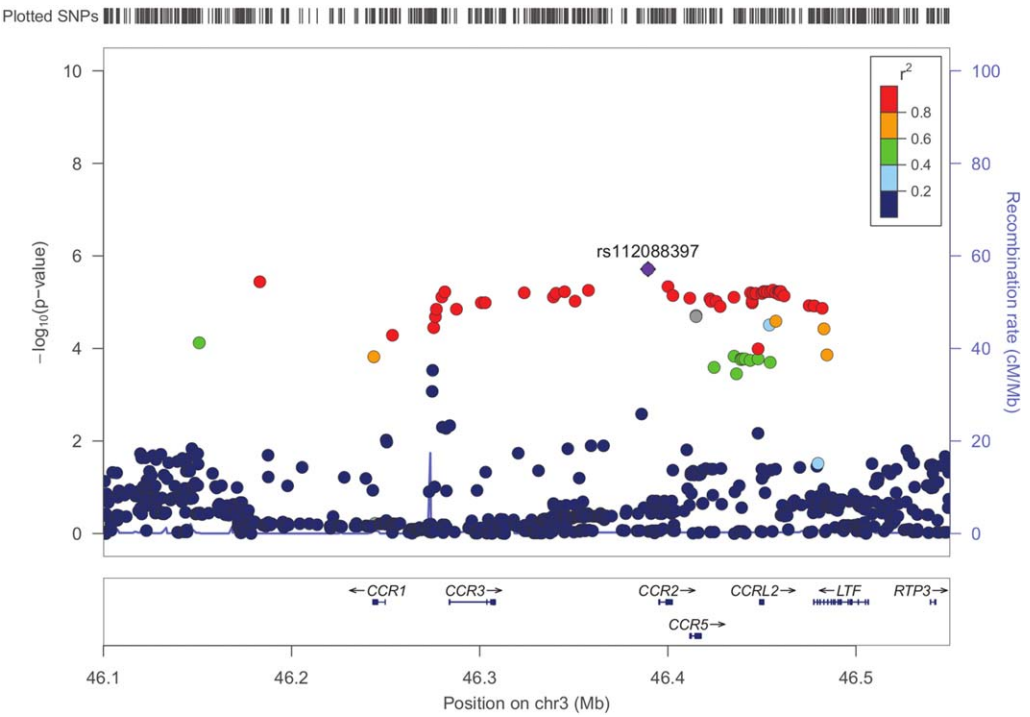

Figure 2. Regional association plot of the chromosome 3 (Chr3) p21.31 region in inclusion body myositis. The plot shows strength of association ($-\log_{10}[P]$) against chromosomal position. The most strongly associated single-nucleotide polymorphism (SNP) is colored purple, with other SNPs colored by the degree of linkage disequilibrium (r^2). Local recombination rates estimated from the HapMap population of Utah residents with ancestry from northern and western Europe are plotted against the secondary y-axis, showing recombination hotspots across the region.

Tables 1–3, http://onlinelibrary.wiley.com/doi/10.1002/art.40045/abstract). Multiple SNPs within the chromosome 3 p21.31 region had evidence for eQTLs for the expression of *CCR5* in monocytes (26). There was 1 missense SNP in the chromosome 3 p21.31 region (rs6441977) that was predicted to be "benign" by PolyPhen-2 (27); however, a frameshift mutation (rs333) is a known variant that results in a 32-bp deletion and a nonfunctional receptor. Conditional analysis on this locus did not identify additional independent variants.

HLA imputation reveals association with HLA–DRB1. To refine associations within the MHC region, HLA alleles were imputed from SNP genotyping information using SNP2HLA (23). Variants reaching statistical significance ($P < 6.8 \times 10^{-6}$) after each round of conditioning are included in Supplementary Tables 4–6, http://onlinelibrary.wiley.com/doi/10.1002/art.40045/abstract. The strongest associations were with alleles that are part of the 8.1 ancestral haplotype, with HLA–DRB1*03:01 reaching $P = 5.77 \times 10^{-34}$ (OR 7.97 [95% CI 5.88–10.95]). Due to strong LD within the MHC, other alleles within this haplotype such as HLA–DQB1*02:02 and HLA–B*08:01 also had strong associations in this analysis; however, these lost significance after conditioning on the effect of HLA–DRB1*03:01. Conducting stepwise conditional analysis on significant HLA–DRB1 alleles, an independent effect was seen with HLA–DRB1*01:01 ($P = 1.56 \times 10^{-16}$, OR 4.64 [95% CI 3.33–6.49]). A further independent effect was seen with HLA–DRB1*13:01 ($P = 3.28 \times 10^{-8}$, OR 3.19 [95% CI 2.14–4.72]).

As risk may lie within multiple HLA alleles, we imputed amino acids to investigate whether shared positions within risk alleles might explain the risk at this locus (see Supplementary Tables 7 and 8, http://onlinelibrary.wiley.com/doi/10.1002/art.40045/abstract). Amino acid position 26 of HLA–DRB1 was associated more significantly than a single classic HLA allele ($P = 5.22 \times 10^{-43}$), with risk attributable to a tyrosine at this position (OR 3.83 [95% CI 2.80–5.29]) (Table 3). This contrasts with PM and DM, where HLA–DRB1 amino acid position 77 was the most strongly associated position (Table 3). Conditioning on the effects of position 26 in IBM revealed an independent effect of position 11 of HLA–DRB1 ($P = 3.80 \times 10^{-13}$). At this position, serine is the most common amino acid in the population and was therefore used as the reference. As many other amino acids are protective at this position, we can infer that serine confers the greatest risk. No further amino acid positions were statistically significant after conditioning on positions 26 and 11 of HLA–DRB1.

Table 3. Independent associations of HLA–DRB1 amino acids in clinical subgroups of idiopathic inflammatory myopathy*

Association, marker	*P*	OR (95% CI)
Most associated in inclusion body myositis		
Position 26	Omnibus 5.22×10^{-43}	
Phenylalanine	Reference†	1
Tyrosine	1.19×10^{-16}	3.83 (2.8–5.29)
Leucine	0.32	0.63 (0.24–1.48)
Position 11	Omnibus 3.80×10^{-13}	
Serine	Reference†	1
Proline	9.06×10^{-5}	0.42 (0.27–0.64)
Valine	2.25×10^{-6}	0.33 (0.2–0.51)
Glycine	4.46×10^{-6}	0.26 (0.14–0.45)
Leucine	0.03	2.75 (1.15–7.5)
Aspartic acid	1.41×10^{-3}	0.13 (0.03–0.39)
Most associated in polymyositis‡		
Position 77	Omnibus 1.65×10^{-80}	
Threonine	Reference†	1
Asparagine	1.65×10^{-80}	2.93 (2.53–3.17)
Most associated in dermatomyositis‡		
Position 77	Omnibus 1.37×10^{-36}	
Threonine	Reference†	1
Asparagine	1.37×10^{-36}	2.14 (1.90–2.41)

* *P* values and odds ratios (ORs) with 95% confidence intervals (95% CIs) were calculated in a logistic regression.
† Reference amino acid is taken as the most frequent in the population.
‡ For comparative purposes, HLA–DRB1 amino acid association statistics for polymyositis and dermatomyositis are shown (from ref. 11).

No distinct HLA association with anti-cN1A positivity. Anti-cN1A antibodies were detected in 36 of the 104 patients serologically tested (35%). After quality control, HLA imputation was conducted on 35 anti-cN1A–positive patients and 140 healthy controls, and the most significant 4-digit classic HLA association was found with HLA–DRB1*03:01 ($P = 5.62 \times 10^{-8}$, OR 11.52 [95% CI 4.95–29.29]) (see Supplementary Table 9, http://onlinelibrary.wiley.com/doi/10.1002/art.40045/abstract). After stepwise conditional analysis, we did not find any additional independent effects. We then compared the 35 anti-cN1A–positive patients with 68 anti-cN1A–negative patients, and we found no significant differences in HLA associations between these groups (data not shown).

No effect of HLA–DRB1 allele interactions on age at onset. Previous studies have suggested that HLA–DRB1 alleles may have disease-modifying effects in IBM, with the HLA–DRB1*03/*01 genotype conferring an earlier age at onset and more severe muscle weakness (5,28). HLA and age at onset data were available for 124 UK patients with IBM. Linear regression was used to analyze the relationship of HLA–DRB1 alleles with age at onset. No significant associations were found with risk alleles HLA–DRB1*01:01, DRB1*03:01, or DRB1*13:01 when these were analyzed separately or in combination (see Supplementary Table 10, http://onlinelibrary.wiley.com/doi/10.1002/art.40045/abstract).

DISCUSSION

This is the largest genetic association study to date in Caucasian patients with IBM. The results confirm that HLA is the most strongly associated region, identify multiple HLA–DRB1 alleles conferring risk, and suggest amino acid positions that may explain the risk in this locus. A novel suggestive association within the chromosome 3 p21.31 locus indicates genetic overlap with other autoimmune diseases and identifies a potentially functional variant that may contribute to the pathogenesis of IBM.

HLA imputation confirmed that the strongest risk within this region lies with HLA–DRB1*03:01. Stepwise conditional analyses revealed additional independent associations with HLA–DRB1*01:01 and HLA–DRB1*13:01, suggesting that the HLA–DRB1 gene is important in susceptibility to IBM. In contrast to previous studies, there were no significant associations of age at onset with HLA–DRB1 alleles. Other reported disease-modifying effects of HLA alleles in IBM, such as with disease severity and lower quadriceps muscle strength, were not investigated due to a lack of consistent clinical data across this multinational, multicenter study. Previous studies have also investigated additional risk factors present on the MHC, such as polymorphisms in the gene for Notch-4 (29) or carriage of secondary HLA–DRB loci such as HLA–DRB3 (30). Although not explicitly investigated in the present study, these associations are in strong linkage with the 8.1 ancestral haplotype, and we do not expect our data to differentiate between these risk factors. Conditioning on the presence of HLA–DRB1, no additional genetic variants within the MHC region were associated with IBM. The frequency of genotypes among patients with IBM (see Supplementary Table 10, http://onlinelibrary.wiley.com/doi/10.1002/art.40045/abstract) suggests that patients homozygous for HLA–DRB1*03:01 and DRB1*01:01 are at lower risk of disease. The contribution of nonadditive effects across HLA alleles has been reported in several autoimmune diseases and may explain higher risk for heterozygote individuals (31). The small numbers in this cohort mean that the study is underpowered to statistically test this in IBM.

As multiple HLA–DRB1 alleles were associated with IBM, we investigated whether there were shared amino acid positions within HLA–DRB1 risk alleles that might explain the risk at this locus. Position 26 of HLA–DRB1 was more strongly associated than a classic HLA allele alone ($P = 5.22 \times 10^{-43}$ versus $P = 5.77 \times 10^{-34}$). An additional independent effect was found

Figure 3. Locations of positions 26 and 11 of HLA–DRB1 within DR β-chain 1. Positions 26 and 11 are independently associated with inclusion body myositis. **Arrows** indicate the locations of the risk-conferring amino acids Tyr^{26} and Ser^{11} within the β-sheet floor of DR β-chain 1. Color figure can be viewed in the online issue, which is available at http://onlinelibrary.wiley.com/journal/doi/10.1002/art.40045/abstract.

with position 11 of HLA–DRB1. Positions 11 and 26 have been associated previously with seropositive autoimmune disease, such as systemic lupus erythematosus (32), which suggests that these positions may determine properties of the HLA–DRB1 peptide-binding groove, allowing it to preferentially bind autoantigenic peptides (Figure 3). Certain amino acids, such as a tyrosine at position 26 and serine at position 11, were associated with risk in this analysis; however, a lack of statistical power means that we were unable to completely characterize the effects of certain amino acids in this molecule. It is interesting to note that while IBM shares HLA–DRB1*03:01 as a significant risk factor with other inflammatory myopathies, such as PM and DM, the amino acid associations differ between these subtypes. In PM and DM, amino acid position 74 of HLA–DRB1 explains almost all of the risk within this gene (11). These differences in amino acid associations may be explained by the additional independent effects of HLA–DRB1*01:01 and HLA–DRB1*13:01 in IBM that are not associated with PM or DM. Understanding the peptide-binding specificities of these risk alleles may inform future research along with the potential identification of unique autoantigens presented to the immune system in IBM.

We investigated potential associations between specific HLA alleles and the newly described anti-cN1A antibody. The significant association observed with HLA–DRB1*03:01 and the anti-cN1A antibody may be due to an increased association with HLA–DRB1*03:01 as a whole in IBM. No significant differences in HLA associations were observed between anti-cN1A–positive and anti-cN1A–negative patients. A recent study in an Australian cohort of patients also failed to show any association with anti-cN1A antibodies and MHC class II alleles other than HLA–DR3 (33). Furthermore, we do not have complete data on co-occurrence of anti-cN1A and other antibodies, such as anti-Ro, which also has a strong HLA–DR3 association (34). It may be that a significantly larger sample size is needed to detect novel HLA associations in patients with anti-cN1A antibodies.

The Immunochip is a custom-designed chip that contains a dense set of SNPs covering 186 loci based on evidence of association with 12 different autoimmune and inflammatory diseases (18). Therefore, the current study tests a specific hypothesis that IBM shares genetic overlap with other autoimmune diseases. The current study has not comprehensively tested other loci that have been purported to be associated with IBM, such as those predisposing to hereditary inclusion body myopathies or loci associated with other degenerative diseases. The observation that the MHC region is strongly associated, and evidence of association with other genes on

this array, suggests an immune-mediated component to IBM. It is not clear whether this represents a primary or secondary involvement.

No non-HLA loci investigated reached genome-wide significance, although this is to be expected in a study of this size. While comparatively large for IBM, this study is underpowered to detect associations of small effect sizes that are expected in genetic studies of conditions with complex etiologies. Three loci did reach a suggestive level of significance ($P < 2.25 \times 10^{-5}$). Of particular interest is the chromosome 3 p21.31 region, which is known to be associated with multiple autoimmune diseases such as celiac disease, type 1 diabetes mellitus, and Behçet's disease and is suggestively associated in juvenile idiopathic arthritis (JIA) (35–38). The strongest association in this region was with rs112088397, which tags a large haplotype block where many additional SNPs reached a suggestive level of significance and is the same risk haplotype as that reported in JIA ($r^2 = 0.87$) (35,39). The variant rs112088397 in our study is found at a higher frequency in controls (minor allele frequency [MAF] of 0.08 for patients versus MAF of 0.16 for controls) and is therefore protective against IBM (OR 0.42 [95% CI 0.29–0.60]). Proxies for rs112088397 fall within multiple candidate genes including *CCR1*, *CCR3*, *CCR2*, *CCR5*, and *CCRL2*, and therefore it is difficult to identify the causal variant in this region. Interestingly, this haplotype contains a frameshift mutation (rs333) that results in a 32-bp deletion variant (CCR5Δ32) and a nonfunctional receptor. The most strongly associated non-HLA SNP in IBM is in high LD with this frameshift mutation ($r^2 = 0.86$); furthermore, a number of SNPs in this region are eQTLs for the expression of *CCR5* in monocytes (26).

CCR5 binds a number of proinflammatory chemokines that are up-regulated in IIMs and IBM, such as CCL3 (macrophage inflammatory protein 1α [MIP-1α]), CCL4 (MIP-1β), and CCL5 (RANTES). CCR5 has been shown to be predominantly expressed on monocytes, macrophages, and T cells, up-regulated in IBM muscle tissue, and localized on inflammatory cells invading nonnecrotic muscle fibers (40,41). Interestingly, in rheumatoid arthritis (RA) the density of CCR5 molecules on the T cell surface determines efficiency of its function as a chemokine receptor and intensity of T cell migration toward RA synoviocytes (42). We hypothesize that CCR5 is important in the pathogenesis of IBM, consistent with studies showing an up-regulation of CCR5 in muscle tissue of patients. Individuals with the protective rs333 frameshift mutation described above will carry a nonfunctional variant and/or decreased expression of CCR5, resulting in reduced migration of T cells into muscle fiber.

It is interesting that the suggestive association with the chromosome 3 p21.31 region in this study was found with only 252 individuals. This may be explained by the stronger effect size in IBM compared to JIA (0.42 versus 0.78, respectively) (35), and although IBM is a rare disease, it may mean that replication of this association is possible with ongoing sample collection. Due to the rarity of IBM, it is difficult to ascertain the sample sizes needed for genome-wide association studies; therefore, next-generation sequencing could be an approach to detect rare, potentially functional variants of large effect size. Sequencing studies are currently underway taking either a candidate gene approach (10) or a hypothesis-free approach sequencing exomes of a large number of patients with IBM (9). The present study has not comprehensively tested other loci that have been purported to be associated with IBM, such as those predisposing to hereditary inclusion body myopathies or loci associated with other degenerative diseases. In a disease in which the etiology is unknown, sequencing could be successful in identifying novel variants and/or pathways involved in disease pathogenesis.

In summary, we have conducted the largest genetic association study to date in Caucasian patients with IBM, confirming the involvement of an immune-mediated genetic component of this understudied disease. Studies in the genetics of IBM are hampered by small sample sizes due to the rarity of this disease. Ongoing sample collection, as well as further international collaborative studies, will allow us to further characterize genetic influences on susceptibility to IBM.

ACKNOWLEDGMENTS

We thank all of the patients and their families who contributed to this study. We thank Mr. Paul New (Salford Royal Foundation Trust) for ethical and technical support. The authors would like to acknowledge the assistance given by IT Services and the use of the Computational Shared Facility at The University of Manchester. A list of other acknowledgments is included in Supplementary Materials, available on the *Arthritis & Rheumatology* web site at http://onlinelibrary.wiley.com/doi/10.1002/art.40045/abstract.

AUTHOR CONTRIBUTIONS

All authors were involved in drafting the article or revising it critically for important intellectual content, and all authors approved the final version to be published. Dr. Rothwell had full access to all of the data in the study and takes responsibility for the integrity of the data and the accuracy of the data analysis.

Study conception and design. Rothwell, Cooper, Lundberg, Gregersen, Ollier, Lamb, Chinoy.

Acquisition of data. Rothwell, Cooper, Lundberg, Gregersen, Hanna, Machado, Herbert, Pruijn, Roberts, Vencovsky, Danko, Limaye, Selva-O'Callaghan, Platt, Molberg, Benveniste, Radstake, Doria, De Bleecker, De Paepe, Gieger, Meitinger, Winkelmann, Padyukov, Lee, Lamb, Chinoy.

Analysis and interpretation of data. Rothwell, Cooper, Lundberg, Lilleker, Bowes, Seldin, Amos, Ollier, Padyukov, Lamb, Chinoy.

REFERENCES

1. Larman HB, Salajegheh M, Nazareno R, Lam T, Sauld J, Steen H, et al. Cytosolic 5′-nucleotidase 1A autoimmunity in sporadic inclusion body myositis. Ann Neurol 2013;73:408–18.
2. Pluk H, van Hoeve BJ, van Dooren SH, Stammen-Vogelzangs J, van der Heijden A, Schelhaas HJ, et al. Autoantibodies to cytosolic 5′-nucleotidase 1A in inclusion body myositis. Ann Neurol 2013;73:397–407.
3. Needham M, Mastaglia FL. Inclusion body myositis: current pathogenetic concepts and diagnostic and therapeutic approaches. Lancet Neurol 2007;6:620–31.
4. Miller FW, Chen W, O'Hanlon TP, Cooper RG, Vencovsky J, Rider LG, et al. Genome-wide association study identifies HLA 8.1 ancestral haplotype alleles as major genetic risk factors for myositis phenotypes. Genes Immun 2015;16:470–80.
5. Rojana-udomsart A, James I, Castley A, Needham M, Scott A, Day T, et al. High-resolution HLA-DRB1 genotyping in an Australian inclusion body myositis (s-IBM) cohort: an analysis of disease-associated alleles and diplotypes. J Neuroimmunol 2012;250:77–82.
6. Sivakumar K, Cervenakova L, Dalakas MC, Leon-Monzon M, Isaacson SH, Nagle JW, et al. Exons 16 and 17 of the amyloid precursor protein gene in familial inclusion body myopathy. Ann Neurol 1995;38:267–9.
7. Needham M, Hooper A, James I, van Bockxmeer F, Corbett A, Day T, et al. Apolipoprotein ϵ alleles in sporadic inclusion body myositis: a reappraisal. Neuromuscul Disord 2008;18:150–2.
8. Gang Q, Bettencourt C, Machado PM, Fox Z, Brady S, Healy E, et al. The effects of an intronic polymorphism in TOMM40 and APOE genotypes in sporadic inclusion body myositis. Neurobiol Aging 2015;36:1766.e1–3.
9. Gang Q, Bettencourt C, Machado P, Hanna MG, Houlden H. Sporadic inclusion body myositis: the genetic contributions to the pathogenesis. Orphanet J Rare Dis 2014;9:88.
10. Weihl CC, Baloh RH, Lee Y, Chou TF, Pittman SK, Lopate G, et al. Targeted sequencing and identification of genetic variants in sporadic inclusion body myositis. Neuromuscul Disord 2015;25:289–96.
11. Rothwell S, Cooper RG, Lundberg IE, Miller FW, Gregersen PK, Bowes J, et al. Dense genotyping of immune-related loci in idiopathic inflammatory myopathies confirms HLA alleles as the strongest genetic risk factor and suggests different genetic background for major clinical subgroups. Ann Rheum Dis 2016;75:1558–66.
12. Griggs RC, Askanas V, DiMauro S, Engel A, Karpati G, Mendell JR, et al. Inclusion body myositis and myopathies. Ann Neurol 1995;38:705–13.
13. Hilton-Jones D, Miller A, Parton M, Holton J, Sewry C, Hanna MG. Inclusion body myositis. MRC Centre for Neuromuscular Diseases, IBM workshop, London, 13 June 2008. Neuromuscul Disord 2010;20:142–7.
14. Rose MR. 188th ENMC International Workshop: inclusion body myositis, 2–4 December 2011, Naarden, The Netherlands. Neuromuscul Disord 2013;23:1044–55.
15. Eyre S, Bowes J, Diogo D, Lee A, Barton A, Martin P, et al. High-density genetic mapping identifies new susceptibility loci for rheumatoid arthritis. Nat Genet 2012;44:1336–40.
16. Wellcome Trust Case Control Consortium. Genome-wide association study of 14,000 cases of seven common diseases and 3,000 shared controls. Nature 2007;447:661–78.
17. International Multiple Sclerosis Genetics Consortium, Beecham AH, Patsopoulos NA, Xifara DK, Davis MF, Kemppinen A, et al. Analysis of immune-related loci identifies 48 new susceptibility variants for multiple sclerosis. Nat Genet 2013;45:1353–60.
18. Trynka G, Hunt KA, Bockett NA, Romanos J, Mistry V, Szperl A, et al. Dense genotyping identifies and localizes multiple common and rare variant association signals in celiac disease. Nat Genet 2011;43:1193–201.
19. Wichmann HE, Gieger C, Illig T, for the MONICA/KORA Study Group. KORA-gen: resource for population genetics, controls and a broad spectrum of disease phenotypes. Gesundheitswesen 2005;67 Suppl 1:S26–30.
20. Gregersen PK, Kosoy R, Lee AT, Lamb J, Sussman J, McKee D, et al. Risk for myasthenia gravis maps to a ^{151}Pro→Ala change in TNIP1 and to HLA-B*08. Ann Neurol 2012;72:927–35.
21. Li MX, Yeung JMY, Cherny SS, Sham PC. Evaluating the effective numbers of independent tests and significant p-value thresholds in commercial genotyping arrays and public imputation reference datasets. Hum Genet 2012;131:747–56.
22. Machiela MJ, Chanock SJ. LDlink: A web-based application for exploring population-specific haplotype structure and linking correlated alleles of possible functional variants. Bioinformatics 2015;31:3555–7.
23. Jia X, Han B, Onengut-Gumuscu S, Chen WM, Concannon PJ, Rich SS, et al. Imputing amino acid polymorphisms in human leukocyte antigens. PLoS One 2013;8:e64683.
24. Herbert MK, Stammen-Vogelzangs J, Verbeek MM, Rietveld A, Lundberg IE, Chinoy H, et al. Disease specificity of autoantibodies to cytosolic 5′-nucleotidase 1A in sporadic inclusion body myositis versus known autoimmune diseases. Ann Rheum Dis 2016;75:696–701.
25. Youden WJ. Index for rating diagnostic tests. Cancer 1950;3:32–5.
26. Zeller T, Wild P, Szymczak S, Rotival M, Schillert A, Castagne R, et al. Genetics and beyond: the transcriptome of human monocytes and disease susceptibility. PLoS One 2010;5:e10693.
27. Adzhubei I, Jordan DM, Sunyaev SR. Predicting functional effect of human missense mutations using PolyPhen-2. Curr Protoc Hum Genet 2013;7:7.20.
28. Mastaglia FL, Needham M, Scott A, James I, Zilko P, Day T, et al. Sporadic inclusion body myositis: HLA-DRB1 allele interactions influence disease risk and clinical phenotype. Neuromuscul Disord 2009;19:763–5.
29. Scott AP, Laing NG, Mastaglia F, Dalakas M, Needham M, Allcock RJ. Investigation of NOTCH4 coding region polymorphisms in sporadic inclusion body myositis. J Neuroimmunol 2012;250:66–70.
30. Rojana-udomsart A, Mitrpant C, James I, Witt C, Needham M, Day T, et al. Analysis of HLA-DRB3 alleles and supertypical genotypes in the MHC class II region in sporadic inclusion body myositis. J Neuroimmunol 2013;254:174–7.
31. Lenz TL, Deutsch AJ, Han B, Hu X, Okada Y, Eyre S, et al. Widespread non-additive and interaction effects within HLA loci modulate the risk of autoimmune diseases. Nat Genet 2015;47:1085–90.
32. Kim K, Bang SY, Lee HS, Okada Y, Han B, Saw WY, et al. The HLA-DRβ1 amino acid positions 11-13-26 explain the majority of SLE-MHC associations. Nat Commun 2014;5:5902.
33. Limaye VS, Lester S, Blumbergs P, Greenberg SA. Anti- C N1A antibodies in South Australian patients with inclusion body myositis. Muscle Nerve 2016;53:654–5.
34. Provost TT, Watson R. Anti-Ro(SS-A) HLA-DR3-positive women: the interrelationship between some ANA negative, SS, SCLE, and NLE mothers and SS/LE overlap female-patients. J Invest Dermatol 1993;100:S14–20.
35. Hinks A, Cobb J, Marion MC, Prahalad S, Sudman M, Bowes J, et al. Dense genotyping of immune-related disease regions identifies 14 new susceptibility loci for juvenile idiopathic arthritis. Nat Genet 2013;45:664–9.
36. Dubois PC, Trynka G, Franke L, Hunt KA, Romanos J, Curtotti A, et al. Multiple common variants for celiac disease influencing immune gene expression. Nat Genet 2010;42:295–302.
37. Kirino Y, Bertsias G, Ishigatsubo Y, Mizuki N, Tugal-Tutkun I, Seyahi E, et al. Genome-wide association analysis identifies new susceptibility loci for Behçet's disease and epistasis between HLA-B*51 and ERAP1. Nat Genet 2013;45:202–7.
38. Onengut-Gumuscu S, Chen WM, Burren O, Cooper NJ, Quinlan AR, Mychaleckyj JC, et al. Fine mapping of type 1 diabetes susceptibility loci and evidence for colocalization of causal variants with lymphoid gene enhancers. Nat Genet 2015;47:381–6.

39. Hinks A, Martin P, Flynn E, Eyre S, Packham J, Childhood Arthritis Prospective Study (CAPS), UKRAG Consortium, BSPAR Study Group, et al. Association of the CCR5 gene with juvenile idiopathic arthritis. Genes Immun 2010;11:584–9.
40. Civatte M, Bartoli C, Schleinitz N, Chetaille B, Pellissier JF, Figarella-Branger D. Expression of the β chemokines CCL3, CCL4, CCL5 and their receptors in idiopathic inflammatory myopathies. Neuropathol Appl Neurobiol 2005;31:70–9.
41. De Paepe B, de Bleecker JL. β-chemokine receptor expression in idiopathic inflammatory myopathies. Muscle Nerve 2005;31:621–7.
42. Desmetz C, Lin YL, Mettling C, Portalès P, Noël D, Clot J, et al. Cell surface CCR5 density determines the intensity of T cell migration towards rheumatoid arthritis synoviocytes. Clin Immunol 2007;123:148–54.

APPENDIX A: MYOGEN INVESTIGATORS

Study investigators of the Myositis Genetics Consortium, in addition to the authors of this article, are as follows: Drs. Christopher Denton (Royal Free Hospital, London, UK), Karina Gheorghe (Karolinska Institutet, Stockholm, Sweden), David Hilton-Jones (John Radcliffe Hospital, Oxford, UK), Patrick Kiely (St. George's Hospital, London, UK), and Herman Mann (Institute of Rheumatology, Prague, Czech Republic).

DOI: 10.1002/art.40078

Clinical Images: Widening of joint spaces in acromegaly

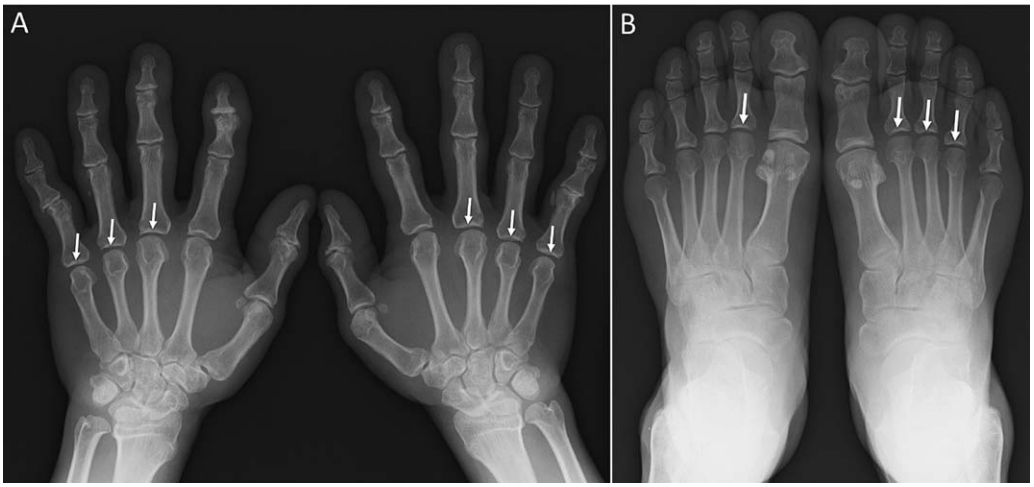

The patient, a previously healthy 51-year-old man, presented with migratory joint pain on the lower extremities lasting for several months. His shoe size had increased by 0.6 inches. Physical examination revealed enlargement of the fingers and toes. Radiography of the hands (**A**) and feet (**B**) showed widening of the joint spaces on some of the metacarpophalangeal and metatarsophalangeal joints (**arrows**), along with tufting of the terminal phalanges. The serum insulin-like growth factor 1 concentration was 1,380 mg/ml (normal 87–243). Magnetic resonance imaging of the pituitary gland (T1-weighted image with contrast) showed a poorly enhanced tumor of 9 mm in the sella turcica. Acromegaly was diagnosed and the brain tumor was resected. Acromegaly is characterized by acral enlargement, with initial presentation sometimes being hypertrophic arthropathy. Radiographs showing widening of joint space due to cartilage enlargement can be a clue to the diagnosis.

Masei Suda, MD
Yasuhiro Suyama, MD
Masato Okada, MD
St. Luke's International University and St. Luke's International Hospital Tokyo, Japan

39. Hinks A, Martin P, Flynn E, Eyre S, Packham J, Childhood Arthritis Prospective Study (CAPS), UKRAG Consortium, BSPAR Study Group, et al. Association of the CCR5 gene with juvenile idiopathic arthritis. Genes Immun 2010;11:584–9.
40. Civatte M, Bartoli C, Schleinitz N, Chetaille B, Pellissier JF, Figarella-Branger D. Expression of the β chemokines CCL3, CCL4, CCL5 and their receptors in idiopathic inflammatory myopathies. Neuropathol Appl Neurobiol 2005;31:70–9.
41. De Paepe B, de Bleecker JL. β-chemokine receptor expression in idiopathic inflammatory myopathies. Muscle Nerve 2005;31:621–7.
42. Desmetz C, Lin YL, Mettling C, Portalès P, Noël D, Clot J, et al. Cell surface CCR5 density determines the intensity of T cell migration towards rheumatoid arthritis synoviocytes. Clin Immunol 2007;123:148–54.

APPENDIX A: MYOGEN INVESTIGATORS

Study investigators of the Myositis Genetics Consortium, in addition to the authors of this article, are as follows: Drs. Christopher Denton (Royal Free Hospital, London, UK), Karina Gheorghe (Karolinska Institutet, Stockholm, Sweden), David Hilton-Jones (John Radcliffe Hospital, Oxford, UK), Patrick Kiely (St. George's Hospital, London, UK), and Herman Mann (Institute of Rheumatology, Prague, Czech Republic).

DOI: 10.1002/art.40078

Clinical Images: Widening of joint spaces in acromegaly

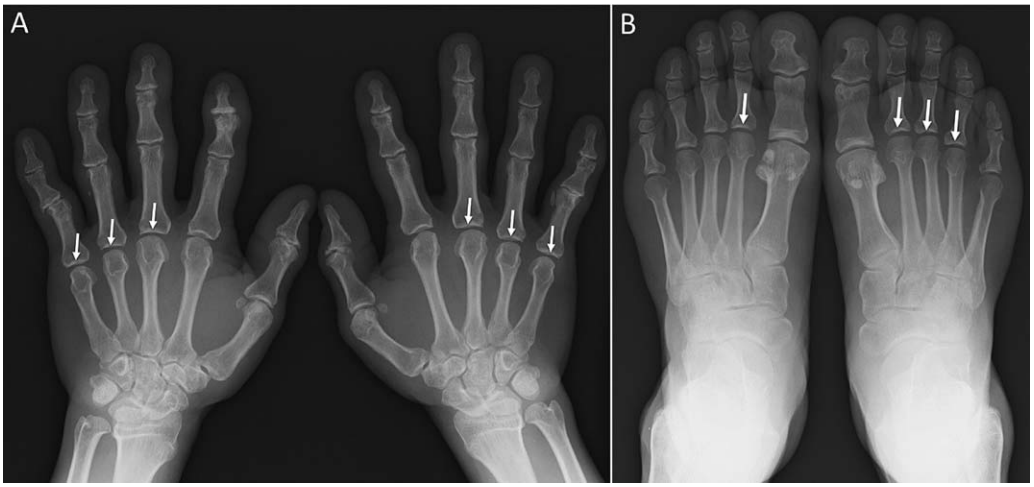

The patient, a previously healthy 51-year-old man, presented with migratory joint pain on the lower extremities lasting for several months. His shoe size had increased by 0.6 inches. Physical examination revealed enlargement of the fingers and toes. Radiography of the hands (**A**) and feet (**B**) showed widening of the joint spaces on some of the metacarpophalangeal and metatarsophalangeal joints (**arrows**), along with tufting of the terminal phalanges. The serum insulin-like growth factor 1 concentration was 1,380 mg/ml (normal 87–243). Magnetic resonance imaging of the pituitary gland (T1-weighted image with contrast) showed a poorly enhanced tumor of 9 mm in the sella turcica. Acromegaly was diagnosed and the brain tumor was resected. Acromegaly is characterized by acral enlargement, with initial presentation sometimes being hypertrophic arthropathy. Radiographs showing widening of joint space due to cartilage enlargement can be a clue to the diagnosis.

Masei Suda, MD
Yasuhiro Suyama, MD
Masato Okada, MD
St. Luke's International University and St. Luke's International Hospital Tokyo, Japan

ARTHRITIS & RHEUMATOLOGY
Vol. 69, No. 5, May 2017, pp 1100–1110
DOI 10.1002/art.40039

MicroRNA Expression Shows Inflammatory Dysregulation and Tumor-Like Proliferative Responses in Joints of Patients With Postinfectious Lyme Arthritis

Robert B. Lochhead,[1] Klemen Strle,[1] Nancy D. Kim,[1] Minna J. Kohler,[1] Sheila L. Arvikar,[1] John M. Aversa,[2] and Allen C. Steere[1]

Objective. **Lyme arthritis (LA) is caused by infection with *Borrelia burgdorferi* and usually resolves following spirochetal killing with antibiotics. However, in some patients, arthritis persists after antibiotic therapy. To provide insights into underlying pathogenic processes associated with antibiotic-refractory LA (postinfectious LA), we analyzed differences in microRNA (miRNA) expression between LA patients with active infection and those with postinfectious LA.**

Methods. **MicroRNA expression was assayed in synovial fluid (SF) from LA patients before and after oral and intravenous antibiotic therapy, and in synovial tissue obtained months after antibiotic therapy from patients with postinfectious LA. SF and tissue from patients with other forms of arthritis, such as rheumatoid arthritis (RA) and osteoarthritis, were used for comparison.**

Results. **SF from LA patients during active infection had marked elevations of white blood cells, particularly polymorphonuclear leukocytes, accompanied by elevated levels of microRNA-223 (miR-223). In contrast, SF from postantibiotic LA patients contained greater percentages of lymphocytes and mononuclear cells. SF from postantibiotic LA patients also exhibited marked inflammatory (miR-146a, miR-155), wound repair (miR-142), and proliferative (miR-17–92) miRNA signatures, and higher levels of these miRNAs correlated with longer arthritis duration. Levels of miR-146a, miR-155, miR-142, miR-223, and miR-17–92 were also elevated in synovial tissue in late postinfectious LA, and levels of let-7a were reduced, similar to RA.**

Conclusion. **During active infection, miRNA expression in SF reflected an immune response associated with bacterial killing, while in postinfectious LA, miRNA expression in SF and synovial tissue reflected chronic inflammation, synovial proliferation, and breakdown of wound repair processes, showing that the nature of the arthritis was altered after spirochetal killing.**

Bacterial infection normally elicits robust and effective immune responses. However, failure to resolve immune responses following pathogen clearance can result in tissue damage. These responses are tightly regulated by microRNAs (miRNAs), which are needed to enhance or limit a large number of biologic processes, including immune responses to infection (1).

MicroRNAs are small noncoding RNAs that bind the 3′-untranslated region of target messenger RNAs (mRNAs) and inhibit translation, thereby acting as fine-tuners of gene expression (2). MicroRNAs provide robustness to gene regulation (3), and defects in miRNAs can contribute to a number of pathologies, including inflammatory and autoimmune diseases (1). For example, a recent miRNA study showed that rheumatoid arthritis (RA), a chronic inflammatory autoimmune disease, had the most significant enrichment of miRNA–target gene risk factors of any disease studied (4). Moreover, mouse

Supported by the NIH (National Institute of Allergy and Infectious Diseases [NIAID] grant R01-AI-101175), the Littauer Foundation, the Roland Foundation, the English, Bonter, Mitchell Foundation, and Massachusetts General Hospital (Lyme Disease and Arthritis Research Fund). Dr. Lochhead's work was supported by National Institute of Arthritis and Musculoskeletal and Skin Diseases (NIAMS) grant T32-AR-007258 and NIAID grant F32-AI-126764 from the NIH. Dr. Strle's work was supported by NIAMS grant K01-AR-062098 from the NIH. Dr. Arvikar's work was supported by the Rheumatology Research Foundation (Scientist Development Award).

[1]Robert B. Lochhead, PhD, Klemen Strle, PhD, Nancy D. Kim, MD (current address: Merck Research Laboratories, Boston, Massachusetts), Minna J. Kohler, MD, Sheila L. Arvikar, MD, Allen C. Steere, MD: Massachusetts General Hospital and Harvard Medical School, Boston, Massachusetts; [2]John M. Aversa, MD: Yale University School of Medicine, New Haven, Connecticut.

Address correspondence to Robert B. Lochhead, PhD, Massachusetts General Hospital, CNY 148/8301, 55 Fruit Street, Boston, MA 02114. E-mail: rlochhead@mgh.harvard.edu.

Submitted for publication September 28, 2016; accepted in revised form January 5, 2017.

studies have shown that microRNA-155 (miR-155) (5), miR-223 (6), and miR-146a (7) directly modulate experimental models of arthritis, consistent with the role of miRNAs and other epigenetic regulatory factors in the pathogenesis of RA in humans (8).

Using mouse models of Lyme disease, we have shown that miR-146a and miR-155 are up-regulated during infection with the Lyme disease spirochete *Borrelia burgdorferi* and that they act as negative (miR-146a) and positive (miR-155) regulators of immune activation (9,10). These 2 miRNAs help to fine-tune the immune response, ensuring effective spirochetal killing while limiting tissue damage. Mice lacking either miR-146a or miR-155 have more severe Lyme arthritis (LA) or carditis, respectively, suggesting important roles for these miRNAs in balancing immune activation and tissue damage (9,10).

Other miRNAs associated with immune regulation and cell proliferation also show altered expression in joints of infected mice that developed severe LA (9). These include miR-142, associated with immune modulation (11,12) and tissue remodeling (13,14); miR-17–92 cluster, associated with cell proliferation and oncogenesis (15–17); and let-7 family members, associated with tumor suppression (18). However, to date, no studies have examined the role of miRNAs in Lyme disease in humans.

LA, the most common late manifestation of Lyme disease, is characterized by intermittent or persistent joint swelling and pain in one or a few large joints, especially the knee (19). In most patients, the arthritis resolves with spirochetal killing with oral or intravenous (IV) antibiotic therapy. However, in some patients, synovitis persists for months or years after antibiotic therapy. The synovial lesion in these patients shows synovial hypertrophy, vascular proliferation, and mononuclear cell infiltrates, which are also observed in other forms of chronic inflammatory arthritis, including RA (20). After antibiotic therapy, patients with antibiotic-refractory LA are treated with disease-modifying antirheumatic drugs (DMARDs), the standard treatment used for other inflammatory arthritides (21).

In this study, we assessed in LA patients the expression of miRNAs that have been previously associated with arthritis pathogenesis (22). We report that during active infection, miRNA expression reflected an immune response associated with bacterial killing, and joint swelling resolved when that was accomplished. However, following antibiotic therapy and in the absence of active infection, a subset of patients developed a marked proliferative synovitis, previously called antibiotic-refractory LA but hereafter termed postinfectious LA. In these patients, miRNA expression profiles reflected inflammatory and proliferative dysregulation involved in pathogenesis of postinfectious LA.

PATIENTS AND METHODS

Patients. The present study was approved by the Human Investigations Committee at Massachusetts General Hospital (MGH). All patients with Lyme disease met the Centers for Disease Control and Prevention criteria for *B burgdorferi* infection (23), and those with RA, psoriatic arthritis (PsA), undifferentiated inflammatory monoarthritis, or osteoarthritis (OA) met validated criteria for those diseases (24–27). LA patients received antibiotic therapy according to an algorithm (28), as detailed in the guidelines of the Infectious Diseases Society of America (29).

Sample collection. Patient synovial fluid (SF) was centrifuged at 300*g* for 10 minutes, then at 3,000*g* for 10 minutes, and stored at −80°C. Synovial tissue was collected from arthritis patients who underwent arthroscopic synovectomies. Tissue was placed immediately in RNA stabilization reagent and stored at −20°C.

RNA purification. RNA was recovered from 200 μl SF using a serum/plasmid miRNeasy kit (Qiagen) or from ~100 mg synovial tissue using an miRNeasy kit. Synovial tissue RNA quality was determined using a Bioanalyzer (Agilent).

SF miRNA expression. MicroRNAs in SF were assayed using miScript Human Serum & Plasma 384HC miRNA polymerase chain reaction (PCR) arrays (MIHS-3106ZG; Qiagen) on an LC-480 light cycler (Roche). Expression levels were normalized to the global geometric mean C_t of levels of all expressed miRNAs (C_t cutoff 35).

Synovial tissue miRNA expression. Small RNA libraries were generated using the NEBNext multiplex small RNA library prep set for Illumina (New England Biolabs). Quality was determined using a Bioanalyzer. Libraries were sequenced to a depth of ~2,500,000 50-bp reads (MiSeq Reagent Kit version 2; Illumina). Library preparation, sequencing, and bioinformatics were performed by the MGH NextGen Sequencing and Bioinformatics Core Facilities.

Statistical and pathway analysis. A Mann-Whitney U test was used to determine differences in clinical data between groups. Welch's *t*-test was used to determine differences in miRNA expression between groups. Pearson's correlation coefficients (r) were determined by correlation analysis. Differential expression analysis was used to determine differences in synovial tissue miRNA expression. MicroRNA/mRNA pathway analysis was performed using DIANA miRPath version 2 (30). Statistical significance ($P < 0.05$) was determined using GraphPad Prism software version 6.

RESULTS

Patient characteristics. During a 1.5-year period from October 2014 through February 2016, 34 LA patients were enrolled in our study, 18 of whom had evaluable SF samples available. Additionally, from 2004 to 2015, 14 LA patients underwent arthroscopic synovectomy, and evaluable synovial tissue from these patients was available. Thus, for this study, we evaluated 32 LA patients from whom we could obtain extracellular miRNA from SF or miRNA from synovial tissue. These patients were representative of the spectrum of disease severity and treatment responses seen in this disease (31). Because inflammation in LA is

Table 1. Characteristics of the study patients*

	Group 1, preantibiotic LA patients (n = 5)	Group 2, postantibiotic LA patients (n = 13)	Group 3, synovectomy patients (n = 14)
No. females/no. males	1/4	4/9	7/7
Age, mean (range) years	49 (34–71)	45 (17–76)	19.5 (11–58)
Borrelia burgdorferi infection			
B burgdorferi IgG titer, median (range) units	6,400 (1,600–25,600)	25,600 (800–25,600)	19,200 (6,400–25,600)
No. PCR positive/no. tested	2/4	0/7	0/14
Arthritis duration, median (range) months			
Prior to start of antibiotics	1 (0.25–2.5)	2 (0.5–13)	0.75 (0.25–20)
Prior to sample collection	1 (0.25–2.5)	6.5 (2.75–17)†	15.5 (4–48)†
Total	3.5 (1–13)	12.5 (8–26)†	15.5 (4–48)†
Arthritis resolved, no./total no. (%)			
After oral antibiotics	3/5 (60)	0/13 (0)	0/14 (0)
After IV antibiotics	2/2 (100)	2/13 (15)	0/14 (0)
After DMARDs‡	NA	9/11 (82)	0/12 (0)
After synovectomy‡	NA	1/1 (100)	12/14 (86)
SF characteristics, median (range)			
Effusion, ml	10 (5–66)	42 (10–95)	NA
Total WBC count, /mm^3	25,760 (11,282–42,793)	7,247 (2,480–22,180)†	NA
PMNs, %	90 (87–92)	63.5 (12–90)†	NA
Lymphocytes, %	4 (1–6)	22.5 (4–57)†	NA
Monocytes, %	7 (5–8)	11 (6–60)†	NA

* PCR = polymerase chain reaction; SF = synovial fluid; NA = not available; WBC = white blood cell; PMNs = polymorphonuclear leukocytes.
† $P < 0.05$ versus preantibiotic Lyme arthritis (LA) patients, by Mann-Whitney U test.
‡ The disease-modifying antirheumatic drug (DMARD) given was usually methotrexate. One patient in group 2 declined DMARD therapy, and her arthritis resolved 6 months following completion of intravenous (IV) antibiotic therapy. Arthritis in another patient in group 2 failed to resolve after 6 months of DMARD therapy, and the patient underwent synovectomy. Two patients in group 3 who declined DMARD therapy prior to synovectomy required a second synovectomy.

localized to affected joints, we present data only for patients from whom SF or synovial tissue was available.

Of the 18 patients from whom SF was collected, 5 were referred prior to antibiotic therapy when they had active *B burgdorferi* infection (group 1, preantibiotic patients) (Table 1). The other 13 patients from whom SF was available were referred because of incomplete responses to oral doxycycline or IV ceftriaxone (group 2, postantibiotic patients). SF was usually collected from these patients soon after oral or IV therapy, when few if any spirochetes remained (32), and prior to starting DMARD therapy, usually methotrexate (MTX). In patients from whom multiple samples were available, the first sample collected was analyzed. MicroRNA from synovial tissue, a target tissue of this disease, was available from 14 patients who underwent arthroscopic synovectomies between 4 and 48 months (median 15.5 months) after oral and IV antibiotics (group 3, synovectomy patients). In these patients, DMARDs were stopped several weeks prior to synovectomy.

Group 1. The 5 patients who were referred prior to antibiotic therapy had mild-to-severe knee swelling and pain for a median duration of 1 month prior to evaluation and the start of antibiotic treatment (Table 1). As was typical in our previous cohorts, titers of antibodies to *B burgdorferi* were high prior to therapy (33), and PCR results for *B burgdorferi* DNA in SF were positive for 2 of the 4 patients tested (50%) (32). In addition, consistent with past experience (19,31), the median white blood cell (WBC) count in SF was 25,760 cells/mm^3 with 90% polymorphonuclear leukocytes (PMNs). Arthritis in 3 of the 5 patients resolved during a 1-month course of oral doxycycline, while the other 2 patients continued to have marked knee swelling. These 2 patients were then treated for 1 month with IV ceftriaxone, and their arthritis resolved.

As determined by quantitative reverse transcription–PCR, the 5 patients with active infection who were seen prior to antibiotic therapy had low levels of 5 of the 6 miRNAs measured in this study, including hematopoietic-specific miR-146a, miR-155, and miR-142 (14,34), which are associated with myeloid cell effector function (Figure 1). Levels of miR-17 and miR-20a, part of the miR-17–92 oncomiR family involved in cell cycle regulation (15), were also low. The notable exception was high levels of miR-223, a hematopoietic-specific miRNA that is abundantly expressed in PMNs (34). MicroRNA-223 is associated with down-regulation of acute inflammation (35) and tissue

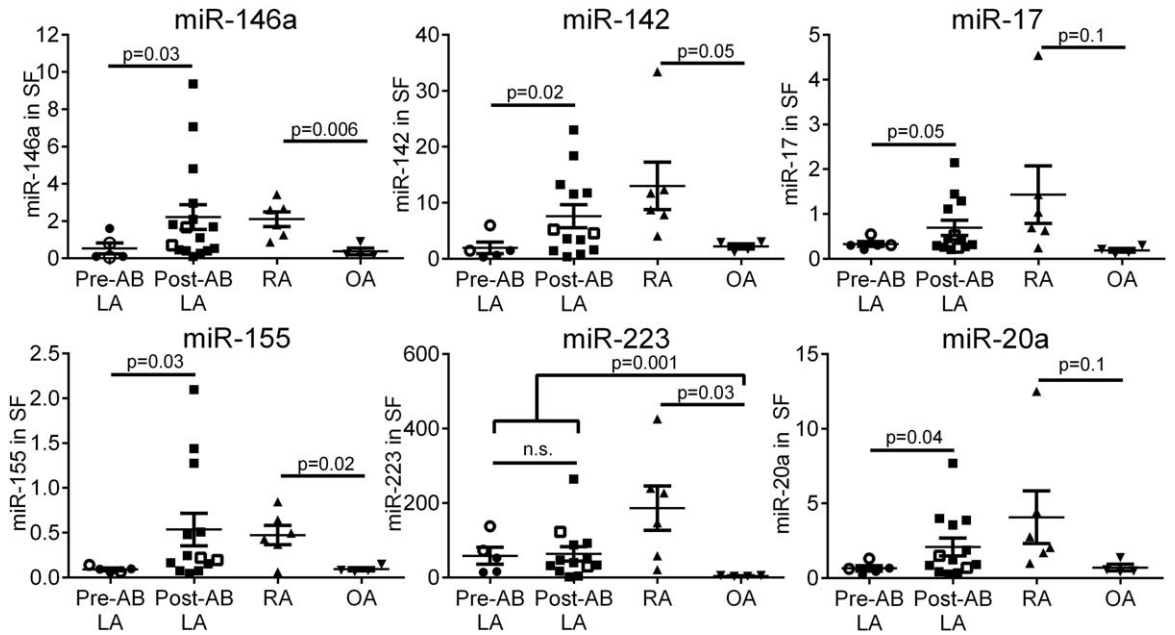

Figure 1. Levels of extracellular microRNAs (miRNAs) in synovial fluid (SF) from patients. Levels of extracellular miRNAs from SF were quantified by quantitative reverse transcription–polymerase chain reaction and normalized to the global geometric mean C_t of levels of all expressed miRNAs (see Patients and Methods). Open circles and squares indicate patients who required intravenous (IV) antibiotic therapy, but not disease-modifying antirheumatic drugs, for resolution of their arthritis; solid circles indicate patients whose arthritis resolved with oral antibiotic therapy; solid squares indicate patients whose arthritis failed to fully resolve with both oral and IV antibiotic therapy. Symbols represent individual patients; bars show the mean ± SE. Statistically significant differences between groups were determined by Welch's *t*-test. Pre-AB LA = Lyme arthritis (LA) in patients referred prior to antibiotic (AB) therapy when they had active *Borrelia burgdorferi* infection; post-AB LA = LA in patients referred because of incomplete responses to oral doxycycline or IV ceftriaxone; RA = rheumatoid arthritis; OA = osteoarthritis; NS = not significant.

remodeling (36). This finding is consistent with high levels of PMNs present in SF from these patients.

Group 2. The 13 patients who continued to have joint swelling after oral or IV antibiotic therapy exhibited marked variability in the severity and duration of their arthritis, which is consistent with heterogeneity of treatment outcomes in LA in humans. These patients were referred because of incomplete responses to oral or IV antibiotic therapy between 2.75 and 17 months after arthritis onset (Table 1). Of the 13 patient samples, 7 were collected after completion of oral antibiotic therapy but before IV antibiotic therapy, and 6 were collected after completion of both oral and IV antibiotic therapy but before DMARD therapy. Compared with patients in group 1, who were seen prior to antibiotic therapy, those in group 2 had significantly lower WBC counts in SF ($P = 0.008$), fewer PMNs ($P = 0.004$), and greater percentages of lymphocytes ($P = 0.008$) and monocytes ($P = 0.028$). Arthritis in 2 of these 13 patients resolved after IV antibiotic therapy; most of the other 11 patients were treated successfully with MTX, and none had reactivation of infection during or after immunosuppressive therapy.

In contrast to the low levels of most miRNAs found in group 1, levels of miR-146a, miR-155, miR-142, miR-17, and miR-20a were higher in group 2 (Figure 1). This suggested that the nature of the arthritis had changed after spirochetal killing. The exception was miR-223, which was typically elevated in patients in both group 1 and group 2. However, of the 5 patients in group 1, the 2 patients who required IV antibiotic therapy for resolution of arthritis had higher levels of miR-142 and miR-223 (open circles in Figure 1) than did the 3 patients whose arthritis was resolved with oral therapy (solid circles in Figure 1). Conversely, of the 13 patients who were seen in the postantibiotic period, the 2 patients whose arthritis resolved with IV therapy (open squares in Figure 1) had low-to-moderate levels of miR-155 and miR-142.

For comparison, miRNAs were also assessed in SF from 4 patients with OA, a minimally inflammatory type of arthritis, and in SF from 6 patients with RA, the prototypic form of chronic inflammatory arthritis. Levels of all 6 miRNAs in RA patients were similar to those in LA patients in group 2, while levels of most of these miRNAs in OA patients were low and similar to those in LA patients in group 1 (Figure 1). Levels of miR-223 were high in all LA patients; they were particularly high in RA patients but very low in OA patients.

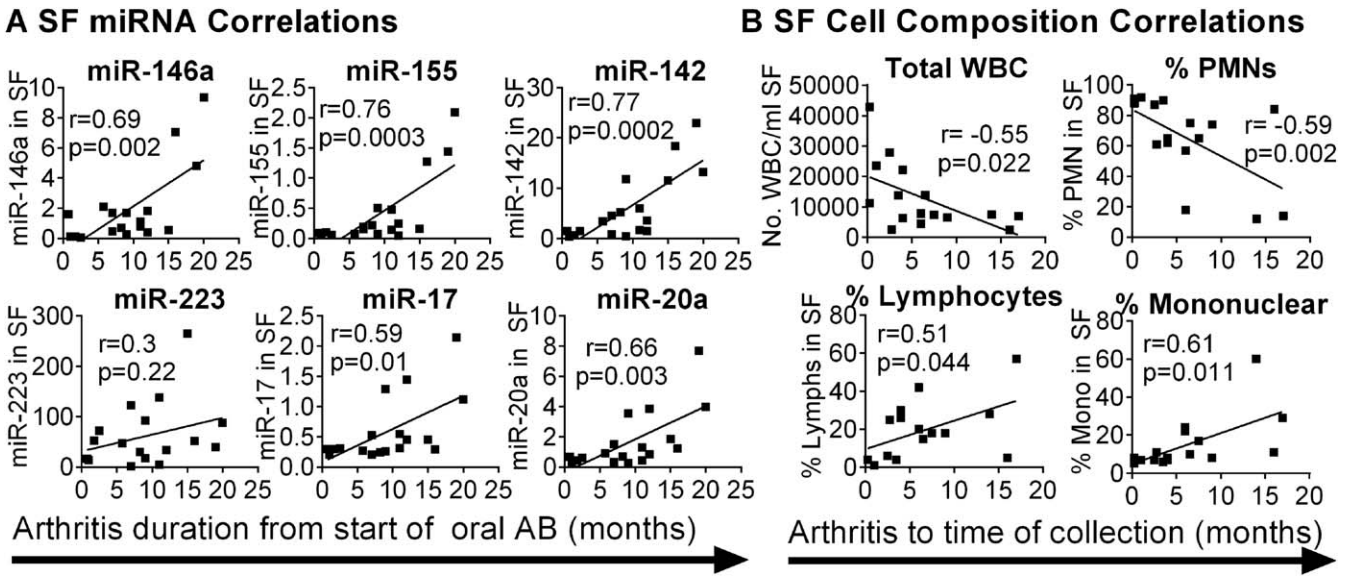

Figure 2. Correlation of arthritis duration with levels of extracellular microRNAs (miRNAs) and with cell composition in synovial fluid (SF). Linear regression analysis was used to determine Pearson's correlation coefficients and *P* values for clinical correlations between expression levels of extracellular miRNAs in SF and arthritis duration after the start of oral antibiotics (AB) (**A**) and between SF cell composition and arthritis duration to the time of SF collection (**B**). WBC = white blood cell; PMNs = polymorphonuclear leukocytes; lymphs = lymphocytes; mono = monocytes.

Correlation of arthritis duration and SF laboratory findings. When patients in groups 1 and 2 were considered together, SF levels of miR-146a, miR-155, miR-142, miR-17, and miR-20a correlated positively with arthritis duration after the start of oral antibiotic therapy (Figure 2A). Similar results were obtained with the estimated total duration of arthritis, but the data are not shown because the date of arthritis onset was not always clear. In contrast, *B burgdorferi* IgG antibody titers correlated negatively with levels of miR-155 ($r = -0.49$, $P = 0.04$), miR-146a ($r = -0.49$, $P = 0.04$), and miR-142 ($r = -0.54$, $P = 0.02$). Levels of miR-223, the only miRNA with high levels in both group 1 and group 2, did not correlate with arthritis duration.

When the cell composition of SF from patients in group 1 was considered together with that of SF from patients in group 2, changes in cellularity correlated with arthritis duration prior to sample collection (Figure 2B). Arthritis duration correlated negatively with the WBC count ($P = 0.022$) and the percentage of PMNs ($P = 0.002$) and positively with the percentages of lymphocytes ($P = 0.044$) and mononuclear cells ($P = 0.011$). These results further suggested that the pathologic characteristics of the arthritis changed during transition from active infection to postinfectious LA and that these miRNAs may have a role in arthritis pathogenesis.

Group 3. RNA from synovial tissue was available from 14 patients who underwent synovectomies for treatment of persistent synovitis a median of 15.5 months (range 4–48 months) after 2–3 months of antibiotic therapy (Table 1). Two patients (14%) required a second synovectomy; both of these patients declined DMARD therapy prior to their first synovectomy, while the other 12 patients did not. All 14 patients had negative culture and PCR results for *B burgdorferi* and *B burgdorferi* DNA (32). SF from these patients was not available for testing.

To assess miRNA expression in synovial tissue, the 14 samples from LA patients were analyzed using miRNA sequencing, allowing a global assessment of all miRNAs. MicroRNA sequencing was not possible with the smaller amounts of RNA in cell-free SF. For comparison, we assessed synovial tissue from 8 patients with other forms of inflammatory arthritis (5 with RA, 2 with PsA, and 1 with undifferentiated inflammatory monoarthritis) and from 5 patients with minimally inflammatory OA. A total of 73 miRNAs were differentially expressed in synovial tissue from patients with postinfectious LA compared with that from OA patients. A complete list of miRNAs differentially expressed in each patient group is provided in Supplementary Table 1, available on the *Arthritis & Rheumatology* web site at http://onlinelibrary.wiley.com/doi/10.1002/art.40039/abstract.

These 73 differentially expressed miRNAs were subjected to further analysis to determine which genes and pathways were predicted to be regulated by them

Table 2. Pathway analysis of miRNA expression in synovial tissue from patients with postinfectious LA versus that in synovial tissue from OA patients*

	P	No. of genes/no. of miRNAs
Regulated in LA		
Pathways in cancer	1.2×10^{-53}	187/34
Wnt signaling	5.0×10^{-26}	91/34
TGFβ signaling	2.9×10^{-18}	57/30
TCR signaling	2.8×10^{-16}	59/31
Cell cycle regulation	5.9×10^{-14}	68/31
BCR signaling	6.6×10^{-12}	42/28
p53 regulation	6.9×10^{-11}	37/29
FcγR-mediated phagocytosis	1.1×10^{-10}	35/30
Regulated in OA		
Focal adhesion	1.3×10^{-47}	102/18
PI3K/Akt signaling	2.4×10^{-33}	149/19
EGFR tyrosine kinase family signaling	4.1×10^{-26}	51/16
Pathways in cancer	3.2×10^{-20}	145/18
Insulin signaling	2.9×10^{-19}	64/16
Ubiquitin-mediated proteolysis	4.7×10^{-18}	65/17
HIF-1 signaling	1.5×10^{-17}	53/17
mTOR signaling	7.5×10^{-16}	33/15

* Genes predicted to be regulated by microRNAs (miRNAs) overexpressed in synovial tissue from patients with postinfectious Lyme arthritis (LA; n = 44) or osteoarthritis (OA; n = 29) were analyzed using DIANA miRPath pathway analysis (see Patients and Methods). The top 8 pathways, ranked by *P* value, are listed along with the number of genes in those pathways (no. of genes) predicted to be targeted by miRNAs (no. of miRNAs). TGFβ = transforming growth factor β; TCR = T cell receptor; BCR = B cell receptor; FcγR = Fcγ receptor; PI3K = phosphatidylinositol 3-kinase; EGFR = epidermal growth factor receptor; HIF-1 = hypoxia-inducible factor 1; mTOR = mechanistic target of rapamycin.

(30) (Table 2). Genes predicted to be regulated by 44 miRNAs overexpressed in synovial tissue from LA patients were involved in cellular proliferation or regulation of inflammatory processes, such as T cell receptor signaling, B cell receptor signaling, and antibody-mediated phagocytosis. In contrast, the 29 miRNAs overexpressed in synovial tissue from OA patients were predicted to be involved in tissue remodeling and cell proliferation but not inflammation, consistent with the nature of OA. Thus, miRNAs in synovial tissue from patients with postinfectious LA predominantly regulated 2 processes, inflammation and proliferation, while miRNAs in this tissue in OA primarily regulated proliferation.

As with all forms of chronic inflammatory arthritis, synovial lesions in the 14 patients with postinfectious LA were characterized by massive, tumor-like proliferation of inflamed synovial tissue that can invade cartilage and bone (Figure 3). MicroRNA sequencing analysis of inflamed synovial tissue showed high expression of many miRNAs that were also abundant in SF from postantibiotic LA patients in group 2. These included antiinflammatory miR-146a and proinflammatory miR-155 (Figure 3A), which are associated with Toll-like receptor (TLR)/NF-κB inflammation (37), as well as hematopoietic-specific miRNAs such as miR-142 and miR-223 (Figure 3B), which are associated with myeloid function, modulation of acute inflammation, and initiation of wound repair (11,12,14,36). While expression levels of most miRNAs were similar between male and female patients, levels of miR-146a were 2.9-fold higher in males and 1.4-fold higher in females in synovial tissue from patients with postinfectious LA compared with that from OA patients.

As in SF, synovial tissue miRNA expression also contained a distinct oncogenic miRNA profile and was similar between male and female patients. Levels of the oncomiRs miR-17 and miR-20a were approximately 2.5-fold to 4-fold higher in synovial tissue from patients with postinfectious LA compared with that from OA patients (Figure 3C); levels of let-7a and let-7c, which are tumor suppressor miRNAs (18), were approximately 2-fold lower (Figure 3D). Thus, in these patients, the transition to the postinfectious phase was blocked by chronic inflammation, which stalled the wound repair process. Both inflammatory and proliferative miRNA responses were altered in these patients, indicative of development of an inflamed, tumor-like synovial lesion, analogous to a chronic synovial wound.

Correlation of miRNA signature in synovial tissue with disease duration. In contrast to findings in SF (Figure 2), expression of the NF-κB–inducible miRNAs miR-146a and miR-155 did not correlate significantly with arthritis duration after the start of antibiotic therapy (Figure 4). However, expression of miR-223 and the oncomiR miR-17–92 cluster in tissue correlated positively with arthritis duration after the start of treatment, while the let-7 family of tumor suppressor miRNAs correlated negatively with posttreatment arthritis duration (Figure 4). Each of these correlations was similar when analyzed with the estimated total arthritis duration (data not shown). Thus, in synovial tissue obtained late in disease, miRNAs involved in proliferative responses correlated with arthritis duration, but chronically elevated inflammatory miRNAs did not.

These synovial tissue results showed that late in postinfectious LA, TLR/NF-κB–dependent miRNAs were constitutively expressed, and the tumor-associated miRNA signature became progressively more pronounced. This suggested that expression of these miRNAs reflected immune dysregulation in the synovial tissue of patients with postinfectious LA, possibly perpetuating chronic inflammation and synovial proliferation in these patients.

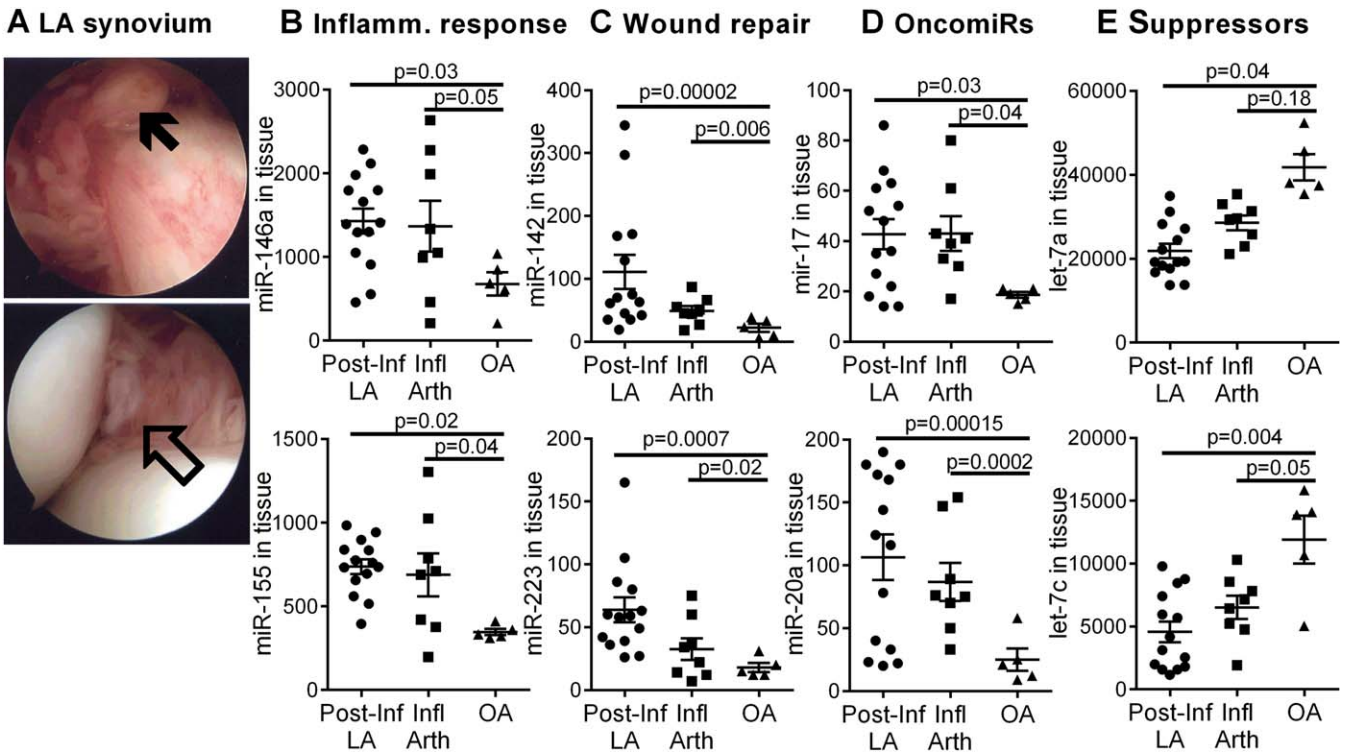

Figure 3. Expression of microRNAs (miRNAs) in synovial tissue. **A**, Arthroscopic images of inflamed synovium in postinfectious Lyme arthritis (Post-Inf LA). **Solid arrow** indicates inflamed villi; **open arrow** indicates invading synovial tissue. **B–E**, Expression levels of microRNA-146a (miR-146a) and miR-155 (inflammatory [Inflamm.] response) (**B**), miR-142 and miR-223 (wound repair) (**C**), miR-17 and miR-20a (oncogenic miRNAs [oncomiRs]) (**D**), and let-7a and let-7c (tumor suppressors) (**E**) in synovial tissue from patients with postinfectious LA, patients with other forms of inflammatory arthritis (Infl Arth), and patients with osteoarthritis (OA), normalized to miRNA copies per million reads. Symbols represent individual patients; bars show the mean ± SD. Statistically significant differences ($P < 0.05$) in expression between groups were determined by differential expression analysis.

DISCUSSION

In this study, patients who were seen prior to antibiotic therapy had a high number of infiltrating leukocytes in SF, primarily PMNs (Table 1), and elevated levels of miR-223, which is highly expressed in PMNs (36). In contrast, they had very low levels of other hematopoietic-specific miRNAs, such as miR-146a, miR-155, and miR-142, similar to levels in SF in patients with OA (Figure 1). Low levels of these miRNAs, especially miR-146a and miR-155, suggested that inflammatory processes such as TLR/NF-κB signaling were tightly regulated in the joints of these patients despite the presence of spirochete-derived TLR ligands. Thus, during active infection, immune responses were focused on bacterial killing, primarily through controlled inflammation, antibody production, and PMN infiltration in SF of infected joints. After antibiotic therapy, arthritis in most patients was resolved by down-regulation of antibacterial responses, allowing for appropriate transition to wound repair and arthritis resolution.

We were unable to obtain SF or synovial tissue from these LA patients in the postinfectious phase, since their arthritis resolved during antibiotic therapy. However, we speculate that in such patients, the transition from infectious LA to the postinfectious phase occurs rapidly, progressing to beneficial wound repair responses after spirochetes have been killed. As a result, we would expect miRNA expression profiles after antibiotic therapy to look similar to those observed in synovial tissue from OA patients, characterized by tissue repair with minimal inflammation.

Animal models of LA provide insights into these processes in LA in humans. When infected with *B burgdorferi*, C57BL/6 mice develop only mildly-to-moderately inflammatory LA (38). They rely on antibody responses to *B burgdorferi* to control the infection, accompanied by robust wound repair responses. In contrast, *B burgdorferi*–infected C3H/HeN mice develop severe arthritis, have a massive cellular immune response dominated by interferon-α/β (IFNα/β)/STAT-1 activation in joint tissue early in infection, and have down-

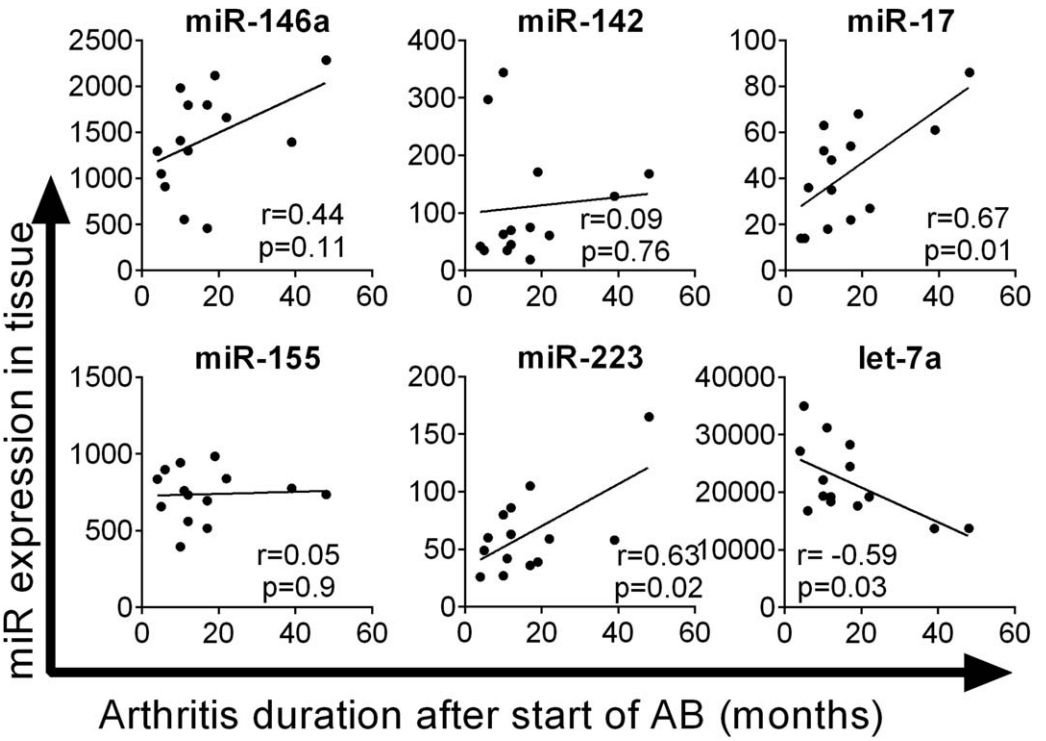

Figure 4. Correlations between microRNA (miRNA) expression in synovial tissue and arthritis duration. Linear regression analysis was used to determine Pearson's correlation coefficients and *P* values for clinical correlations between miRNA expression in tissue and arthritis duration after the start of oral antibiotics (AB).

regulated wound repair responses (39). However, unlike postinfectious LA in humans, neither mouse strain has persistent arthritis after antibiotic therapy.

Despite these differences, joints of C3H/HeN and C57BL/6 mice have similar numbers of spirochetes, indicating that the cellular response in C3H/HeN mice is maladaptive, worsening tissue damage without enhancing host defense (38). We suspect that in humans, genetic variables determine whether *B burgdorferi* infection elicits an appropriate wound repair response (as in C57BL/6 mice) (40,41) or a maladaptive inflammatory cellular response and arrest of wound repair processes (as in C3H/HeN mice) (42). For example, patients who have a polymorphism in the TLR-1 gene (1805GG), found primarily in the European Caucasian population, have higher levels of IFNγ/STAT-1–dependent cytokines when infected with RST1 *B burgdorferi* strains, and they have an increased frequency of postinfectious LA (43).

While arthritis was resolved in all of the pre-antibiotic LA patients from group 1 after completion of 1–3 months of antibiotic therapy, the LA patients from groups 2 and 3 were tested in the postantibiotic phase, when few if any spirochetes remained in affected joints. Compared with patients in group 1, patients in group 2 had longer arthritis duration, fewer WBCs and PMNs in SF, and greater frequencies of lymphocytes and monocytes (Table 1 and Figure 2B). A number of miRNAs associated with NF-κB inflammation (miR-146a, miR-155), myeloid cell function and wound repair (miR-142, miR-223), and Myc-dependent cell cycle regulation (miR-17–92, let-7 family) were highly expressed in SF and synovial tissue in patients from groups 2 and 3 (Figures 1 and 3). These results suggest that the inflammatory and proliferative processes occurring in the synovial environment in postinfectious LA were indeed maladaptive and were consistent with tumor-like characteristics of the synovial lesion, as has been described in RA (44).

The chronically high levels of miR-155 in SF and synovial tissue of patients with postinfectious LA provided valuable insights into the nature of their dysregulated inflammation. In mice, miR-155 is strongly up-regulated upon TLR/NF-κB activation but rapidly down-regulated in the presence of interleukin-10 (IL-10) in a STAT-3–dependent manner (45). When infected with *B burgdorferi*, IL-$10^{-/-}$ mice, which lack this IL-10/STAT-3/miR-155 regulatory mechanism, have very high miR-155 levels as well as a strong IFNγ/STAT-1 cytokine profile, enhancing cellular and humoral responses to infection (10). In contrast, infected C3H/HeN and C57BL/6 mice retain this IL-10/STAT-3/miR-155 regulatory loop and have low miR-155

levels in joint tissue, despite differences between strains in LA severity (9).

While IL-10$^{-/-}$ mice had down-regulated IFNγ/STAT-1 responses in joints after spirochetes had been killed with antibiotics (46), some LA patients have persistent inflammation months or years following completion of antibiotic therapy. We speculate that in postinfectious LA, elevated miR-155 indicates constitutive activation of proinflammatory pathways resulting from elevated cytokines such as IL-1β or tumor necrosis factor, from retained pathogen-associated molecular patterns (47), or from host damage-associated molecular patterns. Mice that chronically overexpress miR-155 spontaneously develop autoimmune T and B cell responses (48). Similarly, chronic overexpression of miR-155 in patients might also be a factor contributing to autoimmunity in LA (49–53) and RA (22) in humans.

In the present study, miRNA expression in patients with postinfectious LA was most similar to expression in RA patients. Consistent with these results, elevated expression of miR-155, miR-146a, and miR-223 has previously been shown in SF, synovial tissue, and synovial fibroblasts from patients with RA (22). Furthermore, studies in mice have demonstrated that miR-155 and miR-223 contribute to more severe experimental arthritis (5,6), and miR-146a limits inflammation and tissue damage in experimental arthritis (7,46). However, while the initial inflammatory triggers in RA are not clear, the initial trigger of LA, infection with *B burgdorferi*, is known with certainty. This makes it possible to study immune responses at their inception, when the stage is being set for subsequent arthritis. Moreover, the comparison of patients with antibiotic-responsive LA and those with postinfectious LA provides a unique opportunity to implicate genetic and regulatory factors that lead to this disadvantageous outcome.

Our study population, which is based on referrals, was representative of the range of possible outcomes in LA. It is unusual that patients are referred prior to therapy with oral doxycycline, and none of the patients referred prior to therapy developed postinfectious LA, which occurs in fewer than 10% of patients with LA (19). Instead, patients are usually referred because of lack of response to oral or IV antibiotic therapy. Therefore, our patient cohort is representative of the severe end of the spectrum of patients who do not respond well to antibiotic therapy. Moreover, SF cannot be obtained from all patients, and synovial tissue, the target tissue of the disease, is nearly always collected late in the postinfectious course in those who undergo arthroscopic synovectomies. Nevertheless, this study provides a novel assessment of miRNA expression in affected joints of patients during the infectious and postinfectious phases of LA.

Finally, the noted similarities in miRNA expression between postinfectious LA and other forms of chronic inflammatory arthritis, including RA, support the practice of treating patients with postinfectious LA with DMARDs after appropriate antibiotic therapy (21). Currently, these patients are usually treated with 2–3 months of oral and IV antibiotic therapy followed by ~6–9 months of DMARD therapy, usually with MTX (21). With this regimen, we have not observed relapse of infection during the period of immunosuppressive DMARD therapy. However, this treatment algorithm requires a total of ≥1 year of therapy, sometimes followed by months of physical therapy to regain normal function. MicroRNAs hold promise as potential biomarkers to identify LA patients who are developing maladaptive immune responses during the period of infection. In such patients, it will be important to learn whether simultaneous treatment with antibiotics and DMARDs, rather than sequential treatment with these medications, will reduce the period of therapy and improve outcome, creating a new paradigm in treatment of this form of chronic inflammatory arthritis.

ACKNOWLEDGMENTS

The authors thank Pauline Schmidt and Kate Sulka for technical assistance; Ann Companiolo (Yale University), Ana Fernandes (MGH), and Fiona Chen (MGH) for help with Institutional Review Board protocols and coordination of study patients; Fei Ji (MGH) and Ruslan Sadreyev (MGH) for sequencing and bioinformatics assistance; and Jameson Crowley (MGH) and Annalisa Pianta (MGH) for their intellectual input and review of the manuscript.

AUTHOR CONTRIBUTIONS

All authors were involved in drafting the article or revising it critically for important intellectual content, and all authors approved the final version to be published. Dr. Lochhead had full access to all of the data in the study and takes responsibility for the integrity of the data and the accuracy of the data analysis.

Study conception and design. Lochhead, Steere.

Acquisition of data. Lochhead, Strle, Kim, Kohler, Arvikar, Aversa.

Analysis and interpretation of data. Lochhead, Strle, Kim, Steere.

REFERENCES

1. O'Connell RM, Rao DS, Baltimore D. microRNA regulation of inflammatory responses [review]. Annu Rev Immunol 2012;30:295–312.
2. Bartel DP. MicroRNAs: target recognition and regulatory functions [review]. Cell 2009;136:215–33.
3. Ebert MS, Sharp PA. Roles for microRNAs in conferring robustness to biological processes [review]. Cell 2012;149:515–24.
4. Okada Y, Muramatsu T, Suita N, Kanai M, Kawakami E, Iotchkova V, et al. Significant impact of miRNA-target gene networks on genetics of human complex traits. Sci Rep 2016;6:22223.
5. Kurowska-Stolarska M, Alivernini S, Ballantine LE, Asquith DL, Millar NL, Gilchrist DS, et al. MicroRNA-155 as a pro-

inflammatory regulator in clinical and experimental arthritis. Proc Natl Acad Sci U S A 2011;108:11193–8.
6. Li YT, Chen SY, Wang CR, Liu MF, Lin CC, Jou IM, et al. Amelioration of collagen-induced arthritis in mice by lentivirus-mediated silencing of microRNA-223. Arthritis Rheum 2012;64:3240–5.
7. Nakasa T, Shibuya H, Nagata Y, Niimoto T, Ochi M. The inhibitory effect of microRNA-146a expression on bone destruction in collagen-induced arthritis. Arthritis Rheum 2011;63:1582–90.
8. Luo X, Ranade K, Talker R, Jallal B, Shen N, Yao Y. microRNA-mediated regulation of innate immune response in rheumatic diseases [review]. Arthritis Res Ther 2013;15:210.
9. Lochhead RB, Ma Y, Zachary JF, Baltimore D, Zhao JL, Weis JH, et al. MicroRNA-146a provides feedback regulation of Lyme arthritis but not carditis during infection with Borrelia burgdorferi. PLoS Pathog 2014;10:e1004212.
10. Lochhead RB, Zachary JF, Dalla Rosa L, Ma Y, Weis JH, O'Connell RM, et al. Antagonistic interplay between MicroRNA-155 and IL-10 during Lyme carditis and arthritis. PloS One 2015;10:e0135142.
11. Annoni A, Brown BD, Cantore A, Sergi LS, Naldini L, Roncarolo MG. In vivo delivery of a microRNA-regulated transgene induces antigen-specific regulatory T cells and promotes immunologic tolerance. Blood 2009;114:5152–61.
12. Sun Y, Oravecz-Wilson K, Mathewson N, Wang Y, McEachin R, Liu C, et al. Mature T cell responses are controlled by microRNA-142. J Clin Invest 2015;125:2825–40.
13. Isobe T, Hisamori S, Hogan DJ, Zabala M, Hendrickson DG, Dalerba P, et al. miR-142 regulates the tumorigenicity of human breast cancer stem cells through the canonical WNT signaling pathway. eLife 2014;3.
14. Fordham JB, Guilfoyle K, Naqvi AR, Nares S. MiR-142-3p is a RANKL-dependent inducer of cell death in osteoclasts. Sci Rep 2016;6:24980.
15. He L, Thomson JM, Hemann MT, Hernando-Monge E, Mu D, Goodson S, et al. A microRNA polycistron as a potential human oncogene. Nature 2005;435:828–33.
16. O'Donnell KA, Wentzel EA, Zeller KI, Dang CV, Mendell JT. c-Myc-regulated microRNAs modulate E2F1 expression. Nature 2005;435:839–43.
17. Pickering MT, Stadler BM, Kowalik TF. miR-17 and miR-20a temper an E2F1-induced G1 checkpoint to regulate cell cycle progression. Oncogene 2009;28:140–5.
18. Johnson SM, Grosshans H, Shingara J, Byrom M, Jarvis R, Cheng A, et al. RAS is regulated by the let-7 microRNA family. Cell 2005;120:635–47.
19. Steere AC, Schoen RT, Taylor E. The clinical evolution of Lyme arthritis. Ann Intern Med 1987;107:725–31.
20. Steere AC, Glickstein L. Elucidation of Lyme arthritis [review]. Nat Rev Immunol 2004;4:143–52.
21. Arvikar SL, Steere AC. Diagnosis and treatment of Lyme arthritis. Infect Dis Clin North Am 2015;29:269–80.
22. Vicente R, Noel D, Pers YM, Apparailly F, Jorgensen C. Deregulation and therapeutic potential of microRNAs in arthritic diseases [published erratum appears in Nat Rev Rheumatol 2016;12:220]. Nat Rev Rheumatol 2016;12:211–20.
23. Centers for Disease Control and Prevention. Recommendations for test performance and interpretation from the Second National Conference on Serologic Diagnosis of Lyme Disease. MMWR Morb Mortal Wkly Rep 1995;44:590–1.
24. Aletaha D, Neogi T, Silman AJ, Funovits J, Felson DT, Bingham CO III, et al. 2010 rheumatoid arthritis classification criteria: an American College of Rheumatology/European League Against Rheumatism collaborative initiative. Arthritis Rheum 2010;62:2569–81.
25. Veale D, Rogers S, FitzGerald O. Classification of clinical subsets in psoriatic arthritis. Br J Rheumatol 1994;33:133–8.
26. Van der Helm-van Mil AH, Detert J, le Cessie S, Filer A, Bastian H, Burmester GR, et al. Validation of a prediction rule for disease outcome in patients with recent-onset undifferentiated arthritis: moving toward individualized treatment decision-making. Arthritis Rheum 2008;58:2241–7.
27. Altman R, Asch E, Bloch D, Bole G, Borenstein D, Brandt K, et al. Development of criteria for the classification and reporting of osteoarthritis: classification of osteoarthritis of the knee. Arthritis Rheum 1986;29:1039–49.
28. Steere AC, Angelis SM. Therapy for Lyme arthritis: strategies for the treatment of antibiotic-refractory arthritis [review]. Arthritis Rheum 2006;54:3079–86.
29. Wormser GP, Dattwyler RJ, Shapiro ED, Halperin JJ, Steere AC, Klempner MS, et al. The clinical assessment, treatment, and prevention of Lyme disease, human granulocytic anaplasmosis, and babesiosis: clinical practice guidelines by the Infectious Diseases Society of America. Clin Infect Dis 2006;43:1089–134.
30. Vlachos IS, Kostoulas N, Vergoulis T, Georgakilas G, Reczko M, Maragkakis M, et al. DIANA miRPath v.2.0: investigating the combinatorial effect of microRNAs in pathways. Nucleic Acids Res 2012;40(Web Server issue):W498–504.
31. Steere AC, Levin RE, Molloy PJ, Kalish RA, Abraham JH III, Liu NY, et al. Treatment of Lyme arthritis. Arthritis Rheum 1994;37:878–88.
32. Li X, McHugh GA, Damle N, Sikand VK, Glickstein L, Steere AC. Burden and viability of Borrelia burgdorferi in skin and joints of patients with erythema migrans or Lyme arthritis. Arthritis Rheum 2011;63:2238–47.
33. Kannian P, McHugh G, Johnson BJ, Bacon RM, Glickstein LJ, Steere AC. Antibody responses to Borrelia burgdorferi in patients with antibiotic-refractory, antibiotic-responsive, or non–antibiotic-treated Lyme arthritis. Arthritis Rheum 2007;56:4216–25.
34. O'Connell RM, Zhao JL, Rao DS. MicroRNA function in myeloid biology [review]. Blood 2011;118:2960–9.
35. Aziz F. The emerging role of miR-223 as novel potential diagnostic and therapeutic target for inflammatory disorders [review]. Cell Immunol 2016;303:1–6.
36. Haneklaus M, Gerlic M, O'Neill LA, Masters SL. miR-223: infection, inflammation and cancer [review]. J Intern Med 2013;274:215–26.
37. Boldin MP, Baltimore D. MicroRNAs, new effectors and regulators of NF-κB [review]. Immunol Rev 2012;246:205–20.
38. Crandall H, Dunn DM, Ma Y, Wooten RM, Zachary JF, Weis JH, et al. Gene expression profiling reveals unique pathways associated with differential severity of Lyme arthritis. J Immunol 2006;177:7930–42.
39. Lochhead RB, Sonderegger FL, Ma Y, Brewster JE, Cornwall D, Maylor-Hagen H, et al. Endothelial cells and fibroblasts amplify the arthritogenic type I IFN response in murine Lyme disease and are major sources of chemokines in Borrelia burgdorferi-infected joint tissue. J Immunol 2012;189:2488–501.
40. Bramwell KK, Ma Y, Weis JH, Chen X, Zachary JF, Teuscher C, et al. Lysosomal β-glucuronidase regulates Lyme and rheumatoid arthritis severity. J Clin Invest 2014;124:311–20.
41. Bramwell KK, Mock K, Ma Y, Weis JH, Teuscher C, Weis JJ. β-glucuronidase, a regulator of Lyme arthritis severity, modulates lysosomal trafficking and MMP-9 secretion in response to inflammatory stimuli. J Immunol 2015;195:1647–56.
42. Ma Y, Bramwell KK, Lochhead RB, Paquette JK, Zachary JF, Weis JH, et al. Borrelia burgdorferi arthritis-associated locus Bbaa1 regulates Lyme arthritis and K/BxN serum transfer arthritis through intrinsic control of type I IFN production. J Immunol 2014;193:6050–60.
43. Strle K, Shin JJ, Glickstein LJ, Steere AC. Association of a Toll-like receptor 1 polymorphism with heightened Th1 inflammatory responses and antibiotic-refractory Lyme arthritis. Arthritis Rheum 2012;64:1497–507.
44. Firestein GS. Invasive fibroblast-like synoviocytes in rheumatoid arthritis: passive responders or transformed aggressors? [review]. Arthritis Rheum 1996;39:1781–90.

45. McCoy CE, Sheedy FJ, Qualls JE, Doyle SL, Quinn SR, Murray PJ, et al. IL-10 inhibits miR-155 induction by toll-like receptors. J Biol Chem 2010;285:20492–8.
46. Lochhead RB. MicroRNAs and type I interferon are critical immune modulators in Lyme arthritis [dissertation]. Salt Lake City (UT): University of Utah; 2014.
47. Bockenstedt LK, Gonzalez DG, Haberman AM, Belperron AA. Spirochete antigens persist near cartilage after murine Lyme borreliosis therapy. J Clin Invest 2012;122:2652–60.
48. Hu R, Kagele DA, Huffaker TB, Runtsch MC, Alexander M, Liu J, et al. miR-155 promotes T follicular helper cell accumulation during chronic, low-grade inflammation. Immunity 2014;41:605–19.
49. Londono D, Cadavid D, Drouin EE, Strle K, McHugh G, Aversa JM, et al. Antibodies to endothelial cell growth factor and obliterative microvascular lesions in the synovium of patients with antibiotic-refractory Lyme arthritis. Arthritis Rheumatol 2014;66:2124–33.
50. Crowley JT, Drouin EE, Pianta A, Strle K, Wang Q, Costello CE, et al. A highly expressed human protein, apolipoprotein B-100, serves as an autoantigen in a subgroup of patients with Lyme disease. J Infect Dis 2015;212:1841–50.
51. Crowley JT, Strle K, Drouin EE, Pianta A, Arvikar SL, Wang Q, et al. Matrix metalloproteinase-10 is a target of T and B cell responses that correlate with synovial pathology in patients with antibiotic-refractory Lyme arthritis. J Autoimmun 2016;69:24–37.
52. Pianta A, Drouin EE, Crowley JT, Arvikar S, Strle K, Costello CE, et al. Annexin A2 is a target of autoimmune T and B cell responses associated with synovial fibroblast proliferation in patients with antibiotic-refractory Lyme arthritis. Clin Immunol 2015;160:336–41.
53. Drouin EE, Seward RJ, Strle K, McHugh G, Katchar K, Londono D, et al. A novel human autoantigen, endothelial cell growth factor, is a target of T and B cell responses in patients with Lyme disease. Arthritis Rheum 2013;65:186–96.

ARTHRITIS & RHEUMATOLOGY
Vol. 69, No. 5, May 2017, pp 1111–1121
DOI 10.1002/art.39982

CRISPR/Cas9 Editing of Murine Induced Pluripotent Stem Cells for Engineering Inflammation-Resistant Tissues

Jonathan M. Brunger,[1] Ananya Zutshi,[1] Vincent P. Willard,[2] Charles A. Gersbach,[1] and Farshid Guilak[3]

Objective. **Proinflammatory cytokines such as interleukin-1 (IL-1) are found in elevated levels in diseased or injured tissues and promote rapid tissue degradation while preventing stem cell differentiation. This study was undertaken to engineer inflammation-resistant murine induced pluripotent stem cells (iPSCs) through deletion of the IL-1 signaling pathway and to demonstrate the utility of these cells for engineering replacements for diseased or damaged tissues.**

Methods. **Targeted deletion of the IL-1 receptor type I (IL-1RI) gene in murine iPSCs was achieved using the RNA-guided, site-specific clustered regularly interspaced short palindromic repeat (CRISPR)/Cas9 genome engineering system. Clonal cell populations with homozygous and heterozygous deletions were isolated, and loss of receptor expression and cytokine signaling was confirmed by flow cytometry and transcriptional reporter assays, respectively. Cartilage was engineered from edited iPSCs and tested for its ability to resist IL-1–mediated degradation in gene expression, histologic, and biomechanical assays after a 3-day treatment with 1 ng/ml of IL-1α.**

Results. **Three of 41 clones isolated possessed the IL-1RI$^{+/-}$ genotype. Four clones possessed the IL-1RI$^{-/-}$ genotype, and flow cytometry confirmed loss of IL-1RI on the surface of these cells, which led to an absence of NF-κB transcription activation after IL-1α treatment. Cartilage engineered from homozygous null clones was resistant to cytokine-mediated tissue degradation. In contrast, cartilage derived from wild-type and heterozygous clones exhibited significant degradative responses, highlighting the need for complete IL-1 blockade.**

Conclusion. **This work demonstrates proof-of-concept of the ability to engineer custom-designed stem cells that are immune to proinflammatory cytokines (i.e., IL-1) as a potential cell source for cartilage tissue engineering.**

Recent progress in the field of regenerative medicine has allowed the development of approaches for restoring the function of a broad range of damaged or diseased tissues, such as skin, bladder, reproductive organs, vascular grafts, and lungs (1–3). However, there is still the challenge of controlling how engineered tissue substitutes or cell therapies respond to the environment of the transplant host. For example, engineered tissues are often implanted in the body in sites characterized by high levels of inflammation due to the underlying disease or injury, potentially leading to stem cell dysfunction. Therefore, developing technologies to precisely govern how a cell therapy or engineered tissue interprets cues from the environment of the recipient may be critical to the long-term success of regenerative medicine.

Major advances in the fields of synthetic biology and genome editing have enabled the facile and highly specific engineering of cellular genomes, opening the

Supported by the Nancy Taylor Foundation for Chronic Diseases, the NIH (grants AR-061042, AR-50245, AR-48852, AG-15768, AR-48182, and OD-008586), the NSF (CAREER Award CBET-1151035), the Collaborative Research Center of the AO Foundation, and the Arthritis Foundation.

[1]Jonathan M. Brunger, PhD, Ananya Zutshi, BS, Charles A. Gersbach, PhD: Duke University, Durham, North Carolina; [2]Vincent P. Willard, PhD: Cytex Therapeutics, Durham, North Carolina; [3]Farshid Guilak, PhD: Washington University and Shriners Hospitals for Children, St. Louis, Missouri.

Drs. Gersbach and Guilak contributed equally to this work.

Drs. Brunger, Gersbach, and Guilak have submitted a patent application for genome engineering stem cells for regenerative medicine applications.

Address correspondence to Charles A. Gersbach, PhD, Department of Biomedical Engineering, Room 1427, FCIEMAS, 101 Science Drive, Box 90281, Duke University, Durham, NC 27708 (e-mail: charles.gersbach@duke.edu); or to Farshid Guilak, PhD, Department of Orthopaedic Surgery, Washington University, Shriners Hospitals for Children - St. Louis, Campus Box 8233, McKinley Research Building, Room 3121, St. Louis, MO 63110 (e-mail: guilak@wustl.edu).

Submitted for publication June 23, 2016; accepted in revised form November 1, 2016.

possibility of precise modification of stem cells at the genomic level. Programmable nucleases based on the clustered regularly interspaced short palindromic repeat (CRISPR)/Cas9 system provide a promising platform for introducing specific, predetermined modifications to chromosomal loci of living cells (4–6). In this RNA-guided nuclease system, a user-defined guide RNA (gRNA) directs the endonuclease Cas9 to a specific genomic target, where it cleaves chromosomal DNA. This cleavage activates endogenous cellular DNA repair pathways and can be exploited to facilitate correction, disruption, or deletion of genes. Engineered nucleases hold great promise for regenerative medicine applications in the area of cell therapy and tissue engineering, since they provide the unique capacity to engineer customized stem cells with user-specified characteristics (7).

Osteoarthritis (OA) is a progressive disease of synovial joints characterized by the destruction of articular cartilage and other joint tissues. While the pathogenesis of OA is not fully understood, increasing evidence suggests that proinflammatory cytokines play an important role in the onset and progression of OA (8,9). Other than total joint replacement with a prosthetic implant, few disease-modifying therapies are available for cartilage injury or OA. Thus, there is increasing interest in tissue engineering as a therapeutic approach for focal cartilage defects as well as total joint resurfacing (10,11). However, chondrocytes or stem cells in injured or OA joints are subjected to increased levels of proinflammatory cytokines such as interleukin-1 (IL-1), IL-6, IL-17, and tumor necrosis factor (TNF) (12). The activity of these cytokines leads to increased production of matrix metalloproteinases (MMPs), aggrecanases, inducible nitric oxide synthase, and prostaglandin E_2 (PGE_2) (8,12,13). These and other factors ultimately lead to suppression of cartilage-specific genes such as type II collagen $\alpha 1$ chain, down-regulation of proteoglycan levels, degeneration of the extracellular matrix (ECM), and chondrocyte apoptosis (12,14). Furthermore, inflammatory signaling mediated by IL-1 inhibits chondrogenic differentiation of stem cells and results in rapid degradation of stem cell–derived cartilage (15–19), suggesting that implantation of engineered tissue replacements in a diseased or injured joint may significantly compromise their potential for success.

To mitigate these effects, gene therapy has been used to ectopically overexpress soluble cytokine antagonists such as IL-1 receptor antagonist (IL-1Ra) with some success (20). A strategy for developing tissue-engineered constructs that are innately resistant to cytokine-induced degradation would be an important advance in the area of orthopedic tissue engineering and regenerative medicine. The goals of this study were to engineer "designer" induced pluripotent stem cells (iPSCs) with specific genomic modifications that confer resistance to IL-1–mediated inflammation and to evaluate the potential of these stem cells as a source for cartilage tissue engineering and regenerative medicine. Owing to their substantial proliferative capacity and their potential to differentiate into a variety of terminal cell types, iPSCs are an attractive cell source for personalized regenerative medicine and the modeling of multifactorial diseases such as OA (21). In this study, we used CRISPR/Cas9 to generate murine iPSCs deficient in IL-1 receptor type I (IL-1RI), the ligand-binding receptor responsible for IL-1 recognition that is necessary for IL-1 signal transduction. We then evaluated the ability of these cells to synthesize a cartilaginous ECM and resist the inflammation-mediated catabolism initiated by IL-1α.

MATERIALS AND METHODS

Induced pluripotent stem cell derivation and culture. Murine iPSCs were derived and cultured as previously described (22). (See Supplementary Methods, available on the *Arthritis & Rheumatology* web site at http://onlinelibrary.wiley.com/doi/10.1002/art.39982/abstract.)

Genome editing and clonal isolation. A plasmid encoding human codon optimized *Streptococcus pyogenes* Cas9 (hCas9) was obtained from Addgene (plasmid no. 41815) (6). Target sequences flanking exon 2 of IL-1RI and corresponding to 5′-GCTTCTGTGTTGAAGACTCA-3′ and 5′-GTAGCTGTGGGCCCACAACC-3′ were selected to generate the deletion of the IL-1RI signal peptide sequence. To produce single chimeric gRNA expression vectors, complementary oligonucleotides containing each of the target sequences were hybridized, phosphorylated, and cloned into an expression vector (23) (Addgene plasmid no. 47108) using a human U6 promoter. Prior to transfection, iPSCs were trypsinized and subjected to a 30-minute feeder subtraction. Lipofectamine 2000 (Life Technologies) was used according to the manufacturer's instructions to cotransfect 400 ng of each gRNA plasmid and 800 ng of hCas9 plasmid into 100,000 iPSCs freshly plated on mouse embryonic fibroblasts (MEFs) in complete, antibiotic-free iPSC medium in a 24-well plate. Cells were then subcultured on MEFs prior to single-cell deposition. In preparation for single-cell deposition, iPSCs were subjected to feeder subtraction prior to overnight culture on 0.1% gelatin. Cells were then trypsinized and subjected to a final feeder subtraction and suspended in calcium- and magnesium-free phosphate buffered saline (PBS), 1 m*M* EDTA, 25 m*M* HEPES, and 1% fetal bovine serum (FBS). A FACSVantage flow cytometer (Becton Dickinson) was used to deposit individual cells into gelatin-coated wells of a 96-well plate. Clones were subcultured on gelatin for 1 additional passage to allow for screening for the appropriate deletion via genomic polymerase chain reaction (PCR) using the following primer pair: IL-1RI determination forward 5′-TCATCTCCTGGTTAGTTATGGTATC-3′ and IL-1RI determination reverse 5′-CCGAGGCCAATGAGATTAAG-3′. A subset of each clone was lysed using QuickExtract (Epicentre Technologies) according to the manufacturer's instructions. The cell lysate was then diluted 8–10-fold prior to use as a template in

Table 1. Primer pairs used in quantitative reverse transcription–polymerase chain reaction gene expression assays

Target	Forward primer	Reverse primer
18S rRNA	5′-CGGCTACCACATCCAAGGAA-3′	5′-GGGCCTCGAAAGAGTCCTGT-3′
Acan	5′-GCATGAGAGAGGCGAATGGA-3′	5′-CTGATCTCGTAGCGATCTTTCTTCT-3′
Adamts4	5′-GACCTTCCGTGAAGAGCAGTGT-3′	5′-CCTGGCAGGTGAGTTTGCAT-3′
Adamts5	5′-GCCCACCCAATGGTAAATCTTT-3′	5′-TGACTCCTTTTGCATCAGACTGA-3′
Ccl2	5′-GGCTCAGCCAGATGCAGTTAA-3′	5′-CCTACTCATTGGGATCATCTTGCT-3′
Col2a1	5′-TCCAGATGACTTTCCTCCGTCTA-3′	5′-AGGTAGGCGATGCTGTTCTTACA-3′
Elf3	5′-GGCCCTCATGGCTGCCACCT-3′	5′-TTGGGATCTTGTCTGAGGTCCTGGA-3′
Il6	5′-GAGGATACCACTCCCAACAGACC-3′	5′-AAGTGCATCATCGTTGTTCATACA-3′
Mmp9	5′-CGAACTTCGACACTGACAAGAAGT-3′	5′-GCACGCTGGAATGATCTAAGC-3′
Mmp13	5′-GGGCTCTGAATGGTTATGACATTC-3′	5′-AGCGCTCAGTCTCTTCACCTCTT-3′

a PCR using Q5 polymerase (New England Biolabs) according to the manufacturer's instructions with the following cycling parameters: initial denaturation at 98°C for 30 seconds followed by 40 cycles of denaturation at 98°C for 8 seconds, annealing at 68°C for 10 seconds, and extension at 72°C for 20 seconds followed by a final extension at 72°C for 2 minutes. Clones of interest exhibiting the IL-1RI$^{+/+}$, IL-1RI$^{+/-}$, and IL-1RI$^{-/-}$ genotypes were passaged on MEFs, and culture was expanded in preparation for micromass culture.

Micromass predifferentiation culture. The iPSCs were subjected to a 15-day, high-density micromass culture as previously described (22) to achieve differentiation toward a mesenchymal state (see Supplementary Methods, available on the *Arthritis & Rheumatology* web site at http://onlinelibrary.wiley.com/doi/10.1002/art.39982/abstract). Predifferentiated cells were subsequently cultured in medium consisting of high-glucose Dulbecco's modified Eagle's medium (DMEM), 10% FBS, nonessential amino acids, 2-mercaptoethanol (2-ME), ITS+ (insulin–transferrin–selenium) premix supplement (BD Biosciences), 25 ng/ml gentamicin, 50 μg/ml L-ascorbic acid–phosphate, 40 μg/ml L-proline, and 4 ng/ml basic fibroblast growth factor (Roche) and used in monolayer assays for functional IL-1RI protein or in cartilage tissue engineering experiments evaluating the utility of these cells as a source for regeneration of tissues immune to IL-1–mediated tissue degradation.

Flow cytometric analysis. Predifferentiated cells were trypsinized, washed in PBS, and resuspended in PBS with 1% FBS supplemented with 5 μg/ml anti-mouse CD16/32 (BioLegend) to block nonspecific immunolabeling. Cells were then immunolabeled with either a phycoerythrin-conjugated Armenian hamster anti-mouse CD121a monoclonal antibody (JAMA-147) or an isotype control (BioLegend). Cells were washed 3 times and then subjected to flow cytometry to determine the presence or absence of IL-1RI.

NF-κB activity assay. A lentiviral construct containing 5 tandem repeats (5′-GGAAATTCCCGGAAAGTCCCCGGAAATTCCCGGAAAGTCCCCGGAAATTCCC-3′) of NF-κB response elements upstream of a firefly luciferase gene was generated by cloning this repeat sequence upstream of the minimal cytomegalovirus promoter in pGL3Basic (Promega) and then subcloning the cassette into a lentiviral expression vector. Lentivirus was generated by cotransfecting 4 μg of the transfer vector, 3 μg of psPAX2 (Addgene catalog no. 12260), and 1.2 μg of pMD2G (Addgene catalog no. 12259) into 293T cells at confluence in the well of a 6-well plate using Lipofectamine 2000. The next day, medium from 293T lentivirus producer cells was changed, and conditioned medium containing lentivirus was collected 36 and 60 hours after transfection. The lentiviral supernatant was filtered through 0.45 μm of cellulose acetate filters and stored at −80°C until used.

Predifferentiated cells were transduced by supplementing culture medium 1:1 with viral supernatant as well as 4 μg/ml Polybrene and incubating the cells in the presence of the virus overnight. Transduced cells were expanded, passaged, and then treated with IL-1α (R&D Systems). At the indicated time points, samples were lysed and assayed for luminescence using a Bright-Glo luminescence kit (Promega) according to the manufacturer's instructions. Luminescence normalized to background levels in untreated cells was used to report induction of NF-κB transcription activity.

Chondrogenesis in aggregate culture system. Passage-2 predifferentiated cells were trypsinized and resuspended in differentiation medium (high-glucose DMEM, nonessential amino acids, 2-ME, ITS+ premix supplement, 25 ng/ml gentamicin, 50 μg/ml L-ascorbic acid–phosphate, and 40 μg/ml L-proline) supplemented with 100 n*M* dexamethasone and 10 ng/ml transforming growth factor β3 (TGFβ3; R&D Systems) at a density of 1×10^6 cells/ml. Aggregate cultures were produced by placing 250,000 cells in each well of a round-bottomed 96-well plate. Cells were pelleted and cultured for 27 days prior to inducing an inflammatory assault using an established in vitro OA model (18). On day 27, cells were cultured in chondrogenic medium lacking the anabolic factors dexamethasone and TGFβ3 and supplemented with 1 ng/ml IL-1α. Control aggregates received no IL-1α. Three days later, pellet cultures and culture supernatant samples were harvested for biochemical, gene expression, and histologic analyses.

Biochemical analyses. Samples used for biochemical analyses were harvested, rinsed with Dulbecco's PBS (DPBS), and stored at −20°C until testing. Pellet culture samples were digested in papain (125 μg/ml; Sigma) at 65°C overnight. Digested samples were then analyzed using the PicoGreen assay (Life Technologies) to measure double-stranded DNA, the orthohydroxyproline assay for measuring total collagen content, and the dimethylmethylene blue (DMMB) assay for measuring the total sulfated glycosaminoglycan (sGAG) content of constructs (n = 4–6 per group).

Gene expression. Samples for gene expression analysis were harvested, rinsed in DPBS, and frozen at −80°C until further processing. Total RNA was isolated according to the recommendations of the manufacturer (Norgen Biotek) following tissue homogenization with a pestle. Reverse transcription was performed using the superscript VILO complementary

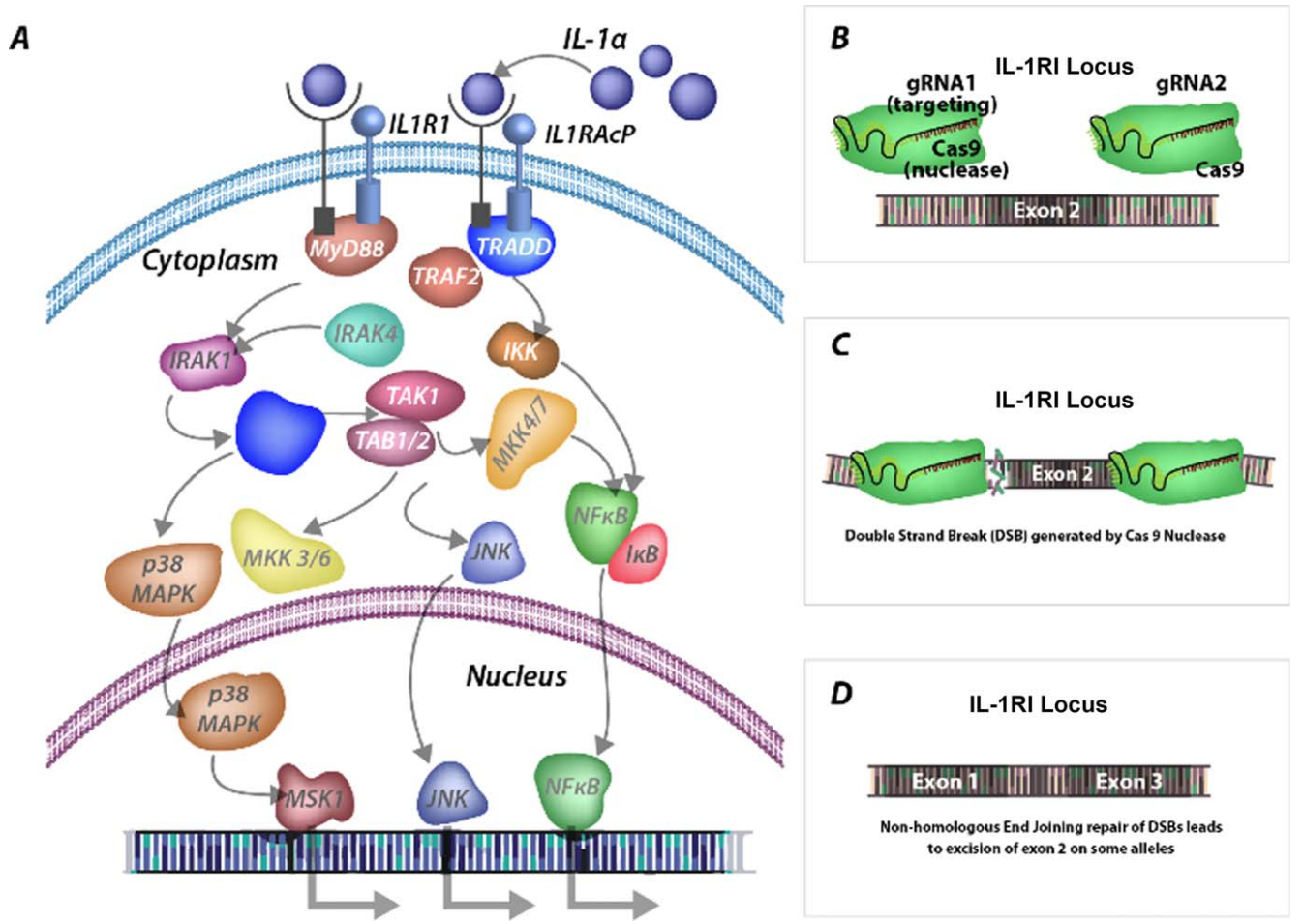

Figure 1. Schematic illustration of our strategy for generating induced pluripotent stem cells (iPSCs) resistant to interleukin-1 (IL-1)–mediated signaling for tissue engineering applications. **A,** Binding of IL-1 ligand to the IL-1 receptor type I (IL-1RI) results in activation of a proinflammatory transcription program involving the transcription factors NF-κB, JNK, and MSK-1. IL-1RAcP = IL-1R accessory protein; MyD88 = myeloid differentiation factor 88; TRAF2 = tumor necrosis factor receptor–associated factor 2; TRADD = tumor necrosis factor receptor type I–associated death domain; IRAK-1 = IL-1 receptor–associated kinase 1; TAK-1 = transforming growth factor β–activated kinase 1; TAB-1/2 = transforming growth factor β–activated kinase 1/2. **B,** Guide RNAs (gRNAs) target the genome-editing nuclease Cas9 to 2 sites flanking exon 2 of IL-1RI, which encodes the signal peptide sequence. **C,** Cas9 induces DNA double-strand breaks (DSBs), which may be repaired via a DNA repair pathway known as nonhomologous end joining. **D,** Nonhomologous end joining leads to a subset of alleles with fully intact IL-1RI, while others may have genomic disruptions at the IL-1RI locus, including excision of the signal peptide sequence, resulting in loss of signaling through IL-1RI.

DNA synthesis kit (Life Technologies) per the manufacturer's instructions. Quantitative reverse transcription–PCR (RT-PCR) was performed with 4 samples per group on a StepOnePlus system using Power SYBR (Applied Biosystems) per the manufacturer's instructions. Cycling parameters were initial denaturation at 95°C for 10 minutes followed by 40 cycles of denaturation at 95°C for 15 seconds and 60°C annealing and extension for 60 seconds. Fold changes were determined relative to a reference group cultured without IL-1α and by using 18S ribosomal RNA as a reference gene. Gene expression was probed using the primer pairs listed in Table 1.

Histologic processing. Samples for histology and immunohistochemistry were rinsed in DPBS upon harvest, fixed in 4% paraformaldehyde for 24 hours, paraffin embedded, and sectioned at 10 μm thickness. Cartilage pellets were stained with Safranin O–fast green/hematoxylin using standard protocols.

Analyses of culture supernatants. Medium samples were analyzed for catabolic byproducts, including nitric oxide, PGE_2, sGAG, and MMP activities. At the time of tissue harvest, cell-conditioned medium samples (n = 4) were collected and stored at −20°C until analysis. As with biochemical samples, sGAG in medium samples was assessed using the DMMB assay. MMP activity was assessed as previously described (24). Briefly, after activating latent MMPs in supernatants with *p*-APMA, total specific MMP activity was measured as the difference in fluorescence arising from cleavage of a quenched fluorogenic substrate (DAB-Gly-Pro-Leu-Gly-

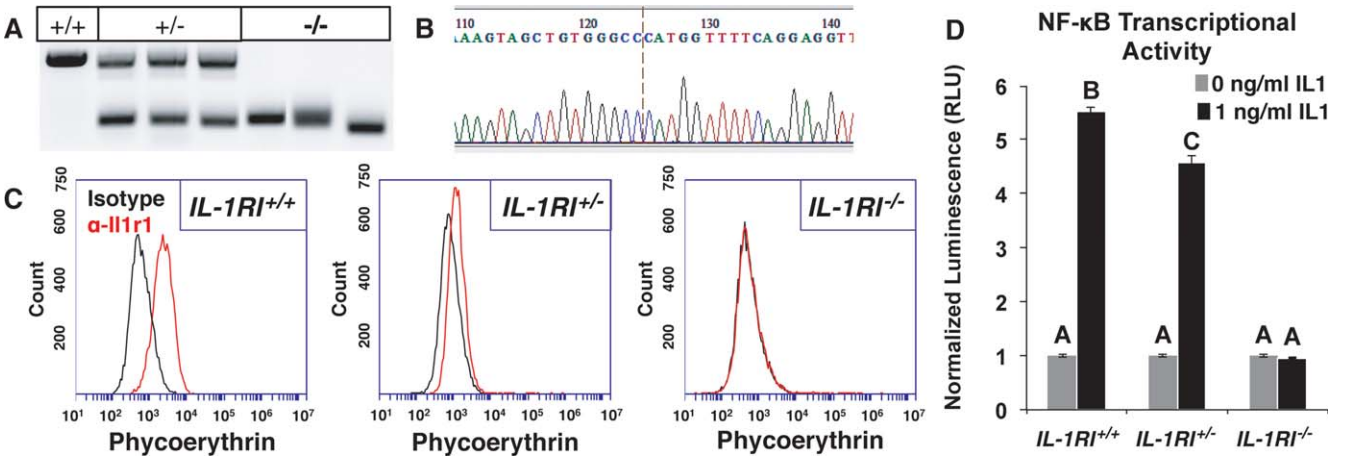

Figure 2. **A,** Genomic polymerase chain reaction (PCR) of clones isolated after single-cell deposition. PCR amplicons indicate the presence or absence of exon 2 in the interleukin-1 receptor type I (IL-1RI) locus. **B,** Sanger sequencing of an allele with clustered regularly interspaced short palindromic repeat/Cas9–mediated deletion of exon 2 from IL-1RI. **C,** Flow cytometry histograms demonstrating differential levels of IL-1RI surface expression in populations derived from each of the IL-1RI$^{+/+}$, IL-1RI$^{+/-}$, and IL-1RI$^{-/-}$ genotypes. a-IL-1RI = anti–IL-1RI antibody. **D,** Luminescence data characterizing the transcription activity of NF-κB in IL-1RI$^{+/+}$, IL-1RI$^{+/-}$, and IL-1RI$^{-/-}$ cells after 24 hours of treatment with 1 ng/ml of IL-1α. Bars show the mean ± SEM (n = 4 samples per group). Groups not sharing the same letter are significantly different ($P < 0.05$). RLU = relative luminescence units.

Met-Arg-Gly-Lys-Flu; Sigma) in samples incubated with a broad-spectrum MMP inhibitor, GM6001, and a scrambled negative control peptide (EMD Biosciences). Nitric oxide and PGE_2 were assayed using commercially available kits (R&D Systems) following the manufacturer's instructions.

Statistical analysis. Statistical analysis was performed in the Statistica 7 software package using analysis of variance with Fisher's protected least significant difference post hoc test with $\alpha = 0.05$. For quantitative RT-PCR comparisons, fold change values were log-transformed prior to statistical analysis. The mean ± SEM was calculated on a logarithmic scale prior to transforming data to linear values for reporting fold changes.

RESULTS

Clonal isolation and confirmation of IL-1RI functional deficit. Our strategy for targeted disruption of IL-1–mediated degradation is illustrated in Figure 1. Two gRNAs were designed to target Cas9 to sites flanking exon 2 of the IL-1RI gene (Figure 1B). Such targeting of the programmable CRISPR/Cas9 nuclease results in the generation of double-strand breaks flanking the signal peptide sequence of IL-1RI in a subset of alleles. Repair of the resultant double-strand breaks via the nonhomologous end-joining pathway results in excision of the signal peptide sequence for both annotated IL-1RI isoforms (Figure 1C).

Plasmids encoding *S pyogenes* Cas9 and gRNAs specific to targets flanking exon 2 of IL-1RI were cotransfected into murine iPSCs, and 41 clones were subsequently isolated and screened after single-cell deposition. Of these, 3 were found to possess the IL-1RI$^{+/-}$ genotype, while 4 possessed the IL-1RI$^{-/-}$ genotype (Figure 2A). Sanger sequencing of the PCR product from the IL-1RI$^{-/-}$ clones verified the expected deletion of ~790 bp (Figure 2B). However, in select clones that underwent chondrogenic differentiation, low but consistent expression of IL-1RI was detected on the surface in the wild-type population (Figure 2C). The IL-1RI$^{+/-}$ population also displayed low levels of expression, with roughly half the intensity of IL-1RI$^{+/+}$ cells, demonstrating reduced expression of IL-1RI protein after editing of 1 allele. Cells possessing the IL-1RI$^{-/-}$ genotype lacked positive staining for IL-1RI (Figure 2C). Absence of IL-1RI on the cell surface resulted in a functional deficiency, as indicated by a decrease in NF-κB transcription activity in IL-1RI$^{+/-}$ cells and loss of NF-κB induction in IL-1RI$^{-/-}$ cells after IL-1α stimulation, as measured in a luminescence transcriptional reporter assay (Figure 2D).

Cartilage engineered from CRISPR/Cas9-edited murine iPSCs is protected against IL-1α. Gene expression assays demonstrated that IL-1α (1 ng/ml) induced significant up-regulation of catabolic gene products and markers of inflammation in engineered cartilage pellets derived from cells with intact IL-1RI (Figure 3). CCL2 and IL-6, soluble mediators of OA and sentinel markers of inflammation, were elevated >50-fold at 72 hours in the IL-1RI$^{+/+}$ and IL-1RI$^{+/-}$ pellets ($P < 10^{-6}$). Expression of catabolic enzymes responsible for cartilage matrix degradation, such as ADAMTS-4, ADAMTS-5,

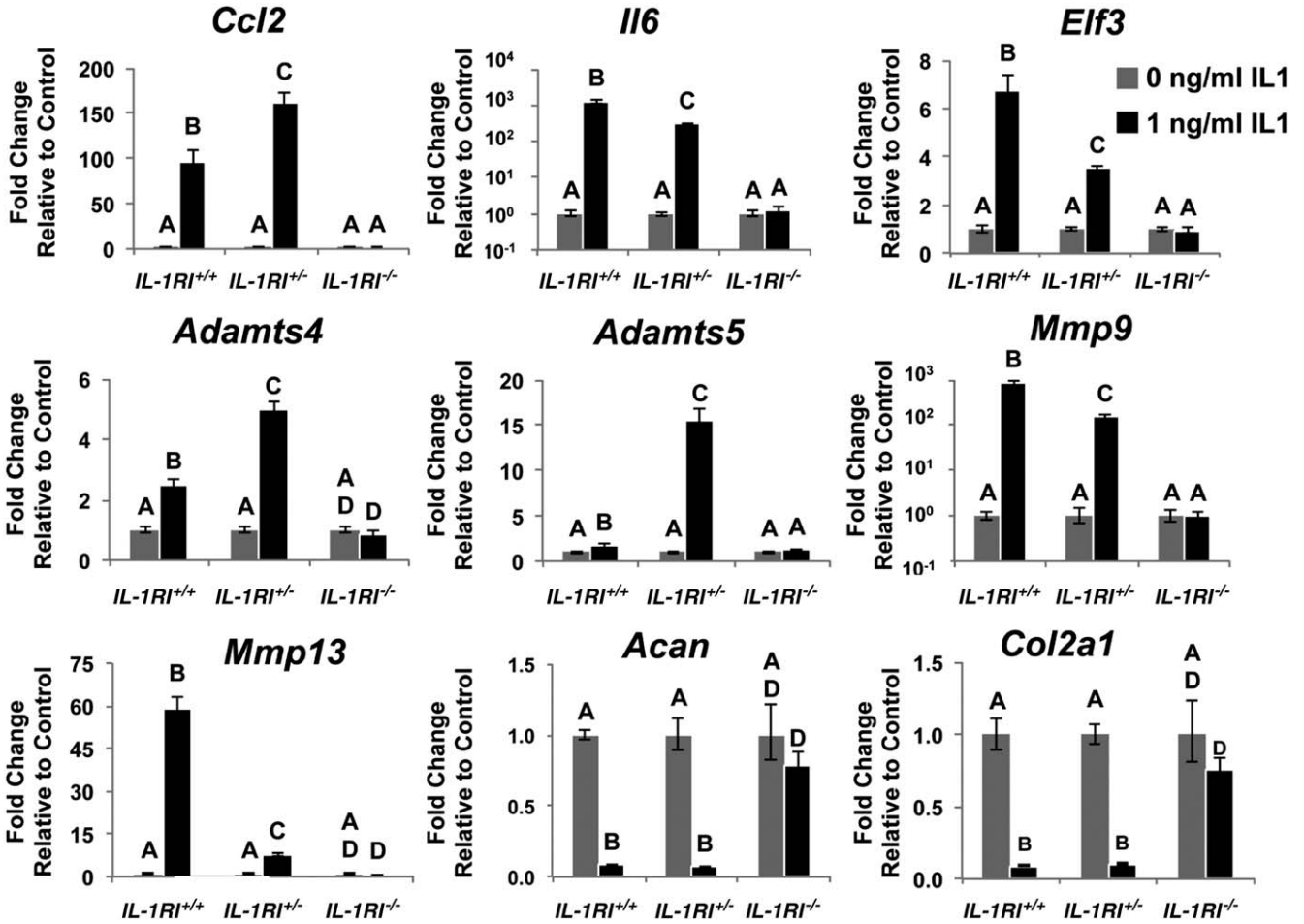

Figure 3. Relative gene expression data, as measured by quantitative reverse transcription–polymerase chain reaction, showing the effects of interleukin-1α (IL-1α) treatment on engineered cartilage derived from IL-1RI$^{+/+}$, IL-1RI$^{+/-}$, or IL-1RI$^{-/-}$ murine cells. Bars show the mean ± SEM fold change (n = 4 samples per group). Groups not sharing the same letter are significantly different ($P < 0.05$).

MMP-9, and MMP-13, were also significantly up-regulated in these cartilage pellets ($P < 0.007$). Expression of Elf-3, a transcription factor that up-regulates IL-1–induced genes such as MMP-13 (25) and suppresses type II collagen expression after cytokine treatment (14), demonstrated a similar response ($P < 10^{-6}$). This corresponded to a concomitant reduction in type II collagen α1 chain expression in the same pellets after IL-1α treatment ($P < 10^{-6}$). Furthermore, expression of aggrecan, a proteoglycan critical for cartilage function, was suppressed after IL-1α treatment in IL-1RI$^{+/+}$ and IL-1RI$^{+/-}$ pellets ($P < 10^{-6}$). In sharp contrast, none of these soluble markers of inflammation ($P > 0.30$), catabolic enzymes ($P > 0.12$), or proinflammatory transcription factors ($P > 0.64$) were significantly altered in pellets generated from the IL-1RI$^{-/-}$ cells. Moreover, the expression of matrix proteins type II collagen α1 chain and aggrecan was not significantly changed by IL-1α treatment in these pellets ($P > 0.07$) (Figure 3).

Consistent with the observed changes at the level of transcription (Figure 3), treatment with IL-1α resulted in an altered biochemical composition of cartilage aggregates generated from the IL-1RI$^{+/+}$ and IL-1RI$^{+/-}$ genotypes. Treatment with IL-1 had no effect on DNA content in aggregates (Figure 4A). Interestingly, DNA content in IL-1RI$^{+/-}$ pellets was significantly higher than DNA content in pellets derived from IL-1RI$^{+/+}$ or IL-1RI$^{-/-}$ cells irrespective of treatment, possibly due to a higher level of proliferation or cell survival in the clone chosen for these experiments. Concomitant with this increased DNA content, aggregates derived from IL-1RI$^{+/-}$ cells displayed increased accumulation of sGAG and total collagen (Supplementary Figures 1A and B, available on the *Arthritis &*

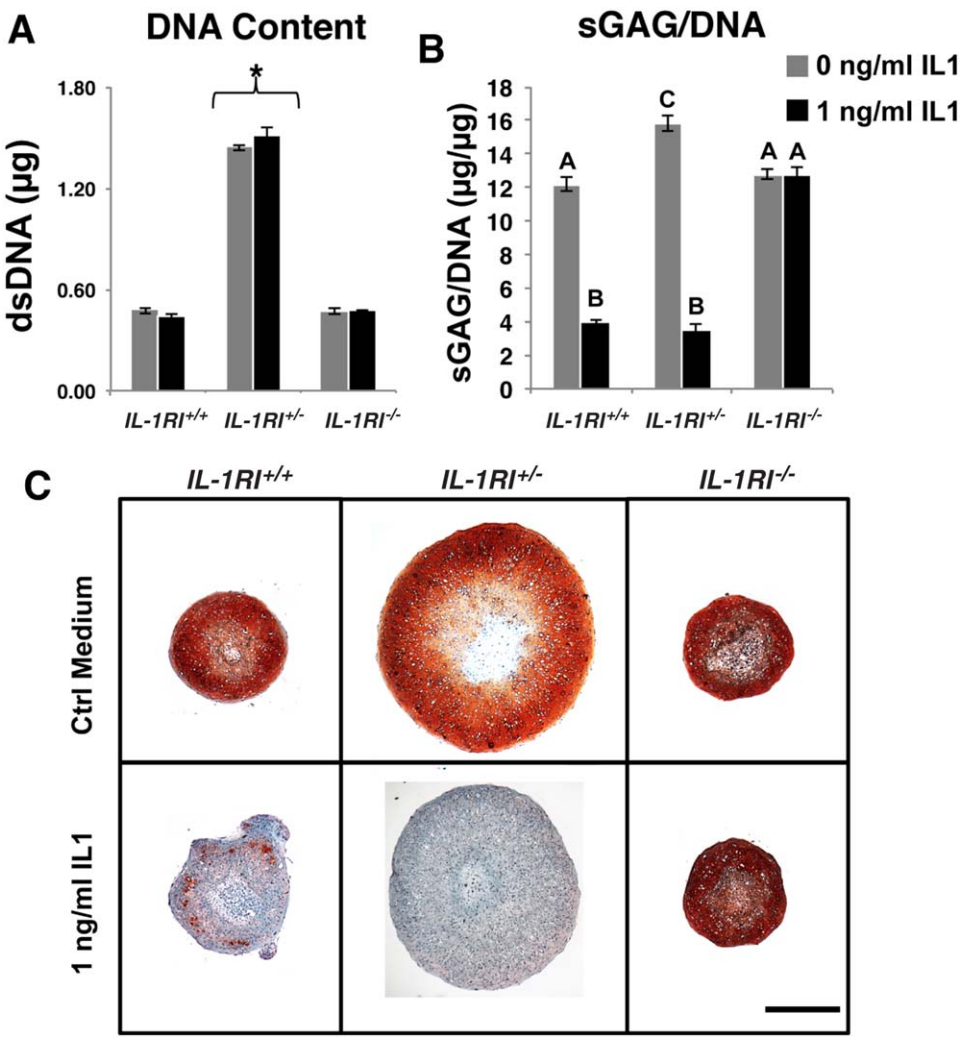

Figure 4. **A** and **B,** Biochemical analyses of engineered cartilage composition. Double-stranded DNA (dsDNA) content, as measured by PicoGreen assay (**A**), and sulfated glycosaminoglycan (sGAG) content per microgram DNA, as measured by dimethylmethylene blue assay (**B**), in engineered cartilage derived from IL-1RI$^{+/+}$, IL-1RI$^{+/-}$, or IL-1RI$^{-/-}$ murine cells are shown. Bars show the mean ± SEM (n = 6 samples per group). In **A,** $* = P < 0.05$, versus the IL-1RI$^{+/+}$ and IL-1RI$^{-/-}$ genotypes. In **B,** groups not sharing the same letter are significantly different ($P < 0.05$). **C,** Representative images of Safranin O–fast green/hematoxylin staining of 10-μm sections of engineered cartilage treated with control or with 1 ng/ml of interleukin-1 (IL-1) for 72 hours. Bar = 500 μm. Color figure can be viewed in the online issue, which is available at http://onlinelibrary.wiley.com/journal/doi/10.1002/art.39982/abstract.

Rheumatology web site at http://onlinelibrary.wiley.com/doi/10.1002/art.39982/abstract). Despite this increased accumulation, IL-1RI$^{+/-}$-derived cartilage remained highly responsive to IL-1α. Sulfated GAG content was found to be significantly dependent on IL-1α treatment and genotype, with cartilage derived from IL-1RI$^{+/+}$ or IL-1RI$^{+/-}$ clones losing >65% of sGAG (Supplementary Figure 1A) or sGAG per microgram DNA ($P < 10^{-6}$) (Figure 4B). Cartilage engineered from CRISPR/Cas9-edited IL-1RI$^{-/-}$ cells was completely protected against IL-1α, with no significant difference in sGAG or sGAG per microgram DNA content associated with IL-1α treatment ($P > 0.95$). No significant effects of IL-1α were found for total collagen or total collagen per microgram DNA (Supplementary Figures 1B and C), consistent with previous studies (26) and possibly due to the retention of partially degraded, large macromolecular constituents from enzymatically degraded tissue (18).

Histologic assessment supported the changes observed in matrix composition in biochemical analyses (Figure 4C). A GAG-rich matrix developed in all genotypes after maturation of engineered cartilage. As suggested by the biochemical data, larger pellets developed from IL-1RI$^{+/-}$ cells. However, a marked reduction in Safranin O

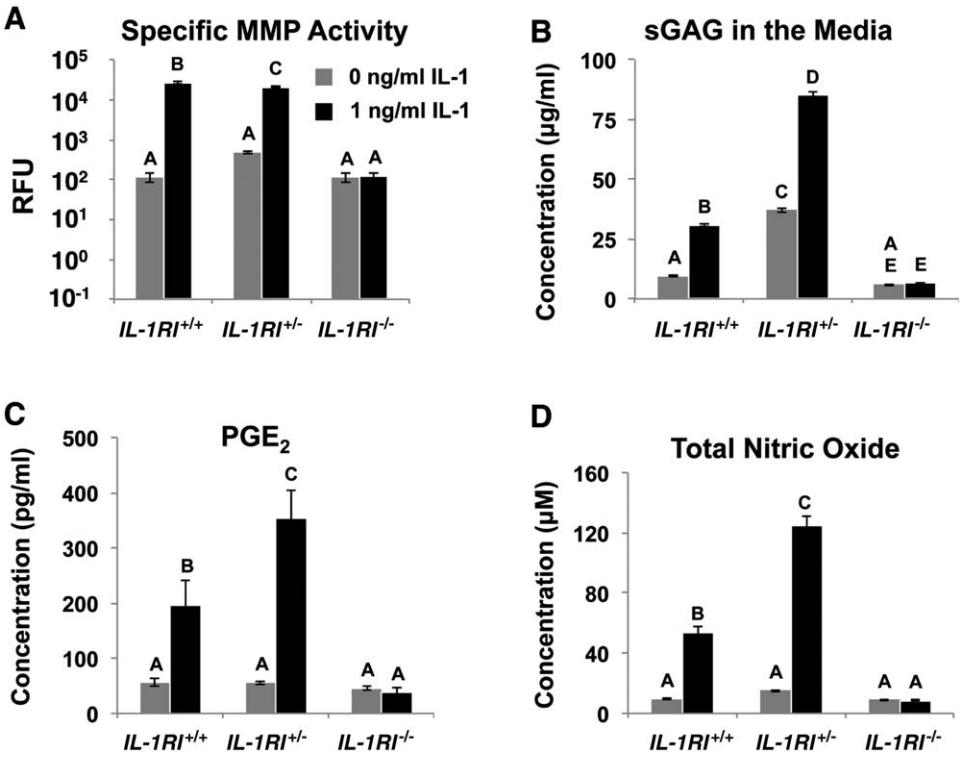

Figure 5. Analysis of medium samples collected from engineered murine cartilage aggregates that were left untreated or cultured with 1 ng/ml of interleukin-1α (IL-1α) for 72 hours. **A,** Specific matrix metalloproteinase (MMP) activity. RFU = relative fluorescence units. **B,** Concentration of sulfated glycosaminoglycan (sGAG) measured in culture medium. **C,** Prostaglandin E_2 (PGE_2) concentration. **D,** Total nitric oxide concentration. Bars show the mean ± SEM (n = 7 samples per group in **A,** 6 samples per group in **B**, and 4 samples per group in **C** and **D**). Groups not sharing the same letter are significantly different ($P < 0.05$).

staining for sGAG was observed in aggregates with intact IL-1RI after IL-1α treatment, consistent with the biochemical measurement of loss of sGAG for both IL-1RI$^{+/+}$ and IL-1RI$^{+/-}$-derived aggregates. In contrast, the cartilage tissues engineered with the IL-1RI$^{-/-}$ cells showed no histologic changes in response to IL-1α treatment.

Culture media collected from IL-1RI$^{+/+}$ and IL-1RI$^{+/-}$ samples displayed increased levels of matrix macromolecules, degradative enzymes, and proinflammatory mediators after a 72-hour treatment with IL-1α, whereas media collected from IL-1RI$^{-/-}$ samples exhibited no signs of tissue degradation or response to IL-1α (Figure 5). Specific MMP activity was significantly elevated in media collected from IL-1α–treated IL-1RI$^{+/+}$ and IL-1RI$^{+/-}$ aggregates (Figure 5A), likely contributing to the elevated levels of sGAG detected in the same medium samples (Figure 5B). The accumulation of significantly higher levels of sGAG in these samples is consistent with the observed loss of sGAG in engineered cartilage derived from IL-1RI$^{+/+}$ and IL-1RI$^{+/-}$ cells. Furthermore, the higher levels of PGE_2 and total nitric oxide species found in IL-1RI$^{+/+}$ and IL-1RI$^{+/-}$ samples (Figures 5C and D) are indicative of the proinflammatory response of IL-1RI–competent cells to IL-1α, whereas IL-1α had no effect on cartilage derived from IL-1RI$^{-/-}$ cells.

DISCUSSION

The findings of this proof-of-concept study show the utility of CRISPR/Cas9-based programmable nucleases for applications in tissue engineering and regenerative medicine by developing stem cells with customized properties via genome engineering. Using targeted gene-editing nucleases, we engineered pluripotent stem cells with the user-specified trait of IL-1 resistance by deleting the IL-1RI signal peptide sequence. CRISPR/Cas9-mediated editing of the IL-1RI locus resulted in complete loss of IL-1 signaling by all measures evaluated. Importantly, cartilage derived from CRISPR/Cas9-edited iPSCs displayed the capacity to withstand treatment with 1 ng/ml of IL-1α. Consistent with our findings, previous studies have shown that treatment with 1 ng/ml of IL-1α results in severe degradation of both engineered cartilage derived from IL-1RI–expressing cells and cartilage from mouse explants (17,18,26). However, in our study, engineered tissue derived from IL-1RI$^{-/-}$ cells

was protected against OA in an in vitro model. Taken together, these results indicate that genome editing can provide a highly effective tool for generating stem cells with custom-designed properties pertinent to tissue regeneration, maintenance, and repair.

In the present study, we examined the effects of IL-1α, but not IL-1β, on engineered stem cells. Primary chondrocytes show higher sensitivity to IL-1α than to IL-1β, possibly due to differences in binding affinity to IL-1RI and/or to the decoy receptor IL-1RII (27). It is important to note that IL-1RI expressed on the cell surface mediates signaling from both proteins, and loss of surface-expressed IL-1RI would be expected to abolish signaling from IL-1α and IL-1β (28). Furthermore, overcoming the proinflammatory effects of not only IL-1, but also TNF, IL-6, and IL-17, and other proinflammatory factors (12,29) represents an important challenge for regenerative medicine. Due to the pleiotropic roles of these cytokines and their involvement in tissue homeostasis, use of antagonistic therapies can lead to significant side effects (30,31). Our goal in this study was to explore avenues for implementing genome engineering technologies to address the challenges presented by the multifaceted proinflammatory niche. To combat the broad panel of factors driving inflammation but also essential for re-establishing homeostasis during tissue repair, future research will need to examine more sophisticated means of delivering cell-based anti-cytokine therapies.

Targeted genome-editing nucleases, including the CRISPR/Cas9 system used in this study as well as zinc-finger nucleases and transcription activator–like effector nucleases, have been extensively characterized for use in gene and cell therapy (7,32,33), and clinical trials have demonstrated the safety and feasibility of transplanting autologous, genome-edited CD4+ T cells (34). By demonstrating the feasibility of stem cell customization to achieve desired features for regenerative medicine, our work extends previous studies exploring the wide utility of programmable nucleases as well as work evaluating the effects of targeted deletions of genes in the IL-1 family. Our findings from knockout of the IL-1RI signal peptide sequence are consistent with a previous study demonstrating the role of IL-1RI in IL-1 signal transduction (28), in which IL-1RI–deficient mice generated by deletion of the signal peptide sequence failed to respond to IL-1, though the mice developed normally and were able to maintain homeostasis.

Interestingly, larger pellets developed in cartilage derived from IL-1RI$^{+/-}$ cells compared with that in cartilage derived from wild-type or IL-1RI$^{-/-}$ cells. Though we did not investigate this further, we attribute this effect to clonal variability, which has been reported to play a role in influencing cellular proliferation (35). Importantly, previous investigations have also shown that IL-1RI$^{-/-}$ mice display no deficits in lymphoid or hematopoietic cell numbers and continue to exhibit normal immune functions with respect to IL-1RI–independent signaling (28,36). Taken together, our findings and previous findings support the utility of CRISPR/Cas9-mediated IL-1RI–knockout for targeted cell and tissue engineering therapy.

The CRISPR/Cas9 system provides an attractive platform for editing mammalian genomes due to high levels of efficiency for generating double-strand breaks at target sites and the ease with which sequence specificity of Cas9 can be reprogrammed with a new gRNA. Our results showed that genome editing with CRISPR/Cas9 yielded the desired genomic modification in $>10\%$ of isolated clones in an unselected population. This method allows for site-specific gene deletion independent of targeting donor vectors that harbor gene traps or loxP sites that facilitate subsequent Cre-mediated excision. Thus, this approach overcomes the need for ectopic overexpression of selectable markers or Cre recombinase, and allows for direct, efficient gene editing.

In addition to these features, recent characterization of CRISPR/Cas9-mediated genome engineering indicates that nuclease activity is highly specific, even in human pluripotent stem cells (37,38). Those studies have shown that off-target mutagenesis occurs at a rate similar to or below that which accumulates simply by serial passaging of unedited cells. Moreover, significant strides have been made toward engineering improved specificity to the *Streptococcus pyogenes* CRISPR/Cas9 system (7), without drastic reductions in targeting efficiency. Such methods involve dual nickase versions of CRISPR/Cas9, the use of truncated gRNAs, the development of catalytically inactive Cas9 fused with RNA-guided FokI nucleases, and engineered variants of Cas9 with enhanced specificity. Use of these techniques has reportedly decreased off-target activity to undetectable levels in some experiments. Though we did not take advantage of these features in the present study, we anticipate that such developments will make the use of designer nucleases even more attractive for regenerative medicine and tissue engineering applications.

The approach of site-specific genome engineering of stem cells not only opens new avenues for conferring user-specified traits such as IL-1 resistance to cells for functional tissue engineering and regenerative medicine, but also may prove complementary to earlier attempts to combat IL-1 in an arthritic joint. Promising

approaches from previous work include the use of the competitive antagonist IL-1Ra via protein delivery (39,40). Other strategies entail ectopic overexpression of IL-1Ra by viral delivery to cells within the synovial joint, by transplantation of cells genetically engineered for constitutive overexpression of IL-1Ra, or by incorporation of IL-1Ra gene delivery vehicles in tissue engineering scaffolds designed for implantation into joint defects (17,20). Existing data suggest that these approaches hold great promise when the presence of IL-1Ra is sufficient to combat pathologic levels of IL-1, which may prove challenging if the transplanted cells or engineered tissues remain susceptible to high levels of IL-1 signaling. However, an important advantage of the current genome editing approach is that the modifications to the stem cell population are precise, as compared to random genomic insertions associated with viral gene therapy. In this regard, not only are IL-1RI$^{-/-}$ cells protected against IL-1 signaling, they also may provide a basal system for a cell-based drug delivery platform through additional engineered genetic modifications, including overexpression of anabolic factors (41–43) or inducible expression of antiinflammatory agents such as IL-4, IL-10, or IL-1Ra (17,44).

An alternative approach to attenuating IL-1RI signal transduction could entail use of either RNA interference (RNAi) or CRISPR interference (CRISPRi) to suppress transcription of IL-1RI. However, unlike approaches relying on RNAi, the targeted gene deletion used in this work abolishes the expression of functional gene product without the risk of toxicity associated with saturating microRNA pathways (45). Additionally, while CRISPRi has proven effective for reducing transcription of many target genes with high specificity (46,47), even low levels of persistent expression of IL-1RI could result in loss of protection against IL-1 stimulation in long-term exposure experiments. The approach of targeted gene disruption abrogates this risk by generating cells with no functional copy of the IL-1RI gene.

In this study, we exploited the ability to clonally expand genome engineered murine iPSCs to show proof-of-principle utility of gene-editing nucleases in cartilage tissue engineering. Implementation of this technique in the clinical setting will require several advances, and future investigation will probe whether the techniques used here can be extended to human iPSCs (48). Such studies will focus on reproducibly differentiating edited human iPSC clones and achieving acceptably low off-target activity of the CRIPSR/Cas9 platform using the methods discussed above. Furthermore, continued development of genome engineering reagents may eventually permit the direct editing of patient-derived mesenchymal stem cells or somatic cells in situ at modification rates adequate for a therapeutic effect, abrogating the need for clonal isolation and cell expansion of iPSCs, allowing the development of custom-designed engineered cells for tissue regeneration.

ACKNOWLEDGMENTS

The authors would like to thank Brian Diekman, PhD and Pablo Perez-Pinera, MD, PhD for helpful technical discussions.

AUTHOR CONTRIBUTIONS

All authors were involved in drafting the article or revising it critically for important intellectual content, and all authors approved the final version to be published. Dr. Guilak had full access to all of the data in the study and takes responsibility for the integrity of the data and the accuracy of the data analysis.

Study conception and design. Brunger, Zutshi, Willard, Gersbach, Guilak.

Acquisition of data. Brunger, Willard.

Analysis and interpretation of data. Brunger, Willard, Gersbach, Guilak.

ADDITIONAL DISCLOSURES

Author Willard is an employee of Cytex Therapeutics.

REFERENCES

1. Atala A, Kasper FK, Mikos AG. Engineering complex tissues. Sci Transl Med 2012;4:160rv12.
2. Dahl SL, Kypson AP, Lawson JH, Blum JL, Strader JT, Li Y, et al. Readily available tissue-engineered vascular grafts. Sci Transl Med 2011;3:68ra9.
3. Petersen TH, Calle EA, Zhao L, Lee EJ, Gui L, Raredon MB, et al. Tissue-engineered lungs for in vivo implantation. Science 2010;329:538–41.
4. Jinek M, Chylinski K, Fonfara I, Hauer M, Doudna JA, Charpentier E. A programmable dual-RNA-guided DNA endonuclease in adaptive bacterial immunity. Science 2012;337:816–21.
5. Cong L, Ran FA, Cox D, Lin S, Barretto R, Habib N, et al. Multiplex genome engineering using CRISPR/Cas systems. Science 2013;339:819–23.
6. Mali P, Yang L, Esvelt KM, Aach J, Guell M, DiCarlo JE, et al. RNA-guided human genome engineering via Cas9. Science 2013;339:823–6.
7. Maeder ML, Gersbach CA. Genome-editing technologies for gene and cell therapy. Mol Ther 2016;24:430–46.
8. Hedbom E, Hauselmann HJ. Molecular aspects of pathogenesis in osteoarthritis: the role of inflammation. Cell Mol Life Sci 2002; 59:45–53.
9. Goldring MB. Chondrogenesis, chondrocyte differentiation, and articular cartilage metabolism in health and osteoarthritis. Ther Adv Musculoskelet Dis 2012;4:269–85.
10. Johnstone B, Alini M, Cucchiarini M, Dodge GR, Eglin D, Guilak F, et al. Tissue engineering for articular cartilage repair: the state of the art. Eur Cell Mater 2013;25:248–67.
11. Moutos FT, Glass KA, Compton SA, Ross AK, Gersbach CA, Guilak F, et al. Anatomically shaped tissue-engineered cartilage with tunable and inducible anticytokine delivery for biological joint resurfacing. Proc Natl Acad Sci U S A 2016;113:E4513–22.

12. Kapoor M, Martel-Pelletier J, Lajeunesse D, Pelletier JP, Fahmi H. Role of proinflammatory cytokines in the pathophysiology of osteoarthritis. Nat Rev Rheumatol 2011;7:33–42.
13. Buckwalter JA, Lotz M, Stoltz JF, editors. Osteoarthritis, inflammation and degradation: a continuum. Amsterdam: IOS Press; 2007.
14. Peng H, Tan L, Osaki M, Zhan Y, Ijiri K, Tsuchimochi K, et al. ESE-1 is a potent repressor of type II collagen gene (COL2A1) transcription in human chondrocytes. J Cell Physiol 2008;215: 562–73.
15. Wehling N, Palmer GD, Pilapil C, Liu F, Wells JW, Muller PE, et al. Interleukin-1β and tumor necrosis factor α inhibit chondrogenesis by human mesenchymal stem cells through NF-κB–dependent pathways. Arthritis Rheum 2009;60:801–12.
16. Heldens GT, Blaney Davidson EN, Vitters EL, Schreurs BW, Piek E, van den Berg WB, et al. Catabolic factors and osteoarthritis-conditioned medium inhibit chondrogenesis of human mesenchymal stem cells. Tissue Eng Part A 2012;18:45–54.
17. Glass KA, Link JM, Brunger JM, Moutos FT, Gersbach CA, Guilak F. Tissue-engineered cartilage with inducible and tunable immunomodulatory properties. Biomaterials 2014;35:5921–31.
18. Willard VP, Diekman BO, Sanchez-Adams J, Christoforou N, Leong KW, Guilak F. Use of cartilage derived from murine induced pluripotent stem cells for osteoarthritis drug screening. Arthritis Rheumatol 2014;66:3062–72.
19. Blasioli DJ, Matthews GL, Kaplan DL. The degradation of chondrogenic pellets using cocultures of synovial fibroblasts and U937 cells. Biomaterials 2014;35:1185–91.
20. Evans CH, Ghivizzani SC, Robbins PD. Arthritis gene therapy and its tortuous path into the clinic. Transl Res 2013;161:205–16.
21. Saha K, Jaenisch R. Technical challenges in using human induced pluripotent stem cells to model disease. Cell Stem Cell 2009;5:584–95.
22. Diekman BO, Christoforou N, Willard VP, Sun H, Sanchez-Adams J, Leong KW, et al. Cartilage tissue engineering using differentiated and purified induced pluripotent stem cells. Proc Natl Acad Sci U S A 2012;109:19172–7.
23. Perez-Pinera P, Kocak DD, Vockley CM, Adler AF, Kabadi AM, Polstein LR, et al. RNA-guided gene activation by CRISPR-Cas9-based transcription factors. Nat Methods 2013;10:973–6.
24. McNulty AL, Miller MR, O'Connor SK, Guilak F. The effects of adipokines on cartilage and meniscus catabolism. Connect Tissue Res 2011;52:523–33.
25. Otero M, Plumb DA, Tsuchimochi K, Dragomir CL, Hashimoto K, Peng H, et al. E74-like factor 3 (ELF3) impacts on matrix metalloproteinase 13 (MMP13) transcriptional control in articular chondrocytes under proinflammatory stress. J Biol Chem 2012;287:3559–72.
26. Lima EG, Tan AR, Tai T, Bian L, Stoker AM, Ateshian GA, et al. Differences in interleukin-1 response between engineered and native cartilage. Tissue Eng Part A 2008;14:1721–30.
27. McNulty AL, Rothfusz NE, Leddy HA, Guilak F. Synovial fluid concentrations and relative potency of interleukin-1 α and β in cartilage and meniscus degradation. J Orthop Res 2013;31:1039–45.
28. Labow M, Shuster D, Zetterstrom M, Nunes P, Terry R, Cullinan EB, et al. Absence of IL-1 signaling and reduced inflammatory response in IL-1 type I receptor-deficient mice. J Immunol 1997;159:2452–61.
29. Marcu KB, Otero M, Olivotto E, Borzi RM, Goldring MB. NF-κB signaling: multiple angles to target OA. Curr Drug Targets 2010;11:599–613.
30. Ramos-Casals M, Brito-Zeron P, Soto MJ, Cuadrado MJ, Khamashta MA. Autoimmune diseases induced by TNF-targeted therapies. Best Pract Res Clin Rheumatol 2008;22:847–61.
31. Kimmerling KA, Furman BD, Mangiapani DS, Moverman MA, Sinclair SM, Huebner JL, et al. Sustained intra-articular delivery of IL-1RA from a thermally-responsive elastin-like polypeptide as a therapy for post-traumatic arthritis. Eur Cell Mater 2015;29: 124–39.
32. Urnov FD, Miller JC, Lee YL, Beausejour CM, Rock JM, Augustus S, et al. Highly efficient endogenous human gene correction using designed zinc-finger nucleases. Nature 2005;435: 646–51.
33. Ousterout DG, Kabadi AM, Thakore PI, Perez-Pinera P, Brown MT, Majoros WH, et al. Correction of dystrophin expression in cells from Duchenne muscular dystrophy patients through genomic excision of exon 51 by zinc finger nucleases. Mol Ther 2015; 23:523–32.
34. Tebas P, Stein D, Tang WW, Frank I, Wang SQ, Lee G, et al. Gene editing of CCR5 in autologous CD4 T cells of persons infected with HIV. N Engl J Med 2014;370:901–10.
35. Liang G, Zhang Y. Genetic and epigenetic variations in iPSCs: potential causes and implications for application. Cell Stem Cell 2013;13:149–59.
36. Glaccum MB, Stocking KL, Charrier K, Smith JL, Willis CR, Maliszewski C, et al. Phenotypic and functional characterization of mice that lack the type I receptor for IL-1. J Immunol 1997; 159:3364–71.
37. Kim S, Kim D, Cho SW, Kim J, Kim JS. Highly efficient RNA-guided genome editing in human cells via delivery of purified Cas9 ribonucleoproteins. Genome Res 2014;24:1012–9.
38. Suzuki K, Yu C, Qu J, Li M, Yao X, Yuan T, et al. Targeted gene correction minimally impacts whole-genome mutational load in human-disease-specific induced pluripotent stem cell clones. Cell Stem Cell 2014;15:31–6.
39. Bresnihan B, Alvaro-Gracia JM, Cobby M, Doherty M, Domljan Z, Emery P, et al. Treatment of rheumatoid arthritis with recombinant human interleukin-1 receptor antagonist. Arthritis Rheum 1998;41:2196–204.
40. Furman BD, Mangiapani DS, Zeitler E, Bailey KN, Horne PH, Huebner JL, et al. Targeting pro-inflammatory cytokines following joint injury: acute intra-articular inhibition of interleukin-1 following knee injury prevents post-traumatic arthritis. Arthritis Res Ther 2014;16:R134.
41. Shi S, Mercer S, Eckert GJ, Trippel SB. Growth factor transgenes interactively regulate articular chondrocytes. J Cell Biochem 2013;114:908–19.
42. Cucchiarini M, Madry H, Ma C, Thurn T, Zurakowski D, Menger MD, et al. Improved tissue repair in articular cartilage defects in vivo by rAAV-mediated overexpression of human fibroblast growth factor 2. Mol Ther 2005;12:229–38.
43. Matthews GL. Disease modification: promising targets and impediments to success. Rheum Dis Clin North Am 2013;39: 177–87.
44. Schukur L, Geering B, Charpin-El Hamri G, Fussenegger M. Implantable synthetic cytokine converter cells with AND-gate logic treat experimental psoriasis. Sci Transl Med 2015;7:318ra201.
45. Grimm D, Streetz KL, Jopling CL, Storm TA, Pandey K, Davis CR, et al. Fatality in mice due to oversaturation of cellular microRNA/short hairpin RNA pathways. Nature 2006;441:537–41.
46. Gilbert LA, Larson MH, Morsut L, Liu Z, Brar GA, Torres SE, et al. CRISPR-mediated modular RNA-guided regulation of transcription in eukaryotes. Cell 2013;154:442–51.
47. Thakore PI, D'Ippolito AM, Song L, Safi A, Shivakumar NK, Kabadi AM, et al. Highly specific epigenome editing by CRISPR-Cas9 repressors for silencing of distal regulatory elements. Nat Methods 2015;12:1143–9.
48. Yamashita A, Morioka M, Kishi H, Kimura T, Yahara Y, Okada M, et al. Statin treatment rescues FGFR3 skeletal dysplasia phenotypes. Nature 2014;513:507–11.

ARTHRITIS & RHEUMATOLOGY
Vol. 69, No. 5, May 2017, pp 1122–1126

LETTERS

DOI 10.1002/art.40023

Lesinurad in combination with allopurinol: risk without reward? Comment on the article by Saag et al

To the Editor:

As I read the recent article by Saag et al on treatment with lesinurad combined with allopurinol in gout patients with inadequate response to allopurinol alone (Saag KG, Fitz-Patrick D, Kopicko J, Fung M, Bhakta N, Adler S, et al. Lesinurad combined with allopurinol: a randomized, double-blind, placebo-controlled study in gout patients with an inadequate response to standard-of-care allopurinol: a US-based study. Arthritis Rheumatol 2017;69:202–11), a single question came to mind: does this medication benefit patients in any meaningful way? The average serum uric acid level in Saag and colleagues' study patients at baseline (at which time all were being treated with allopurinol) was 6.9 mg/dl, not far from the treatment target of <6 mg/dl. However, in >95% of the patients the dosage of allopurinol was only ≤300 mg/day. As the authors of the report well know, allopurinol is approved to be taken in dosages of up to 800 mg/day. The results of the trial demonstrated that this group of patients, whose uric acid levels were at nearly therapeutic levels despite an inadequate dosage of allopurinol, were more likely to achieve uric acid levels of <6 mg/dl with the addition of lesinurad (54% of those with lesinurad 200 mg/day added to the treatment regimen, versus 28% of those who continued to receive only stable doses of allopurinol).

All things being equal, then, the first question a clinician should ask before considering adding lesinurad to allopurinol is, should I not simply increase the prescribed allopurinol dosage first? After all, this is a solution that is less costly and complicated than adding a separate and (presumably) more expensive medication. But all things are not equal: lesinurad also comes with a black box warning about renal impairment. Even at the relatively safer (and approved) daily dose of 200 mg, lesinurad caused a >50% increase in the creatinine level in 12 (6%) of the study patients (versus 1% of those who continued to receive allopurinol alone); in 2 of the 12, renal function had not returned to baseline levels at the time of study close. Considering the unclear benefits of this novel drug, as well as its clear safety concerns, perhaps simply increasing the dosage of allopurinol (or switching to a different urate-lowering agent) would be more appropriate.

Aryeh M. Abeles, MD
University of Connecticut Health Center
Farmington, CT

DOI 10.1002/art.40024

Reply

To the Editor:

My coauthors and I appreciate Dr. Abeles' letter and the question he raises about the need for lesinurad, a new uricosuric agent, as well as its risk/benefit profile. We agree that it is necessary to first maximize urate-lowering therapy before adding a second treatment, such as lesinurad. Regrettably, although allopurinol has been in use in the US for >50 years, and despite continuous efforts by rheumatologists interested in gout care to educate general physicians, most physicians in practice do not dose-titrate allopurinol or febuxostat much (if at all) beyond the starting dose. The main reason they do not up-titrate the xanthine oxidase inhibitor is concern—largely unsubstantiated by data—about the safety of xanthine oxidase inhibitors at higher dosages in certain patients, such as those with kidney disease.

Patients who continue to have active gout and above-target serum urate levels despite maximization of urate-lowering therapy, who are often cared for by rheumatologists, represent another population for whom there is an unmet medical need. It is interesting to note that while there has been a dramatic increase in development of drugs to treat rheumatoid arthritis—with more than a dozen agents currently available—gout, a disease with a greater overall prevalence than rheumatoid arthritis, has had only 3 new drugs (lesinurad, pegloticase, and febuxostat) brought to market in the last 50 years. Thus, there is a considerable need for more treatment options for patients with gout. As lesinurad can lead to increases in creatinine levels, which are reversible in the vast majority of patients studied in clinical trials, always using this drug in combination with a xanthine oxidase inhibitor, and monitoring of renal function during use of this agent, are warranted. We concur with the substantial majority of members of the Food and Drug Administration Arthritis Advisory Panel who voted to endorse this drug for its approval based on what they and we consider an acceptable risk/benefit profile.

Dr. Saag has received consulting fees from Ardea/AstraZeneca and Takeda (less than $10,000 each), and research support from Ardea, Crealta, and Takeda.

Kenneth G. Saag, MD, MSc
University of Alabama
Birmingham, AL

DOI 10.1002/art.40026

Axial spondyloarthritis in relatives of probands with ankylosing spondylitis: comment on the article by Turina et al

To the Editor:

Turina et al (1) recently described a prospective inception cohort study of 51 seemingly healthy first-degree relatives (ages 18–40 years) of 36 HLA–B27–positive probands with ankylosing spondylitis (AS). Seventeen of these 51 first-degree relatives (33%) had clinical and/or imaging abnormalities suggestive of spondyloarthritis (SpA). HLA–B27 was present in only 8 of these 17 relatives with SpA (47%), not different from the 53% prevalence among the remaining 34 relatives without SpA. Moreover, Turina and colleagues report that axial SpA according to the Assessment of SpondyloArthritis international Society (ASAS) classification criteria (2) was present in 5 of 26 HLA–B27–positive relatives (19%) and in 4 of 25 HLA–B27–negative relatives (16%). This almost equal proportion contrasts sharply with the findings of an earlier study with a somewhat similar title ("Spondylitic Disease Without Radiologic

Evidence of Sacroiliitis in Relatives of HLA–B27 Positive Ankylosing Spondylitis Patients") (3). Turina et al did not cite this very relevant report, published in this journal 32 years ago, in which we reported a strong association of HLA–B27 with "spondylitic disease without radiographic sacroiliitis" (which now can be called nonradiographic axial spondyloarthritis, or pre-spondyloarthritis) among HLA–B27–positive, but not HLA–B27–negative, first-degree relatives of HLA–B27–positive patients with AS. Turina and colleagues state in their article "Previous studies have shown that SpA mainly manifests in HLA–B27–positive first-degree relatives," but the results they report contrast with these earlier findings.

How might this surprising finding of approximately equal proportions of axial SpA in HLA–B27–positive and HLA–B27–negative relatives (1) be explained? Two possibilities come to mind. First, Turina and colleagues' pre-spondyloarthritis cohort may have included individuals with clinical entities that do not progress to full-blown axial SpA/AS (by modified New York criteria [4]) in HLA–B27–negative first-degree relatives, implying that the current ASAS classification criteria for axial SpA seem to lack criterion validity because they do not show a strong biologic relationship with AS (5). A second explanation, in accordance with other findings, would be that the current ASAS axial SpA criteria may pick up some "look-alike" nonspecific back pain conditions and (false-positively) label them as axial SpA (5,6).

In an accompanying editorial, Sari and Haroon (7) have very nicely critiqued other aspects of the Pre-SpA cohort study by Turina et al and have also pointed out factors that must be considered in data interpretation and future analysis of the cohort.

Sjef van der Linden, MD, PhD
Maastricht University Medical Center
Maastricht, The Netherlands
Muhammad A. Khan, MD, FRCP, MACP
Case Western Reserve University
MetroHealth Medical Center
Cleveland, OH

1. Turina MC, de Winter JJ, Paramarta JE, Gamala M, Yeremenko N, Nabibux MN, et al. Clinical and imaging signs of spondyloarthritis in first-degree relatives of HLA–B27–positive ankylosing spondylitis patients: the Pre-Spondyloarthritis (Pre-SpA) Cohort Study. Arthritis Rheumatol 2016;68:2444–55.
2. Rudwaleit M, van der Heijde D, Landewé R, Listing J, Akkoc N, Brandt J, et al. The development of Assessment of SpondyloArthritis international Society classification criteria for axial spondyloarthritis (part II): validation and final selection. Ann Rheum Dis 2009;68:777–83.
3. Khan MA, van der Linden SM, Kushner I, Valkenburg HA, Cats A. Spondylitic disease without radiologic evidence of sacroiliitis in relatives of HLA–B27 positive ankylosing spondylitis patients. Arthritis Rheum 1985;28:40–3.
4. Van der Linden S, Valkenburg HA, Cats A. Evaluation of diagnostic criteria for ankylosing spondylitis: a proposal for modification of the New York criteria. Arthritis Rheum 1984;27:361–8.
5. Van der Linden S, Akkoc N, Brown MA, Robinson PC, Khan MA. The ASAS criteria for axial spondyloarthritis: strengths, weaknesses, and proposals for a way forward. Curr Rheumatol Rep 2015;17:62.
6. Van Hoeven L, Luime J, Han H, Vergouwe Y, Weel A. Identifying axial spondyloarthritis in Dutch primary care patients, ages 20–45 years, with chronic low back pain. Arthritis Care Res (Hoboken) 2014;66:446–53.
7. Sari I, Haroon N. Axial spondyloarthritis: the recurrence plot thickens [editorial]. Arthritis Rheumatol 2016;68:2354–6.

DOI 10.1002/art.40075

Bone marrow edema in the sacroiliac joint—degenerative sacroiliac joint disease might be more likely than spondyloarthritis: comment on the article by Turina et al

To the Editor:

We read with interest the report by Turina et al on spondyloarthritis (SpA)–related symptoms in first-degree relatives of SpA patients (1). The authors reported that one-third of first-degree relatives were classified as having SpA according to the Assessment of SpondyloArthritis international Society (ASAS) criteria (2).

Diagnosing early SpA in young patients remains a challenge in routine practice, although it is still unclear whether very early treatment leads to significant improvement in disease outcomes (3) as observed in early rheumatoid arthritis (RA). A pre-RA stage, in which arthralgia is present along with positivity for anti–citrullinated protein antibody and/or rheumatoid factor, has been described (4). Trials evaluating the efficacy of biologic disease-modifying antiinflammatory drug treatment in such patients are ongoing, and it has been suggested that there is a window of therapeutic opportunity early in the disease course, even before the patient can be classified as having definite RA. Such a window of opportunity in SpA has not been demonstrated to date.

Turina and colleagues identified bone marrow edema in the anterior portion of the sacroiliac (SI) joint, which is not specific to SpA. We observed similar bone marrow edema in a 29-year-old patient with chronic back pain (Figure 1). He had left buttock pain with both inflammatory and mechanical features. There were no associated peripheral or extraarticular symptoms. The pain was partially relieved by nonsteroidal antiinflammatory drugs. Clinical examination revealed obesity (body mass index [BMI] 32.7 kg/m^2) and hyperlordosis.

It is commonly believed that limited mobility of the SI joint may prevent cartilage degeneration. However, several studies (5) have shown that hip movement might generate SI joint rotation, explaining the finding of degenerative changes in the SI joint in association with femoroacetabular impingement and hip arthrosis (6). Hence, a significant number of patients meeting strict diagnostic criteria for sacroiliitis, including young patients, exhibit hip or spine conditions causing bone marrow edema of the SI joint (5). Indeed, degenerative changes in the SI joint were observed in 3 of 4 patients with lumbar spine arthrosis (7) and 10% of patients with suspected SpA (8).

Therefore, bone marrow edema in the anterior portion of the SI joint in first-degree relatives of patients with SpA is not necessarily an SpA-related symptom as in back pain cohorts. Degenerative disease of the SI joint is an underrecognized clinical entity (9). The updated definition by the ASAS Magnetic Resonance Imaging Working Group emphasized that bone marrow edema remains the key feature for the definition of active sacroiliitis on magnetic resonance imaging (MRI). This revised definition of active sacroiliitis did not include structural features

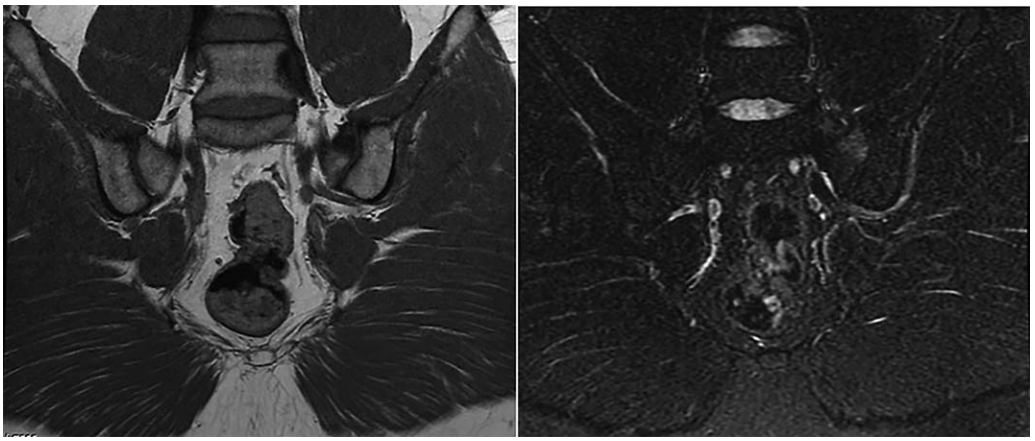

Figure 1. Magnetic resonance images showing bone marrow edema in the sacroiliac joint of a 29-year-old man with chronic back pain without peripheral or extraarticular symptoms. Left, T1-weighted spin-echo image. Right, STIR image.

of the SI joint such as erosion or features of SpA on spine MRI (10). Overlooking degenerative etiologies of SI joint bone marrow edema will lead to overestimation of the prevalence of prespondyloarthritis.

In conclusion, we support the evidence generated by Turina et al that a substantial proportion of seemingly healthy first-degree relatives of HLA–B27–positive SpA patients display imaging abnormalities of the SI joint (11). Degenerative etiologies should be considered, given the high prevalence of age-, sex-, and pregnancy-related SI joint abnormalities shown on MRI. However, we believe additional assessments should also be conducted to evaluate for conditions with a potential impact on SI joint degeneration (such as BMI, spinal curvature, transitional vertebrae, SI joint asymmetry, pregnancy, or microtrauma) in the interpretation of MRI abnormalities of the SI joint, in order to distinguish a degenerative etiology of bone marrow edema in the SI joint from the scope of SpA-related imaging features.

Athan Baillet, MD, PhD
Romain Gastaldi, MD
Université Grenoble Alpes
GREPI AE7405
and Grenoble Hospital
Jean Noel Ravey, MD
Grenoble Alpes Hospital
Philippe Gaudin, MD, PhD
Université Grenoble Alpes
GREPI AE7405
and Grenoble Hospital
Grenoble, France

1. Turina MC, de Winter JJ, Paramarta JE, Gamala M, Yeremenko N, Nabibux MN, et al. Clinical and imaging signs of spondyloarthritis in first-degree relatives of HLA–B27–positive ankylosing spondylitis patients: the Pre-Spondyloarthritis (Pre-SpA) Cohort Study. Arthritis Rheumatol 2016;68:2444–55.
2. Rudwaleit M, van der Heijde D, Landewé R, Listing J, Akkoc N, Brandt J, et al. The development of Assessment of SpondyloArthritis international Society classification criteria for axial spondyloarthritis (part II): validation and final selection. Ann Rheum Dis 2009;68:777–83.
3. Coates LC, Moverley AR, McParland L, Brown S, Navarro-Coy N, O'Dwyer JL, et al. Effect of tight control of inflammation in early psoriatic arthritis (TICOPA): a UK multicentre, open-label, randomised controlled trial. Lancet 2015;386:2489–98.
4. Bos WH, Wolbink GJ, Boers M, Tijhuis GJ, de Vries N, van der Horst-Bruinsma IE, et al. Arthritis development in patients with arthralgia is strongly associated with anticitrullinated protein antibody status: a prospective cohort study. Ann Rheum Dis 2010;69:490–4.
5. Berthelot JM, le Goff B, Maugars Y, Laredo JD. Sacroiliac joint edema by MRI: far more often mechanical than inflammatory? Joint Bone Spine 2016;83:3–5.
6. Morgan PM, Anderson AW, Swiontkowski MF. Symptomatic sacroiliac joint disease and radiographic evidence of femoroacetabular impingement. Hip Int 2013;23:212–7.
7. Hodge JC, Bessette B. The incidence of sacroiliac joint disease in patients with low-back pain. Can Assoc Radiol J 1999;50:321–3.
8. Jans L, van Langenhove C, van Praet L, Carron P, Elewaut D, van den Bosch F, et al. Diagnostic value of pelvic enthesitis on MRI of the sacroiliac joints in spondyloarthritis. Eur Radiol 2014;24:866–71.
9. O'Shea FD, Boyle E, Salonen DC, Ammendolia C, Peterson C, Hsu W, et al. Inflammatory and degenerative sacroiliac joint disease in a primary back pain cohort. Arthritis Care Res (Hoboken) 2010;62:447–54.
10. Lambert RG, Bakker PA, van der Heijde D, Weber U, Rudwaleit M, Hermann KG, et al. Defining active sacroiliitis on MRI for classification of axial spondyloarthritis: update by the ASAS MRI working group. Ann Rheum Dis 2016;75:1958–63.
11. Arnbak B, Jensen TS, Egund N, Zejden A, Hørslev-Petersen K, Manniche C, et al. Prevalence of degenerative and spondyloarthritis-related magnetic resonance imaging findings in the spine and sacroiliac joints in patients with persistent low back pain. Eur Radiol 2016;26:1191–203.

DOI 10.1002/art.40030

Reply

To the Editor:

We thank Drs. van der Linden and Khan for their interest in our recent study, which demonstrated that up to one-third of seemingly healthy (i.e., without axial SpA or any other rheumatologic disorder) first-degree relatives of HLA–B27–positive AS patients display clinical and/or imaging features of SpA, indepen-

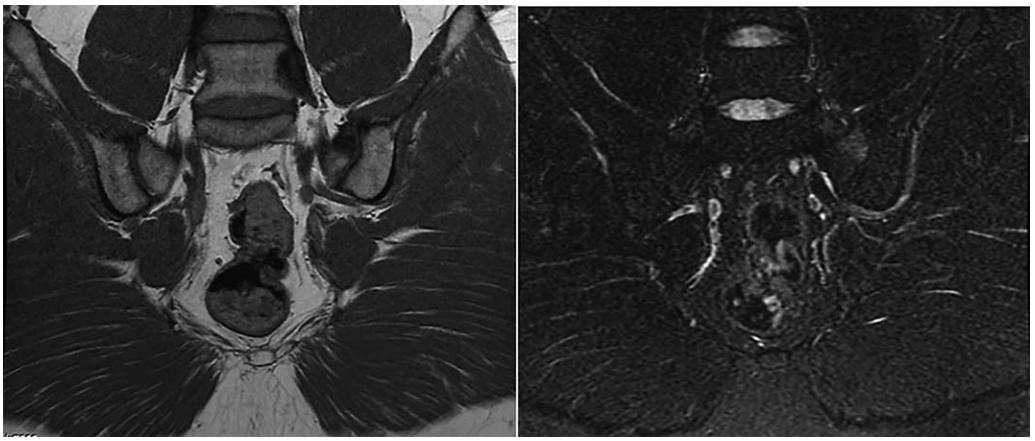

Figure 1. Magnetic resonance images showing bone marrow edema in the sacroiliac joint of a 29-year-old man with chronic back pain without peripheral or extraarticular symptoms. Left, T1-weighted spin-echo image. Right, STIR image.

of the SI joint such as erosion or features of SpA on spine MRI (10). Overlooking degenerative etiologies of SI joint bone marrow edema will lead to overestimation of the prevalence of prespondyloarthritis.

In conclusion, we support the evidence generated by Turina et al that a substantial proportion of seemingly healthy first-degree relatives of HLA–B27–positive SpA patients display imaging abnormalities of the SI joint (11). Degenerative etiologies should be considered, given the high prevalence of age-, sex-, and pregnancy-related SI joint abnormalities shown on MRI. However, we believe additional assessments should also be conducted to evaluate for conditions with a potential impact on SI joint degeneration (such as BMI, spinal curvature, transitional vertebrae, SI joint asymmetry, pregnancy, or microtrauma) in the interpretation of MRI abnormalities of the SI joint, in order to distinguish a degenerative etiology of bone marrow edema in the SI joint from the scope of SpA-related imaging features.

Athan Baillet, MD, PhD
Romain Gastaldi, MD
Université Grenoble Alpes
GREPI AE7405
and Grenoble Hospital
Jean Noel Ravey, MD
Grenoble Alpes Hospital
Philippe Gaudin, MD, PhD
Université Grenoble Alpes
GREPI AE7405
and Grenoble Hospital
Grenoble, France

1. Turina MC, de Winter JJ, Paramarta JE, Gamala M, Yeremenko N, Nabibux MN, et al. Clinical and imaging signs of spondyloarthritis in first-degree relatives of HLA–B27–positive ankylosing spondylitis patients: the Pre-Spondyloarthritis (Pre-SpA) Cohort Study. Arthritis Rheumatol 2016;68:2444–55.
2. Rudwaleit M, van der Heijde D, Landewé R, Listing J, Akkoc N, Brandt J, et al. The development of Assessment of SpondyloArthritis international Society classification criteria for axial spondyloarthritis (part II): validation and final selection. Ann Rheum Dis 2009;68:777–83.
3. Coates LC, Moverley AR, McParland L, Brown S, Navarro-Coy N, O'Dwyer JL, et al. Effect of tight control of inflammation in early psoriatic arthritis (TICOPA): a UK multicentre, open-label, randomised controlled trial. Lancet 2015;386:2489–98.
4. Bos WH, Wolbink GJ, Boers M, Tijhuis GJ, de Vries N, van der Horst-Bruinsma IE, et al. Arthritis development in patients with arthralgia is strongly associated with anticitrullinated protein antibody status: a prospective cohort study. Ann Rheum Dis 2010;69:490–4.
5. Berthelot JM, le Goff B, Maugars Y, Laredo JD. Sacroiliac joint edema by MRI: far more often mechanical than inflammatory? Joint Bone Spine 2016;83:3–5.
6. Morgan PM, Anderson AW, Swiontkowski MF. Symptomatic sacroiliac joint disease and radiographic evidence of femoroacetabular impingement. Hip Int 2013;23:212–7.
7. Hodge JC, Bessette B. The incidence of sacroiliac joint disease in patients with low-back pain. Can Assoc Radiol J 1999;50:321–3.
8. Jans L, van Langenhove C, van Praet L, Carron P, Elewaut D, van den Bosch F, et al. Diagnostic value of pelvic enthesitis on MRI of the sacroiliac joints in spondyloarthritis. Eur Radiol 2014;24:866–71.
9. O'Shea FD, Boyle E, Salonen DC, Ammendolia C, Peterson C, Hsu W, et al. Inflammatory and degenerative sacroiliac joint disease in a primary back pain cohort. Arthritis Care Res (Hoboken) 2010;62:447–54.
10. Lambert RG, Bakker PA, van der Heijde D, Weber U, Rudwaleit M, Hermann KG, et al. Defining active sacroiliitis on MRI for classification of axial spondyloarthritis: update by the ASAS MRI working group. Ann Rheum Dis 2016;75:1958–63.
11. Arnbak B, Jensen TS, Egund N, Zejden A, Hørslev-Petersen K, Manniche C, et al. Prevalence of degenerative and spondyloarthritis-related magnetic resonance imaging findings in the spine and sacroiliac joints in patients with persistent low back pain. Eur Radiol 2016;26:1191–203.

DOI 10.1002/art.40030

Reply

To the Editor:

We thank Drs. van der Linden and Khan for their interest in our recent study, which demonstrated that up to one-third of seemingly healthy (i.e., without axial SpA or any other rheumatologic disorder) first-degree relatives of HLA–B27–positive AS patients display clinical and/or imaging features of SpA, indepen-

dent of their HLA–B27 status. We would like to apologize for our presumed lack of clarity in the text, leading to the incorrect statement by van der Linden and Khan that we report the presence of axial SpA in those relatives. We carefully avoided any statement in this direction throughout the manuscript and wish to emphasize this point once more: the aim of the study (and hence the conclusion drawn) was not to diagnose axial SpA early but, in contrast, to study SpA features in seemingly healthy individuals who do not (yet) have axial SpA. We did not suggest in any way that the presence of features of SpA in these individuals indicates that they have the diagnosis of axial SpA.

Van der Linden and Khan propose, as a potential explanation for the equal prevalence of SpA features in HLA–B27–positive and HLA–B27–negative first-degree relatives, that only a subset of these individuals (presumably those who were HLA–B27 positive) will progress to having full-blown SpA over time. We completely agree, as investigating this question is exactly the reason we have undertaken this prospective cohort study, reporting in our recent article only baseline findings, and why we mention in the article that "Further follow-up will show which first-degree relatives will develop clinically manifest SpA."

Finally, van der Linden and Khan dispute the criterion validity of the ASAS criteria for axial SpA (1). We wish to clearly distance ourselves from this statement as 1) our study was never designed to address this question, 2) the ASAS criteria were developed to classify patients as having axial SpA and not to diagnose axial SpA (2,3), and 3) as clearly indicated in our report and highlighted in the highly relevant editorial by Sari and Haroon (4), we used the ASAS criteria exclusively as a research tool in our study, as the population we studied (healthy first-degree relatives) is not representative of the population in which the criteria were validated.

We wish to clearly reiterate that our study addressed neither the primacy of HLA–B27 nor the validity of the ASAS criteria. The Pre-SpA cohort study is a prospective translational study designed to learn more about early pathophysiologic events in SpA.

We also appreciate the interest and comments of Dr. Baillet and colleagues. Those authors note that treatment in very early SpA has not yet been shown to be efficacious, as it has in RA. In our opinion this highlights the importance of cohort studies investigating the early and very early phases of the disease, such as studies of the Spondyloarthritis Caught Early cohort, the Devenir des Spondyloarthrites Indifférenciées Récentes cohort, and our Pre-SpA family cohort, which even enables identification of the preclinical phases of SpA. Whether such an entity as "pre-spondyloarthritis" can be recognized and if the disease can be halted in such an early phase needs to be determined by careful and ongoing follow-up of the Pre-SpA cohort.

Baillet et al conclude, based on their experience with 1 patient, that inflammation of the anterior portion of the SI joint in a first-degree relative of a patient with SpA is not necessarily an SpA-related symptom. We would like to refer them to Table 2 of our article, comparing participants with and those without imaging abnormalities with regard to a number of features, including risk factors for degenerative disease (higher BMI, female sex, higher age). No differences were found. Additionally, the number of known past pregnancies was comparable in the 2 groups (4 pregnancies among the 39 participants without imaging abnormalities versus 2 pregnancies among the 11 participants with imaging abnormalities; $P = 0.591$). Although the Pre-SpA cohort is a very young cohort (mean $\pm$ SD age 25.2 ± 5.1 years), we agree with Baillet and colleagues that other causes of inflammation of the SI joints should be considered. Since information on MRI findings in the SI joints of asymptomatic individuals is scarce, only by thorough follow-up will we learn which participants will ultimately develop full-blown SpA.

Janneke de Winter, MD
Marleen van de Sande, MD
Robert Landewé, MD, PhD
Dominique Baeten, MD, PhD
Academic Medical Center
University of Amsterdam
Amsterdam, The Netherlands

1. Rudwaleit M, van der Heijde D, Landewé R, Listing J, Akkoc N, Brandt J, et al. The development of Assessment of SpondyloArthritis international Society classification criteria for axial spondyloarthritis (part II): validation and final selection. Ann Rheum Dis 2009;68:777–83.
2. Sepriano A, Landewé R, van der Heijde D, Sieper J, Akkoc N, Brandt J, et al. Predictive validity of the ASAS classification criteria for axial and peripheral spondyloarthritis after follow-up in the ASAS cohort: a final analysis. Ann Rheum Dis 2016;75:1034–42.
3. Van Tubergen A, Weber U. Diagnosis and classification in spondyloarthritis: identifying a chameleon. Nat Rev Rheumatol 2012; 8:253–61.
4. Sari I, Haroon N. Axial spondyloarthritis: the recurrence plot thickens [editorial]. Arthritis Rheumatol 2016;68:2354–6.

DOI 10.1002/art.40011

Facet pain syndrome and nonradiographic axial spondyloarthritis

To the Editor:

Rheumatologists study spondyloarthritis (SpA), but we usually do not study chronic low back pain (1). Facet joint syndrome has been estimated to account for up to 30% of chronic low back pain (2). Despite this high prevalence, the existence of facet pain syndrome was denied in the 1960s and 1970s and only recently confirmed (3). However, it remains poorly understood, and its diagnosis is often difficult (2,3).

In routine practice I frequently see young, thin, HLA–B27–negative women with lumbar hyperlordosis, facet pain syndrome, and nocturnal low back pain. Lumbar facet pain syndrome tends to be eccentric and bilateral, most commonly affecting the lumbosacral area (gluteus). Its onset is usually insidious, and it typically worsens with extension, ipsilateral bending, or rotation of the spine (2–4), improving with lumbar flexion. It causes morning stiffness of the spine (3) and occurs when movement starts and at rest (3,4). In contrast, lumbar hyperlordosis produces overload in its concavity (the facet joints) and is associated with a horizontalized sacrum (5), which, in turn, is associated with female sex (6). Mechanical stress on the horizontalized sacroiliac joints may produce adjacent bone marrow edema (1,7). These patients report that low back pain awakens them at night when they turn over in bed. I believe these patients may sleep in lateral decubitus with their facet joints in slight lumbar flexion, but they awaken when turning over in bed because of a combination of lumbar extension and rotation. In my view, these patients are good candi-

dent of their HLA–B27 status. We would like to apologize for our presumed lack of clarity in the text, leading to the incorrect statement by van der Linden and Khan that we report the presence of axial SpA in those relatives. We carefully avoided any statement in this direction throughout the manuscript and wish to emphasize this point once more: the aim of the study (and hence the conclusion drawn) was not to diagnose axial SpA early but, in contrast, to study SpA features in seemingly healthy individuals who do not (yet) have axial SpA. We did not suggest in any way that the presence of features of SpA in these individuals indicates that they have the diagnosis of axial SpA.

Van der Linden and Khan propose, as a potential explanation for the equal prevalence of SpA features in HLA–B27–positive and HLA–B27–negative first-degree relatives, that only a subset of these individuals (presumably those who were HLA–B27 positive) will progress to having full-blown SpA over time. We completely agree, as investigating this question is exactly the reason we have undertaken this prospective cohort study, reporting in our recent article only baseline findings, and why we mention in the article that "Further follow-up will show which first-degree relatives will develop clinically manifest SpA."

Finally, van der Linden and Khan dispute the criterion validity of the ASAS criteria for axial SpA (1). We wish to clearly distance ourselves from this statement as 1) our study was never designed to address this question, 2) the ASAS criteria were developed to classify patients as having axial SpA and not to diagnose axial SpA (2,3), and 3) as clearly indicated in our report and highlighted in the highly relevant editorial by Sari and Haroon (4), we used the ASAS criteria exclusively as a research tool in our study, as the population we studied (healthy first-degree relatives) is not representative of the population in which the criteria were validated.

We wish to clearly reiterate that our study addressed neither the primacy of HLA–B27 nor the validity of the ASAS criteria. The Pre-SpA cohort study is a prospective translational study designed to learn more about early pathophysiologic events in SpA.

We also appreciate the interest and comments of Dr. Baillet and colleagues. Those authors note that treatment in very early SpA has not yet been shown to be efficacious, as it has in RA. In our opinion this highlights the importance of cohort studies investigating the early and very early phases of the disease, such as studies of the Spondyloarthritis Caught Early cohort, the Devenir des Spondyloarthrites Indifférenciées Récentes cohort, and our Pre-SpA family cohort, which even enables identification of the preclinical phases of SpA. Whether such an entity as "pre-spondyloarthritis" can be recognized and if the disease can be halted in such an early phase needs to be determined by careful and ongoing follow-up of the Pre-SpA cohort.

Baillet et al conclude, based on their experience with 1 patient, that inflammation of the anterior portion of the SI joint in a first-degree relative of a patient with SpA is not necessarily an SpA-related symptom. We would like to refer them to Table 2 of our article, comparing participants with and those without imaging abnormalities with regard to a number of features, including risk factors for degenerative disease (higher BMI, female sex, higher age). No differences were found. Additionally, the number of known past pregnancies was comparable in the 2 groups (4 pregnancies among the 39 participants without imaging abnormalities versus 2 pregnancies among the 11 participants with imaging abnormalities; $P = 0.591$). Although the Pre-SpA cohort is a very young cohort (mean $\pm$ SD age 25.2 ± 5.1 years), we agree with Baillet and colleagues that other causes of inflammation of the SI joints should be considered. Since information on MRI findings in the SI joints of asymptomatic individuals is scarce, only by thorough follow-up will we learn which participants will ultimately develop full-blown SpA.

Janneke de Winter, MD
Marleen van de Sande, MD
Robert Landewé, MD, PhD
Dominique Baeten, MD, PhD
Academic Medical Center
University of Amsterdam
Amsterdam, The Netherlands

1. Rudwaleit M, van der Heijde D, Landewé R, Listing J, Akkoc N, Brandt J, et al. The development of Assessment of SpondyloArthritis international Society classification criteria for axial spondyloarthritis (part II): validation and final selection. Ann Rheum Dis 2009;68:777–83.
2. Sepriano A, Landewé R, van der Heijde D, Sieper J, Akkoc N, Brandt J, et al. Predictive validity of the ASAS classification criteria for axial and peripheral spondyloarthritis after follow-up in the ASAS cohort: a final analysis. Ann Rheum Dis 2016;75:1034–42.
3. Van Tubergen A, Weber U. Diagnosis and classification in spondyloarthritis: identifying a chameleon. Nat Rev Rheumatol 2012; 8:253–61.
4. Sari I, Haroon N. Axial spondyloarthritis: the recurrence plot thickens [editorial]. Arthritis Rheumatol 2016;68:2354–6.

DOI 10.1002/art.40011

Facet pain syndrome and nonradiographic axial spondyloarthritis

To the Editor:

Rheumatologists study spondyloarthritis (SpA), but we usually do not study chronic low back pain (1). Facet joint syndrome has been estimated to account for up to 30% of chronic low back pain (2). Despite this high prevalence, the existence of facet pain syndrome was denied in the 1960s and 1970s and only recently confirmed (3). However, it remains poorly understood, and its diagnosis is often difficult (2,3).

In routine practice I frequently see young, thin, HLA–B27–negative women with lumbar hyperlordosis, facet pain syndrome, and nocturnal low back pain. Lumbar facet pain syndrome tends to be eccentric and bilateral, most commonly affecting the lumbosacral area (gluteus). Its onset is usually insidious, and it typically worsens with extension, ipsilateral bending, or rotation of the spine (2–4), improving with lumbar flexion. It causes morning stiffness of the spine (3) and occurs when movement starts and at rest (3,4). In contrast, lumbar hyperlordosis produces overload in its concavity (the facet joints) and is associated with a horizontalized sacrum (5), which, in turn, is associated with female sex (6). Mechanical stress on the horizontalized sacroiliac joints may produce adjacent bone marrow edema (1,7). These patients report that low back pain awakens them at night when they turn over in bed. I believe these patients may sleep in lateral decubitus with their facet joints in slight lumbar flexion, but they awaken when turning over in bed because of a combination of lumbar extension and rotation. In my view, these patients are good candi-

dates for a diagnosis of nonradiographic axial SpA, and they could help to explain major differences observed between patients with nonradiographic axial SpA according to the Assessment of SpondyloArthritis international Society criteria (8) and patients with ankylosing spondylitis, such as female predominance, lower levels of inflammation markers, lower prevalence of HLA–B27, and nonspecific bone marrow edema adjacent to sacroiliac joints in the former group (1,7,9).

Francisco Javier Olmedo-Garzón, MD
Hospital Clínico de San Carlos
Madrid, Spain

1. Van Hoeven L, Luime J, Han H, Vergouwe Y, Weel A. Identifying axial spondyloarthritis in Dutch primary care patients, ages 25–45 years, with chronic low back pain. Arthritis Care Res (Hoboken) 2014;66:446–53.
2. Cohen SP, Raja SN. Pathogenesis, diagnosis, and treatment of lumbar zygapophysial (facet) joint pain. Anesthesiology 2007;106:591–614.
3. Allegri M, Montella S, Salici F, Valente A, Marchesini M, Compagnone C, et al. Mechanisms of low back pain: a guide for diagnosis and therapy. F1000Res 2016;5:1530.
4. Proietti L, Schiro GR, Sessa S, Scaramuzzo L. The impact of sagittal balance on low back pain in patients treated with zygoapophysial facet joint injection. Eur Spine J 2014;23 Suppl 6:628–33.
5. Been E, Kalichman L. Lumbar lordosis. Spine J 2014;14:87–97.
6. Pries E, Dreischarf M, Bashkuev M, Putzier M, Schmidt H. The effects of age and gender on the lumbopelvic rhythm in the sagittal plane in 309 subjects. J Biomech 2015;48:3080–7.
7. Deodhar A. Sacroiliac joint magnetic resonance imaging in the diagnosis of axial spondyloarthritis: "a tiny bit of white on two consecutive slices" may be objective, but not specific [editorial]. Arthritis Rheumatol 2016;68;775–8.
8. Rudwaleit M, van der Heijde D, Landewé R, Akkoc N, Brandt J, Chou CT, et al. The development of Assessment of SpondyloArthritis international Society classification criteria for axial spondyloarthritis (part II): validation and final selection. Ann Rheum Dis 2009;68:777–83.
9. Arnbak B, Jurik AG, Hørslev-Petersen K, Hendricks O, Hermansen LT, Loft AG, et al. Associations between spondyloarthritis features and magnetic resonance imaging findings: a cross-sectional analysis of 1,020 patients with persistent low back pain. Arthritis Rheumatol 2016;68:892–900.

DOI 10.1002/art.40010

Reply

To the Editor:

We thank Dr. Olmedo-Garzón for an interesting hypothesis on the role of facet joint syndrome in the composition of the nonradiographic SpA patient population. Overall, we agree that with the use of the Assessment of SpondyloArthritis international Society criteria for axial SpA (1), there is a risk that a subgroup of patients with mechanical low back pain may be diagnosed as having SpA. We further agree that a different load distribution in women may influence the presence of bone marrow edema at the sacroiliac joints, and also that it is possible that age and common degenerative disorders may influence the presence of bone marrow edema at the sacroiliac joint. These theories are supported by previous reports from our group (2,3). Likewise, the relatively high prevalence of inflammatory pain characteristics, such as insidious onset, nocturnal pain, and morning stiffness, reported in patients with non-SpA low back pain (4–6) may have various explanations, of which facet joint syndrome might be one.

Unfortunately, diagnosis of facet joint syndrome is difficult, as Olmedo-Garzón points out. The definition is restricted by a lack of objective measurements, compromising the ability to investigate for facet joint syndrome in relation to the diagnosis of SpA. However, the hypotheses proposed by Olmedo-Garzón emphasize the need for further studies aimed at identifying clinical symptoms and imaging findings that would accurately distinguish SpA from other causes of back pain.

Bodil Arnbak, MSc, PhD
Claus Manniche, MD, DMSc
Hospital Lillebaelt
Middelfart, Denmark
and University of Southern Denmark
Odense, Denmark
Anne Grethe Jurik, MD, DMSc
Hospital Lillebaelt
Middelfart, Denmark
University of Southern Denmark
Odense, Denmark
and Aarhus University Hospital
Aarhus, Denmark
Tue Secher Jensen, MSc, PhD
Hospital Lillebaelt
Middelfart, Denmark
and University of Southern Denmark
Odense, Denmark

1. Rudwaleit M, van der Heijde D, Landewé R, Listing J, Akkoc N, Brandt J, et al. The development of Assessment of SpondyloArthritis international Society classification criteria for axial spondyloarthritis (part II): validation and final selection. Ann Rheum Dis 2009;68:777–83.
2. Arnbak B, Jurik AG, Hørslev-Petersen K, Hendricks O, Hermansen LT, Loft AG, et al. Associations between spondyloarthritis features and magnetic resonance imaging findings: a cross-sectional analysis of 1,020 patients with persistent low back pain. Arthritis Rheumatol 2016;68:892–900.
3. Arnbak B, Jensen TS, Egund N, Zejden A, Hørslev-Petersen K, Manniche C, et al. Prevalence of degenerative and spondyloarthritis-related magnetic resonance imaging findings in the spine and sacroiliac joints in patients with persistent low back pain. Eur Radiol 2016;26:1191–203.
4. Keeling SO, Majumdar SR, Conner-Spady B, Battie MC, Carroll LJ, Maksymowych WP. Preliminary validation of a self-reported screening questionnaire for inflammatory back pain. J Rheumatol 2012;39:822–9.
5. Hamilton L, Macgregor A, Newman D, Belkhiri A, Toms A, Gaffney K. Validation of a patient self-reported screening questionnaire for axial spondyloarthropathy in a UK population. Spine (Phila Pa 1976) 2013;38:502–6.
6. Arnbak B, Hendricks O, Hørslev-Petersen K, Jurik AG, Pedersen SJ, Ostergaard M, et al. The discriminative value of inflammatory back pain in patients with persistent low back pain. Scand J Rheumatol 2016;45:321–8.

dates for a diagnosis of nonradiographic axial SpA, and they could help to explain major differences observed between patients with nonradiographic axial SpA according to the Assessment of SpondyloArthritis international Society criteria (8) and patients with ankylosing spondylitis, such as female predominance, lower levels of inflammation markers, lower prevalence of HLA–B27, and nonspecific bone marrow edema adjacent to sacroiliac joints in the former group (1,7,9).

Francisco Javier Olmedo-Garzón, MD
Hospital Clínico de San Carlos
Madrid, Spain

1. Van Hoeven L, Luime J, Han H, Vergouwe Y, Weel A. Identifying axial spondyloarthritis in Dutch primary care patients, ages 25–45 years, with chronic low back pain. Arthritis Care Res (Hoboken) 2014;66:446–53.
2. Cohen SP, Raja SN. Pathogenesis, diagnosis, and treatment of lumbar zygapophysial (facet) joint pain. Anesthesiology 2007;106:591–614.
3. Allegri M, Montella S, Salici F, Valente A, Marchesini M, Compagnone C, et al. Mechanisms of low back pain: a guide for diagnosis and therapy. F1000Res 2016;5:1530.
4. Proietti L, Schiro GR, Sessa S, Scaramuzzo L. The impact of sagittal balance on low back pain in patients treated with zygoapophysial facet joint injection. Eur Spine J 2014;23 Suppl 6:628–33.
5. Been E, Kalichman L. Lumbar lordosis. Spine J 2014;14:87–97.
6. Pries E, Dreischarf M, Bashkuev M, Putzier M, Schmidt H. The effects of age and gender on the lumbopelvic rhythm in the sagittal plane in 309 subjects. J Biomech 2015;48:3080–7.
7. Deodhar A. Sacroiliac joint magnetic resonance imaging in the diagnosis of axial spondyloarthritis: "a tiny bit of white on two consecutive slices" may be objective, but not specific [editorial]. Arthritis Rheumatol 2016;68;775–8.
8. Rudwaleit M, van der Heijde D, Landewé R, Akkoc N, Brandt J, Chou CT, et al. The development of Assessment of SpondyloArthritis international Society classification criteria for axial spondyloarthritis (part II): validation and final selection. Ann Rheum Dis 2009;68:777–83.
9. Arnbak B, Jurik AG, Hørslev-Petersen K, Hendricks O, Hermansen LT, Loft AG, et al. Associations between spondyloarthritis features and magnetic resonance imaging findings: a cross-sectional analysis of 1,020 patients with persistent low back pain. Arthritis Rheumatol 2016;68:892–900.

DOI 10.1002/art.40010

Reply

To the Editor:

We thank Dr. Olmedo-Garzón for an interesting hypothesis on the role of facet joint syndrome in the composition of the nonradiographic SpA patient population. Overall, we agree that with the use of the Assessment of SpondyloArthritis international Society criteria for axial SpA (1), there is a risk that a subgroup of patients with mechanical low back pain may be diagnosed as having SpA. We further agree that a different load distribution in women may influence the presence of bone marrow edema at the sacroiliac joints, and also that it is possible that age and common degenerative disorders may influence the presence of bone marrow edema at the sacroiliac joint. These theories are supported by previous reports from our group (2,3). Likewise, the relatively high prevalence of inflammatory pain characteristics, such as insidious onset, nocturnal pain, and morning stiffness, reported in patients with non-SpA low back pain (4–6) may have various explanations, of which facet joint syndrome might be one.

Unfortunately, diagnosis of facet joint syndrome is difficult, as Olmedo-Garzón points out. The definition is restricted by a lack of objective measurements, compromising the ability to investigate for facet joint syndrome in relation to the diagnosis of SpA. However, the hypotheses proposed by Olmedo-Garzón emphasize the need for further studies aimed at identifying clinical symptoms and imaging findings that would accurately distinguish SpA from other causes of back pain.

Bodil Arnbak, MSc, PhD
Claus Manniche, MD, DMSc
Hospital Lillebaelt
Middelfart, Denmark
and University of Southern Denmark
Odense, Denmark
Anne Grethe Jurik, MD, DMSc
Hospital Lillebaelt
Middelfart, Denmark
University of Southern Denmark
Odense, Denmark
and Aarhus University Hospital
Aarhus, Denmark
Tue Secher Jensen, MSc, PhD
Hospital Lillebaelt
Middelfart, Denmark
and University of Southern Denmark
Odense, Denmark

1. Rudwaleit M, van der Heijde D, Landewé R, Listing J, Akkoc N, Brandt J, et al. The development of Assessment of SpondyloArthritis international Society classification criteria for axial spondyloarthritis (part II): validation and final selection. Ann Rheum Dis 2009;68:777–83.
2. Arnbak B, Jurik AG, Hørslev-Petersen K, Hendricks O, Hermansen LT, Loft AG, et al. Associations between spondyloarthritis features and magnetic resonance imaging findings: a cross-sectional analysis of 1,020 patients with persistent low back pain. Arthritis Rheumatol 2016;68:892–900.
3. Arnbak B, Jensen TS, Egund N, Zejden A, Hørslev-Petersen K, Manniche C, et al. Prevalence of degenerative and spondyloarthritis-related magnetic resonance imaging findings in the spine and sacroiliac joints in patients with persistent low back pain. Eur Radiol 2016;26:1191–203.
4. Keeling SO, Majumdar SR, Conner-Spady B, Battie MC, Carroll LJ, Maksymowych WP. Preliminary validation of a self-reported screening questionnaire for inflammatory back pain. J Rheumatol 2012;39:822–9.
5. Hamilton L, Macgregor A, Newman D, Belkhiri A, Toms A, Gaffney K. Validation of a patient self-reported screening questionnaire for axial spondyloarthropathy in a UK population. Spine (Phila Pa 1976) 2013;38:502–6.
6. Arnbak B, Hendricks O, Hørslev-Petersen K, Jurik AG, Pedersen SJ, Ostergaard M, et al. The discriminative value of inflammatory back pain in patients with persistent low back pain. Scand J Rheumatol 2016;45:321–8.